frontiers | Research Topics

Vegetation, ecosystem processing and carbon budget of wetlands under global change

Edited by
Xiaoming Kang, Yichao Rui, Yangong Du, Rongxiao Che, Yong Li and Bing Song

Published in
Frontiers in Plant Science

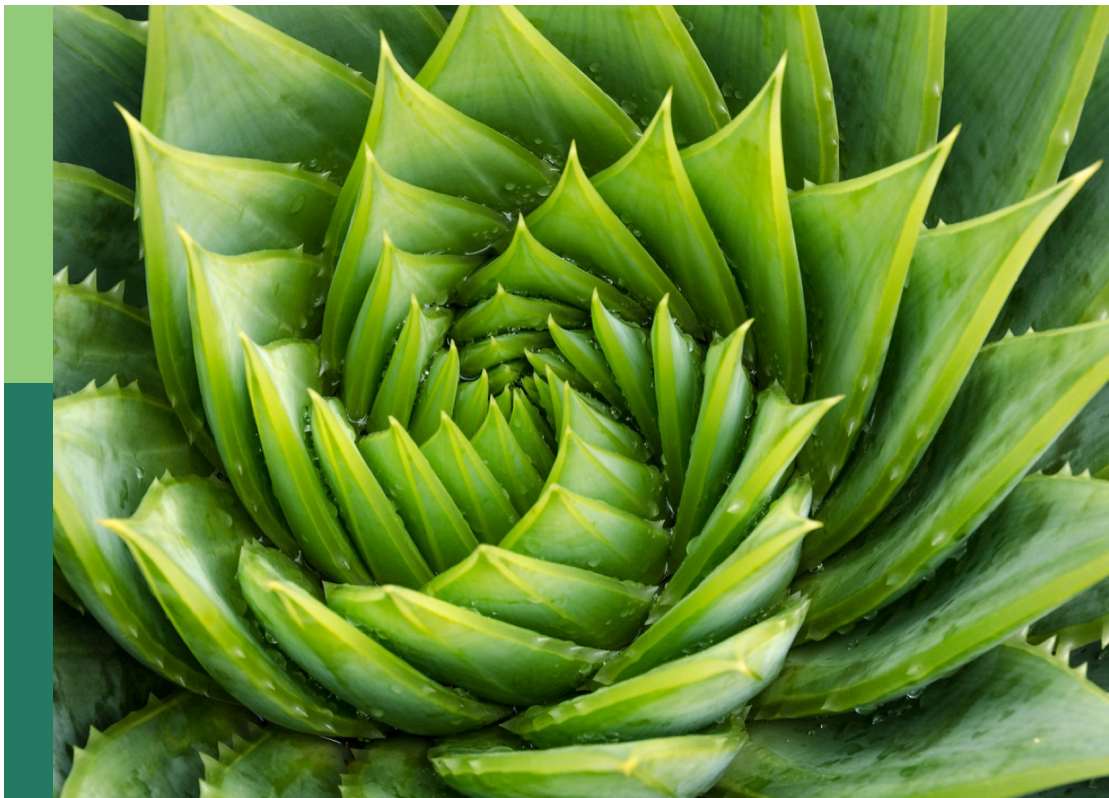

ISSN 1664-8714
ISBN 978-2-83252-170-0
DOI 10.3389/978-2-83252-170-0

About Frontiers

Frontiers is more than just an open access publisher of scholarly articles: it is a pioneering approach to the world of academia, radically improving the way scholarly research is managed. The grand vision of Frontiers is a world where all people have an equal opportunity to seek, share and generate knowledge. Frontiers provides immediate and permanent online open access to all its publications, but this alone is not enough to realize our grand goals.

Frontiers journal series

The Frontiers journal series is a multi-tier and interdisciplinary set of open-access, online journals, promising a paradigm shift from the current review, selection and dissemination processes in academic publishing. All Frontiers journals are driven by researchers for researchers; therefore, they constitute a service to the scholarly community. At the same time, the *Frontiers journal series* operates on a revolutionary invention, the tiered publishing system, initially addressing specific communities of scholars, and gradually climbing up to broader public understanding, thus serving the interests of the lay society, too.

Dedication to quality

Each Frontiers article is a landmark of the highest quality, thanks to genuinely collaborative interactions between authors and review editors, who include some of the world's best academicians. Research must be certified by peers before entering a stream of knowledge that may eventually reach the public - and shape society; therefore, Frontiers only applies the most rigorous and unbiased reviews. Frontiers revolutionizes research publishing by freely delivering the most outstanding research, evaluated with no bias from both the academic and social point of view. By applying the most advanced information technologies, Frontiers is catapulting scholarly publishing into a new generation.

What are Frontiers Research Topics?

Frontiers Research Topics are very popular trademarks of the *Frontiers journals series*: they are collections of at least ten articles, all centered on a particular subject. With their unique mix of varied contributions from Original Research to Review Articles, Frontiers Research Topics unify the most influential researchers, the latest key findings and historical advances in a hot research area.

Find out more on how to host your own Frontiers Research Topic or contribute to one as an author by contacting the Frontiers editorial office: frontiersin.org/about/contact

Vegetation, ecosystem processing and carbon budget of wetlands under global change

Topic editors

Xiaoming Kang — Institute of Wetland Research, Chinese Academy of Forestry, China

Yichao Rui — Rodale Institute, PA, United States

Yangong Du — Northwest Institute of Plateau Biology, Chinese Academy of Sciences (CAS), China

Rongxiao Che — Yunnan University, China

Yong Li — Institute of Wetland Research, Chinese Academy of Forestry, China

Bing Song — Ludong University, China

Citation

Kang, X., Rui, Y., Du, Y., Che, R., Li, Y., Song, B., eds. (2023). *Vegetation, ecosystem processing and carbon budget of wetlands under global change*. Lausanne: Frontiers Media SA. doi: 10.3389/978-2-83252-170-0

The authors declare that the research was conducted in the absence of any commercial or financial relationships that could be construed as a potential conflict of interest.

Table of contents

05 Editorial: Vegetation, ecosystem processing and carbon budget of wetlands under global change
Yong Li, Bing Song and Xiaoming Kang

08 Does a Widespread Species Have a Higher Competitive Ability Than an Endemic Species? A Case Study From the Dongting Lake Wetlands
Yuhang Du, Qiaoqiao Zhou, Zenghui Peng, Fangcheng Peng, Lianlian Xi and Youzhi Li

17 Aboveground Biomass of Wetland Vegetation Under Climate Change in the Western Songnen Plain
Yanji Wang, Xiangjin Shen, Shouzheng Tong, Mingye Zhang, Ming Jiang and Xianguo Lu

27 Water Uptake Tradeoffs of Dominant Shrub Species in the Coastal Wetlands of the Yellow River Delta, China
Jinfang Zhu, Jingtao Liu, Junsheng Li, Caiyun Zhao and Jingkuan Sun

37 Seasonal and Inter-Annual Variations of Carbon Dioxide Fluxes and Their Determinants in an Alpine Meadow
Song Wang, Weinan Chen, Zheng Fu, Zhaolei Li, Jinsong Wang, Jiaqiang Liao and Shuli Niu

49 Soil Respiration of Paddy Soils Were Stimulated by Semiconductor Minerals
Yinping Bai, Ling Nan, Qing Wang, Weiqi Wang, Jiangbo Hai, Xiaoya Yu, Qin Cao, Jing Huang, Rongping Zhang, Yunwei Han, Min Yang and Gang Yang

59 Rising Shallow Groundwater Level May Facilitate Seed Persistence in the Supratidal Wetlands of the Yellow River Delta
Lu Feng, Ling Peng, Qian Cui, Hong-Jun Yang, Jin-Zhao Ma and Jing-Tao Liu

71 Carbon, Nitrogen, and Phosphorus Stoichiometry and Plant Growth Strategy as Related to Land-Use in Hangzhou Bay Coastal Wetland, China
Jing Xiong, Xuexin Shao, Haijing Yuan, Enjun Liu and Ming Wu

83 Degradation reduces the diversity of nitrogen-fixing bacteria in the alpine wetland on the Qinghai-Tibet Plateau
Chengyi Li, Xilai Li, Yuanwu Yang, Yan Shi and Honglin Li

96 Differences in nitrogen and phosphorus sinks between the harvest and non-harvest of *Miscanthus lutarioriparius* in the Dongting Lake wetlands
Zenghui Peng, Yuhang Du, Shiyu Niu, Lianlian Xi, Yandong Niu and Youzhi Li

108 The divergent vertical pattern and assembly of soil bacterial and fungal communities in response to short-term warming in an alpine peatland
Xiaodong Wang, Yong Li, Zhongqing Yan, Yanbin Hao, Enze Kang, Xiaodong Zhang, Meng Li, Kerou Zhang, Liang Yan, Ao Yang, Yuechuan Niu and Xiaoming Kang

122 Can allelopathy of *Phragmites australis* extracts aggravate the effects of salt stress on the seed germination of *Suaeda salsa*?
Jingwen Gao, Bo Guan, Minjia Ge, Franziska Eller, Junbao Yu, Xuehong Wang and Jincheng Zuo

133 Effect of freshwater on plant species diversity and interspecific associations in coastal wetlands invaded by *Spartina alterniflora*
Zhiguo Dou, Lijuan Cui, Wei Li, Yinru Lei, Xueyan Zuo, Yang Cai and Rui Yan

150 Response of vegetation variation to climate change and human activities in semi-arid swamps
Guangyi Deng, Jin Gao, Haibo Jiang, Dehao Li, Xue Wang, Yang Wen, Lianxi Sheng and Chunguang He

166 Response of the fine root morphological and chemical traits of *Tamarix chinensis* to water and salt changes in coastal wetlands of the Yellow River Delta
Jia Sun, Jiangbao Xia, Pengshuai Shao, Jinzhao Ma, Fanglei Gao, Ying Lang, Xianshuang Xing, Mingming Dong and Chuanrong Li

179 Ecological stoichiometry, salt ions and homeostasis characteristics of different types of halophytes and soils
Yinghan Zhao, Tian Li, Junhan Liu, Jingkuan Sun and Ping Zhang

195 Interannual characteristics and driving mechanism of CO_2 fluxes during the growing season in an alpine wetland ecosystem at the southern foot of the Qilian Mountains
Jingbin Zhu, Hongqin Li, Huidan He, Fawei Zhang, Yongsheng Yang and Yingnian Li

205 Response of soil bacterial community to alpine wetland degradation in arid Central Asia
Maidinuer Abulaizi, Mo Chen, Zailei Yang, Yang Hu, Xinping Zhu and Hongtao Jia

frontiers | Frontiers in Plant Science

TYPE Editorial
PUBLISHED 30 March 2023
DOI 10.3389/fpls.2023.1160319

OPEN ACCESS

EDITED BY
Esperança Gacia,
Center for Advanced Studies of Blanes (CSIC), Spain

REVIEWED BY
Salvador Sánchez-Carrillo,
Spanish National Research Council (CSIC), Spain

*CORRESPONDENCE
Xiaoming Kang
xmkang@ucas.ac.cn

SPECIALTY SECTION
This article was submitted to Functional Plant Ecology, a section of the journal Frontiers in Plant Science

RECEIVED 07 February 2023
ACCEPTED 23 March 2023
PUBLISHED 30 March 2023

CITATION
Li Y, Song B and Kang X (2023) Editorial: Vegetation, ecosystem processing and carbon budget of wetlands under global change.
Front. Plant Sci. 14:1160319.
doi: 10.3389/fpls.2023.1160319

Editorial: Vegetation, ecosystem processing and carbon budget of wetlands under global change

Yong Li[1,2,3], Bing Song[4] and Xiaoming Kang[1,2,3]*

[1]Wetland Research Center, Institute of Ecological Conservation and Restoration, Chinese Academy of Forestry, Beijing, China, [2]Beijing Key Laboratory of Wetland Services and Restoration, Beijing, China, [3]Sichuan Zoige Wetland Ecosystem Research Station, Tibetan Autonomous Prefecture of Aba, Sichuan, China, [4]School of Resources and Environmental Engineering, Ludong University, Yantai, China

KEYWORDS

wetland, plant community, vegetation, ecosystem process and function, carbon cycling and sequestration, global change, carbon budget

Editorial on the Research Topic

Vegetation, ecosystem processing and carbon budget of wetlands under global change

The objective of this Research Topic is to synthesize how the components and functions of wetland respond to global change and gain novel insights into the underlying mechanisms. To answer this question, the Research Topic presents a collection of wetland research studies from different biomes to demonstrate how plant population and community, soil microbes, carbon recycling and carbon budget respond to changing environments and human activities.

The papers in this collection explored the coexistence mechanism of plant species in freshwater inland marshes and coastal wetlands. For example, the widespread species *Phragmites australis* had a higher competitive ability during the flooding period, while the endemic species *Triarrhena lutarioriparia* increased the dominance during the non-flooding period in the Dongting Lake wetlands with seasonal flooding, implying the niche differences between the two species enabled their coexistence (Du et al.). Moreover, dominant shrub species *Tamarix chinensis* and *Ziziphus jujuba* showed different water uptake sources during dry and wet seasons in the Yellow River Delta. The difference in interspecific water use strategies demonstrated these species have adapted to the fluctuations of soil moisture, contributing to successful coexistence and increasing the resilience of the coastal wetland ecosystem to drought (Zhu et al.). Furthermore, allelopathy is an important ecological adaptation mechanism for *P. australis* to maintain a high interspecific competitive advantage in the coastal wetlands, as observed in the Yellow River Delta in *P. australis* growing with *Suaeda salsa* (Gao et al.). These findings filled the gap in plant coexistence mechanism in wetlands, which must be important to understand the response of plant species under changing environments.

Responses of seed germinability, root morphological and chemical traits, carbon:nitrogen:phosphorus stoichiometry and plant diversity to changing environments and plant invasion were also investigated (Dou et al.; Feng et al.; Sun et al.; Xiong et al.; Zhao et al.). Seed germinability and viability of seven plant species in response to 90-day storage treatment including different groundwater level and salinity in supratidal wetlands of the Yellow River Delta were explored. It was found that once dispersed into habitats with high groundwater levels and high groundwater salinity in supratidal wetlands, many species of seeds might not germinate but maintain viability, highlighting the adaptation mechanism of seed to environmental changes (Feng et al.). *T. chinensis* responded to the heterogeneity of soil water and salinity induced by groundwater level through trade-offs and changes in root morphological, nutrients and chemical characteristics in coastal wetland of the Yellow River Delta (Sun et al.). The homeostasis results of C, N and P elements in three halophytes (salt-secreting *Aeluropus sinensis*, salt-repellent *Phragmites. communis* and salt-accumulating *S. salsa*) showed that the homeostasis was strongest in *A. sinensis* and weakest in *S. salsa* in the Yellow River Delta (Zhao et al.). These results might be attributable to the differences in plant C, N, P stoichiometry and salt accumulation. Xiong et al. examined the responses of plant-soil stoichiometry and plant growth strategy to land use change (mudflat, native *P. australis*-dominated wetland, invasive *Spartina alterniflora*-dominated wetland, and reclaimed *P. australis*-dominated wetland) in Hangzhou Bay coastal wetland. Land use exerts a strong effect on plant organ and soil depth C:N:P stoichiometry and plant growth strategies. Furthermore, the effects of increased freshwater inputs were explored in coastal wetlands of Yancheng and demonstrated strong benefits in the control of invasive species such as *S. alterniflora*, modifying interspecific plant relationships and increasing plant diversity (Dou et al.). These findings provide insights into responses of plant growth strategies to changing environments.

Beside plants, responses of microbial communities and microbial diversity to wetland degradation and climate warming were also explored (Abulaizi et al.; Li et al.; Wang et al.). Li et al. investigated the diversity of nitrogen-fixing bacteria at different stages of degradation characterized by number and size of freeze-thaw mounds in the alpine wetland of Qinghai-Tibet Plateau. The results showed that the degradation of alpine wetland inhibited the growth of nitrogen-fixing bacteria, leading to the decline of their nitrogen-fixing function. Abulaizi et al. found that the vegetation communities and soil nutrients changed significantly with increasing soil degradation levels, and *Sphingomonas* could be used as a potential biomarker of degradation in mountain wetlands. Moreover, the vertical structure and assembly of the soil bacterial and fungal communities along the soil profile responded differently to short-term warming in Zoige alpine peatland. Results demonstrated that warming significantly influence the vertical structure of the fungal community but not bacterial community and that the vertical structure of the fungal community was driven by a dispersal-based process under control treatment, while the niche and dispersal processes jointly regulated the fungal communities under warming treatment (Wang et al.). These findings could provide insights into the underlying mechanism of microbial communities in response to changing climate and environment in wetlands.

How vegetation responds to climate change and human activities have been discussed in this Research Topic as well (Deng et al.; Wang et al.). Deng et al. found that human activity, rather than climate change was the main reason for vegetation improvement or degradation in the Jilin Momoge marshes of the semi-arid region of northeast China. Wang et al. explored the spatiotemporal change of aboveground biomass and its response to climate change in a marsh wetland of western Songen Plain using MODIS datasets from 2000 to 2020. The increase of summer and autumn precipitation stimulated aboveground biomass by promoting vegetation growth during 2000–2020. These results provide theoretical guidance for the restoration, protection, and adaptive management of wetland vegetation in changing environments.

This Research Topic also explored the responses of ecosystem functions such as nitrogen and phosphorus sinks, carbon recycling and carbon budget to changing environment (Peng et al.; Wang et al.; Zhu et al.). For example, Peng et al. explored the harvest effect on plant nitrogen and phosphorus sinks and these two elements release from litter decomposition of the dominant species *Miscanthus lutarioriparius* in the Dongting Lake wetlands. Non-harvest treatment greatly decreased nitrogen and phosphorus sinks, compared to the harvest treatment. Furthermore, Wang et al. found that Zoige alpine meadow in the Qinghai-Tibet Plateau acted as a faint carbon source during the 5-year observation periods and the annual net CO_2 exchange in the alpine meadow ecosystem was mainly controlled by the maximum CO_2 release rates. Zhu et al. studied the carbon budget of the growing season at long-term and its driving mechanism in a alpine wetland in the Qilian Mountains (northeastern Qinghai-Tibet Plateau) from 2004–2016. Climate warming could be beneficial to the enhancement of gross primary productivity and ecosystem respiration in the alpine wetland, while the increase of precipitation could weaken this effect. These results could advance our understanding of ecosystem function response to various environmental factors in the context of global change.

Overall, this Research Topic provides a synthesis of plant and microbial communities, vegetation, and ecosystem functions of wetlands (including inland lakes, freshwater marshes, mountain wetlands and coastal wetlands) in response to environmental changing because of human activities. We hope these findings could provide new insights into guidance for the conservation and restoration of wetlands under global change.

Author contributions

YL and BS wrote the first version of manuscript. XK revised the manuscript and all the authors contributed to the final version of the manuscript.

Funding

This work was financially supported by the Fundamental Research Funds of CAF (CAFYBB2019QB009), the Second Tibetan Plateau Scientific Expedition and Research Program (STEP) (2019QZKK0304-02), and the National Natural Science Foundation of China (32171597, 32171598, 32271678, and 42041005).

Acknowledgments

We thank Yangong Du, Yichao Rui and Rongxiao Che for their editorial assistance and also thank the authors for their contributions and the reviewers for their insightful comments.

Conflict of interest

The authors declare that the research was conducted in the absence of any commercial or financial relationships that could be construed as a potential conflict of interest.

Publisher's note

frontiers | Frontiers in Plant Science

ORIGINAL RESEARCH
published: 24 May 2022
doi: 10.3389/fpls.2022.864316

Does a Widespread Species Have a Higher Competitive Ability Than an Endemic Species? A Case Study From the Dongting Lake Wetlands

*Yuhang Du[1,2], Qiaoqiao Zhou[1,2], Zenghui Peng[1,2], Fangcheng Peng[1,2], Lianlian Xi[1,2] and Youzhi Li[1,2]**

[1] College of Resources and Environment, Hunan Agricultural University, Changsha, China, [2] Hunan Provincial Key Laboratory of Rural Ecosystem Health in Dongting Lake Area, Hunan Agricultural University, Changsha, China

The distribution range of plants is usually related to their competitiveness. The competitive ability between common widespread, which are generally considered to be invasive, and common endemic species, is still not very clear. Five plant communities were monitored in the field to compare the competitive abilities of widespread species, *Phragmites australis*, and endemic species, *Triarrhena lutarioriparia,* in the Dongting Lake wetlands. The ratios of individual numbers of *T. lutarioriparia* to *P. australis* per square meter were found to be 9:0, 14:1, 10:5, 7:6, and 0:11 in the five respective communities. A manipulation experiment was then performed with five planting modes (*T. lutarioriparia*: *P. australis* was 4:0, 3:1, 2:2, 1:3, and 0:4, respectively). Results from field monitoring showed that the two plant species exhibited similar decreased survival percentages during flooding. *P. australis* had higher aboveground biomass before the flooding and a higher relative elongation rate, whereas *T. lutarioriparia* had higher aboveground biomass after flooding and a higher relative growth rate (RGR). *P. australis* had a higher competitive ability than *T. lutarioriparia* before and after the flooding. The manipulation experiment revealed that *P. australis* had a higher survival percentage than *T. lutarioriparia*, with no differences in plant biomass, RGR, and the relative elongation rate between the two species. *P. australis* was found to have a higher competitive ability than *T. lutarioriparia* in the early growing stage and a lower competitive ability in the middle and later stages. The relative yield total in the field monitoring and manipulation experiment was 1, indicating that *T. lutarioriparia* and *P. australis* occupied different niches in the experimental conditions. It was concluded that, compared with *T. lutarioriparia*, *P. australis* has a higher competitive ability in submerged habitats and a lower competitive ability in the non-submerged habitat. The niche differences between the two species enabled their coexistence in the Dongting Lake wetlands with seasonal flooding.

Keywords: *Triarrhena lutarioriparia*, *Phragmites australis*, competition intensity, interspecific competition, relative growth rate, niche difference

OPEN ACCESS

Edited by:
Bing Song,
Ludong University, China

Reviewed by:
Feng Li,
Institute of Subtropical Agriculture (CAS), China
Guan Bo,
Ludong University, China

***Correspondence:**
Youzhi Li
liyouzhi2004@163.com

Specialty section:
This article was submitted to Functional Plant Ecology, a section of the journal Frontiers in Plant Science

Received: *08 March 2022*
Accepted: *19 April 2022*
Published: *24 May 2022*

Citation:
Du Y, Zhou Q, Peng Z, Peng F, Xi L and Li Y (2022) Does a Widespread Species Have a Higher Competitive Ability Than an Endemic Species? A Case Study From the Dongting Lake Wetlands. Front. Plant Sci. 13:864316. doi: 10.3389/fpls.2022.864316

INTRODUCTION

Plants can be classified as widespread species and endemic species based on their distribution range (Hung et al., 2014; Bai et al., 2018). For example, *Stemona tuberosa*, a traditional medicinal plant, is distributed across more than ten countries in Asia (Chen et al., 2019), and the shrub *Menziesia pentandra* is distributed across Japan, Sakhalin, and the Southern Kuril Islands (Maki et al., 2002). *Cinnamomum kanehirae* is endemic to Taiwan at an elevation range of 200–2,000 m (Hung et al., 2014), and *Pilea carautae* is endemic to the Cabo Frio region in the State of Rio de Janeiro, Southern Brazil (Filho and Alves, 2010). The distribution of a plant is associated with its competitive ability, as it reflects its ability to obtain resources such as light, water, and nutrients, as well as its tolerance to resource stress (Schob et al., 2013). Therefore, widespread plant species appear to have higher competitive abilities than endemic plant species (Zhang and van Kleunen, 2019).

Plant competition includes intraspecific and interspecific competition and is determined by the competition intensity, effects, and outcomes (Connolly, 1987; Weigelt and Jolliffe, 2003). Competitive effects have been used to analyze and predict changes in plant populations and community structure (Goldberg and Werner, 1983; Miller and Werner, 1987; Pan et al., 2021). Under the conditions of water and nitrogen deficiency, the higher competitive ability of the invasive plant *Xanthium italicum* compared with the native plant *Xanthium sibiricum* was the main reason for the succession of *X. sibiricum* by *X. italicum* in its native habitat (Wang, 2018). With an increase in nitrogen levels, *Suaeda salsa* was found to have a higher competitive ability than a congeneric species *Suaeda glauca*, with *S. salsa* gradually dominating the mixed communities (Qi, 2019). Four meta-analyses of hundreds of experiments showed that widespread plant species are more competitive than endemic species (Vilà et al., 2011; Kuebbing and Nunez, 2016; Golivets and Wallin, 2018; Zhang and van Kleunen, 2019). However, the results of these studies may be biased for using common, often invasive, widespread species (Hulme et al., 2013) and rare endemic species (Vilà and Weiner, 2004). It is essential to test the competitive ability between common widespread species and common endemic species to gain a comprehensive understanding of the determinants of invasion success (Maki et al., 2002; Conesa et al., 2008).

Phragmites australis is a widespread species that is commonly distributed across North America (Altartouri et al., 2015; Eller et al., 2017), Europe (Van der Putten, 1997; Klimes, 2000), and Asia (Clevering and Lissner, 1999; Li et al., 2011). *Triarrhena lutarioriparia* is an endemic species that is only distributed along the middle and lower reaches of the Yangtze River, China (Liu et al., 2001; Wang et al., 2019). These two plant species are dominant species in the Dongting Lake, the second-largest freshwater lake in China, and are distributed at the same altitude (24.55–25.10 m above sea level) on the beaches of the lake (Zhuang et al., 2010; Li et al., 2016). These plant species have similar morphological, growth, and propagation characteristics. For example, the specific leaf area of *P. australis* was 280–290 and 290–300 cm^2 g^{-1} for *T. lutarioriparia* (Chen, 2020). Based on field observations in recent years, the area of the lake occupied by *P. australis* has gradually expanded, whereas the area occupied by *T. lutarioriparia* has gradually reduced. We hypothesize that common, widespread plant species, like *P. australis,* have a higher competitive ability than common endemic species like *T. lutarioriparia*. Therefore, to test the hypothesis, a field monitoring and manipulation experiment were conducted to compare the intensity, effect, and outcomes of competition between the two species.

MATERIALS AND METHODS

Study Site

The Yangtze River is connected to Dongting Lake through three inlets (Songzikou, Taipingkou, and Ouchikou) and one outlet (Chenglingji). The Dongting Lake covers an area of 2,625 km^2 (28°38′–29°45′ N, 111°40′–113°10′ E) and is divided into East, South, and West Dongting Lake. The study area has a subtropical monsoon climate, with an average annual temperature of 16.2–17.8°C and 259–277 frost-free days per year. Mean annual precipitation ranges from 1,200 to 1,415 mm, with the rainy season lasting from May to September. The average humidity is 80%, and the average evaporation is 1,270 mm. The annual mean wind speed is 2–3 m s^{-1} and the elevation is 28–35 m above sea level.

Field Monitoring

Fixed Plot Selection

To compare the competitive ability between *T. lutarioriparia* and *P. australis*, in May 2018, five fixed plots comprising three mixed and two single communities were selected on the beach in the Dongting Lake wetlands. The plots were submerged due to flooding from May to September and exposed from October to April the following year. The fixed plot area was 5 m × 5 m, and the key characteristics of the plots are provided in **Table 1**.

Fixed Plot Monitoring

In the fixed plots, the height and number of living individuals were recorded before flooding and after the floodwater had retreated. In the single communities, six individuals across a diagonal section of the plot were selected from each of the five plots. In the mixed communities, six plants, including three *T. lutarioriparia* plants and three *P. australis* plants, were selected in each of the five plots. The aboveground parts (leaves and stems) were collected and taken to the laboratory and dried to constant weight.

Manipulation Experiment

Seed Collection and Germination

A manipulation experiment was performed to accurately control the initial ratio of *T. lutarioriparia* and *P. australis* in communities and continuously compare the competitive ability between the two species. In December 2017, seeds

TABLE 1 | Numbers of *Triarrhena lutarioriparia* (*TL*) and *Phragmites australis* (*PA*) in 1 m^2 area before and after flooding (BF and AF, respectively) in the five fixed communities and geographical coordinates of the communities in the East Dongting Lake wetlands in the field monitoring experiment.

	9:0	14:1		10:5		7:6		0:11
	TL	*TL*	*PA*	*TL*	*PA*	*TL*	*PA*	*PA*
BF	9	14	1	10	5	7	6	11
AF	8	6	0	5	3	5	4	9
Longitude	113°3′56.87	113°4′14.79″		113°5′7.78″		113°6′26.03″		113°7′44.28″
Latitude	29°24′52.12″	29°25′18.77″		29°25′23.75″		29°25′47.90″		29°26′20.40″

The ratios 9:0, 14:1, 10:5, 7:6, and 0:11 are the ratios of individual numbers of TL to PA in a square meter.

of *T. lutarioriparia* and *P. australis* were collected from the bottomland (29°15′15″N, 112°49′20″E) of the East Dongting Lake wetlands and brought back to the laboratory at Hunan Agricultural University. The mean weight of a thousand seeds was 0.35 ± 0.018 g (mean ± standard error) for *T. lutarioriparia* and 0.28 ± 0.004 g for *P. australis*. The mean seed length was 2.33 ± 0.034 mm for *T. lutarioriparia* and 2.03 ± 0.037 mm for *P. australis*. The mean seed width was 0.540 ± 0.014 mm for *T. lutarioriparia* and 0.57 ± 0.013 mm for *P. australis*. In March 2018, the seeds were sown in the field and germinated.

Seedling Transplantation

In April 2018, seedlings with an aboveground height of 6–8 cm were transplanted into basins (12 cm in length, 12 cm in width, and 35 cm in height) filled up to 34 cm with soil (21 g kg^{-1} organic matter, 141 mg kg^{-1} exchangeable N, and 11.4 mg kg^{-1} exchangeable P). In brief, four seedlings were planted in each basin, and five planting patterns (the ratios of seedling numbers of *T. lutarioriparia* to *P. australis* were 4:0, 3:1, 2:2, 1:3, and 0:4, respectively) were used (**Figure 1**). For example, the pattern of 3:1 indicated that there were three *T. lutarioriparia* seedlings and one *P. australis* seedling in the basin. Red and white ropes were tied to the root base of each plant to distinguish between *T. lutarioriparia* and *P. australis* plants, respectively. There were 24 basins for each pattern, making a total of 120 basins. Fifteen basins were placed into a bucket (68 cm in length, 47 cm in width, and 41 cm in height) outdoors, and a total of eight buckets were used in the experiment (**Figure 1**). In total, twelve plants of each species were initially collected and the dry weights were measured. Following the transplantation of seedlings, water was added into the buckets until it reached the soil surface in the basin. This was the only time that water was added artificially into the bucket to simulate the natural environment.

Seedling Harvest

After transplanting the seedlings into basins, the plants were grown for 60, 120, and 180 days, and were then harvested. For a specific planting pattern, eight basins were selected for harvesting. The plants were dug out of the soil and carefully separated to maintain their integrity. The number of living plants, buds, and tillers for each species in the planting pattern was recorded. The dry biomass of the leaves, stems, roots, and buds was determined after drying at 80°C to a constant weight.

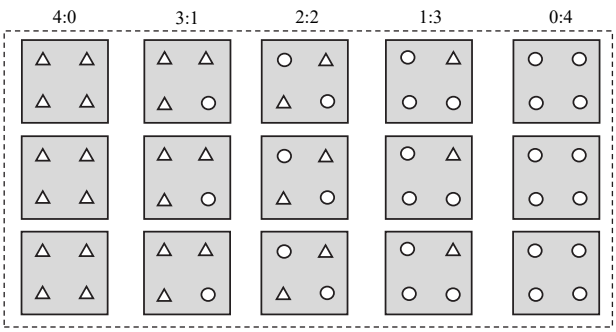

FIGURE 1 | Planting patterns for the two species in each bucket in the manipulation experiment (: bucket, □: basin, Δ: *Triarrhena lutarioriparia*, ○: *Phragmites australis*). The 4:0, 3:1, 2:2, 1:3, and 0:4 were the ratios of seedling numbers of *T. lutarioriparia* to *P. australis* in a basin, respectively.

Data Calculation and Analysis

Plant Growth Parameters

The survival percentage was calculated as the number of living plants divided by the initial number of plants.

The relative growth rate (*RGR*) was calculated using the following equation (Wang, 2013):

$$RGR = \frac{lnY_2 - lnY_1}{t_2 - t_1} \quad (1)$$

where Y_1 is biomass at harvest time t_1, and Y_2 is biomass at harvest time t_2.

The relative elongation rate (*RER*) was calculated using the following equation (Wang, 2013):

$$RER = \frac{lnh_2 - lnh_1}{t_2 - t_1} \quad (2)$$

where h_1 is plant height at harvest time t_1, and h_2 is plant height at harvest time t_2.

Plant Competition Parameters

The relative competition intensity (*RCI*) can reflect plant competitive ability in three mixed communities (14:1, 10:5, and 7:6) in field monitoring, and the three mixed planting patterns (3:1, 2:2, and 1:3) in the manipulation experiment, and was calculated using the following equations (Grace, 1995):

$$RCI_i = (Y_i - Y_{ij})/Y_i \quad (3)$$

$$RCI_j = (Y_j - Y_{ji})/Y_j \quad (4)$$

where Y_i and Y_j are biomass of species i and species j in two single communities (9:0 and 0:11) in field monitoring, and two single planting patterns (4:0 and 0:4) in the manipulation experiment, respectively. Y_{ij} and Y_{ji} are biomass of species i and species j in mixed communities or planting patterns, respectively. $RCI_i > RCI_j$ indicates that species j has a higher competitive ability than species i. $RCI_i = RCI_j$ indicates that species j and i have the same competitive ability; and $RCI_i < RCI_j$ indicates that species i has a higher competitive ability than species j. The known trend is that the lower the relative competition intensity (RCI), the greater the competitive ability.

The relative yield (RY) and the relative yield total (RYT) can reflect plant interspecific or intraspecific competition, and this was calculated using the following equations (Wang, 2013; Jiang et al., 2014):

$$RY_i = Y_{ij}/Y_i \quad (5)$$

$$RY_j = Y_{ji}/Y_j \quad (6)$$

$$RYT = (RY_{\mathrm{i}} + RY_j)/2 \quad (7)$$

where $RY < 1$ indicates that the plants have higher interspecific competition than intraspecific competition. $RY = 1$ indicates that the plants have the same interspecific and intraspecific competition, and $RY > 1$ indicates that plants have lower interspecific competition than intraspecific competition. $RYT < 1$ indicates that plants inhabit the same niches. $RYT = 1$ indicates that plants have partially the same niches. $RYT > 1$ indicates that plants have different niches.

The relative efficiency index (REI) and the expected relative efficiency index (REI_{exp}) are used to predict dynamic changes in plant species in mixed communities or patterns, and were calculated using the following equations (Shipley, 1993; Grace, 1995):

$$REI = (\ln Y_{ij2} - \ln Y_{ij1}) - (\ln Y_{ji2} - \ln Y_{ji1}) \quad (8)$$

$$REI_{exp} = (\ln Y_{i2} - \ln Y_{i1}) - (\ln Y_{j2} - \ln Y_{j1}) \quad (9)$$

where Y_{ij1} and Y_{ij2} are the biomass of species i in mixed communities or planting patterns at harvest times t_1 and t_2, respectively. Y_{ji1} and Y_{ji2} are the biomass of species j in mixed communities or planting patterns at harvest times t_1 and t_2, respectively. Y_{i1} and Y_{i2} are the biomass of species i in single communities or planting patterns at harvest times t_1 and t_2, respectively. Y_{j1} and Y_{j2} are the biomass of species j in single communities or planting patterns at harvest times t_1 and t_2, respectively. $REI < REI_{exp}$ indicates that in mixed communities or planting patterns, species j will show increasing dominance over time. $REI = REI_{exp}$ indicates that in mixed communities or planting patterns, species j will show stable dominance over time, and $REI > REI_{exp}$ indicates that in mixed communities or planting patterns, species j will show decreasing dominance over time.

Multiple comparisons at the significance level of 0.05 were used to analyze the difference in biomass, RGR, relative elongation rate, tiller number, and bud numbers between different species and planting patterns. For these analyses, the IBM SPSS Statistics version 22 software (SPSS Inc., Chicago, IL, United States) was used.

RESULTS

Survival Percentage

In the field monitoring experiment, the number of living individuals for both plant species decreased after flood retreat (**Table 1**). There was a pronounced difference in the survival percentage between the two plant species, except in the basins with a planting ratio of 14:1. With the increase in numbers, the survival percentage of *P. australis* increased, whereas that of *T. lutarioriparia* did not change.

In the manipulation experiment, both species had a decreased survival percentage during the experiment, except for the *P. australis* plants in basins with the planting patterns of 3:1, 1:3, and 0:4 (**Table 2**). At the same harvest time, *T. lutarioriparia* had a lower survival percentage than *P. australis*, except in the basins with the planting pattern of 1:3 on the 60th day.

Plant Biomass, Relative Growth Rate, and Relative Elongation Rate

In the field monitoring experiment, *T. lutarioriparia* had higher aboveground biomass than *P. australis* before flooding and lower aboveground biomass after flood retreat (**Figure 2**). During the flooding, *T. lutarioriparia* had a higher RGR and lower relative elongation rate compared to *P. australis*.

In the manipulation experiment, *T. lutarioriparia* had higher biomass than *P. australis* in the early growth stage, whereas no difference in the biomass was observed between these two species in the later growth stage (**Figure 3**). The plant biomass showed different trends with the change in planting patterns. On the 60th day, there was no significant difference in the plant biomass between the two species for any of the four planting patterns.

TABLE 2 | Survival percentages (%) of *Triarrhena lutarioriparia* (*TL*) and *Phragmites australis* (*PA*) on the 60th, 120th, and 180th days of plant transplantation in the manipulation experiment.

Day	4:0	3:1		2:2		1:3		0:4
	TL	*TL*	*PA*	*TL*	*PA*	*TL*	*PA*	*PA*
60	90.6	95.8	100.0	93.8	100.0	100.0	95.8	100.0
120	87.5	79.2	100.0	68.8	93.8	50.0	95.8	100.0
180	75.0	58.3	100.0	68.8	87.5	37.5	95.8	100.0

The ratios 4:0, 3:1, 2:2, 1:3, and 0:4 are the planting patterns described in ***Figure 1****.*

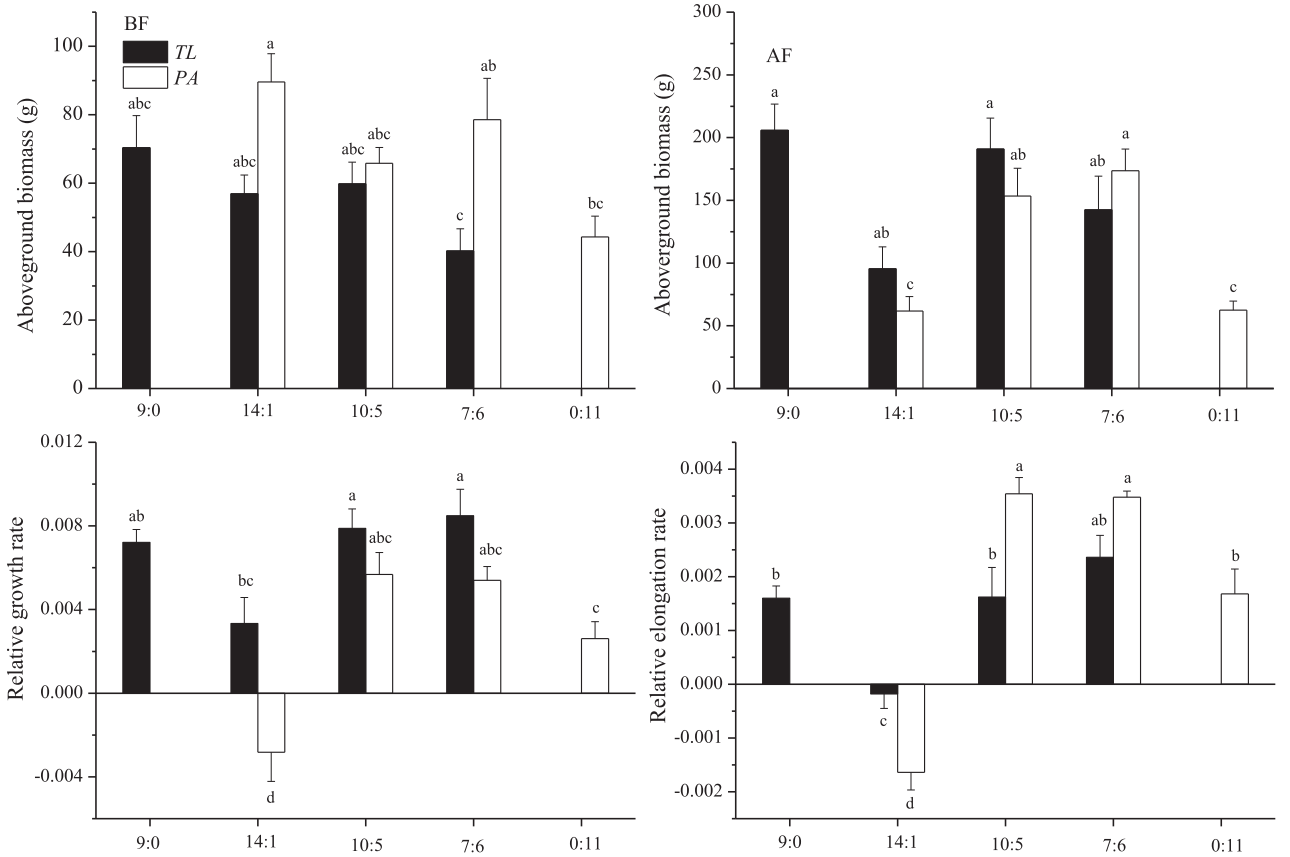

FIGURE 2 | Aboveground biomass of *T. lutarioriparia* (*TL*) and *P. australis* (*PA*) before and after flooding (BF and AF, respectively), and their relative growth and elongation rates during the flooding period in the field monitoring experiment. The ratios 9:0, 14:1, 10:5, 7:6, and 0:11 are the ratios of individual numbers of *TL* to *PA* in a square meter. Different lowercase letters indicate significant differences among planting patterns at the 0.05 significance level.

On the 120th day, the biomass of *T. lutarioriparia* was higher in basins with the 1:3 planting pattern than those with the other three patterns. The *P. australis* biomass was higher in basins with the 3:1 planting pattern than those with the 2:2 planting pattern. On the 180th day, the biomass of *T. lutarioriparia* was higher in the basins with the 2:2 planting pattern than those with the 4:0 and 3:1 planting patterns. However, there were no significant differences in the biomass of *P. australis* between the four planting patterns.

In the manipulation experiment, the relative growth and elongation rates were lower in *T. lutarioriparia* than in *P. australis* over 60–120 days, whereas they were not significantly different over 0–60 and 120–180 days. In the 0–60-day period, there were no significant differences in the relative growth and elongation rates between the four patterns in the two species. Over the 60–120-day period, the relative growth rate of *T. lutarioriparia* was lower in basins with the 3:1 planting pattern and higher in those with the 1:3 planting pattern, and that of *P. australis* was not significantly different in the basins for any of the four patterns. The relative elongation rate of either species did not differ between the four patterns. Over 120–180 days, the relative growth and elongation rates of *T. lutarioriparia* were lower in basins with the 1:3 planting pattern than in the basins with the other patterns, and those of *P. australis* were lower in basins with the 3:1 planting pattern than in the basins with the other patterns.

Relative Competition Intensity and Relative Yield

In the field monitoring experiment, the relative competition intensity of the two plant species was different between two-time points (before and after flooding) and in three mixed communities (**Table 3**). In *T. lutarioriparia*, the flooding increased the relative competition intensity in the basins with the 14:1 and 10:5 patterns and decreased in the basins with the 7:6 pattern. In *P. australis*, flooding increased the relative competition intensity in the basins with the 14:1 and 7:6 patterns and decreased in the basins with the 10:5 pattern. The relative competition intensity of *T. lutarioriparia* was higher than that of *P. australis*. The relative yield of the two plant species also differed between the two-time points (before and after flooding) and the three mixed communities. The relative yield of *T. lutarioriparia* ($\leq$1) was lower than that of *P. australis* ($\geq$1). The relative yield total for the three mixed communities at the two-time points

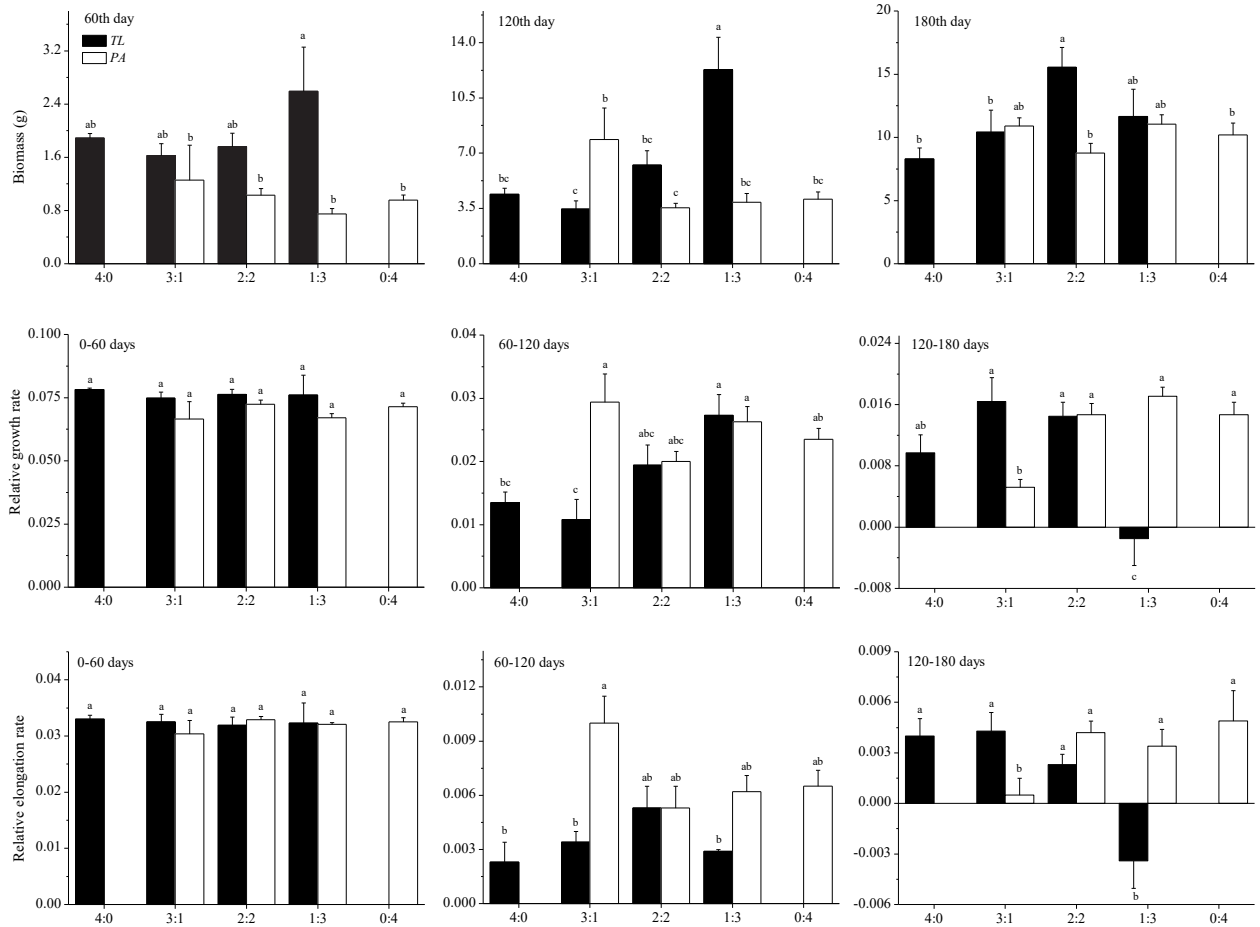

FIGURE 3 | Biomass of *Triarrhena lutarioriparia* (*TL*) and *Phragmites australis* (*PA*) on the 60th, 120th, and 180th days of plant transplantation, and their relative growth and elongation rates in the periods of 0–60, 60–120, and 120–180 days in the manipulation experiment. The ratios 4:0, 3:1, 2:2, 1:3, and 0:4 are the planting patterns described in **Figure 1**. Different lowercase letters indicate significant differences among planting patterns at the 0.05 significance level.

was > 1, indicating that the plants had different niches in the different communities.

In the manipulation experiment, the relative competition intensity of *T. lutarioriparia* decreased in basins with the 3:1 and 2:2 planting patterns and increased over time in those with the 1:3 planting pattern (**Table 3**). However, the relative competition intensity of *P. australis* decreased in the basins with the 3:1 and 1:3 planting patterns and increased in those with the 2:2 planting pattern. *T. lutarioriparia* had a lower relative competition intensity than *P. australis* in basins with the 1:3 planting pattern on the 60th day and in basins with the 2:2 planting pattern on the 120th day, and higher relative competition intensity than *P. australis* in those with the other planting patterns. The relative yield of *T. lutarioriparia* increased over time in basins with the 3:1, 2:2, and 1:3 planting patterns (**Table 4**). However, the relative yield of *P. australis* decreased in basins with the 2:2 planting pattern and increased over time in those with the 3:1 and 1:3 planting patterns. *T. lutarioriparia* had a lower relative yield than *P. australis* in basins with the 1:3 and 2:2 planting patterns on the 60th day and in basins with the 1:3 planting pattern on the 120th day, and a higher relative yield than *P. australis* did in the basins with the other patterns. The total relative yield for both plants in all three patterns and three harvest times was > 1,

TABLE 3 | Relative competition intensity (*RCI*), relative yield (*RY*), and relative yield total (*RYT*) of *Triarrhena lutarioriparia* (*TL*) and *Phragmites australis* (*PA*) before and after flooding (BF and AF, respectively) in the field monitoring experiment.

Time	Communities	*RCI*		*RY*		*RYT*
		TL	*PA*	*TL*	*PA*	
BF	14:1	0.02	−0.53	0.98	1.53	1.26
	10:5	−0.03	−0.13	1.03	1.13	1.08
	7:6	0.31	−0.34	0.70	1.34	1.02
AF	14:1	0.53	0.01	0.47	0.99	0.73
	10:5	0.06	−1.45	0.94	2.46	1.70
	7:6	0.30	−1.78	0.70	2.78	1.74

The ratios 14:1, 10:5, and 7:6 are the individual numbers of TL to PA in a square meter.

indicating that the plants had different niches in different planting patterns.

Relative Efficiency Index and Expected Relative Efficiency Index

In the field monitoring experiment, the relative efficiency index was lower than expected, indicating that *P. australis* would be the dominant species over time (**Table 5**). In the period of 0–60 days, the relative efficiency index was lower than expected in basins with the 3:1 and 2:2 patterns, and higher than expected in the basins with the 1:3 pattern. This indicates that in this period, *P. australis* would be the dominant species in basins with the 3:1 and 2:2 patterns, and *T. lutarioriparia* would be the dominant species in those with the 1:3 pattern (**Table 6**). In the period of 60–120 days, *P. australis* would be the dominant species in basins with the 3:1 pattern, and *T. lutarioriparia* would be the dominant species in those with the 2:2 and 1:3 patterns. In the period of 120–180 days, *T. lutarioriparia* would be the dominant species in basins with the 3:1 and 2:2 patterns, and *P. australis* would be the dominant species in those with the 1:3 pattern. During the whole experimental period (0–180 days), *T. lutarioriparia* would be the dominant species in basins with mixed patterns.

TABLE 4 | Relative competition intensity (*RCI*), relative yield (*RY*), and relative yield total (*RYT*) of *Triarrhena lutarioriparia* (*TL*) and *Phragmites australis* (*PA*) on the 60th, 120th, and 180th days of plant transplantation in the manipulation experiment.

Days	Patterns	*RCI*		*RY*		*RYT*
		TL	*PA*	*TL*	*PA*	
60	3:1	0.14	−0.31*	0.86^{e}	1.31^{a}	1.09
	2:2	0.07	−0.08*	0.93^{e}	1.08^{a}	1.01
	1:3	−0.37*	0.22	1.37^{a}	0.78^{e}	1.08
120	3:1	0.21	−0.92*	0.79^{e}	1.92^{a}	1.36
	2:2	−0.42*	0.14	1.42^{a}	0.86^{e}	1.14
	1:3	−1.80 *	0.05	2.80^{a}	0.95^{e}	1.88
180	3:1	−0.25*	−0.07	1.25^{a}	1.07^{a}	1.16
	2:2	−0.87*	0.14	1.87^{a}	0.86^{e}	1.37
	1:3	−0.40*	−0.08	1.40^{a}	1.08^{a}	1.24

*The ratios 4:0, 3:1, 2:2, 1:3, and 0:4 are the planting patterns described in **Figure 1**. *Indicates that the competition ability was strong.*
[a]Indicates that intraspecific competition was higher than the interspecific competition.
[e]Indicates that intraspecific competition was lower than interspecific competition.

TABLE 5 | Relative efficiency index (*REI*) and expected relative efficiency index (REI_{exp}) during flooding in the field monitoring experiment.

	REI		REI_{exp}
14:1	10:5	7:6	Single communities
0.89^{P}	0.31^{P}	0.47^{P}	1.19

The ratios 14:1, 10:5, and 7:6 are the individual numbers of TL to PA in a square meter. [P]Indicates that Phragmites australis would be the dominant species.

DISCUSSION

Growth Performance

Plant survival is one of the most direct reflections of plant adaptation, especially under environmental stress. In the field monitoring experiment, both *P. australis* and *T. lutarioriparia* showed a decreased survival percentage during flooding, which did not differ between the species. In the Dongting Lake wetlands, deeper submergence led to the death of many wetland plants, such as *Salix triandroides* and *Carex tristachya* (Ding et al., 2017, 2019). However, compared with deeper submergence in the field monitoring, low depth submergence in the manipulation experiment did not lead to variation in the survival percentage of *P. australis* and decreased the survival percentage of *T. lutarioriparia*. This indicated that *P. australis* exhibited a higher survival percentage than *T. lutarioriparia*, suggesting that *P. australis*, a widespread species, is more adaptable to environmental changes than *T. lutarioriparia*, an endemic species (Eller et al., 2017).

Plant growth can also reflect plant adaptation to environmental stress. In the field monitoring experiment, *P. australis* had higher aboveground biomass before flooding and a higher relative elongation rate during flooding, whereas *T. lutarioriparia* had higher aboveground biomass after flooding and a higher relative growth rate during flooding. However, in the manipulation experiment, the plant biomass, relative growth rate, and relative elongation rate were not different between the two species. These differences in plant growth between the field monitoring and the manipulation experiment may be attributed to the difference in water conditions. In the field experiment, a 5-month of flooding caused different response patterns in the plants: the well-developed stem porosity in *T. lutarioriparia* led to increased oxygen transmission from the aboveground parts to the belowground parts and resulted in increased growth, whereas the relatively lower stem porosity in *P. australis* forced rapid vertical stem elongation so that stems were able to reach the water surface and access oxygen from the air (Jackson, 2008; Ding et al., 2017). In the manipulation experiment, the two plants showed similar growth characteristics because of the absence of flooding stress.

TABLE 6 | Relative efficiency index (*REI*) and expected relative efficiency index (REI_{exp}) in the periods of 0–60, 60–120, 120–180, and 0–180 days in the manipulation experiment.

Days	*REI*			REI_{exp}
	3:1	2:2	1:3	Single planting
0–60	-0.03^{P}	0.25^{P}	0.96^{T}	0.39
60–120	-1.08^{P}	0.04^{T}	-0.10^{T}	−0.61
120–180	0.78^{T}	0.01^{T}	-1.09^{P}	−0.28
0–180	-0.33^{T}	0.29^{T}	-0.23^{T}	−0.49

*The ratios 3:1, 2:2, and 1:3 are the planting patterns described in **Figure 1**.*
[T]Indicates that Triarrhena lutarioriparia would be the dominant species.
[P]Indicates that Phragmites australis would be the dominant species.

Competition Performance

Plant competition can be determined by the competitive intensity and is associated with community characteristics, such as biomass, density, and proportion (Zhang and van Kleunen, 2019). The competition performance of *P. australis* and *T. lutarioriparia* also differed between the field monitoring and the manipulation experiment. Overall, *P. australis* showed a higher competitive ability than *T. lutarioriparia* in the field monitoring and a lower competitive ability than *T. lutarioriparia* in the manipulation experiment. Similar to the reasons for differences in plant growth, seasonal flooding reduced the competitive ability of *T. lutarioriparia* and improved the competitive ability of *P. australis*.

Plant competitive ability includes the ability of intraspecific and interspecific competition (Connolly, 1987; Weigelt and Jolliffe, 2003). In the field monitoring experiment, intraspecific competition was higher in *P. australis*, and interspecific competition was higher in *T. lutarioriparia*. However, over time, the competition changed from intraspecific to interspecific in *P. australis* and from intraspecific to interspecific in *T. lutarioriparia*. Competition often leads to species occupying different ecological niches (Sophie and Sylvie, 2012). The total relative yield for the field monitoring and the manipulation experiments was > 1, indicating that the two plant species had different niches. It was found that *P. australis* would become the dominant species in the field monitoring experiment and that *T. lutarioriparia* would become the dominant species in the manipulation experiment.

The present study showed that the competitive ability of plant species varied depending on environmental conditions. In the submerged habitat, the competitive ability of *P. australis* was higher than that of *T. lutarioriparia*, whereas the opposite was true in the non-submerged habitat. In the Dongting Lake wetlands, the 5-month flooding period increased the dominance of *P. australis*, and the 7-month non-flooding period increased the dominance of *T. lutarioriparia*. However, global climate change has led to long-term high-density flooding in recent years. For instance, in 2020, water in the wetlands remained at a high level for 38 consecutive days. This has led to area expansion of *P. australis* in the Dongting Lake wetlands. Therefore, niche differences between these two species enable their coexistence in the Dongting Lake wetlands under the influence of seasonal flooding.

DATA AVAILABILITY STATEMENT

The original contributions presented in the study are included in the article/supplementary material, further inquiries can be directed to the corresponding author.

AUTHOR CONTRIBUTIONS

YL designed the study. YD and ZP performed the field monitoring experiment. QZ, FP, and LX conducted the control experiment. YD and YL wrote the manuscript and other authors revised it. All authors contributed to the article and approved the submitted version.

FUNDING

This study was supported by the Joint Fund for Regional Innovation and Development of NSFC (U21A2009), the Leading Plan for Scientific and Technological Innovation of High-tech Industries in Hunan Province (2020SK2019), the Key Program of Research and Development of Hunan Province (2022SK2088, 2019SK2336, and 2019NK2011), and the Natural Science Foundation of Hunan Province (2021JJ30330).

REFERENCES

Altartouri, A., Nurminen, L., and Jolma, A. (2015). Spatial neighborhood effect and scale issues in the calibration and validation of a dynamic model of *Phragmites australis* distribution–a cellular automata and machine learning approach. *Environ. Model. Softw.* 71, 15–29. doi: 10.1016/j.envsoft.2015.04.010

Bai, G., Guo, H., Zhao, N., Li, S., and Zhang, Y. (2018). The complete chloroplast genome of *Paeonia rockii* (Paeoniaceae), an endangered endemic species to China. *Conserv. Genet. Resour.* 10, 453–456. doi: 10.1007/s12686-017-0847-5

Chen, G., Sun, W., Wang, X., Kongkiatpaiboon, S., and Cai, X. (2019). Conserving threatened widespread species: a case study using a traditional medicinal plant in Asia. *Biodivers. Conserv.* 28, 213–227. doi: 10.1007/s10531-018-1648-1

Chen, M. Z. (2020). *Response of Plant Functional Traits to Environmental Factors and its Relationship with Productivity in West Dongting Lake, floodplain*. Beijing: Beijing Forestry University. (in Chinese).

Clevering, O. A., and Lissner, J. (1999). Taxonomy, chromosome numbers, clonal diversity and population dynamics of *Phragmites australis*. *Aquat. Bot.* 64, 249–250. doi: 10.1016/s0304-3770(00)00094-2

Conesa, M. À, Mus, M., and Rosselló, J. A. (2008). Hybridization between insular endemic and widespread species of Viola in non-disturbed environments assessed by nuclear ribosomal and cpDNA sequences. *Plant Syst. Evol.* 273, 169–177. doi: 10.1007/s00606-008-0006-2

Connolly, J. (1987). On the use of response models in mixture experiments. *Oecologia* 72, 95–103. doi: 10.1007/BF00385051

Ding, X., Luo, J., Li, Y., Ren, B., Bian, H., Yao, X., et al. (2019). Survival of completely submerged Salix triandroides cuttings is associated with non-structural carbohydrate metabolism. *J. Freshw. Ecol.* 34, 395–404. doi: 10.1080/02705060.2019.1618930

Ding, X., Zou, J., Li, Y., Yao, X., Zou, D., Zhang, C., et al. (2017). Acclimation of Salix triandroides cuttings to incomplete submergence is reduced by low light. *Aquat. Ecol.* 51, 321–330. doi: 10.1007/s10452-017-9619-2

Eller, F., Skálová, H., Caplan, J. S., Bhattarai, G. P., Burger, M. K., Cronin, J. T., et al. (2017). Cosmopolitan species as models for ecophysiological responses to global change: the common reed *Phragmites australis*. *Front. Plant Sci.* 8:1833. doi: 10.3389/fpls.2017.01833

Goldberg, D. E., and Werner, P. A. (1983). Equivalence of competitions in plant communities: a null hypothesis and a field experimental approach. *Am. J. Bot.* 70, 1098–1104. doi: 10.1002/j.1537-2197.1983.tb07912.x

Golivets, M., and Wallin, K. F. (2018). Neighbour tolerance, not suppression, provides competitive advantage to non-native plants. *Ecol. Lett.* 21, 745–759. doi: 10.1111/ele.12934

Grace, J. B. (1995). On the measurement of plant competition intensity. *Ecology* 76, 305–308. doi: 10.2307/1940651

Hulme, P. E., Pysek, P., Jarosik, V., Pergl, J., Schaffner, U., and Vila, M. (2013). Bias and error in understanding plant invasion impacts. *Trends Ecol. Evol.* 28, 212–218. doi: 10.1016/j.tree.2012.10.010

Hung, K. H., Lin, C. H., Shih, H. C., Chiang, Y. C., and Ju, L. P. (2014). Development, characterization and cross-species amplification of new microsatellite primers from an endemic species *Cinnamomum kanehirae* (Lauraceae) in Taiwan. *Conserv. Genet. Resour.* 6, 911–913. doi: 10.1007/s12686-014-0239-z

Jackson, M. B. (2008). Ethylene-promoted elongation: an adaptation to submergence stress. *Ann. Bot.* 101, 229–248. doi: 10.1093/aob/mcm237

Jiang, Z. L., Wang, W. Y., Lei, G. S., Gui, F. R., Liu, W. X., and Li, Z. Y. (2014). Root growth characteristics and competitive effects of *Ageratina adenophora* and four functional type herbaceous plants. *Chin. J. Appl. Ecol.* 25, 2833–2839. (in Chinese),

Klimes, L. (2000). *Phragmites australis* at an extreme altitude: rhizome architecture and its modelling. *Folia Geobot.* 35, 403–417. doi: 10.1007/bf02803552

Kuebbing, S. E., and Nunez, M. A. (2016). Invasive non-native plants have a greater effect on neighbouring natives than other non-natives. *Nat. Plants* 2:16134. doi: 10.1038/nplants.2016.134

Li, F., Li, Y., Qin, H., and Xie, Y. (2011). Plant distribution can be reflected by the different growth and morphological responses to water level and shade in two emergent macrophyte seedlings in the Sanjiang Plain. *Aquat. Ecol.* 45, 89–97. doi: 10.1007/s10452-010-9334-8

Li, X., Song, B. B., Li, F., Zeng, J., Hou, Z. Y., Xie, Y. H., et al. (2016). Population distribution patterns and growing status of *Triarrhena* lutarioripa along a gentle elevation gradient of Lake Dongting Wetlands. *J. Lake Sci.* 28, 1039–1046. (in Chinese), doi: 10.18307/2016.0514

Liu, L., Zhu, M., and Zhu, T. (2001). Exploitation and utilization of *Miscanthus* & *Triarrhena*. *J. Nat. Res.* 16, 562–563.

Maki, M., Horie, S., and Yokoyama, J. (2002). Comparison of genetic diversity between narrowly endemic shrub *Menziesia goyozanensis* and its widespread congener *M. pentandra* (Ericaceae). *Conserv. Genet.* 3, 421–425.

Miller, T. E., and Werner, P. A. (1987). Competitive effects and responses between plant species in a first-year old-field community. *Ecology* 68, 1201–1210. doi: 10.2307/1939204

Pan, Y., Yuan, D. Y., Wu, Q. H., Jin, L., Xie, M. L., Gu, Y., et al. (2021). Effect of water exchange rate on interspecies competition between submerged macrophytes: functional trait hierarchy drives competition. *Plant Soil* 466, 631–647. doi: 10.1007/s11104-021-05081-x

Qi, D. H. (2019). *Effects of Nitrogen Level and Reciprocal Neighbour Density on Competition Between Suaeda Salsa and Suaeda Glauca in the Yellow River Delta*. Yantai: University of Chinese Academy of Sciences. (in Chinese).

Schob, C., Armas, C., Guler, M., Prieto, I., and Pugnaire, F. I. (2013). Variability in functional traits mediates plant interactions along stress gradients. *J. Ecol.* 101, 753–762. doi: 10.1111/1365-2745.12062

Shipley, B. (1993). A null model for competitive hierarchies in competition matrices. *Ecology* 74, 1693–1699. doi: 10.2307/1939927

Sophie, T., and Sylvie, D. B. (2012). Coexistence of introduced and native common reed (*Phragmites australis*) in freshwater wetlands. *Ecoscience* 19, 99–105. doi: 10.2980/19-2-3468

Van der Putten, W. H. (1997). Die-back of *Phragmites australis* in european wetlands: an overview of the european research programme on reed die-back and progression (1993-1994). *Aquat. Bot.* 59, 263–275. doi: 10.1016/s0304-3770(97)00060-0

Filho, M. D. M.V, and Alves, R. J. V. (2010). *Pilea* carautae (Urticaceae), a new and endemic species from South-eastern Brazil. *Kew Bull.* 65, 469–474. doi: 10.1007/s12225-010-9222-3

Vilà, M., and Weiner, J. (2004). Are invasive plant species better competitors than native plant species? – Evidence from pair-wise experiments. *Oikos* 105, 229–238. doi: 10.1111/j.0030-1299.2004.12682.x

Vilà, M., Espinar, J. L., Hejda, M., Hulme, P. E., Jarošík, V., Maron, J. L., et al. (2011). Ecological impacts of invasive alien plants: a meta-analysis of their effects on species, communities and ecosystems. *Ecol. Lett.* 14, 702–708. doi: 10.1111/j.1461-0248.2011.01628.x

Wang, J. (2013). *Study on the Eco-physiological Characteristics and Relative Competitive Ability of Two Native Species Under Mixture in Loess Hilly-gully Region*. Yangling: Northwest Agriculture and Forestry University. (in Chinese).

Wang, P. P. (2018). *A Comparative Study on the Competitive Ability of Invasive Plant Xanthium Italicum Moretti and Native Plant X. Sibiricum Patr*. Shihezi: Shihezi University. (in Chinese).

Wang, Y., Molinos, J. G., Shi, L., Zhang, M., Wu, Z., Zhang, H., et al. (2019). Drivers and changes of the Poyang Lake Wetland ecosystem. *Wetlands* 39, 35–44. doi: 10.1007/s13157-019-01180-9

Weigelt, A., and Jolliffe, P. (2003). Indices of plant competition. *J. Ecol.* 91, 707–720. doi: 10.1046/j.1365-2745.2003.00805.x

Zhang, Z., and van Kleunen, M. (2019). Common alien plants are more competitive than rare natives but not than common natives. *Ecol. Lett.* 22, 1378–1386. doi: 10.1111/ele.13320

Zhuang, Y., Sun, Y. X., Wang, Z. S., Yang, L. L., Deng, Z. F., Yao, Z. G., et al. (2010). Research advances in ecotypes of *Phragmites australis*. *Acta Ecologica Sinica* 30, 2173–2181. (in Chinese),

Conflict of Interest: The authors declare that the research was conducted in the absence of any commercial or financial relationships that could be construed as a potential conflict of interest.

frontiers | Frontiers in Plant Science

ORIGINAL RESEARCH
published: 17 June 2022
doi: 10.3389/fpls.2022.941689

Aboveground Biomass of Wetland Vegetation Under Climate Change in the Western Songnen Plain

Yanji Wang[1,2], Xiangjin Shen[1], Shouzheng Tong[1], Mingye Zhang[1,2], Ming Jiang[1] and Xianguo Lu[1]*

[1] Northeast Institute of Geography and Agroecology, Chinese Academy of Sciences, Changchun, China, [2] University of Chinese Academy of Sciences, Beijing, China

Understanding the spatiotemporal dynamics of aboveground biomass (AGB) is crucial for investigating the wetland ecosystem carbon cycle. In this paper, we explored the spatiotemporal change of aboveground biomass and its response to climate change in a marsh wetland of western Songen Plain by using field measured AGB data and vegetation index derived from MODIS datasets. The results showed that the AGB could be established by the power function between measured AGB density and the annual maximum NDVI ($NDVI_{max}$) of marsh: $Y = 302.06 \times NDVI_{max}^{1.9817}$. The averaged AGB of marshes showed a significant increase of 2.04 g·C/m^2/a, with an average AGB value of about 111.01 g·C/m^2 over the entire western Songnen Plain. For the influence of precipitation and temperature, we found that the annual mean temperature had a smaller effect on the distribution of marsh AGB than that of the total precipitation in the western Songnen Plain. Increased precipitation in summer and autumn would increase AGB by promoting marshes' vegetation growth. In addition, we found that the minimum temperature (T_{min}) and maximum temperatures (T_{max}) have an asymmetric effect on marsh AGB on the western Songnen Plain: warming T_{max} has a significant impact on AGB of marsh vegetation, while warming at night can non-significantly increase the AGB of marsh wetland. This research is expected to provide theoretical guidance for the restoration, protection, and adaptive management of wetland vegetation in the western Songnen Plain.

Keywords: marsh wetland, aboveground biomass, vegetation, climate, Songnen Plain

OPEN ACCESS

Edited by:
Xiaoming Kang,
Chinese Academy of Forestry, China

Reviewed by:
Feng Li,
Institute of Subtropical Agriculture (CAS), China
Narendra Kumar Lenka,
Indian Institute of Soil Science (ICAR), India

***Correspondence:**
Shouzheng Tong
tongshouzheng@iga.ac.cn

Specialty section:
This article was submitted to Functional Plant Ecology, a section of the journal Frontiers in Plant Science

Received: *11 May 2022*
Accepted: *27 May 2022*
Published: *17 June 2022*

Citation:
Wang Y, Shen X, Tong S, Zhang M, Jiang M and Lu X (2022) Aboveground Biomass of Wetland Vegetation Under Climate Change in the Western Songnen Plain. Front. Plant Sci. 13:941689. doi: 10.3389/fpls.2022.941689

INTRODUCTION

Marsh is one of the most widely distributed wetland types and plays a vital role in climate regulation and the global carbon cycle (Shen et al., 2021a,b). Biomass is the main input of organic carbon in terrestrial ecosystems (Scurelock et al., 2002; Shen et al., 2020). The aboveground biomass (AGB) is a representative of primary production, which is an important indicator of ecosystem carbon stocks in wetlands (Flombaum and Sala, 2007; Chopping et al., 2008; Wang et al., 2021). Climate change can have a critical effect on marsh biomass, and thus impact regional carbon stocks (Shen et al., 2021a; Wang et al., 2021). In the past several years, numbers of studies on the response of AGB to climate have concentrated on other ecosystems (i.e., grassland and forest ecosystem) (Piao et al., 2004; Fang et al., 2010; Gao et al., 2013; Mitsch et al., 2013; Shen et al., 2021a, 2022a,b; Wang et al., 2021, 2022; Yang et al., 2021). With the rapid development of remote sensing, many studies have

analyzed the correlations between MODIS data and biomass in different regions (Muukkonen and Heiskanen, 2007; Caccamo et al., 2011; Dong et al., 2016; Yin et al., 2019; Gao et al., 2020). Until recently, temporal-spatial changes in the AGB of marsh wetland ecosystems and their response to climate change at the regional scale have not been elucidated. To study the regional carbon cycle and sustainable use of marsh resources, it is important to comprehend the AGB dynamics of marshes and their relation to climate change (Byrd et al., 2018).

The western Songnen Plain, located in an ecologically fragile zone in Northeast China, which is expected to influence marsh growth and productivity, is highly sensitive to climate change (Xie et al., 2020). The area includes large marsh wetlands, which help to regulate the global carbon cycle (Wang et al., 2011, 2020; Shen et al., 2019, 2021b). Therefore, investigating the vegetation AGB changes and the relationship between vegetation AGB and climate change is important for assessing the carbon storage capacity in marsh wetland ecosystems in the western Songnen Plain. Previous studies have explored the changes of marsh vegetation biomass in the western Songnen Plain. For example, Yang and Li (2003) analyzed the biomass of *Phragmites communis* populations in the Songnen Plain, and Guan et al. (2018) studied the vegetation biomass in the Xianghai Wetland. However, most studies have focused on community scales or small study areas because of their limitations in field measurements. With the rapid progress of remote sensing, a combination of remote sensing and ground observations datasets at different scales can be used to effectively estimate vegetation biomass (Myneni et al., 1997, 2001; Piao et al., 2005, 2007; Fang et al., 2007). For instance, Piao et al. (2003) estimated the magnitude and changes in grassland biomass in some ecosystems in China. Yang et al. (2010) investigated the AGB of Tibetan grasslands. Gao et al. (2013) estimated the AGB of Inner Mongolia's grasslands. Several previous studies have also investigated the spatiotemporal dynamic patterns of AGB in the western Songnen marsh Plain by combining remote sensing data and field observation data. To accurately clarify the spatiotemporal change in marsh AGB and its response to climate change on the western Songnen Plain, it is useful to estimate the marsh AGB using large-scale remote-sensing and field observation datasets. Under the background of global warming, previous researchers have found that minimum temperatures at night have increased more rapidly in the past than maximum temperatures during the day (Peng et al., 2013; Shen et al., 2014). This asymmetric warming pattern is more likely to occur during the day and at night (Peng et al., 2013; Qiao et al., 2014). Some studies found that the influences of day and night temperatures on vegetation growth are different. For example, Shen et al. (2021b) found that an increase in minimum temperature significantly promoted the growth of marsh vegetation. Wang et al. (2022) discovered that the increase of maximum temperature has a negative effect on the marsh vegetation growth. At present, whether warming maximum and minimum temperatures had asymmetric impacts on AGB of marsh vegetation in western Songnen Plain is unclear. Therefore, in the context of global asymmetric day and night warming, it is very important to investigate the influences of daytime maximum temperature and night minimum temperature on AGB of marsh vegetation in the western Songnen Plain.

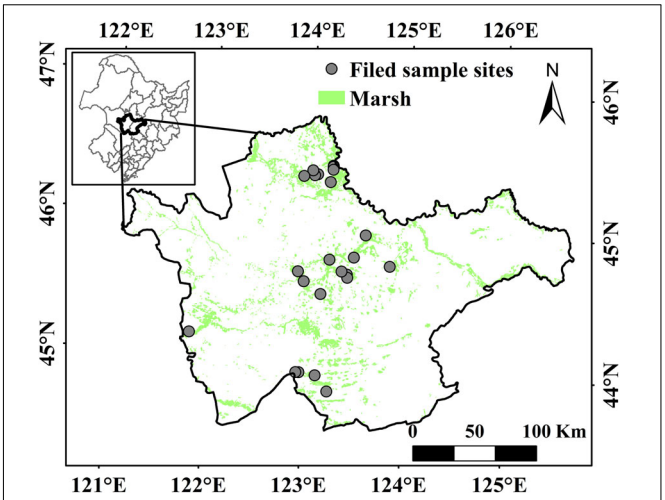

FIGURE 1 | Spatial distribution of marsh and aboveground biomass filed sampling points on the western Songnen Plain.

In the present study, we established an evaluation model of marsh AGB using measured AGB data from the western Songnen Plain marshes and the annual $NDVI_{max}$. Subsequently, we explored the spatiotemporal variation in AGB of marsh vegetation and its relationship with climate factors [including precipitation, mean temperature (T_{mean}), maximum temperature (T_{max}), and minimum temperature (T_{min})]. The objective of this study was to describe the spatiotemporal changes of marshes AGB and their response to climate change, which is crucial for the restoration and protection of wetland plants.

MATERIALS AND METHODS

Study Area

The western Songnen Plain (43°59′–46°18′N, 121°83′–126°30′E) is located in the west of Jilin Province and covers a total area of 46.9×10^3 km^2 (**Figure 1**). The study area is a semi-arid continental monsoon climate zone characterized by four seasons: windy springs, rainy summers, windy autumns, and cold winters. The mean annual temperature spatially increases from north to south (4–6°C). The precipitation is between 350 and 650 mm, 70–80% of which is concentrated in June–August, and gradually decreases from east to west (Wang et al., 2020). The northern edge of the study area includes the Songhua River, the Nenjiang River, and a few river branches (Wang et al., 2009). The vegetation of the area is composed of typical marsh plants distributed in wetlands and mainly includes *Deyeuxia angustifolia*, *Typha orientalis, Bolboschoenus planiculmis,* and *Phragmites australis* (Liu et al., 2018; Zhang et al., 2021).

Data Analysis

Data on monthly climate during 2000–2020 were created from meteorological stations in the western Songnen plain and were

provided by the National Meteorological Information Center.[1] We adopted the ordinary Kriging method to interpolate the meteorological station data into the marsh distribution in western Songnen Plain by using ARCGIS software. The spatial resolution and projected coordinates of the interpolated climate data were unified into the same as the MODIS data information. The MOD13Q1 NDVI dataset for the period from 2000 to 2020 was acquired from the National Aeronautics and Space Administration (NASA), United States. Data for this period with spatial and temporal resolutions of 250 m and 16 days, respectively, were used for the dynamic change analysis. To obtain the maximum annual NDVI ($NDVI_{max}$) values, the maximum value composite (MVC) was used to reconstruct the 16-day NDVI into $NDVI_{max}$ values (Holben, 1986; Stow et al., 2003; Pettorelli et al., 2005; Zhang et al., 2012; Wang et al., 2020). In addition, to obtain the unaltered marshes of the western Songnen Plain, two marsh maps for the year 2000 and 2015 covering the western Songnen Plain were also used in this study (Mao et al., 2019). These marsh wetland distribution data with a spatial resolution of 30 m × 30 m was taken from the National Geographic Resource Science Sub-Center of China.[2] The ground truth points used for verification of the overall accuracy of marsh datasets are generally accurate (Mao et al., 2019). The field biomass sampling survey was collected from July to September of 2012–2016 in the western Songnen plain. In the field survey, we used the AGB data of 24 marsh sites over the entire study area by adopting a comprehensive sampling method to acquire more accurate AGB values (**Figure 1**). In addition, a total of 24 field sample sites in the marsh distribution patches were selected based on the distribution of main marsh patches, and three repeat quadrats of equal size (1 m × 1 m) were set for each site (Shen et al., 2021a). When selecting repeated quadrats, the investigators fully considered the average status of vegetation in the marsh patches. Because the average AGB density of each field site was calculated from the mean AGB density of three quadrats in the same site, the AGB density could basically reflect the mean aboveground biomass density at each field site in the marsh patches. According to a previous study, a conversion coefficient of 0.45 can be used to convert the aboveground biomass values to carbon contents (Wang et al., 2021).

Methods

Analysis of Aboveground Biomass Dynamics

Piao et al. (2004) showed that there is a correlation between the $NDVI_{max}$ and the AGB of grasslands in China. Based on previous studies, we established the relationship between the marsh AGB data from filed-observation at 24 survey sites and the corresponding $NDVI_{max}$ values to estimate the AGB of marsh vegetation at each pixel in western Songnen Plain in the period from 2000 to 2020. For the AGB calculation, we extracted the $NDVI_{max}$ value of each sampling site from the $NDVI_{max}$ according to the corresponding geographic location (Ding et al., 2007).

[1]http://www.nmic.cn/

[2]http://gre.geodata.cn

Evaluation and Analysis of the Modeled Estimates

We calculated the coefficient of determination (R^2) and the Root Mean Square Error (RMSE) to compare the predicted values with observations (Piao et al., 2007).

$$R^2 = 1 - \frac{\sum_{n=1}^{x} (x_{obs} - x_{est})^2}{\sum_{n=1}^{x} (x_{obs} - \overline{x_{est}})^2}$$

$$RMSE = \sqrt{\frac{\sum_{n=1}^{x} (x_{est} - x_{obs})^2}{x}}$$

where x_{est} is the estimated value of the AGB, x_{obs} is the observed value of the AGB, $\overline{x_{est}}$ is the average of the estimated value, and x is the number of samples (24). The RMSE is a measure of prediction accuracy.

Trend Analysis

This study used the simple liner regression to calculate the trends of marsh NPP and climate variables from 2000 to 2020. The calculation formula is as follows (Wang et al., 2020):

$$Slope = \frac{n * \sum_{i=1}^{n} i * AGB_i - \left(\sum_{i=1}^{n} i\right)\left(\sum_{i=1}^{n} AGB_i\right)}{n * \sum_{i=1}^{n} i^2 - \left(\sum_{i=1}^{n} i\right)^2}$$

n is the number of years analyzed; AGB_i is AGB during the i year; *Slope* is the trend of NPP or climate variables for each pixel. If the $Slope < 0$ (> 0), it means a decrease (an increase) of the AGB during 2000–2020; when the *Slope* is zero, it shows that the AGB has no significant change during 2000–2020.

RESULTS

Estimation and Verification of Marsh Aboveground Biomass in the Western Songnen Plain

Regression models (power function) for each paired $NDVI_{max}$ and field-measured AGB of marsh vegetation were estimated (**Figure 2**). The model was evaluated by calculating the RMSE and R^2, and the observed values were compared with the estimates. The RMSE and R^2 were 42.60 and 0.98, respectively. Based on $Y = 302.06 \times NDVI_{max}^{1.9817}$ ($R^2 = 0.73$) the average AGB density of marshes over the entire western Songnen Plain from 2000 to 2020 was estimated (**Figure 3**). Overall, the average estimated marsh AGB was approximately 111.01 g·C/m^2. The R^2 value between the observed and estimated AGB was 0.86, being extremely significant ($P < 0.01$).

Spatiotemporal Variations of Aboveground Biomass in the Western Songnen Plain Marsh Wetland

The temporal changes in marsh AGB density in the western Songnen Plain are shown in **Figure 3**. This study discovered that the AGB density value of marsh vegetation over the entire western Songnen Plain had a significant increase of 2.04 g·C/m^2/a during the study period of 2000–2020 (**Figure 3**). Higher AGB

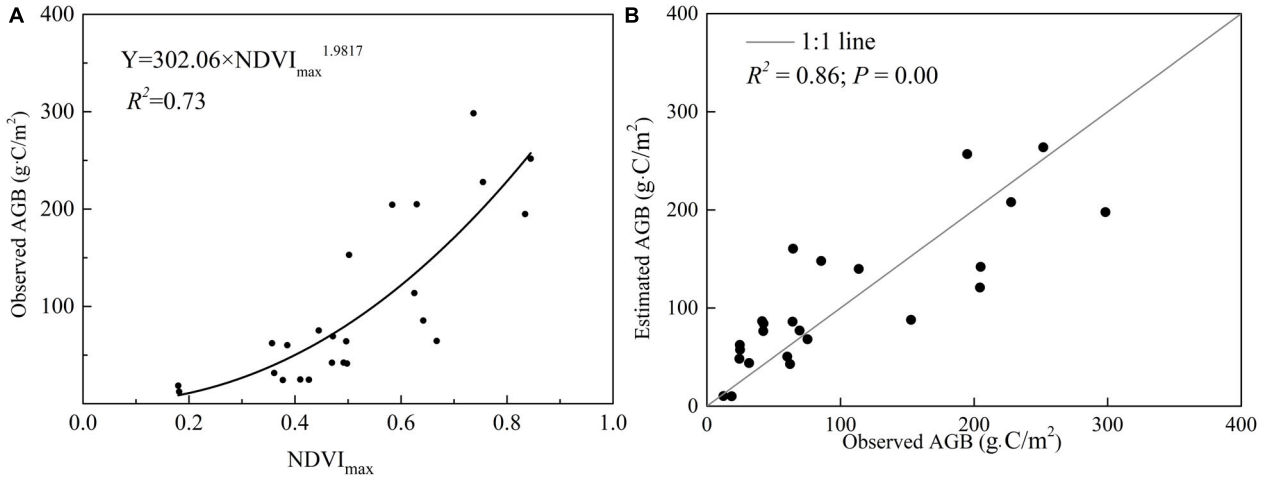

FIGURE 2 | Equation between observed AGB and $NDVI_{max}$ of marsh vegetation **(A)** and relationship between observed AGB and estimated AGB **(B)** in the marsh of western Songnen Plain.

appeared in the northern part of the western Songnen Plain marsh wetland (Momoge Nature Reserve) when compared to the southern part (**Figure 4A**). During the past two decades, the annual trend in AGB of marsh vegetation on the western Songnen Plain showed distinct-obvious spatial heterogeneities; the decreasing marsh AGB trend was mainly observed in the central western Songnen Plain (**Figure 4B**).

Impact of Climate Variables on the Aboveground Biomass of Wetland Vegetation

Figure 5 shows the response of spatial distribution of AGB in the investigated area to annual precipitation and temperature (T_{mean}, T_{max}, and T_{min}) over the western Songnen Plain wetland. We found that the correlation between AGB and climatic factors showed spatial heterogeneity (**Figure 5B**). Moreover, there was a significant positive correlation between marsh AGB and total precipitation ($P < 0.01$), and a weak correlation with T_{mean} (**Table 1** and **Figures 5A,B**). Regarding the maximum and minimum temperatures, our results found that the correlation between marsh AGB and T_{min} was lower than that between marsh AGB and T_{max} (**Table 1** and **Figures 5C,D**). The correlation between AGB and T_{max} was significantly positive ($P < 0.05$) over the study area.

Regarding the impact of seasonal precipitation on marsh AGB, the correlation between aboveground biomass and precipitation during the summer and autumn periods was significantly positive (**Table 1**), indicating that an increasing total precipitation would increase biomass by promoting marsh vegetation growth during the summer and autumn periods. Regarding the influence of T_{max} and T_{min}, marsh AGB has a significant positive correlation with T_{max} in spring (**Table 1**). By contrast, a weak positive relationship was observed between marsh AGB and T_{min} in all seasons (**Table 1**).

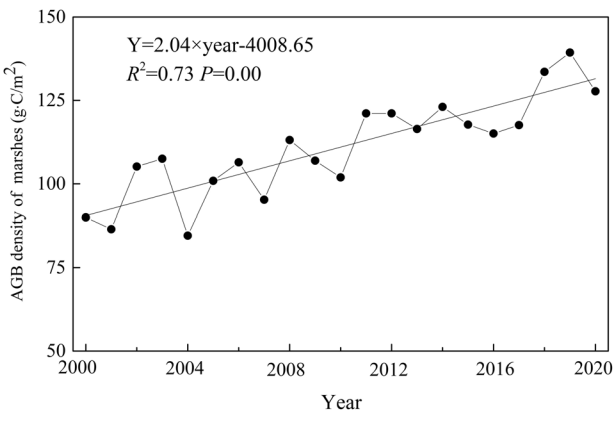

FIGURE 3 | Temporal variation of aboveground biomass density on the western Songnen Plain marshes from 2000 to 2020.

DISCUSSION

Estimation of the Aboveground Biomass in the Western Songnen Plain Wetland

In the present study, we established the fitting equation between marsh AGB and $NDVI_{max}$ for each pixel. The power equation was $Y = 302.06 \times NDVI_{max}^{1.9817}$ (**Figure 2A**; $R^2 = 0.73$). Our findings were similar to those of Piao et al. (2004), who discovered that the grassland aboveground biomass and the $NDVI_{max}$ value had a better power function. However, there are some differences between these functions. Piao et al. (2004) explored AGB of the grassland of China, whereas the present study explored the AGB of temperate semi-arid and semi-humid marshes in the western Songnen Plain. In the present study, the RMSE and R^2-values of the fitted equations were 42.60 and 0.98, respectively. These values indicated that the estimating

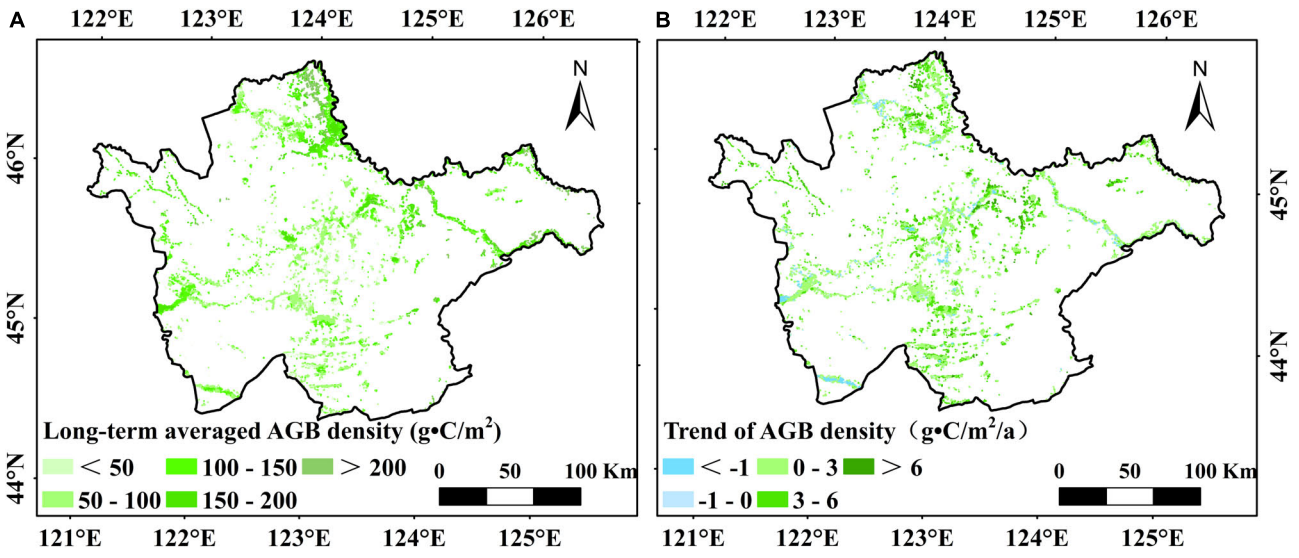

FIGURE 4 | Spatial patterns of the long-term averaged AGB density **(A)** and change trend of AGB density **(B)** in the western Songnen Plain marshes during 2000–2020.

equation could correctly calculate the marsh AGB on the western Songnen Plain. Furthermore, the regression models established between $NDVI_{max}$ and field-measured AGB values in the marsh provided a new method for investigating wetland AGB in the western Songnen Plain.

Based on this equation and $NDVI_{max}$ datasets, we calculated the average AGB density of the studied marsh wetland over a period of 20 years. The results revealed higher marsh AGB in the north of the western Songnen Plain (Momoge Nature Reserve) than in the southern part (**Figure 4A**). The reason for this may be that the abundant precipitation creates favorable environmental conditions for the growth of marsh vegetation in this region. The average marsh AGB showed a significant increasing trend (2.04 $g{\cdot}C/m^2/a$) over the years, with an average AGB density of about 111.01 $g{\cdot}C/m^2$ over the entire western Songnen Plain.

Correlations Between Climate Variables and Vegetation Aboveground Biomass on the Western Songnen Plain Wetland

Multiyear AGB values and the corresponding climate dataset from 2000 to 2020 were used to analyze the annual AGB trends and their relationships with seasonal climate. These trends suggested large spatiotemporal heterogeneity, mainly corresponding to the seasonal changes of climate, indicating that seasonal climate change plays a crucial role in AGB trends. The correlations between marsh AGB and precipitation, T_{mean}, T_{max}, and T_{min} were studied, and the results are shown in **Figure 5**.

In the present study, marsh AGB had a significant positive correlation with total precipitation, especially during the summer and autumn, but it was weakly positively correlated with the mean temperature. Previous studies have shown that the AGB of marsh vegetation in the studied area is less sensitive to mean temperature than to precipitation (Shen et al., 2019; Wang et al., 2020, 2022). Our findings confirmed that increasing precipitation in summer and autumn could be beneficial for marsh vegetation growth on the western Songnen Plain. This result is similar to that obtained by Wang et al. (2013), who discovered that during the growing season on the western Songnen Plain, the NDVI of marsh vegetation has a significant positive relationship with the total precipitation. Relatively good hydrothermal conditions are favorable for wetland vegetation growth in the summer and autumn (Li et al., 2019). Increasing precipitation in these seasons might improve plant light use efficiency, leading to an increase in the AGB of marsh vegetation. In addition, we note that marsh distribution dataset used in this study could contain some seasonal marshes. Precipitation can change the marsh distribution in rainy season. Increasing precipitation in summer and autumn could increase the actual distribution area of marshes and increase moisture availability for marsh vegetation growth, thus increasing marsh aboveground biomass within a certain area (Wang et al., 2021). This may partially account for the positive impacts of precipitation on the AGB in the western Songnen Plain wetland.

Regarding the impact of temperature on marsh AGB, the AGB was positively and significantly correlated with T_{max} but had a weak positive correlation with T_{min}. Our results further showed that T_{min} and T_{max} had an asymmetric effect on the aboveground biomass of the investigated marsh wetland (**Table 1**), suggesting that the increased maximum temperature in spring and winter may be associated with the temporal change in marsh AGB, especially during spring. Furthermore, our findings were consistent with previous studies showing that a warmer climate could lead to increase aboveground biomass as a consequence of enhanced photosynthetic rate and longer growth season (Myneni et al., 1997, 2001; Los et al., 2001; Tucker et al., 2001; Zhou et al., 2001; Hicke et al., 2002; Slayback et al., 2003). First, warming during the day accelerates the reaction

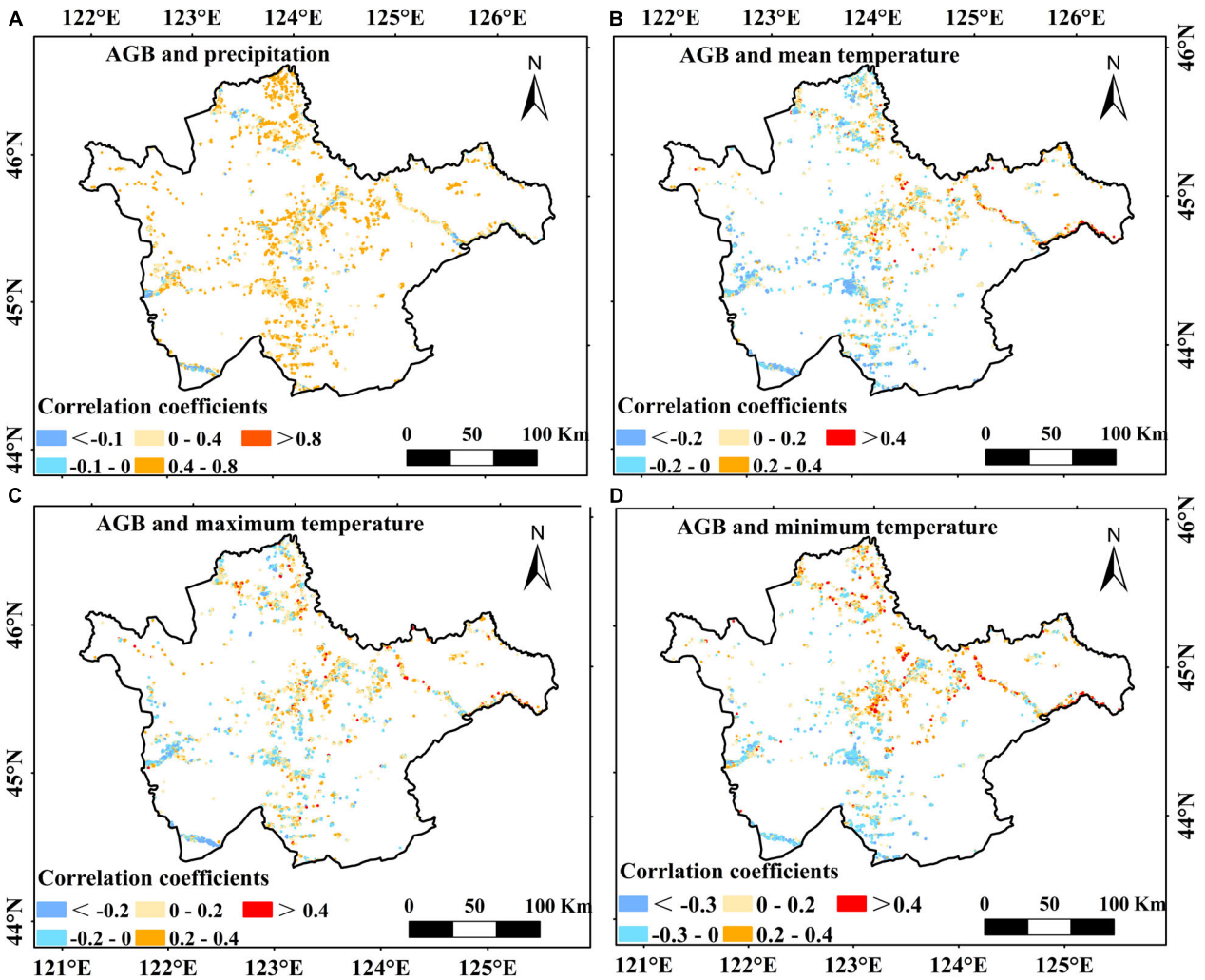

FIGURE 5 | Spatial distributions of correlation coefficients between the annual AGB and annual precipitation **(A)**, annual mean temperature **(B)**, annual maximum temperature **(C)**, and annual minimum temperature **(D)** in the western Songnen Plain marshes.

process of the photosynthetic enzymes, thereby increasing its activity of the photosynthetic enzyme and being conducive to the accumulation of organic matter (Shen et al., 2016). Second, prolonged growing period and early spring phenology may promote carbon sequestration by vegetation (White et al., 1999; Piao et al., 2003). In addition, we found that the minimum temperature showed a significant increase compared to that in maximum temperature but may exert only a slight impact on vegetation growth. Studies have shown that warming at night can be beneficial for vegetation growth as it reduces frost (Shen et al., 2019). Therefore, all these factors may explain why increasing daytime and nighttime temperatures can accelerate the vegetation growth on the western Songnen Plain marsh wetland.

Vegetation Changes in the Western Songnen Plain Marsh Wetlands

In order to further investigate the variation in the AGB of the marshes, we analyzed the spatial-temporal changes in climate factors during the period from 2000 to 2020 (**Table 2** and **Figure 6**). Precipitation showed a significantly increasing trend, at a rate of the 0.919 mm/a ($P < 0.05$), but no significant variation in T_{mean}, T_{max}, and T_{min} was observed. Moreover, precipitation was high in summer and autumn (1.378 mm/a and 1.334 mm/a, respectively) during the entire study period.

TABLE 1 | Correlations between climate factors and AGB of marsh vegetation in the western Songnen Plain marshes.

	Precipitation	T_{mean}	T_{max}	T_{min}
Annual	0.746**	0.316	0.451*	0.166
Spring	0.214	0.178	0.489*	0.400
Summer	0.691**	0.153	0.129	0.303
Autumn	0.446*	–0.041	–0.066	0.225
Winter	0.070	0.114	0.256	0.189

*Levels of significance are set at *p < 0.05 and **p < 0.01.*

TABLE 2 | Temporal trends of precipitation (mm/a), T_{mean} (°C/a), T_{max} (°C/a), and T_{min} (°C/a) on the western Songnen Plain marshes from 2000 to 2020.

	Precipitation	T_{mean}	T_{max}	T_{min}
Annual	0.919**	0.015	0.021	0.013
Spring	0.877	–0.004	0.046	0.088
Summer	1.378*	–0.003	–0.022	0.087*
Autumn	1.334**	0.033	0.001	0.093
Winter	0.088	0.053	0.057	0.130

*Levels of significance are set at *$p < 0.05$ and **$p < 0.01$.*
The symbol "a" indicates per year.

Based on the correlations between marsh AGB and precipitation (**Figure 4** and **Table 1**), we concluded that significant increases in summer and autumn precipitation may have accounted for the increasing marsh AGB. Increased rainfall in summer and autumn can enhance vegetation growth, as discussed in section "Correlations Between Climate Variables and Vegetation Aboveground Biomass on the Western Songnen Plain Wetland." Regarding the temperature changes, the trends of T_{min} were positive in all seasons, suggesting that the T_{min} increased for all seasons during the study period (**Table 2**). In particular, summer T_{min} exhibited an increasing trend (0.087°C/a, $P < 0.05$). This significant summer T_{min} trend in the as well as the one in precipitation during summer and autumn may be beneficial to the increase in marsh AGB throughout the western Songnen Plain.

Regarding the spatial changes in the AGB, the greatest increase of marsh AGB during the study period was observed in the northern Songnen Plain (**Figure 4B**). In particular, our results found that this region had the largest increase in precipitation (**Figure 6A**). According to the spatial correlation between marsh vegetation AGB and total precipitation (**Figure 5A**), the significant increase of total precipitation in the same area may account for the increase in AGB of marsh vegetation in the northern Songnen Plain. In the past 20 years, the local government has strengthened wetland protection and management to restore marsh wetlands in the western Songnen Plain (Wang et al., 2022), which may partly explain the increased AGB of marsh vegetation in this study.

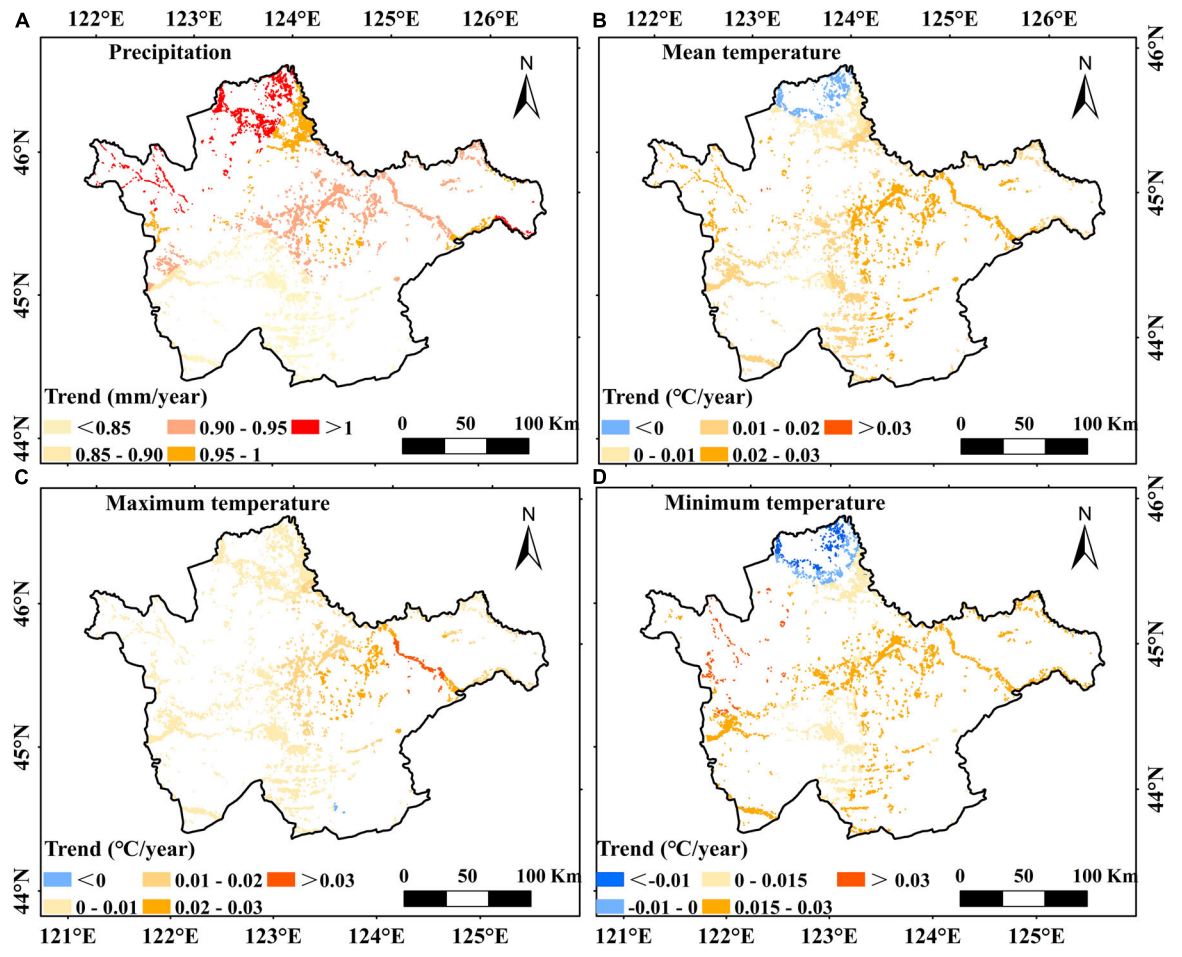

FIGURE 6 | Spatial change trends of annual precipitation **(A)**, annual mean temperature **(B)**, annual maximum temperature **(C)**, and annual minimum temperature **(D)** in the western Songnen Plain marshes during 2000–2020.

Study Limitations

This study has some certain limitations. The first is the uncertainty of marsh data, which may have included some seasonal marshes; therefore, differences from the actual marsh distribution dynamics may lead to some uncertainties in the descriptions of the response of AGB to climate change. For the field-observation data, the ground points were limited and not uniformly distributed, which could cause some uncertainty about the results of this study. Further studies are still needed to verify our results using more field-observation sites. **The** second is the uncertainty of the NDVI time series dataset. In addition, the actual condition of vegetation in a certain area cannot be fully reflected by NDVI data. Third, owing to technical limitations, marsh AGB values cannot be accurately measured under the saturation condition of $NDVI_{max}$. Fourth, we only discussed the impact of precipitation, T_{mean}, T_{max}, and T_{min} on the AGB of marsh vegetation in our studies. In order to reveal the mechanism of marsh AGB variation and simulate biomass results, the influences of various environmental factors on AGB need to be further investigated in the western Songnen Plain marshes in the future.

CONCLUSION

We accurately estimated a power function ($Y = 302.06 \times NDVI_{max}^{1.9817}$), and the aboveground biomass of marsh vegetation on the western Songnen Plain can be well estimated by using the remote sensing and measured biomass datasets. The marsh AGB density showed a significant increasing trend (2.04 g $C/m^2/a$), with an average AGB density value of 111.01 g·C/m^2 during the period 2000–2020 over the entire western Songnen Plain. An especially high AGB value was estimated for the north of the western Songnen Plain marsh wetland (Momoge Nature Reserve). Regarding the influence of precipitation and temperature, the AGB of marsh vegetation is less sensitive to temperature than to precipitation in this region. Increasing precipitation in summer and autumn would increase AGB values by promoting marshes vegetation growth. In addition, we found that the T_{min} and T_{max} have an asymmetric effect on AGB in the western Songnen Plain marsh wetland, with the maximum temperature warming significantly stimulating the vegetation growth. On the other hand, the minimum temperature showed a significant increase but may exert a slight impact on vegetation growth. The findings of the study can affect the protection and management of marshy regions in the future.

DATA AVAILABILITY STATEMENT

The original contributions presented in the study are included in the article/supplementary material, further inquiries can be directed to the corresponding author/s.

AUTHOR CONTRIBUTIONS

ST coordinated the project. YW carried out the data analysis and wrote the manuscript. XS, MZ, MJ, and XL contributed to modifying the manuscript. All authors contributed to the article and approved the submitted version.

FUNDING

This work was funded by the National Natural Science Foundation of China (41871101), the Strategic Priority Research Program of the Chinese Academy of China (XDA23060402), the National Natural Science Foundation of China (41971065), the Youth Innovation Promotion Association, CAS (2019235), the Natural Science Foundation of Jilin Province (20210101104JC), the Key Research Program of Frontier Sciences, CAS (ZDBS-LY-7019), and the Innovation Team Project of Northeast Institute of Geography and Agroecology, CAS (2022CXTD02).

REFERENCES

Byrd, K. B., Ballanti, L., Thomas, N., Nguyen, D., Holmquist, J. R., Simard, M., et al. (2018). A remote sensing-based model of tidal marsh aboveground carbon stocks for the conterminous United States. *ISPRS. J. Photogramm.* 139, 255–271. doi: 10.1016/j.isprsjprs.2018.03.019

Caccamo, G., Chisholm, L., Bradstock, R. A., and Puotinen, M. L. (2011). Assessing the sensitivity of MODIS to monitor drought in high biomass ecosystems. *Remote Sens. Environ.* 115, 2626–2639. doi: 10.1016/j.rse.2001.05.018

Chopping, M., Su, L., Rango, A., Martonchik, J. V., Peters, D. P., and Laliberte, A. (2008). Remote sensing of woody shrub cover in desert grasslands using MISR with a geometric-optical canopy reflectance model. *Remote Sens. Environ.* 112, 19–34. doi: 10.1016/j.rse.2006.04.023

Ding, M., Zhang, Y., Liu, L., Zhang, W., Wang, Z., and Bai, W. (2007). The relationship between NDVI and precipitation on the Tibetan Plateau. *J. Geogr. Sci.* 17, 259–268. doi: 10.1007/s11442-007-0259-7

Dong, T., Liu, J., Qian, B., Zhao, T., Jing, Q., Geng, X., et al. (2016). Estimating winter wheat biomass by assimilating leaf area index derived from fusion of landsat-8 and MODIS data. *Int. J. Appl. Earth Obs. Geoinf.* 49, 63–74. doi: 10.1016/j.jag.2016.02.001

Fang, J., Guo, Z., Piao, S., and Chen, A. (2007). Terrestrial vegetation carbon sinks in China, 1981–2000. *Sci. China Series D.* 50, 1341–1350. doi: 10.1007/s11430-007-0049-1

Fang, J., Yang, Y., Ma, W., Mohammat, A., and Shen, H. (2010). Ecosystem carbon stocks and their changes in China's grasslands. *Sci. China Life Sci.* 5, 757–765. doi: 10.1007/s11427-010-4029-x

Flombaum, P., and Sala, O. E. (2007). A non-destructive and rapid method to estimate biomass and aboveground net primary production in arid environments. *J. Arid. Environ.* 69, 352–358. doi: 10.1016/j.jaridenv.2006.09.008

Gao, T., Xu, B., Yang, X., Jin, Y., Ma, H., Li, J., et al. (2013). Using MODIS time series data to estimate aboveground biomass and its spatio-temporal variation in Inner Mongolia's grassland between 2001 and 2011. *Int. J. Remote Sens.* 34, 7796–7810. doi: 10.1080/01431161.2013.823000

Gao, X., Dong, S., Li, S., Xu, Y., Liu, S., Zhao, H., et al. (2020). Using the random forest model and validated MODIS with the field spectrometer measurement promote the accuracy of estimating aboveground biomass and coverage of alpine grasslands on the Qinghai-Tibetan Plateau. *Ecol. Evol.* 112:106114. doi: 10.1016/j.ecolind.2020.106114

Guan, Q. C., Zhao, H. J., Geng, S. B., and Wang, Y. (2018). Research on vegetation biomass and carbon reserves in the core area of cranes in Xianghai Wetland (in Chinese). *J. Temperate For. Res.* 1, 42–48.

Hicke, J. A., Asner, G. P., Randerson, J. T., Tucker, C., Los, S., Birdsey, R., et al. (2002). Trends in North American net primary productivity derived from satellite observations, 1982–1998. *Global Biogeochem. Cy.* 16:1018. doi: 10.1029/2001GB001550

Holben, B. N. (1986). Characteristic of maximum-value composite images from temporal AVHRR data. *Int. J. Remote Sens.* 7, 1417–1434. doi: 10.1080/01431168608948945

Li, B., Huang, F., Qin, L., Qi, H., and Sun, N. (2019). Spatio-temporal variations of carbon use efficiency in natural terrestrial ecosystems and the relationship with climatic factors in the Songnen Plain. *China. Remote Sens.* 11:2513. doi: 10.3390/rs11212513

Liu, Y., Ding, Z., Bachofen, C., Lou, Y., Jiang, M., Tang, X., et al. (2018). The effect of saline-alkaline and water stresses on water use efficiency and standing biomass of Phragmitesaustralis and Bolboschoenusplaniculmis. *Sci. Total Environ.* 644, 207–216. doi: 10.1016/j.scitotenv.2018.05.321

Los, S. O., Collatz, G. J., Bounoua, L., Sellers, P. J., and Tucker, C. J. (2001). Global interannual variations in sea surface temperature and land surface vegetation, air temperature, and precipitation. *J. Clim.* 14, 1535–1549.

Mao, D., He, X., Wang, Z., Tian, Y., Xiang, H., Yu, H., et al. (2019). Diverse policies leading to contrasting impacts on land cover and ecosystem services in northeast China. *J. Clean. Prod.* 240:117961. doi: 10.1016/j.jclepro.2019.117961

Mitsch, W. J., Bernal, B., Nahlik, A. M., Mander, Ü, Zhang, L., Anderson, C. J., et al. (2013). Wetlands, carbon, and climate change. *Landscape Ecol.* 28, 583–597. doi: 10.1007/s10980-012-9758-8

Muukkonen, P., and Heiskanen, J. (2007). Biomass estimation over a large area based on standwise forest inventory data and ASTER and MODIS satellite data: a possibility to verify carbon inventories. *Remote Sens. Environ.* 107, 617–624. doi: 10.1016/j.rse.2006.10.011

Myneni, R. B., Dong, J., Tucker, C. J., Kaufmann, R. K., Kauppi, P. E., Liski, J., et al. (2001). A large carbon sink in the woody biomass of northern forests. *Proc. Natl. Acad. Sci. U.S.A.* 98, 14784–14789. doi: 10.1073/pnas.261555198

Myneni, R. B., Keeling, C. D., Tucker, C. J., Asrar, G., and Nemani, R. R. (1997). Increased plant growth in the northern high latitudes from 1981 – 1991. *Nature* 386, 698–702. doi: 10.1038/386698a0

Peng, S., Piao, S., Ciais, P., Myneni, R., Chen, A., Chevallier, F., et al. (2013). Asymmetric effects of daytime and night-time warming on Northern Hemisphere vegetation. *Nature* 501, 88–95. doi: 10.1038/nature12434

Pettorelli, N., Vik, J. O., Mysterud, A., Gaillard, J. M., Tucker, C. J., and Stenseth, N. C. (2005). Using the satellite-derived NDVI to assess ecological responses to environmental change. *Trends. Ecol. Evol.* 20, 503–510. doi: 10.1016/j.tree.2005.05.011

Piao, S., Fang, J., He, J., and Xiao, Y. (2004). Spatial distribution of grassland biomass in China (in Chinese). *J. Plant. Ecol.* 28:491.

Piao, S., Fang, J., Zhou, L., Guo, Q., Henderson, M., Ji, W., et al. (2003). Interannual variations of monthly and seasonal normalized difference vegetation index (NDVI) in China from 1982 to 1999. *J. Geophys. Res. Atmos.* 108:4401. doi: 10.1029/2002JD002848

Piao, S., Fang, J., Zhou, L., Tan, K., and Tao, S. (2007). Changes in biomass carbon stocks in China's grasslands between 1982 and 1999. *Global Biogeochem. Cy.* 21:GB2002. doi: 10.1029/2005GB002634

Piao, S., Fang, J., Zhou, L., Zhu, B., Tan, K., and Tao, S. (2005). Changes in vegetation net primary productivity from 1982 to 1999 in China. *Global Biogeochem. Cy.* 19:GB2027. doi: 10.1029/2004GB002274

Qiao, Y., Liu, H., Kellomaki, S., Peltola, H., Liu, Y., Dong, B., et al. (2014). Comparison of the effects of symmetric and asymmetric temperature elevation and CO2 enrichment on yield and evapotranspiration of winter wheat (*Triticum aestivum* L.). *Ecol. Evol.* 4, 1994–2003. doi: 10.1002/ece3.1081

Scurelock, J. M. O., Johnson, K., and Olson, R. J. (2002). Estimating net primary productivity from grassland biomass dynamics measurements. *Global Change Biol.* 8, 736–753. doi: 10.1046/j.1365-2486.2002.00512.x

Shen, M., Piao, S., Chen, X., An, S., Fu, Y. H., Wang, S., et al. (2016). Strong impacts of daily minimum temperature on the green-up date and summer greenness of the Tibetan Plateau. *Global Change Biol.* 22, 3057–3066. doi: 10.1111/gcb.13301

Shen, X., Jiang, M., Lu, X., Liu, X., Liu, B., Zhang, J., et al. (2021a). Aboveground biomass and its spatial distribution pattern of herbaceous marsh vegetation in China. *Sci. China Earth Sci.* 64, 1115–1125. doi: 10.1007/s11430-020-9778-7

Shen, X., Liu, B., Henderson, M., Wang, L., Jiang, M., and Lu, X. (2022a). Vegetation greening, extended growing seasons, and temperature feedbacks in warming temperate grasslands of China. *J. Climate.* 35, 1–51. doi: 10.1175/JCLI-D-21-0325.1

Shen, X., Liu, B., Jiang, M., and Lu, X. (2020). Marshland loss warms local land surface temperature in China. *Geophys. Res. Lett.* 47:e2020GL087648. doi: 10.1029/2020GL087648

Shen, X., Liu, B., Jiang, M., Wang, Y., Wang, L., Zhang, J., et al. (2021b). Spatiotemporal change of marsh vegetation and its response to climate change in china from 2000 to 2019. *J. Geophy. Res. Biogeo.* 126, 1–13. doi: 10.1029/2020JG006154

Shen, X., Liu, B., Li, G., Wu, Z., Jin, Y., Yu, P., et al. (2014). Spatiotemporal change of diurnal temperature range and its relationship with sunshine duration and precipitation in China. *J. Geophys Res-Atmos.* 119, 13163–13179. doi: 10.1002/2014JD022326

Shen, X., Liu, Y., Liu, B., Zhang, J., Wang, L., Lu, X., et al. (2022b). Effect of shrub encroachment on land surface temperature in semi-arid areas of temperate regions of the Northern Hemisphere. *Agr. Forest Meteorol.* 320:108943. doi: 10.1016/j.agrformet.2022.108943

Shen, X., Xue, Z., Jiang, M., and Lu, X. (2019). Spatiotemporal change of vegetation coverage and its relationship with climate change in freshwater marshes of Northeast China. *Wetlands.* 39, 429–439. doi: 10.1007/s13157-018-1072-z

Slayback, D., Pinzon, J., Los, S., and Tucker, C. (2003). Northern Hemisphere photosynthetic trends 1982 – 1999. *Global Change Biol.* 9, 1–15. doi: 10.1046/j.1365-2486.2003.00507.x

Stow, D., Daeschner, S., Hope, A., Douglas, D., Petersen, A., Myneni, R., et al. (2003). Variability of the seasonally integrated normalized difference vegetation index across the north slope of Alaska in the 1990s. *Int. J. Remote Sens.* 24, 1111–1117. doi: 10.1080/0143116021000020144

Tucker, C. J., Slayback, D. A., Pinzon, J. E., Los, S. O., Myneni, R. B., and Taylor, M. G. (2001). Higher northern latitude NDVI and growing season trends from 1982 to 1999. *Int. J. Biometeorol.* 45, 184–190. doi: 10.1007/s00484-001-0109-8

Wang, X., Ma, M., Li, X., Song, Y., Tan, J., Huang, G., et al. (2013). Validation of MODIS-GPP product at 10 flux sites in northern China. *Int. J. Remote Sens.* 34, 587–599. doi: 10.1080/01431161.2012.715774

Wang, Y., Shen, X., Jiang, M., and Lu, X. (2020). Vegetation change and its response to climate change between 2000 and 2016 in marshes of the Songnen Plain, Northeast China. *Sustainability* 12:3569. doi: 10.3390/su12093569

Wang, Y., Shen, X., Jiang, M., Tong, S., and Lu, X. (2021). Spatiotemporal change of aboveground biomass and its response to climate change in marshes of the Tibetan Plateau. *Int. J. Appl. Earth Obs. Geoinf.* 102:102385. doi: 10.1016/j.jag.2021.102385

Wang, Y., Shen, X., Jiang, M., Tong, S., and Lu, X. (2022). Daytime and nighttime temperatures exert different effects on vegetation net primary productivity of marshes in the western Songnen Plain. *Ecol. Indic.* 137:108789. doi: 10.1016/j.ecolind.2022.108789

Wang, Z., Huang, N., Luo, L., Li, X., Ren, C., Song, K., et al. (2011). Shrinkage and fragmentation of marshes in the west Songnen Plain, China, from 1954 to 2008 and its possible causes. *Int. J. Appl. Earth Obs. Geoinf.* 13, 477–486. doi: 10.1016/j.jag.2010.10.003

Wang, Z., Song, K., Zhang, B., Liu, D., Ren, C., Luo, L., et al. (2009). Shrinkage and fragmentation of grasslands in the West Songnen Plain, China. *Agr. Ecosyst. Environ.* 129, 315–324. doi: 10.1016/j.agee.2008.10.009

White, A., Cannell, M. G. R., and Friend, A. D. (1999). Climate change impacts on ecosystems and the terrestrial carbon sink: a new assessment. *Global Environ. Change.* 9, 21–30. doi: 10.1016/S0959-3780(99)00016-3

Xie, Y., Lei, X., and Shi, J. (2020). Impacts of climate change on biological rotation of Larixolgensis plantations for timber production and carbon storage in northeast China using the 3-PGmix model. *Ecol. Model.* 435:109267. doi: 10.1016/j.ecolmodel.2020.109267

Yang, X., Wu, J., Chen, X., Ciais, P., Maignan, F., Yuan, W., et al. (2021). A comprehensive framework for seasonal controls of leaf abscission and productivity in evergreen broadleaved tropical and subtropical forests. *Innovation* 2:100154. doi: 10.1016/j.xinn.2021.100154

Yang, Y., and Li, J. (2003). Biomass allocation and growth analysis on the ramets of Phragmites communis populations in different habitats in the Songnen Plains of China (in Chinese). *J. Appl. Ecol.* 14, 30–34.

Yang, Y., Fang, J., Ma, W., Guo, D., and Mohammat, A. (2010). Large-scale pattern of biomass partitioning across China's grasslands. *Global Ecol. Biogeogr.* 19, 268–277. doi: 10.1111/j.1466-8238.2009.00502.x

Yin, L., Du, P., Zhang, M., Liu, M., Xu, T., and Song, Y. (2019). Estimation of emissions from biomass burning in China based on MODIS fire radiative energy data. *Biogeosciences* 16, 1629–1640. doi: 10.5194/bg-16-1629-2019

Zhang, D., Sun, J., Cui, Q., Jia, X., Qi, Q., Wang, X., et al. (2021). Plant growth and diversity performance after restoration in Carexschmidtii tussock wetlands, Northeast China. *Community Ecol.* 22, 391–401. doi: 10.1007/s42974-021-00062-7

Zhang, G., Dong, J., Xiao, X., Hu, Z., and Sheldon, S. (2012). Effectiveness of ecological restoration projects in Horqin Sandy Land, China based on SPOT-VGT NDVI data. *Ecol. Eng.* 38, 20–29. doi: 10.1016/j.ecoleng.2011.09.005

Zhou, L., Tucker, C. J., Kaufmann, R. K., Slayback, D., Shabanov, N. V., and Myneni, R. B. (2001). Variations in northern vegetation activity inferred from satellite data of vegetation index during 1981 to 1999. *J. Geophys. Res.* 106, 069–083. doi: 10.1029/2000JD000115

Conflict of Interest: The authors declare that the research was conducted in the absence of any commercial or financial relationships that could be construed as a potential conflict of interest.

frontiers | Frontiers in Plant Science

ORIGINAL RESEARCH
published: 23 June 2022
doi: 10.3389/fpls.2022.935025

Water Uptake Tradeoffs of Dominant Shrub Species in the Coastal Wetlands of the Yellow River Delta, China

Jinfang Zhu[1], Jingtao Liu[2], Junsheng Li[1]*, Caiyun Zhao[1] and Jingkuan Sun[2]*

[1] State Key Laboratory of Environmental Criteria and Risk Assessment, Chinese Research Academy of Environmental Sciences, Beijing, China, [2] Shandong Provincial Key Laboratory of Eco-Environmental Science for Yellow River Delta, Binzhou University, Binzhou, China

Tamarix chinensis and *Ziziphus jujuba* are two dominant shrub species on Chenier Island in the Yellow River Delta, China. Water is a restrictive factor determining the plant growth, vegetation composition, and community succession in this coastal zone. We investigated how water uptake tradeoffs of the two shrub species responded to soil water fluctuations caused by seasonal variations of precipitation. The soil water content, salinity and $\delta^{18}O$ values of potential water sources (soil water in 0–20, 20–40, 40–60, and 60–100 cm soil layers, and groundwater) and plant xylem water were measured in wet (July 2013) and dry (July 2014) seasons. The IsoSource model was employed to calculate the contributions of different water sources to plant xylem water. The results showed that $\delta^{18}O$ values of soil water decreased significantly with soil depth in the dry season, while increased significantly with soil depth in the wet season. In the wet season, when the soil water was abundant, *Z. jujuba* mostly used the soil water from the 60–100 cm layer, while *T. chinensis* took up a mixture of groundwater and soil water from the 60–100 cm layer. In the dry season, when the soil water was depleted because of low precipitation, *Z. jujuba* mainly took up a mixture of the soil water from 20 to 100 cm soil layers, while *T. chinensis* mainly used groundwater. *T. chinensis* and *Z. jujuba* showed different ecological amplitudes of water sources during dry and wet seasons. The niche differentiation of major water sources for *T. chinensis* and *Z. jujuba* demonstrated their adaptabilities to the fluctuations of soil moisture in water-limited ecosystems. Water niche differentiations of coexisting shrub species were expected to minimize their competition for limited water sources, contributing to successful coexistence and increasing the resilience of the coastal wetland ecosystem to drought.

Keywords: water use strategy, available soil water, water source, stable oxygen isotope, wetland plants

OPEN ACCESS

Edited by:
Yong Li,
Chinese Academy of Forestry, China

Reviewed by:
Junhong Bai,
Beijing Normal University, China
Xin-Jun Zheng,
Xinjiang Institute of Ecology and Geography (CAS), China

***Correspondence:**
Jingtao Liu
ljteco@126.com
Junsheng Li
lijsh@craes.org.cn

Specialty section:
This article was submitted to Functional Plant Ecology, a section of the journal Frontiers in Plant Science

Received: *03 May 2022*
Accepted: *06 June 2022*
Published: *23 June 2022*

Citation:
Zhu J, Liu J, Li J, Zhao C and Sun J (2022) Water Uptake Tradeoffs of Dominant Shrub Species in the Coastal Wetlands of the Yellow River Delta, China. Front. Plant Sci. 13:935025. doi: 10.3389/fpls.2022.935025

INTRODUCTION

Available water is a key determinant of vegetation composition and community succession (Gazis and Feng, 2004; Xu et al., 2011; Wei et al., 2013; Xia et al., 2014). In coastal wetlands, the available water is extremely limited due to the increasing salinity of soil water and groundwater induced by the seawater intrusion, and this restrict the growth of non-halophytic plants significantly

(Marcelis and Van Hooijdonk, 1999; Osland et al., 2011; Chandrajith et al., 2013; Janousek and Mayo, 2013; Lu et al., 2020). Uneven and stochastic precipitation usually causes temporal–spatial heterogeneity in water availability, increasing the scarcity of the already limited availability (Drake and Franks, 2003; Wu et al., 2014; Gu et al., 2015). Because of the limitation of available water, competition among species in coastal wetlands is likely to be more intense (Asbjornsen et al., 2007; Ewe et al., 2007). This competition is weakened when plants use different water sources (e.g., soil water, groundwater, rainwater, and seawater) (Sternberg and Swart, 1987; Sternberg et al., 1991; Ewe et al., 1999; Corbin et al., 2005). In addition, plant species can adapt to water stress by shifting their main water sources as the soil water conditions change (Ewe et al., 1999; Zhu et al., 2018). Therefore, the tradeoffs in plant water uptake play a critical role in the successful coexistence of dominant species with similar life forms.

Plant water uptake is closely related to the distribution patterns of root systems (Dawson and Pate, 1996; Oliveira et al., 2005; Aroca et al., 2012; Wang et al., 2015). Shallow-rooted plants mainly absorb water from surface soil, and deep-rooted plants can exploit deeper soil water and even groundwater (Williams and Ehleringer, 2000; Yang et al., 2011; Rossatto et al., 2012; Wu et al., 2016). However, some previous studies have shown that the proportions of soil water from different depths for a plant species are not exactly consistent with the distribution patterns of that plant's root systems (Dawson and Pate, 1996; Chimner and Cooper, 2004). This phenomenon is caused by the variations in available water along the soil profile, as the plant often first relies on more dependable water sources. Dawson and Pate's (1996) results showed that plants derived the majority of the water they use from deeper sources via their taproots in dry season, while in the wet season most of the water they use was derived from shallower soil water via their lateral roots. The ability to exploit deeper, dependable water sources makes it possible for plants to survive a long dry period without precipitation (Ehleringer et al., 1991; Dawson and Pate, 1996; Wu et al., 2014; Dai et al., 2015).In coastal wetlands, salinity is also an important factor determining the water uptake patterns of plants (Ewe et al., 2007). A previous study reported that halophytic species were able to use deeper soil water, or groundwater with high salinity, but non-halophytic species depended only on soil water with lower salinity or rainwater stored in the soil (Zhu et al., 2018). The difference in the water sources used by plants contributes to water niche differentiation, which is the key to their successful coexistence.

Chenier Island, one of the world's three large, ancient shell ridges, formed in the Yellow River Delta (YRD) by the accumulation of shells over thousands of years (Zhao et al., 2015).The coastal wetland ecosystem on Chenier Island plays a key role in protection against coastal erosion. It also provides habitats as resting grounds for some migratory bird species and as breeding grounds for others (Zhao et al., 2015). Precipitation is the main freshwater source of soil water recharge and determines the vegetation composition and distribution patterns in this region. Against the background of global climate change, however, precipitation is becoming more uneven and shows significant annual differences which may cause frequent drought (Bai et al., 2020). The movement of precipitation through the soil profile is significantly affected by soil texture, characterized by coarse particle diameter, large porosity, and low water conservation in this area (Zhu et al., 2018). Because of the impact of large porosity, most of the precipitation infiltrates into deep soil layers or groundwater immediately after it falls, and only a small proportion is short-lived in the soil profile available for plant water use (Zhu et al., 2016). On Chenier Island, therefore, soil water is the critical factor limiting the growth and distribution of plants, and its availability will become an even more significant factor in dry seasons with little precipitation. The allocation of water sources is very important to plant survival through a long dry period in this region. Understanding the water tradeoff of dominant plant species is beneficial to the protection and restoration of the coastal wetland ecosystem.

Tamarix chinensis and *Ziziphus jujuba* are two typical xerophytic shrub species that are mainly distributed in the arid and semi-arid areas of China. They have similar life forms and high tolerance to drought stress (Zhu et al., 2018). *T. chinensis*, a common shrub species in YRD, has higher tolerance for salt stress (Zhu et al., 2015). On Chenier Island, *Z. jujuba* and *T. chinensis* are two dominant shrub species coexisting on the dune crest (Zhu et al., 2018). They are ecologically important in protecting the coast from wind and waves (Zhao et al., 2015). The result of our previous study (Zhu et al., 2018) showed that the two species had different water use patterns during growing seasons. Little was known, however, about their water use strategies in wet and dry seasons. Hence, a field experiment was carried out in the same month in different years to investigate (1) whether the two shrub species have differences in water use strategies, and (2) how they shift water sources to adapt to the fluctuations in soil water resulting from precipitation. We hypothesized that (1) *T. chinensis* and *Z. jujuba* have different water use patterns in dry and wet seasons; (2) *T. chinensis*, which has higher salt tolerance than *Z. jujuba*, may use deeper water sources than *Z. jujuba* when the soil water is limited in the dry season.

MATERIALS AND METHODS

Study Area

The study was conducted on Chenier Island lies on the Binzhou National Shell Ridge and Wetland Nature Reserve in the YRD (38°05′–38°21′N, 117°46′–118°05′E) along the northern coast of Wudi county, Shandong province, China (**Figure 1**). A typical temperate continental monsoon climate dominates in the study area. Mean annual temperature is 12.4°C. Mean annual precipitation and mean annual evaporation are 552.4 and 2430.6 mm, respectively (Zhao et al., 2015; Zhu et al., 2016, 2018). Seventy percent of annual precipitation happens between June and September (Zhu et al., 2018).The study area is formed by long-term accumulation of shells brought by tides. The soil matrix consists of shells, mud and sand, and the soil texture is characterized by large porosity, weak water, and fertilizer holding capacity (Zhao et al., 2015). The soil types are mainly shell sand soil and coastal saline soil, and coastal saline soil is dominant on

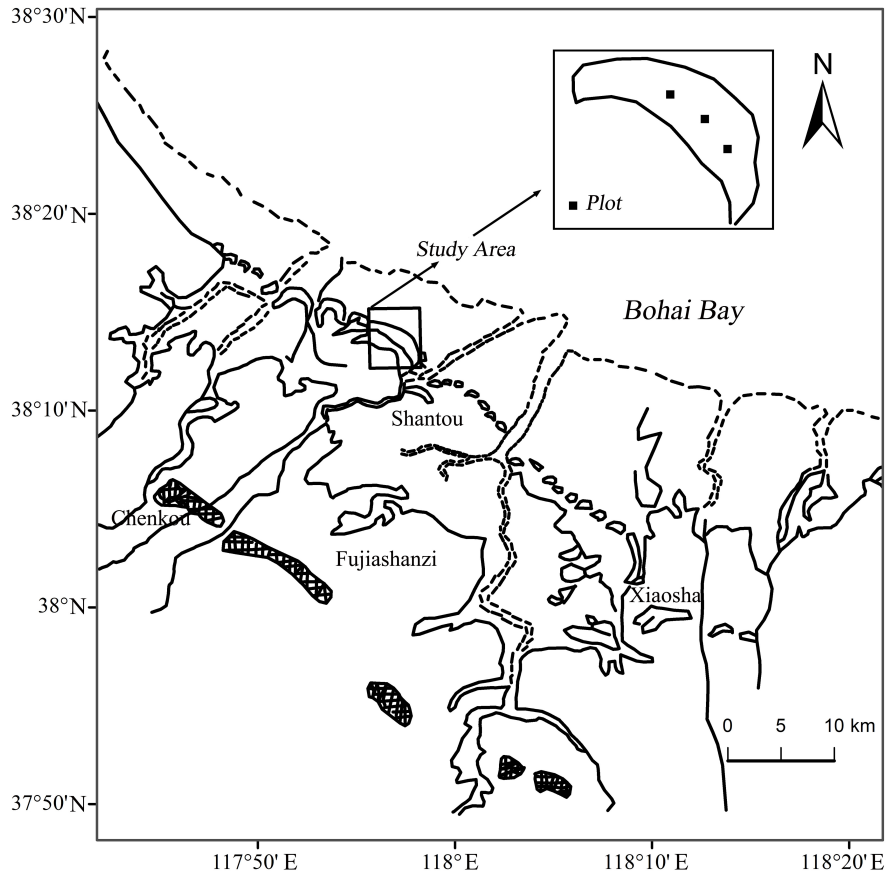

FIGURE 1 | Location map of the study area and sampling sites.

the seaward and landward sides (Zhu et al., 2015; Chen et al., 2019). The groundwater level is very shallow, only 1.8 m depth.

T. chinensis and *Z. jujuba* are two dominant shrub species in the local vegetation communities with the coverage of 75∼90%. The root architectures are clearly different between two shrub species. The root length of *Z. jujuba* is about 1.5 m, with mainly shallow root system. The root length of *T. chinensis* is about 2.2 m, with mainly vertical root system. Associated plants are mainly herbaceous species with shallow roots, such as *Artemisia mongolica* Fisch., *Astragalus adsurgens* Pall., *Messerschmidia sibirica* Linn., *Cayratia japonica* (Thunb.) Gagnep., *Apocynum venetum* L., and *Heteropappus altaicus* (Willd.) Novopokr.

Sample Collection

We conducted a field experiment in shrubland dominated by *T. chinensis* and *Z. jujuba* on Chenier Island in the YRD, China, in July 2013 (wet season) and July 2014 (dry season). Three 10 m × 10 m sample plots were established as the permanent plots in the study area. All plant, soil and groundwater samples were collected on clear days over 5 days after the last rainfall at the end of July 2013 and July 2014. Fully suberized twigs were randomly selected and cut from each species for of xylem water extraction. There were three replicates for each species in each plot. Soil samples were collected for stable isotope, soil water content (SWC) and salinity analyses. Three soil profiles were chosen randomly from different directions within 1 m of the sampled plants in each plot. The soil samples were collected at depths of 0–20, 20–40, 40–60, and 60–100 cm by using a soil auger, respectively. Three groundwater samples were pumped using a 200 cm vitrified-clay tube fixed within 1 m of the sampled plants in each plot. All samples were collected between 06:00 and 08:00 a.m.

To avoid isotopic fractionation caused by evaporation, all samples were placed in individual screw-capped glass vials immediately after collection, sealed with Parafilm and stored in a freezer before water extraction. The soil samples that were used to analyze the SWC were sealed and taken back to the laboratory for determination.

The SWC was determined by the oven-drying method (Gu et al., 2015). Soil and groundwater salinity were measured by the gravimetric method. All laboratory experiments were conducted at Shandong Provincial Key Laboratory of Eco-Environmental Science for Yellow River Delta.

Climatic data of precipitation were continuously recorded at an automatic climate station on Chenier Island which was installed by Shandong Provincial Key Laboratory of Eco-Environmental Science for Yellow River Delta.

Stable Isotope Analysis

Many studies have shown that natural stable isotopes of hydrogen and oxygen are used successfully to trace the water sources of plants (Dawson and Pate, 1996; Ehleringer et al., 2000; Ewe et al., 2007; Wu et al., 2014; Gu et al., 2015), as different water sources have different isotopic compositions because of the isotopic fractionation of hydrogen and oxygen during physical processes (e.g., evaporation and condense) (Ehleringer and Dawson, 1992). The application of isotopic technology on plant water use is based on the assumption that there is no isotopic fractionation of hydrogen and oxygen during water uptake by plant roots (Ewe et al., 2007; Meißner et al., 2014). In most ecosystems the isotopic composition of plant xylem water can reflect the isotopic signatures of water around the root system. However, some studies have shown that certain halophytic or xerophytic plants can fractionate hydrogen isotopes significantly during water uptake, while oxygen isotopic fractionation is negligible during root water uptake (Sternberg and Swart, 1987; Lin and Sternberg, 1993; Ellsworth and Williams, 2007). Consequently, in this study, we used oxygen isotopes to determine plant water uptake patterns. Plant xylem water and soil water were extracted using a cryogenic vacuum distillation system, and the extracted water samples were stored in screw-cap glass vials at 4°C for isotope determination (Zhu et al., 2018). The oxygen isotope ratios ($\delta^{18}O$) of the water samples were determined using a liquid water isotope analyzer (LWIA, DLT-100, Los Gates Research Inc., Mountain View, CA, United States) at the Shandong Provincial Key Laboratory of Eco-Environment Science for the Yellow River Delta. The precision of $\delta^{18}O$ analysis was ±0.25‰. The oxygen isotopic composition can be expressed (Equation 1) as the O isotope ratio ($\delta^{18}O$, ‰):

$$\delta^{18}O = (R_{sample}/R_{standard} - 1) \times 1000 \quad (1)$$

where R_{sample} and $R_{standard}$ are the $^{18}O/^{16}O$ molar ratio of the sample and the standard water (Vienna Standard Mean Ocean Water).

Extracted water of plant often contains organic materials that may cause spectral contamination when using isotope ratio infrared spectroscopy, which result in errors in the measured isotope ratios. In order to eliminate spectral contamination, a calibration curve was used to correct the $\delta^{18}O$ values of the plant xylem water following the method presented by Schultz et al. (2011). The detailed procedures were described in Zhu et al. (2016).

Data Analysis

The feasible contributions of potential water sources to plant xylem water were calculated using the IsoSource mixing model (Phillips and Gregg, 2003). In this study, the increment and the tolerance were set to 1% and 0.05‰ in our calculation, respectively. The mean and possible range of water source proportions were calculated for both species in dry and wet seasons (Phillips and Gregg, 2003; Zhu et al., 2018).

One-way analysis of variance (ANOVA) was used to detect significant differences in salinity of soil and groundwater, SWC of different soil layers or $\delta^{18}O$ values of potential water sources samples in dry or wet seasons ($P < 0.05$). The differences in salinity, SWC or $\delta^{18}O$ values of water sources and plant xylem water between wet and dry seasons were also compared using ANOVA ($P < 0.05$). All statistical analyses of data were performed using SPSS 17.0 (SPSS Inc., Chicago, IL, United States). The charting was processed by Origin 8.5 (Origin Lab Corp., Northampton, MA, United States).

RESULTS

Precipitation Distribution

In the study area, the precipitation showed significant monthly differences, most occurring in summer (**Figure 2**). The total precipitation for 2013 was 629.0 mm, 79.2% occurring during June–August. In 2013, the maximum monthly precipitation was 293.3 mm, occurring in July. In 2014, the total precipitation was 243.6 mm, 91.1% occurring during May–September. Precipitation in July 2014 was only 32.6 mm, significantly lower than that in July 2013 (**Figure 2**).

Soil Water Content

The SWC showed significant vertical variations in the dry season ($F = 21.08$, $P < 0.01$). There was no significant vertical variation in SWC along the soil profile in the wet season ($F = 3.36$, $P = 0.076$) (**Figure 3**). In the dry season, the SWC rose significantly with increasing depth up to 60 cm, but at depths of 60–100 cm the SWC was only 1.627%, and it was significantly lower than that in upper soil layers ($P < 0.05$). In the wet season, the SWC increased gradually along the soil profile. All SWC values at each soil depth in the wet season were significantly higher than at the same soil depth in the dry season ($P < 0.05$) (**Figure 3**).

Salinity of Soil and Groundwater

Soil salinity showed significant vertical variations in dry ($F = 10.69$, $P < 0.01$) and wet ($F = 9.72$, $P < 0.01$) seasons (**Table 1**). In the dry season, the salinity of soil water increased first and then decreased, and there were no significant differences in soil salinity at depths of 0–60 cm ($P > 0.05$). The soil salinity at 60–100 cm was significantly lower than at 0–60 cm depth($P < 0.05$). In the wet season, the soil salinity increased significantly along the soil profile, and the soil salinity of each soil layer and groundwater were higher than in the dry season ($P < 0.05$). The salinity of groundwater in both seasons was significantly higher than that of the soil ($P < 0.05$) (**Table 1**).

$\delta^{18}O$ Values of Soil Water, Groundwater, and Xylem Water

The $\delta^{18}O$ values of soil water showed clear vertical and seasonal variations (**Figure 4**). In the wet season, the $\delta^{18}O$ values of soil water increased significantly with increasing soil depth, and reached a maximum at 60–100 cm. However, there was no significant difference in $\delta^{18}O$ values between soil layers of 20–40 cm and 40–60 cm, with an average of −8.95‰ ($P > 0.05$). In the dry season, the $\delta^{18}O$ values of soil

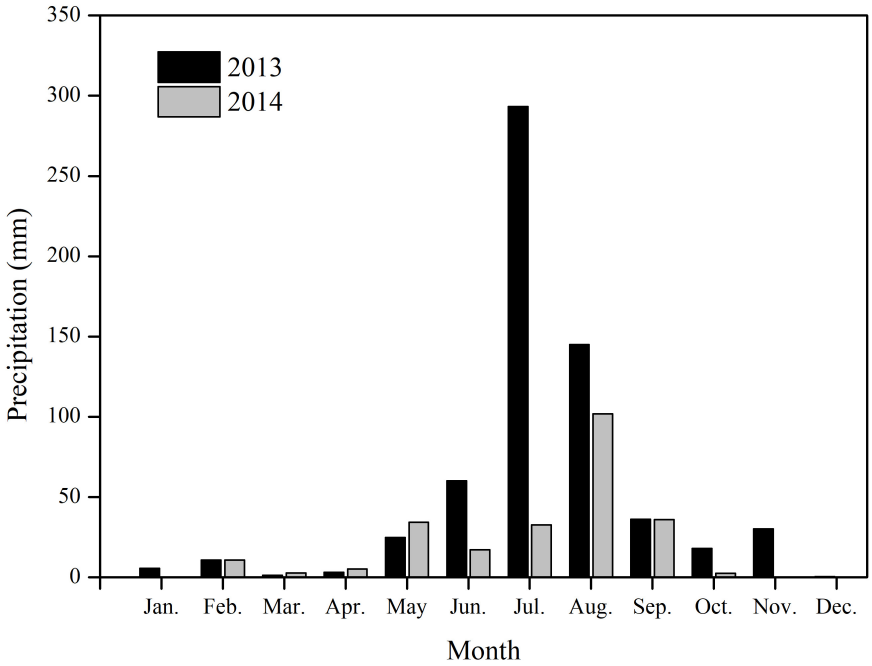

FIGURE 2 | Monthly precipitations for 2013 and 2014 on Chenier Island, Yellow River Delta, China.

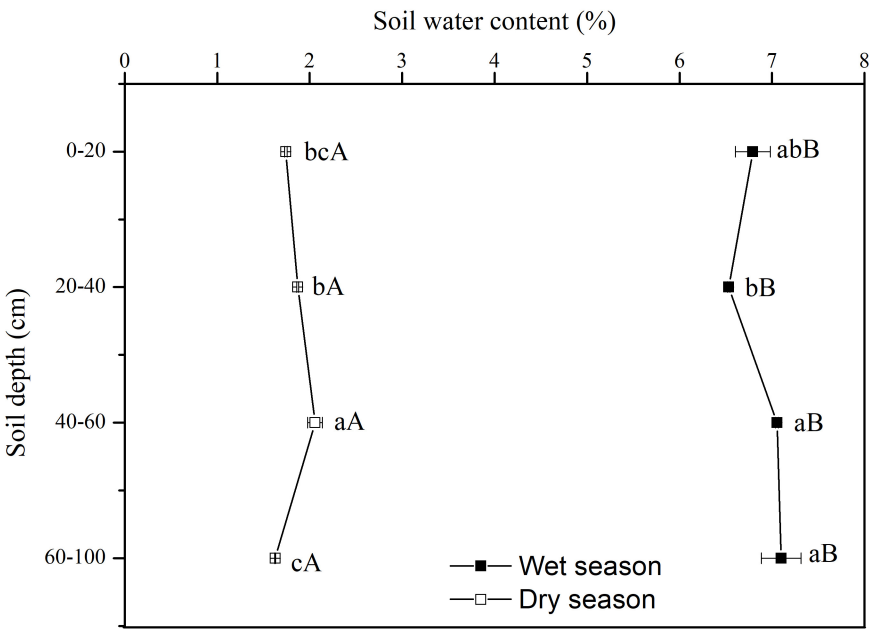

FIGURE 3 | Variation in vertical profile of soil water content (SWC) in dry and wet seasons. Error bars represent standard errors of mean SWC (n = 9).Different lowercase letters represent the significant differences in SWC among different soil depths in dry or wet seasons at the 0.05 level. Different capital letters represent significant differences in SWC at each soil depth between dry and wet seasons at the 0.05 level.

water showed an opposite vertical variation: decreasing with increasing soil depth. There were significant differences in the $\delta^{18}O$ values of soil water among all soil layers ($P < 0.05$). The $\delta^{18}O$ values of soil water in the wet season were significantly lower than those in the dry season ($P < 0.05$), and the differences in $\delta^{18}O$ values of soil water at the same soil layer between wet and dry seasons decreased with increasing soil depth.

TABLE 1 | Salinity of soil and groundwater in dry and wet seasons (average ± standard error).

Water sources		Salinity (%)	
		Wet season	Dry season
Soil depth (cm)	0–20	0.0850 ± 0.0014cA	0.0672 ± 0.0015aB
	20–40	0.0925 ± 0.0014bcA	0.0724 ± 0.0028aB
	40–60	0.0942 ± 0.0022bA	0.0665 ± 0.0021aB
	60–100	0.1058 ± 0.0046aA	0.0573 ± 0.0001bB
Groundwater		1.7454 ± 0.0096A	1.9400 ± 0.0058B

Different lowercase letters represent significant differences in soil salinity at different soil depths in dry or wet season at the 0.05 level. Different capital letters represent significant differences in soil salinity at each soil depth and groundwater between dry and wet seasons at the 0.05 level.

The $\delta^{18}O$ values of groundwater in the wet season were more negative than those in the dry season. In the wet season the $\delta^{18}O$ values of groundwater were significantly lower than those of soil water at 60–100 cm ($P < 0.05$), but they were higher than those of soil water at other soil layers. In dry seasons the $\delta^{18}O$ values of groundwater were significantly lower than those of soil water at all soil layers ($P < 0.05$) (**Figure 4**).

The $\delta^{18}O$ values of xylem water also showed seasonal variations (**Figure 4**). The $\delta^{18}O$ values of xylem water for both species in the dry season were significantly higher than those in the wet season ($P < 0.05$). In the wet season the $\delta^{18}O$ values of xylem water for *Z. jujuba* were close to those of soil water at 60–100 cm and were not significantly different from them ($P > 0.05$). For *T. chinensis*, the $\delta^{18}O$ values of xylem water were intermediate between those of soil water at 60–100 cm and groundwater, and were not significantly different from those of groundwater in the wet season ($P > 0.05$). In the dry season, the $\delta^{18}O$ values of xylem water for *Z. jujuba* were close to those of soil water at 40–60 cm, and those of xylem water for *T. chinensis* were intermediate between those of soil water at 60–100 cm and groundwater. The $\delta^{18}O$ values of xylem water for *Z. jujuba* were all more enriched than those of xylem water for *T. chinensis* in both seasons (**Figure 4**).

Feasible Contributions of Potential Water Sources

The proportions of potential water sources for *T. chinensis* and *Z. jujuba* showed clear seasonal variations (**Table 2**). *Z. jujuba* took up 82.2% of its required water from the 60–100 cm soil layer in the wet season, and only 17.8% of its xylem water was absorbed from other soil layers and groundwater. In the dry season, the proportion of soil water at 60–100 cm for *Z. jujuba* decreased, and contributions of soil water to *Z. jujuba* at other soil layers increased; about 68.3% of xylem water was absorbed from the 20–100 cm soil layer (**Table 2**).

For *T. chinensis*, 51.2% of its xylem water was taken up from the 60–100 cm soil layer, and 18.8% was absorbed from groundwater in the wet season (**Table 2**). In the dry season, *T. chinensis* usage of soil water at 60–100 cm clearly decreased and it shifted its main water sources from deep soil water to groundwater. The proportion of groundwater for *T. chinensis* was up to 67.0% (**Table 2**).

DISCUSSION

Spatial and Temporal Variations of the Soil Water Content and Salinity

Moisture and salinity were two limiting factors for plants growth and distribution in coastal wetlands (Ewe et al., 2007; Yu et al., 2019). The transport of salt was often accompanied by the movement of water. Generally, the recharge of soil water mainly depends on two water sources: precipitation and groundwater. Precipitation is the main water input maintaining plant growth on the surface of the earth (Wu et al., 2014; Walter, 2018). The recharge level of soil water is attributed to the amount, frequency and intensity of precipitation (Walter, 2018). Previous studies have shown that heavy precipitation can recharge deep soil water, but light precipitation just has an impact on the SWC of topsoil (Xu et al., 2012; Zhu et al., 2016). We found that the SWC at 60–100 cm was significantly lower than in the upper soil layers in the dry season, because of low precipitation, which could only recharge shallow soil water.

In coastal area, groundwater is the main source of soil water and salt. It mainly recharges soil water and salt through capillary pores, and so the soil physical properties determine the recharge ability of groundwater (Loik et al., 2004; Wallender et al., 2006; Volodina and Sokolova, 2007; Ma et al., 2011; Xia et al., 2014). However, the most remarkable characteristic of the study area on Chenier Island was its relatively low soil salinity. The soil salinity was significantly lower than that of adjacent soil (1.52%) (Xie et al., 2012). This contributes to plant species survival, especially that of the non-halophytes. The main composition of soil particles – coarse shell particles and fragments—leads to minimal water adsorption and capillarity in study area (Xie et al., 2012). It is difficult, therefore, for salt to be transported through the soil profile, even though the groundwater level is shallow. Our results showed that soil salinity was significantly lower than that of groundwater in both seasons, consistent with the above conclusion. It indicated that groundwater had little effect on the soil moisture and salinity. It also demonstrated that the recruitment of soil water mainly depended on precipitation. Therefore, during seawater intrusion, it mainly affected groundwater and has less effect on soil salinity.

We also found that soil salinity in the dry season was lower than that in the wet season (**Table 1**). This might have been caused by the washing effect of precipitation happened from July 2013 to July 2014. At the same time, specific soil physical properties allowed precipitation to infiltrate to groundwater directly through soil pores (Zhu et al., 2016, 2018). Hence, in our study, the salinity of groundwater in the wet season was lower than in the dry season (**Table 1**), as a large amount of precipitation infiltrated to groundwater and diluted its salinity.

Spatial and Temporal Variations in Isotopic Compositions of Soil Water and Groundwater

The oxygen isotopic composition of soil water was mainly affected by evaporation and precipitation (Drake and Franks, 2003; Dai et al., 2015). Evaporation causes the enrichment of ^{18}O

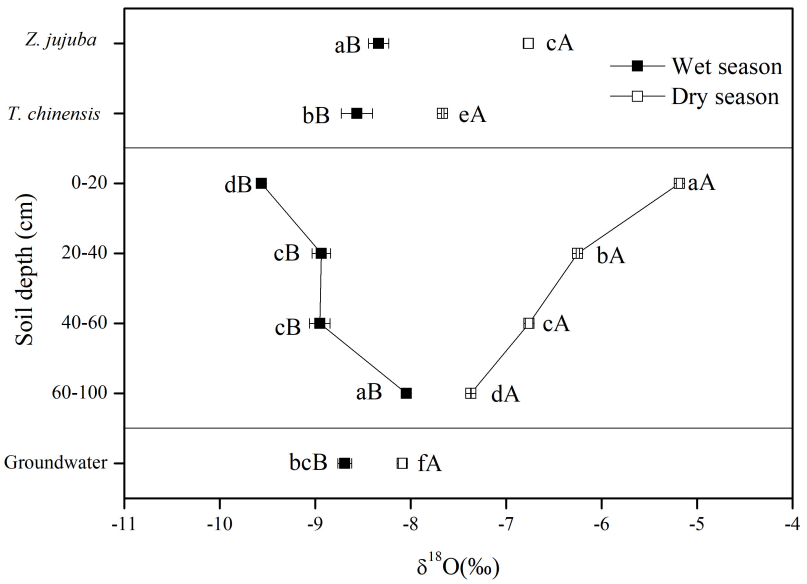

FIGURE 4 | $\delta^{18}O$ values of potential water sources and plant xylem water for dry and wet seasons. Error bars represent standard errors of mean $\delta^{18}O$ (n = 9). Different lowercase letters represent the significant difference in $\delta^{18}O$ values among different samples in dry or wet seasons at the 0.05 level. Different capital letters represent significant difference in $\delta^{18}O$ values of each sample between dry and wet seasons at the 0.05 level.

TABLE 2 | Proportions of potential water sources (%) for *Tamarix chinensis and Ziziphus jujuba* in dry and wet seasons.

Water sources		Wet season		Dry season	
		Z. jujuba	***T. chinensis***	***Z. jujuba***	***T. chinensis***
Soil depth (cm)	0–20	2.1 (0–11)	6.2 (0–28)	15.0 (0–47)	3.4 (0–16)
	20–40	4.4 (0–21)	12.0 (0–54)	21.8 (0–74)	5.8 (0–25)
	40–60	4.3 (0–21)	11.8 (0–52)	25.1 (0–100)	8.2 (0–35)
	60–100	82.2 (67–95)	51.2 (17–78)	21.4 (0–74)	15.6 (0–65)
Groundwater		7.0 (0-33)	18.8 (0–83)	16.8 (0–56)	67.0 (35–87)

Mean source proportions and range of minimum and maximum source proportions (in parentheses) were calculated using the IsoSource model (Phillips and Gregg, 2003).

in soil water. As the depth of the soil layer increased, the influence of evaporation on the $\delta^{18}O$ values of soil water decreased (Barnes and Allison, 1988). Precipitation was the main water source for soil water recharge, so the oxygen isotopic composition of rainwater and its infiltration within the soil profile affected the vertical distribution of ^{18}O in soil water. Generally, the oxygen isotopic composition of precipitation was more depleted owing to Rayleigh distillation of heavy isotopes (Clark and Fritz, 1997; Gu et al., 2015). In the wet season, 293.3 mm precipitation with low $\delta^{18}O$ values recharged the soil water, and recharge reduced with increasing soil depth, so the $\delta^{18}O$ values of soil water rose as soil depth increased (**Figure 4**). This also indicated that the depletion of soil water ^{18}O by precipitation was stronger than the enrichment of soil water ^{18}O by evaporation in the wet season. In contrast, because the precipitation was only 32.6 mm in the dry season, evaporation became the dominant factor enriching the $\delta^{18}O$ values of soil water. Therefore, the $\delta^{18}O$ values of soil water were more enriched and significantly decreased with increasing soil depth in the dry season (**Figure 4**). Therefore, we concluded that the seasonal differences in the $\delta^{18}O$ values of soil water mainly resulted from precipitation and evaporation. In addition, we also found that there were significant differences in $\delta^{18}O$ values between groundwater and deep soil water in both seasons (**Figure 4**). It demonstrated that groundwater had little effect on the $\delta^{18}O$ values of soil water. Consequently, it was difficult for seawater to affect the oxygen isotopic composition of soil water by affecting groundwater.

Previous studies have shown that the oxygen isotopic composition of groundwater is commonly maintained at a stable level (Ewe et al., 2007). However, in this study, we found that the $\delta^{18}O$ values of groundwater showed a clearly seasonal variation. The $\delta^{18}O$ values of groundwater in the wet season were significantly lower than those in the dry season (**Figure 4**). Because the soil had a coarse particle diameter and large porosity, precipitation with depleted $\delta^{18}O$ values could directly recharge the groundwater, leading to a decrease in the $\delta^{18}O$ values of groundwater. At the same time, precipitation in the wet season was obviously greater than that in the dry season. Consequently, precipitation became the main factor causing the seasonal difference in oxygen isotopic composition of groundwater.

Seasonal Patterns of Plant Water Uptake

Previous studies have shown that plant species living in the same habitat often have different water uptake patterns (Ewe et al., 1999; Wu et al., 2014, 2016). This avoids water competition during drought periods when the soil water is limited; they take up similar water sources when soil water is abundant in the environment (Gu et al., 2015). For example, Ewe et al. (2007) reported that all plants used the shallow soil water

in the wet season when the soil water was abundant and less saline. In the dry season, however, *Rhizophora mangle* used a soil–groundwater mix while *Cladium jamaicense* and *Sesuvium portulacastrum* continued to use shallow soil water. In this study, although the shallow soil water was abundant in the wet season, *T. chinensis* and *Z. jujuba* did not take up water from the shallow soil layers. On the contrary, *Z. jujuba* mainly used deep soil water from the 60–100 cm soil layer, and *T. chinensis* used a mixture of deep soil water (60–100 cm) and groundwater. Both dominant shrub species used the deep soil water, and this was of benefit in minimizing water competition with associated plants with shallow root systems. It also improved the use efficiency of available soil water (Yang et al., 2011).

Plant species often explore more stable water sources through extending their roots to deeper soil layers, or even to groundwater when soil water is limited in the dry season (Ewe et al., 2007; Dai et al., 2015). In our study, when the soil water became more depleted because of low precipitation in the dry season, *T. chinensis* shifted its main water sources from deep soil water to groundwater with high salinity (1.94%), indicating that this species could extend its roots to groundwater because it had a strong tolerance to salt. At the same time, *Z. jujuba*—a low salt-tolerance shrub species—found it difficult to extend its roots to deeper layers because of the influence of salt stress. It had to maximize its use of limited water sources stored in the soil profile by expanding its absorption range of soil water from 60–100 to 20–100 cm (**Table 2**). From the side of isotopic composition, the oxygen isotopic composition of xylem water in a plant reflects the isotopic signatures of a mixture of water sources that the plant absorbs (Ehleringer and Dawson, 1992; Ellsworth and Williams, 2007). There was a significant difference in $\delta^{18}O$ values of xylem water between *T. chinensis* and *Z. jujuba* in dry season, indicating that two species had different water sources. All of these results demonstrated that the main water sources of *T. chinensis* and *Z. jujuba* were significantly different when soil water was limited in dry season, supporting our first hypothesis. It helped to avoid competition for water between *T. chinensis* and *Z. jujuba* and promote their coexistence. By comparison, we found that *T. chinensis* could take up more stable and deeper water sources (e.g., groundwater) than *Z. jujuba* in the dry season, and this supported our second hypothesis. The result also demonstrated that *T. chinensis* had stronger drought adaptability than *Z. jujuba*. *T. chinensis* and *Z. jujuba* had the ability to shift their main water sources among different potential water sources, which indicated that they had the advantage of adaptation to a water-limited coastal ecosystem (Zhu et al., 2018).

T. chinensis and *Z. jujuba* showed different water uptake patterns on Chenier Island, and this also supported our first hypothesis. The water uptake patterns of plants are the result of long-term adaptation to fluctuating water conditions (Yang et al., 2011). The different water usage of *T. chinensis* and *Z. jujuba* may lead to their water niche partitioning. The niche differentiation in water uptake among coexisting shrub species is expected to minimize their competition for limited water sources and increase coastal ecosystem resilience to drought (Zhu et al., 2018).

In addition, we found that the effect of salinity on *Z. jujuba* water use was greater than that on *T. chinensis* water use. Therefore, salinity will become a critical factor determining the development of the *Z. jujuba* community as sea levels rise as a result of global warming. This leads us to infer that *Z. jujuba* will gradually disappear from the study area and *T. chinensis* will become to be the only dominant shrub species in the future.

CONCLUSION

In this study, the stable oxygen isotope was used to determine the water uptake of two dominant shrub species and their responses to soil water fluctuations caused by seasonal changes in precipitation. On the Chenier Island, *T. chinensis* and *Z. jujuba* had different water uptake patterns in dry and wet seasons, and they were able to shift their water sources among different potential water sources in fluctuating water environments. In the wet season, when the soil water was abundant, *Z. jujuba* mostly used the soil water from 60 to 100 cm, while *T. chinensis* took up a mixture of groundwater and soil water from 60 to 100 cm. In the dry season, when the soil water was depleted, *Z. jujuba* mainly took up soil water from the 20 to 100 cm soil layers, while *T. chinensis* mainly used groundwater. The shifts in major water sources for *T. chinensis* and *Z. jujuba* demonstrated their adaptations to the fluctuations of soil moisture in water-limited ecosystems. The interspecific differences in water uptake clarified the mechanism of coexistence between two dominant shrub species in a coastal wetland ecosystem.

DATA AVAILABILITY STATEMENT

The original contributions presented in this study are included in the article/supplementary material, further inquiries can be directed to the corresponding authors.

AUTHOR CONTRIBUTIONS

JZ and JTL conceived to the idea. JZ, JTL, JS, and CZ collected the samples in the field, performed the experiments, and collected the data. JZ analyzed the data and wrote the draft manuscript. JTL and JSL revised the manuscript. All authors read and approved the final manuscript.

FUNDING

This study was financially supported by the National Natural Science Foundation of China (41971126 and 41871089).

ACKNOWLEDGMENTS

We are grateful to Liwen Bianji, Edanz Editing China (www.liwenbianji.cn/ac), for editing the English text of a draft of this manuscript.

REFERENCES

Aroca, R., Porcel, R., and Ruiz-Lozano, J. M. (2012). Regulation of root water uptake under abiotic stress conditions. *J. Exp. Bot.* 63, 43–57. doi: 10.1093/jxb/err266

Asbjornsen, H., Mora, G., and Helmers, M. J. (2007). Variation in water uptake dynamics among contrasting agricultural and native plant communities in the Midwestern U.S. *Agric. Ecosyst. Environ.* 121, 343–356.

Bai, J., Yu, L., Ye, X., Yu, Z., Wang, D., Guan, Y., et al. (2020). Dynamics of phosphorus fractions in surface soils of different flooding wetlands before and after flow-sediment regulation in the Yellow River Estuary, China. *J. Hydrol.* 580:124256. doi: 10.1016/j.jhydrol.2019.124256

Barnes, C. J., and Allison, G. B. (1988). Tracing of water movement in the unsaturated zone using stable isotopes of hydrogen and oxygen. *J. Hydrol.* 100, 143–176. doi: 10.1016/0022-1694(88)90184-9

Chandrajith, R., Chaturangani, D., Abeykoon, S., Barth, J. A. C., van Geldern, R., Edirisinghe, E. A. N. V., et al. (2013). Quantification of groundwater–seawater interaction in a coastal sandy aquifer system: a study from Panama, Sri Lanka. *Environ. Earth Sci.* 72, 867–877. doi: 10.1007/s12665-013-3010-y

Chen, Y., Xia, J., Zhao, X., and Zhuge, Y. (2019). Soil moisture ecological characteristics of typical shrub and grass vegetation on Shell Island in the Yellow River Delta, China. *Geoderma* 348, 45–53.

Chimner, R. A., and Cooper, D. J. (2004). Using stable oxygen isotopes to quantify the water source used for transpiration by native shrubs in the San Luis Valley, Colorado USA. *Plant Soil* 260, 225–236.

Clark, I. D., and Fritz, P. (1997). *Environmental Isotopes In Hydrogeology*. New York, NY: Lewis Publishers Press.

Corbin, J. D., Thomsen, M. A., Dawson, T. E., and D'Antonio, C. M. (2005). Summer water use by California coastal prairie grasses: fog, drought and community composition. *Oecologia* 145, 511–521. doi: 10.1007/s00442-005-0152-y

Dai, Y., Zheng, X. J., Tang, L. S., and Li, Y. (2015). Stable oxygen isotopes reveal distinct water use patterns of two Haloxylon species in the Gurbantonggut Desert. *Plant Soil* 389, 73–87. doi: 10.1007/s11104-014-2342-z

Dawson, T. E., and Pate, J. S. (1996). Seasonal water uptake and movement in root systems of Australian phraeatophytic plants of dimorphic root morphology a stable isotope investigation. *Oecologia* 107, 13–20. doi: 10.1007/BF00582230

Drake, P. L., and Franks, P. J. (2003). Water resource partitioning, stem xylem hydraulic properties, and plant water use strategies in a seasonally dry riparian tropical rainforest. *Oecologia* 137, 321–329. doi: 10.1007/s00442-003-1352-y

Ehleringer, J. R., and Dawson, T. E. (1992). Water uptake by plants: perspectives from stable isotope composition. *Plant Cell Environ.* 15, 1073–1082. doi: 10.1111/j.1365-3040.1992.tb01657.x

Ehleringer, J. R., Phillips, S. L., Schuster, W. S. F., and Sandquist, D. R. (1991). Differential utilization of summer rains by desert plants. *Oecologia* 88, 430–434. doi: 10.1007/bf00317589

Ehleringer, J. R., Roden, J., and Dawson, T. E. (2000). "Assessing ecosystem-level water relations through stable isotope ratio analyses," in *Methods in Ecosystem Science*, eds O. Sala, R. Jackson, H. Mooney, and R. Howarth (New York, NY: Springer), 181–198.

Ellsworth, P. Z., and Williams, D. G. (2007). Hydrogen isotope fractionation during water uptake by woody xerophytes. *Plant Soil* 291, 93–107. doi: 10.1007/s11104-006-9177-1

Ewe, S. M. L., Sternberg, L. S. L., and Busch, D. E. (1999). Water-use patterns of woody species in pineland and hammock communities of South Florida. *For. Ecol. Manage.* 118, 139–148.

Ewe, S. M. L., Sternberg, L. S. L., and Childers, D. L. (2007). Seasonal plant water uptake patterns in the saline southeast *Everglades ecotone*. *Oecologia* 152, 607–616. doi: 10.1007/s00442-007-0699-x

Gazis, C., and Feng, X. H. (2004). A stable isotope study of soil water: evidence for mixing and preferential flow paths. *Geoderma* 119, 97–111.

Gu, D., Zhang, Z., Mallik, A., Zhou, A., Mo, L., He, C., et al. (2015). Seasonal water use strategy of *Cyclobalanopsis glauca* in a karst area of southern China. *Environ. Earth Sci.* 74, 1007–1014.

Janousek, C. N., and Mayo, C. (2013). Plant responses to increased inundation and salt exposure: interactive effects on tidal marsh productivity. *Plant Ecol.* 214, 917–928. doi: 10.1007/s11258-013-0218-6

Lin, G., and Sternberg, L. S. L. (1993). "Hydrogen isotopic fractionation by plant roots during water uptake in coastal wetland plants," in *Stable Isotopes and Plant Carbon-water Relations*, ed. J. R. E. E. H. D. Farquhar (San Diego, CA: Academic Press), 497–510.

Loik, M. E., Breshears, D. D., Lauenroth, W. K., and Belnap, J. (2004). A multi-scale perspective of water pulses in dryland ecosystems: climatology and ecohydrology of the western USA. *Oecologia* 141, 269–281. doi: 10.1007/s00442-004-1570-y

Lu, Q., Bai, J., Yan, D., Cui, B., and Wu, J. (2020). Sulfur forms in wetland soils with different flooding periods before and after flow-sediment regulation in the Yellow River Delta, China. *J. Clean. Prod.* 276:122969.

Ma, X., Chen, Y., Zhu, C., and Li, W. (2011). The variation in soil moisture and the appropriate groundwater table for desert riparian forest along the Lower Tarim River. *J. Geogr. Sci.* 21, 150–162. doi: 10.1007/s11442-011-0835-8

Marcelis, L. F. M., and Van Hooijdonk, J. (1999). Effect of salinity on growth, water use and nutrient use in radish (*Raphanus sativus* L.). *Plant Soil* 215, 57–64. doi: 10.1023/A:1004742713538

Meißner, M., Köhler, M., Schwendenmann, L., Hölscher, D., and Dyckmans, J. (2014). Soil water uptake by trees using water stable isotopes (δ2H and δ18O)-a method test regarding soil moisture, texture and carbonate. *Plant Soil* 376, 327–335. doi: 10.1007/s11104-013-1970-z

Oliveira, R. S., Dawson, T. E., Burgess, S. S. O., and Nepstad, D. C. (2005). Hydraulic redistribution in three Amazonian trees. *Oecologia* 145, 354–363. doi: 10.1007/s00442-005-0108-2

Osland, M. J., González, E., and Richardson, C. J. (2011). Coastal freshwater wetland plant community response to seasonal drought and flooding in northwestern Costa Rica. *Wetlands* 31, 641–652. doi: 10.1007/s13157-011-0180-9

Phillips, D. L., and Gregg, J. W. (2003). Source partitioning using stable isotopes: coping with too many sources. *Oecologia* 136, 261–269. doi: 10.1007/s00442-003-1218-3

Rossatto, D. R., Silva, L., de, C. R., Villalobos-Vega, R., Sternberg, L., da, S. L., et al. (2012). Depth of water uptake in woody plants relates to groundwater level and vegetation structure along a topographic gradient in a neotropical savanna. *Environ. Exp. Bot.* 77, 259–266. doi: 10.1016/j.envexpbot.2011.11.025

Schultz, N. M., Griffis, T. J., Lee, X. H., and Baker, J. M. (2011). Identification and correction of spectral contamination in H-2/H-1 and O-18/O-16 measured in leaf, stem, and soil water. *Rapid Commun. Mass Spectr.* 25, 3360–3368. doi: 10.1002/rcm.5236

Sternberg, L. S. L., and Swart, P. K. (1987). Utilization of freshwater and ocean water by coastal plants of southern Florida. *Ecology* 68, 1898–1905. doi: 10.2307/1939881

Sternberg, L., da, S. L., Ish-Shalom-Gordon, N., Ross, M., and O'Brien, J. (1991). Water relations of coastal plant communities near the ocean/freshwater boundary. *Oecologia* 88, 305–310. doi: 10.1007/BF00317571

Volodina, I. V., and Sokolova, T. A. (2007). Changes in the salt status of meadow-chestnut soils under the impact of saline groundwater in a model experiment. *Eurasian Soil Sci.* 40, 839–849. doi: 10.1134/S1064229307080054

Wallender, W. W., Tanji, K. K., Gilley, J. R., Hill, R. W., Lord, J. M., Moore, C. V., et al. (2006). Water flow and salt transport in cracking clay soils of the Imperial Valley, California. *Irrig. Drain. Syst.* 20, 361–387. doi: 10.1007/s10795-006-9013-z

Walter, J. (2018). Effects of changes in soil moisture and precipitation patterns on plant-mediated biotic interactions in terrestrial ecosystems. *Plant Ecol.* 219, 1449–1462. doi: 10.1007/s11258-018-0893-4

Wang, X., Zhu, D., Wang, Y., Wei, X., and Ma, L. (2015). Soil water and root distribution under jujube plantations in the semiarid Loess Plateau region, China. *Plant Growth Regul.* 77, 21–31. doi: 10.1007/s10725-015-0031-4

Wei, L., Lockington, D. A., Poh, S. C., Gasparon, M., and Lovelock, C. E. (2013). Water use patterns of estuarine vegetation in a tidal creek system. *Oecologia* 172, 485–494. doi: 10.1007/s00442-012-2495-5

Williams, D. G., and Ehleringer, J. R. (2000). Intra- and interspecific variation for summer precipitation use in pinyon-juniper woodlands. *Ecol. Monogr.* 70, 517–537. doi: 10.2307/2657185

Wu, H., Li, X. Y., Li, J., Jiang, Z., Chen, H., Ma, Y., et al. (2016). Differential soil moisture pulse uptake by coexisting plants in an alpine Achnatherum splendens grassland community. *Environ. Earth Sci.* 75, 1–13. doi: 10.1007/s12665-016-5694-2

Wu, Y., Zhou, H., Zheng, X. J., Li, Y., and Tang, L. S. (2014). Seasonal changes in the water use strategies of three co-occurring desert shrubs. *Hydrol. Process.* 28, 6265–6275. doi: 10.1002/hyp.10114

Xia, J. B., Zhang, G. C., Wang, R. R., and Zhang, S. Y. (2014). Effect of soil water availability on photosynthesis in *Ziziphus jujuba* var. spinosus in a sand habitat formed from seashells: comparison of four models. *Photosynthetica* 52, 253–261. doi: 10.1007/s11099-014-0030-0

Xie, W., Zhao, Y., Zhang, Z., Liu, Q., Xia, J., Sun, J., et al. (2012). Shell sand properties and vegetative distribution on shell ridges of the Southwestern Coast of Bohai Bay. *Environ. Earth Sci.* 67, 1357–1362. doi: 10.1007/s12665-012-1578-2

Xu, Q., Li, H., Chen, J. Q., Cheng, X. L., Liu, S. R., and An, S. Q. (2011). Water use patterns of three species in subalpine forest, Southwest China: the deuterium isotope approach. *Ecohydrology* 4, 236–244. doi: 10.1002/eco.179

Xu, Q., Liu, S. R., Wan, X. C., Jiang, C. Q., Song, X. F., and Wang, J. X. (2012). Effects of rainfall on soil moisture and water movement in a subalpine dark coniferous forest in southwestern China. *Hydrol. Process.* 26, 3800–3809. doi: 10.1002/hyp.8400

Yang, H., Auerswald, K., Bai, Y., and Han, X. (2011). Complementarity in water sources among dominant species in typical steppe ecosystems of Inner Mongolia, China. *Plant Soil* 340, 303–313. doi: 10.1007/s11104-010-0307-4

Yu, L., Zhuang, T., Bai, J., Wang, J., Yu, Z., Wang, X., et al. (2019). Effects of water and salinity on soil labile organic carbon in estuarine wetlands of the Yellow River Delta, China. *Ecohydrol. Hydrobiol.* 20, 556–569. doi: 10.1016/j.ecohyd.2019.12.002

Zhao, Y., Hu, X., Liu, J., Lu, Z., Xia, J., Tian, J., et al. (2015). Vegetation pattern in shell ridge island in China's Yellow River Delta. *Front. Earth Sci.* 9:567–577. doi: 10.1007/s11707-015-0496-5

Zhu, J. F., Liu, J. T., Lu, Z. H., Sun, J. K., and Xia, J. B. (2015). Water use patterns of Tamarix chinensis in shell island wetland of the yellow river delta (in Chinese). *Wetl. Sci.* 13, 765–771.

Zhu, J., Liu, J., Lu, Z., Li, J., and Sun, J. (2018). Water-use strategies of coexisting shrub species in the Yellow River Delta, China. *Can. J. Forest Res.* 48, 1099–1107. doi: 10.1139/cjfr-2018-0063

Zhu, J., Liu, J., Lu, Z., Xia, J., Sun, J., Shao, H., et al. (2016). Soil-water inter acting use patterns driven by *Ziziphus jujuba* on the Chenier Island in the Yellow River Delta, China. *Arch. Agron. Soil Sci.* 62, 1614–1624. doi: 10.1080/03650340.2016.1155702

Conflict of Interest: The authors declare that the research was conducted in the absence of any commercial or financial relationships that could be construed as a potential conflict of interest.

Publisher's Note: All claims expressed in this article are solely those of the authors and do not necessarily represent those of their affiliated organizations, or those of the publisher, the editors and the reviewers. Any product that may be evaluated in this article, or claim that may be made by its manufacturer, is not guaranteed or endorsed by the publisher.

frontiers | Frontiers in Plant Science

ORIGINAL RESEARCH
published: 23 June 2022
doi: 10.3389/fpls.2022.894398

Seasonal and Inter-Annual Variations of Carbon Dioxide Fluxes and Their Determinants in an Alpine Meadow

Song Wang[1,2], *Weinan Chen*[1,2], *Zheng Fu*[3], *Zhaolei Li*[4], *Jinsong Wang*[1], *Jiaqiang Liao*[1,2] *and Shuli Niu*[1,2*]

[1] *Key Laboratory of Ecosystem Network Observation and Modeling, Institute of Geographic Sciences and Natural Research, Chinese Academy of Sciences, Beijing, China,* [2] *College of Resources and Environment, University of Chinese Academy of Sciences, Beijing, China,* [3] *Laboratoire des Sciences du Climat et de l'Environnement (LSCE), CEA-CNRS-UVSQ, UMR8212, Gif-sur-Yvette, France,* [4] *College of Resources and Environment, and Academy of Agricultural Sciences, Southwest University, Chongqing, China*

The alpine meadow is one of the most important ecosystems on the Qinghai-Tibet Plateau (QTP) due to its huge carbon storage and wide distribution. Evaluating the carbon fluxes in alpine meadow ecosystems is crucial to understand the dynamics of carbon storage in high-altitude areas. Here, we investigated the carbon fluxes at seasonal and inter-annual timescales based on 5 years of observations of eddy covariance fluxes in the Zoige alpine meadow on the eastern Tibetan Plateau. We found that the Zoige alpine meadow acted as a faint carbon source of 94.69 ± 86.44 g C m^{-2} y^{-1} during the observation periods with large seasonal and inter-annual variations (IAVs). At the seasonal scale, gross primary productivity (GPP) and ecosystem respiration (Re) were positively correlated with photosynthetic photon flux density (PPFD), average daily temperature (Ta), and vapor pressure (VPD) and had negative relationships with volumetric water content (VWC). Seasonal variations of net ecosystem carbon dioxide (CO_2) exchange (NEE) were mostly explained by Ta, followed by PPFD, VPD, and VWC. The IAVs of GPP and Re were mainly attributable to the IAV of the maximum GPP rate (GPP_{max}) and maximum Re rate (Re_{max}), respectively, both of which increased with the percentage of *Cyperaceae* and decreased with the percentage of *Polygonaceae* changes across years. The IAV of NEE was well explained by the anomalies of the maximum CO_2 release rate (MCR). These results indicated that the annual net CO_2 exchange in the alpine meadow ecosystem was controlled mainly by the maximum C release rates. Therefore, a better understanding of physiological response to various environmental factors at peak C uptake and release seasons will largely improve the predictions of GPP, Re, and NEE in the context of global change.

Keywords: carbon fluxes, seasonal variation, inter-annual variation, eddy covariance, alpine meadow

OPEN ACCESS

Edited by:
Xiaoming Kang,
Chinese Academy of Forestry, China

Reviewed by:
Liang Yan,
Chinese Academy of Forestry, China
Haijun Peng,
Institute of Geochemistry (CAS), China

***Correspondence:**
Shuli Niu
sniu@igsnrr.ac.cn

Specialty section:
This article was submitted to Functional Plant Ecology, a section of the journal Frontiers in Plant Science

Received: *11 March 2022*
Accepted: *20 May 2022*
Published: *23 June 2022*

Citation:
Wang S, Chen W, Fu Z, Li Z, Wang J, Liao J and Niu S (2022) Seasonal and Inter-Annual Variations of Carbon Dioxide Fluxes and Their Determinants in an Alpine Meadow. Front. Plant Sci. 13:894398. doi: 10.3389/fpls.2022.894398

INTRODUCTION

There are great uncertainties in estimating the carbon dioxide (CO_2) budget of terrestrial ecosystems due to the inadequacies in the observational data and the incomplete conceptual framework (Hawkins and Sutton, 2009; Ito, 2019). Hence, understanding the dynamics of ecosystem carbon fluxes on different time scales and their control mechanisms is of great

significance for accurately simulating and predicting terrestrial ecosystem carbon balances (Jia et al., 2016; Green et al., 2019).

At the seasonal scale, water availability and thermal conditions were considered to affect the dynamics of ecosystem carbon fluxes (Zhang et al., 2018; Li et al., 2019b). For example, in arid and semiarid ecosystems, the amount and distribution of precipitation have been shown to dominate seasonal ecosystem carbon fluxes (Jia et al., 2016; Hao et al., 2018). In contrast, many studies in cold regions found that thermal conditions were the main drivers of the carbon fluxes at the seasonal scale (Fu et al., 2009; Saito et al., 2009). At the annual scale, the temperature fluctuations and water availability have been reported as the most important climate factors in controlling the inter-annual variation (IAV) of the gross primary productivity (GPP), ecosystem respiration (Re), and net ecosystem CO_2 exchange (NEE) at the global scale (Jung et al., 2017; Marcolla et al., 2017; Fernandez-Martinez et al., 2019). Compared to environmental factors, the impact of the biotic mechanisms underlying the IAV of ecosystem CO_2 fluxes has been less explored. Recently, it has been proposed that the maximum daily net ecosystem productivity (NEP) during the CO_2 uptake period (CUP; NEP_{max}) dominated the IAV of NEE at the global scale (Fu et al., 2019), while the summer peak of GPP (GPP_{max}) contributed more to the IAV of GPP than the photosynthetic phenology across North America (Xia et al., 2015). This indicates that community properties related to the maximum C uptake rate are crucial in determining annual C uptakes. However, the controlling factor of CO_2 fluxes may be divergent among different climate and vegetation types. For instance, temperature determines CO_2 fluxes in tropical ecosystems (Wang et al., 2014), but precipitation regulates the annual CO_2 flux of semiarid ecosystems (Poulter et al., 2014), and the soil moisture and species composition have been found to interactively determine CO_2 fluxes in dry meadows (Luan et al., 2016). Thus, the mechanism underlying the seasonal and IAV of ecosystem CO_2 fluxes in those less studied regions still needs further investigation.

The alpine meadow ecosystem is one of the most important ecosystems on the Qinghai-Tibet Plateau (QTP), covering an area of $\approx 70 \times 10^4$ km^2 and accounting for ≈35% of QTP (Ni, 2002; Niu et al., 2017a). It stores about 17.6 Gt carbon, accounting for about 48% of QTP carbon storage (Wang and Zhou, 1999; Lv, 2006). A large amount of carbon was stored in the alpine meadow ecosystem due to the low temperature, high humidity, low soil humus decomposition rate, and high accumulation rate of organic matter (Saito et al., 2009). However, the alpine area is increasingly impacted by climate change with rising temperature and precipitation (Li et al., 2010, 2019a). Meanwhile, the alpine meadow ecosystem is highly susceptible to environmental changes (Liu and Chen, 2000; Wang et al., 2000; Cheng and Wu, 2007; Xu and Liu, 2007). The temperature in the alpine meadow ecosystem increases (0.3–0.4°C per decade) two times faster than the global average (Chen et al., 2013), and the temperature increases more significantly with the increase in altitude (Liu and Chen, 2000). Therefore, studying the carbon fluxes and their response to climate change in the alpine meadow ecosystem is imperative. A few studies about carbon fluxes over alpine meadow ecosystems have been conducted on the QTP. For example, Hao et al. (2011) and Wang et al. (2016) reported that these alpine meadow ecosystems were a weak net CO_2 sink, but the carbon source or sink dynamic has great variations due to the changes in environmental factors. Under the background of increasing air temperature and precipitation (Li et al., 2010, 2019a; Chen et al., 2013), there will be more uncertainty in predicting carbon fluxes in alpine meadow ecosystems in the future. Hence, it is vital to explore the temporal variations of carbon fluxes and their drivers in alpine meadow ecosystems.

Eddy covariance technology provides a reliable approach to measuring the CO_2 fluxes. This approach can measure NEE with precision, contributes to identify the characteristics of source/sink activities of various global ecosystems, and has been widely used to interpret whole-system variability (Braswell et al., 2005; Chen et al., 2019b; Peng et al., 2021). This study focuses on the carbon fluxes dynamic at seasonal and inter-annual timescales based on 5 years (2015–2018, 2020) of eddy covariance flux observation in Zoige alpine meadow on the eastern QTP. The specific objectives of this study are to (1) quantify CO_2 dynamics at seasonal and inter-annual timescales for the Zoige alpine meadow; (2) understand the abiotic and biotic controlling factors for the variations in ecosystem CO_2 fluxes; and (3) explore the key processes associated with plant community species in controlling the inter-annual variability of CO_2 flux. These controlling mechanisms are essential to help us better understand the response of alpine meadows to future climate change.

MATERIALS AND METHODS

Site Description

The study site is at an alpine meadow in the National Zoige Alpine Wetland Ecological Station (32.8°N and 102.6°E; 3,500 m a.s.l), located on the eastern Qinghai-Tibetan Plateau (**Figure 1**). The alpine meadow is characterized by a typical continental plateau monsoon climate with relatively low temperatures and strong solar radiation. Based on the long-term meteorology observation data (1961–2013) from Hongyuan meteorological station (http://101.201.172.75:8888), the annual mean temperature of this site is ≈1.5°C. The coldest month occurs in January with a mean temperature of −9.7°C, while the warmest month occurs in July with a mean temperature of 11.1°C. The mean annual precipitation of this site is ≈761.0 mm, and over 80% of which occurs in the growing season (May to October).

The vegetation at the study site consists of a species mixture of *Deschampsia cespitosa* (Linn.) *Beauv., Koeleria cristata* (Linn.) Pers., *Gentiana sino-ornata* Balf. f., *Potentilla anserina* L., and *Anemone rivularis* Buch.-Ham (Quan et al., 2018). The dominant soil type in this ecosystem is Mat Cry-gelic Cambisol.

Eddy Covariance and Meteorological Measurement

Net ecosystem CO_2 exchange was observed from 2015 to 2020 by an open-path eddy covariance measurement system installed above an alpine meadow at 2 m. The sensor was

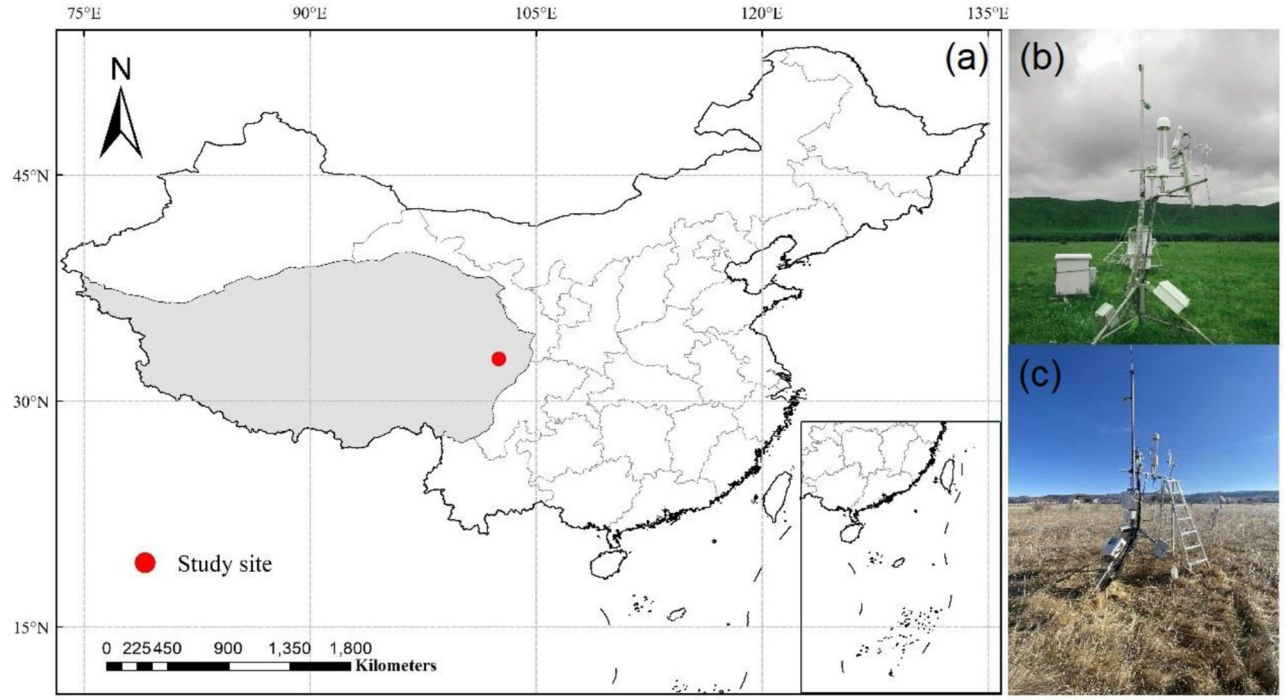

FIGURE 1 | (a) Study site on the Tibetan Plateau and the eddy covariance measurements during the growing season, **(b)** and non-growing season, **(c)** at our study site.

broken at the beginning of 2019, so there was a long data gap in 2019 and the data in 2019 were discarded. The open-path eddy covariance system has a three-dimensional sonic anemometer (CSAT3; Campbell Scientific Inc. (CSI), Logan, USA) and an open-path CO_2/H_2O infrared gas analyzer (LI-7500A; Li-COR Inc, Lincoln, NE, USA). Flux data are logged with a data logger at 10 Hz (CR5000, Campbell Scientific, UT, USA). HMP45C temperature probe (Vaisala, Finland) was used to measure air temperature. Soil volumetric water content (VWC) at a depth of 5 and 10 cm was measured using a CS655 probe (CSI, Logan, USA). Precipitation was measured by a tipping bucket rain gauge (TE525, CSI, Logan, USA). Photosynthetic photon flux density (PPFD) was measured using a photosynthetic active radiation sensor (LI190, LI-Cor, USA). This eddy covariance tower is one of the ChinaFlux (China Flux Observation and Research Network) and FLUXNET long-term observation site.

Aboveground Biomass Measurement

At the peak of annual biomass (usually in August), we randomly placed a quadrat frame (0.50) on each plot × 0.50 m), all the aboveground parts of the plants in the frame together, then separated them into different living species, and dried in the oven at 65°C for 48 h until they reached a constant weight and weighed. In the five replicates of each treatment, the average biomass of all living species in each quadrat was used to calculate aboveground biomass (Ma et al., 2020).

Data Processing

EddyPro 6.2.0 software was used to preprocess and control the quality of the eddy covariance raw data. Data measured during instrument malfunction and severe conditions were filtered out. Specifically, for data quality control, half-hour CO_2 flux data were filtered when: (1) data values were beyond the range of −20 to 20 $\mu mol/m^2/s$; (2) precipitation occurred; and (3) the friction velocity (u^*) was below 0.1 m/s at nighttime. This u^* threshold was determined following Reichstein et al. (2005). The positive values represent CO_2 emission from the underlying surface to the atmosphere, while the negative values represent CO_2 consumption from the atmosphere to soil (plants). Here, we divided CO_2 flux data into two periods: (1) the growing season was between the day with daily mean Tair > 5 and the day with daily mean Tair <5°C for 7 consecutive days, (2) the non-growing season was the days of the year except the growing season (Lund et al., 2010; Song et al., 2015; Peng et al., 2021). GPP and Re data were partitioned from CO_2 flux data (i.e., NEE) using rectangular hyperbolic regression (Falge et al., 2001). More information about missing NEE data gap-filling and partitioning was previously described by Chen et al. (2019b).

Statistical Analysis

We used the daily NEE to calculate the maximum CO_2 uptake rate (MCU), net CUP, and maximum CO_2 release rate (MCR) to quantify the phenological and physiological indicators that determine the annual NEE (Fu et al., 2019) and applied the

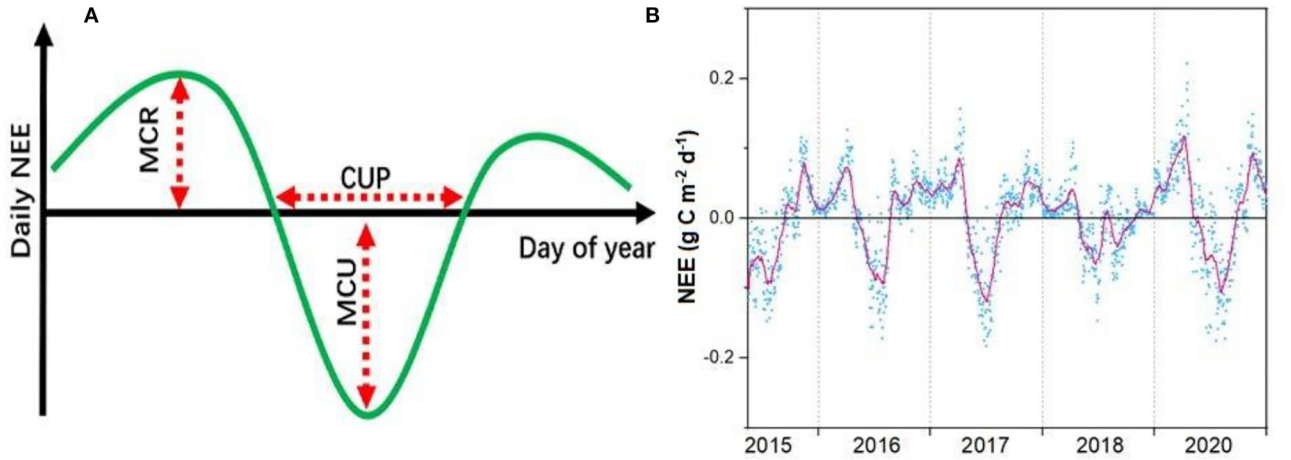

FIGURE 2 | Conceptual figure of maximum CO_2 uptake (MCU), CO_2 uptake period (CUP), and maximum CO_2 release (MCR) in determining the changes in annual net ecosystem CO_2 exchange (NEE) **(A)** with examples of the annual course of observed and filtered NEE **(B)**.

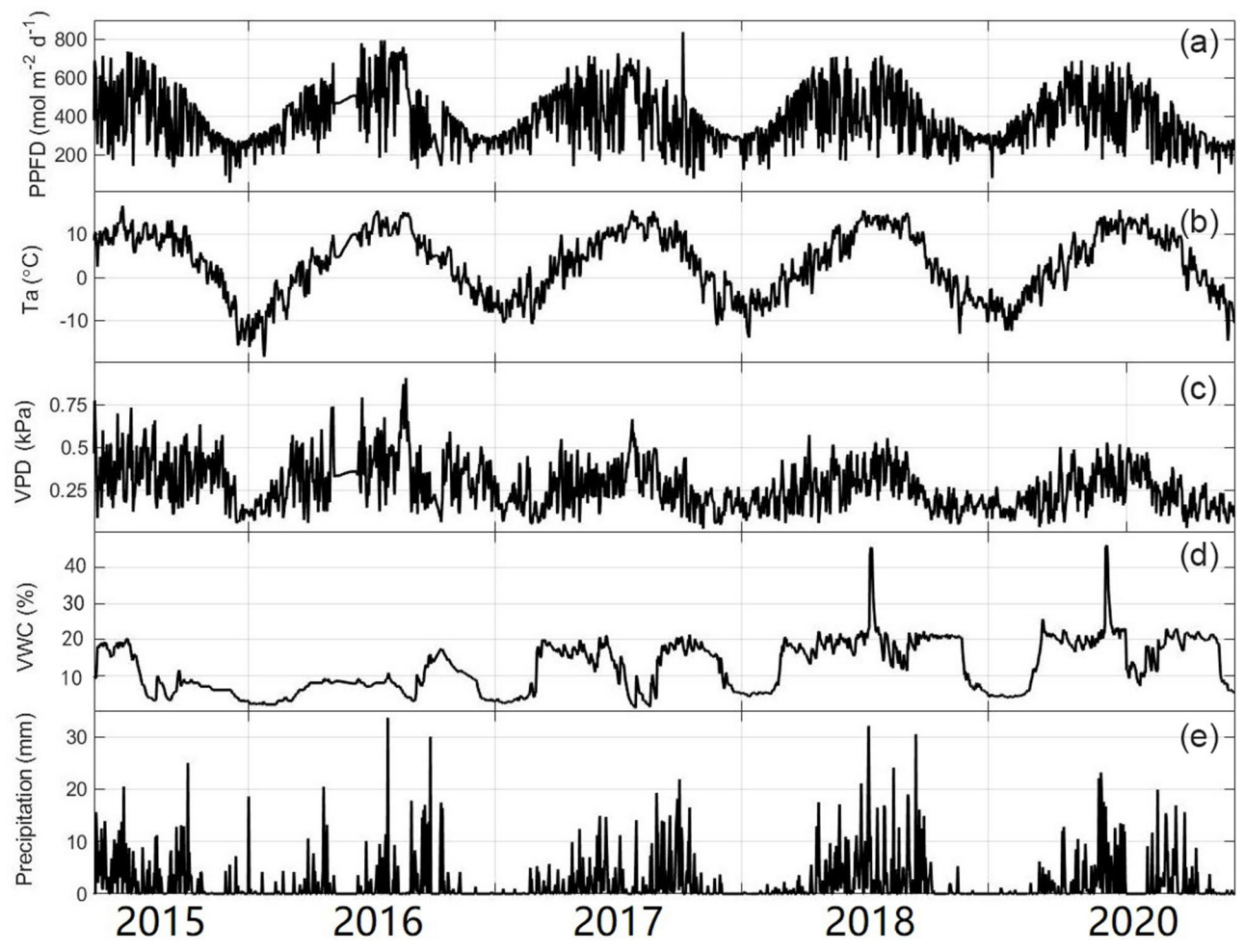

FIGURE 3 | Seasonal variability of **(a)** photosynthetic photon flux density (PPFD), **(b)** average daily temperature (Ta), **(c)** vapor pressure (VPD), **(d)** volumetric water content (VWC), and **(e)** daily total precipitation. The lines are plotted from 1 January 1 to 31 December.

Savitzky–Golay filter to minimize the role of random variability in flux observations (**Figure 2**) (Savitzky and Golay, 1964). We defined the CUP as the number of days with net C uptake (NEE < 0 g C m^{-2} day^{-1}) (Fu et al., 2019). Following this definition, there may be multiple periods across the course of a calendar year that may have net C uptake; these were added for the calculation of CUP on an annual basis. The MCU was defined as the maximum daily net C uptake of the filtered time series. The MCR was defined as the maximum value of the daily net C release of the filtered time series (Fu et al., 2019). To explore the underlying mechanism controlling annual CO_2 exchanges, we split the annual NEE into growing season NEE (NEE_g) and non-growing season NEE (NEE_{ng}). We used the same method as those in Gu et al. (2009) to quantify the canopy photosynthetic phenology and fitted a 9-parameter Weibull function to the data to obtain the GPP_{max} and Re_{max} value of each year.

RESULTS

Environmental Factors

The daily mean Ta showed large seasonal variation, ranging from −18.4 to 15.67°C (**Figure 3**). The average annual temperature in this site from 2016 to 2020 was 0.44°C, of which 2020 was the coldest (0.15°C) year and 2017 was the warmest (0.66°C) year (**Figure 3** and **Table 1**). Similar to temperature, PPFP showed a single peak in late June to early July each year. The maximum daily value could exceed 800 μmol photons m^{-2} d^{-1} (**Figure 3**). There were significant seasonal differences in daily precipitation, and the annual total precipitation amounts

TABLE 1 | Climatic factors and carbon fluxes for 2016–2018 and 2020.

	Year					
	2016	**2017**	**2018**	**2020**	**Average**	**SD**
PPFD (mol m^{-2} d^{-1})	366.89	363.86	357.78	333.87	355.60	14.97
Ta (°C)	0.51	0.66	0.45	0.15	0.44	0.21
VPD (kPa)	0.32	0.22	0.22	0.20	0.24	0.05
VWC (100%)	0.07	0.12	0.14	0.15	0.12	0.04
Rain (mm)	710.40	860.80	995.60	1,032.50	899.82	146.26
ER (g C m^{-2} $year^{-1}$)	869.36	889.89	556.42	1,306.91	905.64	307.37
GPP (g C m^{-2} $year^{-1}$)	777.40	740.41	582.77	1,143.24	810.96	237.06
NEE (g C m^{-2} $year^{-1}$)	91.96	149.48	−26.35	163.67	94.69	86.44

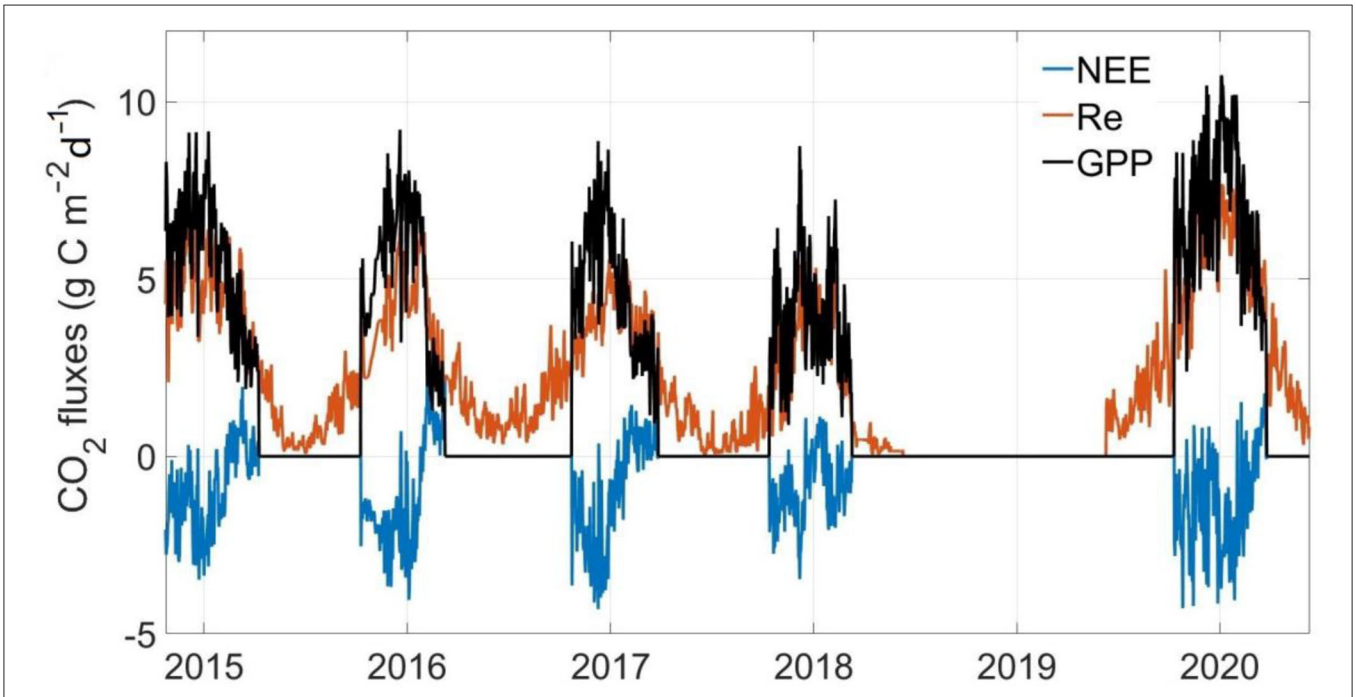

FIGURE 4 | Seasonal and inter-annual variation in the daily average net ecosystem CO_2 exchange (NEE), gross primary productivity (GPP), and ecosystem respiration (Re).

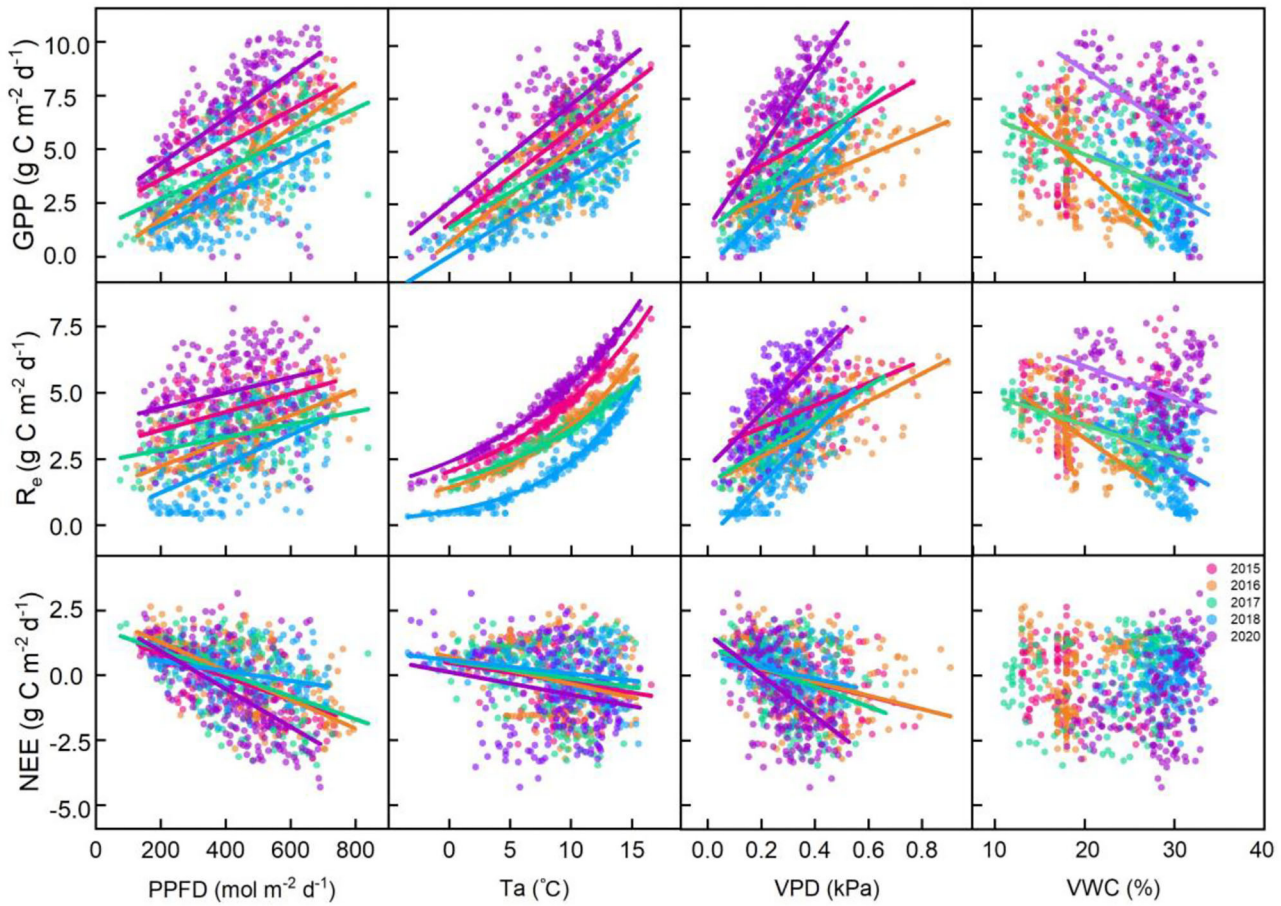

FIGURE 5 | Relationships between daily carbon fluxes (gross primary productivity [GPP], ecosystem respiration [Re], and net ecosystem carbon dioxide (CO_2) exchange [NEE]) and environmental factors (the photosynthetic photon flux density (PPFD), air temperature (Ta), vapor pressure deficit (VPD), and volumetric water content at a depth of 5 cm (VWC at 5 cm)). The fitted lines indicate that the regressions are significant under the confidence of 0.05.

were 710.40, 860.80, 995.60, and 1,032.50 mm for 2016, 2017, 2018, and 2020, respectively (**Table 1**). The variation in the soil water content (SWC) and the mean vapor pressure deficit (VPD) was closely related to the precipitation at the study site. In addition, there were two sharp peaks in the VWC dynamic in 2018 and 2020 because our study site suffered flooding at that time.

Seasonal Variations of GPP, Re, and NEE and Their Controlling Factors

In all observational years, GPP and Re both showed similar curvilinear shapes, with zero GPP and very low Re in the non-growing season (**Figure 4**). The maximum daily GPP values were 4.74–8.60 g C m^{-2} day^{-1} among 4 research years. The daily Re was low in winter (<0.5 g C m^{-2} day^{-1}) with the maximum values of 4.63–6.77 g C m^{-2} day^{-1} in 4 research years. The maximum daily NEE value in the growing season was about −2.39 g C m^{-2} day^{-1}, and the maximum daily NEE value in the non-growing season was about 2.08 g C m^{-2} day^{-1}.

At the seasonal scale, GPP and Re were positively correlated with PPFD, Ta, and VPD and negatively correlated with VWC at 5 cm. Re and Ta showed a significant exponential relationship ($p < 0.001$; **Figure 5**). NEE was negatively correlated with PPFD, Ta, and VPD and positively correlated with VWC ($p < 0.01$; **Figure 5**). We analyzed the relative contributions of six environmental variables to fluxes using the random forest (RF) scheme. The RF of this alpine meadow ecosystem explained 80.01 and 78.93% of the daily GPP and Re variations during the vegetative periods, respectively (**Supplementary Table S1**). Meanwhile, the RF explained 53.11% of the variations in the daily NEE (**Supplementary Table S1**).

IVVs of GPP, Re, and NEE and Their Controlling Factors

In general, the yearly cumulative GPP was 810.96 ± 237.06 g C m^{-2}, and the total accumulative Re was 905.64 ± 307.37 g C m^{-2} over 4 study years (**Figure 4** and **Table 1**). The alpine meadow ecosystem was a faint carbon source during the observation

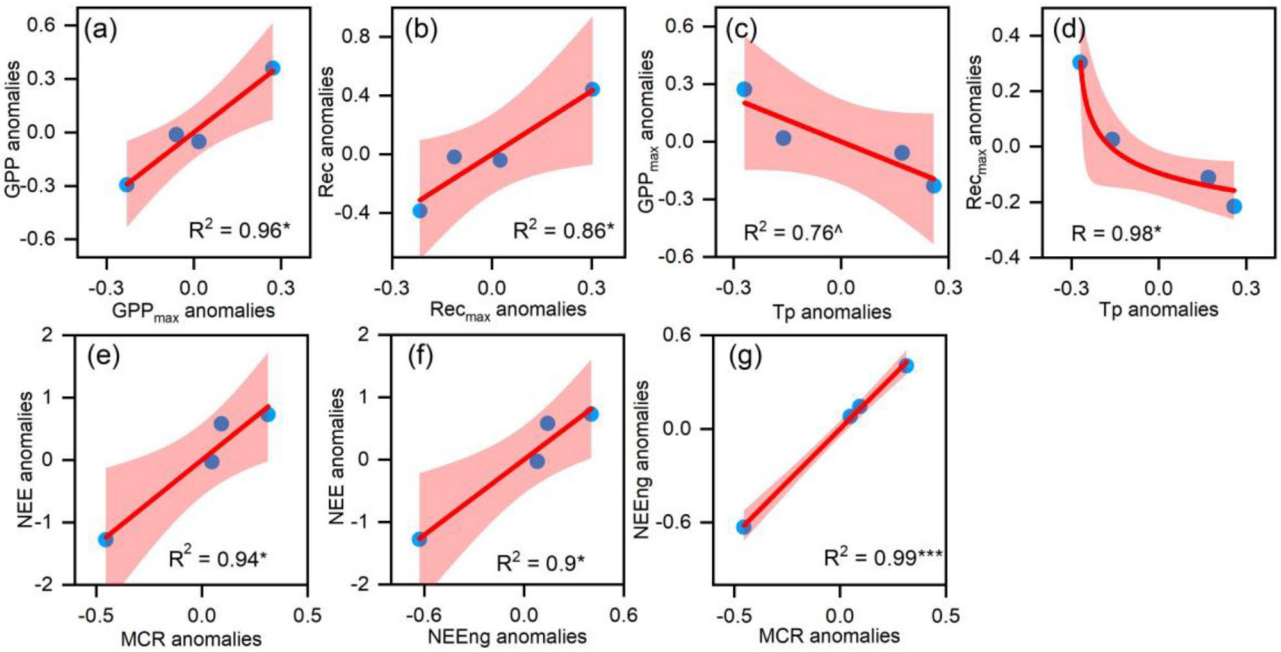

FIGURE 6 | (a) The relationship between the yearly gross primary productivity (GPP) anomalies and the GPP_{max} anomalies; **(b)** the relationship between the yearly Re anomalies and the Re_{max} anomalies; **(c,d)** the relationship between the GPP_{max} anomalies, the Re_{max} anomalies, and the preseason temperature (Tp) anomalies and; **(e–g)** the relationship between the MCR anomalies, the NEE_{ng} anomalies, and the NEE anomalies. ^when $p < 0.1$, * when $p < 0.05$, ** when $p < 0.01$, ***when $p < 0.001$.

period. The mean NEE of these 4 years was 94.69 ± 86.44 C m^{-2} $year^{-1}$ although the NEE in 2018 was negative. The positive NEE values indicated a net emission of CO_2 in the alpine meadow ecosystem during these 4 years.

There were no significant correlations between environmental factors and CO_2 fluxes on the annual scale. The yearly GPP anomalies and Re anomalies were significantly related to GPP_{max} animalizes (**Figure 6a**) and Re_{max} anomalies, respectively (**Figure 6b**). Moreover, the anomalies of GPP_{max} and Re_{max} were negatively correlated with the preseason temperature (Tp, the average temperature from February to April) (**Figures 6c,d**). NEE anomalies were positively correlated with the IAV of MCR (**Figure 6e**) but had no significant corrections with MCU or CUP. Meanwhile, annual NEE anomalies were positively correlated with the IAV of accumulated NEE in the non-growing season (**Figure 6f**), which were significantly related to MCR anomalies (**Figure 6g**).

Biological factors were also considered in this study. Plant community varied considerably during the observation period (**Supplementary Figure S1**). The percentage of *Cyperaceae* had a positive relationship with the GPP_{max} and Re_{max} (**Figure 7a**). The percentage of *Polygonaceae* had a negative relationship with the GPP_{max} and Re_{max} (**Figure 7b**). In addition, the higher Tp had a negative effect on the percentage of *Cyperaceae* (**Figure 7c**) but had a positive effect on the percentage of *Polygonaceae* (**Figure 7c**) on the annual scale.

DISCUSSION

CO_2 Budget at Zoige Alpine Meadow

The carbon budget at Zoige alpine meadow in this study was not consistent with most alpine meadow ecosystems in the Qinghai-Tibet region, which usually acted as a carbon sink (Kato et al., 2006; Zhao et al., 2006; Sun et al., 2019; Wang et al., 2020). Different from the previous opinion that the favorable photosynthetic conditions and a low decomposition rate of organic matter result in carbon accumulation in alpine meadow ecosystems (Kato et al., 2006; Fu et al., 2009), the net carbon balance performed as a weak source among these 4 years in this study. Because the GPP and Re values were comparable in the growing season, the carbon accumulation during the growing season was less than the respiration in the non-growing season.

In this study, both the GPP (810.96 g C m^{-2} $year^{-1}$) and Re (905.64 g C m^{-2} $year^{-1}$) values were very high in comparison with other alpine meadow ecosystems (**Tables 1**, **2**). The relatively high precipitation and temperature led to higher productivity and greater respiration consumption. However, the high productivity did not lead to net carbon uptake accumulation during the observation period because the Re in the cold ecosystem was large and more sensitive to the environmental change than GPP (Illeris et al., 2004; Zhu et al., 2016). For instance, favorable weather increased the Re and GPP, leading to a net carbon emission of 163.67 g C m^{-2} in 2020. However,

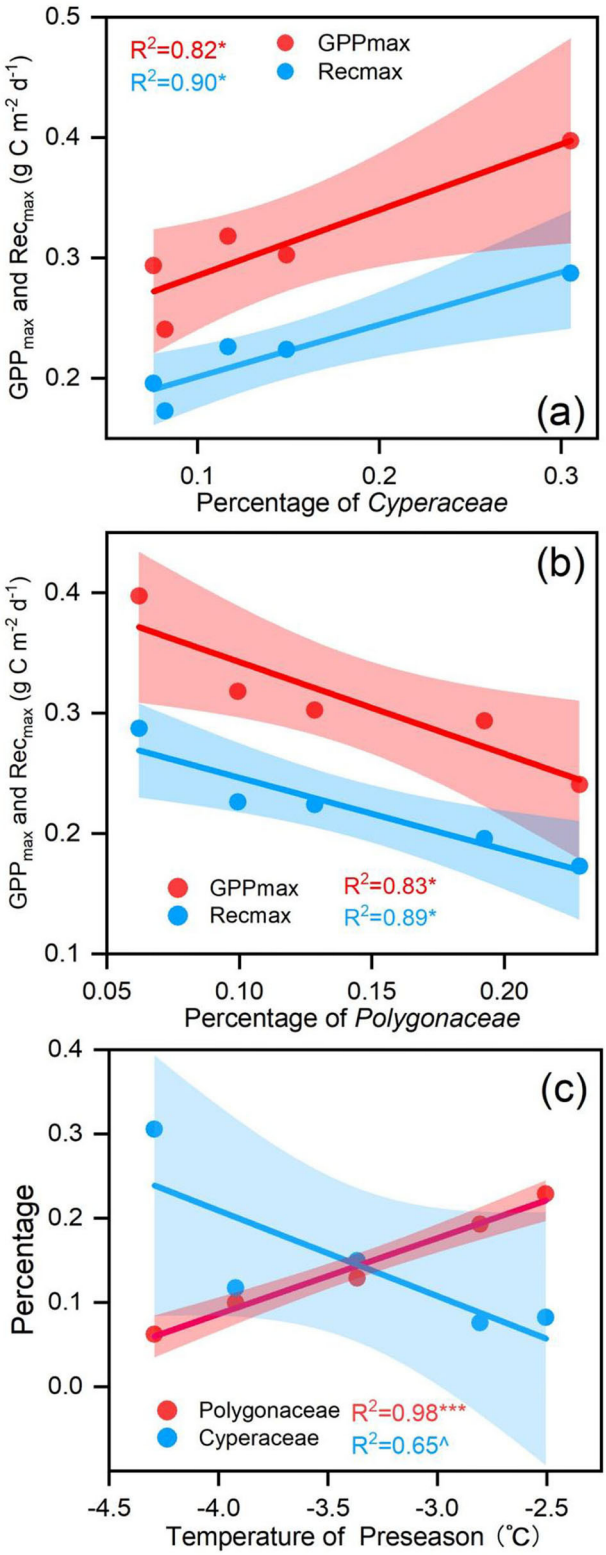

FIGURE 7 | (a) the relationship between the percentage of *Polygonaceae* and carbon fluxes; **(b)** the relationship between the percentage of *Cyperaceae* and carbon fluxes; **(c)** the relationship between the percentage of *Polygonaceae*, *Cyperaceae* and the temperature of the preseason (Tp). ^when $p < 0.1$, * when $p < 0.05$, ** when $p < 0.01$, ***when $p < 0.001$.

unfavorable weather decreased the Re and GPP, leading to a net carbon sink of 26.35 g C m^{-2} in 2018.

Environmental Controls on Seasonal Variation of Ecosystem CO_2 Fluxes

Previous studies have shown that carbon fluxes had a clear seasonal dynamic in temperate and cold ecosystems (Zhao et al., 2010; Niu et al., 2017a; Wang et al., 2020). Alpine meadow ecosystem had a low-temperature condition, and the temperature and thermal conditions were often the limiting factors for vegetation growth, which was typically considered the main factor regulating carbon fluxes (Saito et al., 2009; Li et al., 2019b). The RF analysis suggested that Ta primarily influenced the seasonal changes in GPP, Re, and NEE in this alpine meadow ecosystem, and SWC played subordinate roles in affecting seasonal GPP, Re, and NEE changes (**Supplementary Table S1**).

This result was consistent with previous studies, which found that temperature was the most critical factor for controlling NEE, GPP, and Re for an alpine meadow ecosystem (Kato et al., 2006; Fu et al., 2009; Saito et al., 2009). The reason was that although cold and humid environments provided an adequate soil water supply for plants growth during the growing season, the low temperature often became a limiting factor for plant growth, as temperature affected both the physiology and phenology of plants, which in turn determined the carbon uptake and release. In addition to Ta, SWC played a subordinate role in affecting seasonal GPP, Re, and NEE changes. Previous studies had shown that soil moisture had an important effect on controlling carbon fluxes for a water-limited ecosystem (Wang et al., 2008; Ganjurjav et al., 2016; Zhang et al., 2018) but had little effect on water-rich areas (i.e., wetland) (Zhao et al., 2010; Du et al., 2021). The soil water supply in the Zoige alpine meadow ecosystem was intermediate between grassland and wetland, leading to the subordinate role in seasonal carbon flux variations.

Controlling Factors on IAV in GPP and Re

Our study demonstrated that the IAV of GPP_{max} and Re_{max} mostly determined the IAV of GPP and Re in Zoige alpine meadow, respectively, instead of plant phenology or climates. This result was consistent with previous studies that found the IAV of GPP was best explained by that in GPP_{max} in North America, Europe, and the Tibetan Plateau (Xia et al., 2015; Zhou et al., 2016; Chen et al., 2019a), and the IAV of Re was mainly attributed to Re_{max} at Maoershan forest (Liu et al., 2021a). The control of GPP_{max} on annual GPP variability and the Re_{max} on annual Re variability indicated that environmental changes influenced the IAVs of GPP and Re by affecting vegetation physiology rather than phenology. Hence, given GPP_{max} and Re_{max}'s importance for the alpine region's carbon cycle, it was vital to explore the physiological mechanism underlying GPP_{max} and Re_{max} change in the alpine ecosystem.

The maximum GPP rate was determined by the leaf area index and the leaf photosynthetic capacity of the ecosystem (Hu et al., 2018), and the Re_{max} was also tightly associated with plant biomass and vegetable characteristics (e.g., temperature sensitivity) (Kato et al., 2004a,b; Flanagan and Johnson, 2005; Yashiro et al., 2010). These physiological factors were greatly

TABLE 2 | Ecosystem carbon fluxes in other alpine meadows published in previous studies.

Type	Site	Period	Ta °C	GPP g C m^{-2} y^{-1}	Re g C m^{-2} y^{-1}	NEE g C m^{-2} y^{-1}	Reference
Alpine meadow	Haibei	2003–2004	−1.48	—	—	−282	Zhao et al. (2005)
Alpine shrub meadow				—	—	−53	
Alpine meadows				—	—	478	
Alpine shrub-meadow	Haibei	2004–2005	−1.7	527.7	459.2	−68.5	Fu et al. (2009)
Alpine meadow- steppe	Dangxung		1.3	205.8	253.8	48	
Alpine steppe	Bange	2015	0.02	—	—	21.8	Wang et al. (2018)
Alpine meadow	Lijiang		6.16	—	—	−230	
Alpine meadow	Arou	2013–2016	0.6	818.3	619.6	−198.7	Sun et al. (2019)
Alpine meadow	Dashalong		−3.4	467.5	208.6	−258.9	
Alpine meadow	Yakou	2015–2016	−4.2	228.6	123.3	−105.3	
Alpine wetland	Luanhaizi	2007–2016	−1.1	500.3	620.7	120.4	Zhu et al. (2020)
Alpine meadow	Haibei	2002–2004	−1	634.5	513.6	−120.9	Kato et al. (2006)
Alpine wetland meadow	Haibei	2004–2006	−1.1	629.9	737.1	107.2	Zhao et al. (2010)
Alpine shrubland meadow	Haibei	2003–2004		551.7	484.6	−67.1	Zhao et al. (2006)
Alpine meadow	Hongyuan	2015–2020	0.44	810.96	905.64	94.69	This study

affected by the change in plant community structure (Johnson et al., 2008; Cheng et al., 2015; Xu et al., 2015; Estruch et al., 2018). It had been widely reported that the species composition in the alpine meadow was shifting due to destruction by rodents (Zhou et al., 2005), climate change (Li et al., 2011), or other uncertain causes (Harris, 2010). These interferences could affect ecosystem processes through changing plant species composition (Poulter et al., 2014) and thus ecosystem functions (i.e., GPP and Re) (Sala et al., 2012; Kulmatiski and Beard, 2013).

Our observed changes in species' community support the above explanation. During the study period, the species communities changed significantly from a *Poaceae*-dominated meadow in 2015 to a *Cyperaceae*-dominated meadow in 2020 (**Supplementary Figure S1**). In our study site, *Cyperaceae*, *Polygonaceae*, *Euphorbiaceae*, *Poaceae*, and *Asteraceae* accounted for more than 80% of aboveground biomass (**Supplementary Figure S1**). A previous study had shown that *Cyperaceae* and *Poaceae* had the highest photosynthetic rate and water use efficiency among all of the function groups, and the photosynthetic rate of *Polygonaceae* was the lowest (Liu et al., 2015). Meanwhile, a study based on isotope labeling also found that *Cyperaceae* plants have a stronger ability to assimilate CO_2 and transfer more C to roots and soil, because *Cyperaceae* plants had a high primary carbon assimilation tissue area when compared with *Poaceae* (Mou et al., 2018).

Hence, the percentage of *Cyperaceae* and *Polygonaceae* explained the annual GPP_{max} and Re_{max} variations in Zoige alpine meadow ecosystem. A greater proportion of *Cyperaceae* and a smaller proportion of *Polygonaceae* contributed to a larger annual GPP_{max}. Meanwhile, we found that the temperature before the growing reason had a negative effect on the percentage of *Cyperaceae* ($p < 0.1$; **Figure 7c**) but had a positive effect on the percentage of *Polygonaceae* ($p < 0.01$; **Figure 7c**) on the annual scale. Consequently, a warmer preseason could reduce annual GPP_{max} by increasing the percentage of *Polygonaceae* and decreasing the percentage of *Cyperaceae*.

Controlling Factors on IAV in NEE

Any single environmental factor could not explain the IAV of NEE in this study. Instead, it was explained well by biological processes, such as NEE_{ng} and MCR. The environmental driving factors may ultimately impact the IAV of NEE by changing the phenological and physiological indicators (Fu et al., 2017; Niu et al., 2017b).

Moreover, we found that the IAV of NEE at Zoige alpine meadow was primarily explained by the physiological (MCR) rather than phenological indicators (CUP). Surprisingly, the MCU did not affect the IAV of NEE, which indicated that the IAV of NEE was driven mainly by the net CO_2 release process during the non-growing season rather than the net CO_2 uptake during the growing season in this area, although NEE in growing and non-growing seasons was determined predominately by MCU and MCR, respectively. Meanwhile, the CUP tended to have no significant influence on either NEE_g or NEE_{ng}. A global study also indicated that the CUP contribution to IAV of NEE was lower than the physiological indicator in Zoige alpine meadow area (Fu et al., 2019). Moreover, a study conducted on Siberian tundra also showed that the IAV of NEE had no significant relationship with CUP because of the offset effect between GPP and Re (Parmentier et al., 2011).

However, the driving factor of the IAV of NEE in this study differed from some other studies that indicated the IAV of NEE was determined predominately by MCU (Zscheischler et al., 2016; Gonsamo et al., 2018; Fu et al., 2019). Because most of the study sites in these research studies were carbon sinks, carbon uptake in the growing season was larger than the carbon release in the non-growing season, resulting in the dominant role of MCU in contributing to the IAV of NEE. In our study site, the mean NEE over the 4 years was 94.69 ± 86.44 C m^{-2} $year^{-1}$. The carbon uptake in the growing season was smaller than the carbon release in the non-growing season, leading to the dominant role of MCR in contributing to the IAV of NEE in this study.

We were aware of the possible uncertainty of IAV in GPP and Re due to the short observation periods in this study. The controlling mechanisms for the IAV of GPP and Re could be different in short-term and long-term series because the effects from the influencing factors were changing over time (e.g., legacy effects and accumulation effects) (Bloom et al., 2020; Liu et al., 2021b), and the ecosystems were also acclimating to the changing environments (Luo et al., 2001; Guo et al., 2020). Hence, we suggest that more research should be conducted to explore the processes that control the long-term IAV of GPP, Re, and NEE in the future.

CONCLUSION

The Zoige alpine meadow acted as a faint carbon source during the observation period. GPP, Re, and NEE all showed strongly seasonal and IVVs. The seasonal variations of GPP, Re, and NEE were mostly determined by Ta, followed by PPFD, VPD, and VWC, while GPP_{max} and Re_{max} drove the IAV of GPP and Re. Meanwhile, the higher Tp could decrease the GPP_{max} and Re_{max} by changing the plant species composition in the growing season and decrease GPP and Re in Zoige alpine meadow. The IAV of NEE at the Zoige alpine meadow was largely explained by the MCR, indicating the important role of carbon release in the non-growing season in determining the net C sink in the alpine region. Given the physiological indicators (i.e., GPP_{max}, Re_{max}, and MCR) can best explain the CO_2 exchange variability, future studies need to emphasize the regulatory mechanisms for the dynamics of ecosystem physiological characteristics in the alpine ecosystem.

DATA AVAILABILITY STATEMENT

The raw data supporting the conclusions of this article will be made available by the authors, without undue reservation.

AUTHOR CONTRIBUTIONS

SW, WC, and SN designed this study. SW performed the laboratory analysis and wrote the paper. All authors have revised, discussed, and approved the final manuscript.

FUNDING

This study was supported by the National Natural Science Foundation of China (31988102) and the Second Tibetan Plateau Scientific Expedition and Research (STEP) program (2019QZKK0302).

ACKNOWLEDGMENTS

The authors are grateful to Qiong Wu and Yingjie Yan for helping us get field data, and think Yiheng Wang for polishing our manuscript.

SUPPLEMENTARY MATERIAL

The Supplementary Material for this article can be found online at: https://www.frontiersin.org/articles/10.3389/fpls.2022.894398/full#supplementary-material

REFERENCES

Bloom, A. A., Bowman, K. W., Liu, J., Konings, A. G., Worden, J. R., Parazoo, N. C., et al. (2020). Lagged effects regulate the inter-annual variability of the tropical carbon balance. *Biogeosciences*. 17, 6393–6422. doi: 10.5194/bg-17-6393-2020

Braswell, B. H., Sacks, W. J., Linder, E., and Schimel, D. S. (2005). Estimating diurnal to annual ecosystem parameters by synthesis of a carbon flux model with eddy covariance net ecosystem exchange observations. *Global Change Biol.* 11, 335–355. doi: 10.1111/j.1365-2486.2005.00897.x

Chen, H., Zhu, Q., Peng, C., Wu, N., Wang, Y., Fang, X., et al. (2013). The impacts of climate change and human activities on biogeochemical cycles on the Qinghai-Tibetan Plateau. *Global Change Biol.* 19, 2940–2955. doi: 10.1111/gcb.12277

Chen, S. L., Huang, Y. F., Gao, S., and Wang, G. Q. (2019a). Impact of physiological and phenological change on carbon uptake on the Tibetan Plateau revealed through GPP estimation based on spaceborne solar-induced fluorescence. *Sci. Total. Environ*. 663, 45–59. doi: 10.1016/j.scitotenv.2019.01.324

Chen, W. N., Zhang, F. Y., Wang, B. X., Wang, J. S., Tian, D. S., Han, G. X., et al. (2019b). Diel and Seasonal Dynamics of Ecosystem-Scale Methane Flux and Their Determinants in an Alpine Meadow. *J. Geophys. Res-Biogeo*. 124, 1731–1745. doi: 10.1029/2019JG005011

Cheng, G. D., and Wu, T. H. (2007). Responses of permafrost to climate change and their environmental significance, Qinghai-Tibet Plateau. *J. Geophys. Res-Earth.* 112 doi: 10.1029/2006JF000631

Cheng, S. J., Bohrer, G., Steiner, A. L., Hollinger, D. Y., Suyker, A., Phillips, R. P., et al. (2015). Variations in the influence of diffuse light on gross primary productivity in temperate ecosystems. *Agric. For. Meteorol.* 201, 98–110. doi: 10.1016/j.agrformet.2014.11.002

Du, Q., Liu, H., Liu, Y., Xu, L., and Sun, J. (2021). Water and carbon dioxide fluxes over a "floating blanket" wetland in southwest of China with eddy covariance method. *Agric. For. Meteorol.* 311 doi: 10.1016/j.agrformet.2021.108689

Estruch, C., Lozano, Y. M., Armas, C., and Pugnaire, F. I. (2018). Plant community changes after land abandonment control CO2 balance in a dry environment. *Plant. Soil.* 425, 253–264. doi: 10.1007/s11104-018-3581-1

Falge, E., Baldocchi, D., Olson, R., Anthoni, P., Aubinet, M., Bernhofer, C., et al. (2001). Gap filling strategies for defensible annual sums of net ecosystem exchange. *Agric. For. Meteorol.* 107, 43–69. doi: 10.1016/S0168-1923(00)00225-2

Fernandez-Martinez, M., Sardans, J., Chevallier, F., Ciais, P., Obersteiner, M., Vicca, S., et al. (2019). Global trends in carbon sinks and their relationships with CO2 and temperature. *Nat. Clim. Change.* 9, 73.-+. doi: 10.1038/s41558-018-0367-7

Flanagan, L. B., and Johnson, B. G. (2005). Interacting effects of temperature, soil moisture and plant biomass production on ecosystem respiration in a northern temperate grassland. *Agric. For. Meteorol.* 130, 237–253. doi: 10.1016/j.agrformet.2005.04.002

Fu, Y., Zheng, Z., Hu, Y. u. G., Sun, Z., and Shi, X. P, and Zhao X (2009). Environmental influences on carbon dioxide fluxes over three grassland ecosystems in China. *Biogeosciences*. 6, 2879–2893. doi: 10.5194/bg-6-2879-2009

Fu, Z., Dong, J., Zhou, Y., Stoy, P. C., and Niu, S. (2017). Long term trend and interannual variability of land carbon uptake-the attribution and processes. *Environ. Res. Lett*. 12. doi: 10.1088/1748-9326/aa5685

Fu, Z., Stoy, P. C., Poulter, B., Gerken, T., Zhang, Z., Wakbulcho, G., et al. (2019). Maximum carbon uptake rate dominates the interannual variability

of global net ecosystem exchange. *Global. Change. Biol*. 25, 3381–3394. doi: 10.1111/gcb.14731

Ganjurjav, H., Gao, Q. Z., Schwartz, M. W., Zhu, W. Q., Liang, Y., and Lin, L. i. Y. (2016). Complex responses of spring vegetation growth to climate in a moisture-limited alpine meadow. *Sci. Rep*. 6, 10. doi: 10.1038/srep23356

Gonsamo, A., Chen, J. M., and Ooi, Y. W. (2018). Peak season plant activity shift towards spring is reflected by increasing carbon uptake by extratropical ecosystems. *Global. Change. Biol*. 24, 2117–2128. doi: 10.1111/gcb.14001

Green, J. K., Seneviratne, S. I., Berg, A. M., Findell, K. L., Hagemann, S., Lawrence, D. M., et al. (2019). Large influence of soil moisture on long-term terrestrial carbon uptake. *Nature*. 565, 476.-+. doi: 10.1038/s41586-018-0848-x

Gu, L., Post, W. M., Baldocchi, D. D., Black, T. A., Suyker, A. E., Verma, S. B., et al. (2009). "Characterizing the seasonal dynamics of plant community photosynthesis across a range of vegetation types," in *Phenology of Ecosystem Processes* (https://digitalcommons.unl.edu/cgi/viewcontent.cgi?referer=https://www.google.com/&httpsredir=1&article=1176&context=natrespapers Berlin, Germany: Springer), 35–58.

Guo, X., Gao, Q., Yuan, M., Wang, G., Zhou, X., Feng, J., et al. (2020). Gene-informed decomposition model predicts lower soil carbon loss due to persistent microbial adaptation to warming. *Nat. Commun*. 11, 4897. doi: 10.1038/s41467-020-18706-z

Hao, Y., Zhang, H., Biederman, J. A., Cui, L. i. L., and Xue, X. K, and Wang Y (2018). Seasonal timing regulates extreme drought impacts on CO2 and H2O exchanges over semiarid steppes in Inner Mongolia, China. *Agr. Ecosyst. Environ*. 266, 153–166. doi: 10.1016/j.agee.2018.06.010

Hao, Y. B., Cui, X. Y., Wang, Y. F., Mei, X. R., Kang, X. M., Wu, N., et al. (2011). Predominance of Precipitation and Temperature Controls on Ecosystem CO2 Exchange in Zoige Alpine Wetlands of Southwest China. *Wetlands*. 31, 413–422. doi: 10.1007/s13157-011-0151-1

Harris, R. B. (2010). Rangeland degradation on the Qinghai-Tibetan plateau: a review of the evidence of its magnitude and causes. *J. Arid. Environ*. 74, 1–12. doi: 10.1016/j.jaridenv.2009.06.014

Hawkins, E., and Sutton, R. (2009). The potential to narrow uncertainty in regional climate predictions. *B Am Meteorol Soc*. 90, 1095.-+. doi: 10.1175/2009BAMS2607.1

Hu, Z., Shi, H., Cheng, K., Wang, Y-. P., Piao, S., and Yu, L. i. Y. (2018). Joint structural and physiological control on the interannual variation in productivity in a temperate grassland: A data-model comparison. *Global. Change. Biol*. 24, 2965–2979. doi: 10.1111/gcb.14274

Illeris, L., Christensen, T. R., and Mastepanov, M. (2004). Moisture effects on temperature sensitivity of CO2 exchange in a subarctic heath ecosystem. *Biogeochemistry*. 70, 315–330. doi: 10.1007/s10533-003-0855-2

Ito, A. (2019). Disequilibrium of terrestrial ecosystem CO2 budget caused by disturbance-induced emissions and non-CO2 carbon export flows: a global model assessment. *Earth. System. Dyn*. 10, 685–709. doi: 10.5194/esd-10-685-2019

Jia, X., Zha, T., Gong, J., Wang, B., Zhang, Y., Wu, B., et al. (2016). Carbon and water exchange over a temperate semi-arid shrubland during three years of contrasting precipitation and soil moisture patterns. *Agric. For. Meteorol*. 228, 120–129. doi: 10.1016/j.agrformet.2016.07.007

Johnson, D., Phoenix, G. K., and Grime, J. P. (2008). Plant community composition, not diversity, regulates soil respiration in grasslands. *Biol. Lett*. 4, 345–348. doi: 10.1098/rsbl.2008.0121

Jung, M., Reichstein, M., Schwalm, C. R., Huntingford, C., Sitch, S., Ahlstrom, A., et al. (2017). Compensatory water effects link yearly global land CO2 sink changes to temperature. *Nature*. 541, 516–520. doi: 10.1038/nature20780

Kato, T., Tang, Y. H., Gu, S., Cui, X. Y., Hirota, M., Du, M. Y., et al. (2004a). Carbon dioxide exchange between the atmosphere and an alpine meadow ecosystem on the Qinghai-Tibetan Plateau, China. *Agric. For. Meteorol*. 124, 121–134. doi: 10.1016/j.agrformet.2003.12.008

Kato, T., Tang, Y. H., Gu, S., Hirota, M., Cui, X. Y., Du, M. Y., et al. (2004b). Seasonal patterns of gross primary production and ecosystem respiration in an alpine meadow ecosystem on the Qinghai-Tibetan Plateau. *J. Geophys. Res-Atmos*. 109 doi: 10.1029/2003JD003951

Kato, T., Tang, Y. H., Gu, S., Hirota, M., Du, M. Y., and Zhao, L. i. Y. N. (2006). Temperature and biomass influences on interannual changes in CO2 exchange in an alpine meadow on the Qinghai-Tibetan Plateau. *Global. Change. Biol*. 12, 1285–1298. doi: 10.1111/j.1365-2486.2006.01153.x

Kulmatiski, A., and Beard, K. H. (2013). Woody plant encroachment facilitated by increased precipitation intensity. *Nat. Clim. Change*. 3, 833–837. doi: 10.1038/nclimate1904

Li, D. S., Wen, Z., Cheng, Q. G., Xing, A. G., and Zhang, M. L. (2019a). Thermal dynamics of the permafrost active layer under increased precipitation at the Qinghai-Tibet Plateau. *J. Mt. Sci*. 16, 309–322. doi: 10.1007/s11629-018-5153-5

Li, G. Y., Liu, Y. Z., Frelich, L. E., and Sun, S. C. (2011). Experimental warming induces degradation of a Tibetan alpine meadow through trophic interactions. *J. Appl. Ecol*. 48, 659–667. doi: 10.1111/j.1365-2664.2011.01965.x

Li, H., Zhu, L. i. H., Zhang, J., He, F., Yang, H., and Li, Y. Y, and Zhou H (2019b). Growth stage-dependant variability in water vapor and CO2 exchanges over a humid alpine shrubland on the northeastern Qinghai-Tibetan Plateau. *Agric. For. Meteorol*. 268, 55–62. doi: 10.1016/j.agrformet.2019.01.013

Li, L., Yang, S., Wang, Z. Y., Zhu, X. D., Tang, H. Y. (2010). Evidence of Warming and Wetting Climate over the Qinghai-Tibet Plateau. *Arct. Antarct. Alp. Res*. 42, 449–457. doi: 10.1657/1938-4246-42.4.449

Liu, F., Wang, X., Wang, C., and Zhang, Q. (2021a). Environmental and biotic controls on the interannual variations in CO2 fluxes of a continental monsoon temperate forest. *Agric. For. Meteorol*. 296. doi: 10.1016/j.agrformet.2020.108232

Liu, G., Yan, G., Chang, M., Huang, B., Sun, X., Han, S., et al. (2021b). Long-term nitrogen addition further increased carbon sequestration in a boreal forest. *Eur. J. For. Res*. 140, 1113–1126. doi: 10.1007/s10342-021-01386-9

Liu, M.-x., Liu, Y.-y., Chen, S.-w., An, Q. (2015). Plant Photosynthetic Characteristics along Slope Gradients in an Alpine Meadow Region on the Eastern Edge of Qinghai-Tibetan Plateau. *Soil Crop*. 4:104–12.

Liu, X. D., and Chen, B. D. (2000). Climatic warming in the Tibetan Plateau during recent decades. *Int. J. Climatol*. 20, 1729–1742. doi: 10.1002/1097-0088(20001130)20:14<1729::AID-JOC556>3.0.CO;2-Y

Luan, J., Song, H., Xiang, C., Zhu, D., and Suolang, D. (2016). Soil moisture, species composition interact to regulate CO2 and CH4 fluxes in dry meadows on the Tibetan Plateau. *Ecol. Eng*. 91, 101–112. doi: 10.1016/j.ecoleng.2016.02.012

Lund, M., Lafleur, P. M., Roulet, N. T., Lindroth, A., Christensen, T. R., Aurela, M., et al. (2010). Variability in exchange of CO2 across 12 northern peatland and tundra sites. *Global. Change. Biol*. 16, 2436–2448. doi: 10.1111/j.1365-2486.2009.02104.x

Luo, Y., Wan, S., Hui, D., and Wallace, L. L. J. N. (2001). Acclimatization of soil respiration to warming in a tall grass *prairie*. 413, 622–625. doi: 10.1038/35098065

Lv, C. Q (2006). *Storage Pattern and Influencing Factors of Soil Organic Carbon in Qinghai Xizang Plateau*. Nanjing, http://en.wikipedia.org/wiki/Jiangsu Jiangsu: Nanjing University.

Ma, F., Song, B., Quan, Q., Zhang, F., Wang, J., Zhou, Q., et al. (2020). Light Competition and Biodiversity Loss Cause Saturation Response of Aboveground Net Primary Productivity to Nitrogen Enrichment. *J. Geophys. Res-Biogeo*. 125. doi: 10.1029/2019JG005556

Marcolla, B., Roedenbeck, C., and Cescatti, A. (2017). Patterns and controls of inter-annual variability in the terrestrial carbon budget. *Biogeosciences*. 14, 3815–3829. doi: 10.5194/bg-14-3815-2017

Mou, X. M., Zhao, L. i. X. G., Yu, N., and Kuzyakov, Y. W. Y (2018). Tibetan sedges sequester more carbon belowground than grasses: a C-13 labeling study. *Plant. Soil*. 426, 287–298. doi: 10.1007/s11104-018-3634-5

Ni, J. (2002). Carbon storage in grasslands of China. *J. Arid. Environ*. 50, 205–218. doi: 10.1006/jare.2001.0902

Niu, B., He, Y. T., Zhang, X. Z., Du, M. Y., Shi, P. L., Sun, W., et al. (2017a). CO2 Exchange in an Alpine Swamp Meadow on the Central Tibetan Plateau. *Wetlands*. 37, 525–543. doi: 10.1007/s13157-017-0888-2

Niu, S., Fu, Z., Luo, Y., Stoy, P. C., Keenan, T. F., Poulter, B., et al. (2017b). Interannual variability of ecosystem carbon exchange: From observation to prediction. *Global. Ecol. Biogeogr*. 26, 1225–1237. doi: 10.1111/geb.12633

Parmentier, F., Van Der Molen, M., Van Huissteden, J., Karsanaev, S., Kononov, A., Suzdalov, D., et al. (2011). Longer growing seasons do not increase net carbon uptake in the northeastern Siberian tundra. *J. Geophys. Res. Biogeosci*. 116. doi: 10.1029/2011JG001653

Peng, H., Chi, J., Yao, H., Guo, Q., Hong, B., Ding, H., et al. (2021). Methane emissions offset net carbon dioxide uptake from an alpine peatland on the Eastern Qinghai-Tibetan Plateau. *J. Geophys. Res-Atmos*. 126. doi: 10.1029/2021JD034671

Poulter, B., Frank, D., Ciais, P., Myneni, R. B., Andela, N., and van der Werf, B. i. J. (2014). Contribution of semi-arid ecosystems to interannual variability of the global carbon cycle. *Nature*. 509, 600.-+. doi: 10.1038/nature13376

Quan, Q., Zhang, F. Y., Tian, D. S., Zhou, Q. P., Wang, L. X., and Niu, S. L. (2018). Transpiration Dominates Ecosystem Water-Use Efficiency in Response to Warming in an Alpine Meadow. *J. Geophys. Res-Biogeo*. 123, 453–462. doi: 10.1002/2017JG004362

Reichstein, M., Falge, E., Baldocchi, D., Papale, D., Aubinet, M., Berbigier, P., et al. (2005). On the separation of net ecosystem exchange into assimilation and ecosystem respiration: review and improved algorithm. *Global. Change. Biol*. 11, 1424–1439. doi: 10.1111/j.1365-2486.2005.001002.x

Saito, M., Kato, T., and Tang, Y. (2009). Temperature controls ecosystem CO2 exchange of an alpine meadow on the northeastern Tibetan Plateau. *Global. Change. Biol*. 15, 221–228. doi: 10.1111/j.1365-2486.2008.01713.x

Sala, O. E., Gherardi, L. A., Reichmann, L., Jobbagy, E., and Peters, D. (2012). Legacies of precipitation fluctuations on primary production: theory and data synthesis. *Philos. Trans. R. Soc. B-Biol. Sci*. 367, 3135–3144. doi: 10.1098/rstb.2011.0347

Savitzky, A., and Golay, M. J. E. (1964). Smoothing + differentiation of data by simplified least squares procedures. *Anal. Chem*. 36, 1627. doi: 10.1021/ac60214a047

Song, W. M., Wang, H., Wang, G. S., Chen, L. T., Jin, Z. N., Zhuang, Q. L., et al. (2015). Methane emissions from an alpine wetland on the Tibetan Plateau: Neglected but vital contribution of the nongrowing season. *J. Geophys. Res-Biogeo*. 120, 1475–1490. doi: 10.1002/2015JG003043

Sun, S., Che, T., Wang, L. i. H., Ma, T., and Liu, C. B, and Song Z (2019). 9Water and carbon dioxide exchange of an alpine meadow ecosystem in the northeastern Tibetan Plateau is energy-limited. *Agric. For. Meteorol*. 275, 283–295. doi: 10.1016/j.agrformet.2019.06.003

Wang, L., Liu, H., Shao, Y., Liu, Y., and Sun, J. (2018). Water and CO2 fluxes over semiarid alpine steppe and humid alpine meadow ecosystems on the Tibetan Plateau. *Theor. Appl. Climatol*. 131, 547–556. doi: 10.1007/s00704-016-1997-1

Wang, L., Liu, H. Z., Sun, J. H., and Feng, J. W. (2016). Water and carbon dioxide fluxes over an alpine meadow in southwest China and the impact of a spring drought event. *Int. J. Biometeorol* 60, 195–205. doi: 10.1007/s00484-015-1016-8

Wang, S. L., Jin, H. J., and Zhao, L. i. S. X. (2000). Permafrost degradation on the Qinghai-Tibet Plateau and its environmental impacts. *Permafrost. Periglac*. 11, 43–53. doi: 10.1002/(SICI)1099-1530(200001/03)11:1<43::AID-PPP332>3.0.CO;2-H

Wang, S. Q., and Zhou, C. H. (1999). Estimating soil carbon reservoir of terrestrial ecosystem in China. *Geogr. Res*. 18, 349–356.

Wang, X., Piao, S., Ciais, P., Friedlingstein, P., Myneni, R. B., Cox, P., et al. (2014). A two-fold increase of carbon cycle sensitivity to tropical temperature variations. *Nature*. 506, 212.-+. doi: 10.1038/nature12915

Wang, Y., Ma, Y., and Yuan, L. i. H. (2020). Carbon and water fluxes and their coupling in an alpine meadow ecosystem on the northeastern Tibetan Plateau. *Theor. Appl. Climatol*. 142, 1–18. doi: 10.1007/s00704-020-03303-3

Wang, Y., Zhou, G., and Wang, Y. (2008). Environmental effects on net ecosystem CO2 exchange at half-hour and month scales over Stipa krylovii steppe in northern China. *Agric. For. Meteorol*. 148, 714–722. doi: 10.1016/j.agrformet.2008.01.013

Xia, J., Niu, S., Ciais, P., Janssens, I. A., Chen, J., Ammann, C., et al. (2015). Joint control of terrestrial gross primary productivity by plant phenology and physiology. *Proc. Natl. Acad. Sci. U. S. A*. 112, 2788–2793. doi: 10.1073/pnas.1413090112

Xu, W. X., and Liu, X. D. (2007). Response of vegetation in the Qinghai-Tibet Plateau to global warming. *Chin. Geogr. Sci*. 17, 151–159. doi: 10.1007/s11769-007-0151-5

Xu, X., Shi, Z., Zhou, L. i. D., Sherry, X., and Luo, R. A. Y (2015). Plant community structure regulates responses of prairie soil respiration to decadal experimental warming. *Global. Change. Biol*. 21, 3846–3853. doi: 10.1111/gcb.12940

Yashiro, Y., Shizu, Y., Hirota, M., Shimono, A., and Ohtsuka, T. (2010). The role of shrub (*Potentilla fruticosa*). on ecosystem CO2 fluxes in an alpine shrub meadow. *J. Plant. Ecol-U*. 3, 89–97. doi: 10.1093/jpe/rtq011

Zhang, T., Zhang, Y., Xu, M., Zhu, J., Chen, N., Jiang, Y., et al. (2018). Water availability is more important than temperature in driving the carbon fluxes of an alpine meadow on the Tibetan Plateau. *Agric. For. Meteorol*. 256, 22–31. doi: 10.1016/j.agrformet.2018.02.027

Zhao, L., Xu, L. i. J., Zhou, S., Li, H., Gu, Y., and Zhao, S. X (2010). Seasonal variations in carbon dioxide exchange in an alpine wetland meadow on the Qinghai-Tibetan Plateau. *Biogeosciences*. 7, 1207–1221. doi: 10.5194/bg-7-1207-2010

Zhao, L., Xu, L. i. Y., Zhou, S., Gu, H., Yu, S., and Zhao, G. X (2006). Diurnal, seasonal and annual variation in net ecosystem CO2 exchange of an alpine shrubland on Qinghai-Tibetan plateau. *Global. Change. Biol* 12, 1940–1953. doi: 10.1111/j.1365-2486.2006.01197.x

Zhao, L., Zhao, L. i. Y. N., Xu, X. Q., Tang, S. X., and Yu, Y. H. GR, and Wang QX (2005). Comparative study of the net exchange of CO2 in 3 types of vegetation ecosystems on the Qinghai-Tibetan Plateau. *Chin. Sci. Bull*. 50, 1767–1774. doi: 10.1360/04wd0316

Zhou, H., Zhao, X., Tang, Y., Gu, S., and Zhou, L. (2005). Alpine grassland degradation and its control in the source region of the Yangtze and Yellow Rivers, China. *Grassland. Sci*. 51, 191–203. doi: 10.1111/j.1744-697X.2005.00028.x

Zhou, S., Zhang, Y., Caylor, K. K., Luo, Y. Q., Xiao, X. M., Ciais, P., et al. (2016). Explaining inter-annual variability of gross primary productivity from plant phenology and physiology. *Agric. For. Meteorol*. 226, 246–256. doi: 10.1016/j.agrformet.2016.06.010

Zhu, J., Chen, N., Zhang, Y., and Liu, Y. (2016). Effects of experimental warming on net ecosystem CO_2 exchange in Northern Xizang alpine meadow. *Chin. J. Plant. Ecol*. 40, 1219–1229. doi: 10.17521/cjpe.2016.0186

Zhu, J., Zhang, F., He, L. i. H., Li, H., and Yang, Y. Y, and Luo F (2020). Seasonal and Interannual Variations of CO2 Fluxes Over 10 Years in an Alpine Wetland on the Qinghai-Tibetan Plateau. *J. Geophys. Res-Biogeo*. 125. doi: 10.1029/2020JG006011

Zscheischler, J., Fatichi, S., Wolf, S., Blanken, P. D., Bohrer, G., Clark, K., et al. (2016). Short-term favorable weather conditions are an important control of interannual variability in carbon and water fluxes. *J. Geophys. Res-Biogeo*. 121, 2186–2198. doi: 10.1002/2016JG003503

Conflict of Interest: The authors declare that the research was conducted in the absence of any commercial or financial relationships that could be construed as a potential conflict of interest.

Publisher's Note: All claims expressed in this article are solely those of the authors and do not necessarily represent those of their affiliated organizations, or those of the publisher, the editors and the reviewers. Any product that may be evaluated in this article, or claim that may be made by its manufacturer, is not guaranteed or endorsed by the publisher.

frontiers | Frontiers in Plant Science

ORIGINAL RESEARCH
published: 27 June 2022
doi: 10.3389/fpls.2022.941144

Soil Respiration of Paddy Soils Were Stimulated by Semiconductor Minerals

Yinping Bai[1,2], Ling Nan[3], Qing Wang[2], Weiqi Wang[4], Jiangbo Hai[5], Xiaoya Yu[6], Qin Cao[2], Jing Huang[2], Rongping Zhang[2], Yunwei Han[1], Min Yang[1] and Gang Yang[2]**

[1]School of Environment and Resource, Southwest University of Science and Technology, Mianyang, China, [2]School of Life Science and Engineering, Southwest University of Science and Technology, Mianyang, China, [3]School of Resources and Environmental Engineering, Tianshui Normal University, Tianshui, China, [4]Key Laboratory of Humid Subtropical Eco-geographical Process, Ministry of Education, Fujian Normal University, Fuzhou, China, [5]College of Agronomy, Northwest A&F University, Yangling, China, [6]School of Tourism and Resources Environment, Qiannan Normal University for Nationalities, Duyun, China

OPEN ACCESS

Edited by:
Yong Li,
Chinese Academy of Forestry, China

Reviewed by:
Yinzhan Liu,
Henan University, China
Meirong Zong,
Changzhou University, China

***Correspondence:**
Gang Yang
yanggang903@swust.edu.cn
Qing Wang
qingw@imde.ac.cn

Specialty section:
This article was submitted to Functional Plant Ecology, a section of the journal Frontiers in Plant Science

Received: 11 May 2022
Accepted: 02 June 2022
Published: 27 June 2022

Citation:
Bai Y, Nan L, Wang Q, Wang W, Hai J, Yu X, Cao Q, Huang J, Zhang R, Han Y, Yang M and Yang G (2022) Soil Respiration of Paddy Soils Were Stimulated by Semiconductor Minerals. Front. Plant Sci. 13:941144. doi: 10.3389/fpls.2022.941144

Large quantities of semiconductor minerals on soil surfaces have a sensitive photoelectric response. These semiconductor minerals generate photo-electrons and photo-hole pairs that can stimulate soil oxidation–reduction reactions when exposed to sunlight. We speculated that the photocatalysis of semiconductor minerals would affect soil carbon cycles. As the main component of the carbon cycle, soil respiration from paddy soil is often ignored. Five rice cropping areas in China were chosen for soil sampling. Semiconductor minerals were measured, and three main semiconductor minerals including hematile, rutile, and manganosite were identified in the paddy soils. The identified semiconductor minerals consisted of iron, manganese, and titanium oxides. Content of Fe_2O_3, TiO_2, and MnO in the sampled soil was between 4.21–14%, 0.91–2.72%, and 0.02–0.22%, respectively. Most abundant semiconductor mineral was found in the DBDJ rice cropping area in Jilin province, with the highest content of Fe_2O_3 of 14%. Soils from the five main rice cropping areas were also identified as having strong photoelectric response characteristics. The highest photoelectric response was found in the DBDJ rice cropping area in Jilin province with a maximum photocurrent density of 0.48 μA/cm^2. Soil respiration was monitored under both dark and light (3,000 lux light density) conditions. Soil respiration rates in the five regions were (from highest to lowest): DBDJ > XNDJ > XBDJ > HZSJ > HNSJ. Soil respiration was positively correlated with semiconductor mineral content, and soil respiration was higher under the light treatment than the dark treatment in every rice cropping area. This result suggested that soil respiration was stimulated by semiconductor mineral photocatalysis. This analysis provided indirect evidence of the effect semiconductor mineral photocatalysis has on the carbon cycle within paddy soils, while exploring carbon conversion mechanisms that could provide a new perspective on the soil carbon cycle.

Keywords: semiconductor minerals, soil respiration, rice cropped area, photocatalysis, soil carbon

INTRODUCTION

Soil is the largest global carbon sink, with approximately 3,000 Pg of organic carbon (C) in deep soil layers (Kochy et al., 2015). Soil respiration [Rs, i.e., carbon dioxide (CO_2), which effluxes from the soil surface, including microbial respiration and root respiration; Zhou et al., 2016], contributes large amount of C flux between terrestrial ecosystems and the atmosphere. Approximately, 75–98 Pg of C is released into the atmosphere from the soil each year. That level increases exponentially under global climate change (Schlesinger and Andrews, 2000; Bond-Lamberty and Thomson, 2010; Crowther et al., 2016). Increasing Rs profoundly have been affects global carbon cycling in terrestrial ecosystems and enhance positive feedback loops that contribute to climate warming (Crowther et al., 2016; Wang et al., 2019b). Many previous studies have shown that soil warming accelerates carbon dioxide (CO_2) fluctuation in the atmosphere (Kampman et al., 2012; Valukenko et al., 2017). If the atmospheric temperature increases by one degree Celsius, global soil carbon stocks in surface soil are predicted to fall by 30–203 Pg carbon (Crowther et al., 2016; Melillo et al., 2017). Soil warming has been previously shown to be the main factor controlling Rs levels (Miao et al., 2020; Lu et al., 2022; Yang et al., 2022). Besides soil warming, other factors enhance Rs, including precipitation, increased nitrogen concentration, and phosphorus deposition (Wang et al., 2019a,b; Liu et al., 2021). However, the mechanisms that changing Rs remain primarily unknown. In addition to climate conditions, a recent study found that geochemistry is an essential factor in controlling soil carbon storage capacity. Some researchers have found that metallic oxides increase soil decomposition (Zhang et al., 2018). However, the relationship between metal oxides with the decomposition and transformation of soil organic matter is not yet clear.

Metallic oxides are soil minerals distributed widely throughout the soils (Liu and Liu, 2022). They affect soil organic matter decomposition by promoting adsorbing, catalytic conversion, and other biotic and abiotic processes (Keiluweit et al., 2015). Most metallic oxides are semiconductor minerals that form a thin coating on the earth's surface, have photoelectric conversion capabilities, and provide a driving force for redox geochemistry on the earth's surface through photon-to-electron conversions (Lu et al., 2019b). These inorganic minerals inducing photo catalytic processes have been observed in red soil, which could convert extraneous NO under visible light (Gan et al., 2021). Metallic oxides may also directly impact carbon cycles. It was reported that some kind of metallic oxide were used to enhance humus decomposition (Qi et al., 2019). Humus decomposition accelerated the process of carbon export (Kahkonen and Hakulinen, 2011), however, it remains unclear whether such semiconductor enhanced photocatalysis processes affect soil Rs. Paddy soil is typically rich in semiconductor minerals such as iron and manganese oxides, and has visible light photocatalytic properties affecting soil processes directly (Liu and Liu, 2022). Based on above mentioned analyses, we speculated that the photocatalysis of semiconductor minerals in paddy soils would affect soil carbon cycles. Therefore, the rice cropping region in China was chosen for soil sampling to study the relationship between Rs and semiconductor photocatalysis in paddy soils. This study's objective was to explore whether soil Rs would be positively affected or impeded by semiconductor photocatalysis under sunlight conditions due to enhanced photon to electron conversions.

Abbreviations: HNSJ, Double-cropped rice growing area in Southern China; HZSJ, Double-cropped rice growing area in Central China; XNDJ, Single-cropped rice growing area at Southwestern China; DBDJ, Single-cropped rice growing area in Northeastern China; XBDJ, Single-cropped rice growing area in Northwestern; TC, Total carbon; TN, Total nitrogen; TOC, Total organic carbon; TON, Total organic nitrogen; NH3-N, Ammonium nitrogen; NO3-N, Nitrate nitrogen; GD, Guangdong province; FJ, Fujian province; AH, Anhui province; SC, Sichuan province; YN, Yunnan province; GZ, Guizhou province; JL1 and JL2, Jilin province; NX, Ningxia Hui Autonomous Region.

MATERIALS AND METHODS

Study Site

The study sites were located in five major rice cropping areas in China (**Figure 1**). The sample sites cover the main rice production areas in China. Soils were sampled from double-cropped rice fields in the Guangdong province in Southern China (GD), double-cropped rice fields in Fujian (FJ) and Anhui (AH) province in Center China, single-cropped rice fields in Yunnan (YN) and Guizhou (GZ) province in western China, single-cropped rice fields in Jilin province (JL) in northeastern China, and single-cropped rice fields in the Ningxia (NX) Hui Autonomous Region in Northwestern China.

Data Collection and Laboratory Analysis

Soil Sampling

All soil samples were collected in 2018. Five soil samples were collected at each site from two different layers (0–5 and 5–10 cm deep). The soil samples were divided into two parts. The first fraction was passed through a 2.0 mm mesh sieve and stored at 4°C before measuring soil respiration, total organic carbon (TOC), total organic nitrogen (TON), ammonium nitrogen (NH_3-N), and nitrate nitrogen (NO_3-N) levels. The second fraction was air-dried and passed through a 0.15 mm mesh sieve before measuring total carbon (TC) and total nitrogen (TN) levels, and mineral characteristics.

Measurement of Soil Physicochemical Parameters

Total carbon and total nitrogen were determined using a total organic carbon analyzer (LIQUIL TOCII, Elementar, Germany) and an automatic azotometer (Kjeltec TM 8400 Analyzer Unit, Foss, Sweden). Moist soil (10 g) was weighed and put into a 250 ml conical bottle, with 50 ml 2 mol/L KCl added and centrifuged for 1 h with the rotation speed of 200 r/min. After extraction and filtration of the supernatant, NH_3-N and NO_3-N concentrations were determined using a total organic carbon analyzer (Continuous-Flow Analysis-AA3, SEAL, Germany). The filtered supernatant was then diluted 20 times to determine TOC and TON using a multi N/C 2100 (Analytik Jena, Germany). Soil respiration was determined using a closed culture method in the laboratory. Weigh 25 g of fresh soil and evenly spread

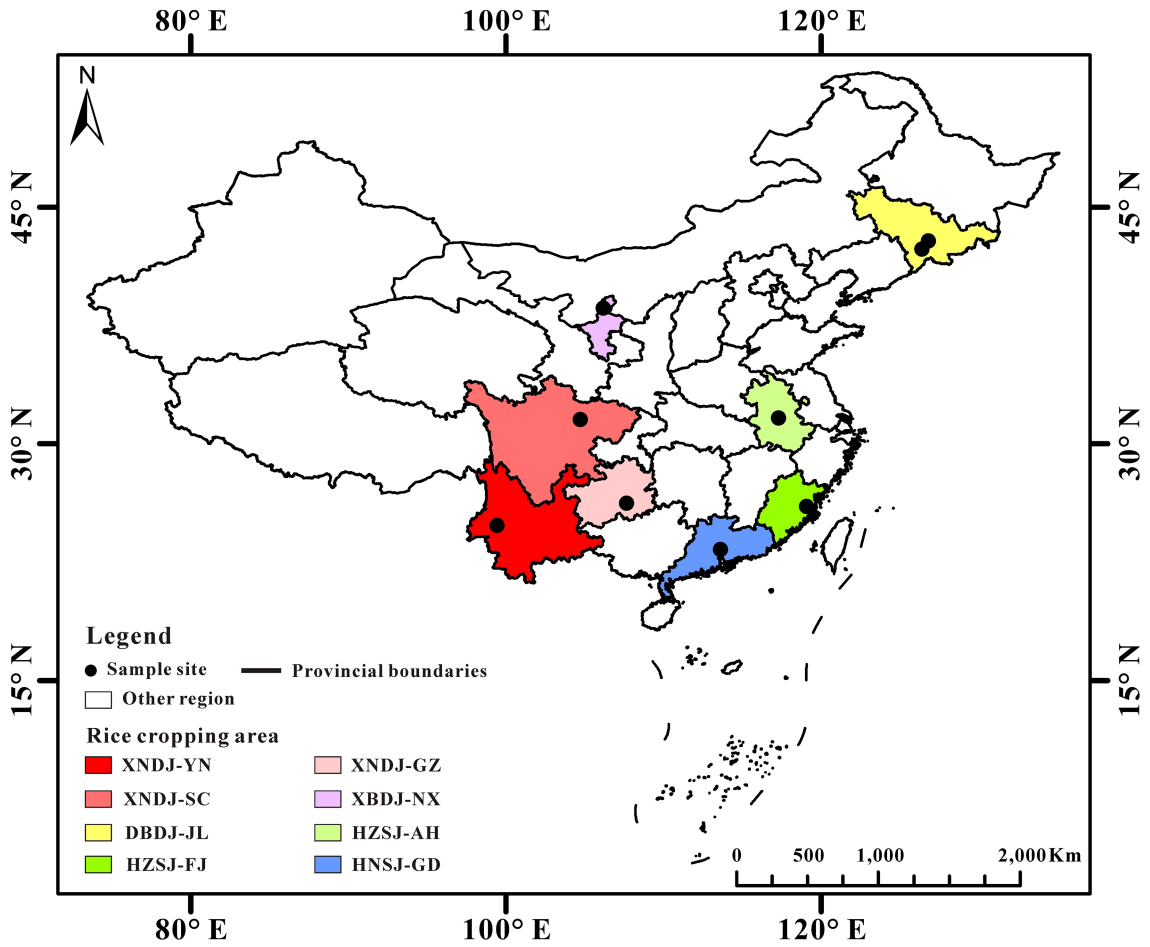

FIGURE 1 | Map of the study sites. Red indicates Yunnan province, Sichuan province, and Guizhou province (part of XNDJ rice cropping area). Yellow indicates Jilin province (part of DBDJ rice cropping area). Green color including Anhui province and Fujian province (part of HZSJ rice cropping area). Blue indicates Guangdong province (part of HNSJ rice cropping area). The five-pointed indicates the location of sample site.

it on the bottom of the 500 ml culture flask. Place a 25 ml beaker with 0.1 mol.L^{-1} NaOH solution in the culture flask, and quickly cover and seal the culture flask. Incubate at a constant temperature of 28°C for 24 h to determine the amount of carbon dioxide released. The CO_2 released from the soil was absorbed by a 0.1 mol.L^{-1} NaOH solution. Then, the NaOH was titrated with standard HCl solution (c = 0.05 mol.L^{-1}) to measure the amount of released CO_2 (Lu, 2002). X-ray fluorescence (XRF) spectrometry was used to determine the most abundant oxides in soil samples. Variations in soil physicochemical characteristics at the different rice cropping sites are shown in **Table 1**.

Semiconductor Minerals Analysis

The properties of the minerals were determined using X-ray diffraction (XRD). XRD patterns were obtained using an X Pert Pro X-ray diffract meter set to 2.2 kW with a Cu target, continuous scanning mode, working voltage of 60 kV, current of 50 mA, scanning range of 5–80°, and a scanning speed of 5°/min. The mineral phase mass fraction was quantitatively analyzed with the *k*-value method, which uses corundum (Al_2O_3) as the universal internal standard. The *K* value on the PDF card is the integral intensity of the strongest peak of the sample divided by the integral intensity of the strongest peak of the corundum after mixing the sample mass with the alumina (corundum) mass fraction in a 1:1 ratio. When corundum is used as an internal standard, the *K* value of the A phase is as follows:

$$K^{A}_{Al_2O_3} = \frac{K^{A}}{K^{Al_2O_3}} = \frac{I_A}{I_{Al_2O_3}}$$

According to the "adiabatic method," if there are *n* phases in the system, the mass fraction of the *X* phase is:

$$W_x = \frac{I_{Xi}}{K^{X}_{A} \sum_{i=A}^{N} \frac{I_i}{K^{i}_{A}}}$$

TABLE 1 | Soil physicochemical characteristics in different rice cropping areas.

Rice cropping area	Sample site	Location	Soil layer cm	pH	Optical band gap	TC %	TN %	TOC mg/kg	TON mg/kg	NH_3-N mg/kg	NO_3-N mg/kg
HNSJ	GD	N 113°15′31″ E 23°18′39″	0–5	6.3	2.54	1.1±0.02	0.16±0.01	42.2±2.2	14.5±0.4	2.9±0.05	17.5±0.23
			5–10	6.4		1.0±0.01	0.15±0.02	37.7±4.1	11.1±0.4	3.2±0.10	7.8±0.07
HZSJ	FJ	N 119°1′00″ E 26°1′00″	0–5	6.4	2.75	1.8±0.01	0.22±0.02	43.4±1.5	27.9±1.0	19.8±0.24	27.5±0.41
			5–10	6.3		1.7±0.05	0.20±0.01	46.9±2.1	25.1±1.6	14.0±0.04	31.8±0.11
HZSJ	AH	N 117°16′31″ E 31°38′11″	0–5	7.1	2.57	1.1±0.01	0.17±0.01	31.9±2.8	10.5±0.7	2.4±0.05	9.2±0.06
			5–10	7.0		0.7±0.01	0.11±0.01	28.5±7.2	10.1±0.9	2.8±0.1	5.8±0.02
XNDJ	SC	N 104°42′00″ E 31°32′00″	0–5	6.6	2.31	1.6±0.04	0.23±0.04	42.8±4.3	12.5±0.8	5.5±0.05	5.9±0.05
			5–10	6.5		1.5±0.01	0.21±0.01	34.3±1.2	12.1±0.4	5.4±0.06	6.2±0.03
XNDJ	YN	N 99°24′31″ E 24°49′7″	0–5	6.9	2.32	3.5±0.01	0.25±0.02	12.7±1.5	4.7±0.2	2.5±0.05	17.9±0.05
			5–10	6.9		3.5±0.09	0.24±0.02	12.3±3.2	14.1±1.1	2.6±0.10	13.3±0.11
XNDJ	GZ	N 107°77′18″ E 26°14′31″	0–5	6.5	2.28	3.5±0.01	0.41±0.01	56.7±1.5	29.1±1.1	3.1±0.05	34.2±0.09
			5–10	6.4		3.7±0.05	0.40±0.02	49.7±0.6	22.5±1.2	3.0±0.88	27.8±0.38
DBDJ	JL1	N 126°47′7″ E 42°51′61″	0–5	7.3	2.92	2.1±0.01	0.25±0.01	117.0±5.2	214.4±11.6	66.5±6.31	82.0±2.23
			5–10	7.3		1.9±0.04	0.19±0.02	117.0±1.5	30.7±0.8	24.7±0.05	9.3±0.20
DBDJ	JL2	N 126°22′6″ E 42°21′1″	0–5	7.0	2.39	5.6±2.7	0.49±0.22	65.5±2.5	20.6±0.7	6.9±0.07	11.0±0.07
			5–10	7.1		6.2±0.06	0.52±0.01	54.5±0.5	21.6±0.3	9.3±0.02	10.3±0.61
XBDJ	NX	N 106°9′18″ E 38°35′30″	0–5	7.0	2.70	2.4±0.01	0.13±0.01	116.0±3.6	10.8±0.5	2.5±0.04	4.7±0.01
			5–10	7.3		2.1±0.01	0.12±0.01	121.6±0.7	10.3±1.3	3.5±0.01	4.5±0.01

TC, total carbon; TN, total nitrogen; TOC, total organic carbon; TON, total organic nitrogen; NH_3-N, ammonium nitrogen; NO_3-N, nitrate nitrogen; HNSJ, double-cropped rice growing area in Southern China; HZSJ, double-cropped rice growing area in Central China; XNDJ, single-cropped rice growing area at Southwestern China; DBDJ, single-cropped rice growing area in Northeastern China; XBDJ, single-cropped rice growing area in Northwestern; GD, Guangdong province; FJ, Fujian province; AH, Anhui province; SC, Sichuan province; YN, Yunnan province; GZ, Guizhou province; JL1 and JL2, Jilin province; and NX, Ningxia Hui Autonomous Region.

Electrochemical Characterization

A soil electrode was used as the working electrode. To prepare the working electrode, 10 mg soil, 1,250 μl, 95% ethanol, and 1,250 μl of deionized water were mixed and were ultrasound for 30 min. Then, 100 μl of 5% naphthol (mass fraction) was added, and the mixture was ultrasound for another 20 min. About 200 μl of ultrasonic solution coating was applied to a 20 mm × 20 mm × 1.1 mm FTO (SnO_2: F) conductive glass, and the film area (10 mm × 20 mm) with even dispersal. After the film was formed, it was dried for 4 h in an oven at 40°C to obtain the soil electrode. A saturated calomel was used as the reference electrode, and a platinum wire was used as the counter electrode. KH_2PO_4 solution was added to a diaphragm three-electrode electrolytic cell. The pH of the solution was 5.33. The electrochemical workstation (CHI760E) was used and the applied voltage was set at 0.3 V to obtain the I-T curve. The light source for photocurrent was a 100 mW/cm^2 Xenon lamp with 50 s interval switch.

Band Gap Analysis

$BaSO_4$ was used as the reference sample, and the film sample was prepared by the integrating sphere method. The full wavelength (200–2,500 nm) diffuse reflectance spectrum was obtained by scanning a solid ultraviolet absorption spectrometer (Soildspec-3700). The semiconductor band gap width was calculated with the following equation using the Tauc plot method, taking hv as the abscissa and $(ahv)^2$ as the ordinate.

$$(\alpha hv)^2 = K\left(hv - E_g\right)$$

where a: light absorption coefficient; h: Planck constant; v: frequency; K: constant; and E_g: band gap width.

Data Analysis

Mean soil physical and chemical properties were calculated by averaging the data from each site. One-way ANOVAs were used to assess the effect of planting location on soil respiration (Duncan's test was used in the ANOVA analysis). Linear regression was used to assess the effect of semiconductor minerals on soil respiration. All sample data were confirmed for normal distribution before ANOVA analysis. SPSS 20.0 for Windows (SPSS Inc., Chicago, IL, United States) was used for all statistical analysis. Graphs were drawn using Sigmaplot 10.0. Differences were considered statistically significant when the value of p was lower than the alpha value ($\alpha = 0.05$).

RESULTS

Soil Physical and Chemical Properties

The concentrations of TC and TN decreased as soil depth increased in most rice cropping areas, except for the TC in XNDJ and TC and TN in the DBDJ rice cropping area within

Jilin province (**Table 1**). The TOC concentration range was from 12.3 to 121.6 mg/kg, and the TON concentration range was from 4.7 to 214.4 mg/kg. The TOC and TON concentrations of the soils sampled in Jilin province were much higher than it in any other province. The highest concentrations of NH_3 and NO_3 (66.5 and 82.0 mg/kg) were also found in Jilin province (**Table 1**).

The oxides identified through XRF analysis included SiO_2, Al_2O_3, Fe_2O_3, K_2O, CaO, TiO_2, MgO, MnO, P_2O_5, BaO, and Rb_2O. SiO_2 was the most abundant oxide with its content varying between 56.01 and 77.91 wt % (**Table 2**). The content of Al_2O_3 ranged between 13.99 and 28.01 wt %. The major semiconductor minerals identified in the five sites were hematile, rutile, and manganosite (**Table 3**; **Figure 2**). Fe_2O_3, TiO_2, and MnO Levels were the highest in the DBDJ rice cropping area in Jilin province (**Table 2**).

Photochemical Properties of the Soil

The prepared samples photo responses to intermittent irradiation with visible light at the bias potential of 0.3 V vs.SCE (**Figure 3**). The maximum photocurrent density of JL1 was 0.48 μA/cm^2 under illumination. Under dark conditions, the photocurrent density of FJ reached 0.46 μA/cm^2 which was the highest value observed. When the light and dark period began, the curves rose and fell sharply, indicating that the photoelectric catalysts in the soil produced electrons and holes that recombined and separated quickly. All the samples showed good reproducibility and stability under bias potential. According to UV/Vis diffuse reflectance, the band gap width ranges from 2.28 to 2.92 eV.

Soil Respiration and Its Relationship With Soil Semiconductors

In this study, soil respiration significantly differed among the rice cropping area (**Figure 4**). The highest soil respiration level found in the DBDJ rice cropping area was five times higher than in the HNSJ rice cropping area. From highest to lowest, measured soil respiration ranks at the sample sites were as follows: DBDJ > XNDJ > XBDJ > HZSJ > HNSJ. Soil respiration was significantly higher in the single cropping rice area was in the double cropping rice area (**Figure 4**). Illumination increased soil respiration levels in all the rice cropping areas. The influence of light was significant in the single cropping rice area (**Figure 5**). The soil respiration was 10.7, 9.2, and 21.7% higher in light treatment than that in dark treatment. Fe_2O_3, TiO_2, MnO_2, and the total concentration of these three oxides were significantly positively related to soil respiration. The R^2 value of this positive correlation was greater for Fe_2O_3 and MnO than for TiO_2 (**Figure 6**).

DISCUSSION

Semiconductor Minerals in Different Rice Cropping Area

Ferromanganese oxide as the main semiconductor minerals, which widely developed on soil surfaces and directly exposed

TABLE 2 | Oxide distributions in soils at different rice growing areas.

Rice cropping area	Sample site	Soil layer	SiO_2	Al_2O_3	Fe_2O_3	K_2O	TiO_2	CaO	P_2O_5	SO_3	MgO	BaO	MnO	Rb_2O
HNSJ	GD	0–5	62.58	26.86	4.26	3.6	1.06	0.56	0.49	0.18	0.14	0.05	0.03	0.02
HNSJ	GD	5–10	61.04	28.01	4.4	3.72	1.03	0.6	0.41	0.16	0.13	0.06	0.02	0.02
HZSJ	FJ	0–5	63.16	24.27	5.96	3.27	0.97	0.65	0.61	0.16	0.34	0.07	0.08	0.02
HZSJ	FJ	5–10	62.8	24.46	6.04	3.39	0.99	0.63	0.66	0.15	0.41	0.06	0.08	0.02
HZSJ	AH	0–5	77.12	14.43	4.26	1.91	0.99	0.77	0.13	0.11	/	0.06	0.06	0.01
HZSJ	AH	5–10	77.91	13.99	4.21	1.83	0.95	0.77	0.07	0.05	/	0.05	0.09	0.01
XNDJ	SC	0–5	70.09	18.31	6.33	3.1	0.91	0.79	0.16	0.11	/	0.07	0.05	0.02
XNDJ	SC	5–10	67.74	18.91	7.52	3.38	1.08	0.94	0.11	0.05	/	0.09	0.06	0.02
XNDJ	YN	0–5	57.52	20.44	8.21	2.91	1.17	7.72	0.56	0.21	0.81	0.06	0.15	0.02
XNDJ	YN	5–10	57.5	20.39	8.22	2.91	1.21	8.18	0.54	0.2	0.33	0.06	0.16	0.02
XNDJ	GZ	0–5	67.24	19.73	6.22	3.74	1.41	0.81	0.3	0.27	0.05	0.06	0.02	0.02
XNDJ	GZ	5–10	66.16	20.1	6.36	3.9	1.38	0.76	0.3	0.26	0.42	0.05	0.02	0.02
DBDJ	JL1	0–5	65.96	18.81	6.08	3.34	0.93	2.77	0.43	0.36	0.45	0.08	0.08	0.02
DBDJ	JL1	5–10	66.41	18.76	6.11	3.13	0.93	3.04	0.21	0.12	0.48	0.07	0.09	0.02
DBDJ	JL2	0–5	57.00	21.26	13.46	1.66	2.66	2.64	0.53	0.3	0.03	0.11	0.19	0.01
DBDJ	JL2	5–10	57.44	19.68	14	1.43	2.72	2.89	0.21	0.19	0.06	0.11	0.22	0.01
XBDJ	NX	0–5	56.01	15.35	5.24	3.05	0.69	12.43	0.36	0.39	4.99	0.09	0.07	0.01
XBDJ	NX	5–10	56.77	14.8	4.88	3.39	0.67	12.22	0.33	0.23	5.25	0.08	0.07	0.01

Oxide levels were measured using XRF technology. HNSJ, double-cropped rice growing area in Southern China; HZSJ, double-cropped rice growing area in Central China; XNDJ, single-cropped rice growing area at Southwestern China; DBDJ, single-cropped rice growing area in Northeastern China; XBDJ, single-cropped rice growing area in Northwestern; GD, Guangdong province; FJ, Fujian province; AH, Anhui province; SC, Sichuan province; YN, Yunnan province; GZ, Guizhou province; JL1 and JL2, Jilin province; and NX, Ningxia Hui Autonomous Region.

TABLE 3 | Phase mass fractions of minerals collected from five different rice soils.

Rice cropping area	Sample site	Soil layer	Rutile	Hematite	Manganosite	Others
HNSJ	GD	0–5 cm	3.59	0.12	3.11	93.18
HZSJ	FJ	0–5 cm	0.96	1.31	5.07	92.66
HZSJ	AH	0–5 cm	11.39	0.78	1.43	86.40
XNDJ	SC	0–5 cm	5.56	0.16	3.12	91.16
XNDJ	YN	0–5 cm	1.61	0.96	3.62	93.81
XNDJ	GZ	0–5 cm	0.86	0.55	4.70	93.89
DBDJ	JL1	0–5 cm	19.88	5.44	0.36	74.32
DBDJ	JL2	0–5 cm	16.89	1.72	3.18	78.22
XBDJ	NX	0–5 cm	10.23	1.50	2.57	85.71

HNSJ, double-cropped rice growing area in Southern China; HZSJ, double-cropped rice growing area in Central China; XNDJ, single-cropped rice growing area at Southwestern China; DBDJ, single-cropped rice growing area in Northeastern China; XBDJ, single-cropped rice growing area in Northwestern; GD, Guangdong province; FJ, Fujian province; AH, Anhui province; SC, Sichuan province; YN, Yunnan province; GZ, Guizhou province; JL1 and JL2, Jilin province; and NX, Ningxia Hui Autonomous Region.

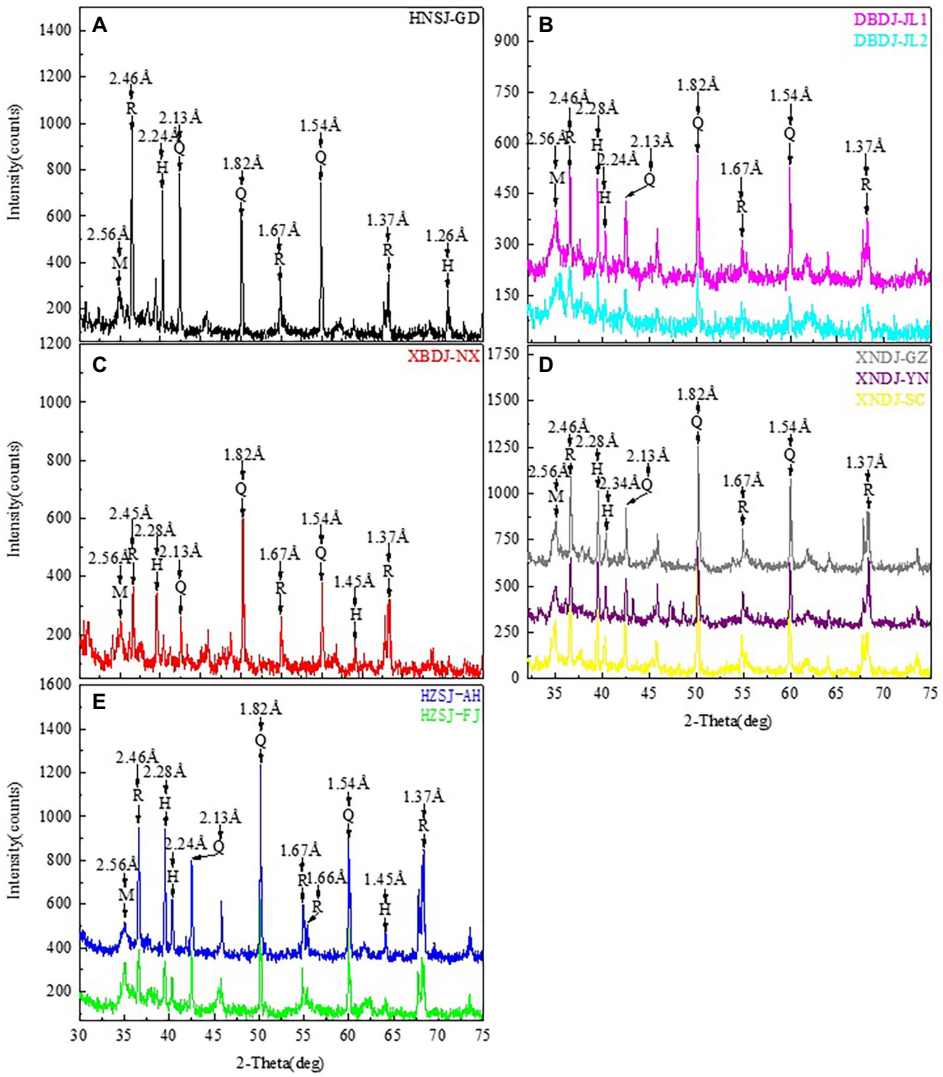

FIGURE 2 | Results of XRD analysis of five different rice soils. **(A–E)** XRD patterns of the 0–5 cm soil layer in HNSJ-GD, DBDJ-JL1, DBDJ-JL2, XBDJ-NX, XNDJ-GZ, XNDJ-YN, XNDJ-SC, HZSJ-AH, and HZSJ-FJ. H, Hematite; R, Rutile; M, Manganosite; and Q, Quartz. HNSJ-GD, double-cropped rice growing area in Guangdong province, Southern China; DBDJ-JL1 and DBDJ-JL2, single-cropped rice growing area in Jilin province, Northeastern China; XBDJ-NX, single-cropped rice growing area in Ningxia Hui Autonomous Region, Northwestern; XNDJ-GD, single-cropped rice growing area at Guangdong province, Southwestern China; XNDJ-YN and XNDJ-SC, single-cropped rice growing area at Yunnan province and Sichuan province, Southwestern China; and HZSJ-AH and HZSJ-FJ, double-cropped rice growing area in Fujian province and Anhui province, Central China.

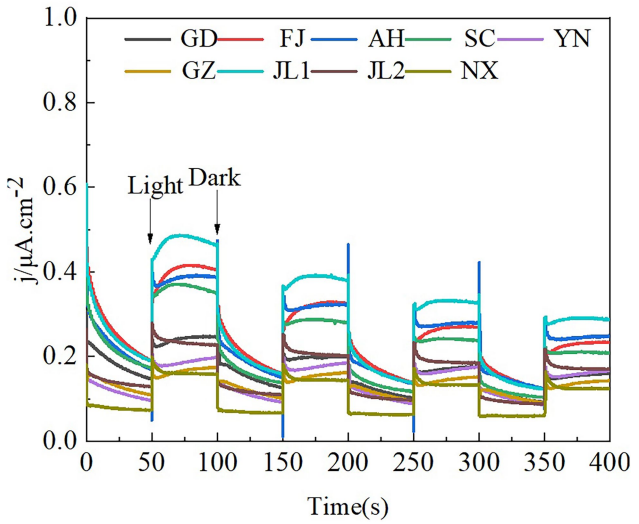

FIGURE 3 | The photocurrent responses of the soil collected from five different rice growing areas. GD, Guangdong province; FJ, Fujian province; AH, Anhui province; SC, Sichuan province; YN, Yunnan province; GZ, Guizhou province; JL1 and JL2, Jilin province; and NX, Ningxia Hui Autonomous Region.

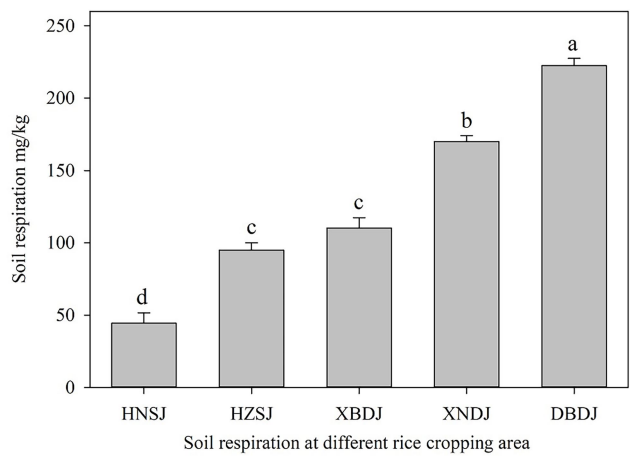

FIGURE 4 | Soil respiration levels (mean ± SE) in five different rice growing areas. Significant differences are indicated by different letters over the error bars ($p < 0.05$).

under sunlight and impact on ecosystem process (Lu et al., 2019a). In this study, semiconductors like hematite, rutile, and manganosite were found in rice paddy soils throughout China. Semiconductor minerals have important environmental properties and is often used to study their adsorption effect on Pollutants (Ma et al., 2018; Wu et al., 2021). Or using as an indicator for forecasting climate changes (Long et al., 2016). In recent years, the photocatalytic properties of semiconductor mineral have gradually attracted the attention of scientists (Xu et al., 2020). In this study, semiconductor minerals were found in high abundance at the single-cropped rice growing area in Jilin province, Northeastern China. And the lower abundance of semiconductor mineral was found in Southwestern and Southern China. The trends of semiconductor distribution in paddy soil probably attributed to China's surface annual sunshine duration because semiconductor minerals is always developed on the surface sides of rock and soils, which direct correspondence with sunlight exposure (Li and He, 2010; Lu et al., 2019a).

Semiconductor Minerals and Soil Respiration

When sunlight hits a semiconductor, photons with energy greater than the forbidden bandwidth can excite the electrons (e^-) in the valence band to the conduction band to leave a positively charged hole (h^+). Electrons and electron holes direct contact with oxygen and water molecules producing reactive oxygen species and hydroxyl radicals, stimulating a series of redox reactions (Gan et al., 2021; Li et al., 2021). Semiconductor mineral photocatalysis mediated redox reactions are widely used in solution systems (Luo et al., 2017), but their mechanisms within a soil system remain ambiguous. However, as the most basal process of a soil system, we posit that soil respiration must be affected by semiconductor mineral photocatalysis. In this study, we found the concentration of Fe_2O_3, TiO_2, MnO, and the sum of these three oxides were positively correlated with Rs. Fe_2O_3 has been identified as one of the most common iron oxides in soil (Gu et al., 1994). Congruently, it has also been reported that approximately 21.5% of the organic carbon in marine sediments are bound to iron oxides (Lalonde et al., 2012). Organic matter combined with iron oxides have been prone to photocatalytic interfacial reactions and accelerated decomposition of organic matter (Zhang et al., 2019; Chen et al., 2020). TiO_2, one of the most common metallic oxides in soil, was also found to stimulate soil mineralization and accelerate soil organic carbon loss (Fan et al., 2020). As shown in **Figures 3**, **5**, our data are consistent with the above mentioned results. Our study observed higher photocurrent and soil respiration in illuminated conditions, indicating that electron–hole pairs generated from the soil surface had a positive effect on soil respiration. Therefore, we can postulate that organic carbon is more easily decomposed in the presence of semiconductor minerals, which, inevitably, accelerate soil respiration rates. Based on the available evidence, we hypothesized that the photocatalytic properties of semiconductor minerals are what stimulated the decomposition of organic matter. Previous research has also produced results that are consistent with the data obtained in this current study (Pan et al., 2020). In this study, similar results were recorded in paddy soils of five different regions in China. These observations suggested that a large quantity of semiconductor minerals in surface soils dramatically affected soil respiration in the presence of light. A possible mechanism was that soil particles from the samples contained many metallic oxides and other semiconductor minerals. When sunlight hits these

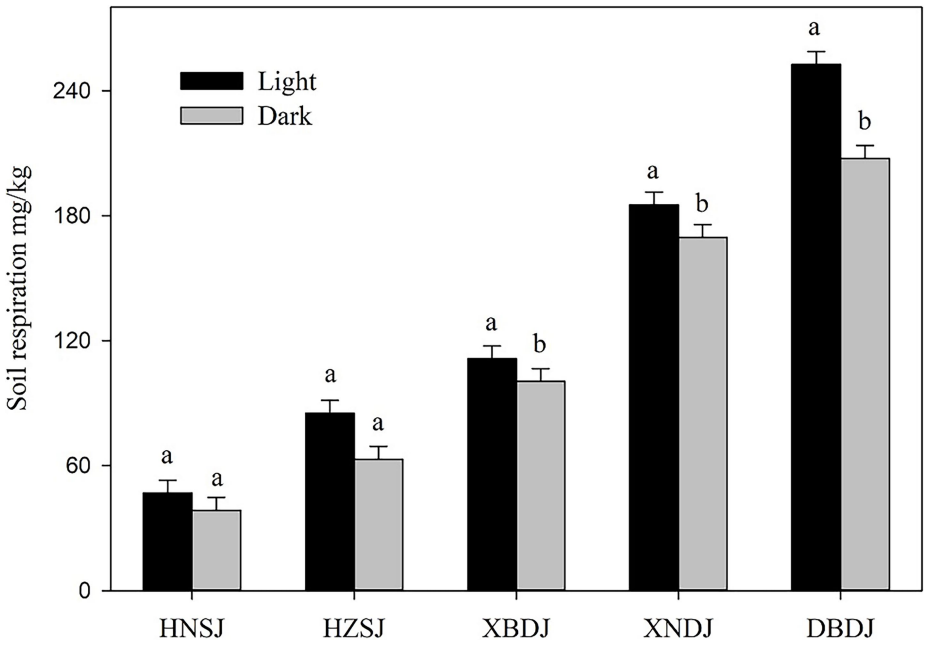

FIGURE 5 | Soil respiration levels (mean ± SE) in different rice growing areas under either dark or light treatments. Significant differences are indicated by different letters over the error bars ($p < 0.05$).

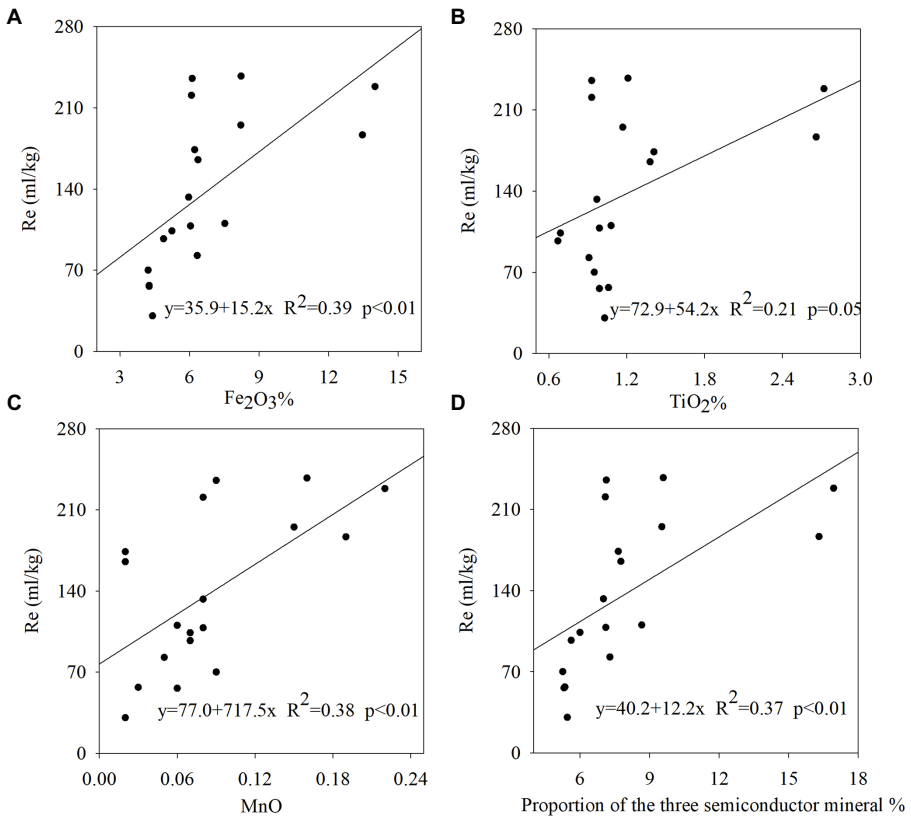

FIGURE 6 | Scatter plots and fitted regression lines for **(A)** soil respiration with Fe_2O_3%; **(B)** soil respiration with TiO_2%; **(C)** soil respiration with MnO%; and **(D)** soil respiration with proportion of the three semiconductor mineral.

semiconductor minerals, an electron–hole pair with strong oxidation–reduction abilities was excited (Liu et al., 2019; Gan et al., 2021). Our results showed that photo-electrons and photo-holes were separated within a certain period, and direct contact with oxygen and water molecules produced reactive oxygen species and hydroxyl radicals resulting in the production of effective photoelectrons that initiated a series of redox reactions that transmitted energy through the electron transport chain (Fan et al., 2016). Ultimately, this process affects all aspects of soil respiration.

The Implication of Semiconductor Minerals on Carbon Cycles

On the soil surface, the interaction between light and minerals occurs all the time. It has been reported that $1\,m^2$ of rock varnish-covered land surface can produce 2.23×10^{16} photoelectrons per second (Lu et al., 2019b), and the photoelectrons produced by these semiconducting minerals rapidly affect organic degradation and gradually impact on soil respiration (Xu et al., 2020). This research provides a new perspective for soil carbon cycle. However, this study ignored the role of microorganisms and the influences of lower valence metals. Previous study has shown that microorganisms are also influenced by the photocatalytic effect of semiconductor minerals (Lu et al., 2012). The evolutionary process of microbial community structure even influenced by photoelectron from semiconducting minerals (Ren et al., 2020). Therefore, future research in this field should examine the effects of semiconductor mineral photocatalysis on soil respiration, while also considering the role of microorganisms play in this process.

DATA AVAILABILITY STATEMENT

The original contributions presented in the study are included in the article/supplementary material; further inquiries can be directed to the corresponding authors.

AUTHOR CONTRIBUTIONS

GY, YB, and QW contributed to conception and design of the experiment. LN, WW, XY, YH, and MY carried out the collection of soil samples. YB analyzed all data, wrote the first draft of the manuscript, and revised it. JHu, RZ, JHa, and QC discussed the first draft. In addition, the natural science fund project applied by GY and QW provided financial support for this research. All authors contributed to the article and approved the submitted version.

FUNDING

This study was financially supported by the National Natural Science Foundation of China (42077038) and the Sichuan Science and Technology Program (2020YFS0020).

ACKNOWLEDGMENTS

We would like to thank Jeffery Hannah at Michigan State University for her assistance with English language and grammatical editing.

REFERENCES

Bond-Lamberty, B., and Thomson, A. (2010). Temperature-associated increases in the global soil respiration record. *Nature* 464, 579–582. doi: 10.1038/nature08930

Chen, C., Hall, S. J., Coward, E., and Thompson, A. (2020). Iron-mediated organic matter decomposition in humid soils can counteract protection. *Nat. Commun.* 11:2255. doi: 10.1038/s41467-020-16071-5

Crowther, T. W., Todd-Brown, K. E. O., Rowe, C. W., Wieder, W. R., Carey, J. C., Machmuller, M. B., et al. (2016). Quantifying global soil carbon losses in response to warming. *Nature* 540, 104–108. doi: 10.1038/nature20150

Fan, F., Zheng, R., Guo, X., Fang, X., Fu, Q., and Liu, S. (2020). Effects of TiO_2 nanoparticles on the mineralization of soil nitrogen in a lakeshore marsh. *Acta Sci. Circumst.* 40, 2220–2228. doi: 10.13671/j.hjkxxb.2020.0024

Fan, D., Zhu, J., Wang, X., Wang, S., and Li, C. (2016). Dual extraction of photogenerated electrons and holes from a ferroelectric Sr0.5Ba0.5Nb2O6 semiconductor. *ACS Appl. Mater. Interfaces* 8, 13857–13864. doi: 10.1021/acsami.6b00809

Gan, Y., Abdellatif, H. R. S., Zhang, J., Wan, Y., Zeng, Q., Chen, J., et al. (2021). Photocatalytic nitrogen-oxide conversion in red soil. *J. Clean. Prod.* 326:129377. doi: 10.1016/j.jclepro.2021.129377

Gu, B., Schmitt, J., Chen, Z., Liang, L., and McCarthy, J. F. (1994). Adsorption and desorption of natural organic matter on iron oxide: mechanisms and models. *Environ. Sci. Technol.* 28, 38–46. doi: 10.1021/es00050a007

Kahkonen, M. A., and Hakulinen, R. (2011). Hydrolytic enzyme activities, carbon dioxide production and the growth of litter degrading fungi in different soil layers in a coniferous forest in Northern Finland. *Eur. J. Soil Biol.* 47, 108–113. doi: 10.1016/j.ejsobi.2010.12.004

Kampman, N., Burnside, N. M., Shipton, Z. K., Chapman, H. J., Nicholl, J. A., Ellam, R. M., et al. (2012). Pulses of carbon dioxide emissions from intracrustal faults following climatic warming. *Nat. Geosci.* 5, 352–358. doi: 10.1038/ngeo1451

Keiluweit, M., Nico, P., Harmon, M. E., Mao, J., Pett-Ridge, J., and Kleber, M. (2015). Long-term litter decomposition controlled by manganese redox cycling. *Proc. Natl. Acad. Sci. U. S. A.* 112, 5253–5260. doi: 10.1073/pnas.1508945112

Kochy, M., Hiederer, R., and Freibauer, A. (2015). Global distribution of soil organic carbon—part 1: masses and frequency distributions of SOC stocks for the tropics, permafrost regions, wetlands, and the world. *Soil* 1, 351–365. doi: 10.5194/soil-1-351-2015

Lalonde, K., Mucci, A., Ouellet, A., and Gélinas, Y. (2012). Preservation of organic matter in sediments promoted by iron. *Nature* 483, 198–200. doi: 10.1038/nature10855

Li, G., Guo, J., Hu, Y., Wang, Y., Wang, J., Zhang, S., et al. (2021). Facile synthesis of the Z-scheme graphite-like carbon nitride/silver/silver phosphate nanocomposite for photocatalytic oxidative removal of nitric oxides under visible light. *J. Colloid Interface Sci.* 588, 110–121. doi: 10.1016/j.jcis.2020.12.063

Li, K., and He, F. (2010). Analysis on mainland China's solar energy distribution and potential to utilize solar energy as an alternative energy source. *Prog. Geogr.* 29, 1049–1054. doi: 10.11820/dlkxjz.2010.09.004

Liu, Y., and Liu, M. (2022). Composition of Typical Soil Minerals and Quantitative Analysis for Influence of Iron and Manganese Forms on Purple Soil Color in Northeastern Sichuan China. *Eurasian Soil Sci.* doi: 10.1134/S1064229322060084 (Epub ahead of print).

Liu, Y., Xie, L., Meng, F., Zhong, X., Dong, F., and Liu, M. (2019). Researches on photocatalytic degradation of methylene blue by birnessite and reaction mechanism. *Environ. Sci. Technol.* 42, 58–64. doi: 10.19672/j.cnki.1003-6504.2019.01.009

Liu, Y., Zhao, C., Guo, J., Zhang, L., Xuan, J., Chen, A., et al. (2021). Short-term phosphorus addition augments the effects of nitrogen addition on soil

respiration in a typical steppe. *Sci. Total Environ.* 761:143211. doi: 10.1016/j.scitotenv.2020.143211

Long, X., Ji, J., Barron, V., and Torrent, J. (2016). Climatic thresholds for pedogenic iron oxides under aerobic conditions: processes and their significance in paleoclimate reconstruction. *Quat. Sci. Rev.* 150, 264–277. doi: 10.1016/j.quascirev.2016.08.031

Lu, R. (2002). *Analysis Methods of Soil Agro-Chemistry (in Chinese)*. Beijing: China agriculture press.

Lu, A., Li, Y., Ding, H., and Wang, C. (2019a). "Mineral membrane" of the surface. *Acta Petrol. Sin.* 35, 119–128. doi: 10.18654/1000-0569/2019.01.08

Lu, A., Li, Y., Ding, H., Xu, X., Li, Y., Ren, G., et al. (2019b). Photoelectric conversion on Earth's surface via widespread Fe- and Mn-mineral coatings. *Proc. Natl. Acad. Sci. U. S. A.* 116, 9741–9746. doi: 10.1073/pnas.1902473116

Lu, A., Li, Y., Jin, S., Wang, X., Wu, X.-L., Zeng, C., et al. (2012). Growth of non-phototrophic microorganisms using solar energy through mineral photocatalysis. *Nat. Commun.* 3:768. doi: 10.1038/ncomms1768

Lu, B., Song, L., Zang, S., and Wang, H. (2022). Warming promotes soil CO2 and CH4 emissions but decreasing moisture inhibits CH4 emissions in the permafrost peatland of the great Xing'an mountains. *Sci. Total Environ.* 829:154725. doi: 10.1016/j.scitotenv.2022.154725

Luo, Z. P., Dong, F. Q., He, H. C., Liu, M. X., Ma, J., Li, G., et al. (2017). Photocatalytic reduction of U(VI) by P25 semiconductor mineral. *J. Nuclear Radiochem.* 39, 30–35. doi: 10.7538/hhx.2017.39.01.0030

Ma, Z., Shan, C., Liang, J., and Tong, M. (2018). Efficient adsorption of selenium(IV) from water by hematite modified magnetic nanoparticles. *Chemosphere* 193, 134–141. doi: 10.1016/j.chemosphere.2017.11.005

Melillo, J. M., Frey, S. D., DeAngelis, K. M., Werner, W. J., Bernard, M. J., Bowles, F. P., et al. (2017). Long-term pattern and magnitude of soil carbon feedback to the climate system in a warming world. *Science* 358, 101–105. doi: 10.1126/science.aan2874

Miao, Y., Liu, M., Xuan, J., Xu, W., Wang, S., Miao, R., et al. (2020). Effects of warming on soil respiration during the non-growing seasons in a semiarid temperate steppe. *J. Plant Ecol.* 13, 288–294. doi: 10.1093/jpe/rtaa013

Pan, Y., Bai, Y., He, H., Hu, W., Wang, Y., Zeng, J., et al. (2020). Paddy soil respiration induced by semiconductor minerals addition and photocatalysis in the red soil region of South China. *Chin. J. Soil Sci.* 51, 1103–1108. doi: 10.19336/j.cnki.trtb.2020.05.13

Qi, H., Wei, Z., Zhang, J., Zhao, Y., Wu, J., Gao, X., et al. (2019). Effect of MnO_2 on biotic and abiotic pathways of humic-like substance formation during composting of different raw materials. *Waste Manag.* 87, 326–334. doi: 10.1016/j.wasman.2019.02.022

Ren, G., Lu, A., Li, Y., Wang, C., and Ding, H. (2020). The evolutionary process of microbial community structure influenced by photoelectron from semiconducting minerals occuring at the "mineral membrane" on the earth surface. *Earth Sci. Front.* 27, 195–206. doi: 10.13745/j.esf.sf.2020.5.53

Schlesinger, W. H., and Andrews, J. A. (2000). Soil respiration and the global carbon cycle. *Biogeochemistry* 48, 7–20. doi: 10.1023/A:1006247623877

Valukenko, N. V., Kotlyakov, V. M., and Sonechkin, D. M. (2017). The connection between the growth of anthropogenic carbon dioxide in the atmosphere and the current climate warming. *Dokl. Earth Sci.* 477, 1307–1310. doi: 10.1134/s1028334x17110083

Wang, R., Hu, Y., Wang, Y., Ali, S., Liu, Q., and Guo, S. (2019a). Nitrogen application increases soil respiration but decreases temperature sensitivity: combined effects of crop and soil properties in a semiarid agroecosystem. *Geoderma* 353, 320–330. doi: 10.1016/j.geoderma.2019.07.019

Wang, Z., McKenna, T. P., Schellenberg, M. P., Tang, S., Zhang, Y., Ta, N., et al. (2019b). Soil respiration response to alterations in precipitation and nitrogen addition in a desert steppe in northern China. *Sci. Total Environ.* 688, 231–242. doi: 10.1016/j.scitotenv.2019.05.419

Wu, X., Hu, J., Wu, F., Zhang, X., Wang, B., Yang, Y., et al. (2021). Application of TiO_2 nanoparticles to reduce bioaccumulation of arsenic in rice seedlings (*Oryza sativa* L.): a mechanistic study. *J. Hazard. Mater.* 405:124047. doi: 10.1016/j.jhazmat.2020.124047

Xu, X., Ding, H., Li, Y., Wang, H., and Lu, A. (2020). The Micro-scaled characterization of natural terrestrial ferromanganese coatings and their semiconducting properties. *CoatingsTech* 10:666. doi: 10.3390/coatings10070666

Yang, J., Jia, X., Ma, H., Chen, X., Liu, J., Shangguan, Z., et al. (2022). Effects of warming and precipitation changes on soil GHG fluxes: a meta-analysis. *Sci. Total Environ.* 827:154351. doi: 10.1016/j.scitotenv.2022.154351

Zhang, Y., Yue, D., Lu, X., Zhao, K., and Ma, H. (2018). Role of ferric oxide in abiotic humification enhancement of organic matter. *J. Mat. Cycles Waste Manag.* 19, 585–591. doi: 10.1007/s10163-015-0435-2

Zhang, L., Zhu, Y., Zhang, J., Zeng, G., Dong, H., Cao, W., et al. (2019). Impacts of iron oxide nanoparticles on organic matter degradation and microbial enzyme activities during agricultural waste composting. *Waste Manag.* 95, 289–297. doi: 10.1016/j.wasman.2019.06.025

Zhou, L., Zhou, X., Shao, J., Nie, Y., He, Y., Jiang, L., et al. (2016). Interactive effects of global change factors on soil respiration and its components: a meta-analysis. *Glob. Chang. Biol.* 22, 3157–3169. doi: 10.1111/gcb.13253

Conflict of Interest: The authors declare that the research was conducted in the absence of any commercial or financial relationships that could be construed as a potential conflict of interest.

Publisher's Note: All claims expressed in this article are solely those of the authors and do not necessarily represent those of their affiliated organizations, or those of the publisher, the editors and the reviewers. Any product that may be evaluated in this article, or claim that may be made by its manufacturer, is not guaranteed or endorsed by the publisher.

frontiers | Frontiers in Plant Science

ORIGINAL RESEARCH
published: 06 July 2022
doi: 10.3389/fpls.2022.946129

Rising Shallow Groundwater Level May Facilitate Seed Persistence in the Supratidal Wetlands of the Yellow River Delta

*Lu Feng, Ling Peng, Qian Cui, Hong-Jun Yang, Jin-Zhao Ma and Jing-Tao Liu**

Shandong Provincial Key Laboratory of Eco-Environmental Science for the Yellow River Delta, Binzhou University, Binzhou, China

The saline groundwater level of many supratidal wetlands is rising, which is expected to continue into the future because of sea level rise by the changing climate. Plant persistence strategies are increasingly important in the face of changing climate. However, the response of seed persistence to increasing groundwater level and salinity conditions is poorly understood despite its importance for the continuous regeneration of plant populations. Here, we determined the initial seed germinability and viability of seven species from supratidal wetlands in the Yellow River Delta and then stored the seeds for 90 days. The storage treatments consisted of two factors: groundwater level (to maintain moist and saturated conditions) and groundwater salinity (0, 10, 20, and 30 g/L). After retrieval from experimental storage, seed persistence was assessed. We verified that the annuals showed greater seed persistence than the perennials in the supratidal wetlands. Overall, seed persistence was greater after storage in saturated conditions than moist conditions. Salinity positively affected seed persistence under moist conditions. Surprisingly, we also found that higher groundwater salinity was associated with faster germination speed after storage. These results indicate that, once dispersed into habitats with high groundwater levels and high groundwater salinity in supratidal wetlands, many species of seeds may not germinate but maintain viability for some amount of time to respond to climate change.

Keywords: sea level rise, groundwater level, groundwater salinity, seed persistence, supratidal wetlands

OPEN ACCESS

Edited by:
Yong Li,
Chinese Academy of Forestry, China

Reviewed by:
Guangxuan Han,
Yantai Institute of Coastal Zone Research (CAS), China
Hongyuan Ma,
Northeast Institute of Geography and Agroecology (CAS), China

***Correspondence:**
Jing-Tao Liu
ljteco@126.com

Specialty section:
This article was submitted to Functional Plant Ecology, a section of the journal Frontiers in Plant Science

Received: *17 May 2022*
Accepted: *20 June 2022*
Published: *06 July 2022*

Citation:
Feng L, Peng L, Cui Q, Yang H-J, Ma J-Z and Liu J-T (2022) Rising Shallow Groundwater Level May Facilitate Seed Persistence in the Supratidal Wetlands of the Yellow River Delta. Front. Plant Sci. 13:946129. doi: 10.3389/fpls.2022.946129

INTRODUCTION

Persistent seeds, as an important component in the soil seed bank, can represent a reserve of genetic potential that accumulates over time (Sallon et al., 2008). Thus, they have been shown to be an important correlate of population persistence (Saatkamp et al., 2009) that play a crucial role in terrestrial ecosystem conservation and restoration (Thompson et al., 1998; Yang et al., 2021).

Coastal vegetation usually exhibits zonation patterns along an environmental gradient caused by the interaction of land and sea (Antunes et al., 2018). Supratidal wetlands lie beyond the reach of tides, and their hydrological regimes are dominated by precipitation and a shallow saline groundwater level in the vertical direction (Han et al., 2015). Sea level rise, which is induced by events such as climate change and anthropogenic activities (e.g., sea reclamation, embanking,

and groundwater pumping), has significant effects on the hydrological conditions of shallow groundwater (Befus et al., 2020). Changes in shallow groundwater directly affect soil moisture and salt conditions, which further affects species distributions (Wilson et al., 2015) and community species diversity (Antonellini and Mollema, 2010; Feng et al., 2018) in supratidal wetlands. It is well-known that persistent soil seed banks play a fundamental role in the assembly of the standing vegetation (Greulich et al., 2019). Mature seeds can therefore be dispersed into conditions that vary along such gradients, which can affect their persistence (Long et al., 2015), however, how soil moisture and salinity caused by groundwater level changes influence seed persistence in supratidal wetlands has received little attention.

The ability of mature seeds to remain viable on the parent plant or on/in the soil referred to as seed persistence (Long et al., 2015; Chen et al., 2021). To some extent, seed persistence varies among species and populations, and depends on reproductive strategies (Rago et al., 2020). Usually, there is formation of a substantial and potentially persistent seed bank when annuals and biennials, which often exhibit r-strategy, produce long-lived seeds with multiyear dormancy; this provides the potential to live through periods of unfavorable conditions (Ooi et al., 2009; Ma et al., 2021). In contrast to annuals and biennials, perennials may have relatively little effect on soil seed banks because their reproductive strategy results in low production of seeds or short-lived seeds (Baskin and Baskin, 2014). Thus, seed persistence can be roughly predicted by species' reproductive strategies.

Knowledge of the main factors that regulate seed persistence in supratidal wetlands is limited. Usually, seed persistence depends on the physical and physiological characteristics of seeds and how they are affected by the biotic and abiotic environment (Long et al., 2015). In supratidal wetlands, soil moisture and salinity induced by groundwater level gradients may be two factors likely to play roles in seed persistence but have received insufficient attention. Generally, soil moisture affects seed persistence by influencing regulation of germination or dormancy (Rubio-Casal et al., 2003; Hu et al., 2018; Garcia et al., 2020). Kaiser and Pirhofer-Walzl (2015) tested the influence of groundwater level on the seed survival rate of eight wet meadow plant species, and they found that more viable seeds survived at lower groundwater levels compared with higher groundwater levels. *Polygonum aviculare* seeds were induced into dormancy by exposure to low moisture conditions (Batlla et al., 2007). Unfortunately, it is difficult to test the effects of groundwater level gradients on persistence of naturally buried seeds in supratidal wetlands because seeds of different species disperse at different times.

High salinity can inhibit seed germination by reducing the water potential of the soil solution to below the threshold water potential for a species (Long et al., 2015), and regulate seed dormancy and germination by triggering significantly lower abundance of seed proteins involved in several biological processes (e.g., primary metabolism, energy, stress response, and stability) (Debez et al., 2018), and enhance reactive oxygen species (ROS) accumulation by activating the transcription of NADPH oxidase genes (Luo et al., 2021). For example, *Calile maritima* is an annual halophyte on Mediterranean coasts which can produce transiently dormant seeds to inhibit germination under high salinity (Debez et al., 2018). Increasing salt decreased seed germination of *Haloxylon stockii*; however, when shifted from salt solution to distilled water, the ungerminated seeds showed high germination recovery (Rasheed et al., 2019). Thus, inhibition of germination allows seeds to become incorporated into the soil, which is the first stage of seed bank formation.

Plants have evolved several unique mechanisms to adapt to environmental changes. Seed dormancy, a nearly ubiquitous feature across all taxa, is a behavior of plants to prevent seeds from germinating under unfavorable environmental conditions (Gremer and Venable, 2014; Nonogaki, 2014), which contributes to adaptive survival under fluctuating ambient environments. Seed dormancy can range from a few weeks or months to decades or centuries (Finch-Savage and Leubner-Metzger, 2006). It is widely assumed that dormancy may be an effective mechanism that facilitates seed persistence in soil (Cao et al., 2014; Collette and Ooi, 2020). For certain species, such as *Arabidopsis thaliana*, water limitation (Auge et al., 2015) and salt stress (Cheng et al., 2016) can suppress seed germination by enhancing dormancy. Past studies found that salinity acted as an environmental filter that could reduce germinable soil seed bank abundance and Shannon diversity (Kottler and Gedan, 2020; Feng et al., 2021); however, seed viability was not tested in these studies. Thus, we cannot confirm whether high salinity prevented seed germination or killed the seeds.

Seed persistence under experimental conditions can be used to represent the potential of a species to form soil seed banks in nature (Saatkamp et al., 2009). This study complements previous descriptive work (Kottler and Gedan, 2020; Feng et al., 2021) by examining seed fate (viability maintenance, germination, or death) after storage by conducting a burial experiment designed to explore how changes of groundwater level and groundwater salinity affect seed persistence. Also, we used the term germinability to indicate seed germination ability, since some viable seeds may not germinate due to dormancy after storage. We observed changes of seed internal ultrastructure before and after the storage treatments to determine if sharp loss of viability during storage was related to internal physiological structure. We hypothesized that: (1) groundwater level and groundwater salinity have varied effects on seed persistence of the tested plant species, and the strength of this effect depends on the seed bank type of the plant species; (2) the negative relationship found between groundwater level and viable seed number (Kaiser and Pirhofer-Walzl, 2015) suggested that we may observe a negative relationship between groundwater level and seed persistence; and (3) high groundwater salinity favors seed persistence in the soil because inhibited germination allows seeds to become incorporated into the soil seed banks.

MATERIALS AND METHODS

Seed Collection

We selected seven of the most frequent and abundant species in supratidal wetlands of the Yellow River Delta. Seeds were obtained from three annual species, *Suaeda salsa*, *Chenopodium*

album, and *Lepidium latifolium*, and four perennial species, *Phragmites australis*, *Cynanchum chinense*, *Apocynum venetum*, and *Imperata cylindrica*. We collected fully ripened seeds of the selected species at maturity in 2019. Seeds were harvested from arbitrarily chosen individuals grown 1 m away from each other and thoroughly mixed. After collection, they were stored in paper bags in the dark at room temperature with 45–50% air humidity until the beginning of the burial experiment. Voucher specimens were deposited at Binzhou University under collection numbers 202006001, 202006002, 202010001, 202010002, 202010003, 202010004, and 202010005.

Experimental Design

The groundwater in the Yellow River Delta is affected by seawater mainly NaCl (average concentration 20 g/L). We used a factorial design with four replicates to test the effects of different groundwater levels and groundwater salinity on seed persistence of seven species. There were two groundwater levels (low groundwater level, in which the vertical distance from the groundwater to the buried seeds was approximately 3 cm to create a moist condition for the buried seeds; and high groundwater level, in which the groundwater submerged the buried seeds to create a saturated condition for the buried seeds) and four groundwater salinity levels (NaCl concentrations: none added, 10, 20, and 30 g/L).

We simulated soil with quartz sand to eliminate the interference of physical and chemical factors. We added 400 g sterile quartz sand (diameter, 2–4 mm) in each 520-mL plastic tissue culture flask and drilled 32 small holes in the body and bottom of the flask. We put each plastic tissue culture flask into matching 1000-mL plastic bowl to simulate different groundwater levels by adding different amounts of water in plastic bowls. In addition, to test the effects of dry storage on seed persistence, seeds were also stored in dry quartz sand without any water storage treatment. The experimental device is shown in **Figure 1**.

Before storage, some seeds were used to determine the initial germination and viability percentages as a baseline for comparison (mean ± 1 SE across Petri dishes: 85.8 ± 1.6 and 87.5 ± 0.8%, for *P. australis*; 76.7 ± 3.0% and 79.7 ± 2.9% for *S. salsa*; 72.5 ± 3.9% and 76.7 ± 2.4% for *C. chinense*; 64.2 ± 1.6% and 72.5 ± 4.3% for *C. album*; 5.0 ± 1.0% and 47.5 ± 1.6% for *A. venetum*; 0.8 ± 0.8% and 61.7 ± 6.3% for *I. cylindrica*; and 5.0 ± 2.2% and 80.8 ± 1.0% for *L. latifolium*, respectively). We put 50 seeds of each species into small packets made of polyamide fabrics with 1-mm mesh width. After being tagged by colored clips, the seed packets were buried 1.5-cm below the top of the quartz sand in each tissue culture flask and stored in the different treatments for 90 days. To decrease the possible effect of strong light on germination, all devices were kept in the shade (20–30 μmol $m^{-2}s^{-1}$).

During storage, the air humidity in the tissue culture flasks was 50–55% for dry storage and 60–65% for low groundwater level storage. After 90 days of storage, the moisture content of the quartz sand with buried seed packets was measured by oven drying. The moisture content of the quartz sand was 0.03% for dry storage, 10.6–11.0% for low groundwater level storage, and 32.9–34.3% for high groundwater level storage. The seed packets were removed from their respective tissue culture flasks, and seed germination and viability percentages were assessed. Although the devices were shaded during the burial experiment, very few seeds germinated. The germinated seeds were considered to have lost persistence. To test germination percentage, we made a culture medium in a 9-cm diameter Petri dish with two layers of filter paper (Feng et al., 2021). We added 2 mL of sterile distilled water to each Petri dish for culturing in a growth chamber (Shanghai Boxun Medical Biological Instrument Co. Ltd., Shanghai, China). The

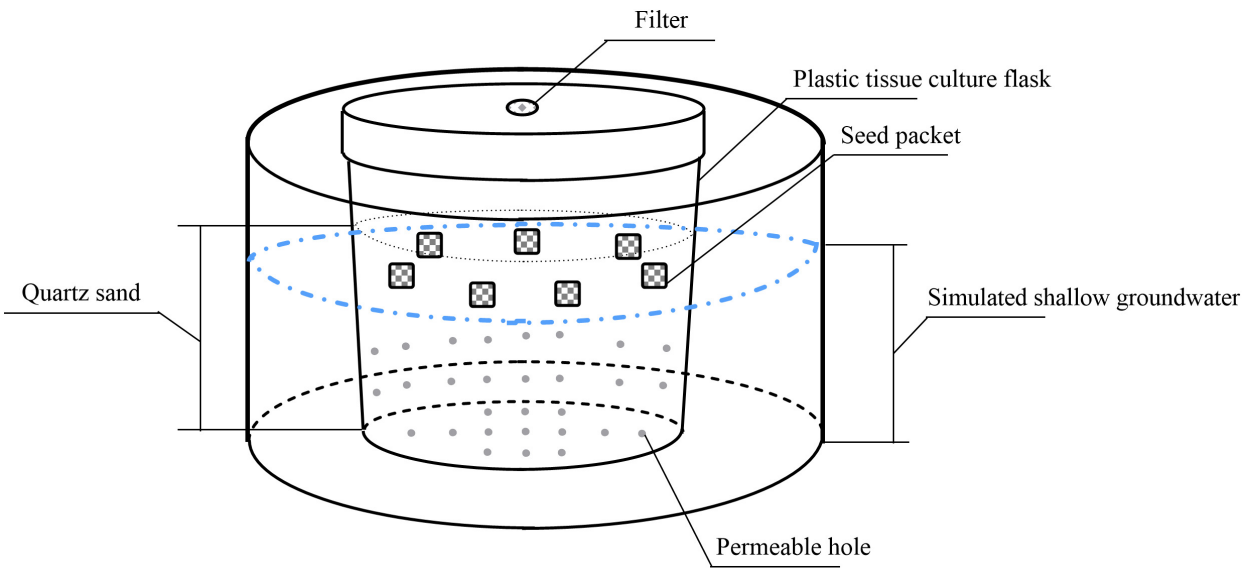

FIGURE 1 | Schematic diagram of the experimental setup showing seed packet layout.

cultivation conditions were: 12: 12 h (day: night), light 60: 0 μmol $m^{-2}s^{-1}$, and temperature 25: 20°C. Germination was recorded upon radicle emergence. The number of germinated seeds was counted every third day during the first 2 weeks; thereafter, scoring was carried out once per week until the germination experiment was concluded after 4 weeks. The Petri dishes were placed in a new randomized sequence when the seeds were counted to minimize the effect of possible unequal abiotic conditions in the artificial climate chamber. At the end of the cultivation period, the viability of seeds that did not germinate was checked by opening the seeds and checking the embryos. Seeds with white and firm endosperms were considered viable. Seeds with black/dark brown or mushy endosperms were scored as inviable (Ooi et al., 2004, 2009; Baskin and Baskin, 2014). The seeds that maintained viability but did not germinate were considered dormant (Chantre et al., 2009).

In addition, we selected the seeds with sharp changes in viability percentage to study the changes of seed internal morphological features. The seeds were fixed in 2.5% glutaraldehyde at room temperature for 2 h for subsequent analysis with a scanning electron microscope (SEM). After an extensive rinse with precooled phosphate buffer (pH 7.0), the samples were post-fixed in 1% OsO_4 overnight at room temperature. The following day, the samples were dehydrated in a graded ethanol series (30, 50, 70, 80, 95, and 100%) and 100% acetone. The samples were then placed overnight in labeled molds that were filled with 100% Spurr's medium. The samples were vertically sectioned on a ultramicrotome (Leica EM UC7, Leica Microsystems, Wetzlar, Germany) at 90 nm and then examined with a Hitachi SU8010 field-emission SEM (Hitachi SU8010, Hitachi Ltd., Tokyo, Japan).

Data Analysis

We analyzed the germination percentage (GP), viability percentage (VP), dormancy percentage (DP), and mean germination time (MGT) of seeds after storages. We used the term "germinability" to represent the ability of seeds to germinate after storages under the lab culture conditions. Germinability was inferred based on the germinability index (GI), which represents the rate of germination conservation. We also used the viability index (VI), which represented the rate of viability conservation, to infer seed persistence based on the ability of seeds to maintain

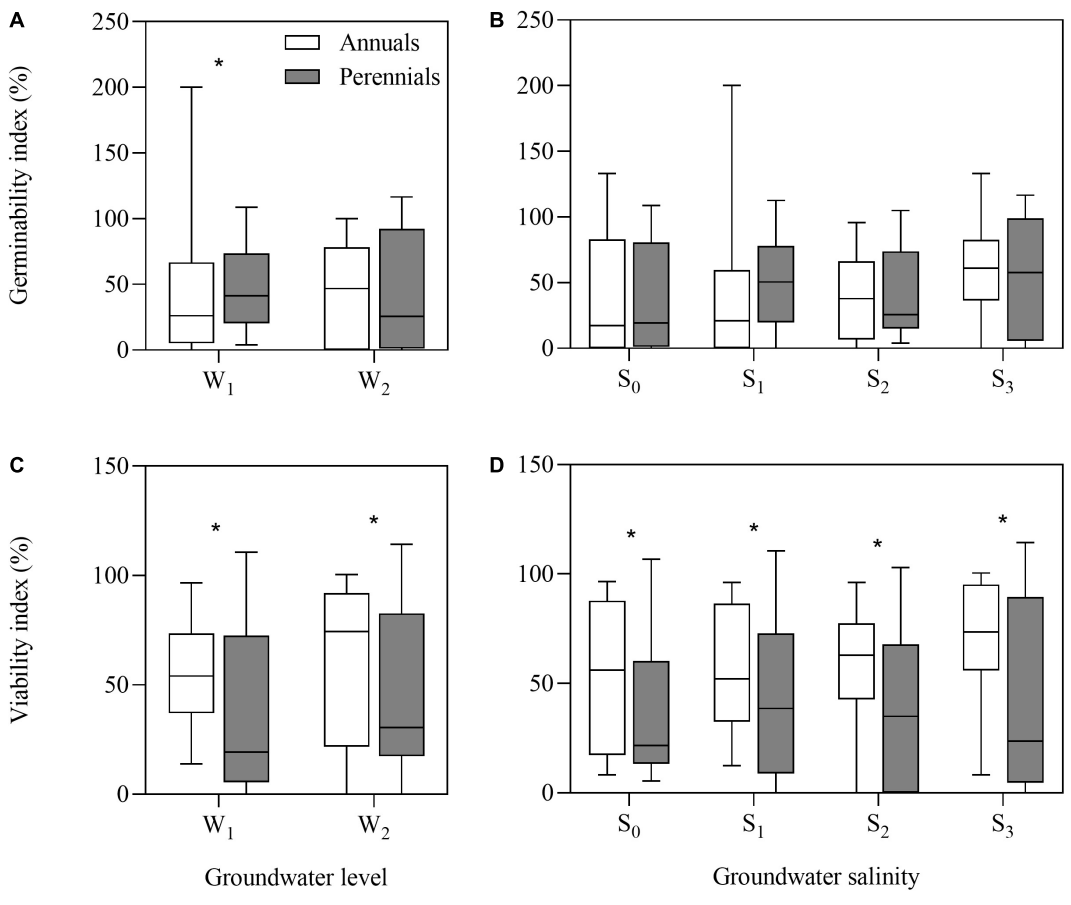

FIGURE 2 | Germinability index **(A,B)** and viability index **(C,D)** of annual and perennial species. W_1, low groundwater level; W_2, high groundwater level; S_0, no added salt; S_1, salt concentration of 10 g/L; S_2, salt concentration of 20 g/L; S_3, salt concentration of 30 g/L. Significant differences between the annual and perennial species are shown by "*." $^*P < 0.05$.

viability under storage conditions. The indexes were calculated as follows:

$$GP(\%) = \frac{\text{Number of germinated seeds}}{\text{Total number of seeds}} \times 100 \quad (1)$$

$$VP(\%) = \frac{\text{Number of dyeing seeds}}{\text{Total number of seeds}} \times 100 \quad (2)$$

$$DP(\%) = \frac{\text{Number of dyeing seeds} - \text{Number of germinated seeds}}{\text{Total number of seeds}} \times 100 \quad (3)$$

$$GI(\%) = \frac{\text{Final GP}}{\text{Initial GP}} \times 100 \quad (4)$$

$$VI(\%) = \frac{\text{Final DP}}{\text{Initial DP}} \times 100 \quad (5)$$

$$MGT(\text{days}) = \frac{\sum(Nt \times Dt)}{\sum Nt} \quad (6)$$

where Nt represents the number of germinated seeds on day t and Dt represents the corresponding number of days.

Statistical analyses were performed using SPSS Statistics version 25.0 (IBM Corp, 2017). Prior to analysis, data were examined for normality, and they were log-transformed as needed. Transformed values were utilized in all subsequent statistical analyses. Untransformed values were presented for all means and standard errors. A two-way Analysis of Variance (ANOVA) was used to examine the effects of groundwater level, groundwater salinity, and their interaction on seed GI and VI (dry treatment was excluded). *T*-tests were used to examine the differences of seed GI and VI between the annual and perennial species, and the effects of groundwater level on GI and VI for each species. One-way ANOVA was used to examine the differences of GI and VI among treatments in each group (W_0S_0, W_1S_0, and W_2S_0; W_1S_0, W_1S_1, W_1S_2, and W_1S_3; W_2S_0, W_2S_1, W_2S_2, and W_2S_3). Group abbreviations are based on groundwater level and groundwater salinity of each set of conditions. For groundwater level, W_0 indicates no water, W_1 indicates low groundwater level, and W_2 indicates high groundwater level. For groundwater salinity, S_0 indicates no added salt; S_1 indicates 10 g/L; S_2 indicates 20 g/L, and S_3 indicates 30 g/L. Tukey HSD tests were used for multiple comparisons when the data satisfied the homogeneity of variance test; otherwise, Games–Howell tests were used. Regression analysis curve estimation was used to build optimal models between DP and VI (dry treatment was included), and between DP, GI, VI, and MGT and groundwater salinity. Significance was set to $P < 0.05$.

RESULTS

Differences Between Annual and Perennial Species

After storage treatments (including dry storage), seed germinability index (GI) of annuals and perennials had no significant differences, but seed viability index (VI) of annuals (average, 63.0%) was significantly higher than that of perennials (average, 35.0%) ($P = 0.024$). After groundwater level and groundwater salinity treatments, the annual species had greater VI than the perennial species (**Figures 2C,D**) (all $P < 0.05$). However, GI of the perennial species was significantly higher than that of the annual species after low groundwater level treatment ($P = 0.032$) (**Figures 2A,B**).

TABLE 1 | Two-way ANOVA results of the effect of groundwater level (GL), groundwater salinity (GS), and interaction between groundwater level and salinity on seed germinability index (GI) and viability index (VI).

	Source	*df*	GI		VI	
			F	*P*	*F*	*P*
P. australis	GL	1	20.2	**0.000**	7.5	**0.009**
	GS	3	4.1	**0.007**	4.1	**0.012**
	GL × GS	3	3.7	**0.003**	2.1	0.073
S. salsa	GL	1	93.8	**0.000**	67.4	**0.000**
	GS	3	9.6	**0.000**	6.5	**0.000**
	GL × GS	3	6.5	**0.000**	7.1	**0.000**
C. chinense	GL	1	42.6	**0.000**	1.4	0.479
	GS	3	6.7	**0.000**	4.0	**0.031**
	GL × GS	3	2.6	0.088	0.9	0.273
C. album	GL	1	44.2	**0.000**	33.7	**0.000**
	GS	3	5.6	**0.000**	4.5	**0.031**
	GL × GS	3	10.3	**0.000**	6.4	**0.013**
A. venetum	GL	1	-	-	42.5	**0.000**
	GS	3	-	-	0.4	0.360
	GL × GS	3	-	-	2.0	0.052
I. cylindrica	GL	1	-	-	14.6	**0.012**
	GS	3	-	-	7.3	**0.001**
	GL × GS	3	-	-	1.5	0.626
L. latifolium	GL	1	8.4	**0.000**	130.3	**0.000**
	GS	3	1.5	0.477	1.1	0.417
	GL × GS	3	1.8	0.152	1.1	0.499

Bold values indicate statistically significant effects ($P < 0.05$).

Effects of Different Groundwater Levels

The two-way ANOVA showed that groundwater level storage treatment had significant effects on GI in five of the seven species and VI in six of the seven species (**Table 1**). Low groundwater level storage generally resulted in decreasing seed GI and VI compared with high groundwater level storage, except for *C. chinense* and *L. latifolium* seeds, which had higher GI and VI after low groundwater level storage (**Figures 3A,B**). When the effect of groundwater level storage treatment without any salinity (W_0S_0, W_1S_0, and W_2S_0) was analyzed, a clear trend in GI and VI was observed: dry storage (95.9% ± 3.6 and 85.9% ± 4.7%, respectively) > high groundwater level storage (49.3% ± 9.9 and 51.9% ± 7.1%) > low groundwater level storage (30.1% ± 9.3 and 35.7% ± 5.4%) (**Figure 4**).

Effects of Varying Salinity

The two-way ANOVA showed that groundwater salinity had a significant effect on GI in four of the seven species and on

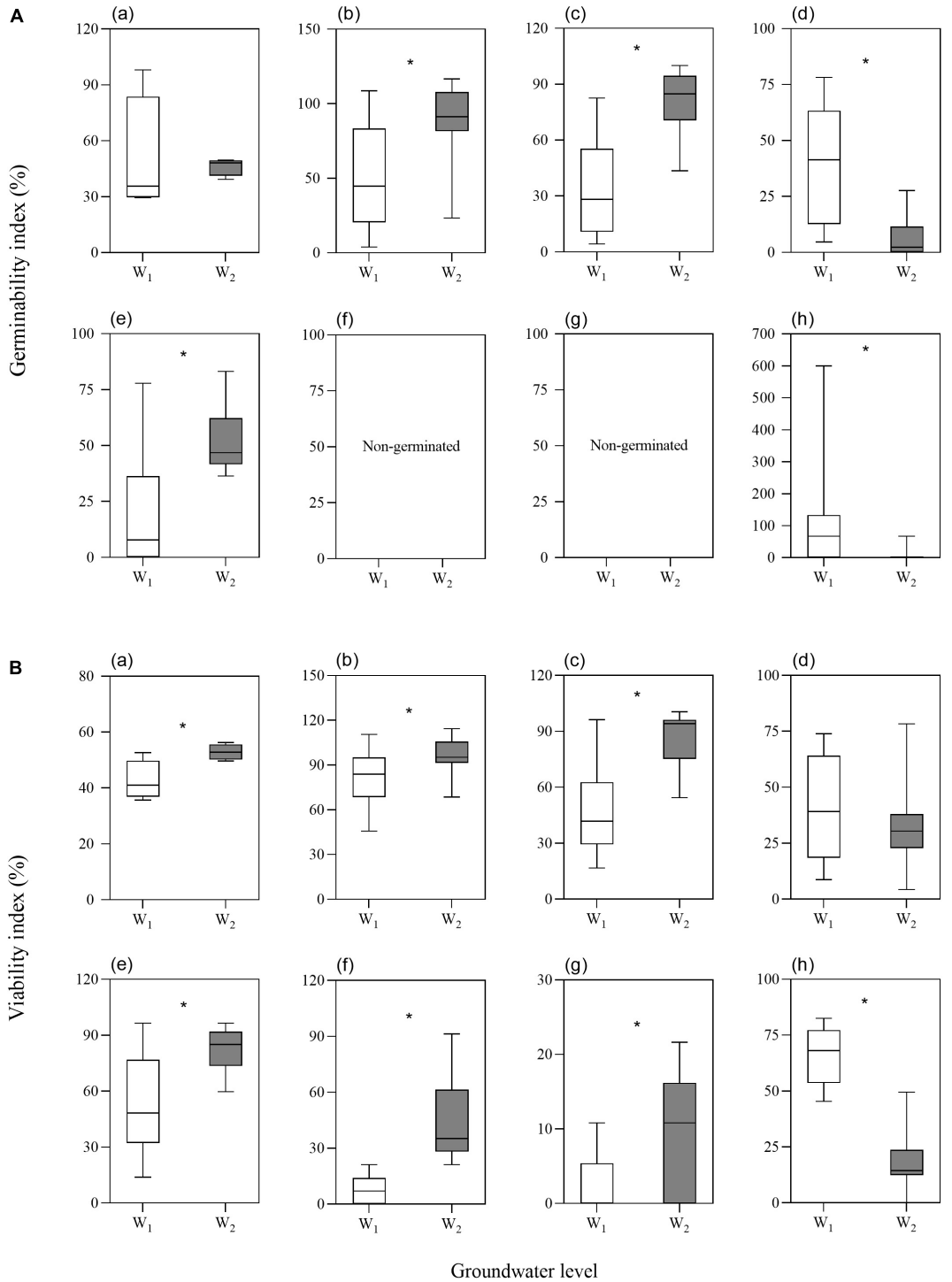

FIGURE 3 | Effects of groundwater level on seed germinability index **(A)** and viability index **(B)** (a. average of the seven species; b. *P. australis*; c. *S. salsa*; d. *C. chinense*; e. *C. album*; f. *A. venetum*; g. *I. cylindrica*; h. *L. latifolium*). Values are the average of GI or VI after storage treatments with the same groundwater level. Significant differences between two groundwater levels are shown by "*" (W_1, low groundwater level; W_2, high groundwater level). *$P < 0.05$.

VI in five of the seven species (**Table 1**). Overall, groundwater salinity had no significant effect on GI and VI when seeds were stored with high groundwater level. However, high salinity generally seemed better for maintenance of germinability and viability under the low groundwater level, except in *I. cylindrica*, whose seeds had better viability when stored in fresh

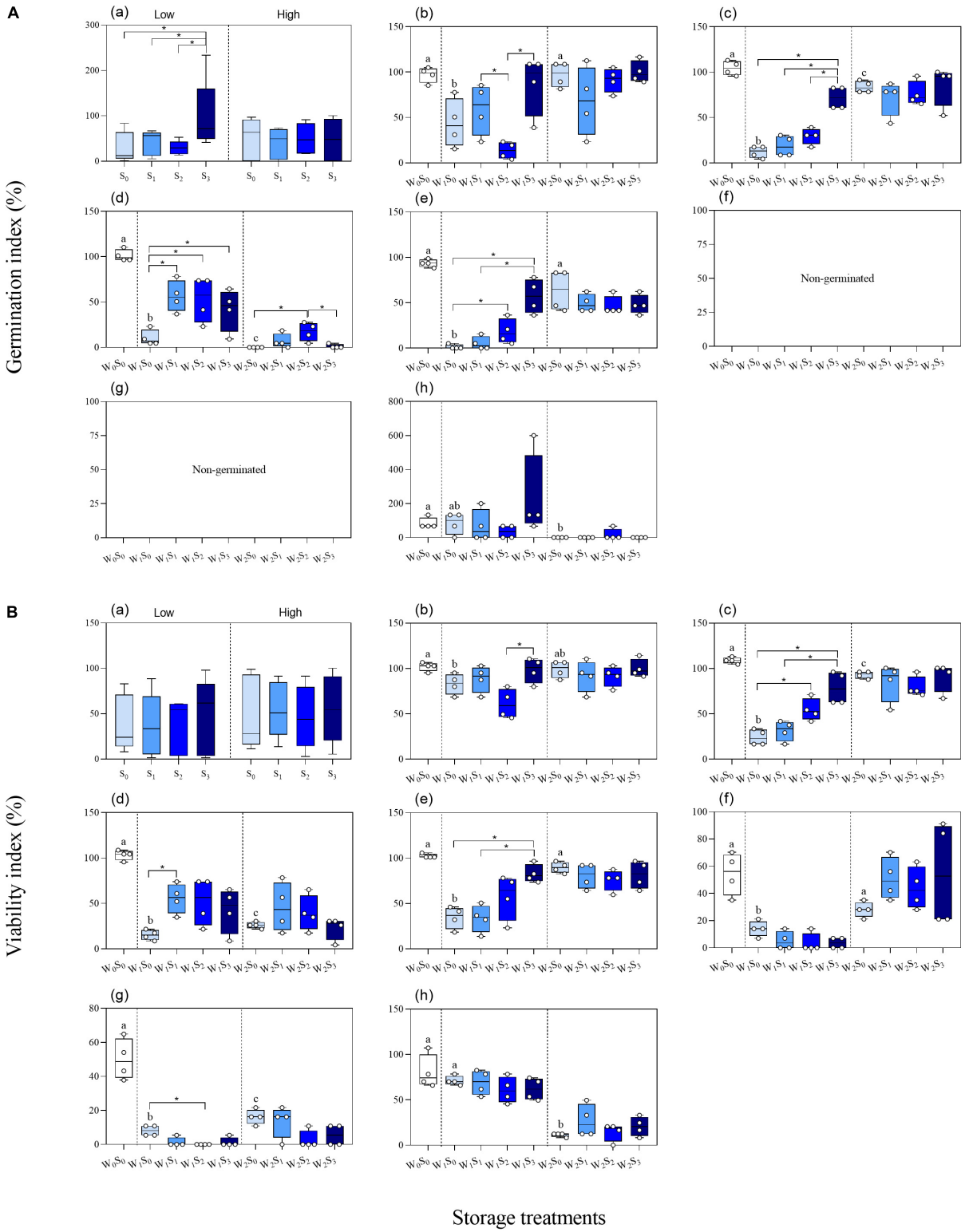

FIGURE 4 | Germinability index **(A)** and viability index **(B)** of seeds (a. average of the seven species; b. *P. australis*; c. *S. salsa*; d. *C. chinense*; e. *C. album*; f. *A. venetum*; g. *I. cylindrica*; h. *L. latifolium*) after different storage treatments. W_0, no water; W_1, low groundwater level; W_2, high groundwater level; S_0, no added salt; S_1, salt concentration of 10 g/L; S_2, salt concentration of 20 g/L; S_3, salt concentration of 30 g/L. Data are mean ± SE (n = 4). Different letters and "*" in each group (W_0S_0, W_1S_0, and W_2S_0; W_1S_0, W_1S_1, W_1S_2, and W_1S_3; W_2S_0, W_2S_1, W_2S_2, and W_2S_3; W_1S_1 and W_2S_1; W_1S_2, and W_2S_2; W_1S_3 and W_2S_3) indicated significant differences in one-way ANOVAs. Note that the scales of the y-axes are different.

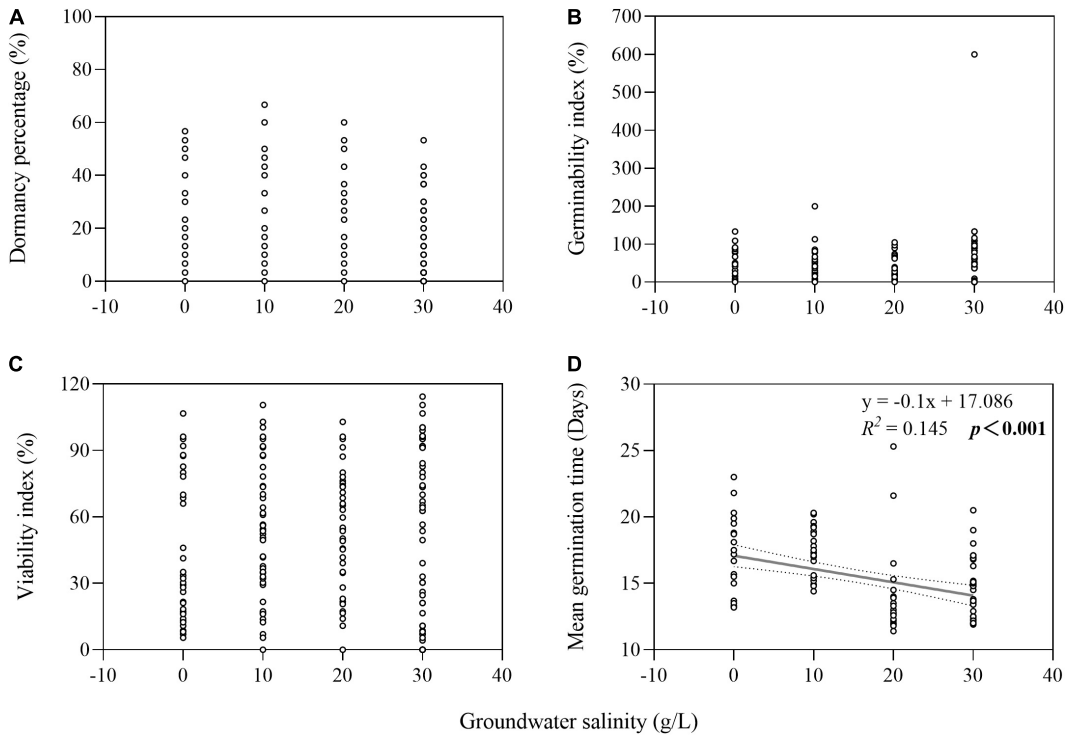

FIGURE 5 | Relationship of groundwater salinity with seed dormancy percentage **(A)**, germinability index **(B)**, viability index **(C)**, and mean germination time **(D)**. The dotted lines indicate the 95% confidence interval of the fit. Note that the x-axes do not start at zero.

groundwater (0 g/L) than higher salinity groundwater (20 g/L) (P = 0.004) (**Figure 4**). Furthermore, groundwater salinity was negatively correlation with seed MGT (average of seven species after storage treatments including dry storage) (R^2 = 0.145; $P < 0.001$) (**Figure 5**).

Interaction Between Groundwater Level and Salinity

We found influence of the interactions between groundwater level and groundwater salinity on seed GI of three species and seed VI of two species (**Table 1**). When the *P. australis*, *S. salsa*, and *C. album* seeds were stored in the low groundwater level treatments, a positive effect on seed GI was clearly observed for groundwater salinity treatments (**Figures 6A–C**). The same effects of groundwater salinity were observed on seed VI of *P. australis* and *C. album* (**Figures 6D,E**). However, the effects disappeared when the seeds were stored in high groundwater level treatments.

Plausible Relationship Between Seed Dormancy and Persistence

Both seed dormancy percentage (not shown in figures) and seed viability index were greater in three perennial species under high groundwater level storage treatment than under low groundwater level storage treatment (all $P < 0.001$) (**Figure 3B**). Overall, we found that seed persistence was positively correlated with seed dormancy percentage (average of seven species after storage treatments including dry storage) (R^2 = 0.321; $P < 0.001$) (**Figure 7**).

Seed Internal Ultrastructure

The internal ultrastructural observations made by SEM analysis were mainly carried out on the seeds that had the greatest changes in seed viability after storage treatment. After certain storage treatments (*P. australis* seeds after W_1S_2 storage; *S. salsa* seeds after W_1S_0 storage; *C. chinense* seeds after W_1S_0 storage; *C. album* seeds after W_1S_1 storage; *A. venetum* seeds after W_1S_2 storage; *I. cylindrica* seeds after W_1S_2 storage; *L. latifolium* seeds after W_2S_0 storage), we found that the sections of seed embryos were reduced (**Figures 8B–D,G**) or their shapes were obviously changed (**Figures 8A,E,F**).

DISCUSSION

In five of the seven species, we found a clear effect of saturated conditions (high groundwater level storage treatment) maintaining greater seed persistence compared with moist conditions (low groundwater level storage treatment). The lower viability after moist storage was similar to the findings of Diantina et al. (2022), who concluded that seeds of five species experienced significant viability loss after aging under controlled laboratory conditions (storage at 60% relative humidity and room temperature). In our study, the moisture content of quartz sand under moist storage treatment was 10.6–11.0% and relative

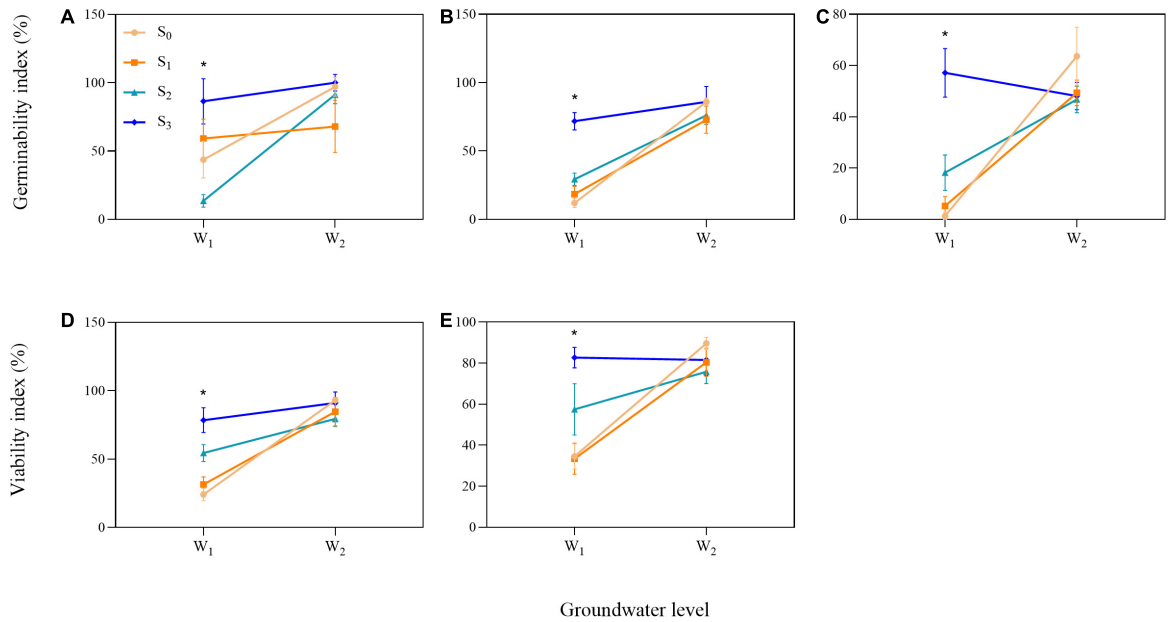

FIGURE 6 | Significant interactions between groundwater level and groundwater salinity on seed germinability index in three species [**(A)** *P. australis*, **(B)** *S. salsa*, and **(C)** *C. album*] and viability index in two species [**(D)** *S. salsa* and **(E)** *C. album*]. W_1, low groundwater level; W_2, high groundwater level; S_0, no added salt; S_1, salt concentration of 10 g/L; S_2, salt concentration of 20 g/L; S_3, salt concentration of 30 g/L. Data are mean ± SE (n = 4). Significant differences among different groundwater salinity treatments are shown. *P < 0.05. Note that the scales of the y-axes are different.

humidity in the tissue culture flasks was approximately 60–65%, which was similar to aging conditions as mentioned above. Moist conditions may have two effects: first, moist conditions can increase seed moisture content, therefore promote seed metabolism, ROS production and cellular damage (Kibinza et al., 2006; Lee et al., 2019; Renard et al., 2020). Second, moisture potentially affects germination of fungal spores and growth of fungi (parasitic or saprobic) that colonize seeds, which may affect seed viability (Maighal et al., 2016). Moist conditions can stimulate more microbial activity, which causes more seed mortality than saturated conditions (Long et al., 2015; Tatsumi et al., 2022). However, when groundwater salinity increased, the negative effects of moist conditions weakened.

Groundwater salinity had significant effects on seed germination conservation in four species and on viability conservation in five species; however, such effects were mainly found when seeds were stored in low groundwater level treatments. Overall, these results indicated that groundwater salinity change had no significant effects on seed persistence when the soil was saturated, but salinity had a positive effect on seed persistence when the soil was moist. Similar result was found by Gu et al. (2018). In their study, 33 ± 10% relative humidity and high salinity were the optimal storage conditions for *Ruppia sinensis* seeds because these conditions could inhibit seed germination. A possible reason for these results is that high salinity played a role in inhibiting microbial activity (Whittle et al., 2022) under moist conditions to maintain higher seed viability. In addition, it was possible that salt stress triggered an increase in the phenolic compounds and flavonoids level (Tlahig et al., 2021) to protect seeds from microorganisms, and this stress may contribute to antioxidant defense under conditions similar to those in the aging experiment as mentioned above. This conclusion was supported by the interaction between groundwater level and salinity. To some extent, our study provides empirical evidence that soil moisture has a greater influence than groundwater salinity on seed persistence in the supratidal wetlands of the Yellow River Delta.

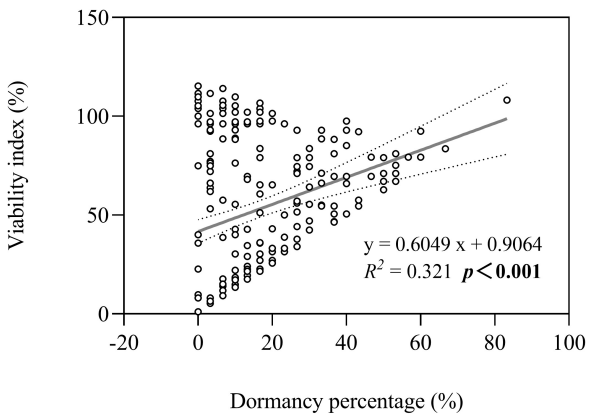

FIGURE 7 | Optimal model for the relationship between seed dormancy percentage and seed viability index. The dotted lines indicate the 95% confidence interval of the fit. Note that the x-axis does not start at zero.

In addition to these factors, our experiment included a test of groundwater without salts compared to dry storage conditions. Overall, seeds maintained greater germinability and

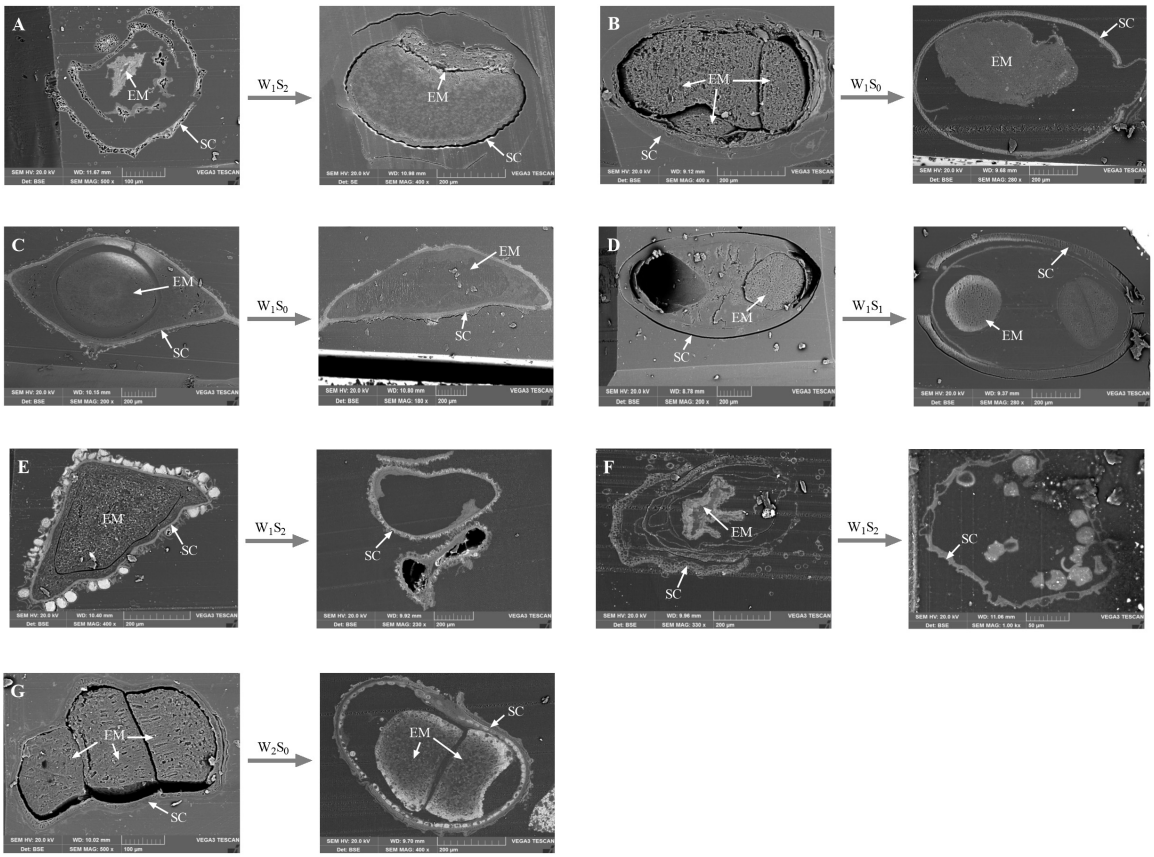

FIGURE 8 | Scanning electron microscopy micrographs of seed vertical sections. The seeds that had sharp change in viability percentage were scanned. **(A)** *P. australis* seeds before and after W_1S_2 storage; **(B)** *S. salsa* seeds before and after W_1S_0 storage; **(C)** *C. chinense* seeds before and after W_1S_0 storage; **(D)** *C. album* seeds before and after W_1S_1 storage; **(E)** *A. venetum* seeds before and after W_1S_2 storage; **(F)** *I. cylindrica* seeds before and after W_1S_2 storage; **(G)** *L. latifolium* seeds before and after W_2S_0 storage. EM, seed embryo; SC, Seed coat.

viability in dry storage compared with moist and saturated conditions without salts added. This might be explained by aging being slowed down in desiccated forms of organisms. The possible reasons were that dry condition was conducive to chemical/enzymatic turnover of lipids (Wiebach et al., 2020); metabolism was reduced because of high viscosity and slow diffusion inside cells (Wood and Jenks, 2008), and therefore the production of ROS and cellular damage are inhibited (Renard et al., 2020).

After 3 months of experimental storage, the seed dormancy percentage of three perennial species was greater under high than low groundwater level storage. These results indicated that, once dispersed into habitats with a high groundwater level, many perennial species will enter dormancy even though the habitats were well-suited for germination. This finding highlighted a mechanism that was potentially responsible for the results found in our previous study, in which perennial plants were not observed aboveground in habitats with high groundwater levels (−20 cm) in the supratidal wetlands of the Yellow River Delta (Feng et al., 2021).

There has been some debate about the relationship between seed dormancy and seed persistence in soil. Thompson et al. (2003) found that there was not a close relationship between seed dormancy and persistence. Some ecologists assumed that seed persistence is phylogenetically related to dormancy because persistent seeds are characterized by some kind of dormancy, being either physical, physiological, or a combination thereof (Long et al., 2015; Gioria et al., 2020). Penfield (2017) noted that dormancy experiments should always be accompanied by analysis of environmental conditions. In our burial experiment, the optimal models showed that seed persistence was positively associated with dormancy percentage. These findings supported previous evidence that seed dormancy was an important mechanism that promoted seed persistence in supratidal wetlands. At the population level, seed dormancy enabled soil seed bank formation in response to environmental disturbances. Additionally, at the individual level, seeds maintained or broke dormancy in response to environmental conditions that limited germination to a specific annual time window (Penfield, 2017).

Previously, much work has been conducted on systematics to identify different species by seed characters using SEM (Ahmad et al., 2020), but there has been little reports on the correlation between seed internal ultrastructure and persistence. It was observed that ABA produced by seed embryos contributed

to germination arrest upon imbibition and then maintained viability (Chahtane et al., 2017). Our results confirmed the importance of seed embryos in maintaining viability. These unique findings resulted in exploration of the seed viability maintenance mechanism. However, our results were based on a subset of seeds and we did not observe internal microstructure changes for all seeds. Therefore, further research is needed to reveal the quantitative relationship between seed ultrastructure and persistence.

Supratidal wetlands are experiencing particularly rapid change as the shallow groundwater level rises (Befus et al., 2020). Our study indicated that, although the species loss from aboveground vegetation as a result of groundwater rising in supratidal wetlands of the Yellow River Delta, seeds of these species may be buried and remain viable (Basto et al., 2015). Following natural or man-made disturbances, seeds may recover (depending on species) from viable seeds by enhanced germination speed and germinability. Once mature seeds are deposited in supratidal wetlands, the seeds may face three fates. First, in habitats with high groundwater level, a lot of seeds, especially perennials, will not germinate but will maintain higher germinability and viability; this may explain the results of our previous study (Feng et al., 2021). Second, in habitats with low groundwater level and low groundwater salinity, seeds will germinate or maintain lower germinability and viability in the soil. Third, in habitats with low groundwater level but high groundwater salinity, seeds will maintain high viability but may germinate soon after the groundwater salinity decreases (Rasheed et al., 2019) or surface soil salinity decreases caused by precipitation.

DATA AVAILABILITY STATEMENT

The raw data supporting the conclusions of this article will be made available by the authors, without undue reservation.

AUTHOR CONTRIBUTIONS

LF and J-TL designed the experiment with the help of H-JY. LF, LP, QC, and J-ZM collected the seeds in the field and performed the lab experiments. All authors contributed significantly to the writing of the manuscript and approved the submitted version.

FUNDING

This study was funded by the National Nature Science Foundation of China (41971126), the Nature Science Foundation of Shandong Province (ZR2019PD008 and ZR2020MD005), and the Youth Innovation Support Program of Shandong Universities (2021KJ081).

ACKNOWLEDGMENTS

We thank Mallory Eckstut, Ph.D. from Liwen Bianji (Edanz) (www.liwenbianji.cn) for editing the English text of a draft of this manuscript.

REFERENCES

Ahmad, S., Zafar, M., Ahmad, M., Ali, M., Sultana, S., Rashid, N., et al. (2020). Seed morphology using SEM techniques for identification of useful grasses in Dera Ghazi Khan, Pakistan. *Microsc. Res. Tech.* 83, 249–258. doi: 10.1002/jemt.23408

Antonellini, M., and Mollema, P. N. (2010). Impact of groundwater salinity on vegetation species richness in the coastal pine forest and wetlands of Ravenna, Italy. *Ecol. Eng.* 36, 1201–1211. doi: 10.1016/j.ecoleng.2009.12.007

Antunes, C., Chozas, S., West, J., Zunzunegui, M., Barradas, M. C. D., Vieira, S., et al. (2018). Groundwater drawdown drives ecophysiological adjustments of woody vegetation in a semi-arid coastal ecosystem. *Glob. Chang. Biol.* 24, 4894–4908. doi: 10.1111/gcb.14403

Auge, G. A., Blair, L. K., Burghardt, L. T., Coughlan, J., Edwards, B., Leverett, L. D., et al. (2015). Secondary dormancy dynamics depends on primary dormancy status in *Arabidopsis thaliana*. *Seed Sci. Res.* 25, 1–17. doi: 10.1017/S0960258514000440

Baskin, C. C., and Baskin, J. M. (2014). *Seeds, Ecology Biogeography and Evolution of Dormancy and Germination*. Burlington, MA: Academic Press.

Basto, S., Thompson, K., Phoenix, G., Sloan, V., Leake, J., and Rees, M. (2015). Long-term nitrogen deposition depletes grassland seed banks. *Nat. Commun.* 6:6185. doi: 10.1038/ncomms7185

Batlla, D., Nicoletta, M., and Benech-Arnold, R. (2007). Sensitivity of *Polygonum aviculare* seeds to light as affected by soil moisture conditions. *Ann. Bot.* 5, 915–924. doi: 10.1093/aob/mcm029

Befus, K. M., Barnard, P. L., Hoover, D. J., Hart, J. A. F., and Voss, C. I. (2020). Increasing threat of coastal groundwater hazards from sea-level rise in California. *Nat. Clim. Chang.* 10, 946–952. doi: 10.1038/s41558-020-0874-1

Cao, D. C., Baskin, C. C., Baskin, J. M., Yang, F., and Huang, Z. Y. (2014). Dormancy cycling and persistence of seeds in soil of a cold desert halophyte shrub. *Ann. Bot.* 113, 171–179. doi: 10.1093/aob/mct256

Chahtane, H., Kim, W., and Lopez-Molina, L. (2017). Primary seed dormancy: a temporally multilayered riddle waiting to be unlocked. *J. Exp. Bot.* 68, 857–869. doi: 10.1093/jxb/erw377

Chantre, G. R., Sabbatini, M. R., and Orioli, G. A. (2009). Effects of burial depth and soil water regime on the fate of *Lithospermum arvense* seeds in relation to burial time. *Weed Res.* 49, 81–89. doi: 10.1111/j.1365-3180.2008.00671.x

Chen, D. L., Chen, X. H., Jia, C. Z., Wang, Y., Yang, L. J., and Hu, X. W. (2021). Effects of precipitation and microorganisms on persistence of buried seeds: a case study of 11 species from the Loess Plateau of China. *Plant Soil* 467, 181–195. doi: 10.1007/s11104-021-04990-1

Cheng, Y., Tian, Q., and Zhang, W. H. (2016). Glutamate receptors are involved in mitigating effects of amino acids on seed germination of *Arabidopsis thaliana* under salt stress. *Environ. Exp. Bot.* 130, 68–78. doi: 10.1016/j.envexpbot.2016.05.004

Collette, J. C., and Ooi, M. K. J. (2020). Evidence for physiological seed dormancy cycling in the woody shrub *Asterolasia buxifolia* and its ecological significance in fire prone systems. *Plant Biol.* 22, 745–749. doi: 10.1111/plb.13105

Debez, A., Belghith, I., Pich, A., Taamalli, W., Abdelly, C., and Braun, H. P. (2018). High salinity impacts germination of the halophyte *Cakile maritima* but primes seeds for rapid germination upon stress release. *Physiol. Plant.* 164, 134–144. doi: 10.1111/ppl.12679

Diantina, S., McGill, C., Millner, J., Nadarajan, J., Pritchard, H. W., Colville, L., et al. (2022). Seed viability and fatty acid profiles of five orchid species before and after ageing. *Plant Biol.* 24, 168–175. doi: 10.1111/plb.13345

Feng, L., Liu, J. T., Han, G. X., Zhang, Q. H., and Peng, L. (2021). Effects of groundwater level fluctuation on characteristics of soil seed banks in coastal wetlands of the Yellow River Delta. *Acta Ecol. Sin.* 41, 3826–3835.

Feng, Y., Sun, T., Zhu, M. S., Qi, M., Yang, W., and Shao, D. D. (2018). Salt marsh vegetation distribution patterns along groundwater table and salinity gradients in yellow river estuary under the influence of land reclamation. *Ecol. Indic.* 92, 82–90. doi: 10.1016/j.ecolind.2017.09.027

Finch-Savage, W. E., and Leubner-Metzger, G. (2006). Seed dormancy and the control of germination. *New Phytol.* 171, 501–523. doi: 10.1111/j.1469-8137.2006.01787.x

Garcia, Q. S., Barreto, L. C., and Bicalho, E. M. (2020). Environmental factors driving seed dormancy and germination in tropical ecosystems: a perspective form *Campo rupestre* species. *Environ. Exp. Bot.* 178:104164. doi: 10.1016/j.envexpbot.2020.104164

Gioria, M., Pysek, P., Baskin, C. C., and Carta, A. (2020). Phylogenetic relatedness mediates persistence and density of soil seed banks. *J. Ecol.* 108, 2121–2131. doi: 10.1111/1365-2745.13437

Gremer, J. R., and Venable, D. L. (2014). Bet hedging in desert winter annual plants: optimal germination strategies in a variable environment. *Ecol. Lett.* 17, 380–387. doi: 10.1111/ele.12241

Greulich, S., Chevalier, R., and Villar, M. (2019). Soil seed banks in the floodplain of a large river: a test of hypotheses on seed bank composition in relation to flooding and established vegetation. *J. Veg. Sci.* 30, 732–745. doi: 10.1111/jvs.12762

Gu, R. T., Zhou, Y., Song, X. Y., Xu, S. C., Zhang, X. M., Lin, H. Y., et al. (2018). Tolerance of *Rupia sinensis* seeds to desiccation, low temperature, and high salinity with special reference to long-term seed stirage. *Front. Plant Sci.* 9:221. doi: 10.3389/fpls.2018.00221

Han, G. X., Chu, X. J., Xing, Q. H., Li, D. J., Yu, J. B., Luo, Y. Q., et al. (2015). Effects of episodic flooding on the net ecosystem CO_2 exchange of a supratidal wetland in the Yellow River Delta. *J. Geophys. Res. Biogeosci.* 120, 1506–1520. doi: 10.1002/2015jg002923

Hu, X. W., Ding, X. Y., Baskin, C. C., and Wang, Y. R. (2018). Effects of soil moisture during stratification on dormancy release in seeds of five common weed species. *Weed Res.* 58, 210–220. doi: 10.1111/wre.12297

Kaiser, T., and Pirhofer-Walzl, K. (2015). Does the soil seed survival of fen-meadow species depend on the groundwater level? *Plant Soil* 387, 219–231. doi: 10.1007/s11104-014-2273-8

Kibinza, S., Vinel, D., Côme, D., Bailly, C., and Corbineau, F. (2006). Sunflower seed deterioration as related to moisture content during ageing, energy metabolism and active oxygen species scavenging. *Physiol. Plant.* 128, 496–506. doi: 10.1111/j.1399-3054.2006.00771.x

Kottler, E. J., and Gedan, K. (2020). Seeds of change: characterizing the soil seed bank of a migrating salt marsh. *Ann. Bot.* 125, 335–344. doi: 10.1093/aob/mcz133

Lee, J. S., Velasco-Punzalan, M., Pacleb, M., Valdez, R., Kretzschmar, T., McNally, K. L., et al. (2019). Variation in seed longevity among diverse Indica rice varieties. *Ann. Bot.* 124, 447–460. doi: 10.1093/aob/mcz093

Long, R. L., Gorecki, M. J., Renton, M., Scott, J. K., Colville, L., Goggin, D. E., et al. (2015). The ecophysiology of seed persistence: a mechanistic view of the journey to germination or demise. *Biol. Rev.* 90, 31–59. doi: 10.1111/brv.12095

Luo, X. F., Dai, Y. J., Zheng, C., Yang, Y. Z., Chen, W., Wang, Q. C., et al. (2021). The ABI4-RbohD/VTC2 regulatory module promotes reactive oxygen species (ROS) accumulation to decrease seed germination under salinity stress. *New Phytol.* 229, 950–962. doi: 10.1111/nph.16921

Ma, M. J., Collins, S. L., Ratajczak, Z., and Du, G. Z. (2021). Soil seed banks, alternative stable state theory, and ecosystem resilience. *Bioscience* 71, 697–707. doi: 10.1093/biosci/biab011

Maighal, M., Salem, M., Kohler, J., and Rillig, M. C. (2016). Arbuscular mycorrhizal fungi negatively affect soil seed bank viability. *Ecol. Evol.* 6, 7683–7689. doi: 10.1002/ece3.2491

Nonogaki, H. (2014). Seed dormancy and germination-emerging mechanisms and new hypotheses. *Front. Plant Sci.* 5:233. doi: 10.3389/fpls.2014.00233

Ooi, M. K. J., Auld, T. D., and Denham, A. J. (2009). Climate change and bet-hedging: interactions between increased soil temperatures and seed bank persistence. *Glob. Chang. Biol.* 15, 2375–2386.

Ooi, M. K. J., Auld, T. D., and Whelan, R. J. (2004). Comparison of the cut and tetrazolium tests for assessing seed viability: a study using Australian native *Leucopogon* species. *Ecol. Manag. Restor.* 5, 141–143. doi: 10.1111/j.1442-8903.2004.201-6.x

Penfield, S. (2017). Seed dormancy and germination. *Curr. Biol.* 27, R853–R909. doi: 10.1016/j.cub.2017.05.050

Rago, M. M., Urretavizcaya, M. F., Orellana, I. A., and Defossé, G. E. (2020). Strategies to persist in the community: soil seed bank and above-ground vegetation in Patagonian pine plantations. *Appl. Veg. Sci.* 23, 254–265. doi: 10.1111/avsc.12482

Rasheed, A., Hameed, A., Gul, B., and Khan, M. A. (2019). Perianth and abiotic factors regulate seed germination of *Haloxylon stocksii*-A cash crop candidate for degraded saline lands. *Land Degrad. Dev.* 30, 1468–1478. doi: 10.1002/ldr.3334

Renard, J., Niñoles, R., Martínez-Almonacid, I., Gayubas, B., Mateos-Fernández, R., Bissoli, G., et al. (2020). Identification of novel seed longevity genes related to oxidative stress and seed coat by genome-wide association studies and reverse genetics. *Plant Cell Environ.* 43, 2523–2539. doi: 10.1111/pce.13822

Rubio-Casal, A. E., Castillo, J. M., Luque, C. J., and Figueroa, E. (2003). Influence of salinity on germination and seeds viability of two primary colonizers of Mediterranean salt pans. *J. Arid Environ.* 53, 145–154. doi: 10.1006/jare.2002.1042

Saatkamp, A., Affre, L., Dutoit, T., and Poschlod, P. (2009). The seed bank longevity index revisited: limited reliability evident from a burial experiment and database analyses. *Ann. Bot.* 104, 715–724. doi: 10.1093/aob/mcp148

Sallon, S., Solowey, E., Cohen, Y., Korchinsky, R., Egli, M., Woodhatch, I., et al. (2008). Germination, genetics, and growth of an ancient date seed. *Science* 320:1464. doi: 10.1126/science.1153600

Tatsumi, C., Taniguchi, T., Du, S., Chen, Q., Yamanaka, N., Otsuki, K., et al. (2022). Differences in the short-term responses of soil nitrogen and microbial dynamics to soil moisture variation in two adjacent dryland forests. *Eur. J. Soil Biol.* 110:103394. doi: 10.1016/j.ejsobi.2022.103394

Thompson, K., Bakker, J. P., Bekker, R. M., and Hodgson, J. G. (1998). Ecological correlation of seed persistence in soil in the north-west European flora. *J. Ecol.* 86, 163–169. doi: 10.1046/j.1365-2745.1998.00240.x

Thompson, K., Ceriani, R. M., Bakker, J. P., and Bekker, R. M. (2003). Are seed dormancy and persistence in soil related? *Seed Sci. Res.* 13, 97–100. doi: 10.1079/SSR2003128

Tlahig, S., Bellani, L., Karmous, I., Barbieri, F., Loumerem, M., and Muccifora, S. (2021). Response to salinity in *Legume* species: an insight on the effects of salt stress during seed germination and seedling growth. *Chem. Biodivers.* 18:e2000917. doi: 10.1002/cbdv.202000917

Whittle, A., Barnett, R. L., Charman, D. J., and Gallego-Sala, A. V. (2022). Low-salinity transitions drive abrupt microbial response to sea level change. *Ecol. Lett.* 25, 17–25. doi: 10.1111/ele.13893

Wiebach, J., Nagel, M., Börner, A., Altmann, T., and Riewe, D. (2020). Age-dependent loss of seed viability is associated with increased lipid oxidation and hydrolysis. *Plant Cell Environ.* 43, 303–314. doi: 10.1111/pce.13651

Wilson, A. M., Evans, T., Moore, W., Schutte, C. A., Joye, S. B., Hughes, A. H., et al. (2015). Groundwater controls ecological zonation of salt marsh macrophytes. *Ecology* 96, 840–849. doi: 10.1890/13-2183.1

Wood, A. J., and Jenks, M. A. (2008). "Plant desiccation tolerance: Dliversity, Distribution, and real-world application," in *Plant Desiccation Tolerance*, eds W. A. Jenks and A. J. Wood (Carlton: Blackwell Publishing). doi: 10.1002/9780470376881.ch1

Yang, X. J., Baskin, C. C., Baskin, J. M., Pakeman, J., Huang, Z. Y., Gao, R., et al. (2021). Global patterns of potential future plant diversity hidden in soil seed banks. *Nat. Commun.* 12:7023. doi: 10.1038/s41467-021-27379-1

Conflict of Interest: The authors declare that the research was conducted in the absence of any commercial or financial relationships that could be construed as a potential conflict of interest.

Publisher's Note: All claims expressed in this article are solely those of the authors and do not necessarily represent those of their affiliated organizations, or those of the publisher, the editors and the reviewers. Any product that may be evaluated in this article, or claim that may be made by its manufacturer, is not guaranteed or endorsed by the publisher.

frontiers | Frontiers in Plant Science

ORIGINAL RESEARCH
published: 06 July 2022
doi: 10.3389/fpls.2022.946949

Carbon, Nitrogen, and Phosphorus Stoichiometry and Plant Growth Strategy as Related to Land-Use in Hangzhou Bay Coastal Wetland, China

Jing Xiong[1,2,3], Xuexin Shao[1,3], Haijing Yuan[1,2,3], Enjun Liu[1,2,3] and Ming Wu[1,3]**

[1]Research Institute of Subtropical Forestry, Chinese Academy of Forestry, Hangzhou, China, [2]College of Landscape Architecture, Nanjing Forestry University, Nanjing, China, [3]Ningbo Wetlands Research Center, Ningbo, China

OPEN ACCESS

Edited by:
Xiaoming Kang,
Chinese Academy of Forestry, China

Reviewed by:
Gang Yang,
Southwest University of Science and Technology, China
Yao-Bin Song,
Hangzhou Normal University, China

***Correspondence:**
Xuexin Shao
shaoxuexin@126.com
Ming Wu
hangzhoubay@126.com

Specialty section:
This article was submitted to Functional Plant Ecology, a section of the journal Frontiers in Plant Science

Received: 18 May 2022
Accepted: 15 June 2022
Published: 06 July 2022

Citation:
Xiong J, Shao X, Yuan H, Liu E and Wu M (2022) Carbon, Nitrogen, and Phosphorus Stoichiometry and Plant Growth Strategy as Related to Land-Use in Hangzhou Bay Coastal Wetland, China. Front. Plant Sci. 13:946949. doi: 10.3389/fpls.2022.946949

Ecological stoichiometry can not only instruct soil nutrient stocks and availability, but also indicated plant growth strategy and adaptability to environmental changes or stress. This study was carried out to examine the plant–soil Carbon (C), Nitrogen (N), and Phosphorus (P) stoichiometry distributions and patterns in three tidal wetlands [mudflat (MF), native *Phragmites australis*-dominated community wetland (NW), invasive *Spartina alterniflora*-dominated community wetland (IW)], and one reclaimed *P. australis*-dominated community wetland (RW) in Hangzhou Bay coastal wetland. The results showed that land-uses have more effect on C and N contents, and C:N and N:P ratios in plant than in soil, P content and C:P ratios more affected by plant organ and soil depth. Compared to land-use, both plant organ and soil depth have stronger effects on C, N, and P stoichiometry. Among tidal wetlands, plant N content and C:P, N:P ratios were significantly higher in NW than in IW. In contrast, plant C, N, and P contents and C:P and N:P ratios were significantly lower in RW, and plant C:N was higher. Soil C, N, and P stocks were similar between tidal wetlands, and were significant higher than those of RW, indicating that reclamation were not beneficial to soil nutrient storage. In the NW, soil N availability was relatively high, and P availability was relatively low; and leaf N:P was 15.33, which means vegetation was co-limited by N and P nutrients. In addition, plants in the NW mainly adopted a conservative growth strategy, with a significantly low aboveground biomass of 1469.35 $g \cdot m^2$. In the RW, soil N availability was relatively low, P availability was relatively high, and leaf N:P was 3, which means vegetation was limited by N nutrient. In addition, plants in the RW mainly adopted a rapid growth strategy, with a significantly high aboveground biomass of 3261.70 $g \cdot m^2$. In the IW, soil N availability was relatively low, soil P availability was relatively high, and leaf N:P was 5.13, which means vegetation was limited by N nutrient. The growth strategy and aboveground biomass (2293.67 $g \cdot m^2$) of the IW were between those of the NW and RW. Our results provide a reference for nutrient management and evaluating the impacts of land-use types on coastal wetland ecosystems.

Keywords: land-use, coastal wetlands, stoichiometry, nutrient stocks, plant strategy, wetland reclamation, plant invasion

INTRODUCTION

Ecological stoichiometry focus on the balance of energy and chemical elements in an ecosystem; and provide a powerful tool for understanding nutrient biogeochemistry and ecological process at individual and ecosystem levels (Reich and Oleksyn, 2004; Elser et al., 2007). Carbon (C), nitrogen (N), and phosphorus (P) are abundant and essential elements for plants and ecosystems (Luo et al., 2020; Hui et al., 2021). Their availabilities and stoichiometric ratios of C, N, and P can significantly affect plant growth and community composition (Högberg et al., 2017; Urbina et al., 2017) and can indicate the nutrient dynamics and limitation of vegetation under changing conditions (Güsewell, 2004; Reich and Oleksyn, 2004; Xiong et al., 2021). Changes in the contents and pools of C, N, and P in soil may alter the C, N, and P ratios of various ecosystem components, thereby affecting the structure and function of an ecosystem (Wang et al., 2019; Crovo et al., 2021). In addition, the C:N, C:P, and N:P ratios of soil are also important indicators of soil quality and nutrient supply capacity. Therefore, these parameters can provide theoretical guidance for managing soil nutrients, and help us understand the response of element changes to global environmental changes and carbon cycle processes (Zhang et al., 2015; Chen and Chen, 2021; Zheng et al., 2021). Compared with the relatively stable C, N, and P stoichiometry of plants, those of soil are more variable (Bui and Henderson, 2013). Therefore, it is helpful to interpret the corresponding ecological effects to study the distribution characteristics of the C, N, and P contents and ratios of different ecosystems.

Changes in land-use caused by natural and human interferences (e.g., forest conversion, farming, and plant invasion) can significantly affect the ecological stoichiometry of C, N, and P both in plants and soils (Wang et al., 2019; Luo et al., 2020; Crovo et al., 2021; Zheng et al., 2021; Tang et al., 2022). C, N, and P stoichiometry of the top soil was more sensitive to land-use (e.g., woodland, upland, and paddy; Tang et al., 2022). Compared to the woodland, soil C was decreased and P was increased of upland agriculture, while soil C, N, and P content were all increased of paddy (Zheng et al., 2021). Land-use changed the competitive relationships of plant through change the soil C, N, P, and K stoichiometry (Wang et al., 2014a). The invasive success of *Spartina alterniflora* may decrease the ecosystem N:P ratio by change the soil N and P capacity and future adjust below- and above-ground trophic chains (Wang et al., 2019). In summary, land-use can result in stoichiometry imbalance and a influence both in soil and plant productivity.

Coastal wetlands have extremely high biodiversity and productivity, and play vitally important functions that cannot be replaced by other ecosystems (Hu et al., 2021). However, global changes, such as reclamation or plant invasion due to human activity, have already change the land-use and degraded and damaged ecosystem functions (Ma et al., 2014). However, how the plant–soil C, N, and P stoichiometry is affected by these changes in coastal wetland remains unknown. The coastal wetland of Hangzhou Bay is the most prominent area for artificial reclamation and utilization; the ecosystem in this region has become extremely unstable and fragile (Yang et al., 2004; Feng and Bao, 2006). Therefore, it is of great significance to explore how different land-use types in this area affect the ecological stoichiometry of plants and soil. Accordingly, this study aims to: (i) investigate the distributions of stoichiometry of C, N, and P in plant organs (leaf, stem, and root) and soil (depths of 0–10, 10–30, 30–60, and 60–100 cm), and (ii) explore their relationships with the environmental conditions of different land-use types (mudflat, native wetland, reclaimed wetland, and invasive wetland). Therefore, we test the following hypotheses: (i) the C, N, and P contents and ratios of plants and soil vary between land-uses, (ii) reclamation and plant invasion are not beneficial soil nutrient stocks, and (iii) land-use can affect the plant growth strategy by changing ecological stoichiometry and habitat.

MATERIALS AND METHODS

Study Area

Hangzhou Bay is a trumpet-shaped tidal estuary located along the north–south demarcation line of coastal wetlands in China. The bay is one of the most abundant areas of waterfowl in eastern China in winter, and is also an important station on the migration route of migratory birds from East Asia to Australasia. The total estimated value of ecosystem services in the southern coastal wetlands of Hangzhou Bay is approximately 1127.83×10^8 Yuan (Ning et al., 2017). This study area is in the southern part of Hangzhou Bay (30°10′ N–30°42′ N, 120°55′ E–121°30′ E), and belongs to the northern subtropical maritime monsoon climate zone, with four distinct seasons. The area has a mean annual temperature of 16°C, a mean annual precipitation of 1,273 mm, an annual sunshine duration of 2,038 h, an annual frost-free period of 244 days, and irregular semi-diurnal tides. The soil type is the littoral salinity subtype.

Reclamation activities and plant invasion are two major ecological issues affecting the "blue carbon" balance. Reclamation activities can lead to habitat destruction in coastal wetlands, while in turn can affect ecosystem health and even lead to habitat loss. *Spartina alterniflora* invaded and rapidly occupied the ecological niche of native plants, resulting in changes in plant communities and affecting the status of invasive ecosystems. Both anthropogenic reclamation and plant invasion have changed the land-use, and may have vital impacts on the balance and cycling of C, N, and P in coastal wetland ecosystems. And mudflat and native plant-dominated community wetland were selected as control. Therefore, mudflat (MF) and native *Phragmites australis*-dominated community wetland (NW), and reclaimed *P. australis*-dominated community wetland (RW), and invasive *S. alterniflora*-dominated community wetland (IW) were selected in the coastal wetland of the southern part of Hangzhou Bay (**Table 1**; **Figure 1**). The MF is in a low-tide flat area with no plants or human activity. The NW is in the middle-high tide flat area, has a single native *P. australis* community, and is unaffected by human management or disturbance. The RW

is in the seawall area and is unaffected by the tide and human management. This area was restored and regenerated with a single native *P. australis* community after it was reclaimed around 2017. The IW is in a low-tidal flat area with a single invasive *S. alterniflora* community. *Spartina alterniflora* (16 m^2) was first planted in the mudflat area of Yuhuan County in Zhejiang Province, China, in 1983. This species, then expanded rapidly and naturally, with its invasive area reaching 5,092 hm^2 in the eastern coastal area (Zhang, 2010).

Field Sampling and Analysis

Plant and soil samples were collected from the MF, NW, RW, and IW in mid-July 2021. At each land-use type, five 20 m × 20 m sample sites were studied. Each sample site was more than 200 m apart, avoiding tidal gullies and edge zones, with large vegetation areas and similar growth status in vegetated samples. A 1 m × 1 m sample plot was randomly selected in each sample site to investigate the vegetation density, height, diameter, and aboveground biomass (**Supplementary Table S1**). Twelve healthy plants were randomly selected in each 1 m × 1 m sample plot, and their root, stem, and leaf were separated and dried to determine their C, N, and P contents, respectively.

In four land use types, the soil physiochemical properties of soil profile were investigated. The temperature was measured by a thermometer; soil moisture was measured by the weighing method; pH and salinity were measured by the multi-functional pH meter and conductivity meter, respectively (**Supplementary Table S2**). According to the response of soil depth to the land-use, root distribution characteristics and soil oxygen status, the soil samples were divided into four layers (Angle et al., 2017; Tang et al., 2022). Five to six disturbed soil samples were collected in each sample plot using a soil drill from each soil depth (0–10, 10–30, 30–60, and 60–100 cm) and combined to form a composite soil sample. The soil C, N, and P stocks in soil layers were determined by the following equations (Tang et al., 2022):

$$\text{Soil C stock (Cs)}\left(\text{Mg}\cdot\text{ha}^{-1}\right)=\frac{\text{C}\times\text{Bulk density}\times\text{soil depth}}{10} \quad (1)$$

$$\text{Soil N stock (Ns)}\left(\text{Mg}\cdot\text{ha}^{-1}\right)=\frac{\text{N}\times\text{Bulk density}\times\text{soil depth}}{10} \quad (2)$$

$$\text{Soil P stock (Ps)}\left(\text{Mg}\cdot\text{ha}^{-1}\right)=\frac{\text{P}\times\text{Bulk density}\times\text{soil depth}}{10} \quad (3)$$

where C is soil C content ($g\cdot kg^{-1}$); N is soil N content ($g\cdot kg^{-1}$); P is soil P content ($g\cdot kg^{-1}$). Total soil C, N, and P stocks within the 100 cm depths were weighed and summed for all four soil layers (0–10, 10–30, 30–60, and 60–100 cm).

The C and N contents of plant organs and soil were determined by the elemental analyzer, and P content of plant organs and soil were determined by a digestion procedure with HNO_3–HF–$HClO_4$ (Jackson, 1958).

Calculation and Statistical Analysis

We log10-transformed all the data before statistical analyses to meet normality of variance requirements. Nested ANOVA were used to examine the effects of three plant organs under three land-use types on the C, N, and P stoichiometry. Nested analysis of variance were used to examine the effects of four soil depths under four land-use types on the C, N, and P stoichiometry. One-way ANOVA were performed to test the effects of three land-use types (NW, RW, IW, and tidal wetlands) with three plant organs on the C, N, and P contents and ratios in plant. And One-way ANOVA were also performed to test the effects of four land-use types (MF, NW, RW, IW, and tidal wetlands) with four soil depths on the C, N, and P contents and ratios. These ANOVA were carried out using the IBM SPSS Statistics 22 software

TABLE 1 | Description of four land-use types in the coastal wetland area of Hangzhou Bay.

Land use	Tidal effect	Longitude and latitude	Mean annual temperature	Mean annual precipitation	Plant type	History and management of land use
Mudflat (MF)	Yes	30.37 N, 121.08 E	16°C	1,273 mm	No plants	Unmanaged
Native *Phragmites australis*-dominated community wetland (NW)		30.32 N, 121.08 E			*Phragmites australis*	Native plants, without human management or disturbance
Invasive *Spartina alterniflora*-dominated community wetland (IW)		30.32 N, 121.08 E			*Spartina alterniflora*	*Spartina alterniflora* rapidly invaded the low-tidal flat area after it was introduction by humans in 1983 and subsequently invaded the study area around 2016
Reclaimed *Phragmites australis*-dominated community wetland (RW)	No	30.36 N, 121.13 E			*Phragmites australis*	Natural restoration occurred after reclamation around 2017, after which there was no tidal flat, human management, or human disturbance

FIGURE 1 | The location of the study area. MF, mudflat; NW, native *Phragmites australis*-dominated community wetland; IW, invasive *Spartina alterniflora*-dominated community wetland; and RW, reclaimed *P. australis*-dominated community wetland.

(SPSS. Inc., Chicago, IL, United States). Pearson's correlation analysis was used to explore the relationships between C, N, and P contents, ratios and stocks of plant organs and soil depths. Principal component analysis (PCA) was used to explore the relationships between C, N, and P stoichiometry and plant growth traits, and soil physiochemical properties under four land-use types. Aggregated boosted tree analysis (ABT) and random forest analysis were used to explore the key factors of soil C, N, and P stocks and plant aboveground biomass. The PCA was conducted using the ggvegan package, Pearson's correlation analysis was conducted using the psych and tidyverse package, the ABT was conducted using the dismo package, and random forest analysis was conducted using the randomForest package in R software (Version 4.1.3), respectively.

RESULTS

Distribution of Plant Organs C, N, and P Contents and Ratios of Three Vegetated Wetlands

Land-uses significantly affected plant C and N contents and plant C:N and N:P ratios ($p < 0.05$), plant organs in the same land-use just did not significantly affected plant C content ($p < 0.05$; **Table 2**). Compared to the RW, the plant C and N contents, and C:P ratios of tidal wetlands were significantly higher, while the C:N ratio was significantly lower ($p < 0.05$; **Supplementary Figures S1A,B,D,E**). In addition, there was a large difference in plant C, N, and P contents and ratios between RW and NW. At the same time, there were relatively small differences between RW and IW ($p < 0.05$; **Supplementary Figure S1**).

The patterns of P content and C:P and N:P among plant organs were contrasting and were not affected by land-use type (**Figures 2C,E,F**). The leaf P content was significantly higher, while the leaf C:P and N:P ratio were significantly lower than those in root and stem ($p < 0.05$). However, land-use type affected the patterns of C and N contents and C:N ratio among plant organs (**Figures 2A,B,D**). Compared to the NW, leaf N allocation was significantly decreased; and root N allocation was significantly increased, while the C:N ratio was higher in leaf than root in RW. In addition, the leaf C allocation was significantly decreased; the stem N allocation were significantly increased in the IW ($p < 0.05$).

Distribution of Soil C, N, and P Contents and Ratios in Different Land-Use Types

Land-uses just significantly affected soil N content and soil C:N ratios ($p < 0.05$), soil depths in the same land-use just did not significantly affected soil P content ($p > 0.05$; **Table 2**). In general, soil C and N contents, and C:P and N:P ratios in tidal wetlands, especially in IW, were significantly higher than those in the RW, while soil C:N was significantly lower ($p < 0.05$; **Supplementary Figures S2A,B,D,E**).

Land use type also affected the distribution characteristics and spatial patterns of soil C and N contents and C:N, C:P, and N:P ratios, but had little influence on soil P content ($p > 0.05$; **Figures 3A–F**). In the MF, soil C and N contents, C:P and N:P ratios first decreased and then decreased with increasing soil depth, while the soil P content and C:N ratio showed the opposite trend. In the NW, the soil C and N contents, and C:N, C:P, and N:P ratios at the 60–100 cm were significantly lower than those at other soil depths ($p < 0.05$). In the RW, the soil C content, and C:N and C:P at the 30–60 cm were significantly lower than those in other soil depths ($p < 0.05$). In the IW, the soil C content, C:N, and C:P ratios first increased and then decreased with the increasing soil depth, and the soil N and N:P ratio at the

TABLE 2 | Nested ANOVA results for the effects of different land-use types, plant organs, and soil depths and on the C, N, and P contents and ratios, and C, N, and P stocks.

	DF	Plant C content	Plant N content	Plant P content	Plant C:N ratio	Plant C:P ratio	Plant N:P ratio			
Land-use	2	29.696**	63.266***	0.110^{ns}	9.209*	1.060^{ns}	11.303**			
Plant organ (Land-use)	6	1.850^{ns}	7.611***	28.048***	21.865***	22.884***	22.423***			
	DF	**Soil C content**	**Soil N content**	**Soil P content**	**Soil C:N ratio**	**Soil C:P ratio**	**Soil N:P ratio**	**Soil C stock**	**Soil N stock**	**Soil P stock**
Land-use	3	0.762^{ns}	5.737*	1.099^{ns}	12.545**	0.811^{ns}	3.120^{ns}	3.400^{ns}	2.245^{ns}	0.200^{ns}
Soil depth (Land-use)	12	32.894***	15.344***	1.180^{ns}	5.860***	4.150**	3.379**	1.640^{ns}	22.056***	27.581***

*DF, degree of freedom for each test. ns, nonsignificant. ***p < 0.001; **p < 0.01; *p < 0.05.*

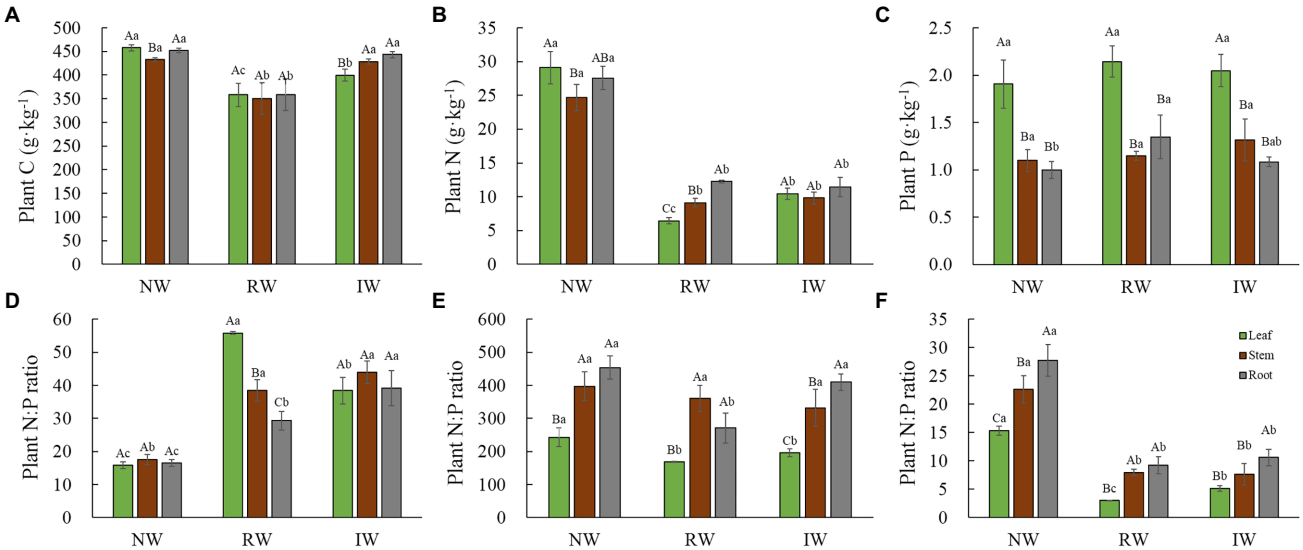

FIGURE 2 | Distributions of the plant Carbon (C) content **(A)**, plant N content **(B)**, plant P contents **(C)**, plant C:N ratio **(D)**, plant C:P ratio **(E)**, and plant N:P ratio (**F**; means ± SD, $n = 3$) under different land-use types in Hangzhou Bay. Different capital letters for the same land-use type indicate a significant difference among plant organs at $p < 0.05$, and different lower-case letters for the same organ indicate a significant difference among land-use types at $p < 0.05$.

0–10 cm depth were significantly higher than those at other soil depths ($p < 0.05$).

In terms of spatial patterns, at the 0–10 and 10–30 cm depth, the soil C and N contents significantly decreased in this order: NW > IW > MF > RW (**Figures 3A,B**). At the 0–10 cm depth, the soil C:N ratio was significantly lower in the NW and significantly higher in the RW ($p < 0.05$; **Figure 3D**). At the 10–30 cm depth, the highest soil C:P ratio and lowest soil C:N ratio were observed in the NW, the highest soil C:N and lowest soil C:P and N:P ratios were observed in the RW, and soil N:P ratio was significantly larger in MF ($p < 0.05$; **Figures 3D–F**). At the 30–60 cm depth, soil C and N contents in the NW were the largest, followed by IW, and MF and RW were the smallest (**Figures 3A,B**). Soil C:P and N:P ratios of the NW and IW were significantly higher than those in MF and RW, while the soil C:N ratio was the opposite ($p < 0.05$; **Figures 3D–F**). At the 60–100 cm depth, the largest soil C and N contents, C:N, C:P, and N:P ratios were observed in the MF and IW, followed by the RW, and were lowest in the NW (**Figures 3A,B,D–F**).

Distributions of Soil C, N, and P Stocks in Different Land-Use Types

Land-uses did not significantly affected Cs, Ns, and Ps ($p > 0.05$), while soil depths in the same land-use did had extremely significant effects on Ns, and Ps ($p < 0.001$; **Table 2**). In general, Cs, Ns, and Ps of each soil depth were lower or significantly lower in RW than tidal wetland ($p < 0.05$). Cs decreased with the increasing soil depth from 0 to 60 cm, and then varied with land-use types at the 60–10 cm depth (**Figure 4A**). Ns and Ps increased with the increasing soil depth from 0 to 100 cm (**Figures 4B,C**). There was no significant difference in total Cs ($p > 0.05$), total Ns and Ps

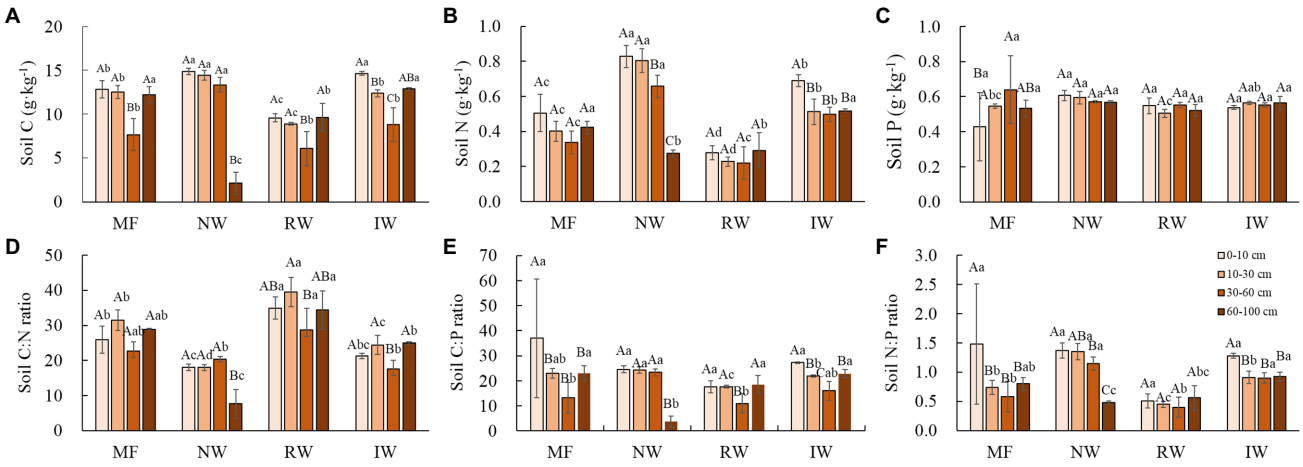

FIGURE 3 | Distributions of the soil C content **(A)**, soil N content **(B)**, soil P contents **(C)**, soil C:N ratio **(D)**, soil C:P ratio **(E)**, and soil N:P ratio (**F**; means ± SD, $n = 3$) under different land-use types in Hangzhou Bay. Different capital letters in the same land-use type indicate a significant difference among soil depths at $p < 0.05$, and different lower-case letters in the same soil depth indicate a significant difference among land-use types at $p < 0.05$.

were significantly lower in the RW than tidal wetland ($p < 0.05$; **Figure 4D**).

Relationships Between C, N, and P Stoichiometry and Stocks and Habitant Conditions

Pearson's analysis showed that C, N, and P contents and ratios in plant or soil all have strong self-correlation. Plant C, N, and P contents and ratios were more likely correlated with soil P content, C:N ratio and Ps ($p < 0.05$; **Figure 5A**). Soil C, N, and P contents and ratios in each soil depth were influenced more by C, N, and P content in the leaf and root than in the stem (**Figure 5B**). And the correlation between C, N, and P contents and ratios in plant organs and soil depths were significantly higher at 10–30 and 30–60 cm depths than at 0–10 and 60–100 cm depths.

The PCA results revealed that the first two axes explained 83.9 and 47.1%, respectively, plant and soil C, N, and P contents and ratios were mainly affected by tidal wetlands (**Figure 6**). Plant and soil C, N, and P contents and ratios were closely related to plant growth traits (e.g., aboveground biomass and diameter; **Figure 6A**) and soil physiochemical properties (e.g., bulk density, temperature, and moisture; **Figure 6B**).

Soil Cs and Ns were more likely to be correlated with C, N, and P contents and ratios in soil than in plants, while soil Ps were both affected (**Figure 5A**). The effects of plant growth traits, especially the height and aboveground biomass, were higher than plant stoichiometry (**Figure 7A**), and the contributions of the soil C content and bulk density were greater than those of the other soil characteristics (**Figure 7B**).

The plant growth traits were closely related to plant N and P contents and N:P ratio, and soil C:N and C:P ratios (**Figure 6A**). Except for plant and soil stoichiometry, the ABT analysis indicated that the plant growth traits were greatly affected by soil properties such as soil bulk density (**Figure 8A**). And the random forest analysis results showed that the aboveground biomass was mainly affected by soil physiochemical properties than soil C, N, and P contents and ratios and stocks (**Figure 8B**).

DISCUSSION

Response of C, N, and P Contents and Allocation Patterns of Plant Organs to Land-Use Types

Coastal wetland can provide many special ecosystem services and products. The changes to Chinese coastal wetlands in the last few decades, such as land-use changes due to human activities, are especially important and universal (Ma et al., 2014; Wang et al., 2014a). Coupled biogeochemical cycles of C, N, and P are fundamental for primary production and organic matter accumulation/decomposition in coastal wetland (Hu et al., 2018, 2020; Wang et al., 2019). Plant nutrient content depends on the dynamic balance between plant demand and soil nutrient supply (Hu et al., 2020). Our results suggest that land-use has an important effect on plant C, N, and P contents and patterns. Compared to the NW, plant C and N of the RW and IW were lower. Firstly, significantly lower soil N contents and stocks in the RW may result in significantly lower plant N content (Chen and Chen, 2021). There was no significant difference in soil N content between the NW and IW; however, as the IW is in a low-tide area, denitrification caused by long-term flooding may reduce the availability of nitrate N, thus significantly reducing their plant N content (Ordoñez et al., 2010). Additionally, according to the growth dilution theory (Townsend et al., 2007), plant nutrient concentration will be diluted with the acceleration of the rapidly increasing biomass and decrease in nutrient content. The higher aboveground biomass in the RW and IW suggests their dilution effects may be stronger than the NW and may lower their C and N contents of plant organs.

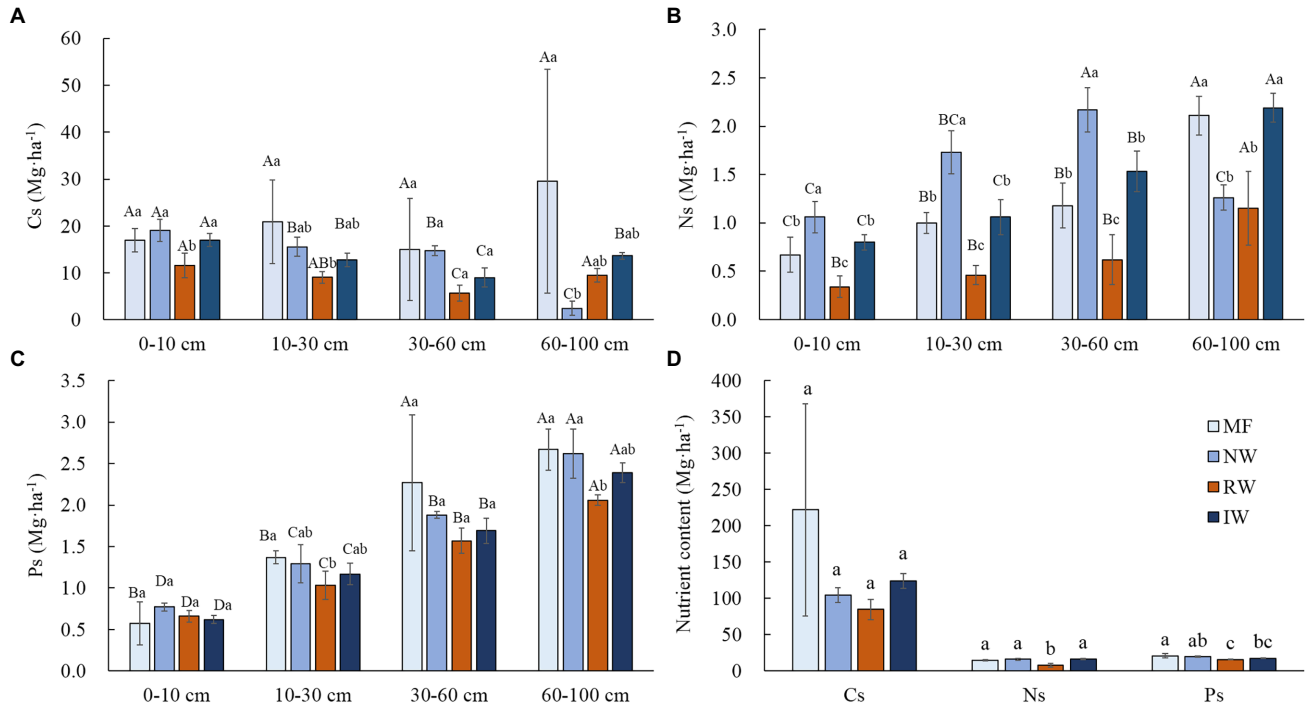

FIGURE 4 | Distributions of the soil C stock **(A)**, soil N stock **(B)**, soil P stock **(C)**, and total soil nutrient stock (**D**; means ± SD, $n = 3$) under different land-use types in Hangzhou Bay. Cs, soil C stock; Ns, soil N stock; and Ps, soil P stock. Different capital letters in the same wetland type indicate a significant difference among soil depths at $p < 0.05$, and different lower-case letters in the same soil depth indicate a significant difference among wetland types at $p < 0.05$.

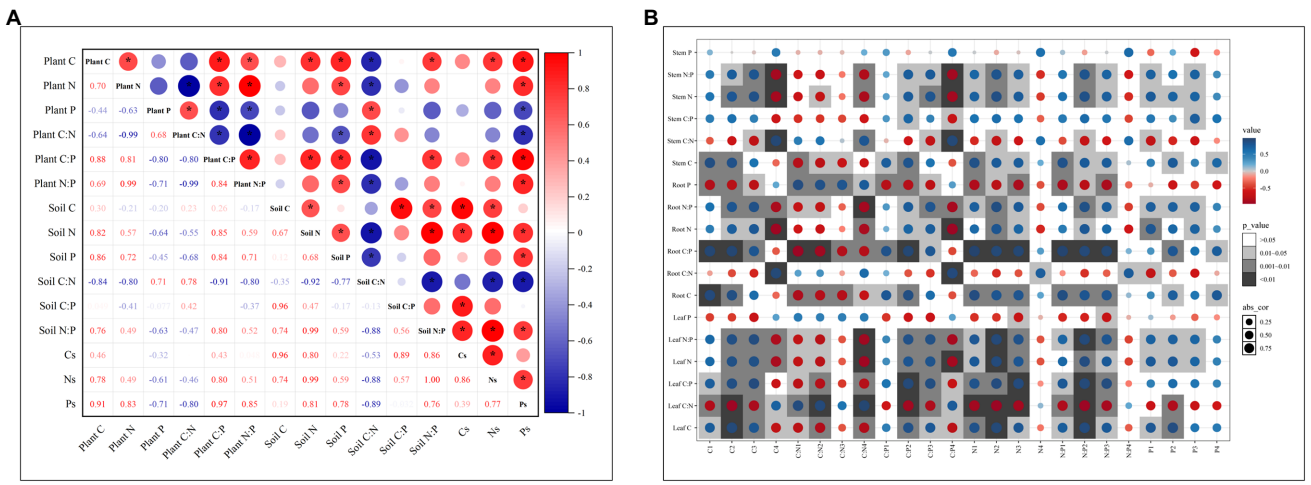

FIGURE 5 | Correlation analysis between C, N, and P contents and ratios of plants and soils **(A)**, and between C, N, P contents and ratios of plant organs and soil depths **(B)**. Cs, soil C stock; Ns, soil N stock; and Ps, soil P stock. C1, N1, P1, C:N1, C:P1, and N:P1 are the soil C, N, and P contents and ratios in 0–10 cm depth. C2, N2, P2, C:N2, C:P2, and N:P2 are the soil C, N, and P contents and ratios in 10–30 cm depth. C3, N3, P3, C:N3, C:P3, and N:P3 are the soil C, N, and P contents and ratios in 30–60 cm depth. C4, N4, P4, C:N4, C:P4, and N:P4 are the soil C, N, and P contents and ratios in 60–100 cm depth.

The allocation patterns of C, N, and P in plant organs are limited by soil nutrient conditions (He et al., 2015; Ma et al., 2019) and are related to tissue structure and functional differentiation (Minden and Kleyer, 2014). During the plant life story, the plant can regulate element allocation in organs to adapt to the living environment and ensure high productivity (Zhang et al., 2020). Leaves have important functions of C assimilation and nutrient gathering, and their nutrient content is generally higher than that of root and stem, and not affected by exogenous nutrient additions (Hu et al., 2014; Xiong et al., 2021). Similarly, P content was significantly higher in leaf than in root and stem, which is conducive to synthesizing

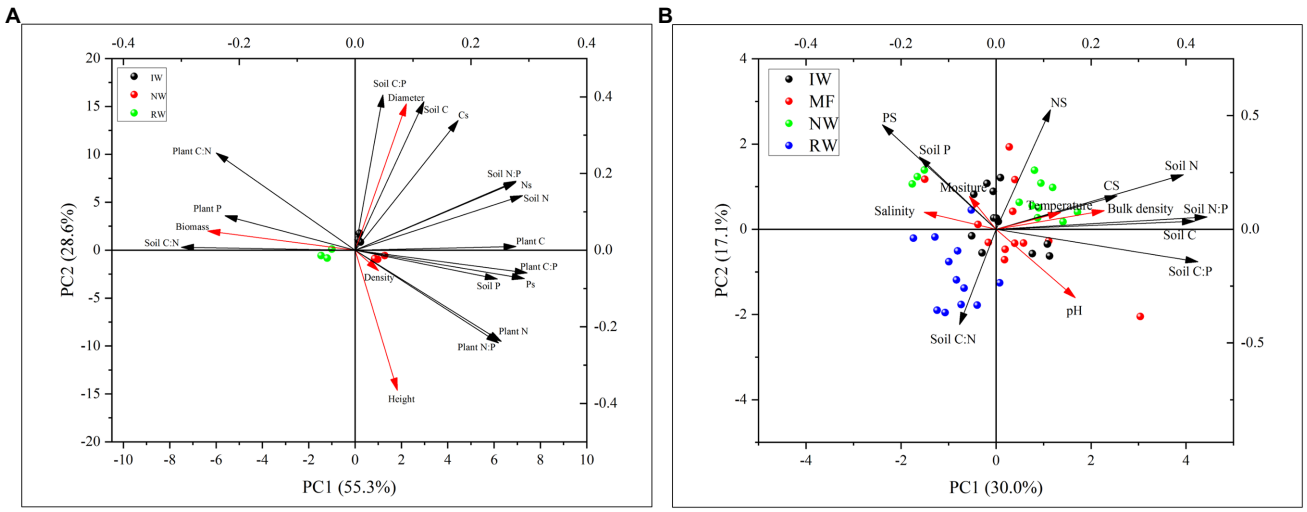

FIGURE 6 | Principal component analysis (PCA) between plant growth traits and the C, N, P stoichiometry and stocks of plants and soils in three land-use types **(A)**. PCA analysis between soil physiochemical properties and the C, N, P stoichiometry and stocks of plants and soils in four land-use types **(B)**. MF, mudflat; NW, native *Phragmites australis*-dominated community wetland; IW, invasive *Spartina alterniflora*-dominated community wetland; and RW, reclaimed *P. australis*-dominated community wetland.

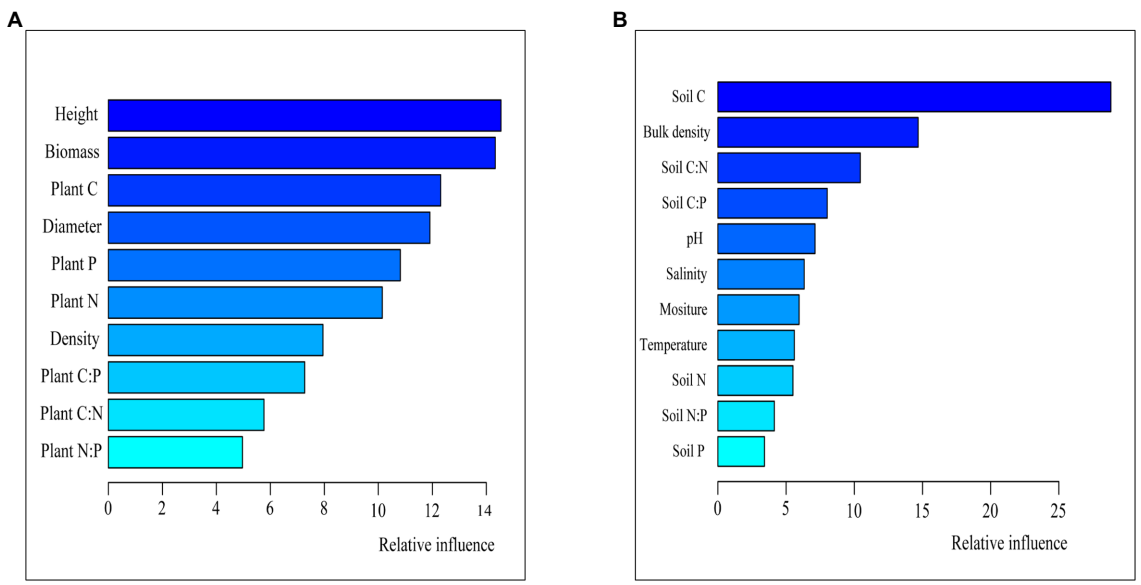

FIGURE 7 | Aggregated boosted tree (ABT) analysis of the soil C, N, and P stocks, plant growth traits, and C–N–P stoichiometry **(A)**. ABT analysis of the soil C, N, and P stocks, soil physiochemical properties, and C–N–P stoichiometries **(B)**.

organic matter and promoting of plant growth and defense system (Wang et al., 2019). However, C and N contents were only significantly higher in leaf than in root and stem in the NW, while there were significantly lower in the RW or were no significant differences in the IW. The higher aboveground biomass may be the main reason leaf C and N contents were smaller than root and stem (Townsend et al., 2007). In addition, when plant growth is limited by nutrients, the nutrients are higher in root than in other organs (Graciano et al., 2005). The higher N allocation in root in the RW and IW will benefit root biomass, and then obtain more N nutrients absorbed.

Response of Soil C, N, and P Contents and Stocks to Land-Use Types

Soil C, N, and P contents and profile patterns are closely related to their sources. Soil C and N contents decrease with

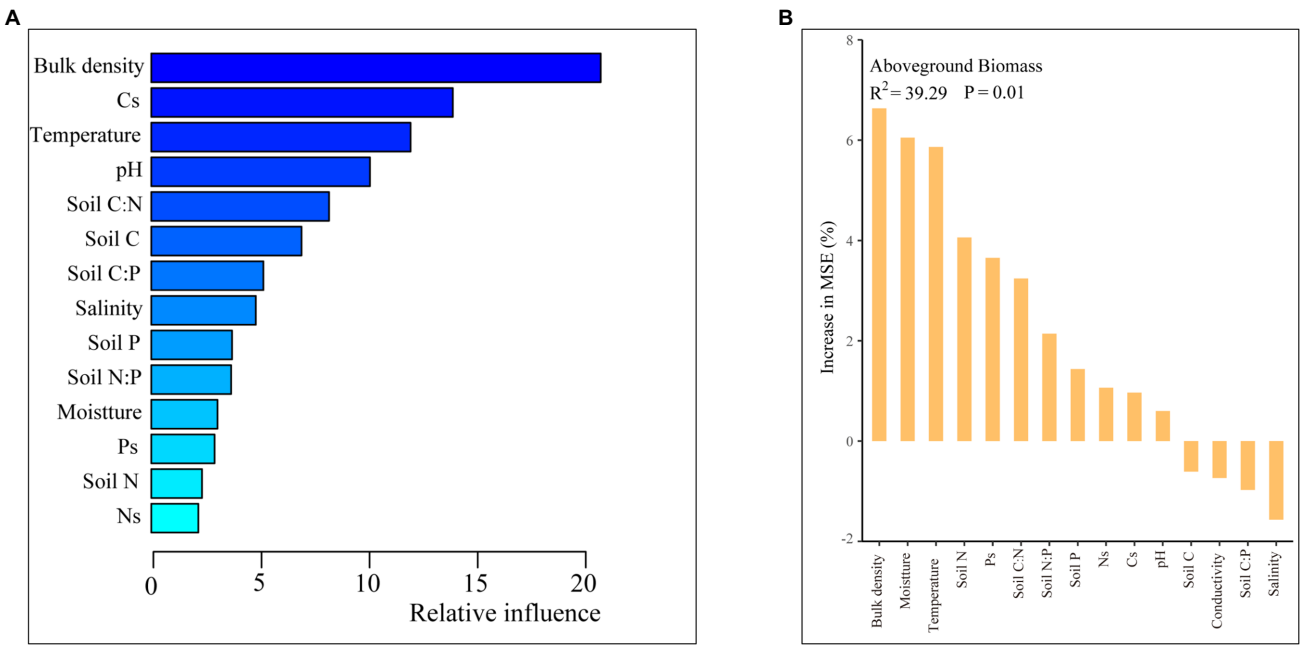

FIGURE 8 | Aggregated boosted tree (ABT) analysis **(A)** and random forest analysis of aboveground plant biomass and soil properties **(B)**.

soil depth and mainly originate from the input of plant litter and root and microbial residues (Yu and Chi, 2019; Zhang et al., 2019). Soil P content is more derived from soil rock weathering and has stable soil profile patterns (Vitousek et al., 2010). Similarly, soil P did not show distinct soil profile patterns, and soil C and N content decreased from 0 to 60 cm. In contrast, soil C and N contents at the 60–100 cm depth were more variable in the four different wetlands, mainly related to whether the root could reach the deep soil and the historic organic carbon accumulation. The soil profile patterns of Cs were similar to soil C content in four land-use types, while soil Ns and Ps were increased at a depth of 100 cm. Soil nutrient stocks were more closely related to soil properties and plant growth traits, indicating that land-use affected soil nutrient stocks by changing soil properties especially the soil bulk density (Wang et al., 2014a, 2015) and plant input (Yu and Chi, 2019). In addition, soil C, N, and P contents and stocks were more affected by tide, and soil total Cs, Ns, and Ps were similar in tidal wetland. Compared to tidal wetlands, soil C, N, and P content and stocks in the RW reached a minimum, indicating that high soil nutrient stocks were mainly attributed to the material exchange by tides (Peñuelas et al., 2012), and that reclamation was detrimental to nutrient storage.

Connection Between Plant and Soil C:N:P Ratios

Soil C:N:P ratios are highly susceptible to human activities and climate factors (Peñuelas et al., 2012; Bui and Henderson, 2013; Yu et al., 2018) and further affect plant stoichiometry (Hu et al., 2020). Demars and Edwards (2010) showed that even under high nutrient supply conditions, the N:P ratios in wild plant tissues of 41 wetland plant species changed only slightly, whereby a strict N:P ratio was determined by the plant endostatic mechanism (Sterner and Elser, 2002). In this study, the N:P ratio pattern of plant organs was not affected by land-use type, indicating that the pattern of N:P ratio in plant organs had a certain internal stability. However, plant N:P was significantly lower after alien plant invasion or wetland reclamation, indicating that land-use types could significantly change the N:P ratio balance in coastal wetland ecosystem, which may change the status of plant nutrient limitation. Given that leaf N:P ratio could be an indicator of nutrient limitation of vegetation (Koerselman and Meuleman, 1996; Vitousek et al., 1996; Güsewell et al., 2003; Wang and Moore, 2014b). Therefore, plants in the NW (10/14 < leaf N:P ratio < 16/20) were co-limited by N and P, plants in the RW and IW (leaf N:P ratio < 10/14) were limited by N in this study.

However, many factors affect leaf N:P ratio. First, wetland herbs have a higher relative growth rate than terrestrial plants (Agren, 2004), which leads to a significant decrease in leaf N content and reducing leaf N:P ratio (Sardans et al., 2012). Second, plant nutrient content is related to soil nutrient availability rather than content (Koerselman and Meuleman, 1996; Cordell et al., 2001). The soil C:N:P ratio greatly determine nutrient availability for plants and soil microorganisms (Vitousek et al., 1996). Stronger correlations were found between the C, N, and P contents and ratios of plant organs and soil depths of 10–30 and 30–60 cm than soil depths of 0–10 and 60–100 cm, suggesting that plant

nutrient content was mainly related to soil nutrient availability of 10–30 and 30–60 cm soil depths. At the 10–30 and 30–60 cm soil depths, significant lower soil C:N ratios and higher soil C:P and N:P ratios in NW means higher N and lower P availability as concluded earlier (Don et al., 2007; Iost et al., 2007; Wang et al., 2014a; Bing et al., 2016). Similarly, in the RW and IW, significantly higher soil C:N ratio and lower soil C:P and N:P ratios indicated lower N and higher P availability. When the availability of soil N and P were relatively low and high, respectively, the plant N:P ratio will be low (Güsewell, 2004). Compared to coastal tidal wetlands in eastern China (leaf N:P ratio was 7.55; Hu et al., 2018), and global coastal wetlands (leaf N:P ratio was 13.40; Hu et al., 2020), leaf N:P ratio of the NW was larger (leaf N:P was 15.33), and leaf N:P ratio of the RW and IW were smaller (leaf N:P were 3.00 and 5.13 respectively). Plant growth in the NW was co-limited by N and P nutrient, while plants in the RW and IW were limited by N nutrient.

The Plant Growth Strategy of Different Land-Use Types

Carbon, N, and P contents and ratios of the plant are helpful in understanding plant growth strategy and its adaptability to environmental changes and stressors, and further contribute to ecological conservation and environmental protection (Elser et al., 2000; Vrede et al., 2004; Hessen et al., 2007; Rong et al., 2015; Zheng et al., 2021). Our results indicated that land-use may significantly alter the balanced C, N, and P contents and ratios in wetland ecosystems and significantly influence plant growth strategy. Moreover, results expressed that plant growth traits were closely related to plant N:P ratio, and soil C:N and C:P ratios. According to the growth rate hypothesis (Sterner and Elser, 2002), fast-growing species tend to have higher plant P content and lower plant C:P and N:P ratios than slow-growing species. In the NW with lower soil P availability and higher N availability, the significant lowest plant P content and highest plant C:P and N:P ratios indicated that plants tend to adopt a conservative resource acquisition strategy, which may lead to significant lowest aboveground biomass. In the RW with lower soil N availability and higher P availability, the significant highest plant P content and lowest plant C:P and N:P ratios indicated that plants tended to adopt a rapid resource acquisition strategy, so its aboveground biomass reached a significant highest value. In the IW, plant P content, C:N and C:P ratios, soil N and P availability, and aboveground biomass were between those of the NW and RW. These findings suggest that the plant growth strategy of the IW was also between that of the NW and RW. However, C, N, and P contents and ratios of plants and soils are all affected by soil physiochemical properties. In addition, plant growth traits were not only affected by soil nutrient limitation and availability, but also by soil physicochemical properties such as bulk density. Therefore, land-use may affect stoichiometry by altering soil physiochemical properties, and then affect vegetation growth strategy.

CONCLUSION

Land-use in Hangzhou Bay coastal wetland affected the C, N, and P contents and ratios of plant and soil by changing the soil's physiochemical properties, thus affecting the nutrient availability and stocks, and eventually affecting plant growth. In tidal wetlands, the difference in soil C, N, and P stocks was not significant, while its N and P availability varied. Compared to the NW, soil P availability of IW was higher, and N availability was lower. Compared to tidal wetland, N stocks and availability of the RW were smaller, while its soil P availability was higher. Moreover, changes in soil C, N, and P stocks and availability ultimately lead to plants taking different growth strategies. In the NW, plants were co-limited by N and P nutrients and took a conservative growth strategy. In the RW, plants were limited by N nutrient and took a rapid growth strategy. In the IW, plants were limited by N nutrient and took a slow-rapid growth strategy. In conclusion, both plant growth and soil nutrient status are closely related to land-use. Reclamation and plant invasion are beneficial to vegetation growth at present, while severe N-limitation and smaller N and P stocks are not beneficial to vegetation community development in the long term. Additionally, the IW is located at the low-tide zone, the lower N availability has negative consequences for water quality since it promotes eutrophication processes. The soil nutrient management, especially N fertilizer, and dynamic monitoring of water quality of different land-use in coastal wetland should be strengthened in the future.

DATA AVAILABILITY STATEMENT

The raw data supporting the conclusions of this article will be made available by the authors, without undue reservation.

AUTHOR CONTRIBUTIONS

All authors contributed to the study and manuscript preparation. XS and MW are responsible for ensuring that the descriptions are accurate and agreed upon by all the authors. JX: conceptualization, methodology, software, data curation, writing—original draft, writing—review and editing, and visualization. XS and MW: conceptualization, methodology, writing—review and editing, validation, project administration, and funding acquisition. HY and EL: methodology, investigation, and resources. All authors contributed to the article and approved the submitted version.

FUNDING

This study was financially supported by the National Natural Science Foundation of China (31870597), the Special Fund

for Cooperation of Zhejiang Province, and the Chinese Academy of Forestry (2021SY03).

ACKNOWLEDGMENTS

We sincerely thank the reviewers for their constructive comments. We also thank Xiaohong Zhu and Xiajuan Xu for help with the fieldwork. We would like to thank editage (www.editage.cn) for English language editing.

SUPPLEMENTARY MATERIAL

The Supplementary Material for this article can be found online at: https://www.frontiersin.org/articles/10.3389/fpls.2022.946949/full#supplementary-material

REFERENCES

Agren, G. I. (2004). The C:N:P stoichiometry of autotrophs theory and observations. *Ecol. Lett.* 7, 185–191. doi: 10.1111/j.1461-0248.2004.00567.x

Angle, J. C., Morin, T. H., Solden, L. M., Narrowe, A. B., Smith, G. J., Borton, M. A., et al. (2017). Methanogenesis in oxygenated soils is a substantial fraction of wetland methane emissions. *Nat. Commun.* 8:1567. doi: 10.1038/s41467-017-01753-4

Bing, H. J., Wu, Y. H., Zhou, J., Sun, H. Y., Luo, J., Wang, J. P., et al. (2016). Stoichiometric variation of carbon nitrogen and phosphorus in soils and its implication for nutrient limitation in alpine ecosystem of eastern Tibetan plateau. *J. Soils Sediments* 16, 405–416. doi: 10.1007/s11368-015-1200-9

Bui, E. N., and Henderson, B. L. (2013). C:N:P stoichiometry in Australian soils with respect to vegetation and environmental factors. *Plant Soil* 373, 553–568. doi: 10.1007/s11104-013-1823-9

Chen, X., and Chen, H. Y. H. (2021). Plant mixture balances terrestrial ecosystem C:N:P stoichiometry. *Nat. Commun.* 12, 4562. doi: 10.1038/s41467-021-24889-w

Cordell, S., Goldstein, G., Meinzer, F. C., and Vitousek, P. M. (2001). Morphological and physiological adjustment to N and P fertilization in nutrient limited Metrosiderospolymorpha canopy trees in Hawaii. *Tree Physiol.* 21, 43–50. doi: 10.1093/treephys/21.1.43

Crovo, O., Aburto, F., Albornoz, M. F., and Southard, R. J. (2021). Soil type modulates the response of C, N, P stocks and stoichiometry after native forest substitution by exotic plantations. *Catena* 197:104997. doi: 10.1016/j.catena.2020.104997

Demars, B., and Edwards, A. C. (2010). Tissue nutrient concentrations in freshwater aquatic macrophytes: high inter-taxon differences and low phenotypic response to nutrient supply. *Freshw. Biol.* 52, 2073–2086. doi: 10.1111/j.1365-2427.2007.01817.x

Don, A., Schumacher, J., Scherer-Lorenzen, M., Scholten, T., and Schulze, E. D. (2007). Spatial and vertical variation of soil carbon at two grassland sites: implications for measuring soil carbon stocks. *Geoderma* 141, 272–282. doi: 10.1016/j.geoderma.2007.06.003

Elser, J. J., Bracken, M. E. S., Cleland, E. E., Gruner, D. S., Harpole, W. S., Hillebrand, H., et al. (2007). Global analysis of nitrogen and phosphorus limitation of primary producers in freshwater, marine and terrestrial ecosystems. *Ecol. Lett.* 10, 1135–1142. doi: 10.1111/j.1461-0248.2007.01113.x

Elser, J., O'brien, W., Dobberfuhl, D., and Dowling, T. (2000). The evolution of ecosystem processes: growth rate and elemental stoichiometry of a key herbivore in temperate and arctic habitats. *J. Evol. Biol.* 13, 845–853. doi: 10.1046/j.1420-9101.2000.00215.x

Feng, L. H., and Bao, Y. X. (2006). Coastal change and tidal flat reclamation in Cixi City. *Geogr. Geogr. Info. Syst.* 22, 75–78.

Graciano, C., Guiamét, J. J., and Goya, J. F. (2005). Impact of nitrogen and phosphorus fertilization on drought responses in *Eucalyptus grandis* seedlings. *For. Ecol. Manag.* 212, 40–49. doi: 10.1016/j.foreco.2005.02.057

Güsewell, S. (2004). N:P ratios in terrestrial plants: Variation and functional significance. *New Phytol.* 164, 243–266. doi: 10.1111/j.1469-8137.2004.01192.x

Güsewell, S., Koerselman, W., and Verhoeven, J. T. A. (2003). BiomassN: P ratios as indicators of nutrient limitation for plantpopulations in wetlands. *Ecol. Appl.* 13, 372–384. doi: 10.1890/1051-0761(2003)013[0372:BNRAIO]2.0.CO;2

He, M. Z., Zhang, K., Tan, H. J., Hu, R., Su, J. Q., Wang, J., et al. (2015). Nutrient levels within leaves, stems, and roots of the xeric species *Reaumuria soongorica* in relation to geographical, climatic, and soil conditions. *Ecol. Evol.* 5, 1494–1503. doi: 10.1002/ece3.1441

Hessen, D., Jensen, T., Kyle, M., and Elser, J. (2007). RNA responses to N- and P-limitation; reciprocal regulation of stoichiometry and growth rate in *Brachionus*. *Funct. Ecol.* 21, 956–962. doi: 10.1111/j.1365-2435.2007.01306.x

Högberg, P., Näsholm, T., Franklin, O., and Högberg, M. N. (2017). Tamm review: on the nature of the nitrogen limitation to plant growth in Fennoscandian boreal forests. *For. Ecol. Manag.* 403, 161–185. doi: 10.1016/j.foreco.2017.04.045

Hu, Y. K., Liu, X. Y., He, N. P., Pan, X., Long, S. Y., Li, W., et al. (2021). Global patterns in leaf stoichiometry across coastal wetlands. *Glob. Ecol. Biogeogr.* 30, 852–869. doi: 10.1111/geb.13254

Hu, M. J., Peñuelas, J., Sardans, J., Sun, Z. G., Wilson, B. J., Huang, J. F., et al. (2018). Stoichiometry patterns of plant organ N and P in coastal herbaceous wetlands along the East China Sea: implications for biogeochemical niche. *Plant Soil* 431, 273–288. doi: 10.1007/s11104-018-3759-6

Hu, M., Sardans, J., Yang, X., Peuelas, J., and Tong, C. (2020). Patterns and environmental drivers of greenhouse gas fluxes in the coastal wetlands of China: A systematic review and synthesis. *Environ. Res.* 186:109576. doi: 10.1016/j.envres.2020.109576

Hu, W. F., Zhang, W. L., Zhang, L. H., Chen, X. Y., Lin, W., Zeng, C. S., et al. (2014). Stoichiometric characteristics of nitrogen and phosphorus in major wetland vegetation of China. *Chin. J. Plant Ecol.* 38, 1041–1052. doi: 10.3724/SP.J.1258.2014.00098

Hui, D. F., Yang, X. T., Deng, Q., and Liu, Q. (2021). Soil C:N: P stoichiometry in tropical forests on Hainan Island of China: spatial and vertical variations. *Catena* 201:105228. doi: 10.1016/j.catena.2021.105228

Iost, S., Landgraf, D., and Makeschin, F. (2007). Chemical soil properties of reclaimed marsh soil from Zhejiang Province P.R China. *Geoderma* 142, 245–250. doi: 10.1016/j.geoderma.2007.08.001

Jackson, M. L. (1958). *Soil Chemical Analysis*. New York: Prentice hall INC

Koerselman, W., and Meuleman, A. F. (1996). The vegetation N:P ratio: a new tool to detect the nature of nutrient limitation. *J. Appl. Ecol.* 33, 1441–1450. doi: 10.2307/2404783

Luo, X. Z., Hou, E. Q., Chen, J. Q., Li, J., Zhang, L. L., Zhang, X. W., et al. (2020). Dynamics of carbon, nitrogen, and phosphorus stocks and stoichiometry resulting from conversion of primary broadleaf forest to plantation and secondary forest in subtropical China. *Catena* 193:104606. doi: 10.1016/j.catena.2020.104606

Ma, X. X., Hong, J. T., and Wang, X. D. (2019). C:N:P stoichiometry of perennial herbs' organs in the alpine steppe of the northern Tibetan plateau. *J. Mt. Sci.* 16, 2039–2047. doi: 10.1007/s11629-018-5299-1

Ma, Z., Melville, D. S., Liu, J., Chen, Y., Yang, H., Ren, W., et al. (2014). Rethinking China's new great wall. *Science* 346, 912–914. doi: 10.1126/science.1257258

Minden, V., and Kleyer, M. (2014). Internal and external regulation of plant organ stoichiometry. *Plant Biol.* 16, 897–907. doi: 10.1111/plb.12155

Ning, X., Hu, M. M., Shao, X. X., and Wu, M. (2017). Assessment of coastal wetland ecosystem services in the south of Hangzhou Bay. *Ecol. Sci.* 36, 166–176. doi: 10.14108/j.cnki.1008-8873.2017.04.023

Ordoñez, J. C., Bodegom, P. M. V., Witte, J. P. M., Bartholomenus, R. P., and Han, D. R. A. (2010). Leaf habit and woodiness regulate different leaf economy traits at a given nutrient supply. *Ecology* 91, 3218–3228. doi: 10.1890/09-1509.1

Peñuelas, J., Sardans, J., Rivasubach, A., and Janssens, J. A. (2012). The human-induced imbalance between C, N and P in Earth's life system. *Glob. Chang. Biol.* 18, 3–6. doi: 10.1111/j.1365-2486.2011.02568.x

Reich, P. B., and Oleksyn, J. (2004). Global patterns of plant leaf N and P in relation to temperature and latitude. *Proc. Natl. Acad. Sci.* 101, 11001–11006. doi: 10.1073/pnas.0403588101

Rong, Q. Q., Liu, J. T., Cai, Y. P., Lu, Z. H., Zhao, Z. Z., Yue, W. C., et al. (2015). Leaf carbon, nitrogen and phosphorus stoichiometry of *Tamarix chinensisLour* in the Laizhou Bay coastal wetland, China. *Ecol. Eng.* 76, 57–65. doi: 10.1016/j.ecoleng.2014.03.002

Sardans, J., Rivas-Ubach, A., and Peñuelas, J. (2012). The elemental stoichiometry of aquatic and terrestrial ecosystems and its relationships with organismic lifestyle and ecosystem structure and function: a review and perspectives. *Biogeochemistry* 111, 1–39. doi: 10.1007/s10533-011-9640-9

Sterner, R. W., and Elser, J. J. (2002). *Ecological Stoichiometry: The Biology of Elements From Molecules to the Biosphere*. Princeton: Princeton University Press.

Tang, X., Hu, J., Qiu, J., Dong, Y., and Li, B. (2022). Soil C, N, P stocks and stoichiometry as related to land use types and Erosion conditions in lateritic red soil region, South China. *Catena* 210:105888. doi: 10.1016/j.catena.2021.105888

Townsend, A. R., Cleveland, C. C., Asner, G. P., and Bustamante, M. M. (2007). Controls over foliar N:P ratios in tropical rain forests. *Ecology* 88, 107–118. doi: 10.1890/0012-9658(2007)88[107:COFNRI]2.0.CO;2

Urbina, I., Sardans, J., Grau, O., Beierkuhnlein, C., Jentsch, A., Kreyling, J., et al. (2017). Plant community composition affects the species biogeochemical niche. *Ecosphere* 8:e01801. doi: 10.1002/ecs2.1801

Vitousek, P. M., Aber, J. D., Howarth, R. W., Likens, G. E., Matson, P. A., Schindler, D. W., et al. (1996). Human alteration of the global nitrogen cycle: sources and consequences. *Nat. Sci. Soc.* 5, 85–750. doi: 10.1016/S1240-1307(97)87738-2

Vitousek, P. M., Porder, S., Houlton, B. Z., and Chadwick, O. A. (2010). Terrestrial phosphorus limitation: mechanisms, implications, and nitrogen-phosphorus interactions. *Ecol. Appl.* 20, 5–15. doi: 10.1890/08-0127.1

Vrede, T., Dobberfuhl, D. R., Kooijman, S., and Elser, J. J. (2004). Fundamental connections among organism C:N:P stoichiometry, macromolecular composition, and growth. *Ecology* 85, 1217–1229. doi: 10.1890/02-0249

Wang, M., and Moore, T. R. (2014b). Carbon, nitrogen, phosphorus, and potassium stoichiometry in an ombrotrophic peatland reflects plant functional type. *Ecosystems* 17, 673–684. doi: 10.1007/s10021-014-9752-x

Wang, W. Q., Sardans, J., Wang, C., Zeng, C. S., Tong, C., Chen, G. X., et al. (2019). The response of stocks of C, N and P to plant invasion in the coastal wetlands of China. *Glob. Chang. Biol.* 25, 733–743. doi: 10.1111/gcb.14491

Wang, W. Q., Sardans, J., Zeng, C. S., Zhong, C., Li, Y., and Peñuelas, J. (2014a). Responses of soil nutrient concentrations and stoichiometry to different human land uses in a subtropical tidal wetland. *Geoderma* 232–234, 459–470. doi: 10.1016/j.geoderma.2014.06.004

Wang, W. Q., Wang, C., Sardans, J., Tong, C., Jia, R. X., Zeng, C. S., et al. (2015). Flood regime affects soil stoichiometry and the distribution of the invasive plants in subtropical estuarine wetlands in China. *Catena* 128, 144–154. doi: 10.1016/j.catena.2015.01.017

Xiong, J., Yu, M. K., Cheng, X. R., Wang, C., and Zou, H. L. (2021). Effects of light and N-P supply ratios on growth and stoichiometric of *Schimasuperba*. *Acta EcologicaSinica* 41, 2140–2150. doi: 10.1016/j.ecoleng.2021.106473

Yang, J. Z., Zhao, Y. L., and Wang, Y. (2004). Remote sensing dynamic monitoring of tidal banks in the Hangzhou Bay. *Geolog. Sci.* 39, 168–177.

Yu, Y. H., and Chi, Y. K. (2019). Ecological stoichiometric characteristics of soil at different depths in a karst plateau mountain area of China. *Pol. J. Environ. Stud.* 29, 969–978. doi: 10.15244/pjoes/102781

Yu, Z., Wang, M., Huang, Z., Lin, T. C., Vadeboncoeur, M. A., Searle, E. B., et al. (2018). Temporal changes in soil C-N-P stoichiometry over the past 60 years across subtropical China. *Glob. Chang. Biol.* 24, 1308–1320. doi: 10.1111/gcb.13939

Zhang, Y. (2010). *The Spatial Distribution and Bioenergy Estimation of an Invasive plant Spartina alterniflora in China*. Hangzhou: Zhejiang university

Zhang, Q. H., Sairebieli, K., Zhao, M. M., Sun, X. H., Wang, W., Yu, X. N., et al. (2020). Nutrients have a different impact on the salt tolerance of two coexisting suaeda species in the Yellow River Delta. *Wetlands* 40, 2811–2823. doi: 10.1007/s13157-020-01382-6

Zhang, K., Su, Y. Z., and Yang, R. (2019). Variation of soil organic carbon, nitrogen, and phosphorus stoichiometry and biogeographic factors across the desert ecosystem of Hexi corridor, Northwestern China. *J. Soils Sediments* 19, 49–57. doi: 10.1007/s11368-018-2007-2

Zhang, W., Zhao, J., Pan, F. J., Li, D. J., Chen, H. S., and Wang, K. L. (2015). Changes in nitrogen and phosphorus limitation during secondary succession in a karst region in Southwest China. *Plant Soil* 391, 77–91. doi: 10.1007/s11104-015-2406-8

Zheng, S. M., Xia, Y. H., Hu, Y. H., Chen, X. B., Rui, Y. C., Gunina, A., et al. (2021). Stoichiometry of carbon, nitrogen, and phosphorus in soil: effects of agricultural land use and climate at a continental scale. *Soil Tillage Res.* 209:104903. doi: 10.1016/j.still.2020.104903

Conflict of Interest: The authors declare that the research was conducted in the absence of any commercial or financial relationships that could be construed as a potential conflict of interest.

The handling editor declared a shared affiliation with the authors at the time of review.

Publisher's Note: All claims expressed in this article are solely those of the authors and do not necessarily represent those of their affiliated organizations, or those of the publisher, the editors and the reviewers. Any product that may be evaluated in this article, or claim that may be made by its manufacturer, is not guaranteed or endorsed by the publisher.

frontiers | Frontiers in Plant Science

TYPE Original Research
PUBLISHED 04 August 2022
DOI 10.3389/fpls.2022.939762

OPEN ACCESS

EDITED BY
Yangong Du,
Northwest Institute of Plateau Biology (CAS), China

REVIEWED BY
Tao Zhang,
Northeast Normal University, China
Lu Wen,
Inner Mongolia University, China
Ning Chen,
Lanzhou University, China

*CORRESPONDENCE
Xilai Li
xilai-li@163.com

SPECIALTY SECTION
This article was submitted to Functional Plant Ecology, a section of the journal Frontiers in Plant Science

RECEIVED 09 May 2022
ACCEPTED 06 July 2022
PUBLISHED 04 August 2022

CITATION
Li C, Li X, Yang Y, Shi Y and Li H (2022) Degradation reduces the diversity of nitrogen-fixing bacteria in the alpine wetland on the Qinghai-Tibet Plateau. *Front. Plant Sci.* 13:939762. doi: 10.3389/fpls.2022.939762

Degradation reduces the diversity of nitrogen-fixing bacteria in the alpine wetland on the Qinghai-Tibet Plateau

Chengyi Li[1], Xilai Li[1,2]*, Yuanwu Yang[1], Yan Shi[3] and Honglin Li[2]

[1]College of Agriculture and Animal Husbandry, Qinghai University, Xining, China, [2]State Key Laboratory of Plateau Ecology and Agriculture, Qinghai University, Xining, China, [3]School of Environment, The University of Auckland, Auckland, New Zealand

Biological nitrogen fixation is a key process in the nitrogen cycle and the main source of soil available nitrogen. The number and diversity of nitrogen-fixing bacteria directly reflect the efficiency of soil nitrogen fixation. The alpine wetland on the Qinghai-Tibet Plateau (QTP) is degrading increasingly, with a succession toward alpine meadows. Significant changes in soil physicochemical properties accompany this process. However, it is unclear how does the soil nitrogen-fixing bacteria change during the degradation processes, and what is the relationship between these changes and soil physicochemical properties. In this study, the *nifH* gene was used as a molecular marker to further investigate the diversity of nitrogen-fixing bacteria at different stages of degradation (none, light, and severe degeneration) in the alpine wetland. The results showed that wetland degradation significantly reduced the diversity, altered the community composition of nitrogen-fixing bacteria, decreased the relative abundance of Proteobacteria, and increased the relative abundance of Actinobacteria. In addition to the dominant phylum, the class, order, family, and genus of nitrogen-fixing bacteria had significant changes in relative abundance. Analysis of Mantel test showed that most soil factors (such as pH, soil water content (SWC), the organic carbon (TOC), total nitrogen (TN), and soil C:P ratio) and abundance had a significant positive correlation. TOC, TN, total phosphorus (TP), soil C:P ratio and Shannon had a significant positive correlation with each other. The RDA ranking further revealed that TOC, SWC, and TN were the main environmental factors influencing the community composition of nitrogen-fixing bacteria. It is found that the degradation of the alpine wetland inhibited the growth of nitrogen-fixing bacteria to a certain extent, leading to the decline of their nitrogen-fixing function.

KEYWORDS

Qinghai-Tibet Plateau, alpine wetland, wetland succession, *nifH* gene, nitrogen-fixing bacteria

Introduction

The nitrogen cycle is one of the globally important biogeochemical processes that are almost entirely mediated by microorganisms in the environment (Wang et al., 2015). As nitrogen fixation is a key process in the microbial nitrogen cycle (Levy-Booth et al., 2014), biological nitrogen fixation reduces atmospheric unavailable N_2 to NH_4^+ that can be absorbed and utilized by plants (Simon et al., 2014). Globally, ~198 Tg of nitrogen per year is fixed by bacteria in natural terrestrial and aquatic ecosystems (Fowler et al., 2018). The fixed nitrogen can alleviate nitrogen constraints on the function of the forest (Deluca et al., 2002), grassland (Regan et al., 2016), desert (Ramond et al., 2018), and marine ecosystems (Zehr, 2011). Therefore, biological nitrogen fixation represents the largest input of non-anthropogenic nitrogen intake to most terrestrial and aquatic ecosystems (Vitousek et al., 1997; Paul et al., 2010), and is also considered to be the largest source of reactive nitrogen on Earth (Cleveland et al., 1999; Galloway et al., 2004). All nitrogen-fixing bacteria discovered so far belong to prokaryotes, and there is a catalytic nitrogenous in these nitrogen-fixing bacteria (Kang et al., 2013). Nitrogenous complexes are composed of MoFeprotein encoded by the *nifD* and *nifK* genes and ferritin encoded by the *nifH* genes (Zehr et al., 2003). The *nifH* gene exists only in nitrogen-fixing bacteria, and its phylogenetic relationship is consistent with 16S rRNA, which is a genetic marker of nitrogen-fixing bacteria (Kang et al., 2013). It is commonly used to prove the existence of nitrogen-fixing bacteria and to reveal the relationship between the community structure of nitrogen-fixing bacteria and the environment (Liu et al., 2017). In addition, the abundance, diversity, and community composition of nitrogen-fixing bacteria have been considered as the key biological factors to determine the nitrogen-fixing capacity of the soil (Lindsay et al., 2010; Reed et al., 2010; Stewart et al., 2011). Therefore, determining them can help to understand the nitrogen cycle in terrestrial ecosystems.

With an average altitude of over 4,000 m, the Qinghai-Tibet Plateau (QTP) is known as the "roof of the world" and the "third pole." It is an important ecological security barrier for China and even Asia, with important functions such as carbon and nitrogen storage, water recharge, and climate regulation (Sun et al., 2012). Its unique geographical location and climatic conditions have nurtured the alpine ecosystems that are sensitive to climate change and human activities (Zhao and Shi, 2020), including grasslands, wetlands, deserts, and forests. Among them, the alpine wetlands cover an area of over 1×10^5 km^2, accounting for nearly 30% of China's wetland area. They are widely distributed in the main region of the QTP, including the headwater of three rivers (Sanjiangyuan region) in China (Xing et al., 2009; Zhao et al., 2014; Zhao and Shi, 2020). Over the past few decades, due to the influence of human activities (drainage and overgrazing), the groundwater level of the alpine wetlands has decreased, and vegetation communities have changed (Straková et al., 2010; Munir et al., 2014; Wu et al., 2021). In addition, global climate change has further exacerbated the human-induced groundwater level decline of the alpine wetlands (Liu et al., 2019). Lower groundwater levels promote the decomposition of organic matter and loss of humus and peat layers in soil (Shuang et al., 2009; Lin et al., 2021), and may simultaneously promote the conversion of soil nitrogen to aerobic processes (Espenberg et al., 2018), resulting in soil nitrogen reduction (Liu L. et al., 2018). The typical regression succession pattern of the alpine wetland is a marsh (intact wetland) → marsh meadow (early degradation stage) → alpine meadow (degraded) (Guo et al., 2013; Luan et al., 2014). The development process of wetland has been transformed into humification and the REDOX process of meadow soil (Yang and Wang, 2001; Liang et al., 2007). It has been experimentally proven that soil microbial communities are more sensitive to environmental changes than plants and animals (Qian and Ricklefs, 2004; Zhou et al., 2008; Zhang et al., 2013). Soil microorganisms are the medium for all soil ecological functions, and their community composition and diversity are key to studying soil ecological balance and soil ecological functions (Shanmugam et al., 2017). Therefore, it is of great scientific importance to study the structure and diversity of soil microbial communities in the alpine wetlands in response to the alpine wetland degradation.

The degradation of the alpine wetland has a significant impact on soil microbial community structure and diversity (Li et al., 2021). However, different microbial taxa show different ecological functions in the biogeochemical cycle of elements, and the specific microbial community structure can affect a variety of ecosystem processes (Allison et al., 2013). At present, there are relatively few studies on the impact of the alpine wetland degradation on soil nitrogen-fixing bacteria community structure, only found by Wu et al. (2016), which reported that nitrogen cycling (nitrogen-fixing, ammonia oxidation, and denitrification), microbial community structure, and relative abundance changed due to the alpine wetland degradation. Even within the same type of ecosystem, soil nitrogen-fixing bacteria abundance, diversity, and community composition varied considerably among the study sites (Che et al., 2017; Wang et al., 2017). So far, many studies have confirmed that complex interactions exist among plant communities, soil physics and chemistry, and soil microorganisms (Tedersoo et al., 2014; Delgado-Baquerizo et al., 2018). The degradation of the alpine wetland is accompanied by significant changes in soil physicochemical properties (Li et al., 2021). The relationship between soil nitrogen-fixing bacteria and soil physicochemical properties during this process is not yet clear. Therefore, studying the changes in nitrogen-fixing bacteria composition and its relationship with the soil environment during the alpine wetland degradation can help us understand the soil microorganisms changing mechanisms and nitrogen-cycling processes of the alpine wetland under human disturbance and climate change.

In this study, none, lightly, and severely degraded alpine wetlands in the source region of the Yellow River on the QTP were selected as research objects, and the diversity of nitrogen-fixing bacteria was identified by using the *nifH* gene as a molecular marker. To reveal the response of nitrogen-fixing bacteria diversity to the degradation of the alpine wetlands, explore the critical environmental factors that affect the community structure of nitrogen-fixing bacteria, and provide scientific theoretical support for the protection and management of the alpine wetlands, this study aims to: (1) explore the structure and composition of the nitrogen-fixing bacteria community in the alpine wetland and its various features in the degraded succession sequence and (2) access the correlation between the diversity of nitrogen-fixing bacteria and environmental factors.

Materials and methods

Description of sample points

The study site is located in Dawu Town, Maqin County, Guoluo Tibetan Autonomous Prefecture, Qinghai Province, western China (34°27′ 48″ N, 100°12′ 49″ E, with an average altitude of 3,730 m) (Figures 1A,B). It has a continental cold and moist climate with an average annual temperature of −3.9 to −3.5°C and average annual precipitation of 423–565 mm (Lin et al., 2021). The alpine wetland in this area is rich in resources, and the plant communities in the experimental sites are mainly composed of *Cyperaceae* and *Gramineae*. The current land-use type is winter grazing. In this area, the wetland gradually changed to swamp meadows due to the increasing number and the decreasing size of freeze-thaw mounds, resulting in a severe degree of degradation. The characteristics of freeze-thaw banks in the alpine wetlands disappeared and transformed into alpine meadows. Dominant species, vegetation coverage, the average height of vegetation, number, and size of freeze-thaw mounds were recorded (Supplementary Table 1). The experimental area is 4 hectares (Figures 1C,D), and the selected sample plot extends outward from the alpine wetland by the sample line method. Three sample lines are randomly selected in different degradation stages (Non-degradation, ND, Figure 1E; Light degradation, LD, Figure 1F; Severe degradation, SD, Figure 1G) to collect soil samples. Each sampling line is sampled at 25 m intervals and tested six times in each location (Figure 1H).

Soil sample collection

In August 2020, during the vigorous growth period of forage grass, according to the principles of "random," "equal amount," and "multi-point mixing" in 18 sample points, five sample plots with specifications of 10 ×10 cm were selected for sampling by five-point sampling method. Because surface soil is more prone to degradation than deep soil (Liu L. et al., 2018), we focused on the changes of nitrogen-fixing bacteria in shallow soil in this study. The sampling tool is disinfected with alcohol, and the ground of 0–20 cm soil layer with the exact weight is evenly mixed. After removing impurities, such as roots and stones, soil samples are put into a sterile tube by the "quartering method." Only 10 g of each soil sample was used for detecting the *nifH* gene (tested by Beijing Allwegene Technology Co., Ltd). These sub-samples were temporarily stored in a liquid nitrogen tank in the field, and the tanks were put into chilly bins filled with dry ice for delivery. The remaining soil samples were taken back to the laboratory, and some fresh soil samples were stored in a low-temperature refrigerator at 4°C. In contrast, others were naturally dried and ground, and sieved to analyze soil's physical and chemical properties.

Analysis and determination of soil samples

Physical and chemical properties

Soil moisture was measured by TDR350 produced by Spectrum Company (USA). The contents of total nitrogen (TN), total phosphorus (TP), available phosphorus (AP), ammonium nitrogen (NH_4^+-N), and nitrate-nitrogen (NO_3^--N) were determined by the AA3 Continuous Flow Analyzer from SEAL company (Germany), and organic carbon content (TOC) was determined by external oxidation heating method of potassium dichromate-concentrated sulfuric acid solution. Soil pH was determined by a pHS-3C pH meter (soil: water = 1: 2.5). There were significant differences in soil physicochemical properties and stoichiometric ratio in the alpine wetlands at different degradation stages (Supplementary Table 2).

Illumina MiSeq sequencing *nifH* gene

The test steps are: genomic DNA extraction—genomic DNA quality inspection—PCR amplification—PCR product electrophoresis detection—PCR product purification—Miseq library construction—Miseq library quality inspection—Illumina Miseq machine sequencing platform.

DNA extraction

Soil microbiome DNA was extracted by the PowerSoil DNA Isolation Kit (MoBio Laboratories, Inc., CA) [Omega E.Z.N.A. Stool DNA Kit (Omega Bio-Tek, Inc., USA)]. The extracted DNA was assayed for DNA quality and concentration using a Nanodrop 2000 (ThermoFisher Scientific, Inc., USA). The samples were stored at −20°C for subsequent experiments.

PCR amplification

Gene primer for *nifH*-F: 5′-AAAGGYGG WATCGGYAARTCCACCAC-3′ and *nifH*-R: 5′-TTGTTSGCSGCRTACATSGCCATCAT-3′

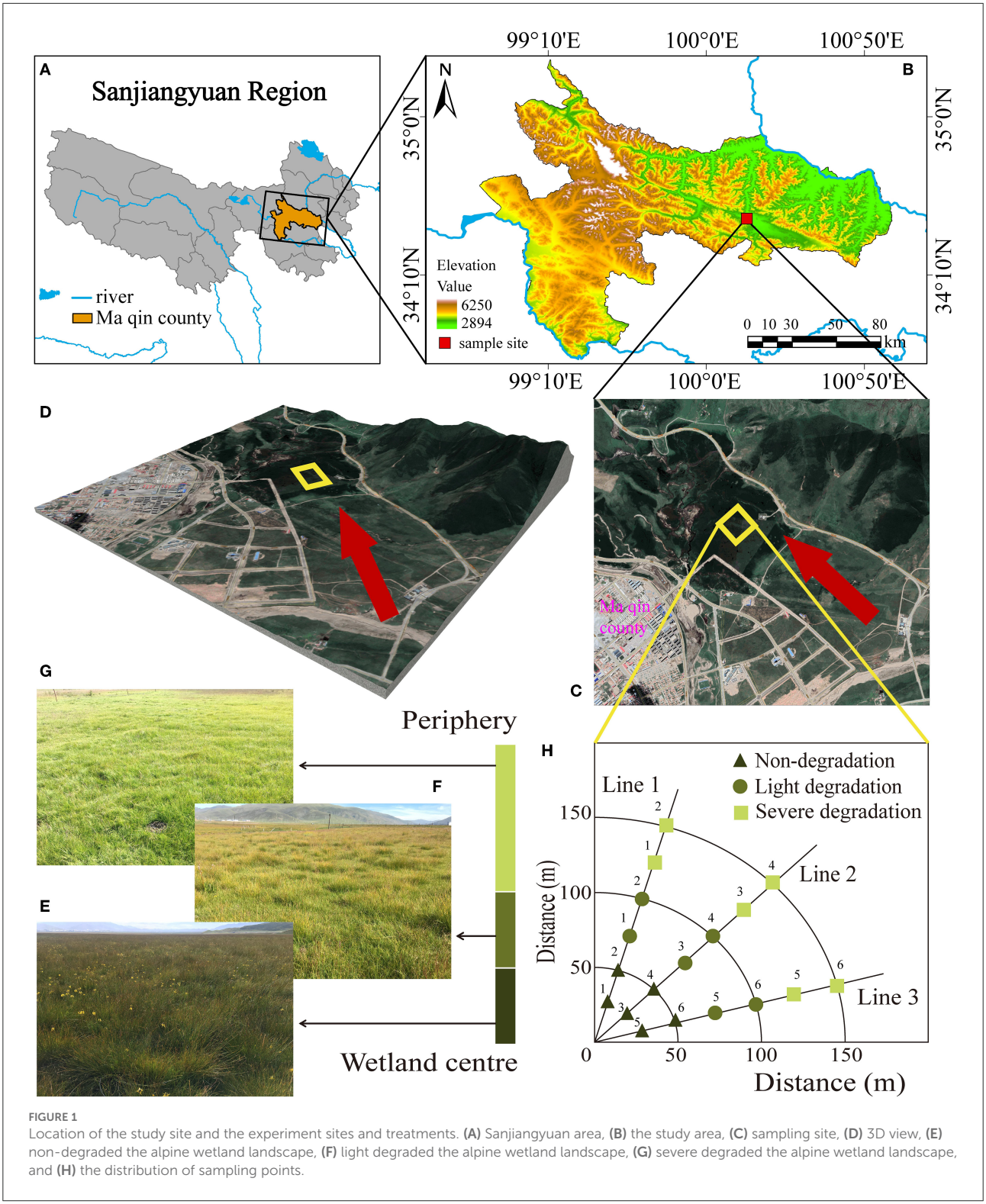

FIGURE 1
Location of the study site and the experiment sites and treatments. **(A)** Sanjiangyuan area, **(B)** the study area, **(C)** sampling site, **(D)** 3D view, **(E)** non-degraded the alpine wetland landscape, **(F)** light degraded the alpine wetland landscape, **(G)** severe degraded the alpine wetland landscape, and **(H)** the distribution of sampling points.

(Rösch and Bothe, 2005). PCR reaction system (total system is 25 μL): 12.5 μL 2xTaq Plus Master Mix II (Vazyme Biotech Co., Ltd, China), 3 μL BSA (2 ng/μL), 1 μL Forward Primer (5 μM), 1 μL Reverse Reaction parameters: 95°C pre-denaturation for 5 min; denaturation at 95°C for 45 s, annealing at 55°C for 50 s, extension at 72°C for 45 s, 28 cycles; extension at 72°C for 10 min. The PCR products were amplified using 1% agarose gel electrophoresis to detect the size of the amplified target bands

and purified using the Agencourt AMPure XP nucleic acid purification kit (Beckman Coulter, Inc., USA).

MiSeq sequencing

PCR products were used to construct microbial diversity sequencing libraries using the NEB Next Ultra II DNA Library Prep Kit (New England Biolabs, Inc., USA). Paired-end sequencing was performed at the Beijing Allwegene Technology Co., Ltd. using the Illumina Miseq PE300 high-throughput sequencing platform (Illumina, Inc., USA). The sequenced raw sequences were uploaded to the NCBI's SRA database.

Data processing

To make the analysis result more accurate and reliable, the off-board data is split by the QIIME (v1.8.0) software according to the Barcode sequence, and the data quality control is carried out by the Pear (v0.9.6) software. After sequence splicing, filtering, and chimerism removal, the optimized sequence is obtained, and then OTUs (operational taxonomic units) clustering and annotation are carried out. The UPARSE method was used to statistically analyze the biological information of OTUs at a 97% similarity level (Edgar, 2013). Based on the clustering results, diversity analysis can be carried out; OTUs were annotated with the database of Silva (Release 128/132 https://www.arb-silva.de/) (Quast et al., 2012). Based on the annotation results, the species information of each classification can be obtained. Then, the correlation analysis of sample composition and community results among samples can be carried out.

Shannon-Wiener is an index reflecting the microbial diversity of samples, and it is constructed by using the microbial diversity index of each sample at different sequencing depths to reflect the microbial diversity of each sample with different sequencing quantities (Quast et al., 2012). The curve tends to be flat, and the sequencing data was large enough to reflect most of the microbial information in the sample (Supplementary Figure 1).

Data analysis

The differences in soil physicochemical properties, nitrogen-fixing bacteria diversity (Chao1, Observed_species, PD_whole_tree, and Shannon), and species abundance in different degradation stages were examined by the one-way ANOVA and multiple comparison (Duncan) analysis with the SPSS Statistics 20.0 statistical analysis software.

The overlap of the number of OTUs in different degradation stages was represented by the Venn diagram. In the R software environment, the differences of *nifH* gene communities in different degradation stages were visualized by principal coordinate analysis (PCoA). To determine whether the degradation of the alpine wetlands changed the community composition of the *nifH* gene, a permutation variance analysis (PERMANOVA) was carried out using the Bray-Curtis similarity index. The effect was analyzed by linear discriminant analysis (LEfSe; Score = 3). Biomarkers with significant differences in abundance among different degradation stages were identified.

The Venn diagram and species composition histogram were counted and plotted by R language, and the Shannon-Wiener index was analyzed by mothur based on OTUs clustering results. The correlation analysis between the Mantel test and Pearson was completed by R language ggplot2, ggcor, and dplyr software package. Conducts the Redundancy analysis (RDA) with Canoco 5.0.

Results

Diversity of nitrogen-fixing bacteria

Chao1, Observed_species, PD_whole_tree, and Shannon indexes decrease with the deterioration of the alpine wetland (Figure 2). Compared with ND, LD Chao1, and Observed_species indexes were significantly decreased by 18.51 and 17.57%, respectively ($P < 0.05$). SD Chao1, Observed_species, PD_whole_tree, and Shannon indexes were significantly reduced by 30.00, 29.33, 23.21, and 4.21%, respectively ($P < 0.05$). Compared with LD, SD Chao1, Observed_species, and Shannon indexes significantly decreased by 14.10, 14.26, and 3.08%, respectively ($P < 0.05$). These results indicate that the degradation of the alpine wetlands is able to decline the diversity of nitrogen-fixing bacteria significantly.

Composition of nitrogen-fixing bacteria community

There were 1,180 common OTUs under different stages of degradation, accounting for 25.3% of the total OTUs. ND, LD, and SD stages had 1,125, 283, and 568 specific OTUs, respectively (Figure 3A). The PCoA results showed that nitrogen-fixing bacteria in different degradation stages gathered strongly (Figure 3B). The PERMANOVA results were consistent with the PCoA results. The PCoA could explain 39.52% of the variation in the communities containing the *nifH* gene. Among these, the first coordinate (PCoA1) distinguished the ND and SD stages, and the second coordinate (PCoA2) explained the remaining 13.73% of the variation.

The sequences obtained from the research were classified into 14 phyla, 19 classes, 49 orders, 95 families, and 177 genera. The proportion of major phylum, class, order, family, and

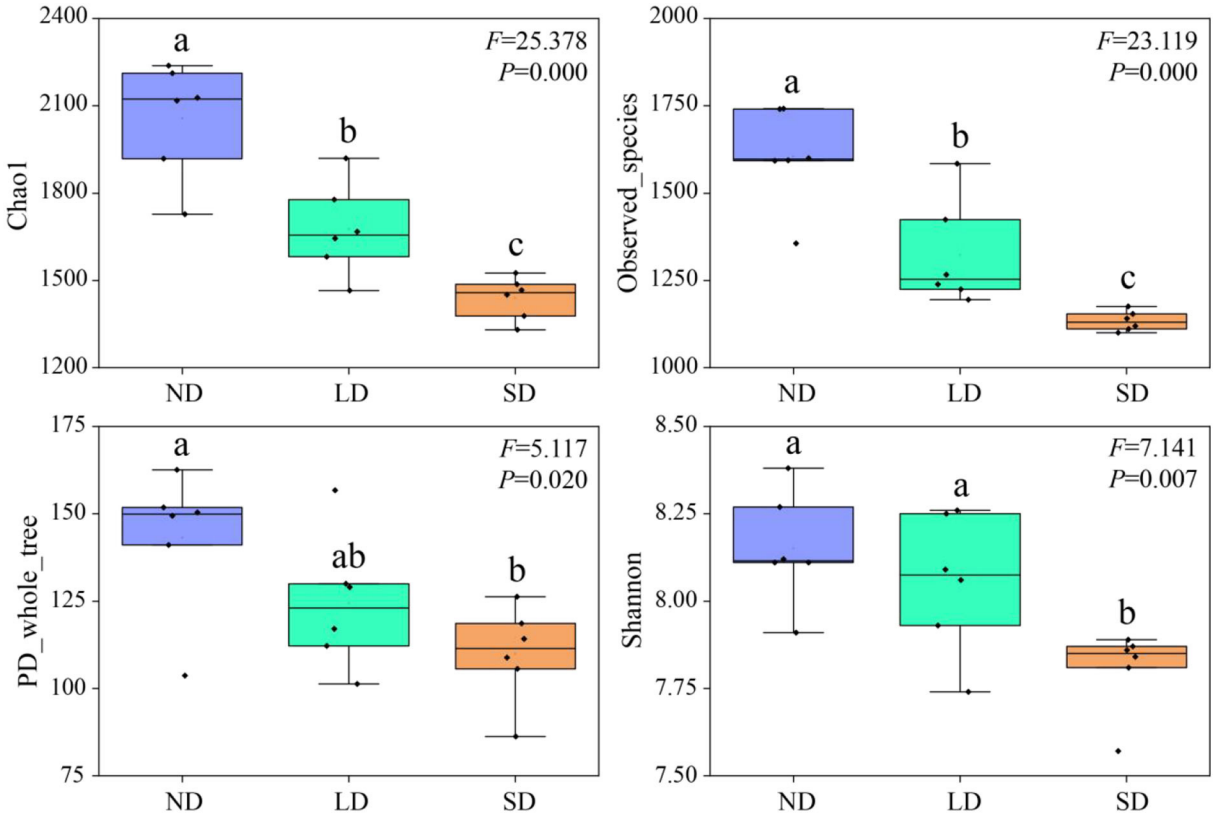

FIGURE 2
Abundance and diversity index of nitrogen-fixing bacteria community. ND is non-degradation and LN and SD are the light and severe degradation stages of the alpine wetland, respectively. The center mark in each box diagram represents the median, and the bottom and top edges of the box represent 25 and 75%, respectively. Different lowercase letters represent significant differences between different degradation stages.

genus is shown in Figure 4. The analysis of LEfSe allowed the identification of species (biomarkers) that were significantly different between groups and species or communities that significantly influenced the variability between groups. The evolution branches of nitrogen-fixing bacteria were different at various stages of degeneration. From phylum to genus, the radiating circle from inside to outside, the proportion of species with no significant difference colored yellow was small. In contrast, there were more *nifH* gene groups reflecting their differences in each degradation stage (Supplementary Figure 2), and the impact of significantly different species is shown in Supplementary Figure 3. At the ND stage of the evolutionary branching diagram, nitrogen-fixing bacteria with obvious directivity appeared at the phylum level, including Proteobacteria and Firmicutes, and Betaproteobacteria and Alphaproteobacteria at the class level, Burkholderiales and Rhizobiales at the order level, and Bradyrhizobiaceae and Burkholderiaceae at the family level. At the LD stage of the evolutionary branching diagram, nitrogen-fixing bacteria that point in a distinct direction do not appear at the phylum level, Deltaproteobacteria at the phylum level, Desulfuromonadales and Sphingomonadales at the order level and Geobacteraceae and Sphingomonadaceae at the family level. At the SD stage of the evolutionary branching diagram, the nitrogen-fixing bacteria that point clearly to the phylum level were Actinobacteria, Actinobacteria at the class level, Frankiales at the order level, and Frankiaceae and Rhizobiaceae at the family level.

The results of the ANOVA test showed significant differences in the abundance of dominant species at phylum, class, order, family, and genus levels at different stages of degradation (Figure 5). ND and LD Proteobacteria were significantly more abundant than SD. The abundance of ND and LD Actinobacteria was significantly lower than SD. ND Betaproteobacteria and Burkholderiales were significantly more abundant than LD and SD. The abundance of Deltaproteobacteria, Desulfuromonadales, Geobacteraceae, and *Geobacter* was significantly higher than that of ND and SD ($P < 0.05$). These results indicate that the degradation of the alpine wetland can significantly change the nitrogen-fixing bacteria community.

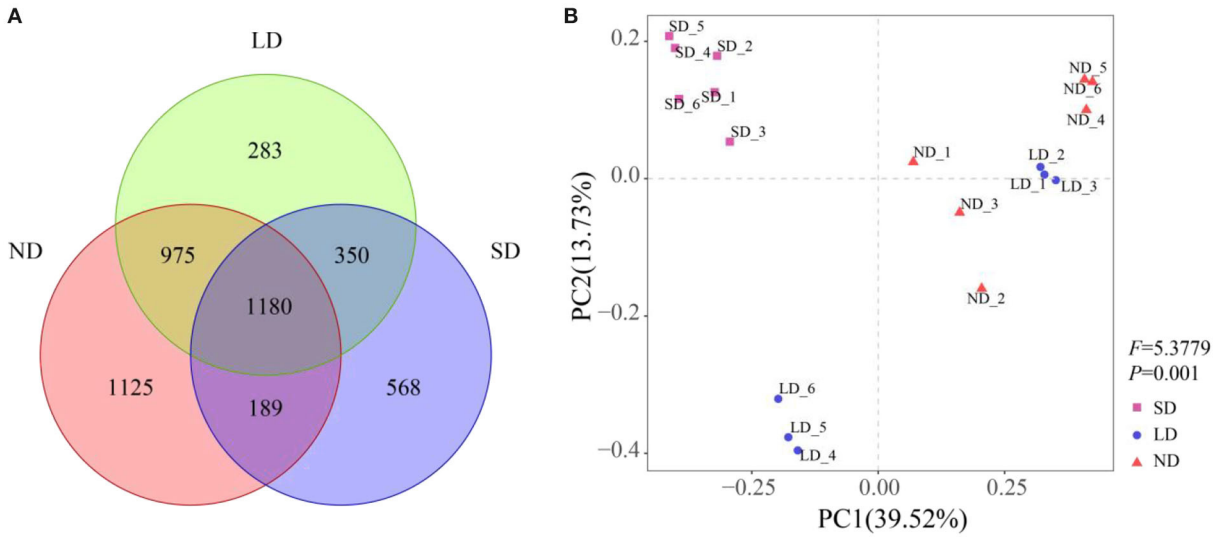

FIGURE 3
Effect of degradation on the community composition of nitrogen-fixing bacteria. **(A)** Venn diagram of different degradation stages, different colors represent different degradation stages, and overlapping areas of different colors represent intersection points (that is, common OTUs appear in areas with overlapping colors, while non-overlapping areas show unique OTUs). **(B)** Application of principal coordinate analysis (PCoA) of nitrogen-fixing bacteria community based on the Bray-Curtis different similarity matrix in different degradation stages. Different shapes represent different degradation stages. The percentage of change explained by principal coordinates is displayed on the coordinate axis, and PERMANOVA results are displayed on the right side of PCoA. ND is non-degradation and LN and SD are the light and severe degradation stages of the alpine wetland, respectively.

Factors affecting nitrogen-fixing bacteria

Analysis of the Mantel test showed that pH, SWC, TOC, TN, C:P, and the abundance of nitrogen-fixing bacteria were significantly positively correlated ($P < 0.05$). SWC, TOC, TN, C:P, N:P, and Chao1 index and species number were significantly positively correlated ($P < 0.05$). TOC, TN, C:P, N:P, and PD_whole_tree diversity were significantly positively correlated ($P < 0.05$). TOC, TN, TP, C:P, and Shannon were significantly positively correlated ($P < 0.05$; Figure 6). In addition, TOC, TP, TN, and SWC were positively correlated.

The RDA ordination results showed that the first- and second-ordination axes explained 26.44 and 13.13% of the total species variables, respectively (Figure 7). TOC, SWC, and TN accounted for 20.1, 17.4, and 15.5% of the prime index, respectively (Supplementary Table 3), as the main environmental factors influencing the abundance of the nitrogen-fixing bacteria phylum.

Discussion

In this study, we selected different degradation stages in an alpine wetland to investigate the responses of nitrogen-fixing bacteria to the degradation severities. Our result is similar to that of Wu et al. (2016), who showed that the degradation of the alpine wetlands significantly altered the community structure of the nitrogen-fixing bacteria. It was found that the degradation of the alpine wetland changed the composition of the nitrogen-fixing bacteria community. In addition, the abundance of nitrogen-fixing bacteria was related to the change of soil properties, especially TOC, SWC, and TN were significantly related to the abundance of nitrogen-fixing bacteria community. The relative abundance of Proteobacteria, which was positively correlated with TOC, SWC, and TN, decreased significantly with the degradation of the wetland. However, the relative abundance of Actinobacteria was negatively correlated with TOC, SWC, and TN. This may be because the soil environment with good water or nutrients is beneficial to the survival and reproduction of Proteobacteria, while Actinobacteria is more suitable for poor soil. We also detected a high proportion of Verrucomicrobia in the soil of the alpine wetland, which may be attributed to its excellent survival ability in extreme environments (Che et al., 2018). However, their abundance did not change significantly during wetland degradation. There was a direct relationship between the changes of nitrogen-fixing dominant bacilli and their dominant classes, orders, families, and genera. For example, the pattern of change in Deltaproteobacteria under Proteobacteria was consistent with changes in abundance of Desulfuromonadales, Geobacteraceae, and *Geobacter*.

Zhang et al. (2020) revealed that the process of transforming a natural marsh into a meadow and then into a sandy area in Zoige on the QTP inhibits the activity of soil nitrogen-fixing

10.3389/fpls.2022.939762

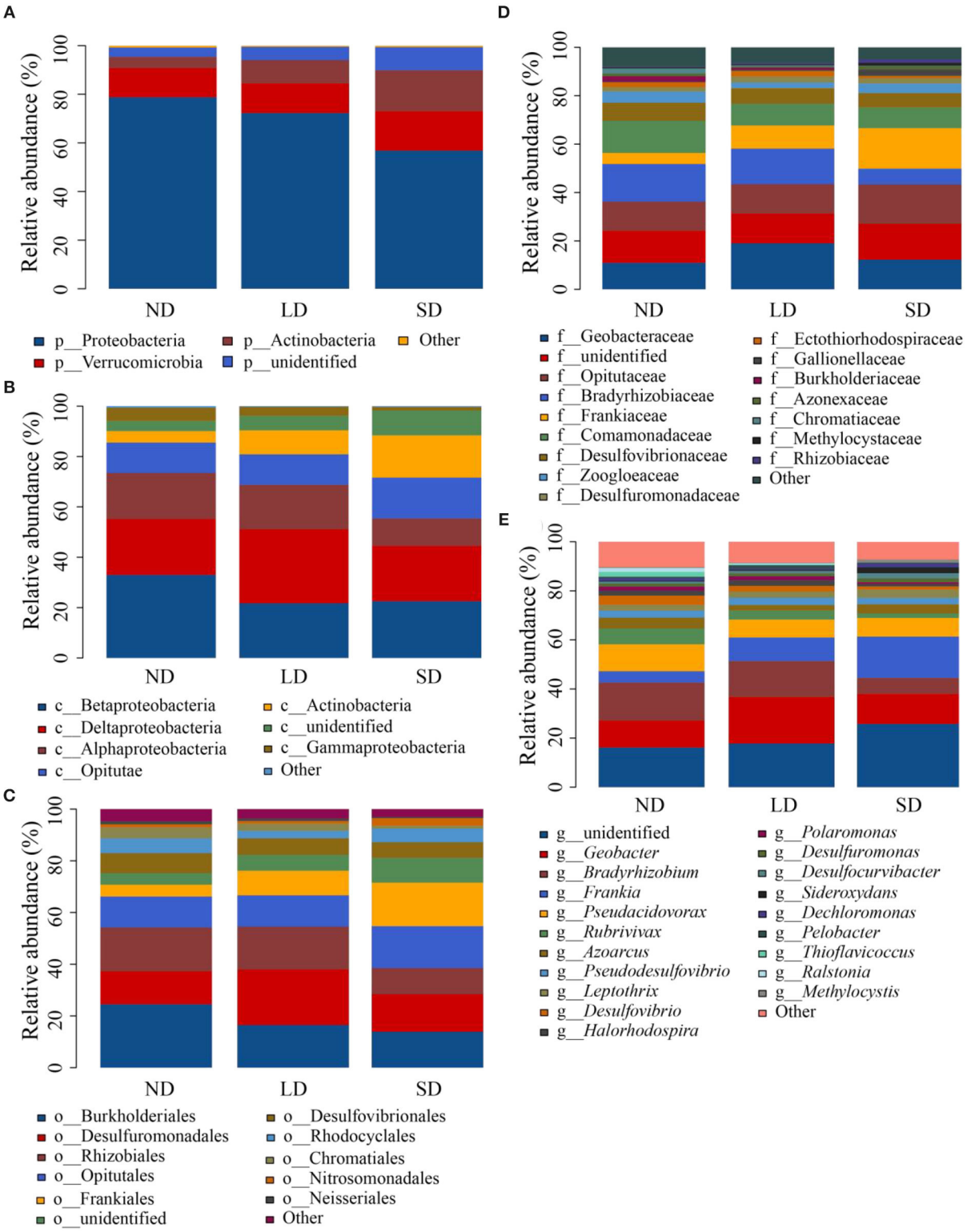

FIGURE 4
Relative abundance of phylum **(A)**, class **(B)**, order **(C)**, family **(D)**, and genus **(E)**. ND is non-degradation and LN and SD are the light and severe degradation stages of the alpine wetland, respectively.

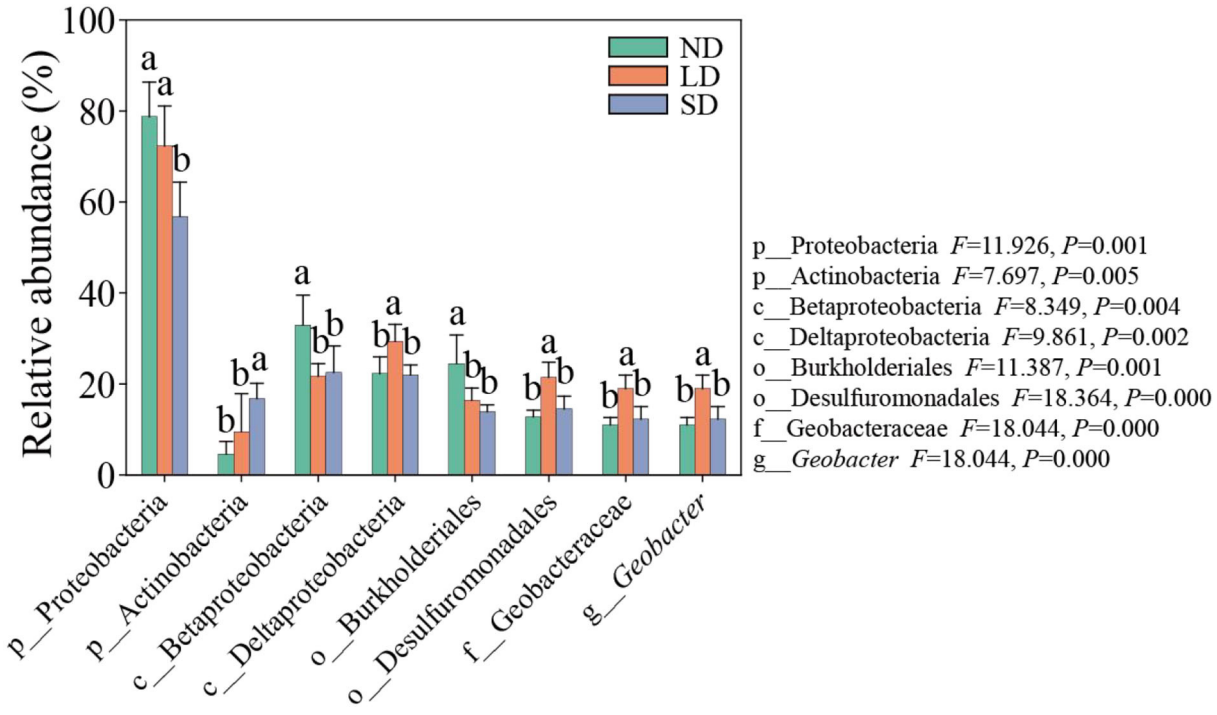

FIGURE 5
Abundance of main species of nitrogen-fixing bacteria. ND is non-degradation and LN and SD are the light and severe degradation stages of the alpine wetland, respectively. Different lowercase letters represent significant differences between different degradation stages.

bacteria. They find that degradation causes a reduction in soil water content, which in turn leads to a reduction in the rate of nitrogen fixation in wetlands through changes in plant communities, soil properties, and the composition of the nitrogen-fixing bacterial communities. In contrast, our results showed that the wetland degradation not only changes the composition of the nitrogen-fixing bacteria community, but also makes soil nitrogen-fixing bacteria more vulnerable, and then, the diversity decreases significantly with the aggravation. However, nitrogen-fixing bacteria diversity is more related to TOC, TN, TP, and soil C:P. First, soil water is widely considered to be the main limiting factor for soil microorganisms and plays a key role in building soil microbial communities (Heděnec et al., 2017; Huang et al., 2017; Noah, 2017). Second, water effectiveness is also a determinant of plant growth and vegetation community composition (Wei et al., 2017; Liu W. et al., 2018). As the underwater decreases, aquatic plants (i.e., the basic vegetation that forms the marsh soil) gradually disappear. At the same time, mesophytes (i.e., meadow vegetation) invaded and became dominant plants, while the changes in vegetation and groundwater broke the balance of soil C, N, and P (Wu et al., 2016). Zhang et al. (2020) find a negative correlation between soil TP and sedge cover, indicating little accumulation of TP as it can be rapidly used by sedge species under flooded conditions. This result also explains well the significant increase in TP when non-degradation wetland was converted to a lightly degraded wetland. In our results, light degradation of wetland reduced the above-ground biomass of Cyperaceae from 85.2 ± 16.8 g·(0.25 m^2)$^{-1}$ to 66.3 ± 15.5 g·(0.25 m^2)$^{-1}$ (Li et al., 2020). In contrast, the significant decrease in TP content from light to severe degradation was due to the strong positive correlation between TP and SOC. At this time, SOC may contribute to TP accumulation, whereas wetland degradation significantly reduces soil SOC content (Zhang et al., 2020); therefore, TP also begins to decline. Many studies have shown that phosphorus is one of the key factors limiting nitrogen fixation due to the high demand for adenosine triphosphate (ATP) by nitrogen-fixing bacteria (Vitousek et al., 2002; Reed et al., 2011). It may be the reason for the significant positive correlation between TP and nitrogen-fixing bacteria diversity. TOC is closely related to the abundance and diversity of nitrogen-fixing bacteria, which reflects the dependence of nitrogen-fixing bacteria on carbon or energy (Reed et al., 2011). The TOC per kg of soil was higher than that of TP, and the TOC of wetland degradation decreased more, so the soil C:P decreases significantly, and it also showed that the soil C:P was positively correlated with the abundance and diversity of nitrogen-fixing bacteria. In addition, TN was positively correlated with the abundance and diversity of

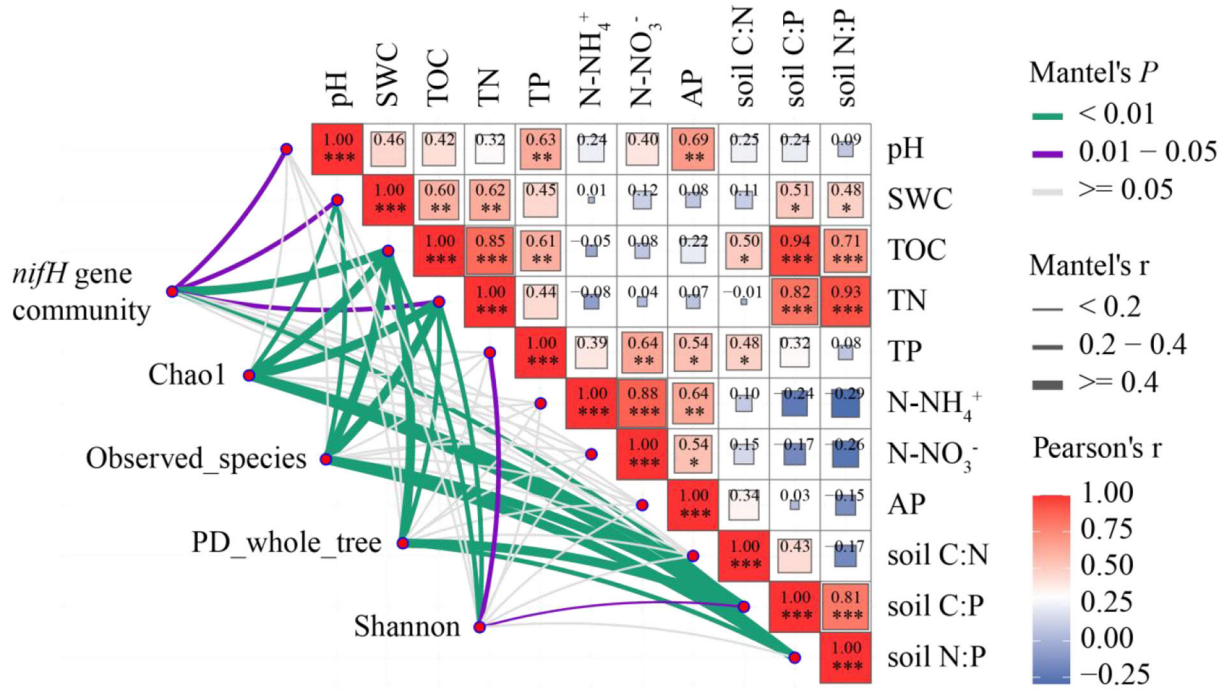

FIGURE 6
Correlations among nitrogen-fixing microbial community and diversity and soil physicochemical properties. Mantel edge width corresponds to Mantel *r*-value, and edge color indicates statistical significance. The color gradient of Pearson correlation coefficient *r* indicates the pairwise correlation of variables. The nitrogen-fixing gene community includes all nitrogen-fixing bacteria phylum. *0.01 < *P* < 0.05, **P* < 0.01, ***P* < 0.001.

nitrogen-fixing bacteria. First, it can be attributed to collinearity between soil nitrogen content and other soil properties (such as moisture, organic carbon, and total phosphorus), which cancels or even reverses the correlation between soil nitrogen content and nitrogen-fixing bacteria abundance (Che et al., 2018). Second, the positive correlation between soil nitrogen content and nitrogen-fixing bacteria may indicate that the community structure of nitrogen-fixing bacteria with different environmental preferences has changed due to the deterioration of the wetland soil environment. The alpine wetland soil in different stages of degradation has different nitrogen-fixing bacteria communities, these changes indicate the adaptability of microorganisms to the new environment and result in the composition of microbial communities once environmental conditions have changed (Wardle et al., 2004). The alpine wetland may be particularly sensitive to the decline of nitrogen-fixing bacteria. In turn, nitrogen inputs to degraded ecosystems will be reduced due to the reduction of soil nitrogen-fixing bacteria. The nitrogen-fixing bacteria are the main source of external nitrogen to these ecosystems, it also suggests that biological nitrogen fixation contributes significantly to the nitrogen input to the alpine wetland on the QTP. Furthermore, the first and second ordination axes of the soil nitrogen-fixing bacteria community explained 26.44% and 13.13% of the total variation in the samples, respectively. This indicates that in addition to soil properties, there are other factors that may cause changes in the community structure of nitrogen-fixing bacteria, one of which is the presence of vegetation (Sarkar, 2022). The more specific details need to be verified by further research.

The alpine wetland degenerates into the alpine meadow, and the diversity of nitrogen-fixing bacteria decreases; it is not conducive to the stability of the soil ecosystem, and it will affect the important ecological role of the alpine wetland in the process of carbon and nitrogen cycle and climate regulation. Our research results show that the degradation and succession of the alpine wetlands into alpine meadows will also lead to a significant decline in plant community productivity and ecosystem carbon sink function (Li et al., 2020). Therefore, it is very important to protect and restore the alpine wetland on the QTP. At the same time, soil microorganisms are closely related to the circulation of many elements such as soil organic matter, nitrogen, and phosphorus. Microbial processes of soil organic carbon and nitrogen transformation involve organic carbon fixation, decomposition, and transformation, organic nitrogen mineralization, nitrification, denitrification, and

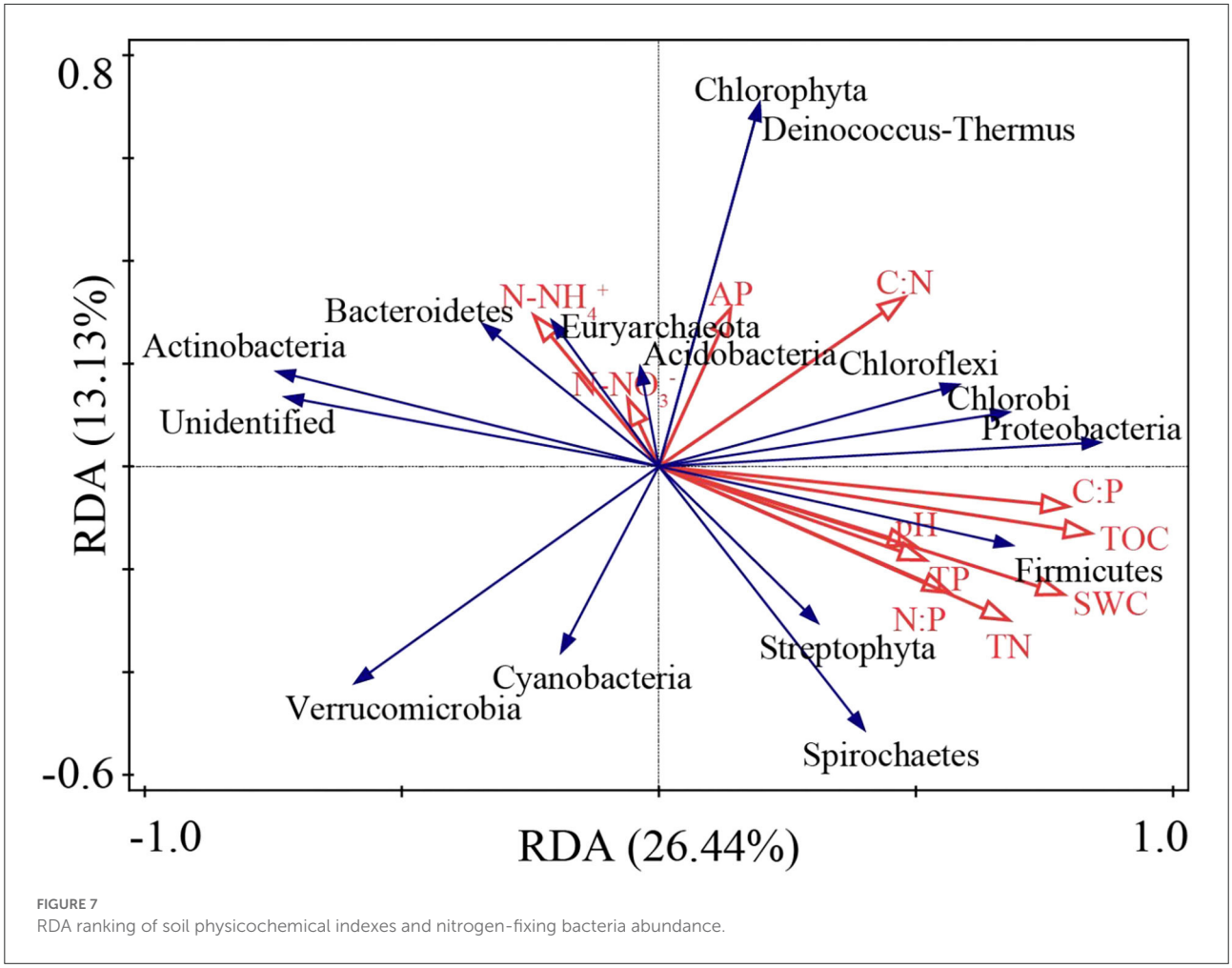

FIGURE 7
RDA ranking of soil physicochemical indexes and nitrogen-fixing bacteria abundance.

others. This study only involves nitrogen-fixing bacteria. The functional microorganisms involved in the carbon-nitrogen cycle also include carbon-fixing bacteria, methanogenic bacteria, methane-oxidizing bacteria, ammonia-oxidizing bacteria, denitrifying bacteria, etc. Therefore, in the future, it is necessary to further explore and analyze the driving effect of different soil functional microorganisms on carbon-nitrogen transformation and their relationship. In addition, freeze-thaw hills are typical features of the alpine wetland, which play an indicative role in the degradation of the alpine wetland. Future research should also pay attention to the changes of soil microbial communities in freeze-thaw hills and between hills during the degradation of the alpine wetland, which will be of great significance to clarify the degradation mechanism in the alpine wetland.

Conclusion

The structure and diversity of nitrogen-fixing bacteria communities in the alpine wetlands changed by degradation severity, and the Proteobacteria were found to be the main phylum of soil nitrogen-fixing bacteria communities. In the processes of wetland degradation, the dominant phylum, class, order, family, and genus of nitrogen-fixing bacteria have changed significantly. Different soil moisture and nutrient conditions in different stages of wetland degradation strongly affected the distribution of nitrogen-fixing bacteria communities. The degradation of the alpine wetlands significantly changed the composition of nitrogen-fixing bacteria communities and reduced their diversity. TOC, SWC, and TN were identified as the main environmental factors that affect the community composition of nitrogen-fixing bacteria.

Data availability statement

The raw sequence data from this study were deposited in the NCBI database with the study accession number: PRJNA854083 that are publicly accessible at http://www.ncbi.nlm.nih.gov/bioproject/854083.

Author contributions

XL and CL carried out the field experiments and sampling and analyzed the data. CL wrote the original manuscript, with contributions from XL, YS, HL, and YY. All authors approved the final version of the manuscript.

Funding

This study was financially supported by the National Natural Sciences Foundation of China (Grant No. U21A20191), the Natural Resources Investigation and Monitoring Project from central funds of Forest-grassland Ecological Protection and Restoration in the Qinghai region of Qilian Mountains National Park (Grant No. QHXH-2021-018), the 111 Project for Introducing Talents through Discipline Innovation in Colleges and Universities (D18013), and the Qinghai Science and Technology Innovation and Entrepreneurship Team Project titled Sanjiangyuan Ecological Evolution and Management Innovation Team.

Conflict of interest

The authors declare that the research was conducted in the absence of any commercial or financial relationships that could be construed as a potential conflict of interest.

Publisher's note

Supplementary material

The Supplementary Material for this article can be found online at: https://www.frontiersin.org/articles/10.3389/fpls.2022.939762/full#supplementary-material

References

Allison, S. D., Ying, L., Weihe, C., Goulden, M. L., Martiny, A. C., and Martiny, T. (2013). Microbial abundance and composition influence litter decomposition response to environmental change. *Ecology* 94, 714–725. doi: 10.1890/12-1243.1

Che, R., Wang, F., Wang, W., Zhang, J., Zhao, X., Rui, Y., et al. (2017). Increase in ammonia-oxidizing microbe abundance during degradation of alpine meadows may lead to greater soil nitrogen loss. *Biogeochemistry* 136, 341–352. doi: 10.1007/s10533-017-0399-5

Che, R. X., Deng, Y. C., Wang, F., Wang, W. J., Xu, Z. H., Hao, Y. B., et al. (2018). Autotrophic and symbiotic diazotrophs dominate nitrogen-fixing communities in Tibetan grassland soils. *Sci. Total Environ.* 639, 997–1006. doi: 10.1016/j.scitotenv.2018.05.238

Cleveland, C., Townsend, A. R., Schimel, D. S., Fisher, H., Howarth, R. W., Hedin, L. O., et al. (1999). Global patterns of terrestrial biological nitrogen (N2) fixation in natural ecosystems. *Glob. Biogeochem. Cycles* 13, 623–645. doi: 10.1029/1999GB900014

Delgado-Baquerizo, M., Oliverio, A. M., Brewer, T. E., Benavent-Gonzalez, A., Eldridge, D. J., Bardgett, R. D., et al. (2018). A global atlas of the dominant bacteria found in soil. *Science* 359, 320–325. doi: 10.1126/science.aap9516

Deluca, T. H., Zackrisson, O., Nilsson, M. C., and Sellstedt, A. (2002). Quantifying nitrogen-fixation in feather moss carpets of Boreal forests. *Nature* 419, 917–920. doi: 10.1038/nature01051

Edgar, R. C. (2013). UPARSE: highly accurate OTU sequences from microbial amplicon reads. *Nat. Methods* 10, 996. doi: 10.1038/nmeth.2604

Espenberg, M., Truu, M., Mander, Ü., Kasak, K., N?Lvak, H., Ligi, T., et al. (2018). Differences in microbial community structure and nitrogen cycling in natural and drained tropical peatland soils. *Sci. Rep.* 8, 4742. doi: 10.1038/s41598-018-23032-y

Fowler, D., Coyle, M., Skiba, U., Sutton, M. A., and Voss, M. (2018). The global nitrogen cycle in the twenty-first century. *Philos. Trans. R. Soc. Lond. B Biol. Sci.* 368, 20130164. doi: 10.1098/rstb.2013.0164

Galloway, J. N., Dentener, F. J., Capone, D. G., Boyer, E. W., and Vosmarty, C. J. (2004). Nitrogen cycles: past, present, and future. *Biogeochemistry* 70, 153–226. doi: 10.1007/s10533-004-0370-0

Guo, X., Du, W., Wang, X., and Yang, Z. (2013). Degradation and structure change of humic acids corresponding to water decline in Zoige peatland, Qinghai-Tibet Plateau. *Sci. Total Environ.* 445–446, 231–236. doi: 10.1016/j.scitotenv.2012.12.048

Heděnec, P., Rui, J., Lin, Q., Yao, M., Li, J., Li, H., et al. (2017). Functional and phylogenetic response of soil prokaryotic community under an artificial moisture gradient. *Appl. Soil Ecol.* 124, 372–378. doi: 10.1016/j.apsoil.2017.12.009

Huang, G., Li, L., Su, Y. G., and Li, Y. (2017). Differential seasonal effects of water addition and nitrogen fertilization on microbial biomass and diversity in a temperate desert. *Catena* 161, 27–36. doi: 10.1016/j.catena.2017.09.030

Kang, W. L., Tai, X. S., Shi-Weng, L. I., Dong, K., Liu, G. X., and Zhang, W. (2013). Research on the number of nitrogen-fixing microorganism and community structure of nitrogen-fixing(nifH) genes in the alkali soils of alpine steppe in the qilian mountains. *J. Glaciol. Geocryol.* 35, 208–216. doi: 10.7522/j.issn.1000-0240.2013.0025

Levy-Booth, D. J., Prescott, C. E., and Grayston, S. J. (2014). Microbial functional genes involved in nitrogen fixation, nitrification and denitrification in forest ecosystems. *Soil Biol. Biochem.* 75, 11–25. doi: 10.1016/j.soilbio.2014.03.021

Li, C., Li, X., Sun, H., Li, D., Zhang, F., Lin, C., et al. (2020). Drought processes of alpine wetland and their influences on CO2 exchange. *Acta Agrestia Sin.* 28, 750–758.

Li, C. Y., Li, X. L., Su, X. X., Yang, Y. W., and Li, H. L. (2021). Effects of alpine wetland degradation on soil microbial structure and diversity on the Qinghai Tibet Plateau. *Euras. Soil Sci.* 54, S33–S41. doi: 10.1134/S1064229322030097

Liang, Y. X., Yi, M. G., Chu, K. Y., Xia, X. J., Chang, C. P., Zhang, J. X., et al. (2007). The Research of the relationship between shrinkage of zoige's wetlands, deterioration and desertification of zoige's grasslands and North Sandy arid Region. *Chin. J. Nat.* 29, 233–238. doi: 10.3969/j.issn.0253-9608.2007.04.009

Lin, C. Y., Li, X. L., Zhang, J., Sun, H. F., and Ma, X. Q. (2021). Effects of degradation succession of alpine wetland on soil organic carbon and total nitrogen in the yellow river source zone, west China. *J. Mount. Sci.* 18, 1–12. doi: 10.1007/s11629-016-3945-z

Lindsay, E. A., Colloff, M. J., Gibb, N. L., and Wakelin, S. A. (2010). The abundance of microbial functional genes in grassy woodlands is influenced more by soil nutrient enrichment than by recent weed invasion or livestock exclusion. *Appl. Environ. Microbiol.* 76, 5547–5555. doi: 10.1128/AEM.03054-09

Liu, L., Chen, H., Lin, J., Ji, H., Wei, Z., He, Y., et al. (2018). Water table drawdown reshapes soil physicochemical characteristics in Zoige peatlands. *Catena* 170, 119–128. doi: 10.1016/j.catena.2018.05.025

Liu, L., He, X. Y., Du, H., and Wang, K. L. (2017). The relationships among nitrogen-fixing microbial communities, plant communities, and soil properties in karst regions. *Acta Ecol. Sin.* 37, 4037–4044. doi: 10.5846/stxb201606141146

Liu, W., Lü, X., Xu, W., Shi, H., Hou, L., Li, L., et al. (2018). Effects of water and nitrogen addition on ecosystem respiration across three types of steppe: the role of plant and microbial biomass. *Sci. Total Environ.* 619–620, 103–111. doi: 10.1016/j.scitotenv.2017.11.119

Liu, X., Zhu, D., Zhan, W., Chen, H., Zhu, Q., Hao, Y., et al. (2019). Five-Year measurements of net ecosystem CO2 exchange at a fen in the zoige peatlands on the Qinghai-Tibetan Plateau. *J. Geophys. Res. Atmosph.* 124, 11803–11818. doi: 10.1029/2019JD031429

Luan, J., Cui, L., Xiang, C., Wu, J., Song, H., and Ma, Q. (2014). Soil carbon stocks and quality across intact and degraded alpine wetlands in Zoige, east Qinghai-Tibet Plateau. *Wetlands Ecol. Manage.* 22, 427–438. doi: 10.1007/s11273-014-9344-8

Munir, T. M., Xu, B., Perkins, M., and Strack, M. (2014). Responses of carbon dioxide flux and plant biomass to water table drawdown in a treed peatland in northern Alberta: a climate change perspective. *Biogeosciences* 11, 807–820. doi: 10.5194/bg-11-807-2014

Noah, F. (2017). Embracing the unknown: disentangling the complexities of the soil microbiome. *Nat. Rev. Microbiol.* 53, 579–590. doi: 10.1038/nrmicro.2017.87

Paul, G., Falkowski, A. N., Glazer, D. E., and Canfield. (2010). The evolution and future of earth's nitrogen cycle. *Science* 330, 192–196. doi: 10.1126/science.1186120

Qian, H., and Ricklefs, R. E. (2004). Taxon richness and climate in angiosperms: is there a globally consistent relationship that precludes region effects? *Am. Nat.* 163, 773–779. doi: 10.1086/383097

Quast, C., Pruesse, E., Yilmaz, P., Gerken, J., and Glckner, F. O. (2012). The SILVA ribosomal RNA gene database project: Improved data processing and web-based tools. *Nucleic Acids Res.* 41, 590–596. doi: 10.1093/nar/gks1219

Ramond, J. B., Woodborne, S., Hall, G., Seely, M., and Cowan, D. A. (2018). Namib Desert primary productivity is driven by cryptic microbial community N-fixation. *Sci. Rep.* 8, 6921. doi: 10.1038/s41598-018-25078-4

Reed, S. C., Cleveland, C. C., and Townsend, A. R. (2011). Functional ecology of free-living nitrogen fixation: a contemporary perspective. *Ann. Rev. Ecol. Evolut. Syst.* 42, 489–512. doi: 10.1146/annurev-ecolsys-102710-145034

Reed, S. C., Townsend, A. R., Cleveland, C. C., and Nemergut, D. R. (2010). Microbial community shifts influence patterns in tropical forest nitrogen fixation. *Oecologia* 164, 521–531. doi: 10.1007/s00442-010-1649-6

Regan, K., Stempfhuber, B., Schloter, M., Rasche, F., Prati, D., Philippot, L., et al. (2016). Spatial and temporal dynamics of nitrogen fixing, nitrifying and denitrifying microbes in an unfertilized grassland soil. *Soil Biol. Biochem.* 109, 214–226. doi: 10.1016/j.soilbio.2016.11.011

Rösch, C., and Bothe, H. (2005). Improved assessment of denitrifying, N2-fixing, and total-community bacteria by terminal restriction fragment length polymorphism analysis using multiple restriction enzymes. *Appl. Environ. Microbiol.* 71, 2026–2035. doi: 10.1128/AEM.71.4.2026-2035.2005

Sarkar, M. (2022). Effect of silver nanoparticles on nitrogen-cycling bacteria in constructed wetlands. *Nanotechnol. Environ. Eng.* 7, 537–559. doi: 10.1007/s41204-021-00192-3

Shanmugam, S. G., Magbanua, Z. V., Williams, M. A., et al. (2017). Bacterial diversity patterns differ in soils developing in sub-tropical and cool-temperate ecosystems. *Microb. Ecol.* 73, 556–569. doi: 10.1007/s00248-016-0884-8

Shuang, X., Guo, R., Wu, N., and Sun, S. (2009). Current status and future prospects of Zoige Marsh in Eastern Qinghai-Tibet Plateau. *Ecol. Eng.* 35, 553–562. doi: 10.1016/j.ecoleng.2008.02.016

Simon, Z., Mtei, K., Gessesse, A., and Ndakidemi, P. A. (2014). Isolation and characterization of nitrogen fixing rhizobia from cultivated and uncultivated soils of Northern Tanzania. *Am. J. Plant Sci.* 05, 4050–4067. doi: 10.4236/ajps.2014.526423

Stewart, K. J., Coxson, D., and Siciliano, S. D. (2011). Small-scale spatial patterns in N 2-fixation and nutrient availability in an arctic hummock–hollow ecosystem. *Soil Biol. Biochem.* 43, 133–140. doi: 10.1016/j.soilbio.2010.09.023

Straková, P., Anttila, J., Spetz, P., Kitunen, V., Tapanila, T., and Laiho, R. (2010). Litter quality and its response to water level drawdown in boreal peatlands at plant species and community level. *Plant Soil* 335, 501–520. doi: 10.1007/s11104-010-0447-6

Sun, H. L., Zheng, D., Yao, T. D., and Zhang, Y. L. (2012). Protection and construction of the national ecological security shelter zone on Tibetan Plateau. *J. Geograph. Sci.* 67, 3–12.

Tedersoo, L., Bahram, M., Polme, S., Koljalg, U., Yorou, N. S., and Al, E. (2014). Global diversity and geography of soil fungi. *Science* 346, 1078. doi: 10.1126/science.1256688

Vitousek, P. M., Aber, J. D., Howarth, R. W., Likens, G. E., and Tilman, D. G. (1997). Human alteration of the global nitrogen cycle: sources and consequences. *Ecol. Applic.* 7, 737–750. doi: 10.1890/1051-0761(1997)007[0737:HAOTGN]2.0.CO;2

Vitousek, P. M., Cassman, K., Leveland, C. C., Crews, T., Field, C. B., Grimm, N. B., et al. (2002). Towards an ecological understanding of biological nitrogen fixation. *Sprin. Netherl.* 57, 1–45. doi: 10.1007/978-94-017-3405-9_1

Wang, H. T., Su, J. Q., Zheng, T. L., and Yang, X. R. (2015). Insights into the role of plant on ammonia-oxidizing bacteria and archaea in the mangrove ecosystem. *J. Soils Sediments* 15, 1212–1223. doi: 10.1007/s11368-015-1074-x

Wang, Y., Li, C., Kou, Y., Wang, J., and Yao, M. (2017). Soil pH is a major driver of soil diazotrophic community assembly in Qinghai-Tibet alpine meadows. *Soil Biol. Biochem.* 115, 547–555. doi: 10.1016/j.soilbio.2017.09.024

Wardle, D. A., Bardgett, R. D., Klironomos, J. N., Setala, H., and Van, W. H. (2004). Ecological linkages between aboveground and belowground biota. *Science* 304, 1629–1633. doi: 10.1126/science.1094875

Wei, X., Zhu, M., Zhang, Z., Ma, Z., and He, J. (2017). Experimentally simulating warmer and wetter climate additively improves rangeland quality on the Tibetan Plateau. *J. Appl. Ecol.* 55, 1486–1497. doi: 10.1111/1365-2664.13066

Wu, G., Li, X., and Gao, J. (2021). The evolution of hummock–depression micro-topography in an alpine marshy wetland in Sanjiangyuan as inferred from vegetation and soil characteristics. *Ecol. Evol.* 11, 3901–3916. doi: 10.1002/ece3.7278

Wu, L. S., Nie, Y. Y., Yang, Z. R., and Zhang, J. (2016). Responses of soil inhabiting nitrogen-cycling microbial communities to wetland degradation on the Zoige Plateau, China. *J. Mount. Sci.* 13, 2192–2204. doi: 10.1007/s11629-016-4004-5

Xing, Y., Jiang, Q. G., Li, W. Q., and Bai, L. (2009). Landscape spatial patterns changes of the wetland in Qinghai-Tibet Plateau. *Ecol. Environ. Sci.* 18, 1010–1015. doi: 10.16258/j.cnki.1674-5906.2009.03.034

Yang, Y. X., and Wang, S. Y. (2001). Human disturbances on mire and peat soils in the Zoige Plateau. *Resourc. Sci.* 23, 37–41. doi: 10.3321/j.issn:1007-7588.2001.02.008

Zehr, J. P. (2011). Nitrogen fixation by marine cyanobacteria. *Trends Microbiol.* 19, 162–173. doi: 10.1016/j.tim.2010.12.004

Zehr, J. P., Jenkins, B. D., Short, S. M., and Steward, G. F. (2003). Nitrogenase gene diversity and microbial community structure: a cross-system comparison. *Environ. Microbiol.* 5, 539–554. doi: 10.1046/j.1462-2920.2003.00451.x

Zhang, X. D., Jia, X., Wu, H. D., Li, J., Yan, L., Wang, J. Z., et al. (2020). Depression of soil nitrogen fixation by drying soil in a degraded alpine peatland. *Sci. Total Environ.* 747, 141084. doi: 10.1016/j.scitotenv.2020.141084

Zhang, Y. G., Lu, Z. M., Liu, S. S., Yang, Y. F., He, Z. L., Ren, Z. H., et al. (2013). Geochip-based analysis of microbial communities in alpine meadow soils in the Qinghai-Tibetan plateau. *BMC Microbiol.* 13, 72. doi: 10.1186/1471-2180-13-72

Zhao, Z. G., and Shi, X. M. (2020). Ecosystem evolution of alpine wetland in Tibetan Plateau and consideration for ecological restoration and conservation. *Sci. Technol. Rev.* 38, 33–41. doi: 10.3981/j.issn.1000-7857.2020.17.003

Zhao, Z. L., Zhang, Y. L., Liu, L. S., Liu, F. G., and Zhang, H. F. (2014). Advances in research on wetlands of the Tibetan Plateau. *Prog. Geogr.* 9, 1218–1230. doi: 10.11820/dlkxjz.2014.09.009

Zhou, J., Kang, S., Schadt, C. W., and Garten, C. T. (2008). Spatial scaling of functional gene diversity across various microbial taxa. *Proc. Nat. Acad. Sci. U.S.A.* 105, 7768–7773. doi: 10.1073/pnas.0709016105

frontiers | Frontiers in Plant Science

TYPE Original Research
PUBLISHED 08 September 2022
DOI 10.3389/fpls.2022.989931

OPEN ACCESS

EDITED BY
Yong Li,
Chinese Academy of Forestry, China

REVIEWED BY
Peng Li,
Hainan Normal University, China
Xinsheng Chen,
Anhui University, China
Yonghong Xie,
Key Laboratory of Agro-Ecological Processes in Subtropical Region, Institute of Subtropical Agriculture (CAS), China

*CORRESPONDENCE
Youzhi Li
liyouzhi2004@163.com

SPECIALTY SECTION
This article was submitted to Functional Plant Ecology, a section of the journal Frontiers in Plant Science

RECEIVED 09 July 2022
ACCEPTED 22 August 2022
PUBLISHED 08 September 2022

CITATION
Peng Z, Du Y, Niu S, Xi L, Niu Y and Li Y (2022) Differences in nitrogen and phosphorus sinks between the harvest and non-harvest of *Miscanthus lutarioriparius* in the Dongting Lake wetlands. *Front. Plant Sci.* 13:989931. doi: 10.3389/fpls.2022.989931

Differences in nitrogen and phosphorus sinks between the harvest and non-harvest of *Miscanthus lutarioriparius* in the Dongting Lake wetlands

Zenghui Peng[1,2], Yuhang Du[1,2], Shiyu Niu[1,2], Lianlian Xi[1,2], Yandong Niu[3,4] and Youzhi Li[1,2]*

[1]College of Resources and Environment, Hunan Agricultural University, Changsha, China, [2]Hunan Provincial Key Laboratory of Rural Ecosystem Health in Dongting Lake Area, Hunan Agricultural University, Changsha, China, [3]Hunan Academy of Forestry, Changsha, China, [4]Hunan Dongting Lake Wetland Ecosystem National Positioning Observation and Research Station, Yueyang, China

Plant non-harvest changes element circulation and has a marked effect on element sinks in the ecosystem. In this study, a field investigation was conducted on the fixation of nitrogen and phosphorus in *Miscanthus lutarioriparius*, the most dominant plant species in the Dongting Lake wetlands. Further, to quantitatively compare the difference in nitrogen and phosphorus sinks between harvest and non-harvest, an *in situ* experiment on the release of the two elements from two types of litters (leaves and stems) was studied. The nitrogen concentrations in the plant had no significant relationship with the environmental parameters. The phosphorus concentrations were positively related to the plot elevation, soil organic matter, and soil total potassium and were negatively related to the soil moisture. The leaves demonstrated a higher decomposition coefficient than that of the stems in the *in situ* experiment. The half decomposition time was 0.61 years for leaves and 1.12 years for stems, and the complete decomposition time was 2.83 years for leaves and 4.95 years for stems. Except for the nitrogen concentration in the leaves, all the concentrations increased during the flood period. All concentrations unsteadily changed in the backwater period. Similarly, except for the relative release index of nitrogen in the leaves, all the relative release indices decreased in the flood period. At the end of the *in situ* decomposition experiment, the relative release indices of both the nitrogen and phosphors were greater than zero, indicating that there was a net release of nitrogen and phosphorus. Under the harvest scenario, the aboveground parts of the plant were harvested and moved from the wetlands, thus increasing the nitrogen and phosphorus sinks linearly over time. The fixed nitrogen and phosphorus in the aboveground parts were released under the non-harvest scenario, gradually accumulating the nitrogen and phosphorus sinks from the first year to the fifth year after non-harvest, reaching a maximum value after the fifth year. This study showed that

the nitrogen and phosphorus sinks greatly decreased after the non-harvest of *M. lutarioriparius* compared to that after harvest. It is recommended to continue harvesting the plant for enhancing the capacity of element sinks.

KEYWORDS

nitrogen sinks, phosphorus sinks, harvest, non-harvest, litter decomposition, relative release indices

Introduction

A large amount of nitrogen and phosphorus has been released into the environment in the past several decades, causing great threats to the ecosystem (Grizzetti et al., 2020). Approximately 605 million moles of nitrogen and 36 million moles of phosphorus are reportedly inputted into the Narragansett Bay each year, eventually getting deposited in the sediment (Nixon et al., 2008). Recently, the nitrogen and phosphorus concentrations in the sediments of the major rivers of China (such as the Yangtze River, Yellow River, and Huai River) were found to be much higher than the soil background values (Yang et al., 2017). This nitrogen and phosphorus will be released from the sediments again and decrease the water quality and accelerate eutrophication (Jin et al., 2006). Due to their important roles in element sinks, plant species such as *Pistia stratiotes*, *Eichhornia crassipes*, and *Phragmites australis* are commonly used to remove the nitrogen and phosphorus from aquatic ecosystems (Lu et al., 2010; Nash et al., 2019; Rezania et al., 2019).

For plants, the capacity of nitrogen and phosphorus sinks depends on the amount of elements fixed in the plant. Nitrogen and phosphorus fixation is a biological process and is associated with certain environmental factors. Studies have shown soil pH to be one of the main factors affecting the fixation of phosphorus (Barrow, 2017). In high soil moisture conditions, low oxygen availability limits nitrogen fixation (Sajedi et al., 2012). Under the comprehensive influence of environmental factors, plant organs exhibit different nitrogen and phosphorus allocation patterns. For example, compared with stems and roots, the leaves in 30 species of desert plants demonstrated higher nitrogen and phosphorus concentrations (Luo et al., 2021). Unlike terrestrial plants, aquatic plants can obtain nitrogen and phosphorus from both soil and water, thus demonstrating higher element concentrations in aboveground parts than in underground parts (Granéli and Solander, 1988). Detailed studies on nitrogen and phosphorus fixation are therefore necessary for quantitatively evaluating the capacity of element sinks.

The fixed nitrogen and phosphorus in plants is released into the environment with the decomposition of litter. The release of nitrogen and phosphorus from litter is also a biological process, and the amount of the released elements can be reflected by the weight of residual litter and elemental concentrations (van der Valk et al., 1991; Kuehn and Suberkropp, 1998). The negative exponential decay model is usually adopted for estimating the mass of residual litters in the decomposition process (Olson, 1963). The nitrogen and phosphorus concentrations in litters show a dynamic balance between element release from litters into the environment and element fixation by litters from the environment (Zhang et al., 2020). A study conducted on the decomposition of forest litter showed that nitrogen concentration in litters increased in the first and second years of the decomposition and decreased in the third year (McClaugherty et al., 1985). Studies on the release process of nitrogen and phosphorus in litter decomposition are therefore also necessary for quantitatively evaluating the capacity of element sinks.

Dongting Lake is the second largest freshwater lake in China and is connected to the Yangtze River and the "four rivers" of Hunan (Xiang, Zi, Yuan, and Li rivers). In the catchment, a large amount of nitrogen, phosphorus, and heavy metals are imported into the lake and deposited in the sediments. *Miscanthus lutarioriparius*, a perennial, emergent macrophyte, is distributed on the beach of the lake and is the most dominant species in this area (Xu et al., 2021). In the past several decades, the aboveground parts of this plant have been harvested as a raw material for papermaking, causing the removal of a great number of elements from the lake (Yao et al., 2018). However, it is now forbidden to harvest *M. lutarioriparius* owing to the important role of the lake in biodiversity protection and the disappearance of papermaking industries in the region. Typically, the aboveground parts of *M. lutarioriparius* will decompose, and the fixed elements will be released into aquatic ecosystems. The non-harvest of the plant, therefore, evokes high concerns regarding the potential ecological risk caused by the possible decline in element sinks. Few studies have quantitatively estimated the difference in element sink between plant harvest and non-harvest to date (Morton et al., 2010). In this context, harvest refers to harvesting the aboveground parts of plants once a year, while non-harvest means removing human disturbance and letting plants fall and decompose in the wild.

To this end, a field investigation and an *in situ* experiment were conducted to explore the fixation of nitrogen and

phosphorus in the aboveground parts of the plants and the release of the two elements to reveal the changes in nitrogen and phosphorus sinks after the policy change from harvest to non-harvest.

Materials and methods

Study area

Dongting Lake has an area of 2,625 km^2 (28(382gt98452gting15402gti30102gting Lake has an area of 2n a by floods from the Yangtze, Xiang, Zi, Yuan, and Li rivers. The annual fluctuation in the water level is approximately 12–14 m, with the maxima in July–August and minima in January–February (Xie et al., 2015). Since the 1960s, *M. lutarioriparius* was planted in Dongting Lake for paper manufacture. This plant generally germinates in March–April and is harvested during November–December. The total distribution area of *M. lutarioriparius* in the lake is approximately 585 km^2 and accounts for 22.3% of the total area of Dongting Lake (Xu et al., 2021). Currently, the lake is a global hotspot for biodiversity conservation, with three international important wetlands and two national wetland nature reserves.

Field investigation on nitrogen and phosphorus fixation

In November 2016, 24 vegetated plots were selected on the beach of Dongting Lake (**Figure 1**). The geographical information of each plot was recorded using a hand-held GPS (UniStrong, China). A quadrat (1 m × 1 m) was chosen for investigation in each vegetated plot. The stems in each sampled quadrat were cut from the soil surface and cut into pieces, and the leaves were collected from the stems. The roots were dug from a soil depth of 0–30 cm and carefully washed such that they were free of soil. The mixed soil samples of 0–30 cm were collected for determining the environmental parameters in the soil. These vegetation and soil samples were sealed in plastic bags and brought back to the laboratory for further analysis.

In situ experiment on nitrogen and phosphorus release

In November 2019, the leaves and stems of *M. lutarioriparius* were collected from the beach of Dongting Lake and air-dried. In April 2020, 5 g each of leaves and stems were put into separate nylon mesh bags (15 cm × 25 cm) with 1 mm apertures. These bags were taken into *M. lutarioriparius* communities on three beaches (Junshan, Beizhouzi, and Luhu) of Dongting Lake. In each plant community, 72 bags, including 36 leaf bags and 36 stem bags, were placed on the soil surface. These bags were placed in the center of the plant communities with an area of 30 width and 50 m length; the distance between bags was 1 m. After the plant bags were put into the plant communities for 30, 210, 240, 270, 300, and 330 days, the samples were taken with six replicates and brought back to the laboratory for further analysis (**Figure 2**).

Measurements of biomass, and nitrogen and phosphorus concentrations in plants

In the field investigation and *in situ* experiment, samples of roots, stems, and leaves were dried separately in an oven at 80°C for 48 h before measuring their dry weight. The biomass of plant organs was defined as dry mass per square meter, and plant total biomass was calculated as the total weight of roots, stems, and leaves. Plant organs were ground to a fine powder and passed through a 0.15 mm mesh. Material less than 0.15 mm was then used to test the concentrations of nitrogen and phosphorus. The nitrogen concentrations in plants were analyzed using a continuous flow analyzer (Auto Analyzer 3 HR, Seal Analytical, Germany), and phosphorus concentrations were measured by the molybdenum-antimony anti-colorimetric method (NY/T 2017-2011).

Measurement of soil properties

In the field investigation, soil properties were measured according to the Chinese national standards (Liu, 1996). Soil moisture was calculated as [(FW - DW)/FW] × 100%, where FW is the soil fresh weight and DW is the soil dry weight after drying in an oven at 105°C for 48 h. The remaining fresh soil was air-dried in the shade for the analysis of soil variables. The pH, electrolyte leakage, organic matter concentration, total nitrogen concentration, alkali-hydrolyzable nitrogen concentration, total phosphorus concentration, available phosphorus concentration, and total potassium concentration were then measured (Yao et al., 2018).

Data calculation

The amount of nitrogen or phosphorus fixed by a plant organ was calculated using the following equation:

$$E_f = M \times C,$$

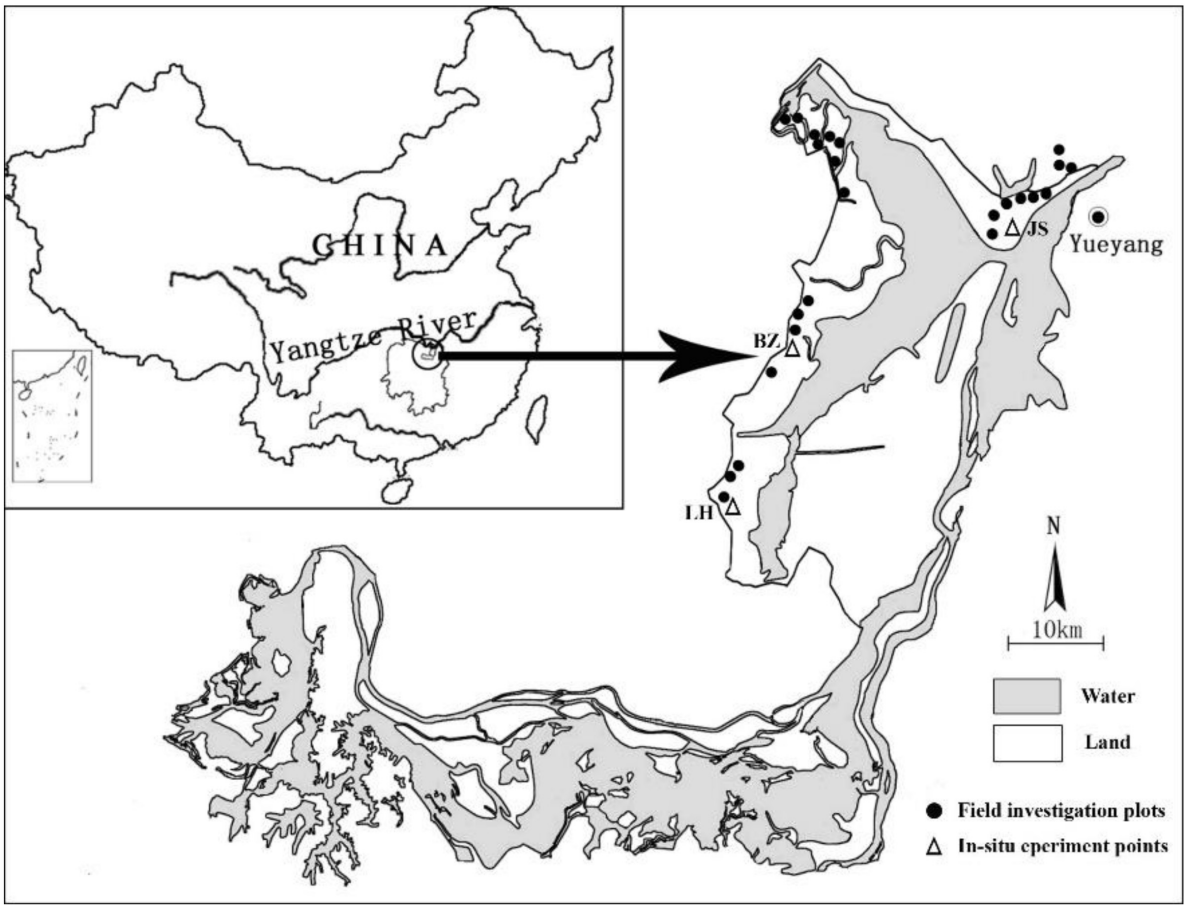

FIGURE 1
The field investigation plots (circles) and *in situ* experiment points (triangles; JS: Junshan; BZ: Beizhouzi; LH: Luhu) in the Dongting Lake wetlands.

where E_f is the amount of an element (nitrogen or phosphorus) fixed in the plant organ (leaf, stem, or root), M is the dry mass of the plant organ, and C is the concentration of an element in the organ. The amount of elements fixed by the aboveground parts of plants was the sum of the amount of the elements fixed by leaves and stems.

The mass residual ratio of litter (leaf or stem) was calculated using the following equation:

$$R = \frac{M_t}{M_0} \times 100\%,$$

where R is the mass residual ratio of litter, M_t is the litter mass after decomposing time t, and M_0 is the initial litter mass.

A negative exponential decay model was used to analyze the mass residual ratio of litter in litter decomposition (Olson, 1963):

$$y = ae^{-kt},$$

where y is the mass residual ratio of litter, a is the fitting parameter, k is the annual decomposition coefficient, and t is the decomposing time.

The amount of an element released in litter decomposition (E_r) and the relative release index (RRI) were calculated using the following equations:

$$E_r = M_0 \times C_0 - M_t \times C_t$$

$$RRI = \frac{M_0 \times C_0 - M_t \times C_t}{M_0 \times C_0} \times 100\%,$$

where M_0 is the initial litter mass, C_0 is the initial concentration of an element in the litter, M_t is litter mass after decomposing time t, and C_t is the concentration of an element in the litter at time t. The litter on the 360th day could not be collected due to uncontrollable factors in the field, and thus, the RRI in the time was calculated according to the regression model of RRI in the leaves and stems (**Figure 3**).

Nitrogen and phosphorus sinks were evaluated for two scenarios. If the plant is harvested, the annual element sinks were considered equal to E_f. If the plant

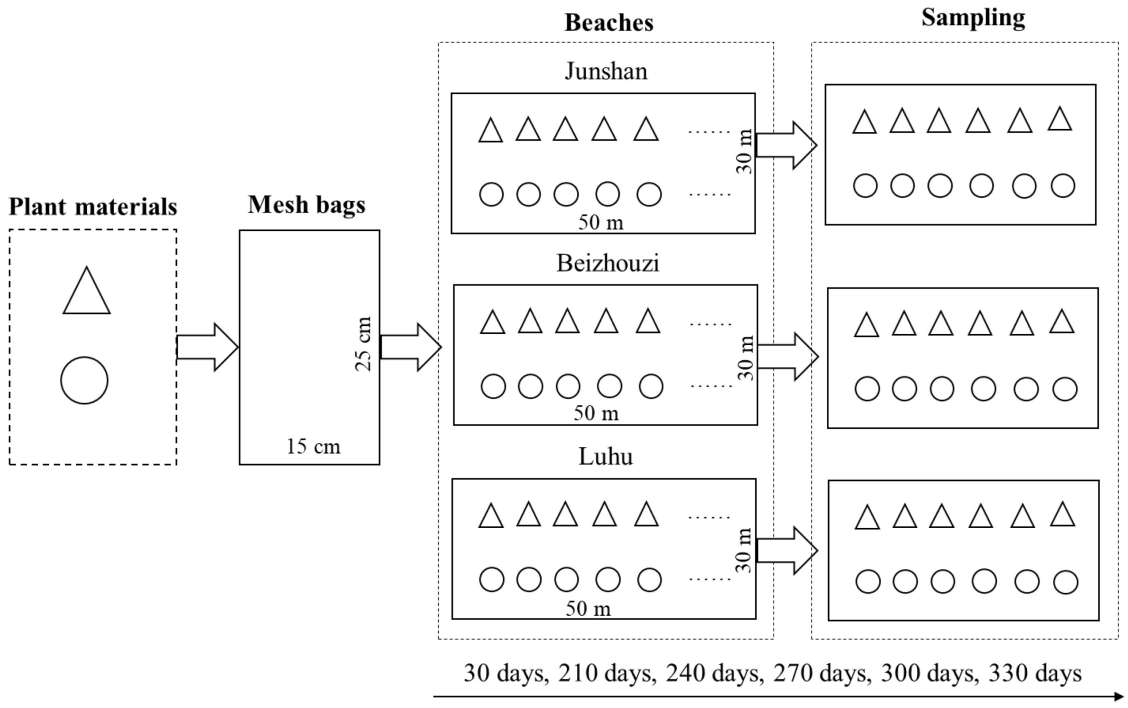

FIGURE 2
Flow picture of the implementation of the *in situ* experiment (triangles, leaves; circles, stems).

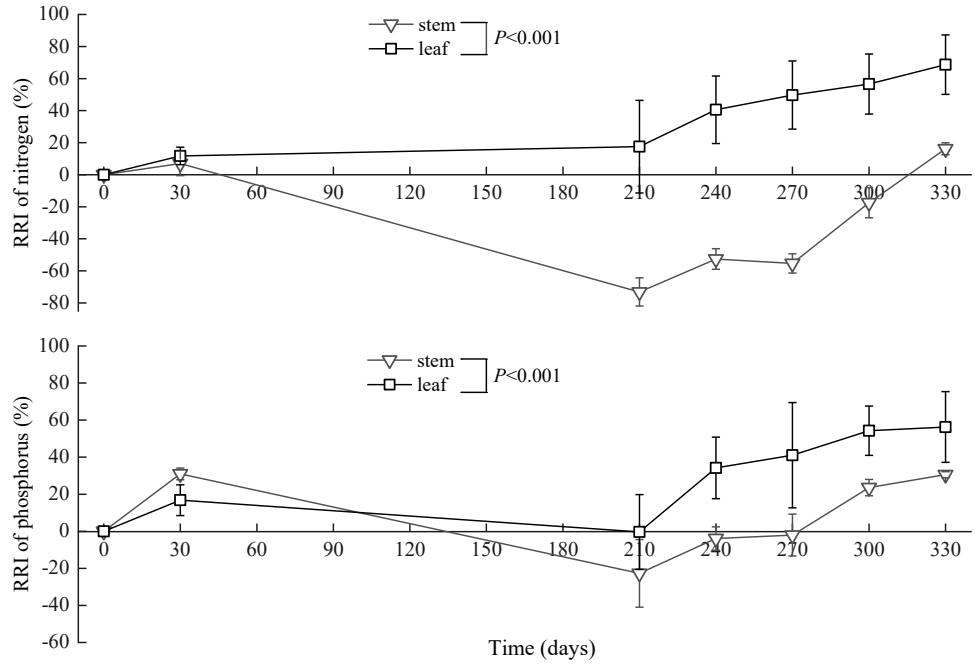

FIGURE 3
Dynamics of relative release indices (RRI, means ± SD) of nitrogen and phosphorus in the *in situ* experiment.

is not harvested, the element sinks were calculated as follows:

$$S_n = \sum_{i=1}^{n} E_{rl} + \sum_{i=1}^{m} E_{rs},$$

where S_n is the element sink in the non-harvest scenario; E_{rl} and E_{rs} are the element contents in residual leaves and stems after a year's litter decomposition, respectively; and n and m are the complete decomposition times of leaves and stems, respectively. Considering that the *in situ* experiment was conducted in 1 year, the amounts of both elements in the residual litters in the following years (the second year, third year, etc.) were estimated as the mean element concentrations in the *in situ* experiment of 1 year multiplied by the weight of residual litters calculated with the exponential decay model of the residual litters ($y = ae^{-kt}$).

Statistical analysis

Multiple comparisons were conducted to test the difference in the biomass, concentrations of nitrogen and phosphorus in plants, and amount of nitrogen and phosphorus fixed in plants using Tukey's test at the 0.05 significance level. Linear regression analysis between mean concentrations of nitrogen and phosphorus in plants and environmental parameters was performed at the 0.05 significance level. Before analysis, the homogeneity of variances was tested using Levene's test, and data were $\log_{10}$-transformed when necessary to reduce the heterogeneity of variances. The statistical analyses were performed using SPSS Statistics 23.0 (IBM Corp., United States) software, and figures were produced using OriginPro 2021 (OriginLab Corp., United States) software.

Results

Concentrations and amount of nitrogen and phosphorus in plants in the field investigation

The concentrations and amounts of nitrogen and phosphorus were significantly different in the three plant organs (Table 1). For concentrations, both nitrogen and phosphorus were the highest in the leaves (16.27 and 1.34 g kg^{-1} for nitrogen and phosphorus, respectively), intermediate in the roots (7.13 and 1.03 g kg^{-1}, respectively), and lowest in the stems (3.83 and 0.44 g kg^{-1}, respectively). However, the amounts of fixed nitrogen and phosphorus were the highest in the roots (9.42 and 1.55 g m^2 for nitrogen and phosphorus, respectively), intermediate in the stems (4.46 and 0.49 g m^2, respectively), and lowest in the leaves (2.66 and 0.21 g m^2, respectively).

The total amounts of elements fixed by plants were 16.544 g m^2 for nitrogen and 2.239 g m^2 for phosphorus. Combined with the area of *M. lutarioriparius* in the Dongting Lake wetlands, approximately 9,680 t nitrogen and 1,310 t phosphorus were fixed by this plant per year, and 4,168 t nitrogen and 404 t phosphorus were fixed by the aboveground parts.

The relationship between nitrogen and phosphorus concentrations in plants and environmental parameters in the field investigation

The mean nitrogen concentrations in the plant did not exhibit a significant relationship with the studied parameters (Table 2). The mean phosphorus concentrations in the plant were positive related to the plot elevation, soil organic matter, and soil total potassium, and were negatively correlated to the soil moisture.

Mass residual ratio of leaves and stems in the *in situ* experiment

There was an obvious difference in the mass residual ratio between leaves and stems (Figure 4). Over time, the mass residual ratio of the leaves and stems demonstrated negative exponential decay models. The decomposition coefficient was 1.037 for stems and 0.6018 for leaves. Based on the negative exponential decay model, it may be deduced that the half decomposition (50% decomposition) time was 0.61 years for leaves and 1.12 years for stems, and the complete decomposition (95% decomposition) time was 2.83 years for leaves and 4.95 years for stems.

Release of nitrogen and phosphorus in leaves and stems in the *in situ* experiment

The concentrations of nitrogen and phosphorus in the leaves and stems changed with time gradually. The nitrogen concentration in the leaves increased in the period from the 0th to the 30th day, decreased from the 30th to the 210th day, and unsteadily changed from the 210th to the 330th day. However, the phosphorus concentration in the leaves increased from the 0th to the 300th day and decreased from the 300th to the 330th day. Overall, the concentrations of nitrogen and phosphorus in the stems increased from the 0th to the 270th day and decreased from the 270th to the 330th day (Figure 5).

The relative release index of nitrogen in the leaves gradually increased in the period from the 0th to the 330th day. However, the relative release index of nitrogen in the stems

TABLE 1 Plant biomass, concentrations, and amounts of nitrogen and phosphorus (means ± SD) fixed in *M. lutarioriparius* in the field investigation.

Plant organs	Plant biomass (g m^{-2})	Element concentrations (g kg^{-1})		Amount of elements (g m^{-2})	
		Nitrogen	Phosphorus	Nitrogen	Phosphorus
Leaf	148.1 ± 102.4[a]	16.27 ± 5.12[c]	1.34 ± 0.32[c]	2.66 ± 2.52[a]	0.21 ± 0.16[a]
Stem	1139.9 ± 467.7[b]	3.83 ± 1.39[a]	0.44 ± 0.20[a]	4.46 ± 2.79[b]	0.49 ± 0.27[b]
Root	1428.7 ± 801.9[c]	7.13 ± 1.56[b]	1.03 ± 0.24[b]	9.42 ± 4.42[c]	1.55 ± 1.03[c]

Different letters in the same column indicate significant differences among plant organs at $P < 0.05$ based on Tukey's test.

TABLE 2 Linear regression analysis of nitrogen (N) and phosphorus (P) concentrations in *M. lutarioriparius* and environmental parameters in the field investigation.

Environmental parameters	N concentration		P concentration	
	Unstandardized coefficients	*t*-Statistic	Unstandardized coefficients	*t*-Statistic
C	4.720	0.158	−1.27	−0.404
PE	−0.292	−1.186	0.068	**2.631***
SM	0.08	0.444	−0.045	**−2.369***
SpH	2.237	0.603	−0.018	−0.047
SEL	−0.00008	−0.01	−0.001	−1.564
SOM	−0.091	−0.473	0.049	**2.41***
SAN	−0.011	−0.214	−0.01	−1.88
STN	3.749	0.637	0.384	0.622
SAP	0.172	0.884	−0.01	−0.471
STP	−13.292	−1.53	0.329	0.361
STK	−0.192	−0.772	0.057	**2.197***
R^2	0.308		0.599	
P	0.805		0.131	

*$P < 0.05$. PE, plot elevation; SM, soil moisture; SpH, soil pH; SEL, soil electrolyte leakage; SOM, soil organic matter; SAN, soil alkali–hydrolyzable nitrogen; STN, soil total nitrogen; SAP, soil available phosphorus; STP, soil total phosphorus; STK, soil total potassium.
Bold values indicate significant correlations.

increased in the period from the 0th to the 30th day, decreased from the 30th to the 210th day (flood period), and then increased from the 210th to the 330th day (backwater period). The relative release index of phosphorus in the leaves and stems increased in the period from the 0th to the 30th day, decreased from the 30th to the 210th day, and then increased from the 210th to the 330th day. At the end of the *in situ* decomposition experiment, the relative release indices of nitrogen and phosphors were greater than zero (Figure 3).

Nitrogen and phosphorus sinks in the scenario of harvest and non-harvest of the plant

In the scenario of the harvest of the plant, the nitrogen and phosphorus sinks increased linearly over time (Figure 6). In the scenario of non-harvest, the nitrogen and phosphorus sinks gradually increased during the period from the first year to the fifth year after non-harvest. However, after the fifth year of non-harvest, the element sinks reached a constant value (4,300 t for nitrogen sinks and 411 t for phosphorus sinks). The nitrogen and phosphorus sinks therefore greatly decreased after the non-harvest of *M. lutarioriparius* for 5 years compared to the harvest scenario.

Discussion

Amount of nitrogen and phosphorus fixed in plants in the field investigation

This study showed that element concentrations differed across plant organs. The concentrations of both nitrogen and phosphorus were the highest in the leaves, intermediate in the roots, and lowest in the stems, which was consistent with observations from previous studies on the wetland plant *P. australis* (Song and Shan, 2012). One possible reason for this may be that leaves are the main photosynthetic organ, with vigorous metabolism and high demand for nitrogen and

10.3389/fpls.2022.989931

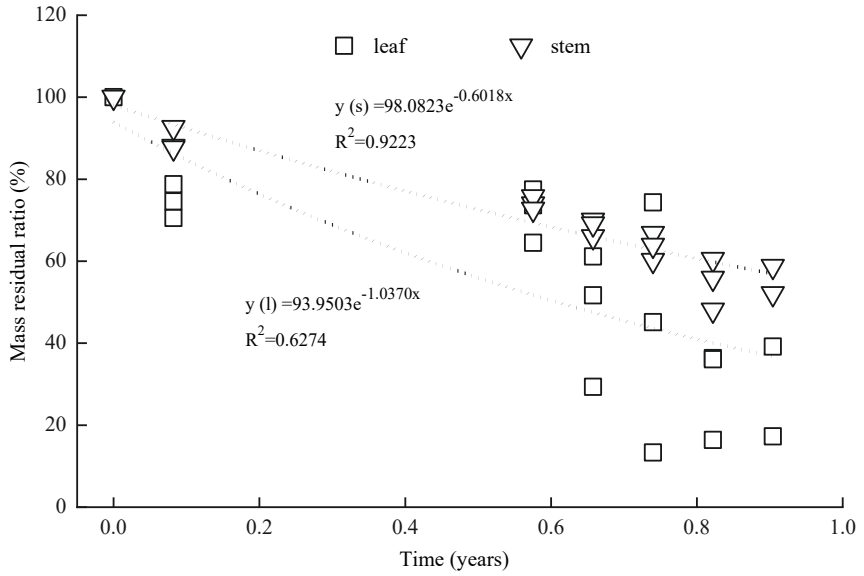

FIGURE 4
Dynamics of mass residual ratio in the leaves and stems in the *in situ* experiment.

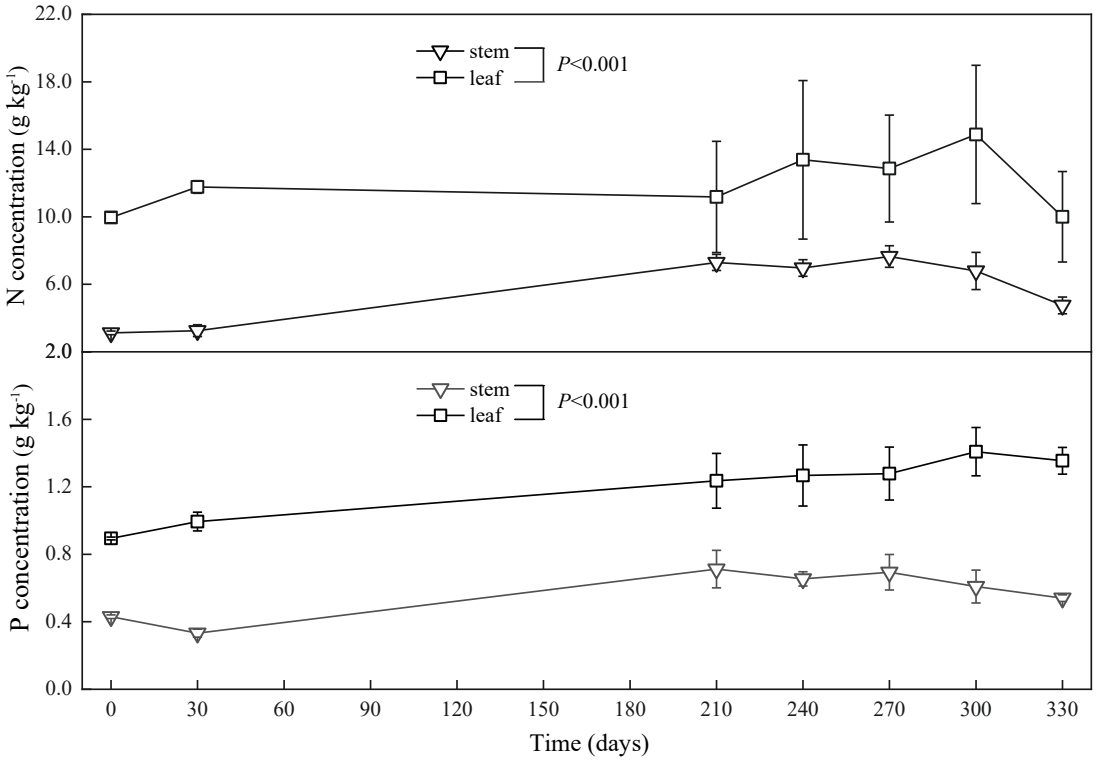

FIGURE 5
Concentrations (means ± SD) of nitrogen (N) and phosphorus (P) in the leaves and stems in the *in situ* experiment.

phosphorus. Another possible reason could be that leaves can absorb some elements from water during prolonged flood periods (Bonanno and Giudice, 2010). Combined with the biomass of plant organs, the amount of nitrogen and phosphorus fixed in the three plant organs was the highest in the roots, intermediate in the stems, and lowest in the leaves. In

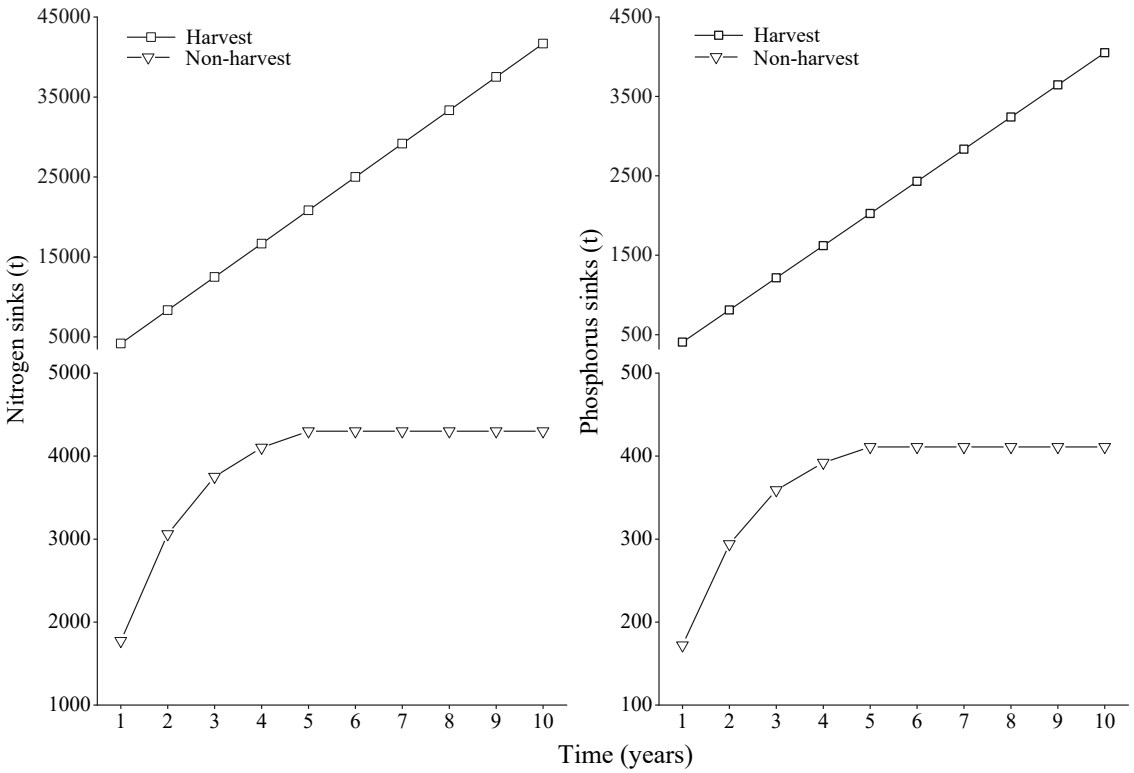

FIGURE 6
Nitrogen and phosphorus sinks in the scenarios of harvest and non-harvest of *M. lutarioriparius* in the Dongting Lake wetlands over time.

Dongting Lake, the annual amount of nitrogen and phosphorus fixed by the aboveground parts of *M. lutarioriparius* reached 4,168 and 404 t, respectively. *M. lutarioriparius* demonstrated great potential for removing nitrogen and phosphorus from the lake as industrial raw materials.

Since elements in plants come from their environment, there is an obvious relationship between the contents of elements in the plants and their environment (Fernández-Aláez et al., 1999; Baldantoni et al., 2004; Chen et al., 2015). However, in this study, we found that the mean nitrogen and phosphorus concentrations in plants were not significantly correlated with their concentrations in soil. Kern-Hansen and Dawson (1978) also found that nutrient concentrations in plants had no obvious correlation with the concentrations in environments. The possible reasons for this may be as follows. Large amounts of nitrogen and phosphorus are deposited in the lake during the flood period from April to October in Dongting Lake, which changes the concentrations of nitrogen and phosphorus in soils and thus weakens the relationship between the element concentrations in plants and those in soils. On the other hand, during the flood period, plants can absorb nitrogen and phosphorus from the water, reducing the links between the element concentrations in plants and soils. Additionally, significant regression coefficients were observed between the mean phosphorus concentrations in plants with plot elevation, soil moisture, soil organic matter concentration, and soil total potassium in this study.

Amounts of nitrogen and phosphorus released in the *in situ* experiment

In this study, the decomposition rate of stems was significantly lower than that of leaves. Similar results were obtained from a study on *Salix triandroides*, a native plant species in the Dongting Lake wetlands (Bian, 2020). Compared with leaves, stems and branches contain higher concentrations of lignin and cellulose, which contribute to the lower decomposition rate in these plant organs (dos Santos Fonseca et al., 2013). The stems, therefore, require a longer time to complete decomposition compared to the leaves (Xie et al., 2017). It was found that the half decomposition time was 1.12 years for stems and 0.61 years for leaves, and the complete decomposition time was 4.95 years for stems and 2.83 years for leaves. Unlike the stems on the soil surface designed in the *in situ* experiment, some stems in the field remained standing in the non-harvest scenario. These stems that remain standing are often colonized slowly by decomposing

organisms (Mäkinen et al., 2006); hence, standing stems have a lower decomposition rate than that of fallen stems. Therefore, the half and complete decomposition time for the stems of *M. lutarioriparius* would be slightly longer than the estimated time.

The relative release indices changed obviously over time. For leaves, the relative release indices of nitrogen and phosphorus were above zero, indicating that there was a net release of nitrogen and phosphorus. This result is consistent with previous research conducted on the wetland plant *Carex cinerascens* (Zhang et al., 2020). Litters were buried during flooding, and many decomposition products were either absorbed on soil exchange surfaces or remained available for direct root uptake (Shure et al., 1986). For stems, the relative release indices of nitrogen and phosphorus were lower than zero in the middle stage of the experiment and higher than zero in the early and later stages, indicating a net fixation of nitrogen and phosphorus in the middle stage. Unlike other experiment conditions, the litter *in situ* experiment in this study was in a special environment condition with alternate flooding and non-flooding. During the long flood period, large amounts of nutrients, such as phosphorus, were carried by water into the lake and deposited into the sediment (Huang et al., 2022). Meanwhile, some nutrients were partially absorbed by the litter (Wang et al., 2018). Exogenous nitrogen and phosphorus supplementation, therefore, leads to increased concentrations of nitrogen and phosphorus in litters in the flood period (**Figure 5**) and contributes to negative relative release indices of the two elements in the period (**Figure 3**).

After litter decomposition of 1 year, the relative release indices of nitrogen and phosphorus in the leaves reached 87.2 and 78.4%, and those in the stems reached 39.7 and 48.6%, respectively. Combined with the distribution area of *M. lutarioriparius* in the Dongting Lake wetlands and the plant biomass in the unit area, the release amounts of nitrogen and phosphorus from the aboveground parts in the first year after the non-harvest of the plant were 2,394, and 232 t, respectively.

Nitrogen and phosphorus sinks between harvest and non-harvest

In the harvest scenario, the aboveground parts of *M. lutarioriparius* were harvested and removed from the Dongting Lake wetlands, and annual element sinks were 4,168 t for nitrogen and 404 t for phosphorus. In the non-harvest scenario, considering that the aboveground parts were not harvested and would decompose in the wetland ecosystems, the element sinks in the first year after the non-harvest were 1,774 t for nitrogen and 172 t for phosphorus. Based on the model of mass residual ratio in litters in the *in situ* experiment, it was found that the nitrogen and phosphorus sinks increased greatly over time in the harvest scenario, while they increased gradually from the first year to the fifth year in the non-harvest scenario and reached a maximum value after the fifth year. Nitrogen and phosphorus sinks therefore greatly decreased after the non-harvest of *M. lutarioriparius* compared to that after harvest.

Besides nitrogen and phosphorus, plant harvest also removes several other pollutants, such as heavy metals. A study conducted by Yao et al. (2018) demonstrated that 0.7 t cadmium, 22.9 t copper, 77.5 t manganese, 3.1 t lead, and 95.9 t zinc were removed per year from the Dongting Lake wetlands through the annual harvest of the aboveground parts of *M. lutarioriparius*. Additionally, a large amount of the fixed elements (nitrogen, phosphorus, heavy metals, etc.) would be released into the environment, leading to new ecological and environmental problems in the non-harvest scenario. A new study demonstrated that the decomposition of *M. lutarioriparius* consumed the dissolved oxygen and increased the carbon, nitrogen, and phosphorus concentrations in the water (Zhao et al., 2021). The non-harvest of *M. lutarioriparius* may therefore have far-reaching impacts on the Dongting Lake wetlands. On the other hand, *M. lutarioriparius* is used to make diverse products, such as acetylated lignin, 2,5-furandicarboxylic acid, and particleboard (Chen et al., 2018; Chai et al., 2021; Liao et al., 2021). It is therefore recommended to continue to harvest *M. lutarioriparius* for ecosystem health and stability.

Data availability statement

The raw data supporting the conclusions of this article will be made available by the authors, without undue reservation.

Author contributions

YL designed the study. ZP and YD conducted the field investigation and the *in situ* experiment. SN, LX, and YN participated the two experiments. ZP and YL wrote the manuscript and other authors revised it. All authors contributed to the article and approved the submitted version.

Funding

This study was supported by the Joint Fund for Regional Innovation and Development of NSFC (U21A2009), the Leading Plan for Scientific and Technological Innovation of High-tech Industries in Hunan Province (2020SK2019), the Key Program of Research and Development of Hunan Province (2022SK2088 and 2019SK2336), and the Natural Science Foundation of Hunan Province (2021JJ30330).

Conflict of interest

The authors declare that the research was conducted in the absence of any commercial or financial relationships that could be construed as a potential conflict of interest.

Publisher's note

All claims expressed in this article are solely those of the authors and do not necessarily represent those of their affiliated organizations, or those of the publisher, the editors and the reviewers. Any product that may be evaluated in this article, or claim that may be made by its manufacturer, is not guaranteed or endorsed by the publisher.

Supplementary material

The Supplementary Material for this article can be found online at: https://www.frontiersin.org/articles/10.3389/fpls.2022.989931/full#supplementary-material

References

Baldantoni, D., Alfani, A., Di Tommasi, P., Bartoli, G., and De Santo, A. V. (2004). Assessment of macro and microelement accumulation capability of two aquatic plants. *Environ. Pollut.* 130, 149–156. doi: 10.1016/j.envpol.2003.12.015

Barrow, N. (2017). The effects of pH on phosphate uptake from the soil. *Plant Soil* 410, 401–410. doi: 10.1007/s11104-016-3008-9

Bian, H. L. (2020). *Carbon sink in Communities of Salix Triandroides and Carex Brevicuspis in Dongting Lake Wetlands*, Ph.D Thesis. Changsha: Hunan Agricultural University.

Bonanno, G., and Giudice, R. L. (2010). Heavy metal bioaccumulation by the organs of Phragmites australis (common reed) and their potential use as contamination indicators. *Ecol. Indic.* 10, 639–645. doi: 10.1016/j.ecolind.2009.11.002

Chai, Y. Z., Yang, H. C., Bai, M., Chen, A. W., Peng, L., Yan, B. H., et al. (2021). Direct production of 2, 5-Furandicarboxylicacid from raw biomass by manganese dioxide catalysis cooperated with ultrasonic-assisted diluted acid pretreatment. *Bioresou. Technol.* 337:125421. doi: 10.1016/j.biortech.2021.125421

Chen, T. Y., Li, Z. W., Zhang, X. M., Min, D. Y., Wu, Y. Y., Wen, J. L., et al. (2018). Effects of hydrothermal pretreatment on the structural characteristics of organosolv lignin from Triarrhena lutarioriparia. *Polymers* 10:1157. doi: 10.3390/polym10101157

Chen, X. S., Li, X., Xie, Y. H., Li, F., Hou, Z. Y., and Zeng, J. (2015). Combined influence of hydrological gradient and edaphic factors on the distribution of macrophyte communities in Dongting Lake wetlands. China. *Wetl. Ecol. Manag.* 23, 481–490.

dos Santos Fonseca, A. L., Bianchini, I., Pimenta, C. M. M., Soares, C. B. P., and Mangiavacchi, N. (2013). The flow velocity as driving force for decomposition of leaves and twigs. *Hydrobiologia* 703, 59–67. doi: 10.1007/s10750-012-1342-3

Fernández-Aláez, M., Fernández-Aláez, C., and Bécares, E. (1999). "Nutrient content in macrophytes in Spanish shallow lakes," in *Shallow Lakes' 98*, eds N. Walz and B. Nixdorf (Dordrecht: Springer), 317–326.

Granéli, W., and Solander, D. (1988). Influence of aquatic macrophytes on phosphorus cycling in lakes. *Hydrobiologia* 170, 245–266. doi: 10.1007/978-94-017-2986-4_35

Grizzetti, B., Billen, G., Davidson, E. A., Winiwarter, W., Vries, W. D., Fowler, D., et al. (2020). "Global nitrogen and phosphorus pollution," in *Just Enough Nitrogen*, eds M. A. Sutton, K. E. Mason, and A. Bleeker (Cham: Springer), 421–431. doi: 10.1007/978-3-030-58065-0_28

Huang, Y., Chen, X. S., Li, F., Hou, Z. Y., Li, X., Zeng, J., et al. (2022). Concurrent effects of flooding regimes and floodwater quality on sediment properties in a Yangtze River-connected floodplain wetland: Insights from field investigations during 2011-2020. *Sci. Total Environ.* 827:154225. doi: 10.1016/j.scitotenv.2022.154225

Jin, X., Wang, S., Pang, Y., and Wu, F. C. (2006). Phosphorus fractions and the effect of pH on the phosphorus release of the sediments from different trophic areas in Taihu Lake. China. *Environ. Pollut.* 139, 288–295. doi: 10.1016/j.envpol.2005.05.010

Kern-Hansen, V., and Dawson, F. H. (1978). "The standing crop of aquatic plants of lowland streams in Denmark and the inter-relationships of nutrients in plant, sediment and water," in *Proceedings 5th EWRS International Symposium on Aquatic Weeds*, (Amsterdam), 143–150.

Kuehn, K. A., and Suberkropp, K. (1998). Decomposition of standing litter of the freshwater emergent macrophyte Juncus effusus. *Freshwater Biol.* 40, 717–727. doi: 10.1046/j.1365-2427.1998.00374.x

Liao, Q. Y., Zhang, J., Yi, Z. L., and Li, Y. Z. (2021). Do Miscanthus lutarioriparius-Based Oriented Strand Boards Provide Environmentally Benign Alternatives? An LCA Case Study of Lake Dongting District in China. *Sustainability* 13:12976. doi: 10.3390/su132312976

Liu, G. S. (1996). *Soil Physical and Chemical Analysis and Description of Profile*. Beijing: China Standards Press.

Lu, Q., He, Z. L., Graetz, D. A., Stoffella, P. J., and Yang, X. (2010). Phytoremediation to remove nutrients and improve eutrophic stormwaters using water lettuce (Pistia stratiotes L.). *Environ. Sci. Pollut. R.* 17, 84–96. doi: 10.1007/s11356-008-0094-0

Luo, Y., Peng, Q. W., Li, K. H., Gong, Y. M., Liu, Y. Y., and Han, W. X. (2021). Patterns of nitrogen and phosphorus stoichiometry among leaf, stem and root of desert plants and responses to climate and soil factors in Xinjiang. China. *Catena* 199:105100. doi: 10.1016/j.catena.2020.105100

Mäkinen, H., Hynynen, J., Siitonen, J., and Sievänen, R. (2006). Predicting the decomposition of Scots pine, Norway spruce, and birch stems in Finland. *Ecol. Appl.* 16, 1865–1879. doi: 10.1890/1051-07612006016

McClaugherty, C. A., Pastor, J., Aber, J. D., and Melillo, J. M. (1985). Forest litter decomposition in relation to soil nitrogen dynamics and litter quality. *Ecology* 66, 266–275. doi: 10.2307/1941327

Morton, C., Cameron, R., and Duinker, P. (2010). Modeling carbon budgets for four protected wilderness areas in Nova Scotia, eds S. Bondrup-Nielsen, K. Beazley, G. Bissix, D. Colville, S. Flemming, *Ecosystem Based Management: Beyond Boundaries*. (Wolfville, NS: Science and Management of Protected Areas Association), 429–440.

Nash, D. A. H., Abdullah, S. R. S., Hasan, H. A., Mushrifah, I., Muhammad, N. F., Al-Baldawi, I. A., et al. (2019). Phytoremediation of Nutrients and Organic Carbon from Sago Mill Effluent using Water Hyacinth (Eichhornia crassipes). *J. Eng. Technol. Sci* 51, 573–584.12. doi: 10.5614/j.eng.technol.sci.2019.51.4.8

Nixon, S. W., Buckley, B. A., Granger, S. L., Harris, L. A., Oczkowski, A. J., Fulweiler, R. W., et al. (2008). *Nitrogen and Phosphorus Inputs to Narragansett Bay: Past, Present, and Future. Science for Ecosystem-Based Management*. New York, NY: Springer, 101–175. doi: 10.1007/978-0-387-35299-2_5

Olson, J. S. (1963). Energy storage and the balance of producers and decomposers in ecological systems. *Ecology* 44, 322–331. doi: 10.2307/1932179

Rezania, S., Park, J., Rupani, P. F., Darajeh, N., Xu, X., and Shahrokhishahraki, R. (2019). Phytoremediation potential and control of Phragmites australis as a green phytomass: An overview. *Environ. Sci. Pollut. R.* 26, 7428–7441. doi: 10.1007/s11356-019-04300-4

Sajedi, T., Prescott, C. E., Seely, B., and Lavkulich, L. M. (2012). Relationships among soil moisture, aeration and plant communities in natural and harvested coniferous forests in coastal British Columbia. *Canada. J. Ecol.* 100, 605–618. doi: 10.1111/j.1365-2745.2011.01942.x

Shure, D. J., Gottschalk, M. R., and Parsons, K. A. (1986). Litter decomposition processes in a floodplain forest. *Am. Midl. Nat* 115, 314–327. doi: 10.2307/2425868

Song, J. Y., and Shan, B. Q. (2012). Nitrogen and phosphorus absorption capacity of Phragmites australis in constructed pond-wetland system for reclaimed water treatment. *Environ. Sci. Technol.* 35, 16–19.

van der Valk, A. G., Rhymer, J. M., and Murkin, H. R. (1991). Flooding and the decomposition of litter of four emergent plant species in a prairie wetland. *Wetlands* 11, 1–16. doi: 10.1007/bf03160837

Wang, L. Z., Liu, Q. J., Hu, C. W., Liang, R. J., Qiu, J. C., and Wang, Y. (2018). Phosphorus release during decomposition of the submerged macrophyte *Potamogeton crispus*. *Limnology* 19, 355–366. doi: 10.1007/s10201-018-0538-2

Xie, Y. H., Tang, Y., Chen, X. S., Li, F., and Deng, Z. M. (2015). The impact of Three Gorges Dam on the downstream eco-hydrological environment and vegetation distribution of East Dongting Lake. *Ecohydrology* 8, 738–746. doi: 10.1002/eco.1543

Xie, Y. J., Xie, Y. H., Xiao, H. Y., Chen, X. S., and Li, F. (2017). Controls on litter decomposition of emergent macrophyte in Dongting Lake wetlands. *Ecosystems* 20, 1383–1389. doi: 10.1007/s10021-017-0119-y

Xu, Y. Z., Fu, G. Y., Tang, N., He, Z. H., Jian, L. C., and Zhao, Y. Y. (2021). Distribution of Triarrhena lutarioriparia and its reserve characteristics of nitrogen and phosphorus in Dongting Lake. In E3S Web of Conferences. *EDP Sci.* 237:01004. doi: 10.1051/e3sconf/202123701004

Yang, Y., Gao, B., Hao, H., Zhou, H. D., and Lu, J. (2017). Nitrogen and phosphorus in sediments in China: A national-scale assessment and review. *Sci. Total Environ.* 576, 840–849. doi: 10.1016/j.scitotenv.2016.10.136

Yao, X., Niu, Y. D., Li, Y. L., Zou, D. S., Ding, X. H., and Bian, H. L. (2018). Heavy metal bioaccumulation by Miscanthus sacchariflorus and its potential for removing metals from the Dongting Lake wetlands. China. *Environ. Sci. Pollut. R.* 25, 20003–20011. doi: 10.1007/s11356-018-2174-0

Zhang, Q. J., Zhang, G. S., Yu, X. B., Liu, Y., Xia, S. X., Meng, Z. J., et al. (2020). Dynamic characteristics of the decomposition rate and carbon, nitrogen and phosphorus release of the dominant plants in Poyang Lake Wetland. *Acta Ecol. Sinaca* 40, 8905–8916. doi: 10.5846/stxb201909161925

Zhao, Y. Y., Xu, Y. Z., Fu, G. Y., Tang, N., and Zhou, S. (2021). Decomposition behavior of Triarrhena lutarioriparia tissues in Dongting Lake water: A laboratory simulation study. *CLEAN–Soil Air Water* 50:2000426. doi: 10.1002/clen.202000426

frontiers | Frontiers in Plant Science

TYPE Original Research
PUBLISHED 08 September 2022
DOI 10.3389/fpls.2022.986034

OPEN ACCESS

EDITED BY
Roberta Pastorelli,
Council for Agricultural and Economics Research (CREA), Italy

REVIEWED BY
Andrea Manfredini,
Council for Agricultural and Economics Research (CREA), Italy
Waqar Islam,
Fujian Agriculture and Forestry University, China
Caroline Fadeke Ajilogba,
North-West University, South Africa

*CORRESPONDENCE
Xiaoming Kang
xmkang@ucas.ac.cn

†These authors have contributed equally to this work and share first authorship

SPECIALTY SECTION
This article was submitted to Functional Plant Ecology, a section of the journal Frontiers in Plant Science

RECEIVED 04 July 2022
ACCEPTED 19 August 2022
PUBLISHED 08 September 2022

CITATION
Wang X, Li Y, Yan Z, Hao Y, Kang E, Zhang X, Li M, Zhang K, Yan L, Yang A, Niu Y and Kang X (2022) The divergent vertical pattern and assembly of soil bacterial and fungal communities in response to short-term warming in an alpine peatland.
Front. Plant Sci. 13:986034.
doi: 10.3389/fpls.2022.986034

The divergent vertical pattern and assembly of soil bacterial and fungal communities in response to short-term warming in an alpine peatland

Xiaodong Wang[1,2,3†], Yong Li[1,2,3†], Zhongqing Yan[1,2,3], Yanbin Hao[4], Enze Kang[1,2,3], Xiaodong Zhang[1,2,3], Meng Li[1,2,3], Kerou Zhang[1,2,3], Liang Yan[1,2,3], Ao Yang[1,2,3], Yuechuan Niu[4] and Xiaoming Kang[1,2,3*]

[1]Wetland Research Center, Institute of Ecological Conservation and Restoration, Chinese Academy of Forestry, Beijing, China, [2]Beijing Key Laboratory of Wetland Services and Restoration, Beijing, China, [3]Sichuan Zoige Wetland Ecosystem Research Station, Tibetan Autonomous Prefecture of Aba, Aba, China, [4]College of Life Sciences, University of Chinese Academy of Sciences, Beijing, China

Soil microbial communities are crucial in ecosystem-level decomposition and nutrient cycling processes and are sensitive to climate change in peatlands. However, the response of the vertical distribution of microbial communities to warming remains unclear in the alpine peatland. In this study, we examined the effects of warming on the vertical pattern and assembly of soil bacterial and fungal communities across three soil layers (0–10, 10–20, and 20–30 cm) in the Zoige alpine peatland under a warming treatment. Our results showed that short-term warming had no significant effects on the alpha diversity of either the bacterial or the fungal community. Although the bacterial community in the lower layers became more similar as soil temperature increased, the difference in the vertical structure of the bacterial community among different treatments was not significant. In contrast, the vertical structure of the fungal community was significantly affected by warming. The main ecological process driving the vertical assembly of the bacterial community was the niche-based process in all treatments, while soil carbon and nutrients were the main driving factors. The vertical structure of the fungal community was driven by a dispersal-based process in control plots, while the niche and dispersal processes jointly regulated the fungal communities in the warming plots. Plant biomass was significantly related to the vertical structure of the fungal community under the warming treatments. The variation in pH was significantly correlated with the assembly of the bacterial community, while soil water content, microbial biomass carbon/microbial biomass phosphorous (MBC/MBP), and microbial biomass nitrogen/ microbial biomass phosphorous (MBN/MBP) were significantly correlated with the assembly of the fungal community. These

results indicate that the vertical structure and assembly of the soil bacterial and fungal communities responded differently to warming and could provide a potential mechanism of microbial community assembly in the alpine peatland in response to warming.

KEYWORDS

soil microbial community, alpine peatland, community assembly, vertical structure, warming

Introduction

The greenhouse effect has been increasing over the past few decades due to the cumulative impact of human activities, leading to global warming (Zandalinas et al., 2021). The global average surface temperature in the first 20 years of the twenty-first century (2001–2020) has increased by 0.99 (0.84–1.10)°C compared with that during 1850–1900 (IPCC, 2021). Peatlands cover only 3% of the Earth's land surface but contain 1,055 Gt of soil carbon (Nichols and Peteet, 2019), which is roughly equivalent to 45% of global soil C (Nichols and Peteet, 2019; Xue D. et al., 2021). Peatlands are a major contributor to global greenhouse gas emissions (Tiemeyer et al., 2016) with a function of buffering the effects of climate warming (Frolking and Roulet, 2007). However, peatlands are suffering massive degradation under climate change and human disturbance, which is affecting the global emissions of greenhouse gases (Chen et al., 2013). Thus, it is necessary to clarify the effects of warming on peatlands.

Warming accelerates carbon emission from subsurface peat, leading to a decreased peatland carbon sink (Dorrepaal et al., 2009; Helbig et al., 2022). The alpine peatlands are more sensitive to warming due to their high altitude (Mclaughlin and Webster, 2018; Zhang et al., 2022). Previous studies have shown that climate warming strongly affects the alpine ecosystem microbial communities on the Qinghai-Tibet Plateau (Zhao et al., 2014; Liu et al., 2016; Zhang K. et al., 2016; Kang et al., 2022). Soil microbes play a vital role in biogeochemical processes and other ecosystem-level decomposition and nutrient cycling processes in peatland and the repose of the microbial community to warming enhances the temperature sensitivity of soil respiration (Bardgett and Van Der Putten, 2014; Anthony et al., 2020). Warming has altered the microbial biomass, community composition, community succession, and network complexity and stability (Blankinship et al., 2011; Guo et al., 2018, 2019; Yuan et al., 2021). However, warming affects the soil bacterial and fungal communities differently. Bacterial communities are more sensitive than fungal communities in topsoil (Guo et al., 2019; De Oliveira et al., 2020; Kanzaki and Takemoto, 2021). Moreover, previous studies focused on the horizontal structure of the soil microbial communities in different soil layers (Du et al., 2017; Jiao et al., 2018; Chen et al., 2020), and the alpha diversity of different microbial taxa varied by depth (Jiao et al., 2018). Soil pH has been reported to be the driving factor for the horizontal structure of the bacterial community (Xia et al., 2016; Liu et al., 2018; Kang et al., 2021). More dimensions must be considered when studying soil microbial communities because of the spatial heterogeneity of the soil and the three-dimensional distribution of microbiomes in soil (Xue R. et al., 2021). However, the vertical responses of soil bacterial and fungal communities to warming remain unclear.

Investigating the ecological processes driving community assembly contributes to disentangling the mechanisms of the microbial communities in response to climate change (Ponisio et al., 2019). Traditional niche theory hypothesizes that community structures are dominated by deterministic factors, such as environmental conditions and the interactions between species, which are referred to as deterministic processes (Chesson, 2000; Fargione et al., 2003; Kraft et al., 2014). In contrast, the neutral theory holds that community structures are determined by stochastic processes, such as birth, death, extinction, speciation, and colonization (Hubbell, 2001; Chave, 2004). The deterministic process and the stochastic process have been recently determined to jointly regulate community assembly (Chase, 2010; Chase and Myers, 2011; Stegen et al., 2016; Cai et al., 2020), but their relative importance in driving community assembly has not been determined (Vellend et al., 2014; Zhou et al., 2014; Tonkin et al., 2018). The dispersal-niche continuum index (DNCI), a standardized effect-size index, has been used to compare the predominance of niche-based vs. dispersal-based processes between multiple datasets (Vilmi et al., 2020), which has a potential ability to reveal the relative importance of ecological processes across soil layers.

The temperature of the Zoige alpine peatland, which is one of the largest and highest plateau peatlands (Chen et al., 2014) in the northeastern part of the Qinghai-Tibet Plateau, has increased significantly (average 0.4°C per decade) (Yang et al., 2014). To investigate how short-term warming affects the vertical distribution and assembly of the soil bacterial and fungal communities, we initiated a field manipulative experiment in the Zoige alpine peatland. We hypothesize that short-term warming has no effects on the diversity of bacterial and fungal communities (hypothesis I); the vertical distribution of bacterial and fungal communities are both altered after short-term warming (hypothesis II); the assembly processes of the bacterial

and fungal communities across soil layers are affected by short-term warming (hypothesis III).

Materials and methods

Study area and experimental design

This experiment was conducted at the Axi Ranch on the Zoige National Wetland Natural Reserve (33°47′56″ N, 102°57′28″ E), which is the largest plateau peat bog in the world. The study region has a typical plateau monsoon climate. The annual average temperature ranges from −1 to 3.3°C, and the annual average precipitation is 650–750 mm. The region has a long frost period (October–April) and a short growing season (May–September) (Yan et al., 2021). The dominant plant species are *Blysmus sinocompressus*, *Carex meyeriana*, *Carex muliensis*, *Carex secbrirostris, Eriophorum gracile*, and *Koeleria tibetica*.

The warming experiment was initiated in June 2021, using a completely random design. Two levels of warming treatments (slight warming, Ws; high warming, Wh) and a control (CK) were set up with three replicates. The warming treatments were carried out in open-top chambers consisting of six transparent acrylic isosceles trapezoidal plates with light transmittance > 95%. Temperatures measured on average every 10 days in the 0–10 cm soil layer over the entire growing season (June–September) rose by 0.9 and 1.8°C on average in the Ws and Wh treatments, respectively compared to CK (Supplementary Figure 1).

Plant and soil sampling

The soil and the above-ground plant biomass were sampled at the end of the growing season in late September 2021 after one growing-season warming treatment. Plant biomass was collected using a square frame (0.5 × 0.5 m) and dried at 65°C for 72 hours before being weighed. Five soil cores (5 cm diameter) were randomly collected at depths of 0–10 cm (up), 10–20 cm (mid), and 20–30 cm (low) from each plot. Then, samples from the same depth at each plot were mixed to form a composite sample. Twenty-seven soil samples (3 treatments × 3 layers × 3 replicates) were taken in total, placed on dry ice, and delivered by express mail to the laboratory in Beijing, China. A subsample of soil from each sample was immediately frozen at −20°C for microbial community analyses and the other subsamples were used to determine the soil physical and chemical indicators.

Soil physicochemical characteristics

A soil subsample was air-dried, finely ground, and passed through a 0.15 mm sieve to measure soil organic carbon (SOC), dissolved organic carbon (DOC), soil pH, total nitrogen (TN), total phosphorus (TP), available phosphorus (AP), ammonium (NH_4^+), nitrate (NO_3^-), microbial biomass carbon (MBC), microbial biomass nitrogen (MBN), and microbial biomass phosphorus (MBP), while another sample was passed through a 2 mm sieve with the roots removed to determine soil water content (SWC). Soil pH was assessed using a pH electrode (PB-10, Sartorius, Germany) in a 1:2.5 soil/water solution. SWC was determined using the oven-drying method. SOC was determined by the rapid dichromate oxidation-titration method. DOC was measured on a total organic C analyzer (Vario TOC Cube, Elementar, Germany). Soil TN was determined full-automatic Kjeldahl apparatus (KJELTEC 8400, FOSS, Danmark), and soil TP was determined by spectrophotometer (TAS-990, Persee, Beijing, China) using the method of Wu et al. (2017). A spectrophotometer was used to assess soil AP by molybdenum blue colorimetry (TAS-990, Persee, Beijing, China). NH_4^+ and NO_3^- concentrations were determined by the extracts of the unfumigated soils using a flow injection auto-analyzer (SANplus, Skalar, Netherlands). The MBC, MBN, and MBP contents were evaluated using the chloroform fumigation extraction method (Brookes et al., 1982, 1985; Vance et al., 1987).

DNA extraction and polymerase chain reaction (PCR) amplification

Microbial community genomic DNA was extracted using the FastDNA® SPIN Kit for Soil (MP Biomedical, Irvine, CA, USA) according to the manufacturer's instructions. The DNA extract was checked by 1% agarose gel electrophoresis, and DNA concentration and purity were determined with the NanoDrop 2000 UV-vis spectrophotometer (Thermo Scientific, Wilmington, DE, USA). The hypervariable V4 region of the bacterial 16S rRNA gene was amplified with the primer pairs 515F (5′-GTGCCAGCMGCCGCGG-3′) and 806R (5′-GGACTACNVGGGTWTCT-3′), while the fungal ITS gene was amplified with the primers ITS1F (5′ CTTGGTCATTTAGAGGAAGTAA-3′) and ITS2R (5′-GCTGCGTTCTTCATCGATGC-3′) using the PCR thermocycler (GeneAmp® 9700, ABI, Thermo Fisher). The reverse primer was combined with the adapter and barcode sequences for multiplexing, and amplification was performed in 20 μl reaction volumes containing 2 μl of 10× *TransStart* FastPfu Buffer, 0.2 μl of FastPfu Polymerase, 0.8 mM of each primer (5 μM), 2 μl of 2.5 mM dNTPs, 0.2 μl of BSA, and 10 ng of template DNA. The PCR program consisted of 30 cycles of initial denaturation at 95°C for 3 min, 95°C for 30 s, 55°C for 30 s, 72°C for 45 s, and a final extension at 72°C for 10 min.

Purified amplicons were sequenced in equimolar concentrations and pair-end read on the Illumina MiSeq PE300 platform/NovaSeq PE250 platform (Illumina, San Diego,

CA, USA) according to the standard protocol of Majorbio Bio-Pharm Technology Co. Ltd. (Shanghai, China).

Bioinformatical analyses

The sequenced reads were demultiplexed, quality-filtered using fastp version 0.20.0 (Chen et al., 2018), and merged with FLASH version 1.2.7 (Magoc and Salzberg, 2011) using the following criteria: (i) only overlapping sequences > 10 bp were assembled according to their overlapped sequence. The maximum mismatch ratio of the overlapping region was 0.2. Reads that could not be assembled were discarded; (ii) Samples were distinguished according to the barcode and primers, and the sequence direction was adjusted using exact barcode matching and 2 nucleotide mismatches for primer matching; (iii) the 300 bp reads were truncated at any site receiving an average quality score < 20 over a 50 bp sliding window, and truncated reads < 50 bp were discarded; reads containing ambiguous characters were also discarded.

UPARSE version 7.1 (Edgar, 2013) was used to cluster the operational taxonomic units (OTUs) with a 97% similarity cutoff (Stackebrandt and Goebel, 1994; Edgar, 2013) and chimeric sequences were identified and removed. The Ribosomal Database Project classifier (version 2.2) with database Silva v138 and UNITE version 10.05.2021 for bacteria and fungi respectively (http://rdp.cme.msu.edu) was used to assign OTU representative sequences at a 70% threshold (Wang et al., 2007; Nilsson et al., 2018).

Statistical analyses

To make abundances comparable between the samples, the *rrarefy* function in the R package "vegan" (The R Foundation for Statistical Computing, Vienna, Austria) was applied. The effects of treatments and soil layers on soil characters and alpha diversity of the bacteria and fungi (richness, Shannon index, and Pielou's evenness) were tested by two-way nested analysis of variance (ANOVA) (soil layers nested in the treatments), followed by multiple comparisons using the LSD method for the treatments and the soil layers. One-way ANOVA was applied to test the effects of the warming treatments on plant biomass. Bray–Curtis metrics were calculated to determine the dissimilarities in the microbial communities at the taxonomic level across soil layers (*vegdist* function in R package "vegan"). Non-metric multidimensional scaling analysis was conducted to visualize distances between communities with the Bray–Curtis dissimilarity measurements (*metaMDS* function in R package "vegan"). Permutational multivariate analysis of variance (PERMANOVA) and ANOSIM was conducted (*adonis* and *anosim* function in R package "vegan") to assess the effects of the treatments and soil layers on the taxonomic composition of the microbial communities. The Mantel test was performed to reveal the relationship between the microbial communities and the environmental variables (*mantel* function in R package "vegan").

The dispersal–niche continuum index (DNCI) was calculated between soil layers and the entire microbial community across soil layers to reveal the ecological processes driving the microbial community across soil layers under the different treatments. Significant positive DNCI values indicate that the community is driven predominantly by the niche process, whereas significant negative values indicate a dispersal-dominated ecological process. If the DNCI distribution does not significantly differ from 0, the dispersal and niche processes were assumed to contribute equally to the community. DNCI analyses were carried out using the R package "DNCImper" available on Github (Vilmi et al., 2020) with 1,000 permutations. Moreover, for each variable (e.g., soil pH), the variation (e.g. |SWCa–SWCb|, where a and b represent samples) and the mean (e.g. [SWCa + SWCb]/2) of each pair of samples was used to calculate Pearson's correlation with the DNCI.

Results

Vertical distribution and variation of environmental variables

In addition to soil SWC, MBC/MBP and MBN/MBP were significantly affected by warming ($p < 0.05$). The majority of the soil characters (SWC, SOC, TN, TP, AP, DOC, and NH_4^+) differed more significantly between soil layers ($p < 0.05$) (Table 1). SWC in the 0–10 cm soil layer decreased by 8.36% and 12.86% in the Ws ($p > 0.05$) and Wh ($p < 0.05$) plots, respectively, compared to CK. Soil NO_3^- concentrations decreased significantly ($p < 0.05$) by 66.55% and 57.10% in the Ws and Wh plots, respectively. Neither Ws nor Wh had significant effects on other soil characters. None of the soil characters in the mid (10–20 cm) or lower (20–30 cm) soil layers were significantly affected by the warming treatments. Plant biomass was not significantly affected by the warming treatments ($p > 0.05$) (Table 1).

Composition of soil bacterial and fungal communities

Approximately 1,365,171 and 1,562,875 sequences (27 samples, average 50,562 and 57,884 sequences) were obtained for the bacterial and fungal communities, respectively. A total of 11,108 bacterial and 3,693 fungi OTUs were obtained at the 97% similarity level based on these sequences.

The dominant groups (>10%) in the bacterial community were Proteobacteria and Actinobacteriota, which were 28.57

TABLE 1 Results of two-way nested ANOVAs for the effects of treatment and soil depth (nested within treatments) on soil characters and the results of one-way ANOVA for plant biomass affected by the treatments.

	Treatments		Layers	
	F	Pr (>F)	*F*	Pr (>F)
SWC	5.011	0.019*	4.830	0.004**
pH	0.880	0.432	2.308	0.079
SOC	0.074	0.929	14.879	0.001***
TN	0.024	0.976	8.724	0.001***
TP	0.741	0.490	4.892	0.004**
AP	0.278	0.760	4.779	0.004**
DOC	0.153	0.859	10.002	0.001***
NH_4^+	0.056	0.946	3.824	0.012*
NO_3^-	2.255	0.134	2.467	0.064
MBC	2.015	0.162	6.938	0.001**
MBN	0.177	0.839	5.493	0.002**
MBP	1.416	0.268	4.322	0.007**
MBC/MBN	1.088	0.358	2.744	0.045*
MBC/MBP	3.906	0.039*	2.046	0.112
MBN/MBP	4.555	0.025*	1.780	0.160
Biomass	3.383	0.104	/	/

MBC, microbial biomass carbon; MBN, microbial biomass nitrogen; MBP, microbial biomass phosphorous; Biomass, plant biomass; *$0.01 < p < 0.05$; **$0.001 < p < 0.01$; ***$p < 0.001$.

and 25.69% of the total (Figure 1A, Supplementary Figure 2), respectively. The relative abundances of Actinobacteriota, Crenarchaeota, Firmicutes, MBNT15, and Verrucomicrobiota were affected by the warming treatments, and the majority of the groups differed significantly ($p < 0.05$) in the soil layers (Supplementary Figure 3). Ascomycota (64.02%), Basidiomycota (12.91%), and Mortierellomycota (10.59%) were the dominant fungal groups (Figure 1B, Supplementary Figure 2). The relative abundance of Mortierellomycota was significantly different between the treatments but no significant effects were observed between the soil layers of the other groups (Supplementary Figure 4).

Alpha and beta diversity of soil bacterial and fungal communities

OTU richness, the Shannon diversity index, and Pielou's evenness were used as indicators of alpha diversity. The results of two-way nested ANOVA showed that the warming treatments had no significant effects on alpha diversity of either the bacterial or the fungal community ($p > 0.05$) but the soil layers had significant effects on richness ($p < 0.01$) of the fungal community (Figure 2).

The Bray-Curtis index for the bacterial communities between mid and low soil layers decreased with temperature, and the dissimilarity of the bacterial communities increased with distance (Supplementary Figure 5A). No significant differences in the Bray-Curtis index of the fungal communities were observed between the treatments or by distance (Supplementary Figure 5B). The results of PERMANOVA and ANOSIM revealed a significant difference between the upper layer (0–10 cm) and the mid (10–20 cm) or lower (20–30) layer bacterial communities, while no significant difference was detected between the mid and lower layers (Figure 3A, Supplementary Tables 2, 3). The fungal communities were significantly different ($p < 0.01$) under the different treatments (Figure 3B). However, the bacterial communities under the different treatments and the fungal communities at different soil depths were not significantly different (Figure 3).

Ecological processes and factors influencing the microbial communities

In the CK plots, SOC, DOC, NO3-, SWC, TN, AP, MBC, MBN and MBP were the important factors contributing to variation in soil bacterial community structure (Figure 4A, Supplementary Table 1). SWC, pH, SOC, TN, DOC, TP, AP, and MBC were the important factors contributing to variation in soil bacterial community structure in Ws plots (Figure 4B, Supplementary Table 1). SWC, SOC, DOC, TN, TP, MBC, MBN, and MBP were the important factors contributing to variation in soil bacterial community structure in the Wh plots (Figure 4C, Supplementary Table 1). In contrast, the vertical structure of the fungal communities in all plots was not significantly affected by the soil characters (Figure 3), while plant biomass was an important factor related to the fungal communities in the Ws and Wh plots (Figures 4E,F, Supplementary Table 1). The ecological processes of the microbial communities across the soil layers were inferred by the DNCI. The DNCI values of the bacterial communities were positive in all treatments, and increased in response to temperature in the upper and lower layers and in total, indicating that niche-based ecology processes were important in bacterial communities and the increased relative importance of the niche process was enhanced by warming (Figure 5A). The DNCI values of the fungal communities were negative in the CK plots but increased close to 0 in the Warming plots, indicating that dispersal was the main process of the fungal communities in the CK plots. The relative importance of dispersal decreased and was close to equal to niche process in the warming plots (Figure 5B). We calculated Pearson's correlation coefficients between the DNCI and soil characters, and the DNCI of the bacterial community was significantly correlated with the variation in pH ($r = 0.747$, $p < 0.05$), while the DNCI of the fungal community was significantly

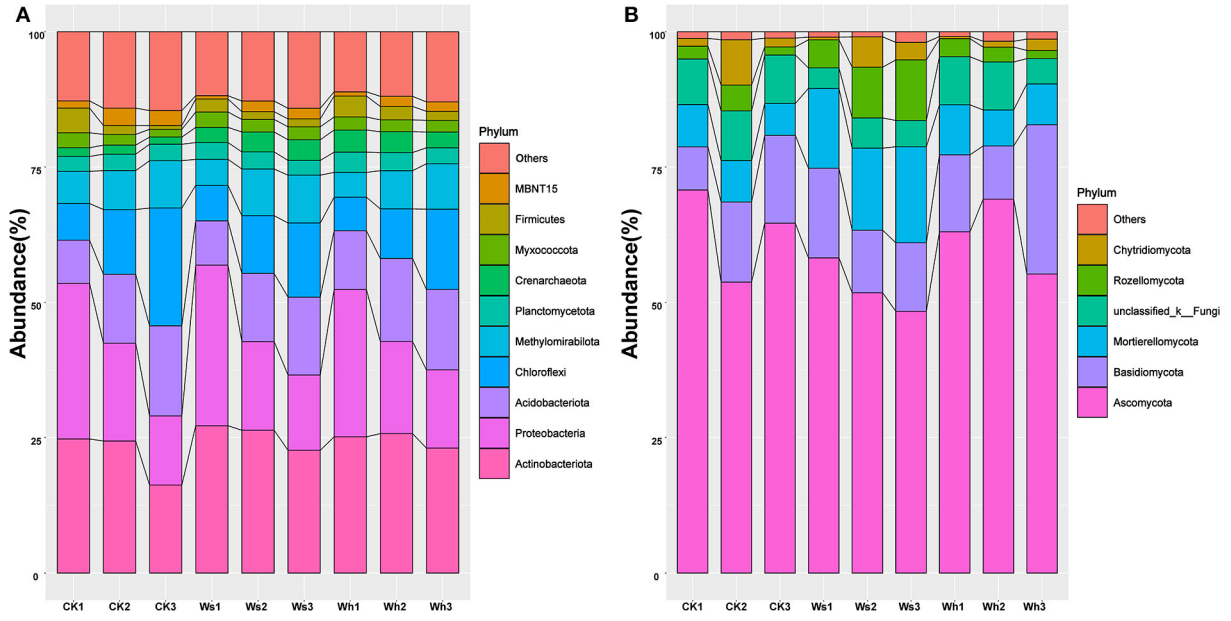

FIGURE 1
Relative abundance of the dominant bacteria **(A)** and fungi **(B)** groups at phylum level at different soil layers. Ws, slight warming; Wh, high warming; CK1, 0–10 cm depth in control plots; CK2, 10–20 cm depth in control plots; CK3, 20–30 cm depth in control plots.

negatively correlated with the mean of the SWC ($r = -0.684$, $p < 0.05$), MBC/MBP ($r = -0.885$, $p < 0.01$) and MBN/MBP ($r = -0.897$, $p < 0.01$) (Table 2).

Discussion

Warming did not affect soil microbial diversity but shifted the fungal community structure

Diversity indices are important indicators of soil microbial diversity. The alpha diversity of the bacterial and fungal communities did not change significantly after the short-term warming treatments in the alpine peatland which support hypothesis I. Previous studies have shown that warming treatments have significant or no effects on microbial communities, which is related to the experimental duration, intensity, frequency of warming, and the availability of substrates for microbial growth (Finlay et al., 1997; Frey et al., 2008; Adair et al., 2019). The same results were reported in alpine grasslands and the cultivated grasslands of the Qinghai-Tibetan Plateau (Zhang Y. et al., 2016). Unlike farmland ecosystems (Sun et al., 2018), the richness of the fungal community was significantly affected by soil depth in this study. Fungi are generally correlated with plants, as they play a critical role in linking below ground with the above ground in the terrestrial ecosystem (Rillig, 2004; Wardle et al., 2004; Hannula and Trager, 2020). The fungal communities could have been affected by roots, as the vegetation type at the study site was herbaceous, which declined with depth.

Proteobacteria and Actinobacteriota were the dominant phyla as reported by a previous study on the Zoige alpine peatland (Fan et al., 2021). The relative abundance of Proteobacteria is also high in moist soils due to its wide adaptability (Jiang et al., 2013; Kang et al., 2021). The bacterial communities did not respond significantly to warming (Figure 3), although several groups in particular soil layers were sensitive to warming (Supplementary Figure 2). The changes in the peatland fungal groups were thought to be related to the magnitude of the temperature increase, as the composition of the fungal communities responded differently to warming at +4 and +8°C (Asemaninejad et al., 2018). In this short-term warming study, the relative abundance of Mortierellomycota was higher under warming at +0.8°C, while it was not significantly different from the control under warming at +1.8°C, indicating that the response of the fungi community to warming was complexed. More experiments with temperature gradients are needed to reveal the mechanisms by which fungal communities respond to warming.

Warming did not affect the vertical structure of bacterial communities but fungal communities

The majority of the bacterial groups were significantly different among the soil layers, while the fungi groups revealed

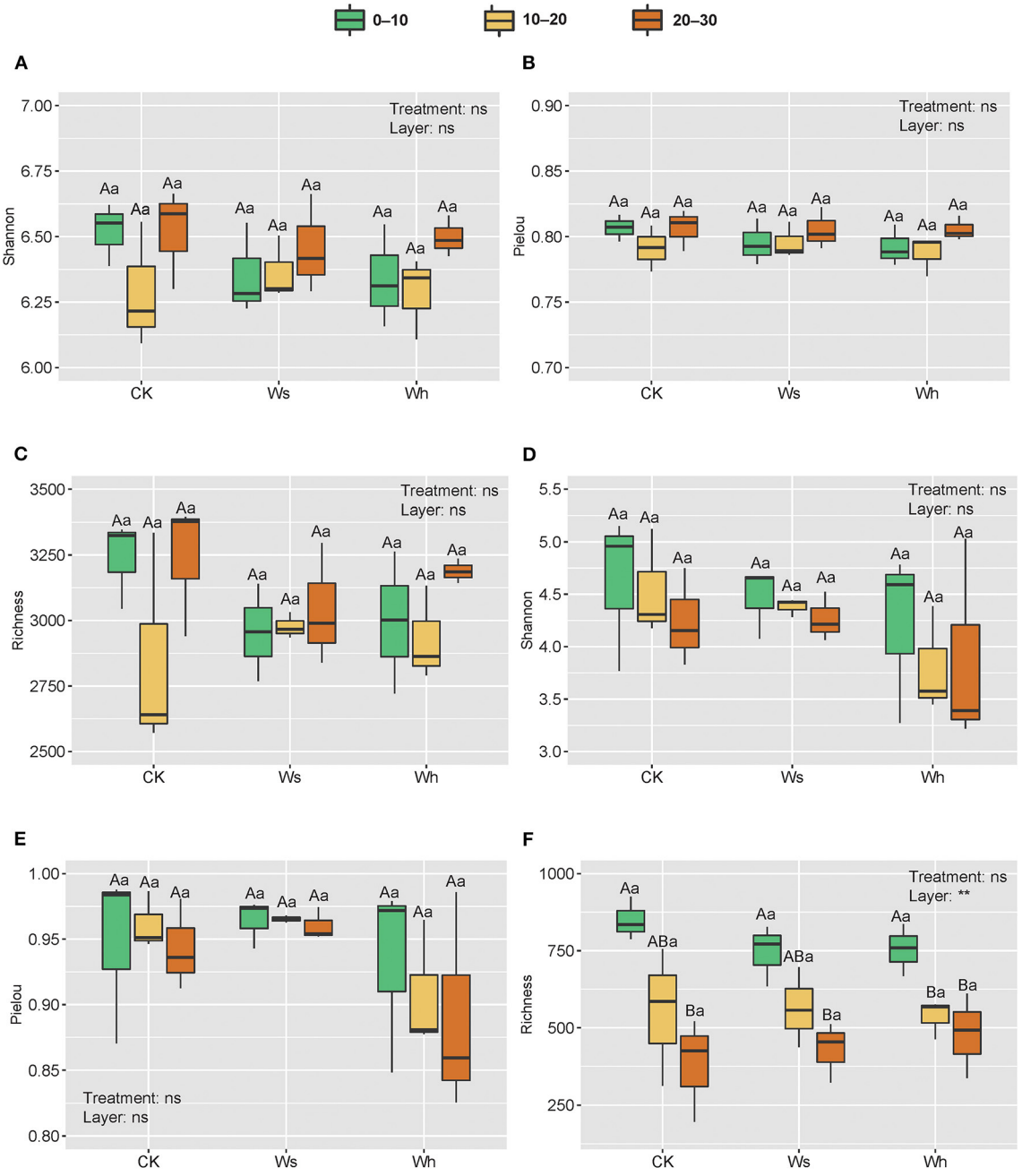

FIGURE 2
Richness and alpha diversity index of soil bacterial **(A–C)** and fungal **(D–F)** communities. Ws, slight warming; Wh, high warming. ** and ns indicate the significant levels for treatments and soil depths (nested within treatments) at 0.01 and non-significant, respectively. Boxplots not sharing a common capital letter are significantly different ($p < 0.05$) among soil layers while different small letters represent significantly different ($p < 0.05$) among treatments.

no distinct vertical patterns. Soil aggregates provide a large number of ecological niches, and the vertical distribution of soil microbial communities that live inside soil aggregates is generally limited by soil environmental factors (Sun et al., 2021). The vertical pattern of the bacterial community is more likely to be correlated with soil C and nutrients (Chu et al., 2016; Du et al., 2017; Sun et al., 2018; Brewer et al., 2019), which was also observed in this study. The structure of the bacterial communities in the warming plots was regulated more strongly by soil moisture and nutrients compared to the

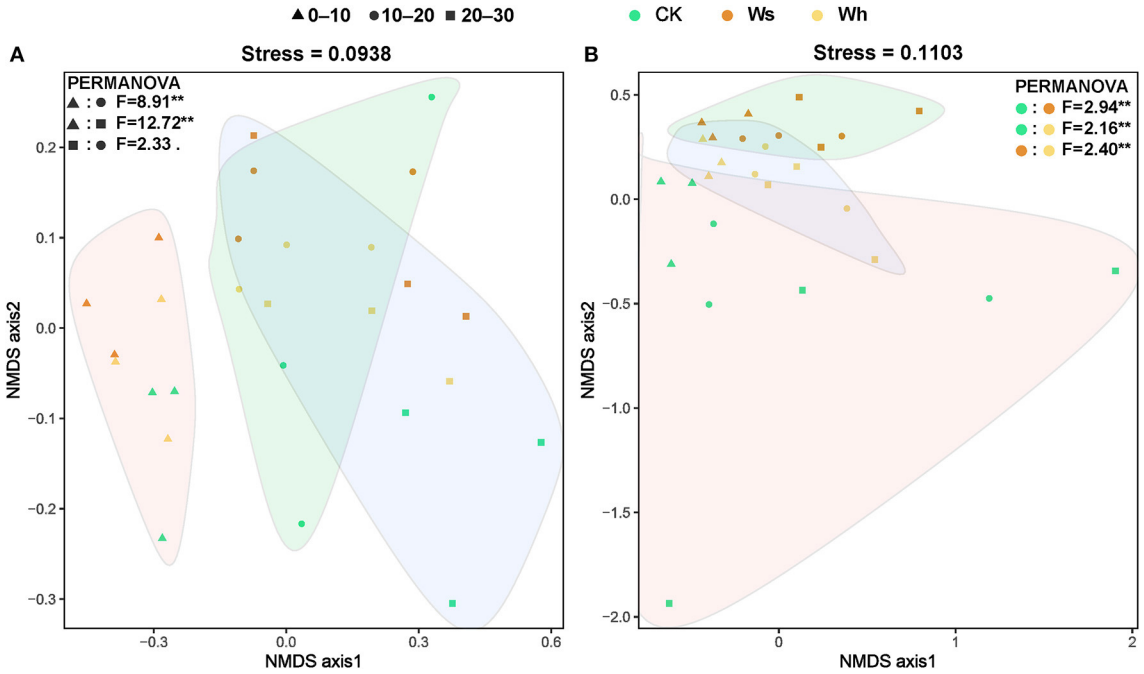

FIGURE 3
Non-metric multidimensional scaling (NMDS) ordination of the soil bacterial **(A)** and fungal **(B)** community structure based on the Bray-Curtis distance. The filled graphs cover significantly different groups of bacteria and fungi communities by PERMANOVA. Ws, slight warming; Wh, high warming; **$0.001 < p < 0.01$.

CK plots (Figure 4). The microbial response to warming may be related to moisture (Sheik et al., 2011; Peltoniemi et al., 2015). Soil bacteria are the main drivers of peatland carbon cycling, and a decrease in wetland soil moisture may increase soil permeability and thus promote the decomposition of soil nutrients (Ladau et al., 2018). The bacterial communities in the lower and middle soil layers became more similar after the temperature increased. Deterministic processes that drive soil prokaryotic communities increase with depth (Du et al., 2021), making it easier for soil microbes in deeper layers to converge as selection increases. However, the structure of the bacterial communities did not differ between the CK and warming plots (Figure 3A), which might be attributed to the delayed response of bacteria to warming (Ladau et al., 2018), differing from hypothesis II. In contrast, the vertical structure of the fungal community responded significantly to warming (Figure 3B). The structure of the fungal community was not significantly related to environmental factors in the CK plots but was significantly correlated with plant biomass in the warming plots (Figure 4). Considering the changes in the fungi community (Figure 5), warming-induced changes in soil moisture may enhance the niche-based processes of the fungal community, thereby enhancing the interactions between the soil fungal community and plants, which needs to be verified by subsequent studies.

Warming enhanced the niche process of bacterial assembly and weakened the dispersal process of fungal assembly

Disentangling ecological processes controlling community assembly is crucial in microbial ecology (Zhou and Ning, 2017). In this study, we focused on the vertical distribution of the soil microbial communities across soil layers. The DNCI index was used to clarify the assembly process of the soil microbial community across soil layers. The results showed that the vertical distribution of the soil microbial community was regulated by the niche process, and the niche process was enhanced by warming (Figure 6). Experiments simulating environmental change have shown that changes in soil bacterial community assembly are usually generated by promoting or inhibiting random processes (Zhang X. et al., 2016). The correlation between the DNCI and environmental factors showed that pH was significantly positively correlated with the niche-based process of soil bacteria, which was similar to the results of Luan et al. (2020). Soil pH is an important factor mediating the balance between the stochastic and deterministic assembly of bacteria in successional soils (Tripathi et al., 2018).

The niche-based process is more important for the bacterial than the fungal community in structuring their vertical distribution (Sun et al., 2018). In this study, the

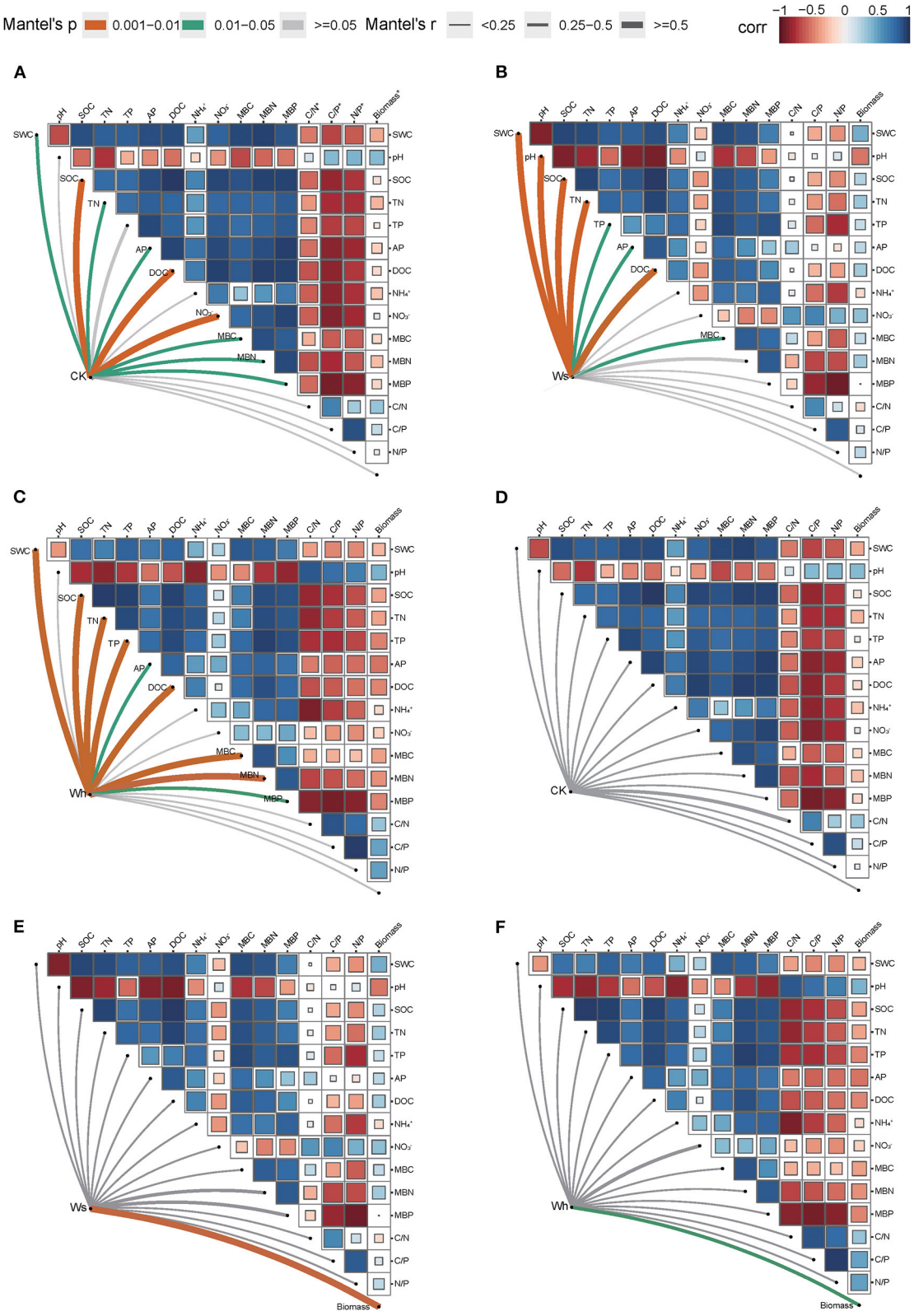

FIGURE 4
Mantel tests between the vertical structure of soil bacterial **(A–C)** and fungal **(D–F)** communities with environmental factors. Ws, slight warming; Wh, high warming; MBC, microbial biomass carbon; MBN, microbial biomass nitrogen; MBP, microbial biomass phosphorous; C/N*, MBC/MBN; C/P*, MBC/MBP; N/P*, MBN/MBP; Biomass*, plant biomass.

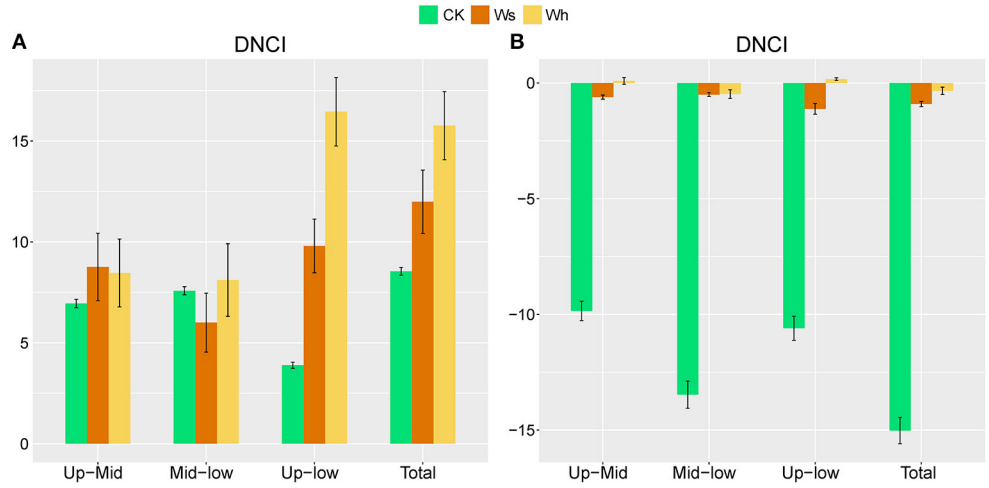

FIGURE 5
Dispersal–niche continuum index (DNCI) of soil bacterial **(A)** and fungal **(B)** communities across soil layers. Means ± standard errors are shown in the figures. The main assembly process is either dispersal (DNCI<0), niche (DNCI>0), or dispersal–niche (DNCI≈0). Ws, slight warming; Wh, high warming. Up, 0–10 cm; Mid, 10–20 cm; Low, 20–30 cm.

TABLE 2 Pearson's correlation coefficients (r values) between the DNCI of the bacterial and fungi communities with the soil characteristics.

	Bacteria		Fungi	
	Variation	**Mean**	**Variation**	**Mean**
SWC	0.509	−0.343	0.740	−0.684*
pH	0.747*	−0.387	0.533	−0.602
SOC	0.538	0.218	0.254	0.157
TN	0.602	0.244	0.276	0.081
TP	0.628	0.387	0.229	0.483
AP	0.039	0.096	−0.202	0.352
DOC	0.443	0.096	0.183	0.020
NH_4^+	0.641	0.101	0.373	−0.047
NO_3^-	−0.659	−0.687	−0.286	−0.579
MBC	0.235	−0.303	0.173	−0.371
MBN	0.558	−0.025	0.060	−0.081
MBP	0.543	0.352	0.252	0.581
MBC/MBN	0.497	−0.518	0.526	−0.539
MBC/MBP	0.136	−0.524	0.130	−0.885**
MBN/MBP	0.210	−0.472	0.916	−0.897**

MBC, microbial biomass carbon; MBN, microbial biomass nitrogen; MBP, microbial biomass phosphorous; Variation, the variation of soil characters; Mean, the mean of soil characters.
*$0.01 < p < 0.05$; **$0.001 < p < 0.01$.

fungal communities were mainly regulated by a dispersal-based process, and warming weakened the effect of random dispersal (Figure 6). The Mantel test indicated no strong correlation between the fungal community structure and soil factors. The results of an alpine meadows study showed that 3 years of warming enhances the deterministic processes of the fungal community (Xu et al., 2022). Unexpectedly, a decrease in the relative importance of random processes of the fungal communities was observed after one growing season of warming in our study, indicating that the fungal communities in alpine peatlands are highly sensitive to temperature change. SWC was correlated with the DNCI, suggesting that the dispersal ability of the fungal communities across soil layers was weakened due to reduced moisture in wet soil. Notably, as the DNCI is calculated based on occurrence data, the potential mechanism driven by the abundance changes may be underestimated (Vilmi et al., 2020).

Conclusion

We investigated the effects on vertical distribution and assembly of soil microbes under one growing season of warming in an alpine peatland. We found that short-term warming had no significant effects on the alpha diversity of either the bacteria or the fungi but altered the structure of fungi community. The vertical pattern of the fungal community in the alpine peatland was sensitive to warming. The vertical assembly of the fungal community was affected by soil moisture during short-term warming, while the relative importance of the niche-based process for bacteria increased with the variation in soil pH. Our results could provide a potential mechanism of microbial community vertical assembly in the alpine peatland in response to warming. Long-term warming and integrative studies are needed to clarify the distinction between the vertical and horizontal distributions and the assembly of soil microbial communities in the future.

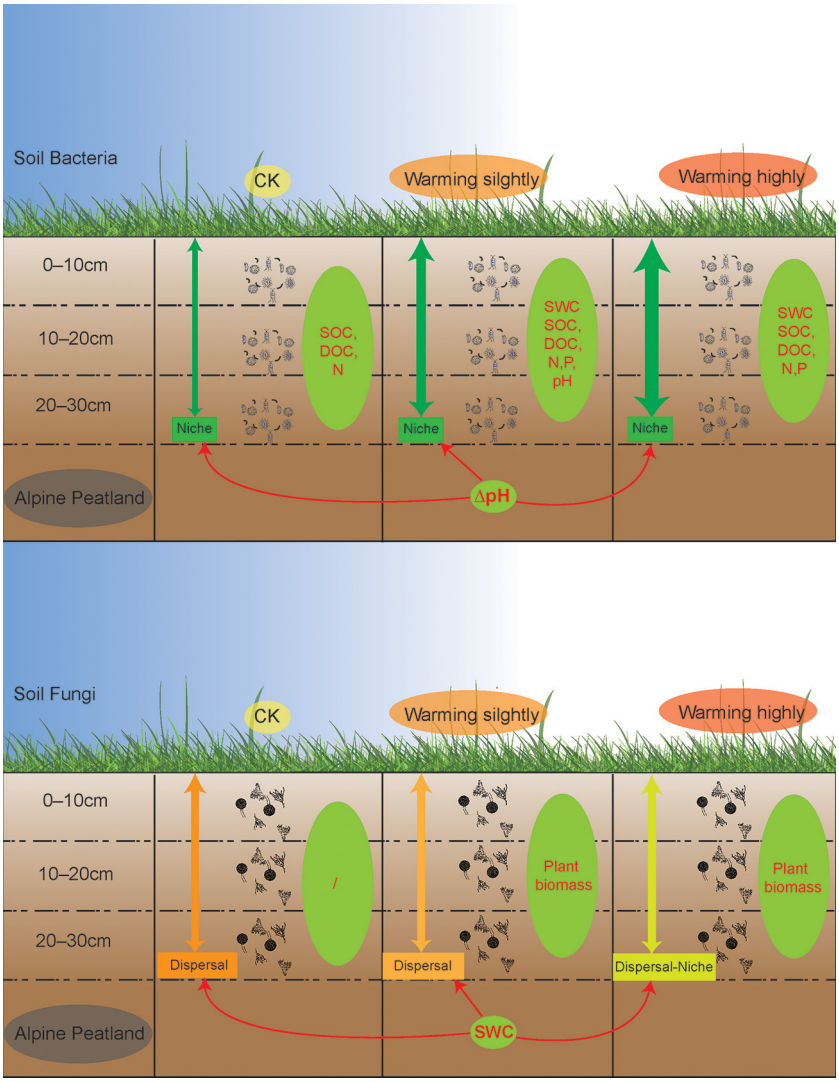

FIGURE 6
A schematic plot to show the vertical assembly of soil bacterial and fungal communities' response to warming in alpine peatland. Thicker green arrows indicate stronger niche processes while darker orange arrows indicate stronger dispersal processes. Green ellipses represent factors driving the vertical structure of the microbial communities, while the red one-way arrows represent factors that influence the vertical assembly of the community.

Data availability statement

The data presented in the study are deposited in the NCBI BioProject under accession number (PRJNA862351).

Author contributions

XW, YL, YH, EK, and XK contributed to the conception and the design of the study. XW, EK, YN, and AY conducted the experiments. XW and YL performed the statistical analysis. XW and XK wrote the first draft of the manuscript. XZ, ZY, ML, LY, and KZ wrote sections of the manuscript. All the authors contributed to the manuscript revision and read and approved the submitted version.

Funding

This study was supported by the National Natural Science Foundation of China (No. 42041005), the Second Tibetan Plateau Scientific Expedition and Research Program (STEP) Grant (No. 2019 QZKK0304), and the National Natural Science Foundation of China (32171597, 32171598).

Conflict of interest

The authors declare that the research was conducted in the absence of any commercial or financial relationships that could be construed as a potential conflict of interest.

Publisher's note

All claims expressed in this article are solely those of the authors and do not necessarily represent those of their affiliated organizations, or those of the publisher, the editors and the reviewers. Any product that may be evaluated in this article, or claim that may be made by its manufacturer, is not guaranteed or endorsed by the publisher.

Supplementary material

The Supplementary Material for this article can be found online at: https://www.frontiersin.org/articles/10.3389/fpls.2022.986034/full#supplementary-material

References

Adair, K. L., Lindgreen, S., Poole, A. M., Young, L. M., Bernard-Verdier, M., Wardle, D. A., et al. (2019). Above and belowground community strategies respond to different global change drivers. *Sci. Rep.* 9, 2540. doi: 10.1038/s41598-019-39033-4

Anthony, M. A., Crowther, T. W., Maynard, D. S., Van Den Hoogen, J., and Averill, C. (2020). Distinct assembly processes and microbial communities constrain soil organic carbon formation. *One Earth.* 2, 349–360. doi: 10.1016/j.oneear.2020.03.006

Asemaninejad, A., Thorn, R. G., Branfireun, B. A., and Lindo, Z. (2018). Climate change favours specific fungal communities in boreal peatlands. *Soil Biol. Biochem.* 120, 28–36. doi: 10.1016/j.soilbio.2018.01.029

Bardgett, R. D., and Van Der Putten, W. H. (2014). Belowground biodiversity and ecosystem functioning. *Nature* 515, 505–511. doi: 10.1038/nature13855

Blankinship, J. C., Niklaus, P. A., and Hungate, B. A. (2011). A meta-analysis of responses of soil biota to global change. *Oecologia* 165, 553–565. doi: 10.1007/s00442-011-1909-0

Brewer, T. E., Aronson, E. L., Arogyaswamy, K., Billings, S. A., Botthoff, J. K., Campbell, A. N., et al. (2019). Ecological and genomic attributes of novel bacterial taxa that thrive in subsurface soil horizons. *Mbio.* 10, e01318–e01319. doi: 10.1128/mBio.01318-19

Brookes, P. C., Landman, A., Pruden, G., and Jenkinson, D. S. (1985). Chloroform fumigation and the release of soil-nitrogen - a rapid direct extraction method to measure microbial biomass nitrogen in soil. *Soil Biol. Biochem.* 17, 837–842. doi: 10.1016/0038-0717(85)90144-0

Brookes, P. C., Powlson, D. S., and Jenkinson, D. S. (1982). Measurement of microbial biomass phosphorus in soil. *Soil. Biol. Biochem.* 14, 319–329. doi: 10.1016/0038-0717(82)90001-3

Cai, W., Snyder, J., Hastings, A., and D'souza, R. M. (2020). Mutualistic networks emerging from adaptive niche-based interactions. *Nat. Commun.* 11, 5470. doi: 10.1038/s41467-020-19154-5

Chase, J. M. (2010). Stochastic community assembly causes higher biodiversity in more productive environments. *Science* 328, 1388–1391. doi: 10.1126/science.1187820

Chase, J. M., and Myers, J. A. (2011). Disentangling the importance of ecological niches from stochastic processes across scales. *Philos. Trans. R. Soc. Lond. B. Biol. Sci.* 366, 2351–2363. doi: 10.1098/rstb.2011.0063

Chave, J. (2004). Neutral theory and community ecology. *Ecol. Lett.* 7, 241–253. doi: 10.1111/j.1461-0248.2003.00566.x

Chen, H., Yang, G., Peng, C., Zhang, Y., Zhu, D., Zhu, Q., et al. (2014). The carbon stock of alpine peatlands on the Qinghai-Tibetan Plateau during the Holocene and their future fate. *Quaternary Sci. Rev.* 95, 151–158. doi: 10.1016/j.quascirev.2014.05.003

Chen, H., Zhu, Q., Peng, C., Wu, N., Wang, Y., Fang, X., et al. (2013). The impacts of climate change and human activities on biogeochemical cycles on the Qinghai-Tibetan Plateau. *Glob. Chang Biol.* 19, 2940–2955. doi: 10.1111/gcb.12277

Chen, S., Zhou, Y., Chen, Y., and Gu, J. (2018). fastp: an ultra-fast all-in-one FASTQ preprocessor. *Bioinformatics* 34, 884–890. doi: 10.1093/bioinformatics/bty560

Chen, W., Jiao, S., Li, Q., and Du, N. (2020). Dispersal limitation relative to environmental filtering governs the vertical small-scale assembly of soil microbiomes during restoration. *J. Appl. Ecol.* 57, 402–412. doi: 10.1111/1365-2664.13533

Chesson, P. (2000). Mechanisms of maintenance of species diversity. *Annu. Rev. Ecol. Syst.* 31, 343–366. doi: 10.1146/annurev.ecolsys.31.1.343

Chu, H., Sun, H., Tripathi, B. M., Adams, J. M., Huang, R., Zhang, Y., et al. (2016). Bacterial community dissimilarity between the surface and subsurface soils equals horizontal differences over several kilometers in the western Tibetan Plateau. *Environ. Microbiol.* 18, 1523–1533. doi: 10.1111/1462-2920.13236

De Oliveira, T. B., De Lucas, R. C., Scarcella, A. S. D., Contato, A. G., Pasin, T. M., Martinez, C. A., et al. (2020). Fungal communities differentially respond to warming and drought in tropical grassland soil. *Mol. Ecol.* 29, 1550–1559. doi: 10.1111/mec.15423

Dorrepaal, E., Toet, S., Logtestijn, R., Swart, E., Weg, M., Callaghan, T. V., et al. (2009). Carbon respiration from subsurface peat accelerated by climate warming in the subarctic. *Nature* 460, 616–619. doi: 10.1038/nature08216

Du, C., Geng, Z., Wang, Q., Zhang, T., He, W., Hou, L., et al. (2017). Variations in bacterial and fungal communities through soil depth profiles in a Betula albosinensis forest. *J. Microbiol.* 55, 684–693. doi: 10.1007/s12275-017-6466-8

Du, X., Deng, Y., Li, S., Escalas, A., Feng, K., He, Q., et al. (2021). Steeper spatial scaling patterns of subsoil microbiota are shaped by deterministic assembly process. *Mol. Ecol.* 30, 1072–1085. doi: 10.1111/mec.15777

Edgar, R. C. (2013). UPARSE: highly accurate OTU sequences from microbial amplicon reads. *Nat. Methods.* 10, 996–998. doi: 10.1038/nmeth.2604

Fan, S., Qin, J., Sun, H., Jia, Z., and Chen, Y. (2021). Alpine soil microbial community structure and diversity are largely influenced by moisture content in the Zoige wetland. *Int. J. Environ. Sci. Te.* 19, 4369–4378. doi: 10.1007/s13762-021-03287-1

Fargione, J., Brown, C. S., and Tilman, D. (2003). Community assembly and invasion: an experimental test of neutral versus niche processes. *Proc. Natl. Acad. Sci. U.S.A.* 100, 8916–8920. doi: 10.1073/pnas.1033107100

Finlay, B. J., Maberly, S. C., and Cooper, J. I. (1997). Microbial diversity and ecosystem function. *Oikos.* 80, 209–213. doi: 10.2307/3546587

Frey, S. D., Drijber, R., Smith, H., and Melillo, J. (2008). Microbial biomass, functional capacity, and community structure after 12 years of soil warming. *Soil Biol. Biochem.* 40, 2904–2907. doi: 10.1016/j.soilbio.2008.07.020

Frolking, S., and Roulet, N. T. (2007). Holocene radiative forcing impact of northern peatland carbon accumulation and methane emissions. *Glob. Change Biol.* 13, 1079–1088. doi: 10.1111/j.1365-2486.2007.01339.x

Guo, X., Feng, J., Shi, Z., Zhou, X., Yuan, M., Tao, X., et al. (2018). Climate warming leads to divergent succession of grassland microbial communities. *Nat. Clim. Change.* 8, 813–818. doi: 10.1038/s41558-018-0254-2

Guo, X., Zhou, X., Hale, L., Yuan, M., Ning, D., Feng, J., et al. (2019). Climate warming accelerates temporal scaling of grassland soil microbial biodiversity. *Nat. Ecol. Evol.* 3, 612–619. doi: 10.1038/s41559-019-0848-8

Hannula, S. E., and Trager, S. (2020). Soil fungal guilds as important drivers of the plant richness-productivity relationship. *New Phytol.* 226, 947–949. doi: 10.1111/nph.16523

Helbig, M., and Živković, T., Alekseychik, P., Aurela, M., El-Madany, T. S., Euskirchen, E. S., et al. (2022). Warming response of peatland CO_2 sink is sensitive to seasonality in warming trends. *Nat. Clim. Change*. 12, 743–749. doi: 10.1038/s41558-022-01428-z

Hubbell, S. P. (2001). *Monographs in Population Biology. The Unified Neutral Theory of Biodiversity and Biogeography*. William Street, Princeton, NJ: Princeton University Press.

IPCC (2021). *Climate Change 2021: The Physical Science Basis*. Contribution of Working Group I to the Sixth Assessment Report of the Intergovernmental Panel on Climate Change. Cambridge: Cambridge University Press, in press.

Jiang, X., Peng, X., Deng, G., Sheng, H., Wang, Y., Zhou, H., et al. (2013). Illumina sequencing of 16S rRNA tag revealed spatial variations of bacterial communities in a mangrove wetland. *Microb. Ecol.* 66, 96–104. doi: 10.1007/s00248-013-0238-8

Jiao, S., Chen, W., Wang, J., Du, N., Li, Q., and Wei, G. (2018). Soil microbiomes with distinct assemblies through vertical soil profiles drive the cycling of multiple nutrients in reforested ecosystems. *Microbiome.* 6, 146. doi: 10.1186/s40168-018-0526-0

Kang, E., Li, Y., Zhang, X., Yan, Z., Wu, H., Li, M., et al. (2021). Soil pH and nutrients shape the vertical distribution of microbial communities in an alpine wetland. *Sci. Total. Environ.* 774, 145780. doi: 10.1016/j.scitotenv.2021.145780

Kang, E., Li, Y., Zhang, X., Yan, Z., Zhang, W., Zhang, K., et al. (2022). Extreme drought decreases soil heterotrophic respiration but not methane flux by modifying the abundance of soil microbial functional groups in alpine peatland. *Catena.* 212, 106043. doi: 10.1016/j.catena.2022.106043

Kanzaki, Y., and Takemoto, K. (2021). Diversity of dominant soil bacteria increases with warming velocity at the global scale. *Diversity-Basel.* 13, 120. doi: 10.3390/d13030120

Kraft, N. J. B., Adler, P. B., Godoy, O., James, E. C., Fuller, S., Levine, J. M., et al. (2014). Community assembly, coexistence and the environmental filtering metaphor. *Funct. Ecol.* 29, 592–599. doi: 10.1111/1365-2435.12345

Ladau, J., Shi, Y., Jing, X., He, J., Chen, L., Lin, X., et al. (2018). Existing climate change will lead to pronounced shifts in the diversity of soil prokaryotes. *mSystems.* 3, e00167–e00118. doi: 10.1128/mSystems.00167-18

Liu, D., Yang, Y., An, S., Wang, H., and Wang, Y. (2018). The biogeographical distribution of soil bacterial communities in the Loess Plateau as revealed by high-throughput sequencing. *Front. Microbiol.* 9, 2456. doi: 10.3389/fmicb.2018.02456

Liu, Y., Priscu, J., Yao, T., Vick-Majors, T., Xu, B., Jiao, N., et al. (2016). Bacterial responses to environmental change on the Tibetan Plateau over the past half century. *Environ. Microbiol.* 18, 1930–1941. doi: 10.1111/1462-2920.13115

Luan, L., Liang, C., Chen, L., Wang, H., Xu, Q., Jiang, Y., et al. (2020). Coupling bacterial community assembly to microbial metabolism across soil profiles. *mSystems.* 5, e00298–e00220. doi: 10.1128/mSystems.00298-20

Magoc, T., and Salzberg, S. L. (2011). FLASH: fast length adjustment of short reads to improve genome assemblies. *Bioinformatics* 27, 2957–2963. doi: 10.1093/bioinformatics/btr507

Mclaughlin, J., and Webster, K. (2018). Effects of climate change on peatlands in the far north of Ontario, Canada: a synthesis. *Arct. Antarct. Alp. Res.* 46, 84–102. doi: 10.1657/1938-4246-46.1.84

Nichols, J. E., and Peteet, D. M. (2019). Rapid expansion of northern peatlands and doubled estimate of carbon storage. *Nat. Geosci.* 12, 917–921. doi: 10.1038/s41561-019-0454-z

Nilsson, R. H., Larsson, K. H., Taylor, A. F. S., Bengtsson-Palme, J., Jeppesen, T. S., Schigel, D., et al. (2018). The UNITE database for molecular identification of fungi: handling dark taxa and parallel taxonomic classifications. *Nucleic Acids Res.* 47, D259–D264. doi: 10.1093/nar/gky1022

Peltoniemi, K., Laiho, R., Juottonen, H., Kiikkila, O., Makiranta, P., Minkkinen, K., et al. (2015). Microbial ecology in a future climate: effects of temperature and moisture on microbial communities of two boreal fens. *Fems Microbiol. Ecol.* 91, fiv062. doi: 10.1093/femsec/fiv062

Ponisio, L. C., Valdovinos, F. S., Allhoff, K. T., Gaiarsa, M. P., Barner, A., Guimaraes, P. R., et al. (2019). A network perspective for community assembly. *Front. Ecol. Evol.* 7, 103. doi: 10.3389/fevo.2019.00103

Rillig, M. C. (2004). Arbuscular mycorrhizae and terrestrial ecosystem processes. *Ecol. Lett.* 7, 740–754. doi: 10.1111/j.1461-0248.2004.00620.x

Sheik, C. S., Beasley, W. H., Elshahed, M. S., Zhou, X., Luo, Y., and Krumholz, L. R. (2011). Effect of warming and drought on grassland microbial communities. *ISME J.* 5, 1692–1700. doi: 10.1038/ismej.2011.32

Stackebrandt, E., and Goebel, B. M. (1994). A place for DNA-DNA reassociation and 16S rRNA sequence analysis in the present species definition in bacteriology. *Int.J.Syst.Bacteriol.* 44, 846–849. doi: 10.1099/00207713-44-4-846

Stegen, J. C., Fredrickson, J. K., Wilkins, M. J., Konopka, A. E., Nelson, W. C., Arntzen, E. V., et al. (2016). Groundwater-surface water mixing shifts ecological assembly processes and stimulates organic carbon turnover. *Nat. Commun.* 7, 11237. doi: 10.1038/ncomms11237

Sun, R., Li, W., Dong, W., Tian, Y., Hu, C., and Liu, B. (2018). Tillage changes vertical distribution of soil bacterial and fungal communities. *Front. Microbiol.* 9, 699. doi: 10.3389/fmicb.2018.00699

Sun, T., Wang, Y., Lucas-Borja, M. E., Jing, X., and Feng, W. (2021). Divergent vertical distributions of microbial biomass with soil depth among groups and land uses. *J. Environ. Manage.* 292, 112755. doi: 10.1016/j.jenvman.2021.112755

Tiemeyer, B., Albiac Borraz, E., Augustin, J., Bechtold, M., Beetz, S., and Beyer, C., et al. (2016). High emissions of green-house gases from grasslands on peat and other organic soils. *Glob. Change Biol.* 22, 4134–4149. doi: 10.1111/gcb.13303

Tonkin, J. D., Altermatt, F., Finn, D. S., Heino, J., Olden, J. D., Pauls, S. U., et al. (2018). The role of dispersal in river network metacommunities: Patterns, processes, and pathways. *Freshwater Biol.* 63, 141–163. doi: 10.1111/fwb.13037

Tripathi, B. M., Stegen, J. C., Kim, M., Dong, K., Adams, J. M., and Lee, Y. K. (2018). Soil pH mediates the balance between stochastic and deterministic assembly of bacteria. *Isme J.* 12, 1072–1083. doi: 10.1038/s41396-018-0082-4

Vance, E. D., Brookes, P. C., and Jenkinson, D. S. (1987). An extraction method for measuring soil microbial biomass-C. *Soil Biol. Biochem.* 19, 703–707. doi: 10.1016/0038-0717(87)90052-6

Vellend, M., Srivastava, D. S., Anderson, K. M., Brown, C. D., Jankowski, J. E., Kleynhans, E. J., et al. (2014). Assessing the relative importance of neutral stochasticity in ecological communities. *Oikos.* 123, 1420–1430. doi: 10.1111/oik.01493

Vilmi, A., Gibert, C., Escarguel, G., Happonen, K., Heino, J., Jamoneau, A., et al. (2020). Dispersal–niche continuum index: a new quantitative metric for assessing the relative importance of dispersal versus niche processes in community assembly. *Ecography.* 44, 370–379. doi: 10.1111/ecog.05356

Wang, Q., Garrity, G. M., Tiedje, J. M., and Cole, J. R. (2007). Naive Bayesian classifier for rapid assignment of rRNA sequences into the new bacterial taxonomy. *Appl. Environ. Microb.* 73, 5261–5267. doi: 10.1128/AEM.00062-07

Wardle, D. A., Bardgett, R. D., Klironomos, J. N., Setala, H., Van Der Putten, W. H., and Wall, D. H. (2004). Ecological linkages between aboveground and belowground biota. *Science.* 304, 1629–1633. doi: 10.1126/science.1094875

Wu, H., Li, Y., Zhang, J., Niu, L., Zhang, W., Cai, W., et al. (2017). Sediment bacterial communities in a eutrophic lake influenced by multiple inflow-rivers. *Environ. Sci. Pollut. Res.* 24, 19795–19806. doi: 10.1007/s11356-017-9602-4

Xia, Z., Bai, E., Wang, Q., Gao, D., Zhou, J., Jiang, P., et al. (2016). Biogeographic distribution patterns of bacteria in typical chinese forest soils. *Front. Microbiol.* 7. doi: 10.3389/fmicb.2016.01106

Xu, X., Qiu, Y., Zhang, K., Yang, F., Chen, M., Luo, X., et al. (2022). Climate warming promotes deterministic assembly of arbuscular mycorrhizal fungal communities. *Glob. Change Biol.* 28, 1147–1161. doi: 10.1111/gcb.15945

Xue, D., Chen, H., Zhan, W., Huang, X. Y., He, Y. X., Zhao, C. A., et al. (2021). How do water table drawdown, duration of drainage, and warming influence greenhouse gas emissions from drained peatlands of the Zoige Plateau? *Land Degrad. Dev.* 32, 3351–3364. doi: 10.1002/ldr.4013

Xue, R., Zhao, K., Yu, X., Stirling, E., Liu, S., Ye, S., et al. (2021). Deciphering sample size effect on microbial biogeographic patterns and community assembly processes at centimeter scale. *Soil Biol. Biochem.* 156. doi: 10.1016/j.soilbio.2021.108218

Yan, Z., Kang, E., Zhang, K., Li, Y., Hao, Y., Wu, H., et al. (2021). Plant and soil enzyme activities regulate CO_2 efflux in alpine peatlands after 5 years of simulated extreme drought. *Front. Plant Sci.* 12:756956. doi: 10.3389/fpls.2021.756956

Yang, G., Chen, H., Wu, N., Tian, J., Peng, C., Zhu, Q., et al. (2014). Effects of soil warming, rainfall reduction and water table level on CH_4 emissions from the Zoige peatland in China. *Soil Biol. Biochem.* 78, 83–89. doi: 10.1016/j.soilbio.2014.07.013

Yuan, M. M., Guo, X., Wu, L., Zhang, Y., Xiao, N., Ning, D., et al. (2021). Climate warming enhances microbial network complexity and stability. *Nat. Clim. Change.* 11, 343–348 doi: 10.1038/s41558-021-00989-9

Zandalinas, S. I., Fritschi, F. B., and Mittler, R. (2021). Global warming, climate change, and environmental pollution: recipe for a multifactorial stress combination disaster. *Trends Plant Sci.* 26, 588–599. doi: 10.1016/j.tplants.2021.02.011

Zhang, K., Peng, C., Zhu, Q., Li, M., Yan, Z., Li, M., et al. (2022). Estimating natural nitrous oxide emissions from the Qinghai–Tibetan Plateau using a process-based model: Historical spatiotemporal patterns and future trends. *Ecol. Model.* 466, 109902. doi: 10.1016/j.ecolmodel.2022.109902

Zhang, K., Shi, Y., Jing, X., He, J., Sun, R., Yang, Y., et al. (2016). Effects of short-term warming and altered precipitation on soil microbial communities in alpine grassland of the Tibetan Plateau. *Front. Microbiol.* 7, 1032. doi: 10.3389/fmicb.2016.01032

Zhang, X., Johnston, E., Liu, W., Li, L., and Han, X. (2016). Environmental changes affect the assembly of soil bacterial community primarily by mediating stochastic processes. *Glob. Change Biol.* 22, 198–207. doi: 10.1111/gcb.13080

Zhang, Y., Dong, S., Gao, Q., Liu, S., Zhou, H., Ganjurjav, H., et al. (2016). Climate change and human activities altered the diversity and composition of soil microbial community in alpine grasslands of the Qinghai-Tibetan Plateau. *Sci. Total Environ.* 562, 353–363. doi: 10.1016/j.scitotenv.2016.03.221

Zhao, C., Zhu, L., Liang, J., Yin, H., Yin, C., Li, D., et al. (2014). Effects of experimental warming and nitrogen fertilization on soil microbial communities and processes of two subalpine coniferous species in Eastern Tibetan Plateau, China. *Plant Soil.* 382, 189–201. doi: 10.1007/s11104-014-2153-2

Zhou, J., Deng, Y., Zhang, P., Xue, K., Liang, Y., Van Nostrand, J. D., et al. (2014). Stochasticity, succession, and environmental perturbations in a fluidic ecosystem. *P. Natl. Acad. Sci. U.S.A.* 111, E836–E845. doi: 10.1073/pnas.1324044111

Zhou, J., and Ning, D. (2017). Stochastic community assembly: does it matter in microbial ecology? *Microbiol. Mol. Biol. R.* 81, e00002-17. doi: 10.1128/MMBR.00002-17

frontiers | Frontiers in Plant Science

TYPE Original Research
PUBLISHED 16 September 2022
DOI 10.3389/fpls.2022.990541

OPEN ACCESS

EDITED BY
Yong Li,
Chinese Academy of Forestry, China

REVIEWED BY
Lei Wang,
Xinjiang Institute of Ecology and Geography (CAS), China
Rong Xiao,
Fuzhou University,
China

*CORRESPONDENCE
Bo Guan
guanbo_99@hotmail.com
Jincheng Zuo
zuo2008@hotmail.com

SPECIALTY SECTION
This article was submitted to Functional Plant Ecology, a section of the journal Frontiers in Plant Science

RECEIVED 10 July 2022
ACCEPTED 29 August 2022
PUBLISHED 16 September 2022

CITATION
Gao J, Guan B, Ge M, Eller F, Yu J, Wang X and Zuo J (2022) Can allelopathy of *Phragmites australis* extracts aggravate the effects of salt stress on the seed germination of *Suaeda salsa*? *Front. Plant Sci.* 13:990541. doi: 10.3389/fpls.2022.990541

Can allelopathy of *Phragmites australis* extracts aggravate the effects of salt stress on the seed germination of *Suaeda salsa*?

Jingwen Gao[1], Bo Guan[2]*, Minjia Ge[3], Franziska Eller[4], Junbao Yu[2], Xuehong Wang[2] and Jincheng Zuo[1]*

[1]Collage of Life Sciences, Ludong University, Yantai, China, [2]The Institute for Advanced Study of Coastal Ecology, Ludong University, Yantai, China, [3]School of Municipal and Environmental Engineering, Jilin Jianzhu University, Changchun, China, [4]Department of Biology, Aarhus University, Ole Worms Allé 1, Aarhus, Denmark

Phragmites australis is highly adaptable with high competitive ability and is widely distributed in the coastal wetland of the Yellow River Delta. However, allelopathic effects of *P. australis* on the growth of neighboring plants, such as *Suaeda salsa*, are poorly understood. In this study, germination responses of *S. salsa* seeds collected from two different habitats (intertidal zone and inland brackish wetland) to the extracts from different part of *P. australis* were compared. Potential allelopathic effects on germination percentage, germination rate, radicle length, and seedling biomass were analyzed. The germination of *S. salsa* was effectively inhibited by *P. australis* extract. Extract organ, extract concentration, and salt concentration showed different effects, the inhibitory rates were highest with belowground extract of *P. australis* between the four different parts. Germination percentage and germination rate were significantly decreased by the interactive effect of salt stress and extract concentration in *S. salsa* from a brackish wetland but not in *S. salsa* from the intertidal zone. The impact of different extracts of *P. australis* on radicle length and seedling biomass of *S. salsa* showed significant but inconsistent variation. The response index results showed that the higher concentration of extract solution (50g·L^{-1}) of *P. australis* had stronger inhibitory effect on the seed germination and seedling growth of *S. salsa* while the belowground extract had the strongest negative effect. Our results indicated that allelopathy is an important ecological adaptation mechanism for *P. australis* to maintain a high interspecific competitive advantage in the species' natural habitat.

KEYWORDS

***Phragmites australis*, *Suaeda salsa*, allelopathy, seed germination, radicle length, biomass**

Introduction

In natural ecosystems, competition exists among plant populations, which is an important factor in shaping ecological structure at different scales (Fowler, 1986, 2013). Competition has been defined in terms of species-level traits and competitive outcomes as the ability of individuals to encroach, grab resources, or otherwise inhibit the fitness of their

neighboring species (Aschehoug et al., 2016). A well-known example of resource competition is the competition for light by rapid length growth to inhibit the growth and survival of neighboring species (Craine and Dybzinski, 2013). Sometimes, competition for resources is considered to be an important driver of plant community diversity and dynamics (Viola et al., 2010). Another factor that affects the ecological patterns of plant communities is allelopathy, the chemically mediated interfering of interplant competition (Raynaud and Leadley, 2004). During allelopathy, plants can release chemicals into the environment and inhibit germination and growth of neighboring species by altering their metabolism, or by affecting their soil community symbionts (Fernandez et al., 2016). An example of a typical allelochemical is Sorgoleone, which is released through root secretions of Sorghum, disrupting several targets in the photosynthetic electron transport chain of neighboring plants (Dayan et al., 2009).

Allelochemicals are released through four pathways: leaching by rain, decomposition of plant residues, exudation from roots, and volatilization (Kulshreshtha and Gopal, 1983; Agami and Waisel, 1985; Elakovich and Wooten, 1989; Gross, 2003). Until now, experiments with plant extracts (i.e., leachates and exudates) have been regarded as an effective method to assess allelopathic effects, although the synthesis of allelochemicals in plants and their concentrations fluctuate throughout the year (Helmig et al., 2013; Santonja et al., 2018). The research on plant allelopathy mostly focuses on alien invasive species, which can affect seed germination, seedling growth, flowering and fruiting of mature bodies, and ultimately causing a decline in species diversity and eventually forming a single dominant species community (Corbin and D'Antonio, 2004). Allelochemicals can be useful as low-cost natural repressors of undesirable vegetation. For example, *Spartina alterniflora*, which is highly invasive in China, has been tested as biological resource against harmful algal blooms. The species' extracts decreased chlorophyll a and weakened photosynthesis of the microalga *Microcystis aeruginosa* at high aqueous extract concentrations, although the allelochemical effect was beneficial for the algae at low extract concentrations (Yuan et al., 2019).

Certain highly competitive native species are able to inhibit the invasion process of alien species through allelopathy, especially if they have not co-evolved and therefore exhibit lower resistance (Callaway and Aschehoug, 2000). Thus, the native species *Sambucus ebulus* was shown to use allelopathy as a biotic containment mechanism against the naturalization of the *Fallopia x bohemica* invasive species (Christina et al., 2015). Conversely, the North American invader *Centaurea diffusa* repressed native grass species to a stronger degree than closely related grass species from communities to which *Centaurea* was native (Callaway and Aschehoug, 2000). *Phragmites australis* is a common rhizomatous graminaceous plant in wetlands. It is widely distributed in coastal marshes and inter-river depressions with shallow groundwater depth (Hellings and Gallagher, 1992; Wang et al., 2017). It has a wide ecological niche and often forms monodominance in its habitat (Zhang et al., 2003). It is also one of the most widespread wetland plants in temperate regions of the world. In the Yellow River Delta (YRD), *P. australis* is a dominant wetland species distributed from intertidal zone to inland brackish wetland. It is widely used for wetland restoration and plays an important role in the maintenance of wetland ecosystem functions of the YRD. *Phragmites australis* is an efficient competitor due to its strong root system, sexual and asexual reproduction, salt tolerance, and a wide range of edaphic niches (Guan et al., 2017, 2021). However, whether allelopathy of *P. australis*, as native species, plays an important role in the process of competition with neighboring plants is still unknown.

Suaeda salsa (L.) is a pioneer species in coastal wetlands of Northern China, covering most forelands in the Yellow River Delta as a part of the natural succession in coastal wetland ecosystems (Guo et al., 2020). Over the past decades, the coastal wetlands of the YRD were suffering serious ecological degradation and soil salinization due to freshwater restriction, neglect of marine areas, and climate change (Zhao et al., 2010; Yu et al., 2014). The area of *S. salsa* is also decreasing with each passing year. *Phragmites australis* is always co-occurring with *S. salsa* in the coastal wetland of the Yellow River Delta, but little is known about a potential competitive or even allelopathic effect of *P. australis* on *S. salsa*.

In this study, germination experiments were conducted to investigate the response of seed germination and early seedling growth of *S. salsa* to the extracts of different organs of *P. australis* within different salinity gradients. The purpose of the study was to solve the following questions: (1) Do the extracts of different organs of *P. australis* have negative effects on seed germination of *S. salsa*? (2) Can salt stress aggravate the potential allelopathic effect of *P. australis* on *S. salsa*? The results can provide insight into the competition mechanism of the two dominant plant communities and give valuable implications for the restoration of degraded wetlands in the Yellow River Delta.

Materials and methods

Study site description

The Yellow River Delta (118°33′–119°20′ E, 37°35′–38°12′ N) is located in the northern part of Shandong Province and the south coast of the Bohai Sea, a warm temperate monsoon climate zone with an average annual temperature of 12.1°C, average annual rainfall of 551.6 mm and average annual evaporation of 1,962 mm (Song et al., 2016). The dominant soil types are classified as Calcaric Fluvisols, Gleyic Solonchaks, and Salic Fluvisols (FAO), which developed on loess material carried by water from the Loess Plateau. *Phragmites australis* and *S. salsa* are dominant species in the YRD (Guan et al., 2013).

Sample collection and treatment

Sample collection

The seeds of two ecotypes of *S. salsa* were collected from, respectively, the intertidal zone and an inland brackish wetland of

the YRD in December 2020 (Figure 1). The seed morphology and 1,000 seed weight of the two habitats were significantly different. The seeds from the intertidal zone were dark brownish-red in color and bigger, with a 1,000-seed weight of 1,453 ± 43.1 mg, while the seeds of the brackish wetland were black-brown and smaller, with a 1,000-seed weight of 376 ± 35.5 mg (Figure 2). Seeds with mature and uniform were randomly selected in this study (both commonly occurring seed-types of each *S. salsa* individual were included), and collected seeds were stored at 4°C until the experiment began.

The *P. australis* samples were collected from the same brackish wetland, which was co-inhabited by *S. salsa* in the YRD. Four parts of the *P. australis* community were collected, which were belowground biomass, aboveground biomass, litter (collected from the ground), and rhizosphere soil. The samples were washed and air dried until being used for extracts.

Aqueous extracts of *Phragmites australis*

The samples were crushed in a grinder and sieved through a 2 mm mesh sieve. The supernatant of the *P. australis* extract was used as the extracting master batch, with a mass concentration of 100 g·L^{-1}. For different parts of the aqueous extracts of *P. australis*, the sample was weighed accurately at 10 g, put into a conical flask, 100 ml of distilled water was added, sealed with a sealing strip, and soaked for 48 h. Then the conical flask was put into a shaker at the speed of 150 r/min and shaken intermittently during soaking. After the soaking, two layers of gauze were used to filter the large residues. The gauze was wrought as much as possible to collect a large amount of solution. For a second filtration, the solution from the previous step was loaded into a centrifuge tube and placed in a centrifuge at 2,500 r/min for 15 min, thus, the supernatant obtained was the extracts at a concentration of 100 g·L^{-1}. All solutions were stored at 4°C.

Germination experimental design

Germination tests were carried out in growth chambers with 16 h light and 8 h dark, at 25°C during the light period (Sylvania cool white fluorescent lamps, 200 μmol m^{-2} s^{-1}, 400–700 nm) and 15°C during the dark period, with a relative air humidity of 75%. Seeds were germinated in a 9 cm diameter petri dish containing two layers of filter paper with 12 ml of test solution. Each petri dish was sealed with parafilm to prevent evaporation. Fifty selected *S. salsa* seeds of full and uniform size were placed evenly on the filter paper after the filter paper had been completely soaked with test solution or water as control, and four replicates of petri dishes were set up for each treatment. Seeds were considered germinated when the radicle protruded 1 mm from seed coat. Germination was recorded daily for 10 days.

To examine the interactive effects of different concentrations of salt stress, different concentrations of *P. australis* extract, and extracts of different organs of *P. australis* were combined with four salt concentrations (0, 100, 300, and 500 mM L^{-1} NaCl solution). Two concentrations of *P. australis* extract (50 and 6.25 g·L^{-1}), and four parts of the *P. australis* community with belowground biomass (rhizome and root), aboveground biomass (shoot and leaf), litter (collected from the ground), and rhizosphere soil were used as different treatments.

After the germination period, the germination was evaluated, seedlings were collected and five seedlings were randomly selected from each replicate and radicle length was measured using a ruler. The seedlings were then wrapped and placed in an oven, dried at 60°C to constant weight and the dry weight was recorded.

Germination percentage (%) was calculated as the number of seeds that germinated in each solution per total number of seeds tested in in each solution, multiplied with 100. Germination rate was calculated as follows:

$$\sum G / t \times 100\%$$

where G is the daily germination rate and t is the total germination time (Khan and Ungar, 1984). The allelopathy was calculated by reference to the response index (*RI*; Williamson and Richardson, 1988)

$$RI = (T - T0) / T0$$

where T is the treatment value of the test item and T0 is the control value. If $RI > 0$, the effect is facilitative; if $RI < 0$, there is an

FIGURE 1
Comparison of plant morphology of *Suaeda salsa* in two habitats, left-Intertidal zone, and right-Brackish wetland.

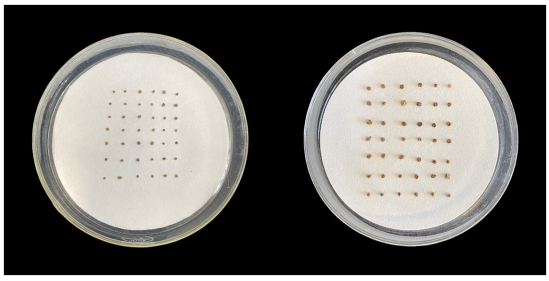

FIGURE 2
Comparison of seed size of *Suaeda salsa* in two habitats, left-Brackish wetland, right-Intertidal zone.

inhibition effect, and the absolute value of *RI* represents the intensity of the effect.

Data analysis

Statistical analysis of data was conducted by SPSS (version 25.0, SPSS Inc., Chicago, Illinois, United States). One-way ANOVA were used to confirm the effects of different extracts of *P. australis* organs on seed germination of *S. salsa* under the same salt concentration and the effects of different salt concentrations on seed germination of *S. salsa* under same organs. Duncan comparison tests were used to compare the differences between different treatments at the 0.05 level. Three-way ANOVA was used to analyze the effect among salt concentration, extract concentration, and extract organ, and the interaction effects between different treatments on seed germination and seedling growth. All acquired data were represented by an average of four replicates and standard deviation (SD).

Results

Germination performance

The extracts of different organs of *P. australis* had significant negative effects on the germination percentage and germination rate of *S. salsa* from two different habitats ($p < 0.05$). At 6.25 g·L^{-1} extract concentration, only extracts of aboveground organs had a significant negative effect on the germination performance of *S. salsa*, relative to the control (Figures 3, 4). At 50 g·L^{-1} extract concentration, the extract of four different parts (belowground, aboveground, litter, and soil) significantly decreased the *S. salsa* seed germination percentage and germination rate of both intertidal zone and brackish wetland ($RI < 0$, Figures 3, 4; Tables 1, 2). Compared with the control treatment, the germination percentage and germination rate of *S. salsa* from the intertidal zone was lower in the different extract treatments ($p < 0.05$). Salt stress significantly affected the germination percentage and germination rate of *S. salsa* from a brackish wetland, but no significant effect was observed on seeds from the intertidal zone (Figures 3, 4). Three-way ANOVA showed that interaction of extract concentration and salt concentration had no significant effect on germination percentage or germination rate of *S. salsa* from the intertidal zone, but it did have a significant effect on *S. salsa* from a brackish wetland. The interaction of extract organ and salt concentration had a significant effect on germination of *S. salsa* from both habitats (Table 3).

Radicle length

The extracts of different organs of *P. australis* had negative effects on the radicle length of *S. salsa* seedlings from the two habitats (Table 4). 6.25 g·L^{-1} belowground extract significantly decreased the radicle length of *S. salsa* seedlings from the brackish wetland ($RI < 0$, Tables 2, 4), but did not significantly affect the seedlings from the intertidal zone (Table 4). At 50 g·L^{-1} extract concentration, belowground extract significantly decreased the radicle length of *S. salsa* seedlings from both habitats ($p < 0.05$, $RI < 0$, Tables 1, 2, 4). However, litter extract significantly increased the radicle length of the seedlings at 100 and 300 mM NaCl concentration (intertidal zone; $RI > 0$, Tables 1, 4), and at 0, 300, and 500 mM NaCl concentration (brackish wetland; $RI > 0$, Tables 2, 4). The response index of *S. salsa* from the intertidal zone showed that 6.25 g·L^{-1} extract concentration of different organs promoted or slightly inhibited the radicle length (Table 1), but 50 g·L^{-1} extract concentration of belowground and aboveground part strongly inhibited the radicle length ($RI < 0$, Table 1). While the response index of *S. salsa* from the brackish wetland showed that belowground extracts of both 6.25 and 50 g·L^{-1} inhibited the radicle length ($RI < 0$, Table 2). With increasing salt concentration, the radicle length decreased significantly (Table 4, $p < 0.05$). Three-way ANOVA showed that there was a significant interaction of extract concentration, salt concentration, and extract organ on the radicle length of *S. salsa* seedlings of the two habitats (Table 3).

Seedling biomass

The extracts from different parts of *P. australis* had different effects on the seedling biomass of *S. salsa* from the two habitats (Table 5). Among them, belowground extract significantly decreased the seedling biomass of *S. salsa* from the two habitats ($p < 0.05$). With increasing salt concentration, the seedling biomass from the intertidal zone increased significantly within the extracts of different parts ($p < 0.05$), except at 50 g·L^{-1} belowground and aboveground extracts (Table 5). The seedling biomass of *S. salsa* from a brackish wetland significantly increased at 50 g·L^{-1} soil extract and 300 mM NaCl ($RI > 0$, Table 2). However, at 50 g·L^{-1} aboveground extracts, all three NaCl concentration (100, 300, and 500 mM) significantly decreased the seedling biomass ($p < 0.05$, $RI < 0$, Tables 2, 5). The salt concentration of 300 mM NaCl with soil extract at 6.25 g·L^{-1} significantly increased the seedling biomass when compared with 0 salt treatment ($p < 0.05$).

The response index of *S. salsa* from the intertidal zone showed that 6.25 g·L^{-1} extract concentration of different organs inhibited the seedling biomass ($RI < 0$, Table 1), expect the litter extract at the 500 mM NaCl treatment ($RI > 0$, Table 1). However, at 50 g·L^{-1} extract concentration, only the belowground extract inhibited the seedling biomass ($RI < 0$, Table 1). The effects of extract of other organs on seedling biomass were different under different salt concentrations (Table 5). For the brackish wetland, both 6.25 and 50 g·L^{-1} extract concentrations of belowground and aboveground parts inhibited the seedling biomass ($RI < 0$, Table 2), but 6.25 g·L^{-1} litter extracts in all salt concentrations promoted the seedling biomass ($RI > 0$, Table 2). Similarly, Three-way ANOVA showed that there was no interaction of extract concentration and salt

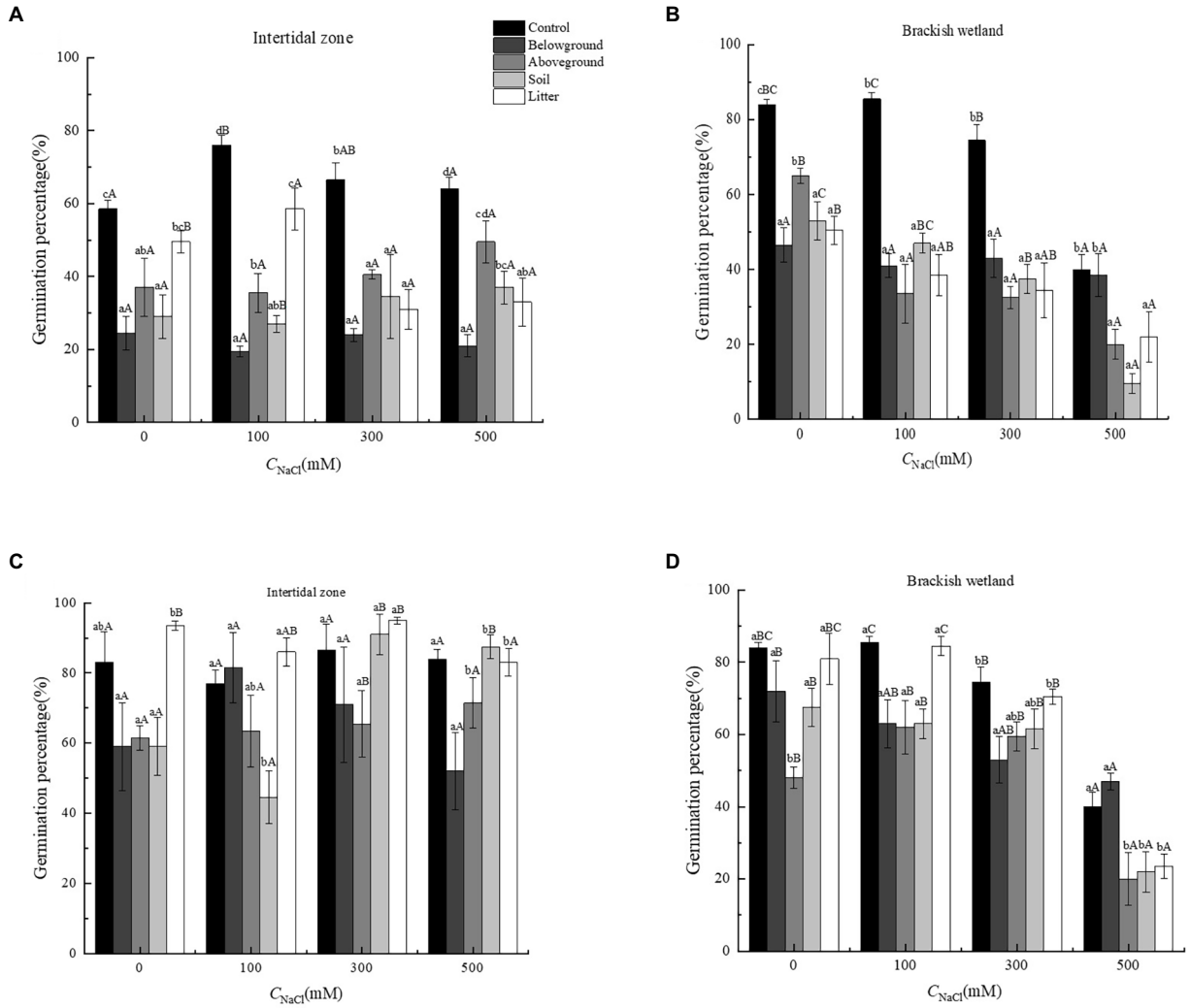

FIGURE 3
Effects of water extracts of *Phragmites australis* on the germination percentage of *Suaeda salsa* in different salt concentrations. **(A)** Germination percentage of *S. salsa* in intertidal zone under 50 g·L^{-1} *P. australis* extracts. **(B)** Germination percentage of *S. salsa* in brackish wetland under 50 g·L^{-1} *P. australis* extracts. **(C)** Germination percentage of *S. salsa* in intertidal zone under 6.25 g·L^{-1} *P. australis* extracts. **(D)** Germination percentage of *S. salsa* in brackish wetland under 6.25 g·L^{-1} *P. australis* extracts. Different lowercase letter means significant differences between different extracts of organs under the same salt concentration (p<0.05); different capital letter means significant differences between different salt concentrations in the same extracts of organ (p<0.05).

concentration on seedling biomass of *S. salsa* from the two different habitats. However, there was a significant interaction of extract organ and salt concentration on seedling biomass, and the inhibition was highest for the belowground extract (Table 3).

Discussion

This study demonstrated that aqueous extracts from aboveground and belowground biomass, soil, and litter of *P. australis* exhibited allelopathic activity on *S. salsa* seed germination and seedling growth, while the strength of the response depended on the habitat of the plants. Especially in halophytes, different habitat conditions can cause seed dimorphism and polymorphism (Khan et al., 2001; Zhang et al., 2021). In the present study, the seed weight of the intertidal zone was greater than that of the brackish wetland. In certain plant species, seed size can positively affect germination and seedling vigor under stressful conditions, since they have higher amounts of starch and other energy reserves needed to counteract the stress (Mut and Akay, 2010; Steiner et al., 2019). In particular, salt stress decreased the germination percentage and germination rate of *S. salsa* of the brackish wetland, but had no significant effect on the seed germination from the intertidal zone. Adaptation to a saline habitat that is the intertidal zone is a likely explanation for our observation (Song et al., 2008). Locally adapted seeds are prone to withstand the harsh conditions of their provenance and preferably used for restoration purposes (Hufford and Mazer, 2003;

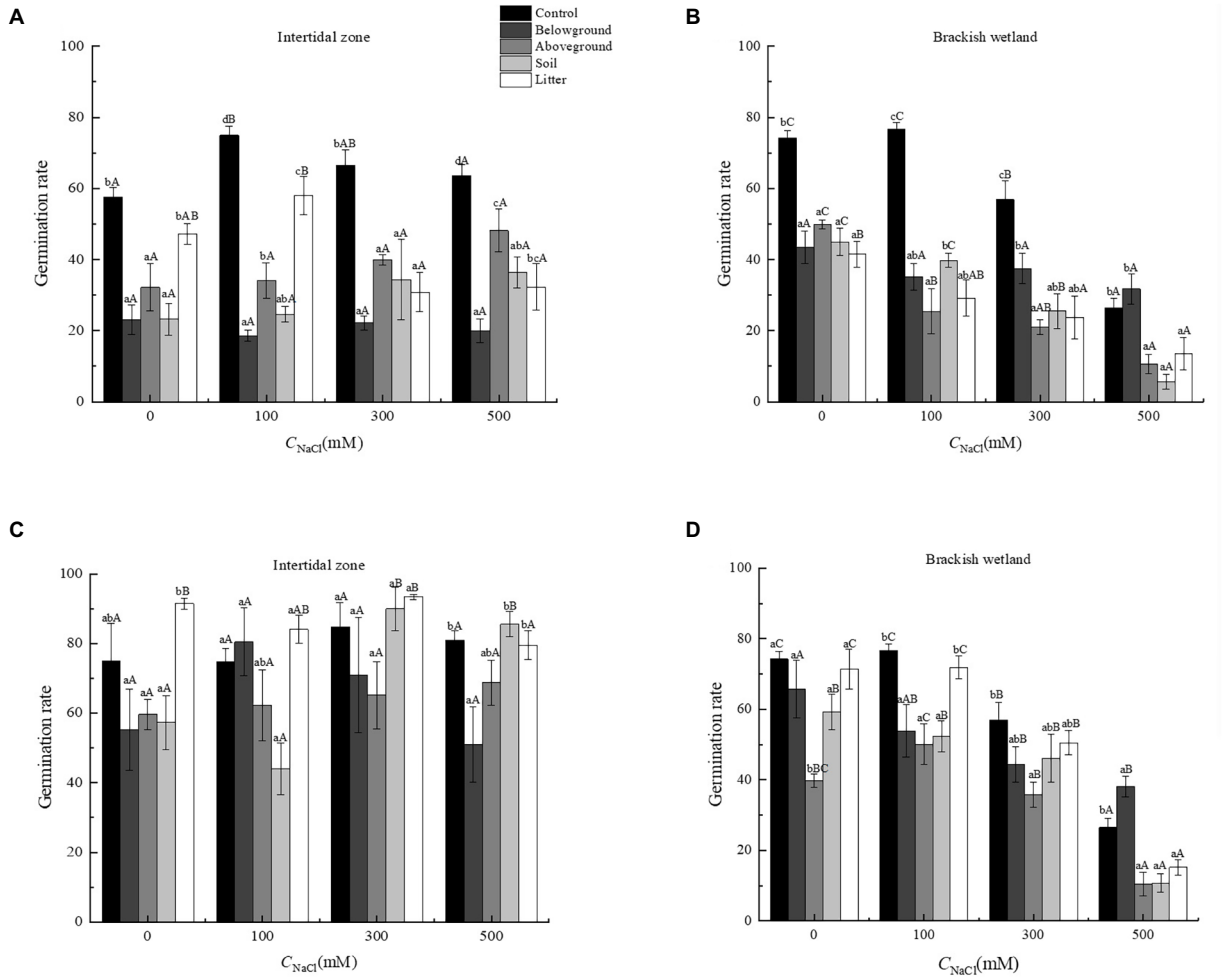

FIGURE 4
Effects of water extracts of *Phragmites australis* on the germination rate of *Suaeda salsa* in different salt concentrations. **(A)** Germination rate of *S. salsa* in intertidal zone under 50 g·L^{-1} *P. australis* extracts. **(B)** Germination rate of *S. salsa* in brackish wetland under 50 g·L^{-1} *P. australis* extracts. **(C)** Germination rate of *S. salsa* in intertidal zone under 6.25 g·L^{-1} *P. australis* extracts. **(D)** Germination rate of *S. salsa* in brackish wetland under 6.25 g·L^{-1} *P. australis* extracts. Different lowercase letter means significant differences between different extracts of organs under the same salt concentration (p<0.05); different capital letter means significant differences between different salt concentrations in the same extracts of organ (p<0.05).

Broadhurst et al., 2008). Hence, the intertidal ecotype responded to a lower degree to salt stress than did the brackish ecotype.

Previous studies on *S. salsa* from brackish wetlands and other halophytes showed that plant height decreased with the increasing salt stress, but biomass production was stimulated at low salinities and only decreased with more intense salt stress (Guan et al., 2013; Parida and Jha, 2014; Parida et al., 2016). In this study, similar trends on radicle length and seedling biomass were observed for the seedlings from both the brackish wetland and the intertidal zone. Generally, when plants encounter salt stress, some growth indicators will decrease (Saddiq et al., 2021), but halophytes, such as *S. salsa*, will invest in longer, thinner roots to gain better access to inorganic nutrients (Wang et al., 2021). In agreement with this, the intertidal ecotype had generally longer roots, and reduced its radicle length to a lesser degree than the brackish ecotype with increasing salinity.

The addition of *P. australis* extract, especially from belowground parts, had an overall stronger inhibitory effect on the seed germination and seedling growth at the higher concentration of extract solution (50 g·L^{-1}), compared to the low concentration (6.25 g·L^{-1}), as could be expected (Tefera, 2002; Bogatek et al., 2006). One aspect of the high inhibition effect of belowground extract could be due to a higher concentration of phenolic acid compounds in the roots of *P. australis*, which suppress the activity of α-amylase that plays an important role for successful seed germination (Uddin et al., 2017; Liu et al., 2018). More importantly, the germination rate, percentage, and radicle length of brackish ecotypes were significantly affected by an interaction of *P. australis* extracts and salinity. The intertidal zone ecotypes also had an interaction, although only with respect to radicle length. For both ecotypes, the negative response to increasing salinity was stronger when exposed to the high extract

TABLE 1 Response index (mean±SE) of *S. salsa* in the intertidal zone under extract from different organs of *P. australis* and different salt concentrations.

Extract concentration		6.25 g·L^{-1}				50 g·L^{-1}			
Items	NaCl (mM)	Response index							
		Belowground	Aboveground	Soil	Litter	Belowground	Aboveground	Soil	Litter
Germination	0	−0.23 ± 0.22	−0.24 ± 0.05	−0.23 ± 0.20	0.17 ± 0.13	−0.59 ± 0.07	−0.37 ± 0.14	−0.51 ± 0.09	−0.15 ± 0.04
percentage	100	0.08 ± 0.17	−0.18 ± 0.12	−0.41 ± 0.13	0.13 ± 0.11	−0.74 ± 0.02	−0.53 ± 0.08	−0.64 ± 0.04	−0.23 ± 0.07
	300	−0.21 ± 0.16	−0.21 ± 0.1	0.09 ± 0.15	0.13 ± 0.11	−0.63 ± 0.04–	−0.38 ± 0.05	−0.49 ± 0.15	−0.53 ± 0.08
	500	−0.37 ± 0.14	−0.15 ± 0.08	0.04 ± 0.04	−0.01 ± 0.06	0.68 ± 0.04	−0.23 ± 0.06	−0.41 ± 0.09	−0.48 ± 0.10
Germination	0	−0.16 ± 0.25	−0.17 ± 0.09	−0.15 ± 0.24	0.30 ± 0.19	−0.60 ± 0.07	−0.44 ± 0.12	−0.61 ± 0.06	−0.18 ± 0.05
rate	100	0.10 ± 0.17	−0.16 ± 0.13	−0.40 ± 0.13	0.14 ± 0.12	−0.75 ± 0.03	−0.54 ± 0.08	−0.67 ± 0.03	−0.23 ± 0.07
	300	−0.20 ± 0.16	−0.20 ± 0.17	0.10 ± 0.16	0.13 ± 0.11	−0.66 ± 0.04	−0.39 ± 0.05	−0.50 ± 0.15	−0.53 ± 0.08
	500	−0.36 ± 0.15	−0.15 ± 0.08	0.06 ± 0.04	−0.01 ± 0.06	−0.69 ± 0.04	−0.25 ± 0.06	−0.42 ± 0.08	−0.49 ± 0.10
Radicle	0	0.01 ± 0.10	0.25 ± 0.08	0.28 ± 0.07	0.36 ± 0.06	−0.81 ± 0.02	−0.15 ± 0.07	−0.13 ± 0.07	0.06 ± 0.13
length	100	−0.01 ± 0.03	0.14 ± 0.06	0.20 ± 0.06	0.22 ± 0.05	−0.81 ± 0.00	−0.28 ± 0.03	0.05 ± 0.07	0.16 ± 0.04
	300	−0.07 ± 0.09	0.04 ± 0.03	0.18 ± 0.06	0.33 ± 0.02	−0.74 ± 0.02	−0.22 ± 0.12	−0.06 ± 0.04	0.22 ± 0.11
	500	0.05 ± 0.05	−0.04 ± 0.03	0.11 ± 0.05	0.65 ± 0.11	−0.74 ± 0.01	−0.29 ± 0.13	0.14 ± 0.18	0.02 ± 0.12
Biomass	0	−0.30 ± 0.07	−0.14 ± 0.07	−0.22 ± 0.06	−0.04 ± 0.07	−0.48 ± 0.09	0.17 ± 0.14	−0.11 ± 0.18	0.09 ± 0.16
	100	−0.24 ± 0.03	−0.14 ± 0.06	−0.25 ± 0.07	−0.05 ± 0.05	−0.68 ± 0.06	−0.26 ± 0.05	−0.20 ± 0.05	0.07 ± 0.04
	300	−0.36 ± 0.04	−0.17 ± 0.03	−0.27 ± 0.04	−0.10 ± 0.07	−0.61 ± 0.06	−0.33 ± 0.08	0.05 ± 0.09	0.14 ± 0.07
	500	−0.39 ± 0.03	−0.08 ± 0.06	−0.19 ± 0.01	0.02 ± 0.08	−0.64 ± 0.05	−0.24 ± 0.07	−0.08 ± 0.13	−0.11 ± 0.10

TABLE 2 Response index (mean±SE) of *S. salsa* in the brackish wetland under extract from different organs of *P. australis* and different salt concentrations.

Extract concentration		6.25 g·L^{-1}				50 g·L^{-1}			
Items	NaCl (mM)	Response Index							
		Belowground	Aboveground	Soil	Litter	Belowground	Aboveground	Soil	Litter
Germination	0	−0.14 ± 0.11	−0.43 ± 0.04	−0.20 ± 0.06	−0.04 ± 0.08	−0.45 ± 0.06	−0.23 ± 0.03	−0.37 ± 0.07	−0.40 ± 0.05
percentage	100	−0.27 ± 0.06	−0.28 ± 0.08	−0.26 ± 0.05	−0.01 ± 0.04	−0.52 ± 0.03	−0.61 ± 0.10	−0.45 ± 0.04	−0.55 ± 0.06
	300	−0.28 ± 0.11	−0.20 ± 0.06	−0.17 ± 0.06	−0.04 ± 0.08	−0.42 ± 0.05	−0.55 ± 0.07	−0.50 ± 0.04	−0.54 ± 0.09
	500	0.19 ± 0.05	−0.53 ± 0.13	−0.47 ± 0.08	−0.41 ± 0.07	−0.13 ± 0.06	−0.48 ± 0.13	−0.53 ± 0.19	−0.48 ± 0.10
Germination	0	−0.11 ± 0.13	−0.46 ± 0.03	−0.20 ± 0.08	−0.04 ± 0.06	−0.41 ± 0.07	−0.33 ± 0.02	−0.39 ± 0.06	−0.44 ± 0.05
rate	100	−0.30 ± 0.08	−0.35 ± 0.07	−0.32 ± 0.05	−0.06 ± 0.06	−0.54 ± 0.05	−0.67 ± 0.09	−0.48 ± 0.04	−0.62 ± 0.06
	300	−0.20 ± 0.12	−0.35 ± 0.09	−0.18 ± 0.10	−0.08 ± 0.14	−0.33 ± 0.07	−0.61 ± 0.08	−0.56 ± 0.06	−0.57 ± 0.11
	500	0.44 ± 0.03	−0.63 ± 0.09	−0.61 ± 0.06	−0.42 ± 0.09	0.22 ± 0.18	−0.58 ± 0.13	−0.77 ± 0.09	−0.51 ± 0.11
Radicle	0	−0.61 ± 0.00	−0.39 ± 0.05	−0.14 ± 0.08	−0.06 ± 0.04	−0.73 ± 0.02	−0.36 ± 0.01	−0.15 ± 0.05	0.13 ± 0.07
length	100	−0.60 ± 0.04	−0.24 ± 0.07	−0.09 ± 0.05	0.00 ± 0.03	−0.76 ± 0.02	−0.04 ± 0.05	0.00 ± 0.06	0.03 ± 0.06
	300	−0.57 ± 0.03	0.04 ± 0.08	0.23 ± 0.15	0.17 ± 0.07	−0.71 ± 0.03	0.17 ± 0.12	0.17 ± 0.12	0.40 ± 0.15
	500	−0.50 ± 0.03	−0.20 ± 0.07	−0.14 ± 0.05	0.45 ± 0.05	−0.54 ± 0.05	0.51 ± 0.07	0.10 ± 0.12	0.54 ± 0.04
Biomass	0	−0.02 ± 0.12	−0.28 ± 0.07	−0.03 ± 0.18	0.33 ± 0.18	−0.47 ± 0.11	−0.36 ± 0.03	−0.01 ± 0.11	0.42 ± 0.19
	100	−0.41 ± 0.07	−0.33 ± 0.02	−0.19 ± 0.09	0.05 ± 0.22	−0.71 ± 0.03	−0.37 ± 0.06	−0.17 ± 0.08	−0.19 ± 0.13
	300	−0.38 ± 0.10	−0.24 ± 0.09	0.31 ± 0.29	0.19 ± 0.16	−0.50 ± 0.09	−0.12 ± 0.09	0.28 ± 0.15	0.04 ± 0.13
	500	−0.25 ± 0.15	−0.19 ± 0.15	0.12 ± 0.12	0.09 ± 0.12	−0.41 ± 0.15	−0.07 ± 0.14	−0.22 ± 0.20	−0.13 ± 0.12

concentration, while the control with zero extract stayed similar. Hence, allelopathy can potentially worsen abiotic stresses, although it has been shown that high soil salinity can also lower allelopathic substances due to a reduction of secondary metabolite production in the source plant (Kotzamani et al., 2021). Weeds and invasive plants have been shown to be quite salt tolerant when compared to crops (Cirillo et al., 2018). *Phragmites australis* often behaves like a weed, with its high intraspecific genetic variation, remarkable phenotypic plasticity, ecological niche breadth, and high productivity (Eller et al., 2017). A salt-tolerant weed like

TABLE 3 Three-way ANOVA of the response of different stress factors to the seed germination and growth of *S. salsa* in the intertidal zone.

Index	Germination percentage		Germination rate		Radicle length		Biomass	
	F	*P*	*F*	*P*	*F*	*P*	*F*	*P*
Intertidal zone								
Extract concentration (EC)	259.917	**0.000**	255.957	**0.000**	263.230	**0.000**	92.962	**0.000**
Salt concentration (SC)	1.058	0.370	2.254	**0.000**	14.915	**0.000**	44.580	**0.000**
Organ	27.113	**0.000**	26.793	**0.000**	13.267	**0.000**	95.911	**0.000**
EC × SC	2.350	0.076	2.326	0.078	13.537	**0.000**	2.217	0.090
EC × Organ	7.443	**0.000**	8.591	**0.000**	19.518	**0.000**	13.535	**0.000**
SC × Organ	3.146	**0.001**	3.380	**0.000**	31.071	**0.005**	2.866	**0.002**
EC × SC × Organ	1.857	**0.047**	1.700	0.075	35.627	**0.000**	2.869	**0.002**
Brackish wetland								
Extract concentration (EC)	87.826	**0.000**	77.705	**0.000**	12.118	**0.001**	8.597	**0.004**
Salt concentration (SC)	116.529	**0.000**	153.108	**0.000**	44.450	**0.000**	3.883	**0.000**
Organ	43.226	**0.004**	50.865	**0.000**	279.291	**0.000**	32.768	**0.000**
EC × SC	7.264	**0.000**	7.041	**0.006**	2.880	**0.039**	0.575	0.633
EC × Organ	9.457	**0.000**	9.585	**0.000**	12.656	**0.000**	2.951	**0.023**
SC × Organ	3.735	**0.000**	4.642	**0.003**	10.452	**0.000**	2.880	**0.002**
EC × SC × Organ	3.300	**0.000**	2.690	**0.003**	2.289	**0.012**	0.921	0.529

Significant effects ($p < 0.05$) are in bold.

TABLE 4 Effects of water extracts of *P. australis* on the radicle length of *S. salsa* in different salt concentrations (mean±SE).

NaCl (mM)	Organ	Intertidal zone		Brackish wetland	
		Radicle length (cm)			
		50 g·L^{-1}	6.25 g·L^{-1}	50 g·L^{-1}	6.25 g·L^{-1}
0	Control	5.99 ± 0.24cA	5.34 ± 0.18aA	4.67 ± 0.13dA	4.67 ± 0.13dA
	Belowground	1.11 ± 0.03aA	5.28 ± 0.17aA	1.25 ± 0.05aAB	1.80 ± 0.06aAB
	Aboveground	5.05 ± 0.22bA	6.58 ± 0.13bA	2.98 ± 0.14bA	2.83 ± 0.12bB
	Soil	5.23 ± 0.32bA	6.78 ± 0.13bcA	3.94 ± 0.15cAB	4.02 ± 0.15cB
	Litter	6.21 ± 0.21cA	7.19 ± 0.12cA	5.29 ± 0.19eA	4.39 ± 0.16cdA
100	Control	5.87 ± 0.13cA	5.26 ± 0.11aA	4.88 ± 0.12bA	4.88 ± 0.12dA
	Belowground	1.10 ± 0.02aA	5.22 ± 0.10aA	1.16 ± 0.07aAB	1.95 ± 0.09aA
	Aboveground	4.21 ± 0.22bB	6.00 ± 0.13bB	4.66 ± 0.20bB	3.69 ± 0.17bC
	Soil	6.16 ± 0.31cB	6.28 ± 0.12bcB	4.87 ± 0.13bC	4.45 ± 0.17cC
	Litter	6.81 ± 0.22dA	6.42 ± 0.12cB	5.04 ± 0.20bA	4.88 ± 0.13 dB
300	Control	4.64 ± 0.09cB	5.11 ± 0.08abA	3.84 ± 0.16bB	3.84 ± 0.16bB
	Belowground	1.22 ± 0.05aB	4.74 ± 0.17aB	1.09 ± 0.07aA	1.62 ± 0.07aBC
	Aboveground	3.64 ± 0.29bB	5.35 ± 0.12bC	4.39 ± 0.12cB	3.92 ± 0.13bC
	Soil	4.38 ± 0.30cA	5.98 ± 0.12cA	4.43 ± 0.19cBC	4.62 ± 0.17cC
	Litter	5.68 ± 0.27 dB	6.83 ± 0.15 dB	5.27 ± 0.19dA	4.42 ± 0.17cA
500	Control	4.19 ± 0.18cB	4.10 ± 0.08aB	2.93 ± 0.10bC	2.93 ± 0.10cC
	Belowground	1.07 ± 0.03aA	4.28 ± 0.11abC	1.35 ± 0.03aB	1.45 ± 0.06aC
	Aboveground	2.87 ± 0.20bC	3.95 ± 0.10aD	4.41 ± 0.30cB	2.35 ± 0.16bA
	Soil	4.61 ± 0.30cA	4.56 ± 0.10bC	3.15 ± 0.53cA	2.50 ± 0.12bA
	Litter	4.14 ± 0.20cC	6.72 ± 0.19cA	4.50 ± 0.17cB	4.25 ± 0.13cA

Different lowercase letter means significant differences between different extracts of organs under the same salt concentration ($p < 0.05$); different capital letter means significant differences between different salt concentrations in the same extracts of organ ($p < 0.05$).

P. australis can be expected to have augmented inhibitory effects by enhanced phytotoxicity of its allelochemicals under high salt concentrations (Khalid et al., 2002; El-Darier and Youssef, 2017; Cirillo et al., 2018), as we observed here. In salt-tolerant plants, enzymatic activity associated with reactive oxygen species (ROS) scavenging is high, as a means of stress defense (Munns and

TABLE 5 Effects of water extracts of *P. australis* on the biomass of *S. salsa* in different salt concentrations (mean±SE).

NaCl (mM)	Organ	Intertidal zone		Brackish wetland	
		Biomass(mg/plant)			
		50 g·L^{-1}	6.25 g·L^{-1}	50 g·L^{-1}	6.25 g·L^{-1}
0	Control	1.38 ± 0.11bcA	1.79 ± 0.12dA	0.68 ± 0.07bA	0.68 ± 0.07abA
	Belowground	0.69 ± 0.09aA	1.25 ± 0.08aA	0.34 ± 0.06aA	0.67 ± 0.11abA
	Aboveground	1.58 ± 0.09cA	1.52 ± 0.05bcA	0.43 ± 0.02acA	0.48 ± 0.04aA
	Soil	1.18 ± 0.16bA	1.38 ± 0.03abA	0.65 ± 0.04bA	0.64 ± 0.09abA
	Litter	1.45 ± 0.08bcA	1.70 ± 0.08cdA	0.92 ± 0.06cA	0.89 ± 0.06bA
100	Control	1.94 ± 0.04cB	2.03 ± 0.07cA	0.97 ± 0.05cB	0.97 ± 0.05bB
	Belowground	0.62 ± 0.13aA	1.53 ± 0.06bA	0.28 ± 0.03aA	0.57 ± 0.07aA
	Aboveground	1.43 ± 0.08bA	1.74 ± 0.10abA	0.61 ± 0.05bB	0.65 ± 0.03aA
	Soil	1.55 ± 0.09bAB	1.50 ± 0.09aA	0.81 ± 0.12bcAB	0.78 ± 0.08abAB
	Litter	2.08 ± 0.06cB	1.94 ± 0.11bcAB	0.77 ± 0.09bcA	0.99 ± 0.18bA
300	Control	1.93 ± 0.11cB	2.44 ± 0.09 dB	0.79 ± 0.07bcAB	0.79 ± 0.07bcAB
	Belowground	0.73 ± 0.09aA	1.56 ± 0.11aB	0.38 ± 0.05aA	0.49 ± 0.11aA
	Aboveground	1.29 ± 0.15bA	2.04 ± 0.07bcB	0.68 ± 0.05bB	0.58 ± 0.02abA
	Soil	2.00 ± 0.12cB	1.78 ± 0.12abB	0.98 ± 0.10cB	0.98 ± 0.14cB
	Litter	2.18 ± 0.10cB	2.20 ± 0.10cdBC	0.81 ± 0.09bcA	0.91 ± 0.06cA
500	Control	2.17 ± 0.14bB	2.47 ± 0.10cB	0.85 ± 0.08bAB	0.85 ± 0.08abAB
	Belowground	0.78 ± 0.11aA	1.50 ± 0.03aB	0.47 ± 0.09aA	0.62 ± 0.11aA
	Aboveground	1.66 ± 0.22bA	2.26 ± 0.12abB	0.77 ± 0.08bB	0.67 ± 0.11abA
	Soil	1.96 ± 0.18bB	2.00 ± 0.07bB	0.64 ± 0.12abA	0.93 ± 0.08bAB
	Litter	1.88 ± 0.15bB	2.51 ± 0.17cC	0.72 ± 0.05abA	0.90 ± 0.04abA

Different lowercase letter means significant differences between different extracts of organs under the same salt concentration ($p < 0.05$); different capital letter means significant differences between different salt concentrations in the same extracts of organ ($p < 0.05$).

Tester, 2008). Although allelochemicals can suppress specific scavenging enzymes, the antioxidant defense system of salt-tolerant plants may be constituted to counteract the harmful effects of ROS generated during seed germination and initial growth in the presence of toxic allelochemicals (Coelho et al., 2017).

Few studies have compared the effects of allelopathic extracts from different parts of the plant community. Among all the extracts, the belowground and aboveground parts showed the overall strongest inhibition, which were well aligned with previous studies of phytotoxic evaluation of *P. australis* (Uddin et al., 2012). *Phragmites australis* is a persistent grass with a long rootstock (rhizome) and high growth rates. The rhizomes and roots in soil keep their viability for many years and the robust rhizome is of great importance in the life of this plant (Uddin and Robinson, 2017). In this study, the strong allelopathic effect of belowground extracts could be another important reason for its high competitiveness to other, coexisting species. *Phragmites australis* root secretions contain gallic acid, which induces the production of reactive oxygen species and disrupts plant root growth by causing peroxidation of membrane lipids and membrane damage, thereby impeding neighboring plant growth and development (Rudrappa et al., 2007).

Interestingly, not all the extracts of *P. australis* showed allelopathic effects on the radicle length and seedling biomass. The low concentration of litter extract significantly promoted seedling radicle length of the intertidal zone ecotype, especially in higher salt concentrations, suggesting that nutrient elements in the extract could provide some nutrients for the seedling growth.

Conclusion

We found that the extracts of different organs of *P. australis*, with the strongest inhibition caused by belowground and aboveground extracts, had an allelopathic effect on the germination and growth of *S. salsa* from two habitats. With increasing salt stress, the germination performance of the seeds from the intertidal zone showed high salt tolerance, but seeds from the brackish wetland showed salt stress, which was enhanced by the allelochemical extracts. Our study suggests that allelopathy is one of the important reasons of high competitiveness and invasive capacity of *P. australis* in its habitats. As the allelopathic potential was mainly exerted at higher extract concentrations, we suggest that allelopathic chemicals should be analyzed in natural soils, where *P. australis* and *S. salsa* co-occur. Moreover, it is possible that extracts from reed ecotypes differ, in addition to our observation of different stress tolerance of *S. salsa* ecotypes. Cross-testing of *P. australis* extracts from different provenances with *S. salsa* ecotypes could provide

insights for this assumption. *Phragmites australis* is commonly used for restoration in Chinese wetlands. Understanding its allelochemical effects is crucial to avoid undesired inhibition of coexisting flora. This study represents a valuable step forward in our understanding of allelopathic effects from different parts of the *P. australis* community.

Data availability statement

The original contributions presented in the study are included in the article/supplementary material, further inquiries can be directed to the corresponding authors.

Author contributions

BG and JZ designed the study. JG and MG conducted the control experiment. JG and BG carried out the data analysis and wrote the manuscript. FE, JY, and XW revised the manuscript. BG, XW, and JY coordinated the project. All authors contributed to the article and approved the submitted version.

Funding

This work was financially supported by the National Natural Science Foundation of China (41871091, 42171111, and U1806218).

Conflict of interest

The authors declare that the research was conducted in the absence of any commercial or financial relationships that could be construed as a potential conflict of interest.

Publisher's note

All claims expressed in this article are solely those of the authors and do not necessarily represent those of their affiliated organizations, or those of the publisher, the editors and the reviewers. Any product that may be evaluated in this article, or claim that may be made by its manufacturer, is not guaranteed or endorsed by the publisher.

References

Agami, M., and Waisel, Y. (1985). Inter-relationships between *Najas marina* L. and three other species of aquatic macrophytes. *Hydrobiologia* 126, 169–173. doi: 10.1007/BF00008684

Aschehoug, E. T., Brooker, R., Atwater, D. Z., Maron, J. L., and Callaway, R. M. (2016). The mechanisms and consequences of interspecific competition among plants. *Ann. Rev. Ecol. Evol. Sci.* 47, 263–281. doi: 10.1146/annurev-ecolsys-121415-032123

Bogatek, R., Gniazdowska, A., Zakrzewska, W., Oracz, K., and Gawronski, S. (2006). Allelopathic effects of sunflower extracts on mustard seed germination and seedling growth. *Biol. Plant.* 50, 156–158. doi: 10.1007/s10535-005-0094-6

Broadhurst, L. M., Andrew, L., David, J., Coates, S. A., Cunningham, M. M., Peter, A., et al. (2008). Seed supply for broadscale restoration: maximizing evolutionary potential. *Evol. Appl.* 1, 587–597. doi: 10.1111/j.1752-4571.2008.00045.x

Callaway, R. M., and Aschehoug, E. T. (2000). Invasive plants versus their new and ole neighbors: a mechanism for exotic invasion. *Science* 290, 521–523. doi: 10.1126/science.290.5491.521

Christina, M., Rouifed, S., Puijalon, S., Vallier, F., Meiffren, G., Bellvert, F., et al. (2015). Allelopathic effect of a native species on a major plant invader in Europe. *Sci. Nat.* 102, 12–18. doi: 10.1007/s00114-015-1263-x

Cirillo, V., Masin, R., Maggio, A., and Zanin, G. (2018). Crop-weed interactions in saline environments. *Eur. J. Dermatol.* 99, 51–61. doi: 10.1016/j.eja.2018.06.009

Coelho, É. M. P., Barbosa, M. C., Mito, M. S., Mantovanelli, G. C., Olivetra, R. S. Jr., and Lshii, E. L. (2017). The activity of the antioxidant defense system of the weed species *Senna obtusifolia* L. and its resistance to allelochemical stress. *J. Chem. Ecol.* 43, 725–738. doi: 10.1007/s10886-017-0865-5

Corbin, J. D., and D'Antonio, C. M. (2004). Competition between native perennial and exotic annual grasses: implications for an historical invasion. *Ecology* 85, 1273–1283. doi: 10.1890/02-0744

Craine, J. M., and Dybzinski, R. (2013). Mechanisms of plant competition for nutrients, water and light. *Funct. Ecol.* 27, 833–840. doi: 10.1111/1365-2435.12081

Dayan, F. E., J'Lynn, H., and Weidenhamer, J. D. (2009). Dynamic root exudation of sorgoleone and its in *planta* mechanism of action. *J. Exp. Bot.* 60, 2107–2117. doi: 10.1093/jxb/erp082

Elakovich, S. D., and Wooten, J. W. (1989). Allelopathic potential of sixteen aquatic and wetland plants. *J. Aquat. Plant Manag.* 27, 78–84.

El-Darier, S. M., and Youssef, R. S. (2017). Does salinity enhance allelopathic effects of *Tribulus terrestris* L. in *Citrullus vulgaris* schrad, agroecosystems at Nobaria, Egypt? *Exper. Invest. Int. Stand. J.* 5, 1–8. doi: 10.9734/bpi/rppsr/v5/15282D

Eller, F., Skálová, H., Caplan, J. S., Bhattarai, G. P., Burger, M. K., Cronin, J. T., et al. (2017). Cosmopolitan species as models for ecophysiological responses to global change: the common reed *Phragmites australis*. *Front. Plant Sci.* 8:1833. doi: 10.3389/fpls.2017.01833

Fernandez, C., Monnier, Y., Santonja, M., Gallet, C., Weston, L. A., Prevosto, B., et al. (2016). The impact of competition and allelopathy on the trade-off between plant defense and growth in two contrasting tree species. *Front. Plant Sci.* 7:594. doi: 10.3389/fpls.2016.00594

Fowler, N. (1986). The role of competition in plant communities in arid and semiarid regions. *Ann. Rev. Ecol. Sci.* 17, 89–110. doi: 10.1146/annurev.es.17.110186.000513

Fowler, M. S. (2013). The form of direct interspecific competition modifies secondary extinction patterns in multi-trophic food webs. *Oikos* 122, 1730–1738. doi: 10.1111/j.1600-0706.2013.00346.x

Gross, E. M. (2003). Allelopathy of aquatic autotrophs. *Crit. Rev. Plant Sci.* 22, 313–339. doi: 10.1080/713610859

Guan, B., Gao, N., Chen, M., Cagle, G. A., Hou, A., Han, G., et al. (2021). Seedling adaptive characteristics of *Phragmites australis* to nutrient heterogeneity under salt stress using a split-root approach. *Aquat. Sci.* 83, 1–11. doi: 10.1007/s00027-021-00811-w

Guan, B., Yu, J., Cao, D., Li, Y., Han, G., and Mao, P. (2013). The ecological restoration of heavily degraded saline wetland in the Yellow River Delta. *CLEAN Soil Air Water* 41, 690–696. doi: 10.1002/clen.201200569

Guan, B., Yu, J., Hou, A., Han, G., Wang, G., Qu, F., et al. (2017). The ecological adaptability of *Phragmites australis* to interactive effects of water level and salt stress in the Yellow River Delta. *Aquat. Ecol.* 51, 107–116. doi: 10.1007/s10452-016-9602-3

Guo, J., Liu, L., Du, M., Tian, H., and Wang, B. (2020). Cation and Zn accumulation in brown seeds of the euhalophyte *Suaeda salsa* improves germination under saline conditions. *Front. Plant Sci.* 11:602427. doi: 10.3389/fpls.2020.602427

Hellings, S. E., and Gallagher, J. L. (1992). The effects of salinity and flooding on *Phragmites australis*. *J. Appl. Ecol.* 29, 41–49. doi: 10.2307/2404345

Helmig, D., Daly, R. W., Milford, J., and Guenther, A. (2013). Seasonal trends of biogenic terpene emissions. *Chemosphere* 93, 35–46. doi: 10.1016/j.chemosphere.2013.04.058

Hufford, K. M., and Mazer, S. J. (2003). Plant ecotypes: genetic differentiation in the age of ecological restoration. *Trends Ecol. Evol.* 18, 147–155. doi: 10.1016/S0169-5347(03)00002-8

Khalid, S., Tahira, A., and Shad, R. (2002). Use of allelopathy in agriculture. *Asian J. Plant Sci.* 1, 292–297. doi: 10.3923/ajps.2002.292.297

Khan, M. A., Gul, B., and Weber, D. J. (2001). Germination of dimorphic seeds of *Suaeda moquinii* under high salinity stress. *Aus. J. Bot.* 49, 185–192. doi: 10.1071/BT00020

Khan, M. A., and Ungar, I. A. (1984). The effect of salinity and temperature on the germination of polymorphic seeds and growth of *Atriplex triangularis* Willd. *Am. J. Bot.* 71, 481–489. doi: 10.1002/j.1537-2197.1984.tb12533.x

Kotzamani, A., Vasilakoglou, I., Dhima, K., Moulas, A. N., Vaiou, M., and Stefanou, S. (2021). Impact of soil salinity on barley allelopathic potential and main secondary metabolites gramine and hordenine. *J. Plant Growth Regul.* 40, 137–146. doi: 10.1007/s00344-020-10084-6

Kulshreshtha, M., and Gopal, B. (1983). Allelopathic influence of *Hydrilla verticillata* (L.F.) Royle on the distribution of *Ceratophyllum* species. *Aquat. Bot.* 16, 207–209. doi: 10.1016/0304-3770(83)90095-5

Liu, L., Xia, W., Li, H., Zeng, H., Wei, B., Han, S., et al. (2018). Salinity inhibits rice seed germination by reducing α-amylase activity via decreased bioactive gibberellin content. *Front. Plant Sci.* 9:275. doi: 10.3389/fpls.2018.00275

Munns, R., and Tester, M. (2008). Mechanisms of salinity tolerance. *Annu. Rev. Plant Biol.* 59, 651–681. doi: 10.1146/annurev.arplant.59.032607.092911

Mut, Z., and Akay, H. (2010). Effect of seed size and drought stress on germination and seedling growth of naked oat (*Avena sativa* L.). *Bulg. J. Agric. Sci.* 9, 764–770. doi: 10.1016/S1671-2927(09)60153-X

Parida, A. K., and Jha, B. (2014). Inductive responses of some organic metabolites for osmotic homeostasis in peanut (*Arachis hypogaea* L.) seedlings during salt stress. *Acta Physiol. Plant.* 35, 2821–2835. doi: 10.1007/s11738-013-1315-9

Parida, A. K., Veerabathini, S. K., Asha, K., and Agarwal, P. K. (2016). Physiological, anatomical and metabolic implications of salt tolerance in the halophyte *Salvadora persica* under hydroponic culture condition. *Front. Plant Sci.* 7:351. doi: 10.3389/fpls.2016.00351

Raynaud, X., and Leadley, P. W. (2004). Soil characteristics play a key role in modeling nutrient competition in plant communities. *Ecology* 85, 2200–2214. doi: 10.1890/03-0817

Rudrappa, T., Bonsall, J., Gallagher, J. L., Seliskar, D. M., and Bais, H. P. (2007). Root-secreted allelochemical in the noxious weed *Phragmites Australis* deploys a reactive oxygen species response and microtubule assembly disruption to execute rhizotoxicity. *J. Chem. Ecol.* 33, 1898–1918. doi: 10.1007/s10886-007-9353-7

Saddiq, M. S., Iqbal, S., Hafeez, M. B., Ibrahim, A. M., Raza, A., Fatima, E. M., et al. (2021). Effect of salinity stress on physiological changes in winter and spring wheat. *Agronomy* 11, 1–16. doi: 10.3390/agronomy11061193

Santonja, M., Rouzic, B., and Thiébaut, G. (2018). Seasonal dependence and functional implications of macrophyte–phytoplankton allelopathic interactions. *Freshw. Biol.* 63, 1161–1172. doi: 10.1111/fwb.13124

Song, J., Fan, H., Zhao, Y., Jia, Y., Du, X., and Wang, B. (2008). Effect of salinity on germination, seedling emergence, seedling growth and ion accumulation of a euhalophyte *Suaeda salsa* in an intertidal zone and on saline inland. *Aquat. Bot.* 88, 331–337. doi: 10.1016/j.aquabot.2007.11.004

Song, D., Yu, J., Wang, G., Han, G., Guan, B., and Li, Y. (2016). Change characteristics of average annual temperature and annual precipitation in costal wetland region of the Yellow River Delta from 1961 to 2010. *Wetland Sci.* 14, 248–253. doi: 10.13248/j.cnki.wetlandsci.2016.02.016

Steiner, F., Zuffo, A. M., Busch, A., Sousa, T. D. O., and Zoz, T. (2019). Does seed size affect the germination rate and seedling growth of peanut under salinity and water stress? *Pesq. Agropec. Trop. Goiânia.* 49, 1–9. doi: 10.1590/1983-40632019v4954353

Tefera, T. (2002). Allelopathic effects of *Parthenium hysterophorus* extracts on seed germination and seedling growth of *Eragrostis tef. J. Agro. Crop Sci.* 188, 306–310. doi: 10.1046/j.1439-037X.2002.00564.x

Uddin, M. N., Caridi, D., and Robinson, R. W. (2012). Phytotoxic evaluation of *Phragmites australis*: an investigation of aqueous extracts of different organs. *Mar. Freshw. Res.* 63, 777–787. doi: 10.1071/MF12071

Uddin, M. N., and Robinson, R. W. (2017). Changes associated with *Phragmites australis* invasion in plant community and soil properties: a study on three invaded communities in a wetland, Victoria, Australia. *Limnologica* 66, 24–30. doi: 10.1016/j.limno.2017.07.006

Uddin, M. N., Robinson, R. W., Buultjens, A., Harun, M. A. Y. A., and Shampa, S. H. (2017). Role of allelopathy of *Phragmites australis* in its invasion processes. *J. Exp. Mar. Biol. Ecol.* 486, 237–244. doi: 10.1016/j.jembe.2016.10.016

Viola, D. V., Mordecai, E. A., Jaramillo, A. G., Sistla, S. A., Albertson, L. K., Gosnell, J. S., et al. (2010). Competition–defense trade-offs and the maintenance of plant diversity. *Proc. Natl. Acad. Sci. U.S.A.* 107, 17217–17222. doi: 10.1073/pnas.1007745107

Wang, X., Zhang, D., Guan, B., Qi, Q., and Tong, S. (2017). Optimum water supplement strategy to restore reed wetland in the Yellow River Delta. *PLoS One* 12, e0177692–e0177611. doi: 10.1371/journal.pone.0177692

Wang, S., Zhao, Z., Ge, S., Peng, B., Zhang, K., Hu, M., et al. (2021). Root morphology and rhizosphere characteristics are related to salt tolerance of *Suaeda salsa* and *Beta vulgaris* L. *Front. Plant Sci.* 12:677767. doi: 10.3389/fpls.2021.677767

Williamson, G. B., and Richardson, D. (1988). Bioassays for allelopathy: measuring treatment responses with independent controls. *J. Chem. Ecol.* 14, 181–187. doi: 10.1007/BF01022540

Yu, J., Li, Y., Han, G., Zhou, D., Fu, Y., Guan, B., et al. (2014). The spatial distribution characteristics of soil salinity in coastal zone of the Yellow River Delta. *Environ. Earth Sci.* 72, 589–599. doi: 10.1007/s12665-013-2980-0

Yuan, R., Li, Y., Li, J., Ji, S., Wang, S., and Kong, F. (2019). The allelopathic effects of aqueous extracts from *Spartina alterniflora* on controlling the *Microcystis aeruginosa* blooms. *Sci. Total Environ.* 66, 24–30. doi: 10.1016/j.limno.2017.07.006

Zhang, H., Hu, M., Ma, H., Jiang, L., Zhao, Z., Ma, J., et al. (2021). Differential responses of dimorphic seeds and seedlings to abiotic stresses in the halophyte *Suaeda salsa*. *Front. Plant Sci.* 12:630338. doi: 10.3389/fpls.2021.630338

Zhang, S., Wang, R., Zhang, Z., Guo, W., and Song, B. (2003). Study on morphological variation of *Phragmites Australis* in the Yellow River downstream wetland. *Acta Phytoecol. Sin.* 27, 78–85. doi: 10.17521/cjpe.2003.0012

Zhao, X., Cui, B., Sun, T., and He, Q. (2010). The relationship between the spatial distribution of vegetation and soil environmental factors in the tidal creek areas of the Yellow River Delta. *Ecol. Environ. Sci.* 36, 1150–1156. doi: 10.3724/SP.J.1035.2010.01150

frontiers | Frontiers in Plant Science

TYPE Original Research
PUBLISHED 21 September 2022
DOI 10.3389/fpls.2022.965426

OPEN ACCESS

EDITED BY
Bing Song,
Ludong University, China

REVIEWED BY
Bin Chen,
Nanjing Forestry University, China
Demin Zhou,
Capital Normal University, China

*CORRESPONDENCE
Lijuan Cui
wetlands108@126.com;
lkyclj@126.com

SPECIALTY SECTION
This article was submitted to Functional Plant Ecology, a section of the journal Frontiers in Plant Science

RECEIVED 09 June 2022
ACCEPTED 31 August 2022
PUBLISHED 21 September 2022

CITATION
Dou Z, Cui L, Li W, Lei Y, Zuo X, Cai Y and Yan R (2022) Effect of freshwater on plant species diversity and interspecific associations in coastal wetlands invaded by *Spartina alterniflora*.
Front. Plant Sci. 13:965426.
doi: 10.3389/fpls.2022.965426

Effect of freshwater on plant species diversity and interspecific associations in coastal wetlands invaded by *Spartina alterniflora*

Zhiguo Dou[1,2,3], Lijuan Cui[1,2]*, Wei Li[1,2,3], Yinru Lei[1,2,3], Xueyan Zuo[1,2], Yang Cai[1,2] and Rui Yan[4]

[1]Institute of Wetland Research, Chinese Academy of Forestry, Beijing, China, [2]Beijing Key Laboratory of Wetland Services and Restoration, Beijing, China, [3]Institute of Ecological Conservation and Restoration, Chinese Academy of Forestry, Beijing, China, [4]Yancheng Milu Institute, Jiangsu Dafeng Père David's Deer National Nature Reserve, Yancheng, China

Plant invasions in coastal wetlands lead to the degradation of native vegetation; the introduction of freshwater in coastal wetlands would prevent the spread of invasive plants and facilitate the restoration of native vegetation. In this study, we evaluated the effects of freshwater on plant communities in the coastal wetlands of Yancheng, China, invaded by *Spartina alterniflora* Loisel. Two field investigations were conducted in 2008 and 2018 before and after the introduction of freshwater (started in 2011). The characteristics of plant communities were subjected to hierarchical cluster analysis and compared using several diversity indices. In addition, differences in habitat community composition and interspecific relationships of dominant species were analyzed. The results showed that *S. alterniflora* reduced the overall species diversity in the region. Plant species diversity increased after freshwater was introduced into the study site when compared to the areas without freshwater introduction. The introduction of freshwater caused a shift often changes in the interspecific relationships between *Suaeda salsa* (L.) Pall. and other species. The intensified invasion of *S. alterniflora* changed the interspecific relationship of native halophytes from negative to positive. Although freshwater effectively inhibited further invasion of *S. alterniflora*, it also increased the risk of expansion of the glycophytes in the community. The results of this study highlight the need for early intervention for restoration of coastal wetlands, preservation of biodiversity, and management of plant resources.

KEYWORDS

coastal wetland, invasive plants, biodiversity, freshwater, restoration

Introduction

Biological invasions drive global changes in ecosystems (Vitousek, 1997; Mooney and Hobbs, 2000), which cause huge economic losses (Pimentel et al., 2000; Courtois et al., 2017) and lead to serious ecological and evolutionary consequences (Li et al., 2009; Ehrenfeld, 2010; He et al., 2020; Ren et al., 2021), including loss of biodiversity and alteration of the structure and function of the invaded ecosystem (Schirmel et al., 2016; Osborne and Gioria, 2018; Stephanie et al., 2018; Vaz et al., 2018; Giulio et al., 2022). Coastal wetland ecosystems are one of the habitats most vulnerable to alien species invasion (Zedler and Kercher, 2004; Bradley et al., 2010; Gillard et al., 2021). *Spartina alterniflora* Loisel. is a common invasive plant occurring in coastal salt marsh ecosystems (Daehler and Strong, 1996; Takahashi et al., 2019), the invasion range of which includes the coastal areas of China, France, the United Kingdom, Spain, Australia, New Zealand, and South Africa (Riddin et al., 2016; Meng et al., 2020; Yan et al., 2022). Efforts have been made worldwide to reduce the impact of *S. alterniflora* invasion and to restore local ecosystems (Diefenderfer et al., 2018; Zhao et al., 2019; Chen et al., 2020).

Wetland ecological restoration engineering is an important field that focuses on restoring wetland ecology and improving its ecological structure, processes, and functions (Daily et al., 2009; Glenn et al., 2013; Davies et al., 2014; Xie et al., 2021). Wetland ecological water replenishment has significantly enhanced the regulation and support of plant species in wetland ecosystems (Cui et al., 2009; Restrepo and Cantera, 2013; Demarco et al., 2022). In coastal wetlands, the introduction of freshwater facilitates the biodiversity restoration in addition to ecological replenishment (Proosdij et al., 2010; Cui et al., 2018; Yang et al., 2019; Huang et al., 2020). Ecological management practices have shifted the focus from removing the invasive species alone to monitoring and restoring the entire ecosystem (Zavaleta et al., 2001; Remm et al., 2019). In wetland ecosystem monitoring, plant communities are among the main indicators of invasion in comparative studies before and after restoration (Giljohann et al., 2011; Nicol et al., 2017; Arnoldi et al., 2022). Therefore, it is essential to investigate the characteristics of the coastal wetland plant communities invaded by *S. alterniflora* before and after restoration.

S. alterniflora has been studied extensively as an invasive species; however, most of the studies have focused on the impact of *S. alterniflora* invasion on native species in coastal wetlands without ecological restoration measures (Minchinton et al., 2006; Gerwing et al., 2021; Yue et al., 2021). Some studies have found that freshwater introduction leads to more obvious community zonality of coastal wetlands (Cui et al., 2018). After the introduction of freshwater, the diversity of plant communities first increased and then decreased, whereas the dominant salt-tolerant and halophytic plant species were gradually replaced by glycophytic plants (Cui et al., 2009; Duarte et al., 2015). Studies on the long-term invasion of *S. alterniflora* have focused on quantifying the temporal dynamics where the spread of S. alterniflora and subsequent elimination of native species was monitored over a period of time (Tang et al., 2012; Liu et al., 2017; Zhang et al., 2020; Yan et al., 2021). However, few studies have focused on the effects of freshwater introduction measures on plant diversity and interspecific associations in coastal wetlands invaded by *S. alterniflora*.

S. alterniflora was first artificially introduced in Yancheng, China, in 1979 (Li et al., 2005). After long-term expansion, the coastal wetlands of Yancheng currently experience a significant biological invasion by *S. alterniflora* (Gu et al., 2018; Meng et al., 2020; Zuo et al., 2021). To preserve the biodiversity and to control *S. alterniflora* invasion in the region, the Chinese government has been implementing ecological hydrological engineering, including freshwater introduction, in Dafeng Père David's Deer National Nature Reserve since 2011 (Yan et al., 2021). In this study, we documented the plant community composition in the region by *in situ* investigation in 2008 and 2018. To assess the possible consequences of freshwater introduction on the plant communities invaded by *S. alterniflora,* we analyzed species diversity and interspecific associations at the study sites. The results of this study will help to develop strategies for controlling of *S. alterniflora* invasion and improve the management of coastal wetland ecosystem biodiversity.

Materials and methods

Study sites

Dafeng Père David's Deer (*Elaphurus davidianus*) National Nature Reserve (32°58′-33°03′N, 120°47′-120°53′E) is a Ramsar site located in the Yellow Sea in the eastern part of Yancheng City, Jiangsu Province, China (Figure 1A), covering an area of 26.67 km^2. This region experiences a marine monsoon climate and belongs to the transition zone between the north subtropical and a warm temperate zone; it is characterized by an average annual precipitation of 1,068 mm and an average annual temperature of 14.1°C (Zuo et al., 2021; Yan et al., 2022).

Through the central wetland subsidy project, ecological hydrological engineering measures were implemented by the government in the coastal wetland (third core) area of the reserve. In 2011, a dyke with a length of approximately 2.3 km was built in the middle of the third core area (Yan et al., 2021), dividing the third core area into sites A and B (Figure 1A). Freshwater was introduced into site A, whereas site B remained in its natural state. Site A was not completely enclosed and thus could still be affected by high tidal action. To enhance the restoration effect of freshwater introduction, a 10 km artificial freshwater ditch was built at site A in 2016. In

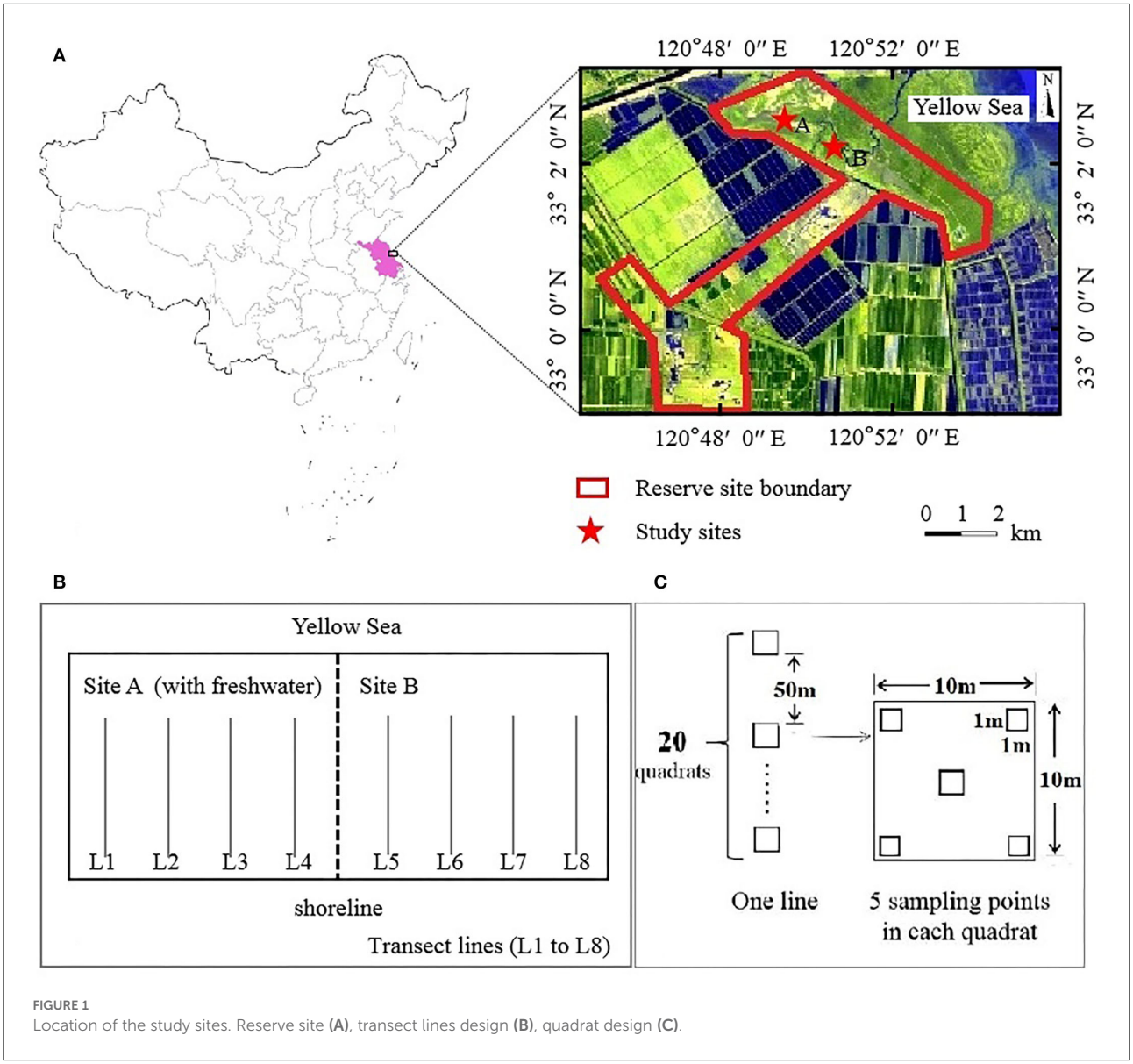

FIGURE 1
Location of the study sites. Reserve site **(A)**, transect lines design **(B)**, quadrat design **(C)**.

summary, site A had a continuous influx of freshwater, which is occasionally affected by seawater. Site B was maintained in a tidal-action environment.

Field investigation

Eight parallel transect lines (L1–L8) running perpendicular to the shoreline were marked for sampling at the study sites A and B; four transect lines were used per study site (Figure 1B). All parallel transect lines had 20 quadrats (Q01–Q20, with an area of 10 × 10 m) with a 50 m gap between each quadrat. Five uniformly spaced sampling points with an area of 1 m × 1 m were marked within each quadrat (Figure 1C). The quadrat was named as L×Q××. The plant species, total coverage, partial coverage, plant height, and number of plants (clumps) were recorded in each quadrat. Based on the changes in the dominant species, we estimated growth gradients among plant communities extending from the shoreline to nearshore. Two surveys were conducted in mid-August 2008 (before the introduction of freshwater) (completed by engineers working in the reserve) and mid-August 2018 (after the introduction of freshwater).

Statistical analysis

The importance value (*IV*) was calculated to characterize the wetland plant communities. Hierarchical clustering analysis was used to study the community types of coastal wetland

vegetation (Lemein et al., 2017; Gaberščik et al., 2018). The following four indices were calculated to assess the species diversity: species richness (S), Shannon–Wiener index (H), Simpson's diversity index (D), and Pielou evenness index (J). The differences in the species diversity indices between different study sites were analyzed using one-way analysis of variance with the level of significance defined at 0.05. The interspecific relationship of the dominant species was analyzed using the dominant species pair correlation test and the degree of inter-species association (Stachowicz, 2001; Turnbull et al., 2004). Between-habitat diversity (beta diversity, β) and principal coordinate analysis (PCoA) (Bray–Curtis coefficient was used as the similarity index) were used to compare the community composition of different habitats (Costa et al., 2011). The distribution and changes in the communities were analyzed by calculating the ratio of the number of each vegetation type to the total number of quadrats. All the above parameters were computed using IBM SPSS Statistics (version 22.0; SPSS Inc., Chicago, IL, USA) and R (version 3.5.2, R Foundation for Statistical Computing).

$$\begin{aligned} IV &= (\text{relative density} + \text{relative coverage} \\ &+ \text{relative frequency})/3 \\ H &= -\sum_{i=1}^{s} P_i \log_2 P_i \\ D &= 1 - \sum_{i=1}^{s} \frac{N_i\,(N_i - 1)}{N\,(N-1)} \\ J &= \frac{-\sum P_i \ln P_i}{\ln S} \end{aligned}$$

where S is the number of species (mean among quadrats), P_i is the ratio of individuals of species i to total individuals of all species, N_i is the number of individuals of species i, and N is the individual number of all species in the community.

The interspecific relationship of the dominant species was assessed using the dominant species pair correlation test—chi-square test (Table 1).

$$x^2 = \frac{N\left(|ad - bc| - \frac{N}{2}\right)^2}{(a+b)\,(c+d)\,(a+c)\,(b+d)}$$

where ad - $bc > 0$, the two species are positively related; ad - $bc < 0$, the two species are negatively related; and ad - $bc = 0$, the two species are independent of each other. If $x^2 > 6.635$, the connection between the two species is extremely significant; if $3.841 < x^2 < 6.635$, the connection between the two species is significant; and if $x^2 < 3.841$, the connection between the two species is not significant.

The degree of inter-species association was calculated using the association coefficient (AC), as follows:

$$\begin{aligned} ad \geq bc, \text{then AC} &= (ad - bc)/[(a+b)(b+d)], \\ ad < bc, \text{and } d \geq a, \text{then AC} &= (ad - bc)/[(a+b)(a+c)], \\ ad < bc, \text{and } d < a, \text{then AC} &= (ad - bc)[(b+d)(d+c)], \end{aligned}$$

where AC represents the strength of inter-species association. An AC value closer to 1 represents a strong positive association between two species, whereas that close to −1 indicates a negative association; for AC = 0, the two species appear alone.

The between-habitat diversity index was calculated using the β_{jk}, as follows:

$$\beta_{jk} = \frac{e+f}{2d+e+f}$$

where d is the number of species shared by the two quadrats, e is the number of species present in quadrat j but not in quadrat k, and f is the number of species present in quadrat k but not in quadrat j.

Results

Characteristics and changes of species composition

The field investigation in 2008 performed before the introduction of freshwater recorded 13 species, belonging to five families and 12 genera of site A; similar results were observed in site B (Figure 2). All plants were herbaceous angiosperms comprising four halophytes, four salt-tolerant species, and five glycophytes. Poaceae species were the most common, and they included *S. alterniflora*, *Zoysia macrostachya* Franch. et. Sav., *Phragmites australis* Trin., *Imperata cylindrica* (L.) P. Beauv., and *Aeluropus sinensis* (Debeaux) Tzvelev. Three species belonged to Asteraceae [*Aster subulatus* (Michx.) G. L. Nesom, *Erigeron annuus* (L.) Pers., and *Ixeris japonica* (Burm. f.) Nakai], two species were from Amaranthaceae [*Suaeda salsa* (L.) Pall. and *Suaeda glauca* (Bunge) Bunge], and Polygonaceae, Plumbaginaceae, and Cyperaceae were each represented by one species [*Persicaria lapathifolium* (L.) S. F. Gray, *Limonium sinense* (Girard) Kuntze, and *Carex scabrifolia* Steud., respectively].

In 2018, 26 species were identified in site A, which is a significant increase in species number from that observed in 2008. The 26 species belonged to eight families and 25 genera, including those identified in 2008. The 13 newly species identified in 2018 were included in Apocynaceae (*Cynanchum chinense* R. Br.), Asteraceae (*Artemisia capillaris*

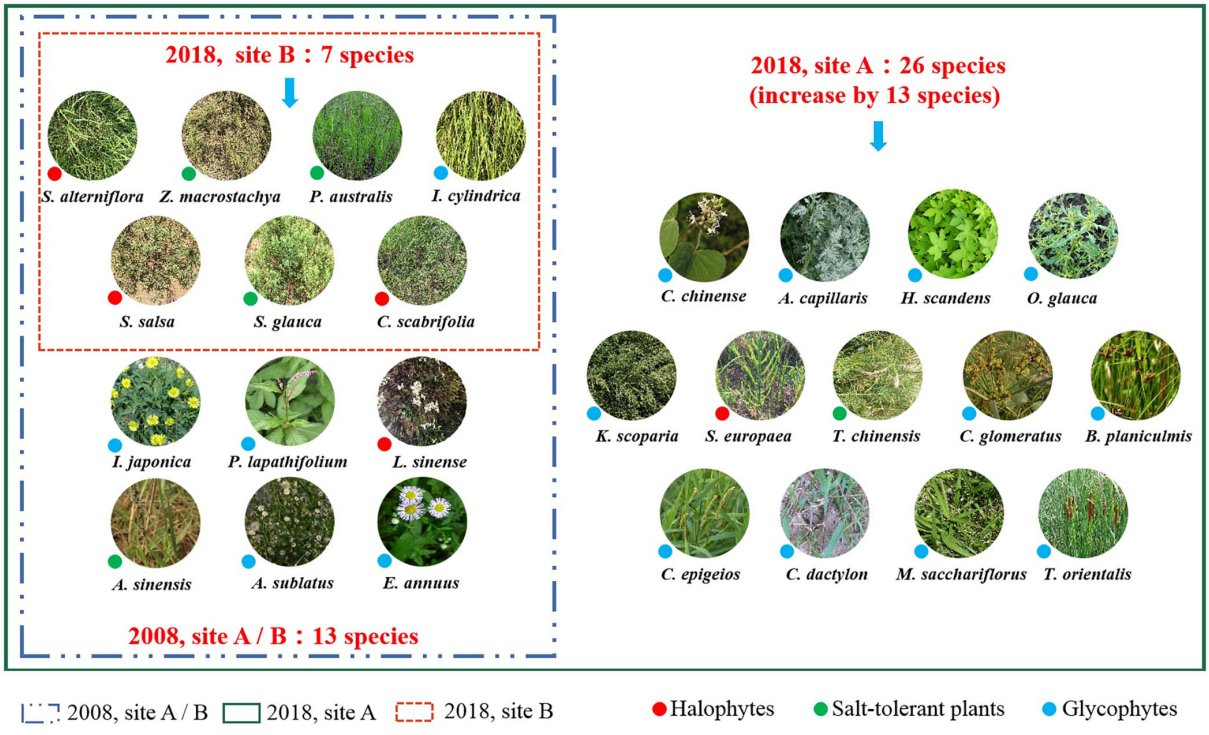

FIGURE 2
Differences in species composition between 2008 and 2018.

Thunb.), Cannabaceae [*Humulus scandens* (Lour.) Merr.], Amaranthaceae [*Oxybasis glauca* (L.) S. Fuentes, Uotila & Borsch, *Kochia scoparia* (L.) Schrad., and *Salicornia europaea* L.], Tamaricaceae (*Tamarix chinensis* Lour.), Cyperaceae [*Cyperus glomeratus* L. and *Bolboschoenus planiculmis* (F. Schmidt) T. V. Egorova], Poaceae [*Calamagrostis epigejos* (L.) Roth, *Cynodon dactylon* (L.) Persoon, and *Miscanthus sacchariflorus* (Maxim.) Benth. & Hook. f. ex Franch.], and Typhaceae (*Typha orientalis* C. Presl). After the introduction of freshwater, the number of halophytes and salt-tolerant plants increased from four to five, and the number of glycophytes increased from five to 16 (Figure 2).

In site B in 2018, seven species belonging to three families and six genera were identified. Four species belonged to Poaceae (*S. alterniflora*, *P. australis*, *I. cylindrica,* and *A. sinensis*), two species belonged to Amaranthaceae (*S. salsa* and *S. glauca*), and one species belonged to Cyperaceae (*C. scabrifolia*). The species composition of the wetland plant communities in site B was relatively simpler compared to that measured in 2008. After the distribution of *S. alterniflora* expanded, the number of halophytes and salt-tolerant species decreased by one species (*L. sinense* and *A. sinensis*, respectively), and the number of glycophytes decreased by four species (*I. japonica*, *P. lapathifolium*, *A. subulatus,* and *E. annuus*) (Figure 2).

Changes in types of plant communities

The plant communities were categorized according to the importance values (*IV*) of the species within each quadrat. In 2008, seven settlement clusters (Figure 3) were identified: *S. salsa* (site A, 30%; site B, 28.75%), *P. australis* (site A, 22.5%; site B, 7.5%), *S. alterniflora* (site A, 15%; site B, 15%), *Z. macrostachya* (site A, 12.5%; site B, 18.75%), *I. cylindrica* (site A, 7.5%; site B, 10%), *C. scabrifolia* (site A, 7.5%; site B, 11.25%), and *A. sinensis* (site A, 5%; Site B, 8.75%).

The first settlement cluster (A) contained 48 quadrats (site A, 25; site B, 23). *S. salsa* was the dominant species in this community. There were 28 quadrats (site A, 13; site B, 15) in which *S. salsa* was the only species detected. There were nine quadrats (site A, 2; site B, 7) of *P. australis* associated with *S. salsa* and seven quadrats (site B) of *S. glauca* associated with *S. salsa*. The remaining five quadrats (site A, 4; site B, 1) contained the association of *P. lapathifolium*, *A. subulatus,* and *L. sinense*. The community represented in cluster (A) was located far from the nearshore environment at an average distance of 800 m.

The second settlement cluster (B) consisted of 36 quadrats (site A, 30; site B, 6). *P. australis* was the dominant species in the community, with 19 quadrats (site A) containing only *P. australis*. Four quadrats (site A, 3; site B, 1) contained *P. australis*

10.3389/fpls.2022.965426

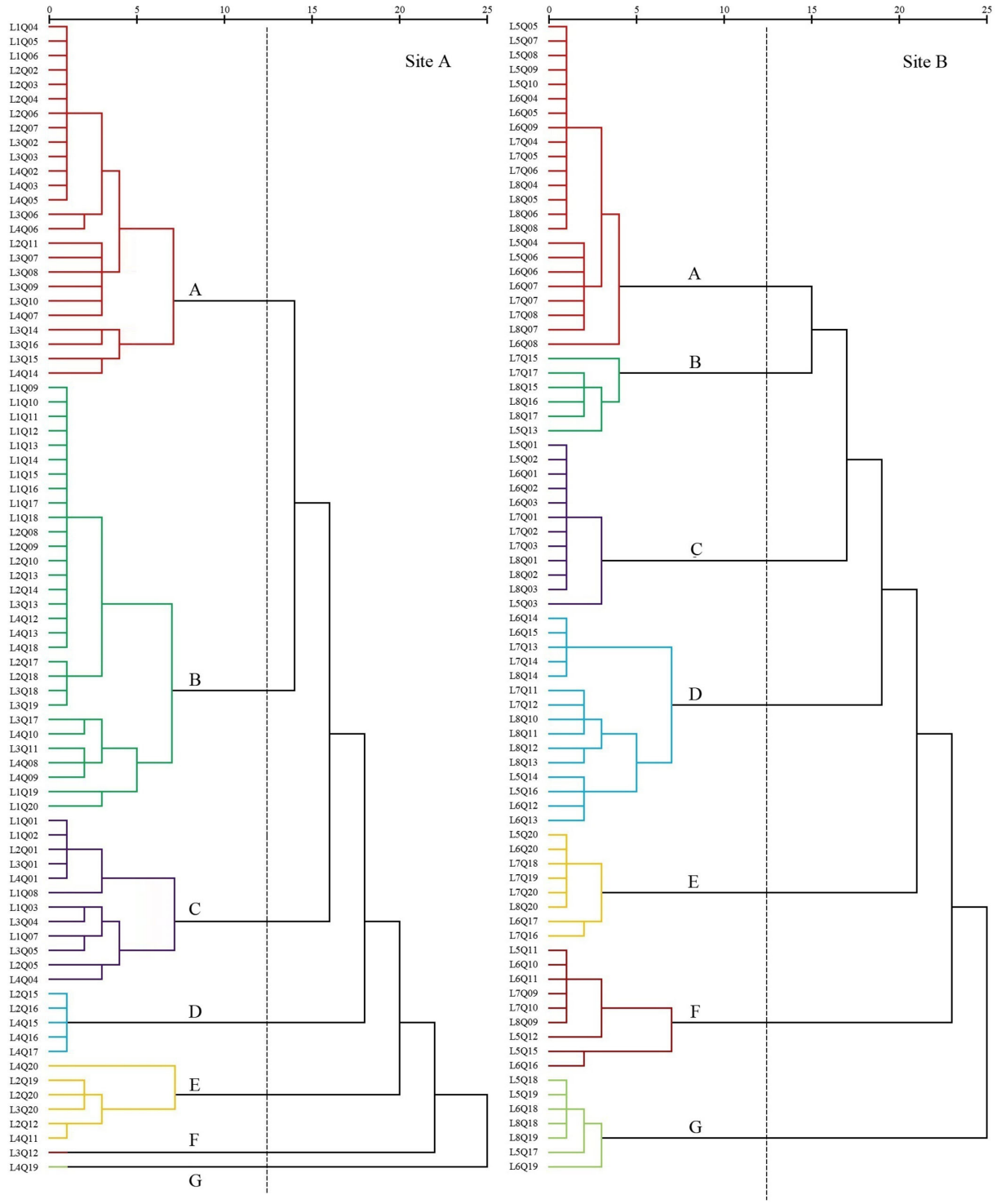

FIGURE 3
Dendrogram of coastal wetland vegetation based on cluster analysis of data collected in 2008.

associated with *S. glauca,* and nine quadrats (site A, 5; site B, 4) included *P. australis* associated with *S. salsa* or *I. cylindrica*. The remaining three quadrats (site A, 2; site B, 1) contained associations of *E. annuus*, *A. subulatus*, *I. japonica,* and *Z. macrostachya*. Settlement cluster (B) was located proximally to the nearshore.

The third settlement cluster (C) consisted of 24 quadrats (site A, 12; site B, 12). *S. alterniflora* was the dominant species in the community, and 16 quadrats (site A, 5; site B, 11) contained only *S. alterniflora*. The other eight quadrats (site A, 7; site B, 1) included *S. salsa*, *S. glauca*, *C. scabrifolia,* and *P. australis*. Settlement cluster (C) was located farthest from the nearshore of all the defined groups.

The fourth settlement cluster (D) included 20 quadrats (site A, 5; site B, 15). *Z. macrostachya* was the dominant species in the community, with 10 quadrats (site A, 5; site B, 5) of *Z. macrostachya* as a single species. The other 10 quadrats (site B) contained the association of *S. salsa*, *S. glauca,* and *C. scabrifolia*. This community was centrally located in the sample line.

The fifth settlement cluster (E) contained 14 quadrats (site A, 6; site B, 8). *I. cylindrica* was the dominant species in the community, and eight quadrats (site A, 2; site B, 6) contained only *I. cylindrica.* The remaining six quadrats (site A, 4; site B, 2) contained an association of *P. australis*, *C. scabrifolia,* and *L. sinense*. This community was located closest to the nearshore.

The sixth settlement cluster (F) included 10 quadrats (site A, 1; site B, 9). *C. scabrifolia* was the dominant species in the community, accounting for seven single-species quadrats (site A, 1; site B, 6). The remaining three quadrats (site B) were associated with *I. cylindrica* and *S. salsa*. This community was centrally located in the sample line.

The seventh settlement cluster (G) contained eight quadrats (site A, 1; site B, 7). *A. sinensis* was the dominant species in the community, and six quadrats (site A, 1; site B, 5) contained only *A. sinensis*. The other two quadrats (site B) were *A. sinensis* associated with *I. cylindrica* and *S. salsa*. This community was located proximally to the nearshore. The average distance is less than 100 m.

In site A in 2018, freshwater introduction resulted in 10 settlement cluster (Figure 4) with dominant species including *S. salsa* (20%), *P. australis* (20%), *S. alterniflora* (13.75%), *Z. macrostachya* (2.5%), *I. cylindrica* (18.75%), *C. scabrifolia* (8.75%), *A. sinensis* (1.25%), *M. sacchariflorus* (7.5%), *T. chinensis* (3.75%), and *S. europaea* (3.75%).

The first settlement cluster (A) included 16 quadrats. *S. salsa* was the dominant species in the community. There were 10 quadrats containing only *S. salsa*, accounting for 63%. The remaining six quadrats were *S. salsa* associated with *S. europaea*, *P. lapathifolium*, *P. australis*, and *L. sinense*. This community was located far from the nearshore.

The second settlement cluster (B) contained 16 quadrats. *P. australis* was the dominant species in the community. There were six quadrats containing only *P. australis*. There were four quadrats of *P. australis* associated with *I. cylindrica* and two quadrats of *P. australis* associated with *S. salsa*. The remaining four quadrats were associated with *E. annuus*, *A. subulatus*, *I. japonica*, *O. glauca*, *K. scoparia*, *T. orientalis*, and *Z. macrostachya*. This community was located proximally to the nearshore.

The third settlement cluster (E) included 15 quadrats. *I. cylindrica* was the dominant species in the community. Seven quadrats contained only *I. cylindrica*. The remaining eight quadrats were associated with *P. australis*, *C. scabrifolia*, *M. sacchariflorus*, *C. epigejos*, *A. capillaris*, *G. aparine*, *E. annuus*, *H. scandens*, and *C. chinense*. This community was closest to the nearshore.

The fourth settlement cluster (C) contained 11 quadrats. *S. alterniflora* was the dominant species in the community. Six quadrats contained only *S. alterniflora*, accounting for 55%. The remaining five quadrats were associated with *S. salsa*, *S. glauca*, and *C. scabrifolia*. This community was located the farthest from the nearshore.

The fifth settlement cluster (F) contained seven quadrats. *C. scabrifolia* was the dominant species in the community. The remaining four quadrats were associated with *S. europaea*, accounting for 57%. The remaining three quadrats were associated with *I. cylindrica*, *S. europaea*, *B. planiculmis*, *C. glomeratus*, and *S. salsa*. This community was centrally located in the sample line.

The sixth settlement cluster (H) contained six quadrats. *M. sacchariflorus* was the dominant species in the community, and four quadrats contained only *M. sacchariflorus*, accounting for 67%. The remaining two quadrats were associated with *I. cylindrica* and *P. australis*. This community was close to the nearshore.

The seventh settlement cluster (I) included three quadrats. *S. europaea* was the dominant species in the community, and all quadrats included *S. salsa*. This community was close to the nearshore.

The eighth settlement cluster (J) included three quadrats. *T. chinensis* was the dominant species in the community, and all quadrats included *I. cylindrica* and *S. salsa*. This community was close to the nearshore.

The ninth settlement cluster (D) consisted of two quadrats. *Z. macrostachya* was the dominant species in the community, and all quadrats also contained *C. dactylon*. This community was located in the middle of the sample line.

The tenth settlement cluster (G) consisted of one quadrat. *A. sinensis* was the dominant species in the community, and the quadrat contained only *A. sinensis*. This community was close to the nearshore.

In site B in 2018, without freshwater introduction contained six settlement cluster (Figure 4), with dominant species including *S. salsa* (20%), *P. australis* (5%), *S. alterniflora* (60%), *C. scabrifolia* (7.5%), *I. cylindrica* (3.75%), and *Z. macrostachya* (3.75%).

The first settlement cluster (C) contained 48 quadrats. *S. alterniflora* was the dominant species in the community, and 39 quadrats contained only *S. alterniflora*, accounting for 81% of the quadrats. The other nine quadrats were associated with *S. salsa*, *S. glauca*, and *C. scabrifolia*. This community was farthest from the nearshore.

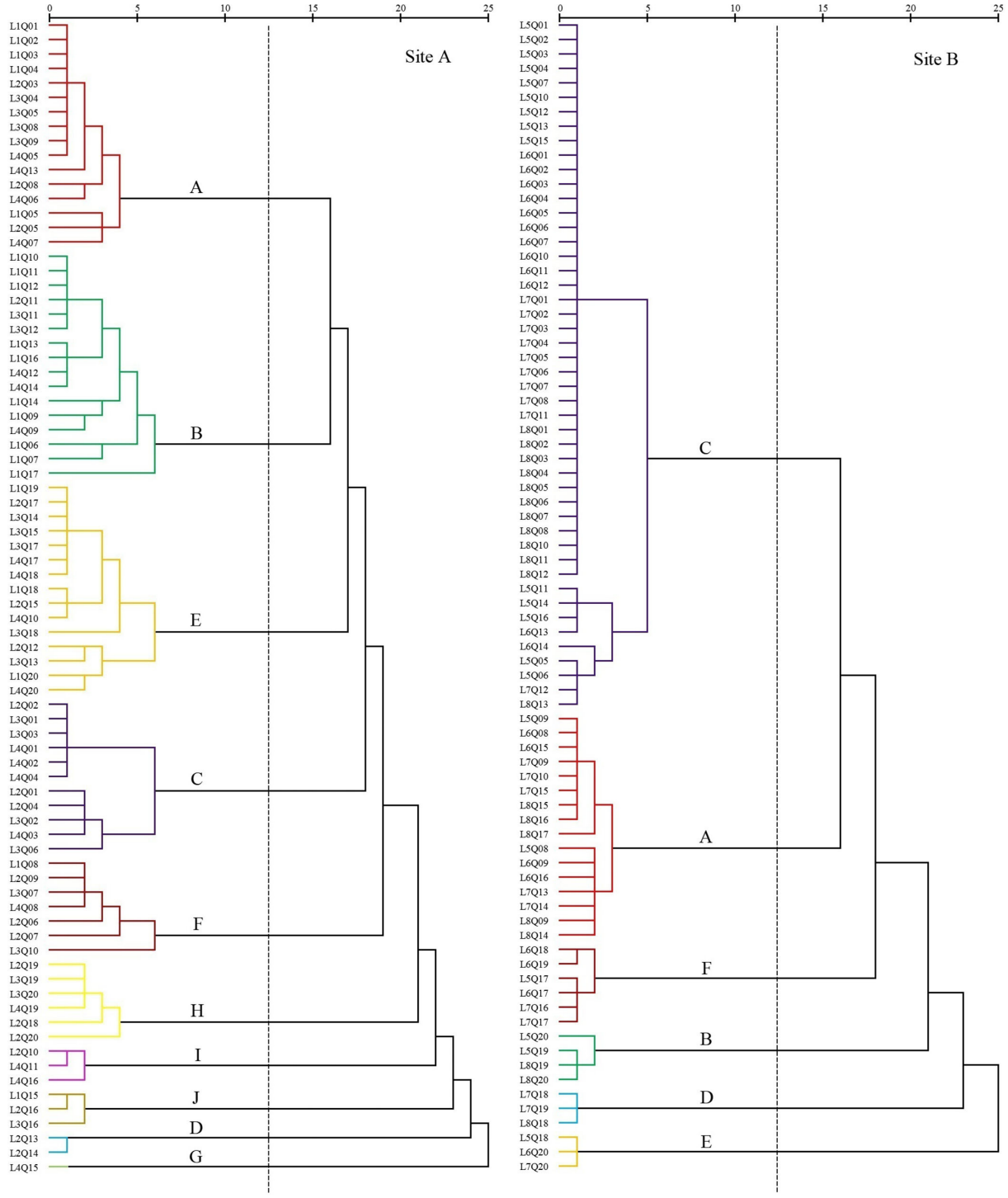

FIGURE 4
Dendrogram of coastal wetland vegetation based on cluster analysis of data collected in 2018.

The second settlement cluster (A) contained 16 quadrats. *S. salsa* was the dominant species, and eight quadrats contained only *S. salsa*, accounting for 50%. There were seven quadrats of *S. alterniflora* associated with *S. salsa* and one quadrat containing *Z. macrostachya* associated with *S. salsa*. This community was far from the nearshore. This community was located in the middle of the sample line.

10.3389/fpls.2022.965426

TABLE 1 Determination of inter-species association 2×2 contingency table.

Species		Species B		Statistics
		Occurring (1)	Not occurring (0)	
Species A	Occurring (1)	a	b	a+b
	Not occurring (0)	c	d	c+d
	Statistics	a+c	b+d	N=a+b+c+d

The third settlement cluster (F) contained six quadrats. *C. scabrifolia* was the dominant species, and two quadrats contained only *C. scabrifolia*. The other four quadrats contained *C. scabrifolia* associated with *S. salsa*. This community was close to the nearshore. The average distance is less than 150 m.

The fourth settlement cluster (B) contained four quadrats. *P. australis* was the dominant species in the community, and one quadrat contained only *P. australis*. There are three quadrats of *P. australis* associated with *I. cylindrica*. This community was very close to the nearshore.

The fifth settlement cluster (D) consisted of three quadrats. *Z. macrostachya* was the dominant species in the community, and one quadrat contained *A. sinensis* as a single species. The other two quadrats were *Z. macrostachya* associated with *C. scabrifolia* and *S. salsa*. This community was close to the nearshore. The average distance is less than 150 m.

The sixth settlement cluster (E) consisted of three quadrats. *I. cylindrica* was the dominant species in the community. There were three quadrats of *I. cylindrica* as a single species. This community was closest to the nearshore.

Changes in plant species diversity

As shown in Table 2, species diversity in the coastal wetland plant communities was generally low. In 2018, although the plant species diversity at site A increased (based on the *S* index for settlement clusters B, C, D, E, and F; *H* index for settlement clusters B, C, E, and F; and *D* index for settlement clusters B, C, and E) following the introduction of freshwater, the overall species diversity of the coastal wetland vegetation remained low. In addition, in site B, we observed a reduction in species diversity (*S* index for settlement clusters A, B, C, and E and *H* index and *D* index for settlement clusters C and E) without freshwater introduction compared with that in 2008.

In 2008, there was no significant difference in the species diversity of plant communities at sites A and B. We observed differences in diversity indices of different communities (Table 2). There were no significant differences in species richness (*S*) among the communities. According to the Shannon–Wiener index (*H*) and Simpson's diversity index (*D*), the species diversity of the *S. alterniflora* and *Z. macrostachya*

TABLE 2 Species diversity of plant communities in coastal wetlands invaded by *S. alterniflora*.

Settlement cluster	*S*				*H*				*D*				*J*			
	2008		2018		2008		2018		2008		2018		2008		2018	
	Site A	Site B	Site A	Site B	Site A	Site B	Site A	Site B	Site A	Site B	Site A	Site B	Site A	Site B	Site A	Site B
A (*S. salsa*)	1.52 ± 0.54 ns	1.52 ± 0.48 ns	1.41 ± 0.49 *	1.50 ± 0.50 ns	0.20 ± 0.24 ns	0.21 ± 0.22 ns	0.15 ± 0.18 *	0.45 ± 0.46 *	0.12 ± 0.15 ns	0.12 ± 0.12 ns	0.08 ± 0.11 *	0.28 ± 0.29 *	0.84 ± 0.19 ns	0.86 ± 0.17 ns	0.80 ± 0.25 *	0.95 ± 0.07 *
B (*P. australis*)	1.70 ± 0.82 ns	1.65 ± 0.82 ns	1.81 ± 0.75 *	1.63 ± 0.43 ns	0.29 ± 0.32 ns	0.27 ± 0.35 ns	0.33 ± 0.28 *	0.67 ± 0.39 *	0.19 ± 0.21 ns	0.18 ± 0.18 ns	0.21 ± 0.18 ns	0.43 ± 0.25 *	0.92 ± 0.11 ns	0.89 ± 0.14 ns	0.84 ± 0.17 *	0.95 ± 0.04 ns
C (*S. alterniflora*)	1.33 ± 0.47 ns	1.33 ± 0.47 ns	1.45 ± 0.50 *	1.17 ± 0.37 *	0.19 ± 0.27 ns	0.18 ± 0.32 ns	0.23 ± 0.25 *	0.12 ± 0.27 *	0.13 ± 0.18 ns	0.16 ± 0.17 ns	0.15 ± 0.16 ns	0.11 ± 0.26 ns	0.94 ± 0.09 ns	0.97 ± 0.10 ns	0.88 ± 0.13 *	0.95 ± 0.11 ns
D (*Z. macrostachya*)	1.28 ± 0.45 ns	1.50 ± 0.50 ns	1.50 ± 0.50 ns	2.00 ± 0.82 *	0.30 ± 0.30 ns	0.32 ± 0.20 ns	0.14 ± 0.14 *	0.49 ± 0.40 *	0.21 ± 0.21 ns	0.23 ± 0.25 ns	0.08 ± 0.08 *	0.31 ± 0.22 *	0.94 ± 0.07 ns	0.95 ± 0.06 ns	0.71 ± 0.29 *	0.97 ± 0.03 ns
E (*I. cylindrica*)	1.41 ± 0.41 ns	1.43 ± 0.48 ns	1.80 ± 0.98 *	1.00 ± 0.00 *	0.21 ± 0.25 ns	0.19 ± 0.18 ns	0.25 ± 0.25 ns	0.00 ± 0.00 *	0.13 ± 0.16 ns	0.12 ± 0.14 ns	0.14 ± 0.13 ns	0.00 ± 0.00 *	0.88 ± 0.15 ns	0.90 ± 0.15 ns	0.76 ± 0.23 *	1.00 ± 0.00 *
F (*C. scabrifolia*)	1.00 ± 0.00 ns	1.34 ± 0.46 ns	1.43 ± 0.49 ns	1.67 ± 0.47 *	0.17 ± 0.24 ns	0.22 ± 0.25 ns	0.18 ± 0.21 ns	0.56 ± 0.39 *	0.11 ± 0.16 ns	0.11 ± 0.10 ns	0.11 ± 0.13 ns	0.41 ± 0.29 *	0.91 ± 0.12 ns	0.90 ± 0.11 ns	0.83 ± 0.19 *	0.89 ± 0.08 ns
G (*A. sinensis*)	1.00 ± 0.00 ns	1.29 ± 0.43 ns	1.00 ± 0.00 ns	—	0.14 ± 0.24 ns	0.15 ± 0.16 ns	0.00 ± 0.00 *	—	0.09 ± 0.16 ns	0.09 ± 0.15 ns	0.00 ± 0.00 *	—	0.95 ± 0.08 ns	0.98 ± 0.07 ns	1.00 ± 0.00 ns	—
H (*M. sacchariflorus*)	—	—	1.33 ± 0.47	—	—	—	0.17 ± 0.24	—	—	—	0.11 ± 0.16	—	—	—	0.91 ± 0.13	—
I (*S. europaea*)	—	—	1.33 ± 0.47	—	—	—	0.14 ± 0.20	—	—	—	0.09 ± 0.12	—	—	—	0.87 ± 0.18	—
J (*T. chinensis*)	—	—	1.33 ± 0.50	—	—	—	0.18 ± 0.26	—	—	—	0.06 ± 0.08	—	—	—	0.93 ± 0.10	—

"ns," not significant; asterisk indicates significant differences at $P < 0.05$.

communities was higher than that of other communities. Each community had a higher Pielou's evenness index (*J*).

In 2018, among the 80 quadrats at site A, 43 quadrats (accounting for 53.75%) contained a single species. The *S* index of the *S. salsa* communities decreased slightly; no change was detected in the case of *Z. macrocephala* and *A. sinensis* communities, whereas *S* of the other communities increased significantly. According to the diversity indices *H* and *D*, the diversity of the *P. australis* community was higher than that of other communities. Compared with the values in 2008, the species diversity of the other three vegetation communities was not high. *J* index was high, but compared to 2008, it was reduced in all communities except that of *A. sinensis*.

In 2018, among the 80 quadrats in site B, 55 quadrats (accounting for 68.75%) comprised a single species. The *S* index of the *P. australis*, *Z. macrostachya*, and *C. scabrifolia* communities increased, while that of *S. salsa*, *S. alterniflora*, and *I. cylindrica* communities decreased. According to *H* and *D* indices, the diversity of the *S. alterniflora* and *I. cylindrica* communities decreased significantly, whereas other communities showed a significant increase in diversity. Only the *J* of *C. scabrifolia* decreased slightly and that of the other communities was >0.95, indicating a significant increase.

Analysis of between-habitat diversity values showed a value of zero between site A and site B in 2008; the value of site A between 2008 and 2018 was 0.33, the value of site B between 2008 and 2018 was 0.30, and the value between site A and site B in 2018 was 0.40. Both the introduction of freshwater and further invasion by *S. alterniflora* resulted in the replacement of native community, with the introduction of the freshwater

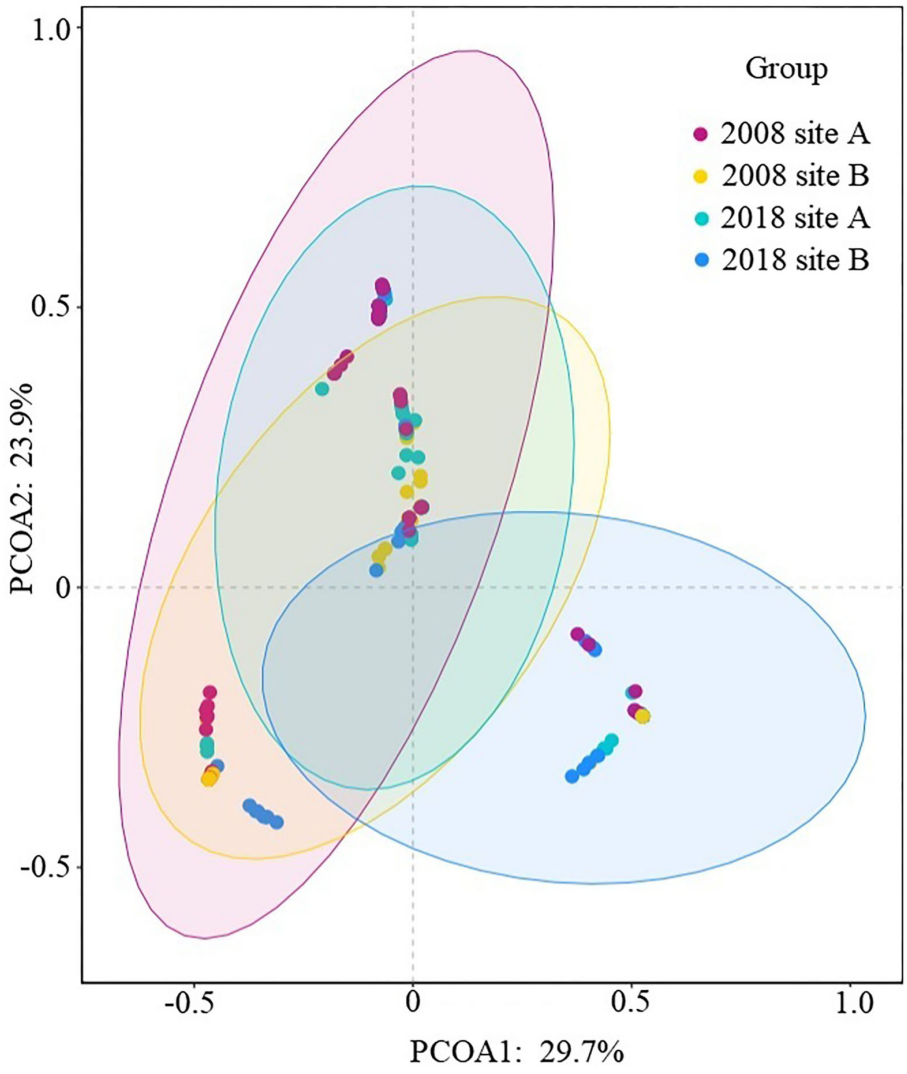

FIGURE 5
Similarity in species composition in coastal wetlands.

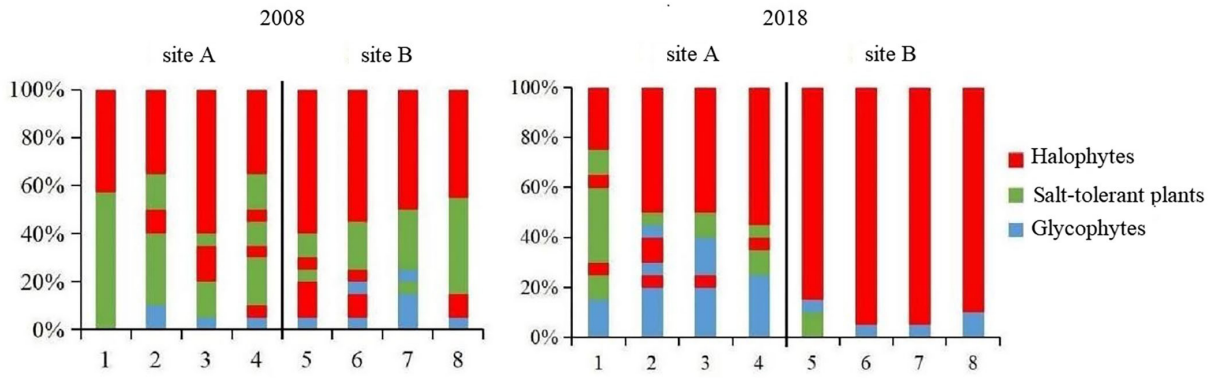

FIGURE 6
Distribution of vegetation types in coastal wetlands.

showing a faster replacement rate. Analysis of similarity in species composition in the coastal wetlands (Figure 5) showed that the plant species composition in site B in 2018 was markedly separated from that of the other three groups, thus indicating a different species composition.

Growth gradient among plant communities

The dominant species in the coastal wetland vegetation can be divided into three types, namely halophytes, salt-tolerant plants, and glycophytes, as it extends from the shoreline to the nearshore. *S. salsa*, *S. alterniflora*, *C. scabrifolia*, *S. europaea,* and *L. sinense* are halophytes. *P. australis*, *Z. macrostachya*, *T. chinensis*, *S. glauca,* and *A. sinensis* are salt-tolerant plants, and the other species such as *I. cylindrica*, *A. sublatus*, *E. annuus*, *I. japonica*, *P. lapathifolium,* and *M. sacchariflorus* are glycophytes.

The plant communities between 2008 and 2018 in the region with freshwater introduction (site A) were compared (Figure 6). The glycophytic plant communities were distinctly enlarged. There was no evident change in the halophyte community; the habitat of salt-tolerant plants appeared compressed. In a case of the vegetation in the area without freshwater introduction (site B), because of the further expansion of *S. alterniflora* (Figure 6), the halophyte community was significantly expanded, whereas the habitats of the glycophytic and salt-tolerant plant communities were compressed.

The proportion of samples with different vegetation types between 2018 and 2008 were analyzed (Figure 7). The proportion of invasive plants increased in areas without freshwater introduction (site B), whereas the proportion of glycophytes increased in areas with freshwater introduction (site A).

Changes in interspecific relationships among species

The dominant species pair correlation test showed a significant negative correlation among the plant communities in the coastal wetland invaded by *S. alterniflora* (Figure 8); the positive–negative association ratio was less than 1. In site A, the ratio increased in 2018 (0.31) compared to that in 2008 (0.22) after the introduction of freshwater. In site B, the ratio decreased in 2018 (0.19) compared to that in 2008 (0.22) following the continued invasion of *S. alterniflora*.

In site A, the introduction of freshwater significantly altered the interspecific relationships of *S. salsa* with other species. For example, we observed a shift in the interspecific relationships among *S. salsa*, *S. alterniflora,* and *Z. macrostachya* from negative to positive. The interspecific relationships among *S. salsa*, *S. glauca*, *A. subulatus*, and *P. lapathifolium* shifted from positive to negative. In site B (without freshwater introduction), the interspecific relationships of native halophytes (*S. salsa*, *C. scabrifolia*, and *Z. macrostachya*) changed from negative to positive or positive to negative. The interspecific relationships between the glycophytes *A. sublatus* and *S. salsa*, *P. australis*, and *S. alterniflora* shifted from negative to positive.

Determination of the degree of inter-species association revealed a stronger negative association among plant communities in the coastal wetlands invaded by *S. alterniflora* (Figure 9). The results indicate that that the probability of two species appearing in the same habitat is low and that there is usually a negative correlation or no obvious interspecific relationship between two species. In site A, freshwater introduction reduced the strength of the negative associations between species. In site B, further expansion of *S. alterniflora* increased the strength of the negative associations between species; most species in the communities were relatively independent.

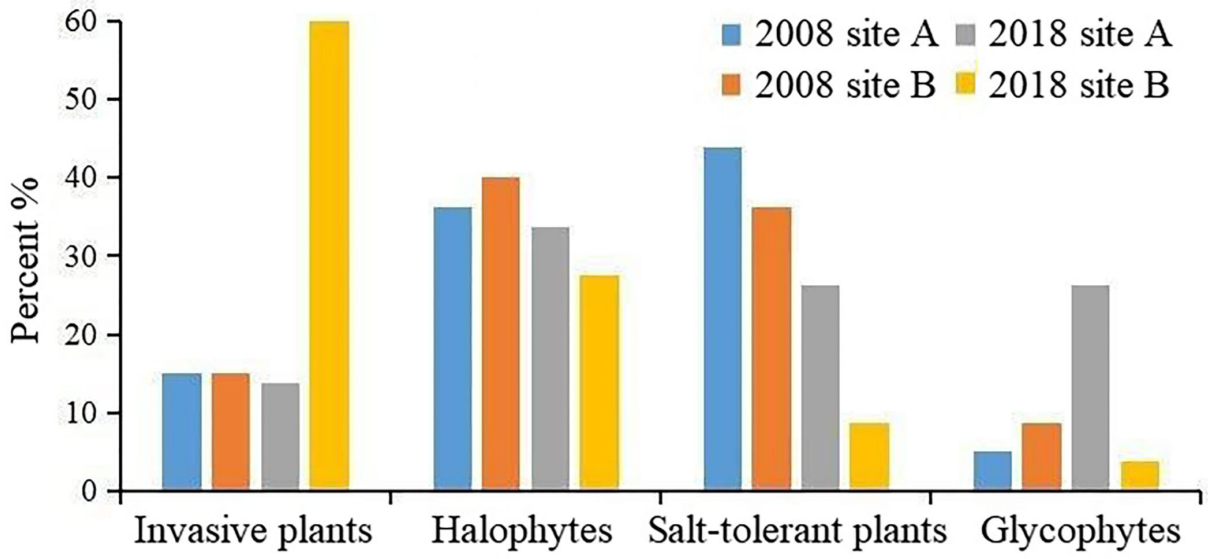

FIGURE 7
Changes in the proportion of coastal wetland vegetation types.

Discussion

Effects of *S. alterniflora* invasion on coastal wetland vegetation

S. alterniflora is one of the most dominant invasive species in coastal wetlands of China (Liu et al., 2020; Meng et al., 2020). Unless control measures are implemented, *S. alterniflora* would cause damage to coastal wetland ecosystems and negatively affect their biodiversity. Following the invasion of *S. alterniflora*, the coastal wetland plant communities in the 2008 investigation comprised dominant species and a few associated species with low species diversity, ecological dominance, and community evenness. In site B, where *S. alterniflora* further expanded in 2018, the species composition and types of plant communities appeared simpler than those in 2008. In addition to the relatively simple habitat conditions of the coastal wetland, the species composition of the quadrats was modest, and the associated species were limited owing to the influence of the invasive plant (Lemein et al., 2017; Li et al., 2020).

The niche theory states that the construction of a community is the result of species interactions under the pressure of a specific environment. Interspecific relationships are closely related to the degree of niche overlap during the process of colonization and coexistence in local habitats. Native plants in the invasive coastal wetland community of *S. alterniflora* were negatively correlated; this is an indication that the community in this area is unstable, immature, and prone to fluctuations.

The distribution of coastal wetland vegetation from the shorelines to nearshore showed evident changes in the species composition (Lemein et al., 2017), including *S. alterniflora*, *S. salsa*, *C. scabrifolia*, *S. salina*, *Z. macrostachya*, *T. chinensis*, *P. australis*, *A. sinensis*, *I. cylindrica*, and *M. sacchariflorus* communities. In 2018, in site B, where there was no influx of freshwater, we observed an increase in the growth expansion of *S. alterniflora*. According to the proportion of samples with different vegetation community types between 2018 and 2008, the survival pressure of native salt-tolerance plants was the greatest in coastal wetlands invaded by *S. alterniflora*, which significantly encroached the growth space of the native vegetation. This resulted in a sharp decrease or even the disappearance of certain native species. The biogeomorphic feedback of invasive species can alter the selection pressure of local species at the population and community levels, leading to changes in the evolutionary process (Wang et al., 2019; Gerwing et al., 2021).

Effect of freshwater on plant species diversity in coastal wetlands invaded by *S. alterniflora*

Studies have shown that hydrology is a key factor for the restoration of coastal wetlands (Zhao et al., 2016; Yang et al., 2017; Gaberščik et al., 2018; Liu et al., 2021). Freshwater is an effective measure for controlling the growth of *S. alterniflora*. Similarly, our findings indicated that freshwater introduction exhibited positive effects on the diversity of plant communities in the coastal wetlands invaded by *S. alterniflora*. In 2018,

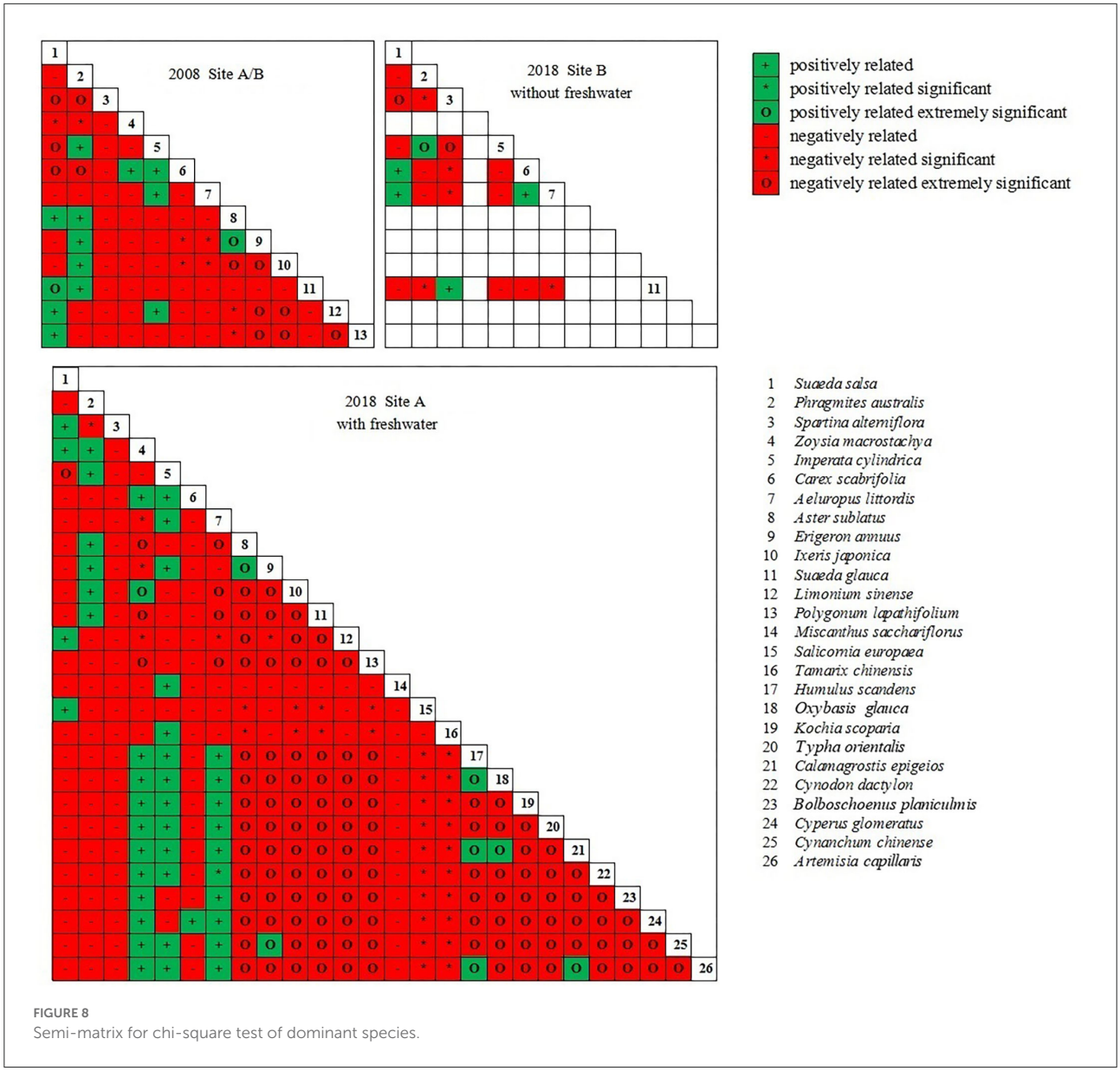

FIGURE 8
Semi-matrix for chi-square test of dominant species.

the species diversity increased at the study site with the introduction of freshwater. The number of species in the coastal wetland vegetation increased from 13 to 26 species, and there was a significant reduction in the area occupied by the invasive species. After freshwater introduction, three vegetation community types were added in 2018, leading to an increase in plant species diversity. These results indicated that freshwater introduction positively influenced the native plant communities of the coastal wetlands invaded by *S. alterniflora*. Although the similarity of species composition after freshwater introduction in site A was not markedly separated from that in 2008, it was markedly separated from that in site B (without freshwater introduction) in 2018. From the perspective of species composition similarity, freshwater introduction significantly contributed to the biodiversity maintenance of plant communities in coastal wetlands invaded by *S. alterniflora*. These results highlight the importance of early intervention in controlling the spread of invasive species, such as *S. alterniflora*, in coastal wetlands.

Moreover, in 2018, we identified certain wetland plants that prefer freshwater environments (such as *T. orientalis* and *M. sacchariflora*). Future vegetation monitoring should thus follow these patterns. Although the freshwater introduction restoration project had clear positive effects on the biodiversity of the invaded coastal wetland, it had potential shortcomings that require control measures. At the freshwater introduction site, we observed an increase in species diversity in terms of glycophyte expansion. Future studies should monitor

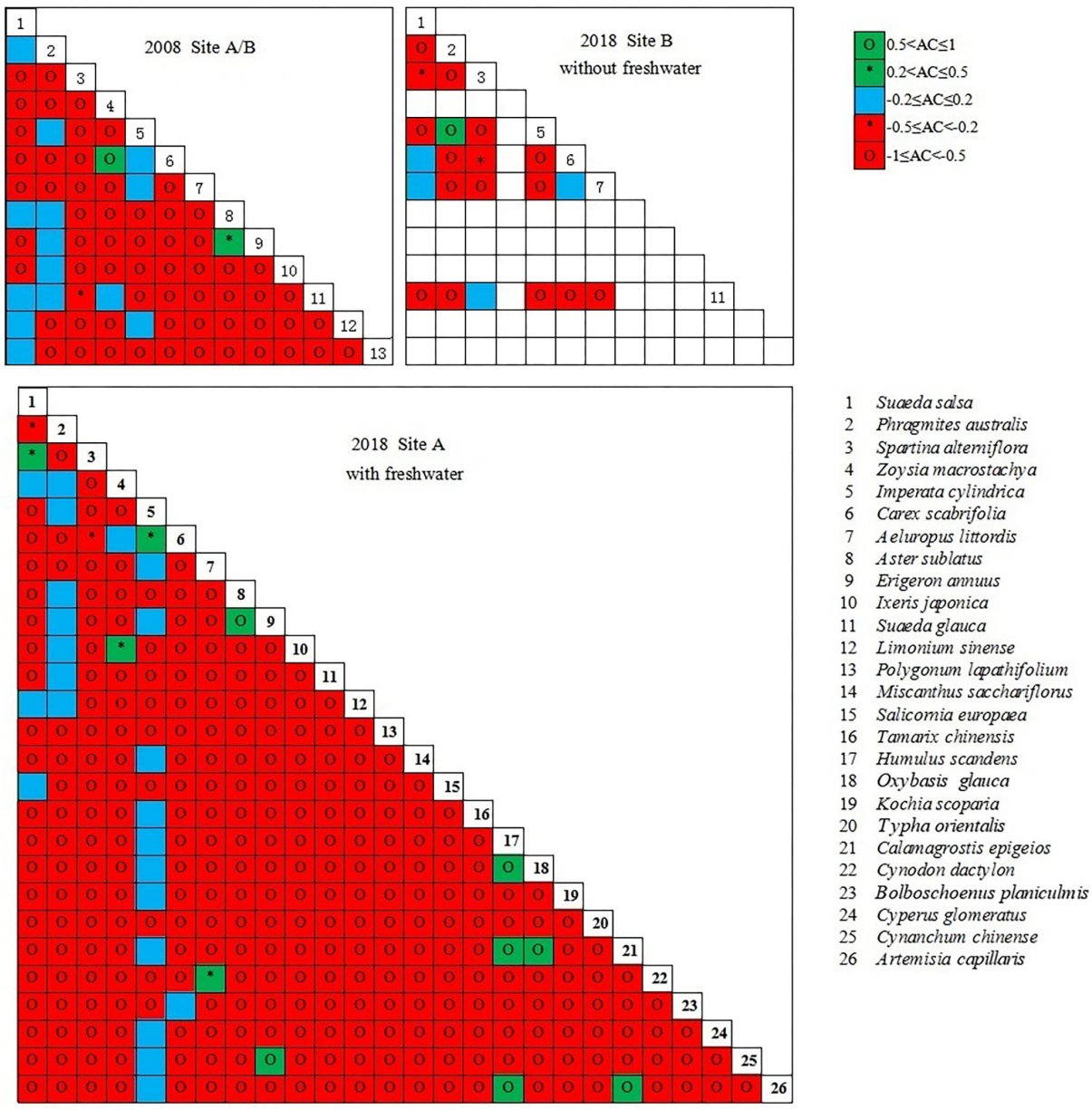

FIGURE 9
Dominant species AC value semi-matrix.

glycophytes as indicator species to determine their impact on native halophyte communities.

Effect of freshwater on plant interspecific associations in coastal wetlands invaded by *S. alterniflora*

The results of the dominant species pair correlation test suggested that freshwater introduction did not reverse the positive–negative associations among coastal wetland plant communities. The value of the positive–negative association ratio was increased compared to that in 2008; however, it remained < 1, indicating that the vegetation in the Yancheng coastal wetlands invaded by *S. alterniflora* was unstable. Furthermore, during the same period, the positive–negative association ratio of the site where freshwater was introduced (0.31) was significantly higher than that of the site where freshwater was not introduced (0.19). Moreover, the development of the existing plant communities was in

the initial stages and thus showed strong instability (Callaway, 1995; Wang et al., 2012; García-Cervigón et al., 2013). The interspecific relationships between *S. salsa* and other species were significantly altered after the introduction of freshwater. Therefore, *S. salsa* should be used as an indicator species to monitor the restoration of coastal wetlands invaded by *S. alterniflora* using freshwater introduction. Furthermore, the measurements of the degree of inter-species association suggested that freshwater introduction reduced the strength of negative associations between species. Without the introduction of freshwater, an increase in the strength of negative associations between species was observed. The introduction of freshwater thus promoted the stability of the plant communities in the coastal wetlands invaded by *S. alterniflora*.

Environmental factors, particularly soil salinity, significantly influence the distribution of vegetation (Amores et al., 2013; Telesh et al., 2013; Archer et al., 2021; Danihelka et al., 2022). Because our investigations did not account for environmental indicators such as soil, this study did not analyze the environmental impact on different vegetation communities. This study offers a preliminary judgment based on the type of vegetation, and the introduction of freshwater to the changes in soil salinity requires further analysis. Future research should include sampling and analysis of various environmental factors to explain the effects of plant invasions and coastal wetland restoration on native plant communities.

Conclusion

This study comprehensively investigated the influence of freshwater introduction on vegetation in coastal wetlands invaded by *S. alterniflora*. There was an overall reduction in plant species diversity in the coastal wetlands invaded by *S. alterniflora*. Without freshwater introduction, *S. alterniflora* would further occupy the space of native vegetation communities, resulting in a sharp reduction or even disappearance of native species. Although freshwater introduction increased the number and diversity of plants and effectively inhibited further invasion of *S. alterniflora*, it also increased the risk of expansion of the glycophyte community. Both freshwater introduction and intensified invasion of *S. alterniflora* introduced a shift in the interspecific relationship between *S. salsa* and other species. Thus, *S. salsa* is the most important native species in Yancheng coastal wetlands. Future studies should focus on observing community changes in *S. salsa* and glycophytes by setting up fixed monitoring points to regulate the influx of freshwater in the wetlands. This study emphasizes the need for early intervention by implementing restoration measures in coastal wetlands invaded by *S. alterniflora* and calls for a follow-up monitoring and meticulous management.

Data availability statement

The original contributions presented in the study are included in the article/supplementary material, further inquiries can be directed to the corresponding author.

Author contributions

LC, WL, and ZD conceived the ideas and designed methodology. ZD, XZ, YC, and RY collected the data. ZD analyzed the data. ZD and YL wrote the manuscript. All authors contributed critically to the drafts and gave final approval for publication.

Funding

This work was supported by the Project Fund Research Grant of Yellow Sea Academy of Wetland Research (20210109) and the National Key R&D Program of China (2017YFC0506200).

Acknowledgments

We thank Zhimin Dou for helping us conduct experiments in the field.

Conflict of interest

The authors declare that the research was conducted in the absence of any commercial or financial relationships that could be construed as a potential conflict of interest.

Publisher's note

References

Amores, M. J., Verones, F., Raptis, C., Juraske, R., Pfister, S., Stoessel, F., et al. (2013). Biodiversity impacts from salinity increase in a coastal wetland. *Environ. Sci. Technol.* 47, 6384–6392. doi: 10.1021/es3045423

Archer, M. J., Pitchford, J. L., Biber, P., and Underwood, W. (2021). Assessing vegetation, nutrient content and soil dynamics along a coastal elevation gradient in a mississippi estuary. *Estuar. Coast.* 45, 1217–1229. doi: 10.1007/s12237-021-01012-2

Arnoldi, J.-F., Barbier, M., Kelly, R., Barabás, G., and Jackson, A. L. (2022). Invasions of ecological communities: hints of impacts in the invader's growth rate. *Methods Ecol. Evol.* 13, 167–182. doi: 10.1111/2041-210X.13735

Bradley, B. A., Blumenthal, D. M., Wilcove, D. S., and Ziska, L. (2010). Predicting plant invasions in an era of global change. *Trends Ecol. Evol.* 25, 310–318. doi: 10.1016/j.tree.2009.12.003

Callaway, R. M. (1995). Positive interactions among plants. *Bot. Rev.* 61, 306–349. doi: 10.1007/BF02912621

Chen, X., Huang, Y., Yang, H., Pan, L., Perry, D. C., Xu, P., et al. (2020). Restoring wetlands outside of the seawalls and to provide clean water habitat. *Sci. Total Environ.* 721, 137788. doi: 10.1016/j.scitotenv.2020.137788

Costa, J. C., Neto, C., Martins, M., and Lousã, M. (2011). Annual dune plant communities in the Southwest coast of Europe. *Plant Biosyst.* 145, 91–104. doi: 10.1080/11263504.2011.602729

Courtois, P., Figuieres, C., Mulier, C., and Weill, J. (2017). A cost-benefit approach for prioritizing invasive species. *Ecol. Econ.* 146, 607–620. doi: 10.1016/j.ecolecon.2017.11.037

Cui, B., Yang, Q., Yang, Z., and Zhang, K. (2009). Evaluating the ecological performance of wetland restoration in the Yellow River Delta, China. *Ecol. Eng.* 35, 1090–1103. doi: 10.1016/j.ecoleng.2009.03.022

Cui, L., Li, G., Ouyang, N., Mu, F., Yan, F., Zhang, Y., et al. (2018). Analyzing coastal wetland degradation and its key restoration technologies in the coastal area of Jiangsu, China. *Wetlands* 38, 525–537. doi: 10.1007/s13157-018-0997-6

Daehler, C. C., and Strong, D. R. (1996). Status, prediction and prevention of introduced cordgrass spartina spp. invasions in pacific estuaries, USA. *Biol. Conserv.* 78, 51–58. doi: 10.1016/0006-3207(96)00017-1

Daily, G. C., Polasky, S., Goldstein, J., Kareiva,P., Mooney, H. A., Pejchar, L., et al. (2009). Ecosystem services in decision making: time to deliver. *Front. Ecol. Environ.* 7, 21–28. doi: 10.1890/080025

Danihelka, J., Chytrý, K., Harásek, M., Hubatka, P., Klinkovsk,á, K., Krato,š, F., et al. (2022). Halophytic flora and vegetation in southern Moravia and northern Lower Austria: past and present. *Preslia* 94, 13–110. doi: 10.23855/preslia.2022.013

Davies, P. M., Naiman, R. J., Warfe, D. M., Pettit, N. E., Arthington, A. H., and Bunn, S. E. (2014). Flow-ecology relationships: closing the loop on effective environmental flows. *Mar. Freshwater Res.* 65, 133–141. doi: 10.1071/MF13110

Demarco, K. E., Hillmann, E. R., Nyman, J. A., Couvillion, B., and Peyre, M. L. (2022). Defining aquatic habitat zones across northern gulf of mexico estuarine gradients through submerged aquatic vegetation species assemblage and biomass data. *Estuar. Coast.* 45, 148–167. doi: 10.1007/s12237-021-00958-7

Diefenderfer, H. L., Sinks, I. A., Zimmerman, S. A., Cullinan, V. I., and Borde, A. B. (2018). Designing topographic heterogeneity for tidal wetland restoration. *Ecol. Eng.* 123, 212–225. doi: 10.1016/j.ecoleng.2018.07.027

Duarte, B., Santos, D., Marques, J. C., and Caçador, I. (2015). Ecophysiological constraints of two invasive plant species under a saline gradient: halophytes versus glycophytes. *Estuar. Coast. Shelf S.* 167, 154–165. doi: 10.1016/j.ecss.2015.04.007

Ehrenfeld, J. G. (2010). Ecosystem consequences of biological invasions. *Annu. Rev. Ecol. Evol. S.* 41, 59–80. doi: 10.1146/annurev-ecolsys-102209-144650

Gaberščik, A., Lea Krek, J., and Zelnik, I. (2018). Habitat diversity along a hydrological gradient in a complex wetland results in high plant species diversity. *Ecol. Eng.* 118, 84–92. doi: 10.1016/j.ecoleng.2018.04.017

García-Cervigón, A. I., Gazol, A., Sanz, V., Camarero, J. J., and Olano, J. M. (2013). Intraspecific competition replaces interspecific facilitation as abiotic stress decreases: the shifting nature of plant-plant interactions. *Perspect. Plant Ecol.* 15, 226–236. doi: 10.1016/j.ppees.2013.04.001

Gerwing, T. G., Thomson, H. M., Brouard-John, E. K., Kushneryk, K., Davies, M., and Lawn, P. (2021). Observed dispersal of invasive yellow flag iris (*Iris pseudacorus*) through a saline marine environment and growth in a novel substrate, shell hash. *Wetlands* 41, 1. doi: 10.1007/s13157-021-01421-w

Giljohann, K. M., Hauser, C. E., Williams, N. S. G., and Moore, J. L. (2011). Optimizing invasive species control across space: willow invasion management in the Australian Alps. *J. App. Ecol.* 48, 1286–1294. doi: 10.1111/j.1365-2664.2011.02016.x

Gillard, M. B., Castillo, J. M., Mesgaran, M., Futrell, C. J., and Grewell, B. J. (2021). High aqueous salinity does not preclude germination of invasive *Iris pseudacorus* from estuarine populations. *Ecosphere.* 12, e03486. doi: 10.1002/ecs2.3486

Giulio, S., Pinna, L. C., and Jucker, T. (2022). Invasion dynamics and potential future spread of sea spurge (*Euphorbia paralias*) across Australia's coastal dunes. *J. Biogeogr.* 49, 378–390. doi: 10.1111/jbi.14308

Glenn, E. P., Flessa, K. W., and Pitt, J. (2013). Restoration potential of the aquatic ecosystems of the Colorado River Delta, Mexico: introduction to special issue on "Wetlands of the Colorado River Delta". *Ecol. Eng.* 59, 1–6. doi: 10.1016/j.ecoleng.2013.04.057

Gu, J., Luo, M., Zhang, X., Christakos, G., Agust,í, S., Duarte, C. M., et al. (2018). Losses of salt marsh in China: trends, threats and management. *Estuar. Coast. Shelf. S.* 214, 98–109. doi: 10.1016/j.ecss.2018.09.015

He, T., Sun, Z., Hu, X., Chen, B., Wang, H., and Wang, J. (2020). Effects of *Spartina alterniflora* invasion on spatial and temporal variations of total sulfur and inorganic sulfur fractions in sediments of salt marsh in the Min River estuary, southeast China. *Ecol. Indic.* 113, 106253. doi: 10.1016/j.ecolind.2020.106253

Huang, L., Zhang, G., Bai, J., Xia, Z., Wang, W., and Jia, J. (2020). Desalinization via freshwater restoration highly improved microbial diversity, co-occurrence patterns and functions in coastal wetland soils. *Sci. Total Environ.* 765, 142769. doi: 10.1016/j.scitotenv.2020.142769

Lemein, T., Albert, D. A., and Tuttle, E. D. G. (2017). Coastal wetland vegetation community classification and distribution across environmental gradients throughout the laurentian great lakes. *J. Great Lakes Res.* 43, 658–669. doi: 10.1016/j.jglr.2017.04.008

Li, B., Liao, C., Zhang, X., Chen, H., Wang, Q., and Chen, Z. (2009). *Spartina alterniflora* invasions in the Yangtze River estuary, China: an overview of current status and ecosystem effects. *Ecol. Eng.* 35, 511–520. doi: 10.1016/j.ecoleng.2008.05.013

Li, X., Yang, W., Li, S., Sun, T., Bai, J., Pei, J., et al. (2020). Asymmetric responses of spatial variation of different communities to a salinity gradient in coastal wetlands. *Mar. Environ. Res.* 158, 105008. doi: 10.1016/j.marenvres.2020.105008

Li, Y., Zhu, X., Zou, X., and Gao, J. (2005). Study on landscape ecosystem of coastal wetlands in Yancheng, Jiangsu Province. *B. Mar. Sci.* 24, 46–51. doi: 10.1111/j.1745-7254.2005.00209.x

Liu, J., Liu, Y., Xie, L., Zhao, S., Dai, Y., and Zhang, Z. (2021). A threshold-like effect on the interaction between hydrological connectivity and dominant plant population in tidal marsh wetlands. *Land Degrad. Dev.* 32, 2922–2935. doi: 10.1002/ldr.3913

Liu, L., Wang, H., and Yue, Q. (2020). China's coastal wetlands: ecological challenges, restoration, and management suggestions. *Reg. Stud. Mar. Sci.* 37, 101337. doi: 10.1016/j.rsma.2020.101337

Liu, X., Liu, H., Gong, H., Lin, Z., and Lv, S. (2017). Appling the one-class classification method of maxent to detect an invasive plant *Spartina alterniflora* with time-series analysis. *Remote Sens.* 9, 1120. doi: 10.3390/rs9111120

Meng, W., Feagin, R. A., Innocenti, R. A., Hu, B., He, M., and Li, H. (2020). Invasion and ecological effects of exotic smooth cordgrass *Spartina alterniflora* in China. *Ecol. Eng.* 143, 105670. doi: 10.1016/j.ecoleng.2019.105670

Minchinton, T. E., Simpson, J. C., and Bertness, M. D. (2006). Mechanisms of exclusion of native coastal marsh plants by an invasive grass. *J. Ecol.* 94, 342–354. doi: 10.1111/j.1365-2745.2006.01099.x

Mooney, H. A., and Hobbs, R. J. (2000). *Invasive Species in a Changing World*. Washington, DC: Island Press.

Nicol, S., Sabbadin, R., Peyrard, N., and Chadès, I. (2017). Finding the best management policy to eradicate invasive species from spatial ecological networks with simultaneous actions. *J. App. Ecol.* 54, 1989–1999. doi: 10.1111/1365-2664.12884

Osborne, B., and Gioria, M. (2018). Plant invasions. *J. Plant. Ecol.* 11, 1–3. doi: 10.1093/jpe/rtx070

Pimentel, D., Lach, L., Zuniga, R., and Morrison, D. (2000). Environmental and economic costs of nonindigenous species in the United States. *Bioscience* 50, 53–65. doi: 10.1641/0006-3568(2000)050[0053:EAECON]2.3.CO;2

Proosdij, D. V., Lundholm, J., Neatt, N., Bowron, T., and Graham, J. (2010). Ecological re-engineering of a freshwater impoundment for salt marsh restoration in a hypertidal system. *Ecol. Eng.* 36, 1314–1332. doi: 10.1016/j.ecoleng.2010.06.008

Remm, L., Lhmus, A., Leibak, E., Kohv, M., Salm, J.-O., Lõhmus, P., et al. (2019). Restoration dilemmas between future ecosystem and current species values: the concept and a practical approach in estonian mires. *J. Environ. Manage.* 250, 109439. doi: 10.1016/j.jenvman.2019.109439

Ren, J., Chen, J., Xu, C., de Koppel, J. V., Thomsen, M. S., Qiu, S., et al. (2021). An invasive species erodes the performance of coastal wetland protected areas. *Sci. Adv.* 42, eabi8943. doi: 10.1126/sciadv.abi8943

Restrepo, J. D., and Cantera, J. R. (2013). Discharge diversion in the Patía River delta,the Colombian Pacific: geomorphic and ecological consequences for mangrove ecosystems. *J. S. Am. Earth Sci.* 46, 183–198. doi: 10.1016/j.jsames.2011.04.006

Riddin, T., Van Wyk, E., and Adams, J. (2016). The rise and fall of an invasive estuarine grass. *S. Afr. J. Bot.* 107, 74–79. doi: 10.1016/j.sajb.2016.07.008

Schirmel, J., Bundschuh, M., Entling, M. H., Kowarik, I., and Buchholz, S. (2016). Impacts of invasive plants on resident animals across ecosystems, taxa, and feeding types: a global assessment. *Global Change Biol.* 22, 594–603. doi: 10.1111/gcb.13093

Stachowicz, J. J. (2001). Mutualism, facilitation, and the structure of ecological communities: positive interactions play a critical, but underappreciated, role in ecological communities by reducing physical or biotic stresses in existing habitats and by creating new habitats on which many species depend. *Bioscience* 51, 235–246. doi: 10.1641/0006-3568(2001)051[0235:MFATSO]2.0.CO;2

Stephanie, P., Davis, A. J. S., Mangiante, M. J., and Darling, J. A. (2018). Assessing threats of non-native species to native freshwater biodiversity: conservation priorities for the united states. *Biol. Conserv.* 224, 199–208. doi: 10.1016/j.biocon.2018.05.019

Takahashi, D., Seung-Woo, S., and Eun-Jin, P. (2019). Colonial population dynamics of *Spartina alterniflora*. *Ecol. Model* 395, 45–50. doi: 10.1016/j.ecolmodel.2019.01.013

Tang, L., Yang, G., Wang, C., Zhao, B., and Li, B. (2012). A plant invader declines through its modification to habitats: a case study of a 16-year chronosequence of *spartina alterniflora* invasion in a salt marsh. *Ecol. Eng.* 49, 181–185. doi: 10.1016/j.ecoleng.2012.08.024

Telesh, I., Schubert, H., and Skarlato, S. (2013). Life in the salinity gradient: discovering mechanisms behind a new biodiversity pattern. *Estuar. Coast. Shelf. S.* 135, 317–327. doi: 10.1016/j.ecss.2013.10.013

Turnbull, L. A., Coomes, D., and Rees, H. M. (2004). Seed mass and the competition/colonization trade-off: competitive interactions and spatial patterns in a guild of annual plants. *J. Ecol.* 92, 97–109. doi: 10.1111/j.1365-2745.2004.00856.x

Vaz, A. S., Alcaraz-Segura, D., Campos, J. C., Campos, J. C., and Honrado, C. (2018). Managing plant invasions through the lens of remote sensing: a review of progress and the way forward. *Sci. Total Environ.* 642, 1328–1339. doi: 10.1016/j.scitotenv.2018.06.134

Vitousek, P. M. (1997). Introduced species: a significant component of human-induced global change. *New Zeal. J. Ecol.* 21, 1–16.

Wang, Y., Chen, D., Yan, E., Yu, F., and van Kleunen, M. (2019). Invasive alien clonal plants are competitively superior over co-occurring native clonal plants. *Perspect. Plant Ecol.* 40, 125484. doi: 10.1016/j.ppees.2019.125484

Wang, Y., Ellwood, M. D. F., Maestre, F. T., Yang, Z., Wang, G., and Chu, C. (2012). Positive interactions can produce species-rich communities and increase species turnover through time. *J. Plant Ecol.* 5, 417–421. doi: 10.1093/jpe/rts005

Xie, T., Wang, Q., Ning, Z., Chen, C., Cui, B., Bai, J., et al. (2021). Artificial modification on lateral hydrological connectivity promotes range expansion of invasive *Spartina alterniflora* in salt marshes of the Yellow River delta, China. *Sci. Total Environ.* 769, 144476. doi: 10.1016/j.scitotenv.2020.144476

Yan, D., Li, J., Yao, X., and Luan, Z. (2021). Quantifying the long-term expansion and dieback of *Spartina alterniflora* using google earth engine and object-based hierarchical random forest classification. *IEEE J Stars* 4, 9781–9793. doi: 10.1109/JSTARS.2021.3114116

Yan, D., Li, J., Yao, X., and Luan, Z. (2022). Integrating UAV data for assessing the ecological response of *Spartina alterniflora* towards inundation and salinity gradients in coastal wetland. *Sci. Total Environ.* 814, 152631. doi: 10.1016/j.scitotenv.2021.152631

Yang, M., Lu, K., Batzer, D. P., and Wu, H. (2019). Freshwater release into estuarine wetlands changes the structure of benthic invertebrate assemblages: a case study from the Yellow River Delta. *Sci. Total Environ.* 687, 752–758. doi: 10.1016/j.scitotenv.2019.06.154

Yang, W., Li, X., Sun, T., Yang, Z., and Li, M. (2017). Habitat heterogeneity affects the efficacy of ecological restoration by freshwater releases in a recovering freshwater coastal wetland in China's yellow river delta. *Ecol. Eng.* 104, 1–12. doi: 10.1016/j.ecoleng.2017.04.007

Yue, S., Zhou, Y., Xu, S., Zhang, X., Liu, M., Qiao, Y., et al. (2021). Can the Non-native Salt Marsh Halophyte *Spartina alterniflora* Threaten Native Seagrass (*Zostera japonica*) Habitats? A Case Study in the Yellow River Delta, China. *Front. Plant Sci.* 12, 643425. doi: 10.3389/fpls.2021.643425

Zavaleta, E. S., Hobbs, R. J., and Mooney, H. A. (2001). Viewing invasive species removal in a whole-ecosystem context. *Trends Ecol. Evol.* 16, 454–459. doi: 10.1016/S0169-5347(01)02194-2

Zedler, J. B., and Kercher, S. (2004). Causes and consequences of invasive plants in wetlands: opportunities, opportunists, and outcomes. *Crit. Rev. Plant Sci.* 23, 431–452. doi: 10.1080/07352680490514673

Zhang, X., Xiao, X., Wang, X., Xu, X., Chen, B., Wang, J., et al. (2020). Quantifying expansion and removal of *Spartina alterniflora* on Chongming island, China, using time series Landsat images during 1995-2018. *Remote Sens. Environ.* 247, 111916. doi: 10.1016/j.rse.2020.111916

Zhao, C., Li, J., and Zhao, X. (2019). Mowing plus shading as an effective method to control the invasive plant *Spartina alterniflora*. *Flora* 257, 151408. doi: 10.1016/j.flora.2019.05.007

Zhao, Q., Bai, J., Huang, L., Gu, B., Lu, Q., and Gao, Z. (2016). A review of methodologies and success indicators for coastal wetland restoration. *Ecol. Indic.* 60, 442–452. doi: 10.1016/j.ecolind.2015.07.003

Zuo, X., Cui, L., Li, W., Lei, Y., Dou, Z., Liu, Z., et al. (2021). *Spartina alterniflora* leaf and soil eco-stoichiometry in the yancheng coastal wetland. *Plants* 10, 13. doi: 10.3390/plants10010013

frontiers | Frontiers in Plant Science

TYPE Original Research
PUBLISHED 27 September 2022
DOI 10.3389/fpls.2022.990592

OPEN ACCESS

EDITED BY
Xiaoming Kang,
Chinese Academy of Forestry, China

REVIEWED BY
Xiangjin Shen,
Northeast Institute of Geography and Agroecology, (CAS), China
Xiaodong Zhang,
Chinese Academy of Forestry, China

*CORRESPONDENCE
Haibo Jiang
jianghb625@nenu.edu.cn
Chunguang He
he-cg@nenu.edu.cn

SPECIALTY SECTION
This article was submitted to Functional Plant Ecology, a section of the journal Frontiers in Plant Science

RECEIVED 10 July 2022
ACCEPTED 07 September 2022
PUBLISHED 27 September 2022

CITATION
Deng G, Gao J, Jiang H, Li D, Wang X, Wen Y, Sheng L and He C (2022) Response of vegetation variation to climate change and human activities in semi-arid swamps.
Front. Plant Sci. 13:990592.
doi: 10.3389/fpls.2022.990592

Response of vegetation variation to climate change and human activities in semi-arid swamps

Guangyi Deng[1], Jin Gao[1], Haibo Jiang[1]*, Dehao Li[1], Xue Wang[1], Yang Wen[2], Lianxi Sheng[1] and Chunguang He[1]*

[1]State Environmental Protection Key Laboratory of Wetland Ecology and Vegetation Restoration, Key Laboratory for Vegetation Ecology Ministry of Education, Northeast Normal University, Changchun, China, [2]Key Laboratory of Environmental Materials and Pollution Control, The Education Department of Jilin Province, School of Engineering, Jilin Normal University, Siping, China

Vegetation is a sensitive factor in marsh ecosystems, which can provide nesting sites, foraging areas, and hiding places for waterfowl and can affect their survival environment. The Jilin Momoge National Nature Reserve, which consists of large areas of marshes, is located in the semi-arid region of northeast China and is an important stopover site for the critically endangered species of the Siberian Crane (*Grus leucogeranus*). Global climate change, extreme droughts and floods, and large differences in evaporation and precipitation in this region can cause rapid vegetation succession. In recent years, increased grain production and river-lake connectivity projects carried out in this area to increase grain outputs and restore wetlands have caused significant changes in the hydrological and landscape patterns. Therefore, research on the response of variation trends in vegetation patterns to the main driving factors (climate change and human activities) is critical for the conservation of the Siberian Crane. Based on the Google Earth Engine (GEE) platform, we obtained and processed the Normalized difference vegetation index (NDVI) data of the study area during the peak summer vegetation period for each year from 1984 to 2020, estimated the annual vegetation cover using Maximum value composites (MVC) method and the image dichotomy method, calculated and analyzed the spatial and temporal trends of vegetation cover, explored the response of vegetation cover change in terms of climate change and human activities, and quantified the relative contribution of both. The results revealed that first, from the spatial and temporal changes, the average annual growth rate of regional vegetation was 0.002/a, and 71.14% of the study area was improved. The vegetation cover showed a trend of degradation and then recovery, in which the percentage of high vegetation cover area decreased from 51.22% (1984–2000) to 28.33% (2001–2005), and then recovered to 55.69% (2006–2020). Second, among climate change factors, precipitation was more correlated with the growth of vegetation in the study area than temperature, and the increase in precipitation during the growing season could promote the growth of marsh vegetation in the Momoge Reserve. Third, overall, human activities have

contributed to the improvement of vegetation cover in the study area with the implementation of important ecological projects, such as the return of farmland to wetlands, the return of grazing to grass, and the connection of rivers and lakes. Fourth, climate change and human activities jointly drive vegetation change, but the contribution of human activities in both vegetation improvement and degradation areas (85.68% and 78.29%, respectively) is higher than that of climate change (14.32% and 21.71%, respectively), which is the main reason for vegetation improvement or degradation in the study area. The analysis of vegetation pattern change within an intensive time series in semi-arid regions can provide a reference and basis for studying the driving factors in regions with rapid changes in vegetation and hydrological conditions.

KEYWORDS

temporal and spatial changes in vegetation, migration stopover, Momoge National Nature Reserve of Jilin Province, Google Earth Engine, anthropogenic activities, climate variation

1 Introduction

Wetlands are one of the most productive ecosystems in the world and have irreplaceable ecological value for the conservation of species and the maintenance of biodiversity (Mas et al., 2021). As the core part of wetland ecosystems, wetland vegetation plays an important role in the balance of Earth's ecosystem, climate change, the water cycle, and energy flow (e.g., Guntenspergen et al., 1989; Shen et al., 2021; Zhang et al., 2021; Shen et al., 2022c; Yan et al., 2022). At the same time, vegetation is also a sensitive factor for ecological changes and is considered to be an important part of migratory waterfowl habitat, providing food, hiding places, and breeding sites for waterfowl, directly affecting their living environment (Barchiesi et al., 2022; Wang et al., 2022c; Yuan et al., 2022). To ensure that waterfowl are provided with a suitable habitat at each stopover point along the migration corridor, it is important to effectively monitor vegetation changes and drivers of waterfowl habitat over time.

The Jilin Momoge National Nature Reserve (hereinafter referred to as Momoge Reserve), located in the western part of the Songnen Plain in China, is a long-term supply stop on the East Asia¬–Australia migratory bird route, providing *Bolboschoenus planiculmis*, an important food source for whooping cranes, before they fly to their wintering grounds (Wang et al., 2022d). The Momoge Nature Reserve is a typical climate change-sensitive area. In the context of long-term global warming and economic development, the region has suffered continuous drought and wetland development in recent years, which has continuously changed the distribution pattern of vegetation, thus affecting the distribution pattern and resting population of whooping cranes (Jiang et al., 2015a; Haverkamp et al., 2022). Although the mechanisms of vegetation dynamics are complex and multifaceted, climate change and human activities have been identified as the main drivers (Qi et al., 2022; Wu et al., 2022). Many studies have been conducted on the response of vegetation to climate change and human activities (Hu et al., 2011; Liu et al., 2015; Yuan et al., 2019; Bai et al., 2022), however, few studies have been able to quantitatively assess the long-term response of vegetation to climate change and human activities, and there is a lack of effective differentiation between the effects of climate factors and human activities on vegetation and quantification of their respective relative contributions to vegetation change (Wang et al., 2022b). Therefore, studying the mechanisms of climate change and human activities on the dynamics of vegetation change in waterfowl habitats has become a key issue for the restoration and conservation of food resources in whooping crane resting habitats.

To elucidate the vegetation changes in whooping crane stopover sites and their response to climate change and human activities, this study was conducted in the western half of the Momoge Reserve to investigate the three following aspects: (1) how vegetation patterns have changed dynamically over the past 37 years, (2) the relationship between vegetation dynamics and climate change at spatial and temporal scales, and (3) the relative contribution of climate change and human activities to vegetation dynamics and provision of theoretical guidance for ecological management and sustainable development of wetlands in the Momoge Reserve.

2 Materials and methods

2.1 Study area

The study area was located within the Momoge Reserve in northeastern China, a region where the maximum number of whooping cranes at rest represents more than 95% of the world's population (Figure 1). The study area is located in the western semi-arid region of the Songnen Plain, China, and is an important stopover area along the East Asia–Australia migratory route for migratory birds (Tian et al., 2019). It was included in the list of internationally important wetlands in 2013. The region has a temperate continental monsoon climate with an annual average temperature of 4.2°C (Wang et al., 2020), annual evaporation of 1200–1900 mm, and annual average precipitation of 378.14 mm, with an extremely uneven distribution of precipitation during the year, mainly concentrated in June–August, accounting for 79% of the total annual precipitation. The Tao'er and Erlongtao Rivers flow through the area. The plant and animal resources in the reserve are rich, with more than 600 species of seed plants, including herbaceous species such as reeds, small-leafed adults, moss grasses, and fragrant cattails, which have a high population density and biomass, are the dominant species in the reserve, and are distributed in slightly different areas (Zhao et al., 2022).

2.2 Data source and pre-processing

The NDVI data were obtained from GEE platform, spanning 1984–2020, with a spatial resolution of 30 m. The downloaded data were pre-processed using software for stitching, projection, and format conversion. Maximum value composites (MVC) method was used to obtain the monthly NDVI data, which reduced the effects of clouds, atmosphere, and solar altitude angle (Holben, 1986), which were averaged to obtain the growing season NDVI data. And then the monthly NDVI data were extracted by the mean method from April to October each year to obtain the year-by-year growing season NDVI data.

The meteorological data were obtained from the China Meteorological Data Network(http://cdc.cma.gov.cn/), and the month-by-month hydrological and temperature data from 1984 to 2020 were extracted from the nearest meteorological stations in Baicheng City. The meteorological data were projected and resampled by ArcGIS 10.6 software to obtain the meteorological factor raster data with the same resolution as NDVI data.

Landuse/landcover (LULC) data were obtained from the Resource and Environment Science and Data Centre of the Chinese Academy of Sciences(http://www.resdc.cn), and were divided into seven phases of images (1980, 1990, 2000, 2005, 2010, 2015, and 2020) with a spatial resolution of 30 m. The land use types were grassland, swampy wetland, water surface, paddy field, dry field, artificial surface, sandy land, saline land, and woodland

2.3 Methods

2.3.1 Fractional vegetation cover

A like-element dichotomous model was used to estimate the fractional vegetation cover (FVC) in the study area (Gong et al., 2017) to explore the spatial and temporal variation characteristics of vegetation cover using the following equation:

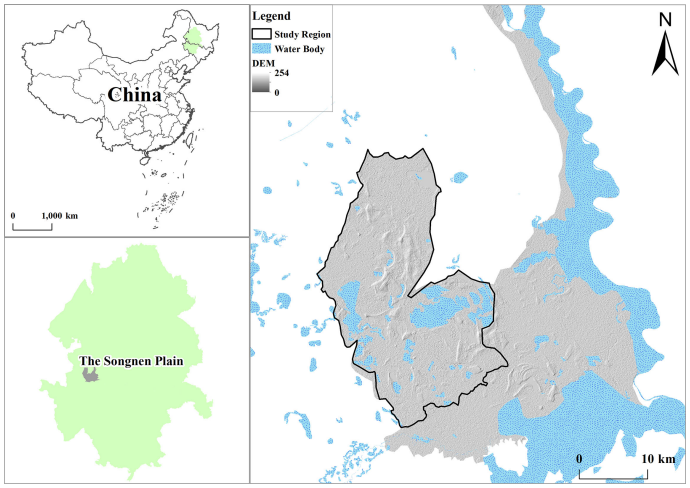

FIGURE 1
Location of study area.

$$FVC = \frac{(NDVI - NDVI_{soil})}{(NDVI_{veg} - NDV_{soil})} \quad (1)$$

where FVC is the vegetation cover, $NDVI_{soil}$ is the NDVI value of bare land, and $NDVI_{veg}$ is the NDVI value of high cover. In this study, the normalized vegetation index with a cumulative frequency of 5% was selected as $NDVI_{soil}$, and the normalized vegetation index with a cumulative frequency of 95% was selected as $NDVI_{veg}$. Based on the grading standards of vegetation cover in the northeastern black soil area in the Soil Erosion Classification and Grading Standards issued by the Ministry of Water Resources of China in 2008, and combined with the characteristics of the local ecological environment (Jiang et al., 2017), the proportional standards of vegetation cover were developed and classified into five categories: low coverage, low to medium coverage, medium coverage, medium to high coverage, and high coverage (Table 1).

2.3.2 Trend analysis

The Theil–Sen Median trend analysis estimation was used to explore the trend of NDVI of the vegetation in the study area (Jiang et al., 2015b; Jiang et al., 2022) to reveal its change characteristics on the time scale. The formula used is as follows:

$$\theta_{NDVI} = Median\left(\frac{NDVI_j - NDVI_i}{j - i}\right) \quad (2)$$

Where i and j represent years, $i \le j$, and takes values between 1984 and 2020. $NDVI_i$ and $NDVI_j$ represent NDVI in years i and j, respectively. θ_{NDVI} represents the slope of the change in NDVI of vegetation during the study period. When $\theta_{NDVI} > 0$, the NDVI of vegetation during the study period was considered to be increasing and the vegetation cover was improving. When $\theta_{NDVI} > 0$, the vegetation NDVI remained unchanged and the vegetation cover was more stable; when $\theta_{NDVI} > 0$, the vegetation NDVI decreased, and the vegetation cover was degraded during the study period.

The Mann–Kendall significance test was used to determine whether the slope of change in vegetation NDVI over the study period was significant and the degree of significance (Mann, 1945; Kendall, 1948). The results of θ_{NDVI} and Mann–Kendall significance test were combined to obtain six scenarios of vegetation NDVI: when $\theta_{NDVI} > 0$ and passed α=0.05 significance test, vegetation NDVI showed a significant increasing trend; when α=0.05 significance test was not passed, vegetation NDVI showed a non-significant increasing trend; similarly, vegetation NDVI showed a decreasing trend. Two scenarios with decreasing trends in NDVI were obtained.

2.3.3 Partial correlation analysis

The partial correlation between vegetation cover and each climate factor was analyzed using image-based spatial analysis (Yuan et al., 2019). The simple correlation coefficient was calculated first, and then the partial correlation coefficient was obtained. The correlation coefficients of NDVI, temperature, and rainfall were calculated as follows:

$$r_{xy} = \frac{\sum_{1=1}^{n}(x_1 - \overline{x})(y_1 - \overline{y})}{\sqrt{\sum_{1=1}^{n}(x_1 - \overline{x})^2(y_1 - \overline{y})^2}} \quad (3)$$

where r_{xy} is the correlation coefficient between NDVI and climate factor, x_i, y_i are the values of climate factor and vegetation NDVI in year i respectively, x_i, yi are the mean values of each variable, i is the year number, and n is the monitoring year.

Partial correlation analysis was used to analyze the degree of correlation between two variables, without considering the effect of the third variable. The partial correlation coefficient is calculated based on a linear correlation using the following formula:

$$r_{xy,z} = \frac{r_{xy} - r_{xz}r_{yz}}{\sqrt{(1 - r_{xy}^2)(1 - r_{yz}^2)}} \quad (4)$$

where $r_{xy,z}$ denotes the partial correlation coefficient of x and y variables after the fixed variable z; r_{xy}, r_{xz}, r_{yz} are the correlation coefficients between the respective variables, and the partial correlation coefficients take values in the range of –1 to 1.

The test of correlation coefficient is often done by T-test and according to the test results we can classify the bias correlation into 6 levels: highly significant positive correlation ($r_{xy,z} > 0, p < 0.01$), highly significant negative correlation ($r_{xy,z} < 0, p < 0.01$), significant positive correlation ($r_{xy,z} > 0, 0.01 \le p < 0.05$), significant negative correlation($r_{xy,z} < 0, 0.01 \le p < 0.05$), no significant positive correlation ($r_{xy,z} > 0, p \ge 0.05$), no significant negative correlation ($r_{xy,z} < 0, p \ge 0.05$).

TABLE 1 The classification standard of FVC.

Grade	FVC	Classification features
Low	<10%	Basically no vegetation
Low to medium	10%-30%	Sparse vegetation
Medium	30%-45%	Better vegetation
Medium to high	45%-60%	Well-vegetated
High	≥60%	Lush vegetation

2.3.4 Relative role analysis

Residual analysis has been used to discern the effects of human activities on vegetation changes (Wessels et al., 2007). NDVI predictions were obtained by fitting precipitation and air temperature data to obtain a time series of NDVI for the vegetation growing season with only climatic effects, thus obtaining the residual value, which is the effect of human activity on NDVI for the vegetation growing season, using the following equation:

$$NDVI_{Pre} = a \times P \times b \times T + C \quad (5)$$

$$NDVI_{Rre} = NDVI_{Real} - NDVI_{Pre} \quad (6)$$

where $NDVI_{Pre}$ denotes the predicted value of NDVI, $NDVI_{Real}$ denotes the real value of NDVI; α and b denote the regression coefficients of NDVI on precipitation and temperature, respectively; C denotes the regression constant term; P denotes precipitation; and T denotes temperature. An $NDVI_{Res} > 0$ indicates a positive effect of human activities, whereas an $NDVI_{Res} = 0$ indicates a negative effect of human activities. An $NDVI_{Res} = 0$ indicates a relatively weak effect of human activities.

The test of residual values is often done by T-test and according to the test results we can classify residual values into 4 levels: significant positive correlation ($NDVI_{Res} > 0$,$p<0.05$), significant negative correlation ($NDVI_{Res} < 0$,$p<0.0)5$, no significant positive correlation ($NDVI_{Res} > 0$,$p \geq 0.05$), no significant negative correlation. ($NDVI_{Res} < 0$,$p \geq 0.05$).

2.3.5 Driving factor determination

Using the simulation assessment method (Cheng et al., 2021), the trends of $NDVI_{Real}$, $NDVI_{Pre}$, and $NDVI_{Res}$ ($\theta_{NDVI_{Real}}$, $\theta_{NDVI_{Pre}}$, $\theta_{NDVI_{Res}}$) were calculated using residual analysis, and the spatial distribution of the drivers was calculated using ArcGIS 10.6 (Table 2).

2.3.6 Relative action method

Relative contribution analysis was used to quantify the relative contributions of climate change and human activity to vegetation changes (Sun et al., 2020). Residual analysis was used to establish the evaluation method of the relative contribution of climate change and human activities to the vegetation change process under different possible scenarios (Table 3). When $\theta_{NDVI_{Real}} > 0$, it indicates that vegetation tends to improve, and vice versa; when $\theta_{NDVI_{Pre}} > 0$, it indicates that climate change promotes vegetation growth, and vice versa; and when $\theta_{NDVI_{Res}} > 0$, it indicates that human activities promote vegetation growth, and vice versa.

2.3.7 LULC transfer matrix analysis

The spatial transformation of land use types was analyzed for the study area in 1980, 1990, 2000, 2005, 2010, 2015, and 2020 using a transfer matrix (Yao et al., 2021). The wetland transfer matrix was visualized using a Sankey diagram with the following equation.

$$S_{ij} = \begin{pmatrix} S_{11} & S_{12} & \cdots & S_{1n} \\ S_{21} & S_{22} & \cdots & S_{2n} \\ \cdots & & \cdots & \cdots \quad \cdots \\ S_{n1} & S_{n2} & \cdots & S_{nn} \end{pmatrix} \quad (7)$$

Where S is the area; n is the number of landscape types; and i, j in S_{ij} denote the landscape types at the beginning and end of the study period, respectively.

3 Results

3.1 FVC change characteristics

3.1.1 Temporal and spatial analysis of FVC

The overall vegetation cover in the study area from 1984 to 2020 was good, and the area was dominated by medium to high vegetation cover. Additionally, there was heterogeneity in the spatial cover of vegetation between different years (Figure 2). The first period (1984–2000) had a wide area of vegetation cover and more areas of high and medium vegetation cover, which were evenly distributed in the study area. Medium vegetation

TABLE 2 Determination criteria of driving factors.

$\theta_{NDVI_{Real}}$	Driving Factors	$\theta_{NDVI_{CC}}$	$\theta_{NDVI_{HA}}$	Contribution of drivers (%)	
CC	HA				
>0	CC&HA	>0	>0	$\frac{\theta_{NDVI_{CC}}}{\theta_{NDVI_{Real}}}$	$\frac{\theta_{NDVI_{HA}}}{\theta_{NDVI_{Real}}}$
	CC	>0	<0	100	0
	HA	<0	>0	0	100
<0	CC&HA	<0	<0	$\frac{\theta_{NDVI_{CC}}}{\theta_{NDVI_{Real}}}$	$\frac{\theta_{NDVI_{HA}}}{\theta_{NDVI_{Real}}}$
	CC	<0	>0	100	0
	HA	>0	<0	0	100

HA, human activity; CC, natural factor; $\theta_{NDVI_{CC}}$ refers to the trend of climate change impact ($\theta NDVI_{Real}$), $\theta_{NDVI_{HA}}$ refers to the trend of human activity impact ($\theta NDVI_{Pre}$), and $\theta NDVI_{Real}$ refers to the trend of actual NDVI change.

TABLE 3 Methods for evaluating the relative roles of climate change and human activities in the process of vegetation change under different scenarios.

Zoning	Scenario	$\theta_{NDVI_{Pre}}$	$\theta_{NDVI_{Res}}$	The relative role of climate change $\times 100^0/_0$	The relative role of human activities $\times 100^0/_0$	Description
Vegetation improvement	1	>0	>0	$\theta_{NDVI_{Real}} \frac{\lvert\Delta NDVI_{Pre}}{\lvert\Delta NDVI_{Pre} + \Delta NDVI_{Res}}$	$\frac{\lvert\Delta NDVI_{Res}}{\lvert\Delta NDVI_{Pre} + \Delta NDVI_{Res}}$	Common driven
	2	>0	<0	100%	0%	CC driven
	3	<0	>0	0%	100%	HA driven
Vegetation degradation	4	<0	<0	$\frac{\lvert\Delta NDVI_{Pre}}{\lvert\Delta NDVI_{Pre} + \Delta NDVI_{Res}}$	$\frac{\lvert\Delta NDVI_{Res}}{\lvert\Delta NDVI_{Pre} + \Delta NDVI_{Res}}$	Common driven
	5	<0	>0	100%	0%	CC driven
	6	>0	<0	0%	100%	HA driven

$\Delta NDVI_{Pre}$ is the difference between $NDVI_{Pre}$ and in year t+1 under the influence of climate change; is the difference between. $NDVI_{Res}$ and $NDVI_{Res}$ in year t+1 under the influence of human activities.

cover was distributed in the northern part of the study area, while there were less low and medium vegetation cover areas, which were mainly scattered in the southern part of the study area and the western part, and the low vegetation cover areas were scattered. In the second period (2001–2005), there was a decrease in vegetation cover in the study area, low vegetation cover, medium-low vegetation cover, and medium vegetation cover gradually expanded, medium vegetation cover areas were evenly distributed in the study area, medium-low vegetation cover spread to the northern part of the study area, and low vegetation cover was mainly in the west, especially in 2001; the medium-low vegetation cover area was the highest. The third period covered the period from 2006–2020, and the high vegetation cover and medium vegetation cover in this time period again increased significantly each year. The vegetation in the northern area grew and returned to the high vegetation area and medium-high vegetation cover area. Compared with the first period, the medium vegetation cover and medium-low vegetation cover area were less, and the medium-low vegetation cover was mainly located in the southern part of the study area.

The differences in the different classes of vegetation cover in the different years were more obvious (Figure 3). Overall, high vegetation cover was the most distributed, with an average of 49.94%, followed by medium-high vegetation cover with an average of 22.97%, medium value cover with an average of 16.99%, medium-low vegetation with an average of 9.81%, and low vegetation cover with an average of 0.28%. The study period is divided into 3 stages. The first period spanned 1984–2000. During this period, the average percentage of high vegetation cover area was 51.22%, the average percentage of higher vegetation cover was 21.21%, average percentage of medium vegetation cover was 15.02%,

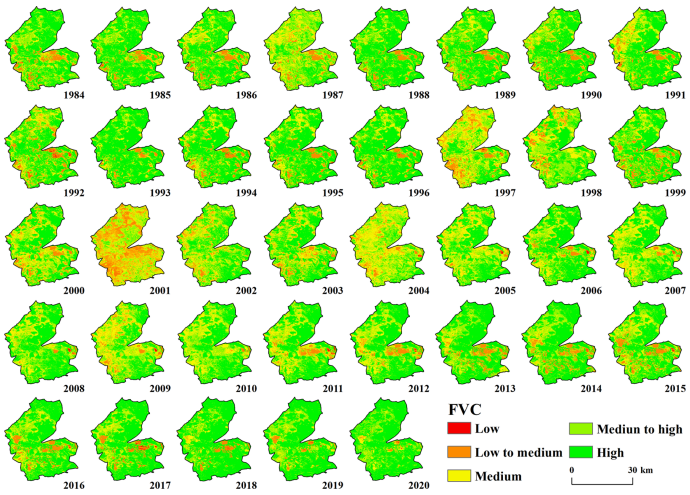

FIGURE 2
Spatial distribution characteristics of FVC in the study area from 1984–2020.

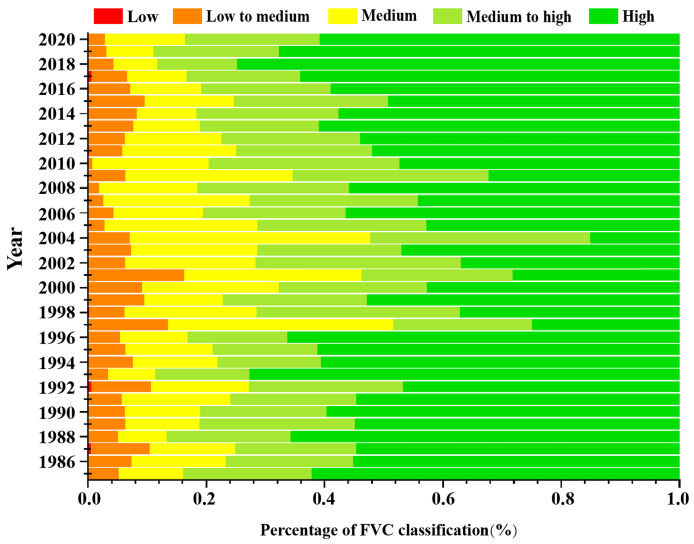

FIGURE 3
The proportion of FVC of different grades in the study area from 1984–2020.

average percentage of medium and low vegetation cover area was 12.09%, and average percentage of low vegetation cover area was 0.47%. It can be seen that the percentage of high vegetation cover is the highest. In the second period, from 2001 to 2005, the average value of high vegetation cover area was 28.33%, average value of higher vegetation cover area was 26.23%, average value of medium vegetation cover area was 29.19%, average value of medium and low vegetation cover area was 16.18%, and average value of low vegetation cover area was 0.05%. Thus, it was found that the high vegetation cover area was still the highest, but with a decreasing trend; the mean value is 16.7% less than in the first stage, but the distribution of medium vegetation and medium-high vegetation increased significantly and the proportion of medium-low vegetation cover decreased. The third period was from 2006 to 2020; in this period, the mean value of the high vegetation cover area was 55.69%, the mean value of higher vegetation cover was 23.89%, proportion of medium vegetation cover average value was 15.16%, the average value of the medium-low vegetation cover area was 5.12%, and the average value of the low vegetation cover area was 0.15%. The distribution of the high vegetation area increased significantly, and the percentage of medium-low vegetation cover continued to show a decreasing trend. In summary, the change in low vegetation cover was small in the three stages, medium-low vegetation cover showed a decreasing trend, medium vegetation cover and medium-high vegetation cover showed roughly the same trend, that is, increasing and then decreasing, while high vegetation cover showed a decreasing and then increasing trend.

3.1.2 NDVI trend analysis

The spatial and temporal variation of vegetation NDVI in the study area from 1984 to 2020 showed obvious spatial heterogeneity (Figure 4). The multi-year average NDVI change rate was –0.026–0.031/a, with a mean value of 0.002/a. 71.14% of the vegetation cover in the study area was improved, among which, 37.54% of the significantly improved areas were evenly dispersed in the study area; while The degraded areas accounted for 28.86% and only 7.2% of the significantly degraded areas, which were mainly concentrated in the central part of the study area.

3.2 Response of vegetation change to climatic factors

3.2.1 Analysis of interannual variability of climatic factors

The vegetation growing seasons in the study area from 1984 to 2020 were generally consistent with temperature changes during the same period (Figure 5). The growing season NDVI trend in the study area shifted in 2000, that is, increasing and then decreasing, and then shifted a second time in 2006, from decreasing to increasing, and the rate of increase was higher than the rate of increase before the 1990s. The growing season temperature in the study area also showed decreasing, increasing, and substantially increasing trends from to 1984–2000, 2001–2005, and 2006–2020, respectively, which were almost consistent with the fluctuations and trends of NDVI.

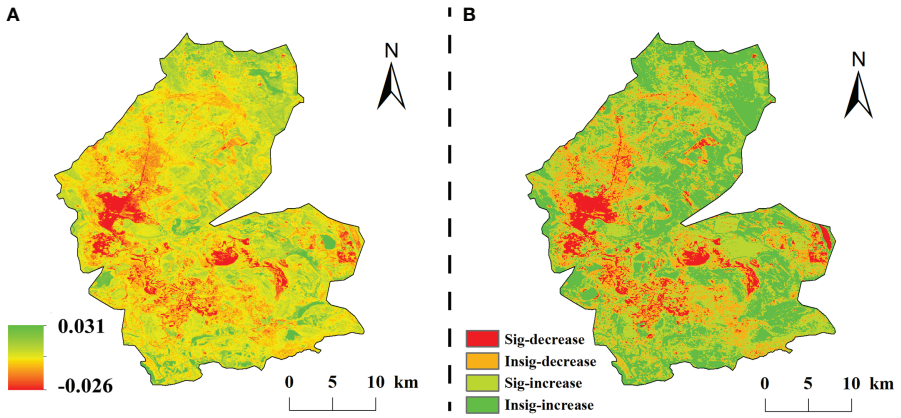

FIGURE 4
The classification of change trend in the study area from 1984 to 2020. **(A)** is the slope of interannual variation of NDVI, **(B)** is the spatial distribution of significance.

3.2.2 Correlations of NDVI with temperature and precipitation

The correlation coefficient between the NDVI and precipitation for the entire study area was 0.19. The correlation coefficient between NDVI and precipitation in the growing season of vegetation in the study area was mainly positive, ranging from −0.546 to 0.755, with positive and negative correlations accounting for 53.89% and 46.11% of the study area, respectively. Significant negative correlations accounted for 3.68% and were sporadically distributed within the study area. Insignificant positive and negative correlations accounted for 50.66% and 42.43%, respectively, and were evenly distributed in the study area (Figure 6).

The NDVI and temperature in the study area mainly showed a positive correlation during the growing season, with correlation coefficients of −0.654 to 0.752, of which the proportion of positive and negative correlation areas were 52.79% and 47.21% of the whole study area, respectively; among them, a significant positive correlation accounted for 2.14% and was scattered in the study area; a significant negative correlation accounted for 4.78% and was mainly distributed in the central part of the study area; an insignificant positive correlation accounted for 50.66%, mainly in the western and eastern regions of the study area, and 42.43% of the insignificant negative correlations were scattered in the study area (Figure 6).

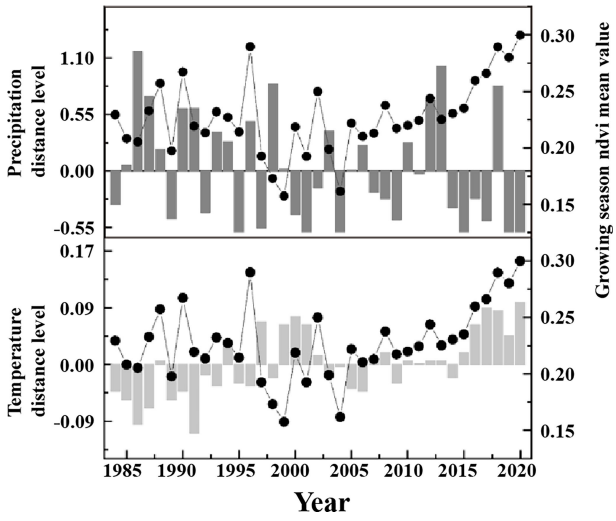

FIGURE 5
The interannual variations of NDVI, precipitation and temperature in June of 1984-2020.

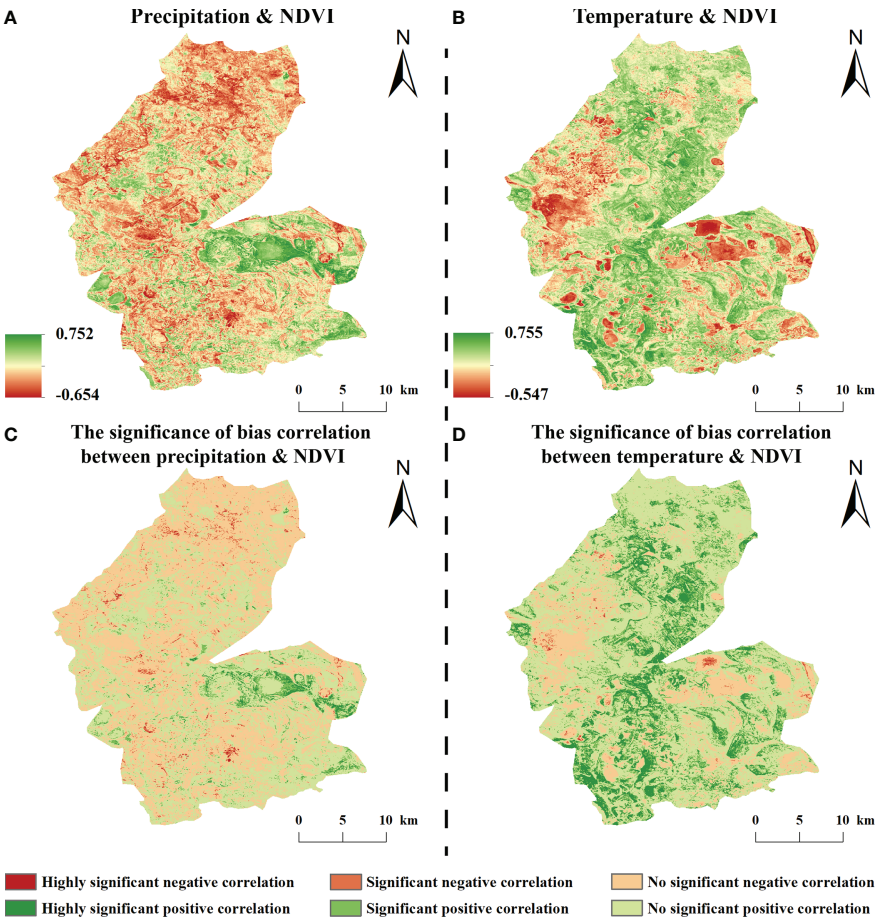

FIGURE 6
Bias correlation between NDVI and climatic factors from 1984-2020 (**A, B** are the bias off NDVI with precipitation and temperature, respectively; **C, D** are the respective significance).

3.3 Response of vegetation change to human activities

3.3.1 Residual analysis

On a time scale, the mean values of NDVI residuals of vegetation in the study area were mainly negative in the early period and positive beginning in 2010. The residuals showed an overall increasing trend at a rate of $0.0021a^{-1}$. Spatially (Figure 7), the NDVI residual values in the study area varied from –0.0.028 to 0.025 a^{-1}, and the areas with positive residuals accounted for 71.50% of the total area, of which 34.42% of the total area was significantly increased and concentrated in the northern and eastern parts of the study area.

3.3.2 LULC impacts on vegetation pattern changes

The correlation between land use change and vegetation change in the study area from 1980 to 2020 was clearly characterized (Figure 8A). The area changes of herbaceous wetlands, water bodies and woodlands were consistent with the trend of NDVI change, decreasing first and then increasing, while the area changes of grassland, dryland and saline land were opposite to the trend of NDVI change. In addition, land use types with different NDVI transformed into each other to different degrees during this period (Figure 8B). From 1980 to 1990, a total of 95.12 km^2 was transferred from grassland, swampy wetland, water, saline land and forest land to dryland, indicating that there was more agricultural reclamation during this period; from 1990 to 2000, the transfer from swampy wetland, water, dryland and sandy land to saline land 57.68 km^2, indicating that a part of the land began to be saline in that period; from 2000 to 2005, the areas of marsh wetland to water surface, grassland and dryland were 32.71 km^2, 20.08 km^2 and 9.45 km^2, indicating that a large area of marsh wetland was degraded in that period; from 2005 to 2010, the areas of grassland to dryland and marsh wetland were 15.33 km^2, 13.19 km^2;

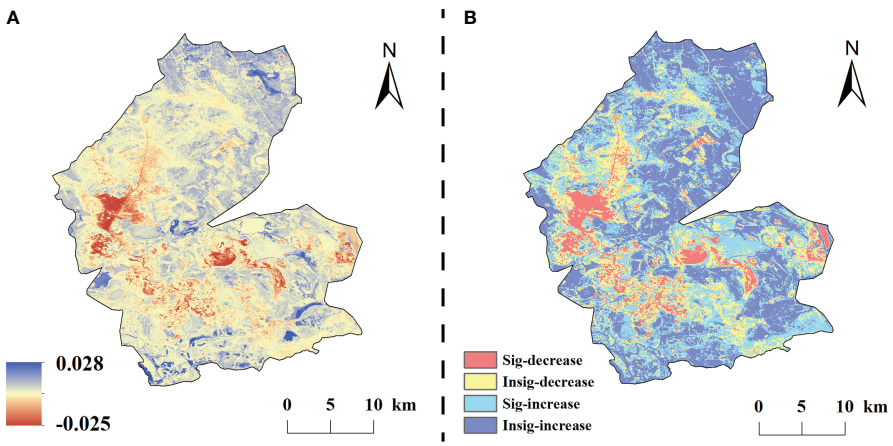

FIGURE 7
Trends in NDVI residuals under the influence of human change from 1984–2020 (**A** is the residual trend, **B** is the residual significance).

indicating that both agricultural reclamation and ecological water replenishment projects existed simultaneously in this period; from 2010 to 2015, the area shifted from marsh wetland, dryland and saline land to water bodies was 48.50 km^2, 21.23 km^2, 16.60 km^2, indicating that ecological restoration efforts were stronger in this period; from 2015 to 2020, water surface to marsh wetland shifted 11.12 km^2, indicating the existence of vegetation protection in this period.

3.4 Vegetation change driving mechanisms

3.4.1 Spatial distribution of drivers of vegetation change

The percentage of areas where the NDVI of vegetation in the study area was driven by both climate change and human activity was 43.23%, which was mainly distributed in the eastern part of the study area. The percentages of NDVI

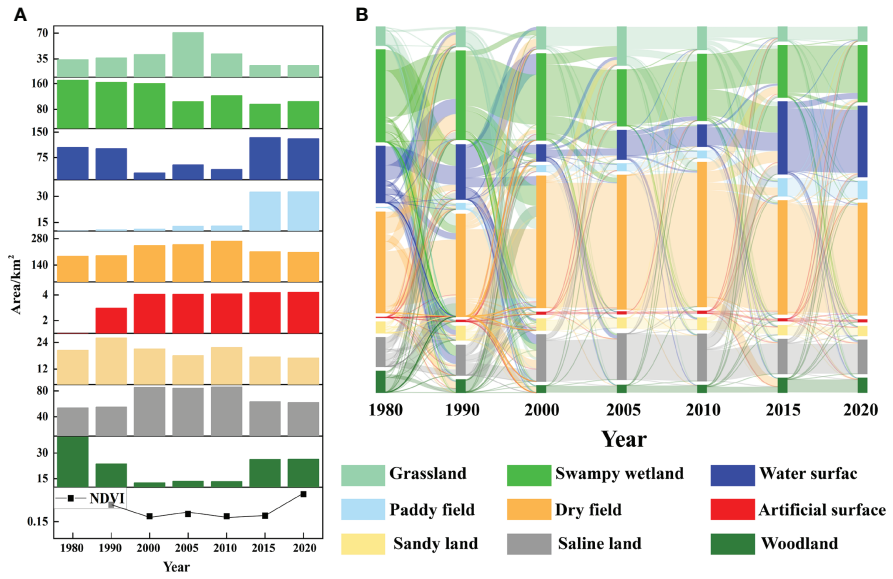

FIGURE 8
The change of land use types and NDVI values in the study area (**A** is the trends in land use area and NDVI values, **B** is the sankey diagram of landscape transfer matrix).

increase in vegetation driven by climate change alone and by human activity alone were 1.78% and 26.72%, respectively. By contrast, 15.12%, 1.71%, and 11.44% of the areas driven by climate change and human activities, climate change alone, and human activities alone, respectively, were distributed in the western part of the study area (Figure 9).

3.4.2 Relative contribution of different drivers to vegetation change

Climate change and human activities have contributed to vegetation growth in most areas of the study area but have also resulted in a decreasing trend in local vegetation vigor (Figure 10). The relative contributions of climate change and human activities to vegetation improvement in the study area from 1984 to 2020 were 14.32% and 85.68%, respectively. In the vegetation improvement area of the study area, the relative contribution of climate change within 40% accounted for 91.72% of the vegetation improvement area; compared with natural factors, the contribution of human activities to vegetation improvement was mainly concentrated in the range of 80–100%, accounting for 78.20% of the vegetation improvement area and mainly distributed at the edge of the study area.

There was a large spatial variation in the magnitude of the relative contributions of climate change and climate change to vegetation degradation (Figure 10). In the degraded areas, although the contribution of climate change to vegetation change increased compared with the improved areas, it was still lower than the contribution of human activities (21.71% and 78.29% of the relative contribution of the two, respectively). Among them, the area where the contribution of climate change to the vegetation NDVI degradation was in the range of 0–20% respectively was the largest, accounting for 60.98% of the vegetation degradation area and mainly distributed in the western part of the study area; the area where the relative contribution of human activities was above 60% accounted for 82.64% of the vegetation degradation area and was evenly distributed in the inner part of the study area.

4 Discussion

4.1 Temporal and spatial characteristics of vegetation cover

On the time scale, the vegetation NDVI in the study area of Momoge showed a fluctuating upward trend from 1984 to 2020, and the vegetation growth status was generally good; however, the vegetation NDVI continued to decline in the middle of the study, which is consistent with the conclusion obtained by other researchers (Xue et al., 2022). In addition, the trend of high vegetation cover in the study area increased before 2000 and decreased after 2005, whereas the trend of vegetation cover and middle and high vegetation cover changed in the opposite direction. In the early stage, the study area had good vegetation cover due to abundant precipitation, sufficient heat, less human disturbance, low exploitation, and longitudinal water systems. In the middle stage, the vegetation cover decreased due to agricultural reclamation, water conservation projects, and increased extreme drought, which is consistent with the results of previous studies (Wang et al., 2022a). At the spatial scale, at least 70% of the study area showed an increasing vegetation

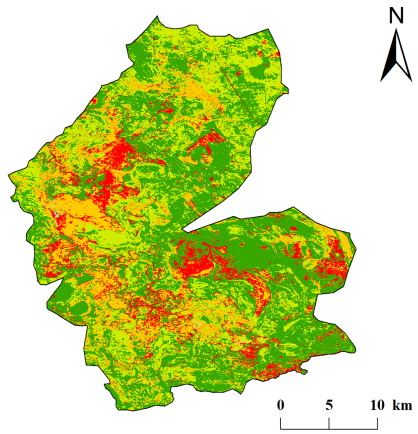

FIGURE 9
Spatial distribution of driving mechanisms of vegetation NDVI change in the study area.

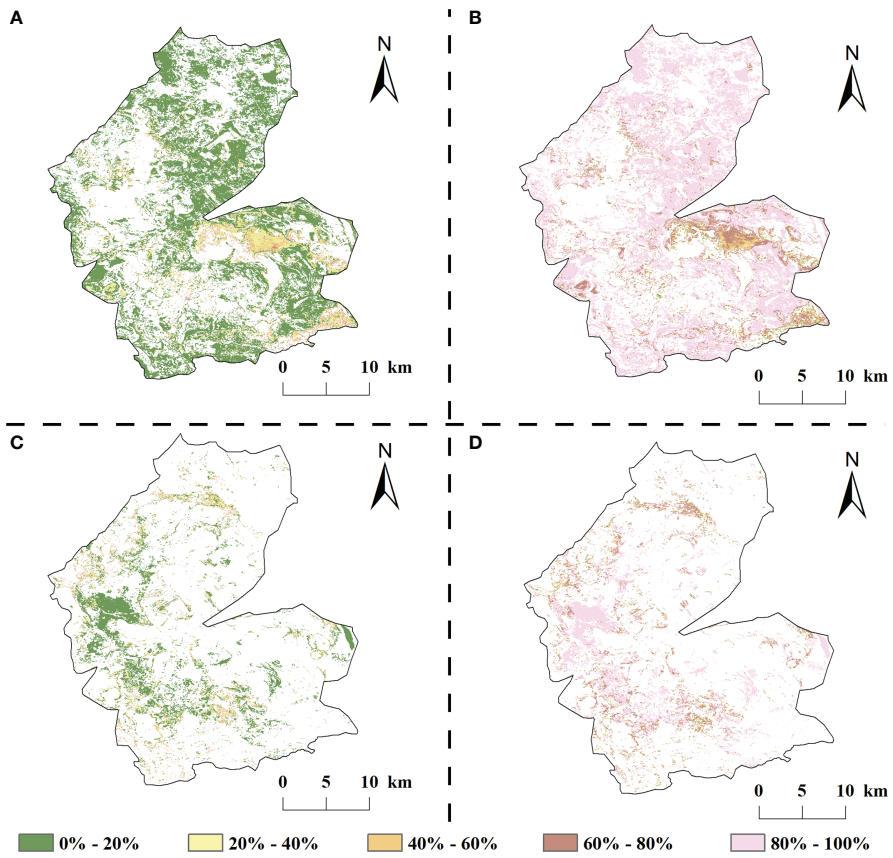

FIGURE 10
Relative contribution of climate change and human activities study areas, 1984-2020 (**A**, **B** are the relative contribution of climate change, human activities to vegetation improvement areas, respectively; **C**, **D** are the relative contribution of climate change, human activities to vegetation degradation areas, respectively).

trend from 1984 to 2020. The other decreasing areas were distributed in several villages, towns, and surrounding areas in the study area of Momo, mainly because the above areas had a poor vegetation base owing to the high intensity of human activities, and the negative human disturbance destroyed the vegetation growth environment, resulting in a decreasing vegetation cover trend.

4.2 Drivers and mechanisms of vegetation change

Previous studies have shown that vegetation cover change is a complex process, with long term vegetation cover change mainly influenced by natural geographic processes such as climate change, while short term vegetation change is significantly influenced by human activities such as deforestation, overgrazing and ecological engineering (Chapman et al., 2014; Qu et al., 2018). Based on the results of the driving analysis of vegetation change, we found that vegetation growth in the study area from 1984 to 2020 was driven by both climate change and human activities in 58.35% of the total study area, which shows that the joint driving factors of climate change and human activities is the main reason for the change in vegetation NDVI in the Momoge Reserve. Among them, human activities contributed more to the vegetation cover change in the study area than climate change.

4.2.1 Climate change

The overall trend of vegetation versus precipitation and temperature during the growing season showed that the study area suffered from multi-year drought in the middle of the season, with precipitation below the multi-year average, temperature increased, and vegetation cover decreased; in the later season, the climate improved and vegetation cover increased as precipitation increased. The positive correlation between vegetation cover and precipitation in the study area was higher than that of temperature. The reasons for this are as follows: (1) Precipitation is a key constraint on vegetation growth and distribution in semi-arid areas

(Huang and Wang, 2010). Precipitation can replenish soil moisture and promote plant growth (Shen et al., 2019). In the study area, there is severe water shortage in drought years, soil salinization is severe, water retention is poor and water content is low, and plants depend on precipitation to replenish water to maintain survival. (2) Temperature is a limiting factor affecting vegetation cover (Mao et al., 2012). In arid and semi-arid regions, increasing temperature will accelerate vegetation transpiration, resulting in increased evapotranspiration and reduced soil moisture, which will inhibit vegetation growth (Vicente-Serrano et al., 2013). With global warming, the trend of warming and drying of swampy wetlands in semi-arid areas has increased, and the frequent occurrence of drought is not conducive to local vegetation recovery.

The spatial correlation between vegetation and precipitation and temperature during the growing season showed that the NDVI response to precipitation and temperature was spatially unevenly distributed, with both positive and negative correlation coefficients. the precipitation-related areas were mostly located in meadows and croplands, where increased precipitation helped to relieve plants from water stress (Lou et al., 2015), while the temperature-related areas were mostly located in swampy wetlands or around water bubbles, where water and heat conditions were abundant and conducive to plant growth (Cai et al., 2021). The land use types in the study area are mainly swampy wetlands and croplands, unlike the more stable forest ecosystems, which are more sensitive to climate change (Piao et al., 2020; Masao et al., 2022), however, we noticed that there are fewer areas of significant correlation between vegetation cover and temperature and precipitation, and the influence of hydrothermal factors on vegetation growth activities is smaller. This is related to the implementation of ecological water recharge projects in recent years. The availability of water resources in the study area is not controlled by climatic factors but by human activities, and nowadays vegetation is rarely affected by water stress, therefore, vegetation growth is less sensitive to climatic factors, which is consistent with the results of existing studies (Shi et al., 2021).

4.2.2 Human activities

In addition to climate change, human activities are also a key factor in determining the spatial distribution patterns and dynamics of vegetation in the study area, as strongly evidenced by NDVI residuals. The human land use patterns characterize the impact of human activities on the surface vegetation to a certain extent. The Momog Reserve is located in the transition zone between East Asian broadleaf forests and Eurasian steppes, where natural and artificial vegetation coexist in the reserve (Ning et al., 2014). In the study area, in the middle period, the area of swampy wetlands, woodlands and water bodies decreases with the consequent decrease in NDVI; in the later period, NDVI increases with the increase in the area of swampy wetlands, woodlands and grasslands, which is consistent with the findings of existing studies (Yang et al., 2022).

It is worth mentioning that human activities have caused a shift in land use type and use pattern in Momoge Reserve, which in turn has a positive or negative impact on vegetation cover area and quality. Irrational human cultivation and urban expansion degrade vegetation, while the implementation of ecological engineering improves it (He et al., 2021). We can see from the results of land use conversion that in the medium term, with over-exploitation by humans, a large number of vegetation NDVI high value areas (swampy wetlands, woodlands and grasslands) were converted to NDVI low value areas (water bodies, unused land and built-up land) in the study area (Mao et al., 2019); in recent years, with the implementation of ecological projects such as returning wetlands to farmland, forests to farmland, grazing to grass, and river and lake linkages (Huang et al., 2022), a large number of vegetation areas with low NDVI values (cropland and unused land) have been transformed into areas with high NDVI values (grassland and woodland) in the study area. Coupled with the gradual stabilization of cropland size in recent years, with high NDVI crops such as rice and soybean, the study area maintains a high and stable vegetation cover (Geng and Zhou, 2022). The human-driven NDVI increase in the study area is higher than the human-driven NDVI decrease in the study area, which indicates that human conservation efforts in the study area have been effective.

4.3 Limitations of this study

In this study, NDVI was used as a parameter to quantitatively evaluate the method of climate change and anthropogenic contribution to vegetation cover in a typical arid and semi-arid swampy region of China. However, we should also recognize the limitations of this study. First, this study used the Landsat dataset to calculate NDVI for long time series, which does not have a high spatial resolution (30 m), which may affect the study results and can be improved in the future by fusing multi-source data at a higher spatial resolution and long-term scale (Decuyper et al., 2020; Shen et al., 2022a; Shen et al., 2022b). Second, since natural factors affecting vegetation change include precipitation, temperature, topography and soil, only precipitation and temperature were considered when conducting the natural factor analysis in this paper, and multiple natural factors should be considered in the future to explore the causes of vegetation change in an integrated manner. Finally, the climate data used in this study were obtained by spatial interpolation based on sparse site data, which may be another potential source of uncertainty.

5 Conclusions

In this study, we found that the average NDVI of the vegetation growing season in the study area from 1984 to 2020 was 0.55, and the average annual growth rate was 0.002/a. The NDVI of 71.14% of the area increased, and there was spatial and temporal heterogeneity of vegetation cover in the study area, with a decreasing trend of low and medium vegetation cover, a generally consistent trend of medium and high vegetation cover (i.e. increasing first and then decreasing), and a decreasing trend of high vegetation cover. Spatial and temporal heterogeneity of vegetation cover in the study area was found. Among the climate change factors, precipitation is the most important factor for vegetation growth in the study area, and it is positively correlated with the NDVI in the study area as a whole and has a greater influence. Human activities also have a dual effect on vegetation change, and a series of ecological restoration measures have effectively improved the ecological environment of the area in recent years. The vegetation cover change in the study area was mainly driven by both human activities and climate change; however, the promotion in the conclusion effect of human activities on vegetation growth was greater than that of climate change, and the relative effect on the vegetation improvement area was 85.68%.

Data availability statement

The original contributions presented in the study are included in the article/supplementary material. Further inquiries can be directed to the corresponding authors.

Author contributions

GD: Data Analysis, writing-original draft. JG: Writing-review and editing. HJ: Project administration. DL: Formal analysis. XW and YW: Visualization. LS and CH: Investigation, Validation. All authors have read and agreed to the published version of the manuscript.

Funding

This research was funded by the National Natural Science Foundation of China, grant numbers 41901116 and U19A2042, and the Foundation of Jilin Educational Committee, grant numbers JJKH20220448KJ.

Acknowledgments

The authors would like to acknowledge the contributions of colleagues, institutions, and agencies that aided their efforts.

Conflict of interest

The authors declare that the research was conducted in the absence of any commercial or financial relationships that could be construed as a potential conflict of interest.

Publisher's note

References

Bai, Z., Dong, Z., Xue, L., Cui, Y., Shi, W., Chen, G., et al. (2022). An analysis of the effects of anthropogenic factors on vegetation cover change in guanzhong, China. *Front. Earth Sci.* 10. doi: 10.3389/feart.2022.831904

Barchiesi, S., Alonso, A., Pazmiño-Hernandez, M., Serrano-Sandí, J. M., Muñoz-Carpena, R., and Angelini, C. (2022). Wetland hydropattern and vegetation greenness predict avian populations in Palo Verde, Costa Rica. *Ecol. Appl.* 32, e2493. doi: 10.1002/eap.2493

Cai, H., Guang, R., Gang, L., Yun, Y., Qiang, W., Deng, H., et al. (2021). The effects of rainfall characteristics and land use and cover change on runoff in the yellow river basin, China. *J. hydrology hydromechanics* 69, 29–40. doi: 10.2478/johh-2020-0042

Chapman, S., Mustin, K., Renwick, A. R., Segan, D. B., Hole, D. G., Pearson, R. G., et al. (2014). Publishing trends on climate change vulnerability in the conservation literature reveal a predominant focus on direct impacts and long time-scales. *Diversity Distributions* 20, 1221–1228. doi: 10.1111/ddi.12234

Cheng, D. ,. D., Qi, G. ,. Z., Song, J. ,. X., Zhang, Y. ,. X., Bai, H. ,. Y., and Gao, X. ,. Y. (2021). Quantitative assessment of the contributions of climate change and human activities to vegetation variation in the qinling mountains. *Front. Earth Sci.* 9. doi: 10.3389/feart.2021.782287

Decuyper, M., Chávez, R. O., Čufar, K., Estay, S. A., Clevers, J. G. P. W., Prislan, P., et al. (2020). Spatio-temporal assessment of beech growth in relation to climate extremes in Slovenia – an integrated approach using remote sensing and tree-ring data. *Agric. For. Meteorology* 287, 107925. doi: 10.1016/j.agrformet.2020.107925

Geng, G., and Zhou, H. (2022). Assessing the relationship between drought and vegetation dynamics in northern China during 1982–2015. *Theor. Appl. Climatol* 148, 467–479. doi: 10.1007/s00704-022-03956-2

Gong, Z. ,. N., Zhao, S. ,. Y., and Gu, J. ,. Z. (2017). Correlation analysis between vegetation coverage and climate drought conditions in north China during 2001–2013. *J. Geogr. Sci.* 27, 143–160. doi: 10.1007/s11442-017-1369-5

Guntenspergen, G. R., Stearns, F., and Kadlec, J. A. (1989). "Wetland vegetation," in *Constructed wetlands for wastewater treatment* (Boca Raton, FL: CRC Press), 2020 73–88.

Haverkamp, P. J., Bysykatova-Harmey, I., Germogenov, N., and Schaepman-Strub, G. (2022). Increasing Arctic tundra flooding threatens wildlife habitat and survival: Impacts on the critically endangered Siberian crane (Grus leucogeranus). *Front. Conserv. Sci.* 25. doi: 10.3389/fcosc.2022.799998

He, X. ,. H., Yu, Y. ,. P., Cui, Z. ,. P., and He, T. (2021). Climate change and ecological projects jointly promote vegetation restoration in three-river source region of China. *Chin. Geogr. Sci.* 31, 1108–1122. doi: 10.1007/s11769-021-1245-1

HOLBEN, B. N. (1986). Characteristics of maximum-value composite images from temporal AVHRR data. *Int. J. Remote Sens.* 7, 1417–1434. doi: 10.1080/01431168608948945

Huang, F., and Wang, P. (2010). Vegetation change of ecotone in west of northeast China plain using time-series remote sensing data. *Chin. Geogr. Sci.* 20, 167–175. doi: 10.1007/s11769-010-0167-0

Huang, J., Yang, H., He, W., and Li, Y. (2022). Ecological service value tradeoffs: An ecological water replenishment model for the jilin momoge national nature reserve, China. *Int. J. Environ. Res. Public Health* 19, 3263. doi: 10.3390/ijerph19063263

Hu, M. Q., Mao, F., Sun, H., and Hou, Y. Y. (2011). Study of normalized difference vegetation index variation and its correlation with climate factors in the three-river-source region. *Int. J. Appl. Earth Observation Geoinformation* 13, 24–33. doi: 10.1016/j.jag.2010.06.003

Jiang, F., Deng, M. L., Yong, Y., and Sun, H. (2022). Spatial pattern and dynamic change of vegetation greenness from 2001 to 2020 in Tibet, China. *Front. Plant Sci.* 13, 892625. doi: 10.3389/fpls.2022.892625

Jiang, H., He, C., Sheng, L., Tang, Z., Wen, Y., Yan, T., et al. (2015a). Hydrological modelling for Siberian crane grus leucogeranus stopover sites in northeast China. *PLoS One* 10, e0122687. doi: 10.1371/journal.pone.0122687

Jiang, M. ,. C., Tian, S. ,. F., Zheng, Z. ,. J., Zhan, Q., and He, Y. ,. X. (2017). Human activity influences on vegetation cover changes in Beijing, China, from 2000 to 2015. *Remote Sens.* 9, 271. doi: 10.3390/rs9030271

Jiang, W. ,. G., Yuan, L. ,. H., Wang, W. ,. J., Cao, R., Zhang, Y. ,. F., and Shen, W. ,. M. (2015b). Spatio-temporal analysis of vegetation variation in the yellow river basin. *Ecol. Indic.* 51, 117–126. doi: 10.1016/j.ecolind.2014.07.031

Kendall, M. G. (1948). *Rank correlation methods* (Oxford, England: Griffin).

Liu, Y., Li, Y., Li, S., and Motesharrei, S. (2015). Spatial and temporal patterns of global NDVI trends: Correlations with climate and human factors. *Remote Sens.* 7, 13233–13250. doi: 10.3390/rs71013233

Lou, Y. ,. J., Zhao, K. ,. Y., Wang, G. ,. P., Jiang, M., Lu, X. ,. G., and Rydin, H. (2015). Long-term changes in marsh vegetation in sanjiang plain, northeast China. *J. Vegetation Sci.* 26, 643–650. doi: 10.1111/jvs.12270

Mann, H. B. (1945). Nonparametric tests against trend. *Econometrica* 13, 245–259. doi: 10.2307/1907187

Mao, D. ,. H., He, X. ,. Y., Wang, Z. ,. M., Tian, Y. ,. L., Xiang, H. ,. X., Yu, H., et al. (2019). Diverse policies leading to contrasting impacts on land cover and ecosystem services in northeast China. *J. Cleaner Production* 240, 117961. doi: 10.1016/j.jclepro.2019.117961

Mao, D. ,. H., Wang, Z. ,. M., Luo, L., and Ren, C. ,. Y. (2012). Integrating AVHRR and MODIS data to monitor NDVI changes and their relationships with climatic parameters in northeast China. *Int. J. Appl. Earth Observation Geoinformation* 18, 528–536. doi: 10.1016/j.jag.2011.10.007

Masao, C. A., Igoli, J., and Liwenga, E. T. (2022). Relevance of neglected and underutilized plants for climate change adaptation & conservation implications in semi-arid regions of Tanzania. *Environ. Manage.* 69, 1–17. doi: 10.1007/s00267-022-01656-1

Mas, M., Flaquer, C., Rebelo, H., and López-Baucells, A. (2021). Bats and wetlands: synthesising gaps in current knowledge and future opportunities for conservation. *Mammal Rev.* 51, 369–384. doi: 10.1111/mam.12243

Ning, Y., Zhang, Z. ,. X., Cui, L. ,. J., and Sun, X. ,. W. (2014). Vegetation composition of momoge wetland and its implications for succession in alkaline wetland. *J. Beijing Forestry Univ.* 36, 1–8. doi: 10.13332/j.cnki.jcnki.jbfu.2014.06.007

Piao, S. ,. L., Wang, X. ,. H., Park, T., Chen, C., Lian, X., He, Y., et al. (2020). Characteristics, drivers and feedbacks of global greening. *Nat. Rev. Earth Environ.* 1, 14–27. doi: 10.1038/s43017-019-0001-x

Qi, Q., Zhang, M. ,. Y., Tong, S. ,. Z., Liu, Y., Zhang, D. ,. J., Zhu, G. ,. L., et al. (2022). Evolution of potential spatial distribution patterns of carex tussock wetlands under climate change scenarios, northeast China. *Chin. Geogr. Sci.* 32, 142–154. doi: 10.1007/s11769-022-1260-x

Qu, S., Wang, L. ,. C., Lin, A. ,. W., Zhu, H. ,. J., and Yuan, M. ,. X. (2018). What drives the vegetation restoration in Yangtze river basin, China: Climate change or anthropogenic factors? *Ecol. Indic.* 90, 438–450. doi: 10.1016/j.ecolind.2018.03.029

Shen, X. ,. J., Jiang, M., Lu, X. ,. G., Liu, X. ,. T., Liu, B., Zhang, J. ,. Q., et al. (2021). Aboveground biomass and its spatial distribution pattern of herbaceous marsh vegetation in China. *Sci. China Earth Sci.* 64, 1115–1125. doi: 10.1007/s11430-020-9778-7

Shen, X. ,. J., Liu, B. ,. H., Henderson, M., Wang, L., Jiang, M., and Lu, X. ,. G. (2022a). Vegetation greening, extended growing seasons, and temperature feedbacks in warming temperate grasslands of China. *J. Climate* 35, 5103–5117. doi: 10.1175/JCLI-D-21-0325.1

Shen, X. ,. J., Liu, Y. ,. W., Liu, B. ,. H., Zhang, J. ,. Q., Wang, L., Lu, X. ,. G., et al. (2022b). Effect of shrub encroachment on land surface temperature in semi-arid areas of temperate regions of the northern hemisphere. *Agric. For. Meteorology* 320, 108943. doi: 10.1016/j.agrformet.2022.108943

Shen, X. ,. J., Liu, B. ,. H., Xue, Z. ,. S., Jiang, M., Lu, X. ,. G., and Zhang, Q. (2019). Spatiotemporal variation in vegetation spring phenology and its response to climate change in freshwater marshes of northeast China. *Sci. Total Environ.* 666, 1169–1177. doi: 10.1016/j.scitotenv.2019.02.265

Shen, X. ,. J., Liu, Y. ,. W., Zhang, J. ,. Q., Wang, Y. ,. J., Ma, R., Liu, B. ,. H., et al. (2022c). Asymmetric impacts of diurnal warming on vegetation carbon sequestration of marshes in the qinghai Tibet plateau. *Global Biogeochemical Cycles* 36, e2022GB007396. doi: 10.1029/2022GB007396

Shi, S. ,. Y., Yu, J. ,. J., Wang, F., Wang, P., Zhang, Y. ,. C., and Jin, K. (2021). Quantitative contributions of climate change and human activities to vegetation changes over multiple time scales on the loess plateau. *Sci. Total Environ.* 755, 142419. doi: 10.1016/j.scitotenv.2020.142419

Sun, Y. ,. L., Shan, M., Pei, X. ,. R., Zhang, X. ,. K., and Yang, Y. ,. L. (2020). Assessment of the impacts of climate change and human activities on vegetation cover change in the haihe river basin, China. *Phys. Chem. Earth Parts A/B/C* 115, 102834. doi: 10.1016/j.pce.2019.102834

Tian, Y. ,. L., Wang, Z. ,. M., Mao, D. ,. H., Li, L., Liu, M. ,. Y., Jia, M. ,. M., et al. (2019). Remote observation in habitat suitability changes for waterbirds in the West songnen plain, China. *Sustainability* 11, 1552. doi: 10.3390/su11061552

Vicente-Serrano, S. M., Gouveia, C., Camarero, J. J., Camarero, Jesús Julio, Trigo, R., López-Moreno, J. L., et al. (2013). Response of vegetation to drought time-scales across global land biomes. *Proc. Natl. Acad. Sci.* 110, 52–57. doi: 10.1073/pnas.1207068110

Wang, Y. ,. H., Gong, M. ,. H., Zou, C. ,. L., Zhou, T. ,. Y., Wen, W. ,. Y., Liu, G., et al. (2022d). Habitat selection by Siberian cranes at their core stopover area during migration in northeast China. *Global Ecol. Conserv.* 33, e01993. doi: 10.1016/j.gecco.2021.e01993

Wang, S., Ping, C., Wang, N., Wen, J., Zhang, K., Yuan, K., et al. (2022b). Quantitatively determine the dominant driving factors of the spatial-temporal changes of vegetation-impacts of global change and human activity. *Open Geosciences* 14, 568–589. doi: 10.1515/geo-2022-0374

Wang, Y. ,. J., Shen, X. ,. J., Jiang, M., and Lu, X. ,. G. (2020). Vegetation change and its response to climate change between 2000 and 2016 in marshes of the songnen plain, northeast China. *Sustainability* 12, 3569. doi: 10.3390/su12093569

Wang, H., Zhang, C., Yao, X. ,. C., Yun, W. ,. J., Ma, J. ,. N., Gao, L. ,. L., et al. (2022a). Scenario simulation of the trade off between ecological land and farmland in black soil region of northeast China. *Land Use Policy* 114, 105991. doi: 10.1016/j.landusepol.2022.105991

Wang, X., Zhao, J. ,. M., Xu, W. ,. J., and Ye, X. ,. X. (2022c). Effects of waterbird herbivory on dominant perennial herb carex thunbergii in shengjin lake. *Diversity* 14, 331. doi: 10.3390/d14050331

Wessels, K. J., Prince, S. D., Malherbe, J., Small, J., Frost, P. E., and VanZyl, D. (2007). Can human-induced land degradation be distinguished from the effects of rainfall variability? A case study in south Africa. *J. Arid Environments* 68, 271–297. doi: 10.1016/j.jaridenv.2006.05.015

Wu, H., Fang, S. ,. M., Yang, Y. ,. Y., and Cheng, J. (2022). Changes in habitat quality of nature reserves in depopulating areas due to anthropogenic pressure: Evidence from northeast china 2000–2018. *Ecol. Indic.* 138, 108844. doi: 10.1016/j.ecolind.2022.108844

Xue, L., Kappas, M., Wyss, D., Wang, C., Putzenlechner, B., Thi, N. P., et al. (2022). Assessment of climate change and human activities on vegetation development in northeast China. *Sensors* 22, 2509. doi: 10.3390/s22072509

Yang, S. ,. L., Wang, H. ,. M., Tong, J. ,. P., Bai, Y., Alatalo, J. M., Liu, G., et al. (2022). Impacts of environment and human activity on grid-scale land cropping suitability and optimization of planting structure, measured based on the MaxEnt model. *Sci. Total Environ.* 836, 155356. doi: 10.1016/j.scitotenv.2022.155356

Yan, W. ,. C., Wang, Y. ,. Y., Chaudhary, P., Ju, P. ,. J., Zhu, Q. ,. A., Kang, X. ,. M., et al. (2022). Effects of climate change and human activities on net primary production of wetlands on the zoige plateau from 1990 to 2015. *Global Ecol. Conserv.* 35, e02052. doi: 10.1016/j.gecco.2022.e02052

Yao, Z. ,. H., Wang, B., Huang, J., Zhang, Y., Yang, J. ,. C., Deng, R. ,. X., et al. (2021). Analysis of land use changes and driving forces in the yanhe river basin from 1980 to 2015. *J. Sensors* 2021, e6692333. doi: 10.1155/2021/6692333

Yuan, L., Liu, D. ,. Y., Tian, B., Yuan, X., Bo, S., Ma, Q., et al. (2022). A solution for restoration of critical wetlands and waterbird habitats in coastal deltaic systems. *J. Environ. Manage.* 302, 113996. doi: 10.1016/j.jenvman.2021.113996

Yuan, J., Xu, Y. ,. P., Xiang, J., Wu, L., and Wang, D. ,. Q. (2019). Spatiotemporal variation of vegetation coverage and its associated influence factor analysis in the Yangtze river delta, eastern China. *Environ. Sci. pollut. Res.* 26, 32866–32879. doi: 10.1007/s11356-019-06378-2

Zhang, M., Lin, H., Long, X. ,. R., and Cai, Y. ,. T. (2021). Analyzing the spatiotemporal pattern and driving factors of wetland vegetation changes using 2000-2019 time-series landsat data. *Sci. Total Environ.* 780, 146615. doi: 10.1016/j.scitotenv.2021.146615

Zhao, Y. ,. X., Mao, D. ,. H., Zhang, D. ,. Y., Wang, Z. ,. M., Du, B. ,. J., Yan, H. ,. Q., et al. (2022). Mapping phragmites australis aboveground biomass in the momoge wetland ramsar site based on sentinel-1/2 images. *Remote Sens.* 14, 694. doi: 10.3390/rs14030694

frontiers | Frontiers in Plant Science

TYPE Original Research
PUBLISHED 11 October 2022
DOI 10.3389/fpls.2022.952830

OPEN ACCESS

EDITED BY
Bing Song,
Ludong University,
China

REVIEWED BY
Liping Shan,
Northeast Institute of Geography and Agroecology (CAS), China
Jian Liu,
Shandong University,
China

*CORRESPONDENCE
Jiangbao Xia
xiajb@163.com
Ying Lang
langying115@163.com

†These authors have contributed equally to this work

SPECIALTY SECTION
This article was submitted to Functional Plant Ecology, a section of the journal Frontiers in Plant Science

RECEIVED 25 May 2022
ACCEPTED 25 August 2022
PUBLISHED 11 October 2022

CITATION
Sun J, Xia J, Shao P, Ma J, Gao F, Lang Y, Xing X, Dong M and Li C (2022) Response of the fine root morphological and chemical traits of *Tamarix chinensis* to water and salt changes in coastal wetlands of the Yellow River Delta. *Front. Plant Sci.* 13:952830. doi: 10.3389/fpls.2022.952830

Response of the fine root morphological and chemical traits of *Tamarix chinensis* to water and salt changes in coastal wetlands of the Yellow River Delta

Jia Sun[1,2†], Jiangbao Xia[1*†], Pengshuai Shao[1], Jinzhao Ma[1], Fanglei Gao[1], Ying Lang[3*], Xianshuang Xing[4], Mingming Dong[4] and Chuanrong Li[2]

[1]Shandong Key Laboratory of Eco-Environmental Science for the Yellow River Delta, Binzhou University, Binzhou, China, [2]College of Forestry, Shandong Agricultural University, Tai'an, China, [3]College of Agriculture and Forestry Science, Linyi University, Linyi, China, [4]Shandong Hydrology Center, Jinan, China

To explore the adaptation of the fine root morphology and chemical characteristics of *Tamarix chinensis* to water–salt heterogeneity in the groundwater–soil system of a coastal wetland zone, *T. chinensis* forests at different groundwater levels (high: GW1 0.54 m and GW2 0.83 m; medium: GW3 1.18 m; low: GW4 1.62 m and GW5 2.04 m) in the coastal wetland of the Yellow River Delta were researched, and the fine roots of *T. chinensis* standard trees were excavated. The fine roots were classified by the Pregitzer method, and the morphology, nutrients, and nonstructural carbohydrate characteristics of each order were determined. The results showed that the groundwater level had a significant indigenous effect on the soil water and salt conditions and affected the fine roots of *T. chinensis*. At high groundwater levels, the specific root length and specific surface area of fine roots were small, the root tissue density was high, the fine root growth rate was slow, the nutrient use efficiency was higher than at low groundwater levels, and the absorption of water increased with increasing specific surface area. With decreasing groundwater level, the N content and C/N ratio of fine roots first decreased and then increased, and the soluble sugar, starch, and nonstructural carbohydrate content of fine roots first increased and then decreased. At high and low groundwater levels, the metabolism of fine roots of *T. chinensis* was enhanced, and their adaptability to high salt content and low water content soil environments improved. The first- and second-order fine roots of *T. chinensis* were mainly responsible for water and nutrient absorption, while the higher-order (from the third to fifth orders) fine roots were primarily responsible for the transportation and storage of carbohydrates. The fine root morphology, nutrients, nonstructural carbohydrate characteristics, and other aspects of the water and salt environment heterogeneity cooperated in a synergistic response and trade-off adjustment.

KEYWORDS

coastal wetland, fine root order, groundwater level, morphology, nonstructural carbohydrate, nutrient, water and salt

Introduction

The Yellow River Delta (YRD) is an alluvial plain formed by the sediment carried by the Yellow River and deposited in the Bohai Sea depression. It is located at the junction of the river, sea, and land. The ecosystem is unique and has significant ecological functions (Zhao et al., 2020). Due to sea level rises and seawater intrusion caused by global warming, the groundwater level in this region is generally high, with an average groundwater level between 0.5 and 2.5 m, making the shallow groundwater in the YRD more complex and variable than in other areas (An et al., 2013). In areas of the YRD where the groundwater level is shallow, the upwards flow of water from the groundwater to the soil root zone plays an important role in plant growth (Xie et al., 2011). The distribution and evolution of the salinity of the soil in coastal wetlands are closely related to groundwater dynamics, and rising groundwater levels aggravate the degree of soil salinization (Fan et al., 2012). Research has shown that a groundwater level of 3.5 m was the minimum limit to maintain a safe level of soil salinity in the YRD, but at this groundwater level, the decrease in the soil water content exacerbated environmental pressure on *Phragmites australis* growth (Xie et al., 2011). The characteristics of the spatial distributions of soil water and salt were affected by the fluctuations in the groundwater level, and these fluctuations could further affect the growth, development, and succession of vegetation through their root systems.

Fine roots are crucial for the absorption of water and nutrients at both the individual and community levels (Li et al., 2019), and they generally account for 22% to 76% of the net primary productivity of terrestrial ecosystems (McCormack et al., 2015; Ma and Chen, 2016). Moreover, the functional traits of fine roots are commonly considered good predictors of plant adaptation and ecosystem function in response to environmental changes (Freschet et al., 2021). Studies have shown that fine root biomass (FRB) is mainly regulated by the interactions between groundwater and root trait diversity, followed by groundwater, root trait diversity, and soil moisture (Wang et al., 2021a). Although the mean and seasonality of the groundwater depth had substantial effects on FRB, the groundwater affected the FRB mainly through indirect pathways mediated by root trait diversity (Wang et al., 2021a). Important findings of fine root N, P, and N/P ratios were mainly determined by groundwater (Wang et al., 2021b). Salt stress significantly inhibited the growth of absorbing roots (diameter < 0.5 mm), including the root length, surface area, volume, root length density, and the number of root tips, resulting in the inhibition of the growth and development of the whole root system (Li et al., 2021).

Many scholars have studied the structure and function of fine roots from the perspective of root order and found that the same root order in different plant root systems has similar functions, and the root order is directly related to its function (Wang et al., 2006; Withington et al., 2006). Fine roots are classified according to their root order, i.e., the branch position. First-order roots are the most distal, and second-order roots begin at the junction of two first-order roots, and so on, up to fifth-order roots (Pregitzer et al., 2002; Wang et al., 2006; Rewald et al., 2014; Eissenstat et al., 2015). This classification method not only can minimize the internal heterogeneity of fine roots but also can more accurately describe the physiological and ecological processes of underground roots (Pregitzer et al., 2002; Guo et al., 2008). Therefore, studying the relationship between the morphology and function of fine roots from the perspective of root order is of great significance for understanding the heterogeneity within a root system.

Prairie shrubland is a typical type of wetland landscape present in the YRD. The halophyte *Tamarix chinensis* is the most widely distributed shrub species, and it is also the main tree species preferred for the construction of shelter forests in coastal wetlands. *T. chinensis* is a significant component of the YRD wetland ecosystem, and it plays an important role in the process of vegetation restoration and ecological remediation. A study found that, at a high groundwater level, the root topological structure tended to be dichotomous, and the fractal dimension and fractal abundance values were both large. The topological structure of medium and low groundwater level *T. chinensis* tended to be herringbone like, and the fractal dimension and fractal abundance values were small. The *T. chinensis* root system has strong phenotypic plasticity to the heterogeneous water–salt habitat of the groundwater–soil system (Sun et al., 2022). The root morphology and architecture of *T. chinensis* are highly plastic with respect to changes in the soil water and salt content caused by groundwater salinity (Peng et al., 2022). The root systems of *T. chinensis* with different densities were mainly distributed near the ground surface and expanded outwards onto the beach of the YRD. Low-density *T. chinensis* expands its root growth space mainly by increasing the number of branches, while medium- and high-density *T. chinensis* have fewer branches and strengthen the use of internal resources to reduce competition with neighboring plants (Sun et al., 2021). Song et al. (2017) found that, under different salinity levels, the root–shoot ratio of *T. chinensis* was significantly different, the rooting depth differed, and the root system biomass decreased in a negative logarithmic relationship with increasing soil depth. In conclusion, research on the response of the root system of *T. chinensis* to environmental heterogeneity

has mainly focused on root growth and architecture, and there have been few studies of the morphology and function of different orders of fine roots. It is unclear how *T. chinensis* fine roots adapt to heterogeneous groundwater–soil water and salt habitats, which affect the tending and management of low-efficiency forests and the planting and water–salt management of *T. chinensis* seedlings.

We hypothesized that the groundwater level affects the morphological and chemical traits of the fine roots of *T. chinensis* by affecting the content of soil water and salt. Given this background, 7a *T. chinensis* was the subject of research at different groundwater levels formed by microtopographic changes and tidal action in the YRD coastal wetland. To investigate the response and adaptation strategy of the different orders of fine root traits of *T. chinensis* and the trade-off relationship of fine root functional traits under different groundwater levels, this study was expected to provide a theoretical basis and technological support for water–salt management of *T. chinensis* seedlings and improvements in forest stand quality in the YRD.

Materials and methods

Study site

The study site is located in the *T. chinensis* Shrub Farm (118°2′–118°4′ E, 38°9′–38°10′ N) in Binzhou Port, Binzhou Beihai New Area, Shandong Province. This area has a continental climate in the temperate East Asian monsoon region. The average temperature is 12.6°C, the average maximum temperature is 31.4°C (July), and the monthly average minimum temperature is −7.99°C (January). The average annual precipitation is 543.2 mm, and it mainly occurs from June to September, accounting for approximately 75% of the total annual precipitation, with less precipitation from November to March. The test area has a shallow groundwater level of 0.5–2.5 m, high salinity, and a flat terrain. The tidal flat soil is alluvial loess parent material. The mechanical composition is mainly silt. The sand is interlaced and easy to compact and has poor air permeability. The vegetation types primarily include shrubs and grasses, among which the shrubs are mainly *T. chinensis*, and the herb distribution includes *Suaeda glauca*, *Suaeda salsa*, *Phragmites australis*, *Imperata cylindrica*, *Setaria viridis*, *Cynanchum chinense*, and *Echinochloa crus-galli* (L.) Beauv.

Experimental design

In July 2020, a field survey of a *T. chinensis* forest in Binzhou Port, Beihai New Area, Binzhou City, Shandong Province, was conducted, and groundwater level observation tubes were buried. Three PVC pipes with a diameter of 5 cm and a length of 1–3 m were buried in each plot to observe the groundwater level. One end of each PVC pipe was drilled and wrapped with gauze mesh with a diameter of 0.5 mm. The pipes were buried underground, and the groundwater level was measured 24 h later. The groundwater level was measured by a physical water level gauge; the specific groundwater level conditions of each plot are shown in Supplementary Table 1. The groundwater level was divided into five groundwater level conditions: GW1, GW2, GW3, GW4, and GW5. For each groundwater level condition, three quadrats of 10 m × 10 m were randomly set. The mean groundwater levels of GW1, GW2, GW3, GW4, and GW5 were 0.54 ± 0.07, 0.83 ± 0.06, 1.18 ± 0.10, 1.62 ± 0.07, and 2.04 ± 0.05 m, respectively. 7a *T. chinensis* was the subject of this research. The base diameter, plant height, and crown width of each *T. chinensis* specimen were measured in each plot, and one standard tree was selected; i.e., three standard trees were selected at each groundwater level.

Fine root sample collection and processing

The whole root system containing more than 3 branch grades closest to the standard tree taproot was taken and placed in a liquid nitrogen tank to maintain its activity. The impurities and soil on the surface were removed with low-temperature deionized water before root scanning. According to the Pregitzer root order grading method, the first root of the outer layer is the first level, two first-level roots meet at the second level, two second-level roots meet at the third level, and so on. If different root levels meet, then the higher level is taken as the root level. After the roots were graded, they were placed in labeled containers and stored in a refrigerator for root scanning.

According to the fine root morphology indicator measured by analysis software (Win-RhIZO 2008a) and the measured fine root biomass, the average diameter, SRL, specific surface area (SSA), and RTD of the fine roots were calculated.

$$\mathrm{SRL}\left(\mathrm{m/g}\right) = \mathrm{Root\ length}\left(\mathrm{m}\right) / \mathrm{Root\ biomass}\left(\mathrm{g}\right).$$

$$\mathrm{SSA}\left(\mathrm{cm^2/g}\right) = \mathrm{Surface\ area}\left(\mathrm{cm^2}\right) / \mathrm{Root\ biomass}\left(\mathrm{g}\right).$$

$$\mathrm{RTD}\left(\mathrm{g/cm^3}\right) = \mathrm{Root\ biomass}\left(\mathrm{g}\right) / \mathrm{Root\ volume}\left(\mathrm{cm^3}\right).$$

Fine root nutrients and nonstructural carbohydrate determination

After drying and pulverizing samples of different order-level fine roots, the total C and total N contents were determined by an elemental analyzer (Elementar, vario EL III). The content of soluble sugar and starch was determined by the anthrone colorimetric method, and the nonstructural carbohydrate (NSC) content was the sum of the content of soluble sugar and starch.

Soil sample collection and determination

Soil samples were collected near the standard trees, and three soil samples were collected from the 0–60 cm soil layer of the

concentrated root distribution layer in each plot for the determination of soil water and salt parameters. The soil water content was determined by the oven drying method, the soil salt content was measured by the residue drying method, and the soil to water ratio was 5:1. The absolute concentration of the soil solution (%) = soil salt content (proportion to dry soil mass)/soil water content (proportion to dry soil mass) × 100%.

Data processing and analysis

Microsoft Office Excel 2010, Origin 2019, and RStudio software applications were used for data processing and mapping. Two-way ANOVA was implemented to detect the effects of GW levels and various fine root orders on fine root traits. When interactions were not significant, independent effects were then considered. When the effects were significant, the LSD test was used to compare the mean values. Data were analyzed with SPSS software, version 26.0. Principal component analysis (PCA) and drawing with Origin 2021. We used the generalized least squares estimation method to fit the measured data to the model. Adequate model goodness of fit was tested by the root-mean-square error of approximation (RMSEA). The statistical results of indirect, direct, and total effects were selected and output to assess groundwater level effects on fine roots using AMOS software (AMOS 23.0 student version). The data in the chart are the mean ± standard deviation.

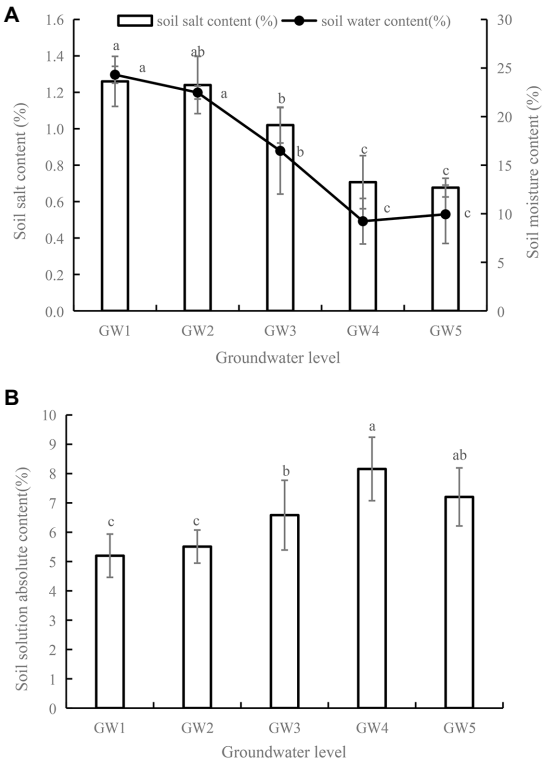

FIGURE 1
Soil water, salinity **(A)** and soil solution absolute content **(B)** of *Tamarix chinensis* shrubland for different groundwater levels. The lower case letters indicate significant and non-significant differences at $p<0.05$. The same as below.

Results

Soil water and salt characteristics

With decreasing GW levels, soil salt content generally decreased (Figure 1A). Soil salt contents for GW3, GW4, and GW5 were significantly lower than that for GW1 (1.26%; $p < 0.05$). With decreasing GW levels, the soil water content showed a decreasing trend. There was no statistically significant difference in the soil water content between GW1 and GW2 ($P > 0.05$). The soil water content for GW3, GW4, and GW5 was significantly lower than that for GW1 ($p < 0.05$) by 32.25%, 61.21%, and 59.10%, respectively. With decreasing GW levels, the absolute concentration of the soil solution first increased and then decreased (Figure 1B).

Tamarix chinensis fine root morphology characteristics

The effects of groundwater level on root morphological traits

The GW level had a significant effect on the average diameter of the *T. chinensis* fine roots ($p < 0.05$; Supplementary Table 2). There were no significant differences in the average diameter of the fine roots at GW1, GW3, GW4, and GW5 ($P > 0.05$; Figure 2A). With decreasing GW levels, the average diameters of the first-, second-, third-, fourth-, and fifth-order fine roots all showed increasing, decreasing, increasing, and decreasing trends and reached their maximum for GW2 (Figure 2A).

The GW level had a significant effect on the SSAs of the fine roots of *T. chinensis* ($p < 0.05$; Supplementary Table 2). The SSAs of the fine roots at GW1 and GW2 were significantly lower than those at GW5 ($p < 0.05$) by 35.38% and 27.57%, respectively (Figure 2B). With decreasing GW levels, the SSAs of the third- and fourth-order fine roots showed a decreasing, increasing, and decreasing trend, and the SSAs of the first-, second-, and fifth-order fine roots showed an increasing, decreasing, and increasing trend. They all reached the maximum values for GW5 (Figure 2B). The GW level had no significant effect on the RTDs of *T. chinensis* fine roots ($P > 0.05$; Figure 2C; Supplementary Table 2).

Differences in root morphological traits across root orders

Root order had an extremely significant effect on the average diameter, SRL, SSA, and RTD of *T. chinensis* fine roots ($p < 0.01$; Supplementary Table 2). The average diameters of the first-, second-, and third-order roots were significantly lower than those of the fifth-order roots by 57.43%, 42.49%, and 35.49%,

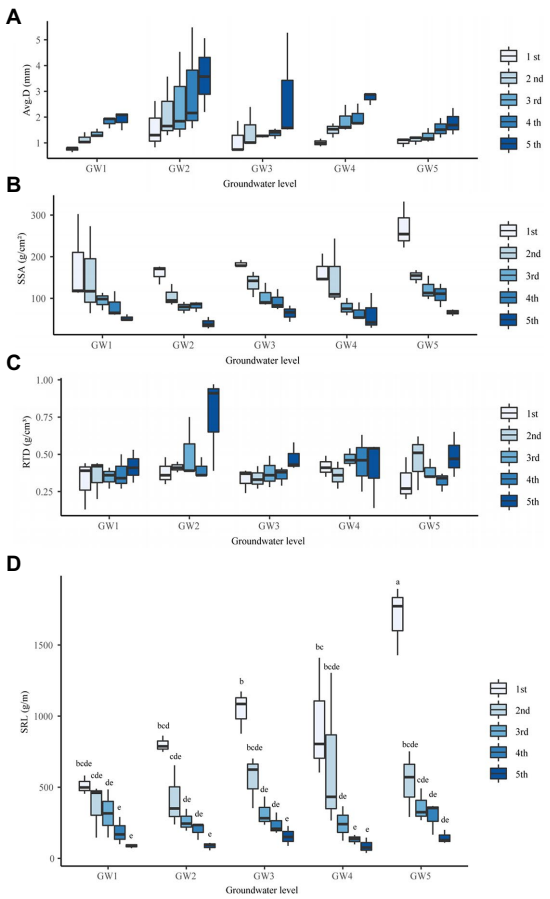

FIGURE 2
The Avg.D **(A)**, SSA **(B)**, RTD **(C)**, and SRL **(D)** of different orders of fine roots of *Tamarix chinensis* at different groundwater levels. SSA, Specific surface area; RTD, Root Tissue Density; SRL, Specific Root Length.

respectively ($p < 0.05$; Supplementary Table 2). The SSAs of the second-, third-, fourth-, and fifth-order roots were significantly lower than those of the first-order roots ($p < 0.05$) by 27.30%, 50.16%, 55.14%, and 70.32%, respectively (Supplementary Table 2). The RTDs of the first-, second-, third- and fourth-order roots were significantly lower than those of the fifth-order roots ($p < 0.05$) by 30.60%, 24.15%, 17.64%, and 25.47%, respectively (Supplementary Table 2).

The interaction effects of groundwater level and root order on root morphological traits

The interaction of GW level and root order had an extremely significant effect on SRL ($p < 0.01$). At groundwater level GW5, the SRL of first-order roots was significantly higher than that of other groundwater levels and other root orders ($p < 0.05$). At different groundwater levels, with the increase in root order, the specific root length of fine roots showed a downward trend. Under GW5 conditions, the second-, third-, fourth-, and fifth-order fine roots were reduced by 49.06%, 69.95%, 78.99%, and 88.78% compared with the first-order fine roots, respectively (Figure 2D). The interaction effects of GW level and root order on the average diameter, SSA, and RTD were not significant ($p > 0.05$; Supplementary Table 2).

Nutrient traits of the fine roots of *Tamarix chinensis*

Effects of groundwater level on root nutrient traits

The GW level had a significant effect on the C content of the fine roots of *T. chinensis* ($p < 0.05$; Supplementary Table 3). The C content for GW1, GW2, and GW4 was significantly lower than that for GW3 ($p < 0.05$) by 3.62%, 2.99%, and 4.17%, respectively (Supplementary Table 3). The C content of the fourth-order fine roots reached the maximum value at GW1 (499.31 g/kg; Figure 3A).

The GW level had a significant effect on the N content of *T. chinensis* fine roots ($p < 0.05$; Supplementary Table 3). The N content for GW1 and GW5 was significantly higher than that for GW2 and GW3 ($p < 0.05$), but the difference was not significant with respect to GW4 ($p > 0.05$; Supplementary Table 3). The N content of the first- and second-order fine roots reached the maximum values for GW1, which were 12.50 and 10.57 g/kg, respectively. The N content of the third- and fourth-order fine roots reached maximum values at GW5, which were 10.08 and 9.20 g/kg, respectively. The N content of the fifth-order fine roots reached the maximum value at GW4 (9.04 g/kg; Figure 3B).

The GW level had a significant effect on the C/N ratio of the fine roots of *T. chinensis* ($p < 0.05$; Supplementary Table 3). The C/N values for GW1, GW4, and GW5 were significantly lower than those for GW2 and GW3 ($p < 0.05$; Supplementary Table 3). With decreasing GW levels, the C/N of the first- and fourth-order fine roots reached their maximum values at GW2 (44.23) and GW3 (65.07), respectively (Figure 3C). The C/N ratios of the second-, third-, and fifth-order fine roots reached their maximum values at GW5 (45.92), GW3 (52.82), and GW3 (77.87), respectively (Figure 3C).

Differences in root nutrient traits across root orders

Root order had no significant effect on the C content of *T. chinensis* fine roots but had an extremely significant effect on the N content and C/N ratio ($p < 0.01$; Supplementary Table 3). The N content of the second-, third-, fourth- and fifth-order roots was significantly lower than that of the first-order roots ($p < 0.05$) by 9.94%, 14.98%, 29.15%, and 31.70%, respectively (Supplementary Table 3). The C/N values of the second-, third-, fourth- and fifth-order roots were significantly lower than those of the first-order roots ($p < 0.05$; Supplementary Table 3).

The interaction effects of GW level and root order on the C content, N content, and C/N ratio of fine roots were not significant ($p > 0.05$; Supplementary Table 3).

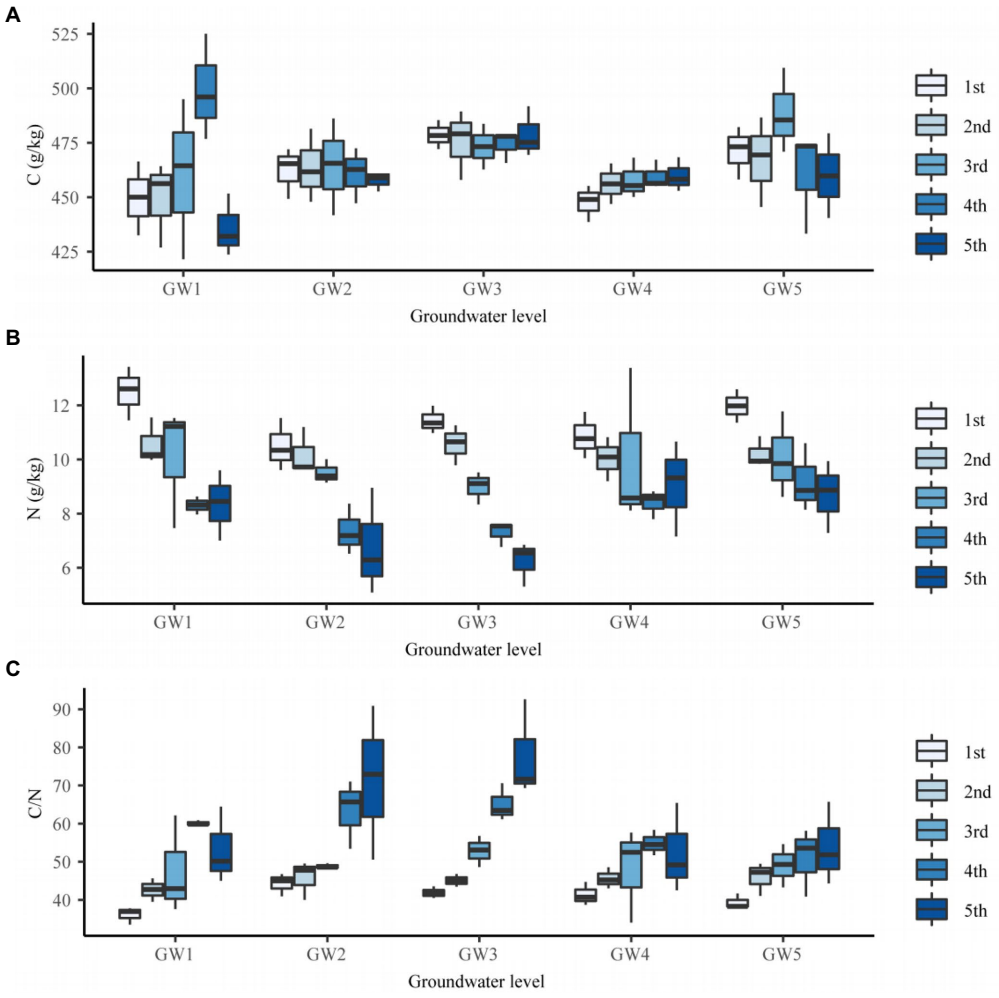

FIGURE 3
The C content **(A)**, N content **(B)**, and C/N **(C)** of fine roots of different orders of *Tamarix chinensis* at different groundwater levels.

Tamarix chinensis fine root nonstructural carbohydrate traits

Effects of groundwater level on root nonstructural carbohydrate traits

The GW level had an extremely significant effect on the soluble sugar, starch, and NSC content of *T. chinensis* fine roots ($p < 0.01$) but no significant effect on the soluble sugar/starch content ($p > 0.05$; Supplementary Table 4). The soluble sugar content at GW1, GW3, GW4, and GW5 was significantly lower than that at GW2 ($p < 0.05$) by 31.14%, 27.82%, 23.91%, and 33.62%, respectively (Figure 4A).

At GW1 and GW5, the NSC content of fine roots was significantly lower than that of GW2 ($p < 0.05$) by 20.75% and 30.55%, respectively (Supplementary Table 4). With decreasing GW levels, the NSC content of the first-, second-, third-, and fourth-order fine roots showed an increasing, decreasing, increasing, and decreasing trend, and all reached their maximum values at GW2. The NSC content of the fifth-order fine roots first increased and then decreased and reached its maximum value at GW4 (173.98 g/kg; Figure 4C).

Differences in root nonstructural carbohydrate traits across root orders

Root order had a significant effect on the soluble sugar and starch content of *T. chinensis* fine roots ($p < 0.05$) and an extremely significant effect on the NSC content ($p < 0.01$) but no significant effect on the soluble sugar/starch ($p > 0.05$; Supplementary Table 4).

The soluble sugar content of the third-, fourth-, and fifth-order roots was significantly higher than those of the first-order roots ($p < 0.05$; Supplementary Table 4). The soluble sugar content of fine roots at GW2 first increased and then decreased, and that of the third-order roots was the highest (Figure 4A).

The starch content of different order fine roots was between 32.23 and 59.97 g/kg, and the starch content of the third-, fourth-, and fifth-order roots was significantly higher than those of the first-order roots ($p < 0.05$; Supplementary Table 4). With increasing root orders, the soluble sugar content of fine roots at

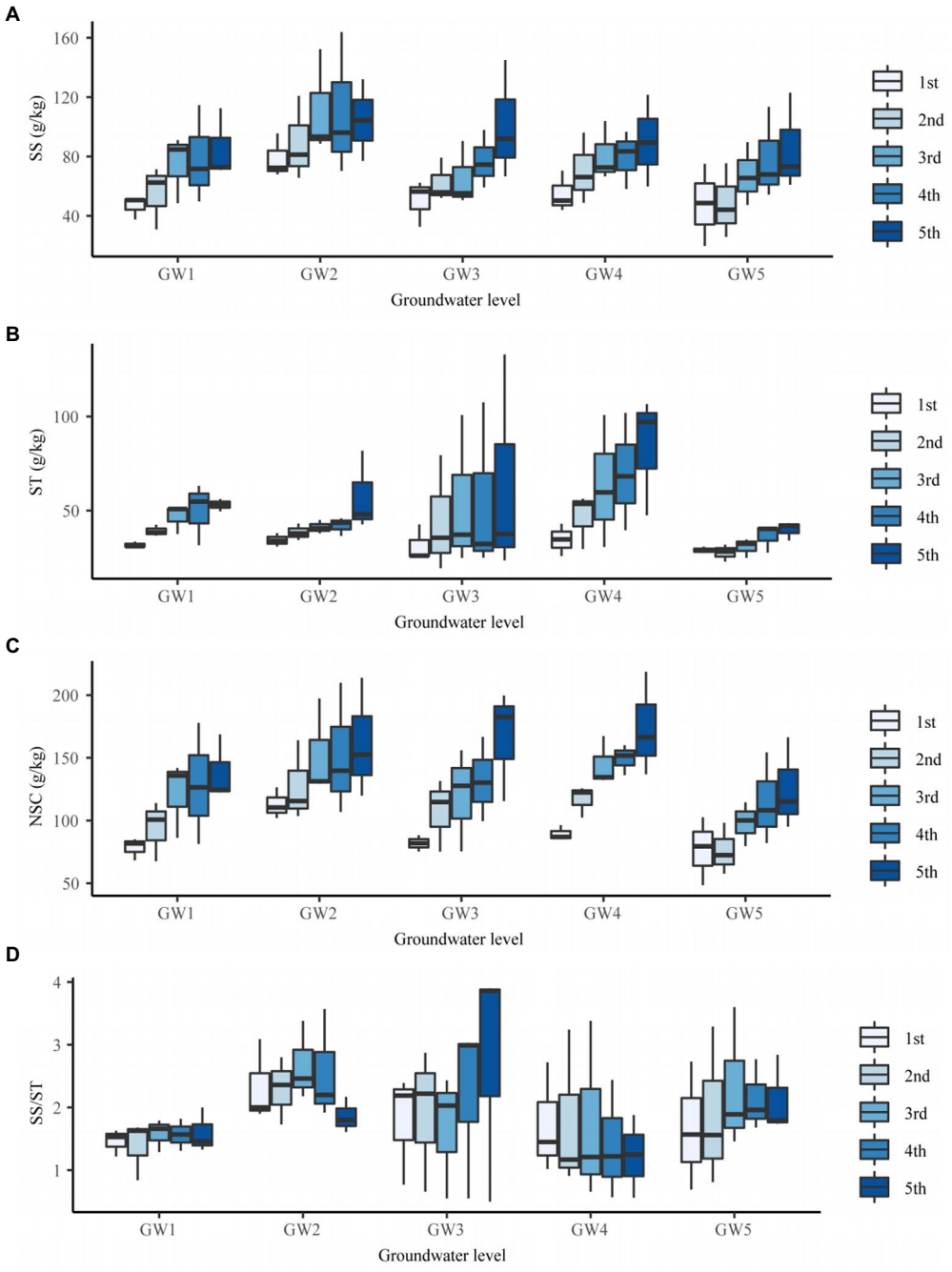

FIGURE 4
The SS content **(A)**, ST content **(B)**, NSC content **(C)**, and SS/ST **(D)** of fine roots of different order of *Tamarix chinensis* at different groundwater levels. SS, Soluble Sugar; ST, Starch; NSC, nonstructural carbohydrate; SS/ST, Soluble Sugar/Starch.

GW1, GW2, GW3, GW4, and GW5 increased, and the soluble sugar content of the fifth-order roots was the highest (Figure 4B).

The NSC content of the third-, fourth-, and fifth-order roots was significantly higher than those of the first-order roots ($p < 0.05$; Supplementary Table 4). With increasing root orders, the NSC content of the fine roots at GW1, GW2, GW3, GW4, and GW5 increased, and the NSC content of fifth-order roots was the highest (Figure 4D).

The interaction effects of groundwater level and root order on the soluble sugar content, starch content, NSC content, and soluble sugar/starch of fine roots were not significant ($p > 0.05$; Supplementary Table 4).

Correlation analysis of *Tamarix chinensis* fine root morphology and chemical characteristics and environmental factors

The correlation analysis showed that the groundwater level was significantly negatively correlated with the SRL of *T. chinensis* fine roots ($p < 0.05$). The root order was extremely significantly

positively correlated with the average diameter, C/N, and soluble sugar, starch, and NSC content of the fine roots ($p < 0.01$) and was significantly negatively correlated with the SRL, SSA, and N content of the fine roots ($p < 0.05$; Figure 5).

The average diameter was extremely significantly positively correlated with the C/N ratio of the fine roots ($p < 0.01$), significantly positively correlated with the RTD, soluble sugar, and NSC content of the fine roots ($p < 0.05$), extremely significantly negatively correlated with the SSA and N content of the fine roots ($p < 0.01$) and significantly negatively correlated with the SRL of the fine roots ($p < 0.05$). The SRL was extremely significantly positively correlated with the SSA and N content of the fine roots ($p < 0.01$), extremely significantly negatively correlated with the C/N ratio, soluble sugar, and NSC content of the fine roots ($p < 0.01$) and significantly negatively correlated with the starch content of the fine roots ($p < 0.05$). The SSA was extremely significantly positively correlated with the N content of the fine roots ($p < 0.01$), extremely significantly negatively correlated with the RTD, C/N ratio, soluble sugar, and NSC content of the fine roots ($p < 0.01$) and significantly negatively correlated with the starch content of the fine roots ($p < 0.05$). The RTD was extremely significantly positively correlated with the C/N ratio, soluble sugar, and NSC content of the fine roots ($p < 0.01$) and extremely significantly negatively correlated with the NSC content of the fine roots ($p < 0.01$; Figure 5).

The N content was extremely significantly negatively correlated with the C/N, soluble sugar, and NSC content of the fine roots ($p < 0.01$) and significantly negatively correlated with the starch content of the fine roots ($p < 0.05$). The C content was extremely significantly positively correlated with the soluble sugar/starch content of the fine roots ($p < 0.01$) and significantly positively correlated with the C/N ratio and soluble sugar content of the fine roots ($p < 0.05$). The C/N ratio was extremely significantly positively correlated with the soluble sugar and NSC content of the fine roots ($p < 0.01$) and significantly positively correlated with the soluble sugar/starch of the fine roots ($p < 0.05$). The soluble sugar content was extremely significantly positively correlated with the soluble sugar/starch and NSC of the fine roots ($p < 0.01$; Figure 5).

A structural equation model was used to adapt and analyze the groundwater level, soil salt content, soil water content, morphology of fine roots, nutrients, and NSC characteristics of *T. chinensis*, and finally, the following structural equation model was established (Figure 6). During modeling, dimension reduction was performed on the morphology (D, SRL, SSA, RTD), nutrients (C, N, C/N), and nonstructural carbohydrates (SS, ST, NSC, SS/ST) of the fine roots. The first-dimension data were extracted, and the interpretation rates were 61.00%, 67.50%, and 53.50%, respectively. The results showed that the structural equation model could explain 41% of the fine root morphology, 35% of the fine root nutrients, and 9% of the fine root nonstructural carbohydrates. Groundwater level had a significantly positive impact on soil salinity and soil water content. Soil salinity had direct and significant positive effects on fine root NSCs, and fine root NSCs had direct and indirect positive effects on morphological characteristics.

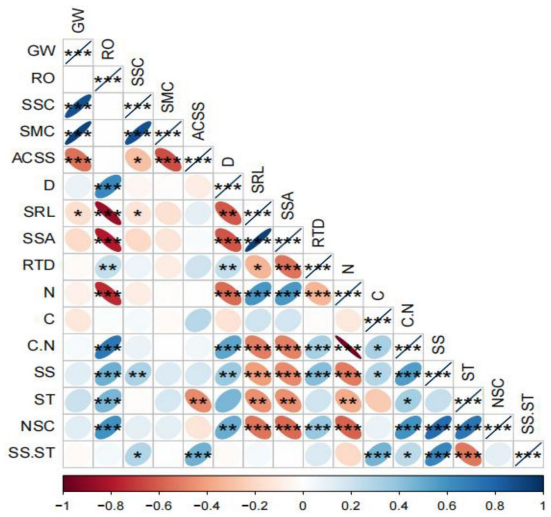

FIGURE 5
Correlation analysis between environmental factors and the morphology and chemical indices of the fine roots of *Tamarix chinensis*. *p<0.05; **p<0.01; ***p<0.001. WG, groundwater level; RO, root order; SSC, soil salinity content; SMC, soil moisture content; ACSS, soil solution absolute content; D, fine root average diameter; SRL, specific root length; SSA, specific surface area; RTD, root tissue density; N, nitrogen; C, carbon; C/N, nitrogen/carbon; SS, soluble sugar; ST, starch; NSC, nonstructural carbohydrate; SS/ST, soluble sugar/starch. The same applies below.

Discussion

The variations in *Tamarix chinensis* fine root morphology, nutrient, and nonstructural carbohydrate characteristics for different groundwater levels in the coastal wetland

Variation in fine root traits can often be described based on shifts in resource foraging that range from acquisitive (i.e., roots that are inexpensively constructed but that proliferate and acquire resources more rapidly) to conservative (i.e., roots that require greater investment and live longer but acquire resources more slowly). For example, larger diameter roots and higher RTDs are both associated with greater tissue construction costs and longer average fine root life spans, reflecting a more conservative strategy (Caplan et al., 2019). With decreasing groundwater levels, the *T. chinensis* fine root SRL and SSA gradually increased, the RTD gradually decreased, and the average diameter did not undergo an obvious regular change. This outcome indicated that the high groundwater levels of GW1 (0.54 m) and GW2 (0.81 m) were relatively rich in soil salt-based ions compared with the low groundwater levels of GW4 (1.62 m) and GW5 (2.04 m); A

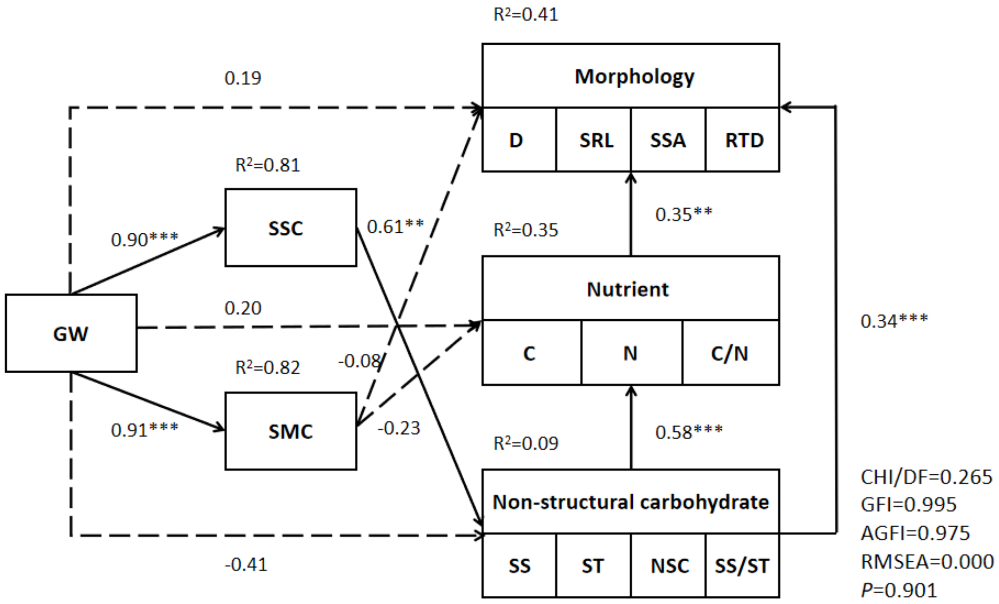

FIGURE 6
Structural equation model of *Tamarix chinensis* fine root characteristics and environmental factors. **significant at 0.01 level and ***significant at 0.001 level.

relatively high soil salinity generally causes osmotic stress in plants and disrupts their nutrient ion balance, thereby affecting physiological and biochemical processes such as growth, osmotic adjustment synthesis, and lipid metabolism (Zhang et al., 2017), and ultimately limits the growth rate of the fine roots; the SSA and SRL of the fine roots were low; the RTD was high; and the nutrient absorption rate per unit of dry weight of fine roots was low (Xu et al., 2011). At the low groundwater levels of GW4 (1.62 m) and GW5 (2.04 m), *T. chinensis* improved its water use efficiency by increasing the SSA and SRL of the fine roots and accelerated growth turnover by reducing the RTD of the fine roots.

Increasing the SSA and SRL of the fine roots at the low groundwater levels of GW4 (1.62 m) and GW5 (2.04 m) can improve the water utilization efficiency of *T. chinensis* by reducing the RTD of fine roots to accelerate growth turnover, reduce water loss, and improve the absorption of water. However, studies have shown that, for the conditions of high groundwater levels in the sinking zone of Shengjin Lake in the Tongjiang Lake wetland, the SRL and RTD of *Carex thunbergii* fine roots were significantly reduced, while the average diameter and SSA were significantly increased. The difference between this study of *C. thunbergii* and the results for the average diameter of fine roots may occur because wetland plants have more developed ventilation tissues, which can expand the diameter of their air cavities to increase oxygen acquisition under hypoxic stress caused by high groundwater level conditions, significantly affecting the morphological structure characteristics of fine roots (Yuan and Huangpu, 2020). The decrease in groundwater level had no significant effect on the root length or root surface area of *Haloxylon ammodendron* in the arid desert areas, but the SRL decreased significantly (Liu et al., 2022). Short-term water treatment significantly affected the different orders of fine root average diameter, SRL, and RTD of *Machilus pauhoii*, and drought stress significantly increased the diameter of the third-order fine roots and decreased the RTD of the first- and second-order fine roots (Zou et al., 2018). *H. ammodendron*, *M. pauhoii*, and *T. chinensis* are all woody plants. Due to their dissimilar tolerance characteristics, their fine root morphology changes in response to water also showed great differences with the variety of species and habitat conditions.

The content of C and N in fine roots is an important part of nutrient cycling and energy flow in the ecosystem and an index for measuring the cost of fine root biomass construction and maintenance. The C content of fine roots is associated with construction costs (Withington et al., 2006; Terzaghi et al., 2013), whereas the N content is associated with metabolic activity, respiration, and root longevity (Withington et al., 2006; McCormack et al., 2012). As a consequence, the C/N ratio can indicate the life span of fine roots (Withington et al., 2006), i.e., the higher the fine root C/N ratio, the longer the life span, and the lower the fine root turnover rate (Pregitzer et al., 2002; McCormack et al., 2012). With the decrease in GW levels, the C content of fine roots of *T. chinensis* in coastal beaches did not show an obvious change trend, while the N content first decreased and then increased, and the C/N ratio first increased and then decreased. At the groundwater level of GW3 (1.18 m), the soil water and salt conditions of the *T. chinensis* forest were relatively suitable, the respiration of the fine roots of *T. chinensis* decreased, and the fine root life increased. Under relatively high and low groundwater levels, the fine roots had higher N content and lower C/N ratios, it could improve its adaptability to high salinity and

low water content soil environments by increasing the turnover rate of fine roots and enhancing their metabolism (Di et al., 2018).

Nonstructural carbohydrates are composed of starch and soluble sugar, which are synthesized by plant leaves through photosynthesis and transported to the root system. Nonstructural carbohydrates not only can provide raw materials for building root structures but also are important substances that enable a root system to resist stress related to adversity (Zhang et al., 2020). With decreasing groundwater levels, the soluble sugar, starch, and NSC content and the soluble sugar/starch of *T. chinensis* fine roots first increased and then decreased. The soil salt content was higher at the high groundwater level, but the NSC characteristics of fine roots did not respond in a sensitive manner to it. It was previously assumed that a high groundwater level, GW1 (0.54 m), increased the soluble sugar content and soluble sugar/starch ratio of the fine roots of *T. chinensis* and increased the osmotic potential of the cell solution to resist physiological stress due to drought, which was caused by high concentrations of salt ions. However, the study found that the soluble sugar content and soluble sugar/starch ratio of GW1 (0.54 m) were low under high groundwater level conditions, which may have been due to the dilution of soil salts by high soil water content for high groundwater level conditions, resulting in the low absolute concentrations of soil solution or the limited adaptability of *T. chinensis* fine roots to salt stress. Further experimental studies are needed to investigate the specific reasons. For the GW5 (2.04 m) low groundwater level, the starch and NSC content of the fine roots of *T. chinensis* was the lowest, but the soluble sugar/starch ratio was higher. This result could have been due to the stronger growth and photosynthesis ability of *T. chinensis* at low groundwater levels and the increased amount of photosynthetic products (Xia et al., 2018). However, this result may have been due to the low soil water content at the GW5 (2.04 m) low groundwater level and the rapid growth of plant roots in a short time to obtain sufficient water. To meet the needs of respiratory metabolism, NSCs are more involved in physiological activities, such as metabolism, in the form of soluble sugar, and the amount of starch converted into soluble sugar is greater than the consumption of soluble sugar (Meghan and Robin, 2020). It may be that *T. chinensis* can meet its water demand by increasing the soluble sugar content in its fine roots and increasing the osmotic potential of cells under the condition of relatively scarce water. Under mild drought stress, the changes in soluble sugar content in the roots of *Caragana microphylla* in Khorchin Sandy Land were similar to the results of this study. With the increase in drought stress, the starch content of *C. microphylla* increased to synthesize defensive substances and resist drought-related stress (Lei et al., 2017). The specific root respiration and NSC content of *Cunninghamia lanceolata* did not change under the condition of isolated precipitation, but the starch content of fine roots with diameters of 1–2 mm increased, and the soluble sugar content and soluble sugar/starch ratio decreased significantly, showing that *C. lanceolata* responded to drought-related stress caused by reduced precipitation by increasing the proportion of NSC storage (Zhong et al., 2016). However, the changes in starch content in the fine roots of *T. chinensis* in coastal wetlands were not consistent with the changes in the above two drought-related stress conditions, which simulated drought-induced stress conditions. In this study, the groundwater level was extremely significantly positively correlated with the soil salt content ($p < 0.01$), so the changes in soil water and salt conditions caused by groundwater level affected the fine root starch content of *T. chinensis*. Additionally, due to the different plant species and degrees of soil moisture reduction, the research results were inconsistent. However, Zheng et al. (2014) also found that the increase in NSCs in plants was not related to resistance to drought-induced stress, but the lack of water in plants affected the structural construction of plant tissues when the starch content increased as the premise because starch is a nonpermeable active substance. Therefore, there should be some differences in the responses of physiological and biochemical processes of plants to water-related stress.

The structural equation model showed that soil salinity had a significant, positive effect on the NSCs in the fine roots of *T. chinensis*. Fine root NSCs had direct significant effects on fine root nutrients and fine root morphology. Fine root nutrients had an indirect effect on morphology, while soil moisture had no significant effect on fine root indicators. It was concluded that the groundwater–soil salt conditions played a major role in the fine roots of *T. chinensis* in the groundwater–soil salt system, and water was a secondary factor. In arid regions, groundwater mainly affects the growth of plant roots through the soil water content, and the water deficit is the limiting factor. The groundwater level in the YRD is high, and water is not the main limiting factor. However, since the rise in groundwater level will aggravate the degree of soil salinization, salinity is the main factor affecting the fine roots of *T. chinensis*. Fine root morphology and function coordinate to adapt to changes in groundwater and soil water and salt. *T. chinensis* is a typical halophyte. Under salt stress, osmotic adjustment substances, such as NSCs, increase; fine root nutrient content increases; and stress resistance is enhanced. Fine root morphology is adjusted accordingly to improve root construction costs. With the increase in stress, *T. chinensis* fine roots changed from an acquisition strategy to a conservative strategy. In summary, there was not a single response of the fine root morphology and functional indicators of *T. chinensis* to groundwater levels, but the fine root morphology, chemical characteristics, and other aspects of water and salt environment heterogeneity showed a synergistic response, and there were trade-offs and adjustments.

The variation in *Tamarix chinensis* fine root morphology, nutrient, and nonstructural carbohydrate characteristics of different orders in the coastal wetland

Morphological plasticity is a manifestation of plant survival strategies in heterogeneous habitats. Fine roots have high

morphological and functional heterogeneity at the root-order level (Kong et al., 2019). Affected by the order of growth and development, the root traits related to plant function change strongly and nonlinearly with increasing root orders, reflecting the functional transformation from resource absorption to transportation (Pregitzer et al., 2002; McCormack et al., 2015). In this study, with increasing fine root orders, the average diameter and RTD of fine roots increased, the SRL and SSA decreased, the C/N ratio gradually increased, the N content gradually decreased, and the soluble sugar, starch, and NSC content gradually increased. For example, Yu et al. (2021) studied the morphological characteristics of the first five fine roots of *Pinus koraiensis* at different latitudes in China, Pregitzer et al. (2002) studied the first three fine roots of nine coniferous and broad-leaved species in North America, and Shi (2008) studied the first five fine roots of 20 broad-leaved species in the natural secondary forest of Maoer Mountain in Northeast China, all of which revealed similar changes to this study, further confirming that there were certain functional differences between fine roots of different orders. The morphological structural heterogeneity of fine roots follows a general rule in plants. The root order method can distinguish the heterogeneity of fine roots (Pregitzer et al., 2002). First- and second-order fine roots mainly provide nutrient acquisition in the root system, without secondary growth processes, short life cycles, strong metabolic activity, and fast respiration rates, and they consume more NSCs. Therefore, they have higher SRLs, SSAs, and N content, increase land use area with less carbon input, and meet the needs of plants with high metabolic rates for nutrient resources (Chen et al., 2017). Third-, fourth-, and fifth-order fine roots have secondary growth processes, large diameters, and high RTDs, and they can better undertake nutrient transport and storage functions (Guo et al., 2008; McCormack et al., 2015); therefore, they also have a higher NSC content.

Conclusion

With decreasing groundwater levels, the soil salinity and water content gradually decreased in the coastal wetland of the YRD. Changes in soil salinity caused by groundwater levels in this region are the main factors affecting fine roots. The fine roots of *T. chinensis* in the coastal wetland of the Yellow River Delta responded to the heterogeneity of different groundwater–soil water–salt systems through trade-offs and changes in morphological, nutrient, and chemical characteristics. With decreasing groundwater levels, the specific root length, specific surface area, and root tissue density of fine roots of *T. chinensis* increased gradually, indicating that the growth rate of fine roots was slower at a high groundwater level than at a low groundwater level. *T. chinensis* increased the opportunity for root-specific surface area to improve water absorption at a low groundwater level. Under a medium groundwater level, the content of N and C/N decreased, and the content of soluble sugar, starch, and nonstructural carbohydrates increased to inhibit the respiration of fine roots, and the utilization of soluble sugar and starch was lower. At high groundwater and low groundwater levels, the fine roots of *T. chinensis* must enhance their metabolism and improve their adaptability to environments with high salt and low groundwater content. The fine roots of *T. chinensis* at different orders were significantly different in morphology, nutrients, and chemical characteristics, and the morphological changes of fine roots were compatible with their functions.

Data availability statement

The raw data supporting the conclusions of this article will be made available by the authors, without undue reservation.

Author contributions

JS contributed to writing—original draft, writing—review and editing, investigation, and data curation. JX contributed to supervision and funding acquisition. PS contributed to methodology and investigation. JM, FG, and YL contributed to investigation and data curation. XX contributed to investigation and validation. MD contributed to investigation and analysis. CL contributed to writing—review and editing and methodology. All authors contributed to the article and approved the submitted version.

Funding

This research was financially supported by the Joint Funds of the National Natural Science Foundation of China (no. U2006215), the Forestry Science and Technology Innovation Project of Shandong Province (no. 2019LY006), the Basic Investigation Project for the Development Quality of Wetland Park in Shandong Province (no. SDGP202202001808A_001), and the Taishan Scholars Program of Shandong Province, China (no. TSQN201909152).

Conflict of interest

The authors declare that the research was conducted in the absence of any commercial or financial relationships that could be construed as a potential conflict of interest.

Publisher's note

All claims expressed in this article are solely those of the authors and do not necessarily represent those

of their affiliated organizations, or those of the publisher, the editors and the reviewers. Any product that may be evaluated in this article, or claim that may be made by its manufacturer, is not guaranteed or endorsed by the publisher.

Supplementary material

The Supplementary material for this article can be found online at: https://www.frontiersin.org/articles/10.3389/fpls.2022.952830/full#supplementary-material

References

An, L. S., Zhao, Q. S., and Xu, Y. (2013). Dynamic characteristics of the shallow groundwater table and its genesis in the Yellow River Delta. *Environ. Sci. Technol.* 36, 1–56. doi: 10.3969/j.issn.1003-6504.2013.09.011

Caplan, J. S., Meiners, S. J., Habacuc, F. M., and Mccormack, M. L. (2019). Fine-root traits are linked to species dynamics in a successional plant community. *Ecology* 100, 1–14. doi: 10.1002/ecy.2588

Chen, G. T., Zheng, J., Peng, T. C., Li, S., Qiu, X. R., Chen, Y. Q., et al. (2017). Fine root morphology and chemistry characteristics in different branch orders of Castanopsis platyacantha and their responses to nitrogen addition. *Chin. J. Appl. Ecol.* 28, 3461–3468. doi: 10.13287/j.1001-9332.201711.004

Di, N., Liu, Y., Mead, D. J., Xie, Y. Q., Jia, L. M., and Xi, B. Y. (2018). Root-system characteristics of plantation-grown *Populus tomentosa* adapted to seasonal fluctuation in the groundwater table. *Trees* 32, 137–149. doi: 10.1007/s00468-017-1619-2

Eissenstat, D. M., Kucharski, J. M., Zadworny, M., Adams, T. S., and Koide, R. T. (2015). Linking root traits to nutrient foraging in arbuscular mycorrhizal trees in a temperate forest. *New Phytol.* 208, 114–124. doi: 10.1111/nph.13451

Fan, X., Pedroli, B., Liu, G., Liu, Q., Liu, H., and Shu, L. (2012). Soil salinity development in the yellow river delta in relation to groundwater dynamics. *Land Degrad. Dev.* 23, 175–189. doi: 10.1002/ldr.1071

Freschet, G. T., Roumet, C., Comas, L. H., Weemstra, M., Bengough, A. G., Rewald, B., et al. (2021). Root traits as drivers of plant and ecosystem functioning: current understanding, pitfalls and future research needs. *New Phytol.* 232, 1123–1158. doi: 10.1111/nph.17072

Guo, D., Xia, M., Wei, X., Chang, W., Liu, Y., and Wang, Z. (2008). Anatomical traits associated with absorption and mycorrhizal colonization are linked to root branch order in twenty-three Chinese temperate tree species. *New Phytol.* 180, 673–683. doi: 10.1111/j.1469-8137.2008.02573.x

Kong, D. L., Wang, J. J., Wu, H. F., Valverde-Barrantes, O. J., and Feng, Y. (2019). Nonlinearity of root trait relationships and the root economics spectrum. *Nat. Commun.* 10:2203. doi: 10.1038/s41467-019-10245-6

Lei, H., Wang, K., Tian, H., Gao, X., and Zhao, L. R. (2017). Responses of non-structural carbohydrates accumulation and distribution of *Caragana microphylla* seedlings to drought stress. *Chin. J. Ecol.* 36, 3168–3175. doi: 10.13292/j.1000-4890.201711.016

Li, F., Hu, H., Mccormlack, M. L., Feng, D. F., Liu, X., and Bao, W. (2019). Community-level economics spectrum of fine roots driven by nutrient limitations in subalpine forests. *J. Ecol.* 107, 1238–1249. doi: 10.1111/1365-2745.13125

Li, X. Q., Wang, X. D., Fan, Y., Liu, Q., and Wang, S. J. (2021). Effects of salt stress on the growth index of absorbing roots of *Pyrus betulifolia*. *J. Shanxi Agric. Univ. (Nat. Sci. Ed.)* 41, 62–67. doi: 10.13842/j.cnki.issn1671-8151.202105048

Liu, S. S., Xu, G. Q., Chen, T. Q., Mi, X. J., Liu, Y., Ma, J., et al. (2022). Effects of groundwater depth on functional traits of young *Haloxylon ammodendron*. *Chin. J. Appl. Ecol.* 33, 733–741. doi: 10.13287/j.1001-9332.202202.025

Ma, Z., and Chen, H. Y. H. (2016). Effects of species diversity on fine root productivity in diverse ecosystems: a global meta analysis. *Glob. Ecol. Biogeogr.* 25, 1387–1396. doi: 10.1111/geb.12488

McCormack, M. L., Adams, T. S., Smithwick, E. A. H., and Eissenstat, D. M. (2012). Predicting fine root lifespan from plant functional traits in temperate trees. *New Phytol.* 195, 823–831. doi: 10.1111/j.1469-8137.2012.04198.x

McCormack, M. L., Dickie, I. A., Eissenstat, D. M., Fahey, T. J., Fernandez, C. W., Guo, D., et al. (2015). Redefining fine roots improves understanding of below-ground contributions to terrestrial biosphere processes. *New Phytol.* 207, 505–518. doi: 10.1111/nph.13363

Meghan, B., and Robin, H. (2020). Adaptive variation and plasticity in nonstructural carbohydrate storage in a temperate tree species. *Plant Cell Environ.* 44, 2494–2505. doi: 10.1111/pce.13959

Peng, G. W., Sun, J., Zhao, X. M., Fang, Y., and Xia, J. B. (2022). The influence of groundwater salinity on the growth and architecture of *Tamarix chinensis* root system. *J. Southwest Forest. Uni. (Nat. Sci.)* 42, 1–7. doi: 10.11929/j.swfu.202106037

Pregitzer, K. S., DeForest, J. L., Burton, A. J., Allen, M. F., Ruess, R. W., and Hendrick, R. L. (2002). Fine root architecture of nine north American trees. *Ecol. Monogr.* 72, 293–309. doi: 10.1890/0012-9615

Rewald, B., Rechenmacher, A., and Godbold, D. (2014). It's complicated: intraroot system variability of respiration and morphological traits in four deciduous tree species. *Plant Physiol.* 166, 736–745. doi: 10.1104/pp.114.240267

Shi, W. (2008). *Comparison of root morphology and leaf morphology of twenty hardwood species in Maoershan natural secondary forest* Northeast Forestry University.

Song, X. J., Li, S. N., Wei, W., Guo, J., Yu, Y. L., and Liu, Z. W. (2017). Distribution characteristics of root f system of *Tamarix chinensis* in Yellow River Delta and its influence factors. *Wetland Sci.* 15, 716–723. doi: 10.13248/j.cnki.wetlandsci.2017.05.011

Sun, J., Xia, J. B., Dong, B. T., Gao, F. L., Chen, P., Zhao, W. L., et al. (2021). Root morphology and growth characteristics of *Tamarix chinensis* with different densities on the beach of the Yellow River Delta. *Acta Ecol. Sin.* 41, 3775–3783. doi: 10.5846/stxb202007081779

Sun, J., Zhao, X. M., Fang, Y., Xu, W. G., Gao, F. L., Zhao, W. L., et al. (2022). Root growth and architecture of *Tamarix chinensis* in response to the groundwater level in the Yellow River Delta. *Mar. Pollut. Bull.* 179:113717. doi: 10.1016/j.marpolbul.2022.113717

Terzaghi, M., Montagnoli, A., and Di, I. A. (2013). Fine-root carbon and nitrogen concentration of European beech (*Fagus sylvatica* L.) in Italy Prealps: possible implications of coppice conversion to high forest. *Front. Plant Sci.* 4:192. doi: 10.3389/fpls.2013.00192

Wang, Z. Q., Guo, D. L., Wang, X. R., Gu, J. C., and Mei, L. (2006). Fine root architecture, morphology, and biomass of different branch orders of two Chinese temperate tree species. *Plant and Soil* 288, 155–171. doi: 10.1007/s11104-006-9101-8

Wang, Y., Wang, J. M., Wang, X. L., He, Y. C., Li, G. J., and Li, J. W. (2021b). Dominant roles but distinct effects of groundwater depth on regulating leaf and fine-root N, P and N: P ratios of plant communities. *J. Plant Ecol.* 14, 1158–1174. doi: 10.1093/jpe/rtab062

Wang, Y., Wang, J. M., Yang, H., Li, G. J., Chen, C., and Li, J. W. (2021a). Groundwater and root trait diversity jointly drive plant fine root biomass across arid inland river basin. *Plant and Soil* 469, 369–385. doi: 10.1007/s11104-021-05182-7

Withington, J. M., Reich, P. B., Oleksyn, J., and Eissenstat, D. M. (2006). Comparisons of structure and life span in roots and leaves among temperate trees. *Ecol. Monogr.* 76, 381–397. doi: 10.1890/0012-9615

Xia, J. B., Ren, J. Y., Zhao, X. M., Zhao, F. J., and Liu, J. H. (2018). Threshold effect of the groundwater depth on the photosynthetic efficiency of Tamarix chinensis in the Yellow River Delta. *Plant and Soil* 433, 157–171. doi: 10.1007/s11104-018-3829-9

Xie, T., Liu, X. H., and Sun, T. (2011). The effects of groundwater table and flood irrigation strategies on soil water and salt dynamics and reed water use in the Yellow River Delta, China. *Ecol. Model.* 222, 241–252. doi: 10.1016/j.ecolmodel.2010.01.012

Xu, Y., Gu, J. C., Dong, X. Y., Liu, Y., and Wang, Z. Q. (2011). Fine root morphology, anatomy and tissue nitrogen and carbon contents of the first five orders in four tropical hardwood species in Hainan Island, China. *Chin. J. Plant Ecol.* 35, 955–964. doi: 10.3724/SP.J.1258.2011.00955

Yu, Q., Gao, C. L., Jin, G. Z., Liu, Z. L., and Shi, B. K. (2021). Latitude patterns in fine root morphological and anatomical traits across root orders of *Pinuskoraiensis*. *Scand. J. For. Res.* 36, 539–549. doi: 10.1080/02827581.2021.1981430

Yuan, Y. S., and Huangpu, C. H. (2020). Effects of nitrogen addition and groundwater level interaction on the growth of the wet plant *Carex thunbergii* in the lakes connecting the Yangtze River. *Res. Environ. Sci.* 33, 2838–2847. doi: 10.13198/j.issn.1001-6929.2020.04.13

Zhang, W. T., Shan, L. S., Li, Y., Bai, Y. M., and Ma, J. (2020). Effects of nitrogen addition and precipitation change on non-structural carbohydrates in *Reaumuria soongorica* seedlings. *Chin. J. Ecol.* 39, 803–811. doi: 10.13292/j.1000-4890.202003.017

Zhang, X. X., Yin, X. L., Li, H. L., Su, D., Jia, S. Y., and Dong, Z. (2017). Effect of salt stress on the biomass and photosynthetic characteristics of *Ulmuspumila* L. strains. *Acta Ecol. Sin.* 37, 7258–7265. doi: 10.5846/stxb201608091632

Zhao, Q. Q., Bai, J. H., Gao, Y. C., Zhao, H. X., Zhang, G. L., and Cui, B. S. (2020). Shifts of soil bacterial community along a salinity gradient in the Yellow River Delta. *Land Degrad. Dev.* 31, 2255–2267. doi: 10.1002/ldr.3594

Zheng, Y. P., Wang, H. X., Lou, X., Yang, Q. P., and Xu, M. (2014). Changes of non-structural carbohydrates and its impact factors in trees: a review. *Chin. J. Appl. Ecol.* 25, 1188–1196. doi: 10.13287/j.1001-9332.2014.0110

Zhong, B. Y., Xiong, D. C., Shi, S. Z., Feng, J. X., Xu, C. S., Deng, F., et al. (2016). Effects of precipitation exclusion on fine-root biomass and functional traits of *Cunninghamia lanceolata* seedlings. *Chin. J. Appl. Ecol.* 27, 2807–2814. doi: 10.13287/j.1001-9332.201609.023

Zou, Y. X., Zhong, Q. L., You, Y. L., Yu, H., Zheng, W. T., Chen, J. J., et al. (2018). Short-term effects of nitrogen and water treatments on fine root order morphology of *Machilus pauhoi* seedlings. *Chin. J. Appl. Ecol.* 29, 2323–2329. doi: 10.13287/j.1001-9332.201807.014

frontiers | Frontiers in Plant Science

TYPE Original Research
PUBLISHED 13 October 2022
DOI 10.3389/fpls.2022.990246

OPEN ACCESS

EDITED BY
Xiaoming Kang,
Chinese Academy of Forestry, China

REVIEWED BY
Puchang Wang,
Guizhou Normal University, China
Feng Li,
Institute of Subtropical Agriculture, (CAS), China

*CORRESPONDENCE
Tian Li
912litian@163.com

SPECIALTY SECTION
This article was submitted to Functional Plant Ecology, a section of the journal Frontiers in Plant Science

RECEIVED 09 July 2022
ACCEPTED 21 September 2022
PUBLISHED 13 October 2022

CITATION
Zhao Y, Li T, Liu J, Sun J and Zhang P (2022) Ecological stoichiometry, salt ions and homeostasis characteristics of different types of halophytes and soils.
Front. Plant Sci. 13:990246.
doi: 10.3389/fpls.2022.990246

Ecological stoichiometry, salt ions and homeostasis characteristics of different types of halophytes and soils

Yinghan Zhao[1,2], Tian Li[1]*, Junhan Liu[1,2], Jingkuan Sun[1] and Ping Zhang[3]

[1]Shandong Key Laboratory of Eco-Environmental Science for Yellow River Delta, Binzhou University, Binzhou, China, [2]College of Forestry, Shandong Agricultural University, Taian, China, [3]College of Life Sciences, Ludong University, Yantai, China

Studying eco-stoichiometric and salt ions characteristics of halophytes and soils is helpful to understand the distribution mechanism of nutrients and salts in halophytes and their adaptation strategies to salinized habitats. In this study, three different types of halophytes (*Phragmites communis*-salt repellent, *Suaeda salsa*-salt accumulating, and *Aeluropus sinensis*- salt secreting) and soils were selected to analyze the differences and correlations of C, N, P stoichiometry and salt accumulation. Results showed that: (1) the total nitrogen (TN) and total phosphorus (TP) contents of the three halophytes' leaves were significantly higher than those of the roots and stems, and the C: N ratios were contrary to the difference mentioned above. The growth of *P. communis* and *S. salsa* was mainly limited by P, whereas *A. sinensis* was limited by both N and P. *S. salsa* had a stronger absorption capacity for Na^+ and Mg^{2+} than *P. communis* and *A. sinensis*. The interrelationship between salt ions and C, N and P ecological stoichiometry of halophyte organs was influenced by the type of halophytes. (2) The TC, TN, and N: P contents of the three halophyte communities in the surface soil (0-20 cm) were significantly higher than the other soil layers, while P did not differ significantly among soil layers. The planting of different halophytes affected the TC, TN, C: N, N: P values and the content of seven ions in the surface soil. $SO_4^{2-}$was positively correlated with soil TC, TN, N:P, and Na^+ were positively correlated with soil TC in three halophytes. (3) The *P. communis* TC and *A. sinensis* TN contents were negatively correlated with soil TC, TN, C: P, and N: P, whereas TC contents of *S. salsa* were positively correlated with the aforementioned soil indicators. The *P. communis* and *A. sinensis* TC contents were negatively correlated with soil K^+, while this correlation was opposite between *S. salsa* and soil. (4) The homeostasis of C, N, and P elements in all three halophytes showed that C > N > P, the homeostasis was strongest in *A. sinensis* and weakest in *S. salsa*. The results provide a theoretical basis for the restoration of saline land in the Yellow River Delta.

KEYWORDS

ecological chemometrics, halophyte, salt ions, homeostasis, Yellow River delta

1 Introduction

In terrestrial ecosystems, the balance of energy and nutrients is called ecological stoichiometry (Yang et al., 2018), which represents the demand of organisms for natural resources and mainly connects biogeochemical cycles at different levels through carbon(C), nitrogen(N), and phosphorus(P) (Hu et al., 2018). Stoichiometric homeostasis is the core of ecological chemometrics (Koojiman, 1995), which refers to the ability of organisms to maintain their chemical composition relatively constant by adjusting the concentration of chemical elements and the proportion of different chemical elements in their organisms when external environmental conditions change. The strength of homeostasis can reflect the adaptability of organisms to environmental changes (Sterner and Elser, 2002). The elements C, N, and P are the basis for the composition of all living substances on earth (Jordi et al., 2012). For plants, C constitutes the basic structure of plants, accounting for about 50% of their biomass (Schade et al., 2003; Liu et al., 2011); N is the basic component of enzymes and plays a crucial role in plant production and photosynthesis (Elser et al., 2000); P is an essential element for nucleic acids and cell membranes, responsible for the composition of cellular structural DNA and RNA (Tilman, 2004; Bai et al., 2012).

Plant and soil ecological stoichiometric ratios are used to represent important ecological processes in terrestrial ecosystems. For example, the concept of leaf N: P ratios to assess nutrient limitations in plant growth has been demonstrated in a variety of plants (Koerselman and Meuleman, 1996; Schreeg et al., 2014); The C: N and C: P ratios in plants indicate the ability of the plant to assimilate and accumulate C and the degree of nutrient utilization, which can be used as an indicator of plant growth rate (Agren, 2004). Soil quality plays a decisive role in plant growth as an important means of obtaining nutrients for plant growth and development. When soil nutrients are insufficient and restrict plant growth, plants will continuously adjust the physiological and ecological processes of various nutrient organs to meet their growth and development needs (Schreeg et al., 2014). Therefore, it is of great significance to analyze the relationship of the ecological stoichiometric characteristics of C, N, and P elements between plants and soil in the ecosystem, to clarify the correlation between plants and soils ecological stoichiometric, to reveal the interaction between C, N and P elements and the relationship between restriction and balance.

The Yellow River Delta Nature Reserve is the youngest and most complete wetland ecosystem in the world (Li et al., 2021). However, due to natural factors and anthropogenic activities in recent years, the water and salt balance of wetland soil in the Yellow River Delta has been destroyed and the degree of soil salinization has increased (Zhao et al., 2022), limiting the growth of many plants in the area, which is a key factor affecting the sustainable development of agriculture. Halophytes are the main vegetation type in this saline-alkali area. According to plants' different salt tolerance modes, halophytes are divided into three types: salt repellent, salt accumulating, and salt secreting. They all have unique physiological processes of salt tolerance, which can affect the physicochemical properties of soil and the structure of the rhizosphere microbial community by adjusting the salt content of the soil, forming a microenvironment conducive to plant growth and development, it has an important impact on soil improvement of saline-alkali land (Lau and Lennon, 2012; Lareen et al., 2016). At present, most studies on the ecological stoichiometry of halophytes have focused on the changes in the stoichiometric ratio between plants and soil surface ecosystems under different external environments (Wang et al., 2010; Wen et al., 2021), while studies on nutrient organs and soil profile stoichiometry changes and salt accumulation in different types of halophytes are relatively limited.

Therefore, three different types of halophyte communities, *Phragmites communis* (salt repellent), *Suaeda salsa* (salt accumulating), and *Aeluropus sinensis* (salt secreting), were selected in the Yellow River Delta to explore the ecological stoichiometry, salt characteristics, and intrinsic relationships in the plant-soil system, and to comprehensively assess the homeostasis characteristics of nutrient organ stoichiometry of the three halophytes, as well as to reveal the allocation strategies of different types of halophytes for nutrients and salinity in saline habitats from the perspective of the effect of salinity on ecological stoichiometric characteristics. To this end, we have the following three hypotheses: First, the salt tolerance mechanisms of halophytes influence the ecological stoichiometry and salt ion content characteristics at the soil profile level and among plant nutrient organs; Second, the correlation between ecological stoichiometry characteristics and salt ion content of halophytes varies depending on the salt tolerance mechanisms of halophytes; Third, due to the different salt tolerance strategies developed by halophytes as a result of their long-term adaptation to saline soils, their growth-limiting elements as well as their internal stability therefore differ somewhat and show different patterns in the internal stability of their nutrient organs.

2 Materials and methods

2.1 Study area

The study area (N 37°55'26", E 118°34'37") is located in Dongying City, Yellow River Delta, as shown in Figure 1. The region has a semi-humid continental monsoon climate with four distinct seasons. The annual average temperature is 12.1 °C, and the regional average precipitation is about 550 mm; the terrain is relatively flat, mostly sandy and argillaceous soils, which are easy to compact and with poor nutrient conditions. The vegetation types are mainly *P. communis*, *S. salsa*, *A. sinensis*, and *Tamarix*

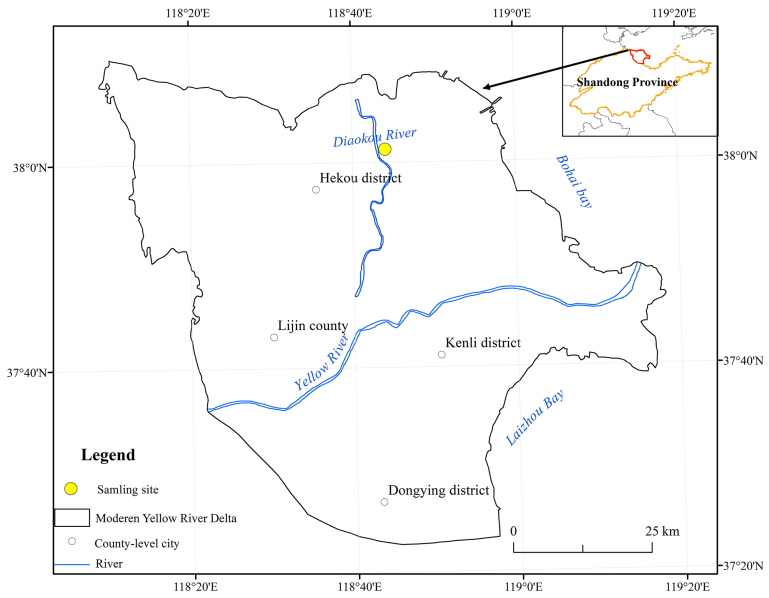

FIGURE 1
Location of the study area (Zhao et al., 2022).

chinensis. The area was classified as a moderately saline soil area based on the results of soil salinity determination at the above sampling sites and the forestry industry-standard (LY/T2959-2018) released in 2018.

2.2 Plant and soil sample collection

Plants: Three fixed sites of 30 m × 30 m were selected in the study area. According to the serpentine distribution method, three small plots of 1 m × 1 m were set in each plot based on the distribution of three types of halophytes. We selected the intact roots, stems, and leaves of three healthy plants in each small sample square, took them back to the laboratory with zip lock bags, and immediately cleaned the soil on the roots, stems, and leaves of the plants until they were free of mud. After drying, removing any impurities such as withered material and rotten roots; placing the clean plant organs in a 105°C oven for 30 min, and then continue drying in a 65°C oven for 2-3 days to achieve a constant weight. The dried plant roots, stems, and leaves were crushed with a plant crusher and ground with a mortar for storage.

Soil: A soil sampling point was set at each plant sampling point, and the soil samples were sampled from three soil layers by soil drill: 0-20 cm, 20-40 cm, and 40-60 cm, 5 drills of soil were taken from each soil layer. After evenly mixing, keep about 1 kg by quartering, placing them in zip lock bags and returning to the laboratory, air-drying them naturally for 10-15 days, and picking out the plant residues. After grinding, they screened through 10 a mesh sieve and a 60 mesh sieve respectively for standby.

2.3 Plant and soil sample determination

Plants: TC and TN were determined by an elemental analyzer; TP was determined by the molybdenum antimony anti-colorimetric method; K^+, Ca^{2+}, Na^+, and Mg^{2+} contents were digested with concentrated sulfuric acid-perchloric acid and determined by an inductively coupled plasma emission spectrometer.

Soil: soil salinity was determined by the residue drying method; pH was determined by the potentiometric method; TC and TN were determined by an elemental analyzer; TP was determined by the molybdenum antimony anti-colorimetric method; K^+, Ca^{2+}, Na^+, and Mg^{2+} contents were digested with concentrated sulfuric acid-perchloric acid and determined by an inductively coupled plasma emission spectrometer; Cl^-, SO_4^{2-}, and NO_3^- contents were determined by ion chromatography (Bao, 2000).

2.4 Comprehensive evaluation method of plant homeostasis

2.4.1 Calculation of homeostasis index

The homeostasis index was calculated using the model (Sterner and Elser, 2002): $y=cx^{1/H}$. In this study, y is the

nutrient elements and stoichiometric ratios (C, N, P, C: N, C: P, N: P) of plant roots, stems, and leaves; x is the corresponding nutrient elements and stoichiometric ratios of plant surface soil, c is a constant, and H is the homeostasis index. The homeostasis index H was calculated by the power function index formula in Excel 2016. For the convenience of statistics, this study also uses 1/H to measure the strength of homeostasis (Hood and Sterner, 2010). And classified 1/H into four types: 0 < 1/H < 0.25, steady-state; 0.25 < 1/H < 0.5, weakly steady-state; 0.5 < 1/H < 0.75 weakly sensitive; and 1/H > 0.75, sensitive (Persson et al., 2010).

2.4.2 Comprehensive evaluation method of homeostasis

In this study, the fuzzy mathematics subordinate method was used to evaluate plant homeostasis (Xu et al., 2021). The formula was: $X(\mu)=\frac{X-X_{min}}{X_{max}-X_{min}}$. In the formula, X is the H value of a certain element or stoichiometric ratio of the plant, Xmax is the maximum H value of a certain index of the roots, stems and leaves in the halophyte, and Xmin is the minimum value. Based on calculating the homeostasis index H, the subordinate values of the three halophyte nutrient elements and the stoichiometric ratios were calculated in different organs, and then the subordinate values of each indicator in different halophyte organs were accumulated and averaged. Finally, the subordinate values of each indicator of each plant were accumulated to obtain the average value. The homeostasis of the three halophytes was evaluated comprehensively by comparing the magnitude of the total mean value of the homeostasis subordinate to the halophytes (Sun et al., 2006)

2.5 Data analysis

Excel 2016 was used to perform statistics and calculations on the data, and the SPSS 20.0 Duncan (D) method was used to perform ANOVA one-way analysis. The paper's data were expressed as mean ± standard error, with a significance level of $P = 0.05$. Origin 2019b was used for box and histogram plotting.

3 Results

3.1 Ecological stoichiometry and salt ions characteristics of different halophytes

3.1.1 Characteristics of TC, TN, and TP content distribution in nutrient organs

There were great differences in TC content among the three nutrient organs of halophytes (Figure 2), with the *P. communis* showing: leaf > stem > root, the *S. salsa*: root = stem > leaf, and the *A. sinensis*: stem > leaf > root. TN and TP contents in leaves were significantly higher than those in roots and stems in the three halophytes. *P. communis* stems had significantly lower TN content than roots, while *S. salsa* and *A. sinensis* stems had significantly higher TN content than roots ($P < 0.05$).

Comparing the same nutrient organs of different plants, it was found that the TC content of *P. communis* roots was significantly higher than that of *S. salsa* and *A. sinensis*, and the TC content of *P. communis* and *A. sinensis* stems and leaves was significantly higher than that of *S. salsa* ($P < 0.05$). Among the different halophytes, roots and leaves TN content showed as follows: *S. salsa* >

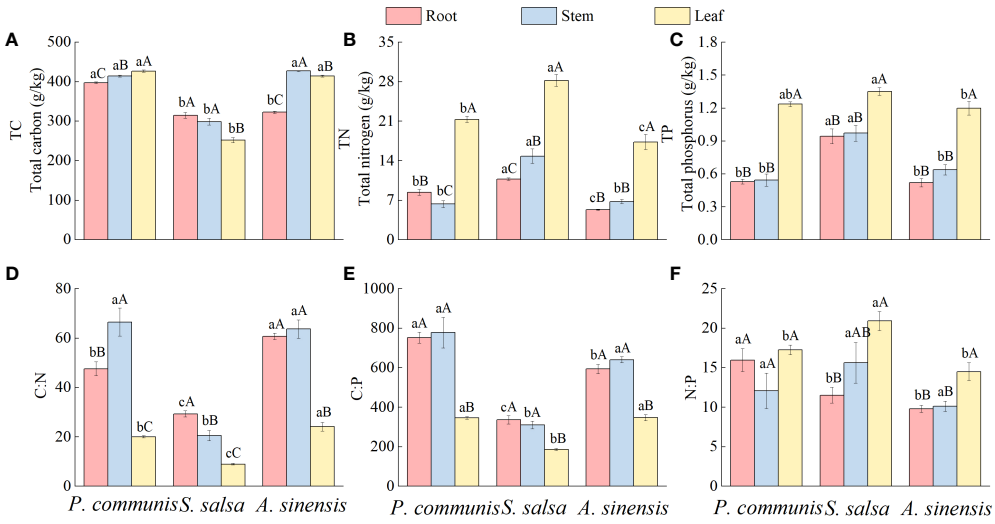

FIGURE 2
Characteristics of TC **(A)**, TN **(B)** and TP **(C)** contents and C:N **(D)**, C:P **(E)** and N:P **(F)** stoichiometric ratios in halophyte organs. Capital letters indicate the difference between different organs in the same halophyte, and lowercase letters donate the difference of different halophytes of the same organ ($P < 0.05$).

P. communis > *A. sinensis*, stem: *S. salsa* > *P. communis* = *A. sinensis*; the TP content of *S. salsa* roots and stems was significantly higher than that of *P. communis* and *A. sinensis*, and the TP content of leaves was significantly higher than that of *A. sinensis* ($P < 0.05$).

3.1.2 Eco-stoichiometric ratio characteristics of nutrient organs

Significant differences in C: N among different organs of the same halophytes (Figure 2), *P. communis*: stem > root > leaf, *S. salsa*: root > stem > leaf, *A. sinensis*: root = stem > leaf; C: P content of the roots and stems in the three halophytes was significantly higher than that of the leaves; N: P was significantly higher in *S. salsa* leaves than in roots, and in *A. sinensis* leaves than in roots and stems ($P < 0.05$), but there was no significant difference in N: P in different organs of *P. communis*($P > 0.05$).

The differences in root and leaf C: N among different halophytes were as follows: *A. sinensis* > *P. communis* > *S. salsa*, stem: *A. sinensis* = *P. communis* > *S. salsa*; C: P difference in stems and leaves was: *P. communis* = *A. sinensis* > *S. salsa*, root: *P. communis* > *A. sinensis* > *S. salsa*; N: P in roots of three halophytes was: *P. communis* > *S. salsa* = *A. sinensis*, leaf: *S. salsa* > *P. communis* = *A. sinensis*, and there was no significant difference in N: P between stems.

3.1.3 Total cation content of nutrient organs of halophytes

The different ion contents of plant roots, stems, and leaves varied under the same halophyte type (Figure 3), where the variability of K^+ content in *P. communis* nutrient organs showed: leaf > stem > root, *S. salsa*: root > stem = leaf, *A. sinensis*: stem = leaf > root; The Ca^{2+} content was significantly different among the three organs of *S. salsa* and *A. sinensis* ($P < 0.05$), *S. salsa*: stem = leaf > root, *A. sinensis*: root > stem = leaf, and no significant difference in *P. communis*; the difference in Na^+ content of different organs of *P. communis* was: root > stem > leaf, while *A. sinensis* was the opposite: root < stem < leaf, and *S. salsa*: leaf > root = stem; The differences in Mg^{2+} content of nutrient organs of *P. communis* were as follows: root > stem, *S. salsa*: leaf > stem > root, and *A. sinensis*: leaf > stem = root.

Comparing the same nutrient organs of different halophytes (Figure 3), it was found that the K^+ and Na^+ contents in the roots of *S. salsa*, Ca^{2+}, Na^+, and Mg^{2+} contents of stems and leaves were significantly higher than those in *P. communis* and *A. sinensis*. In addition, the K^+ contents of *P. communis* leaves were significantly higher than those of *S. salsa* and *A. sinensis* ($P < 0.05$), and the Ca^{2+} and Mg^{2+} contents of *A. sinensis* roots were significantly higher than those of *P. communis* ($P < 0.05$).

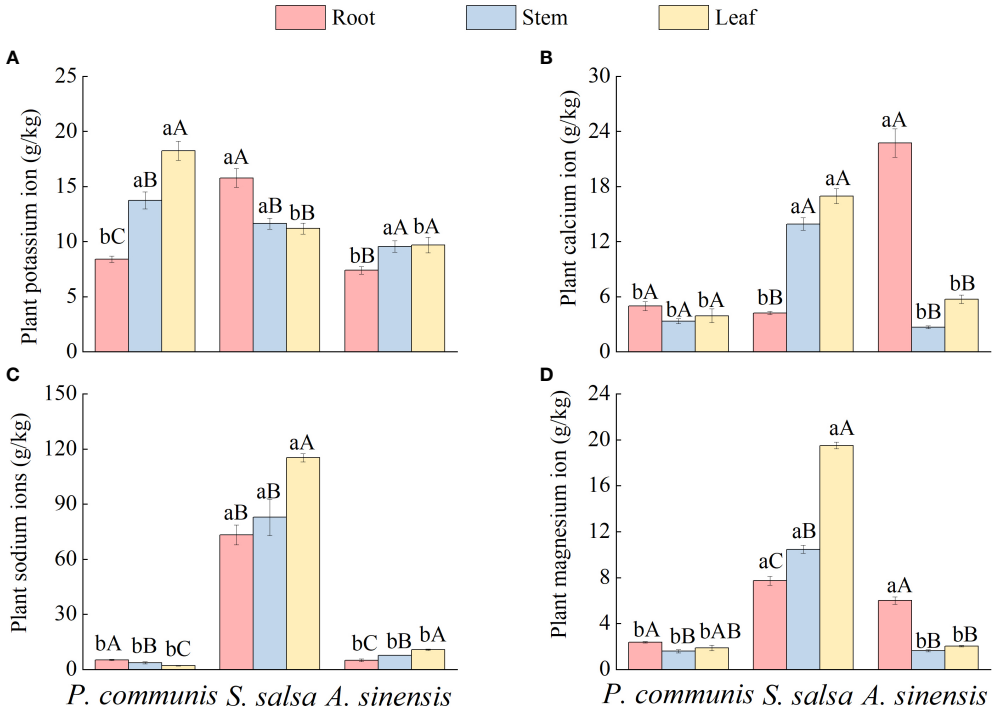

FIGURE 3
K+ **(A)**, Ca2+ **(B)**, Na+ **(C)**, Mg2+ **(D)** cation content in organs of halophyte. Capital letters indicate the difference between different organs in the same halophyte, and lowercase letters donate the difference of different halophytes of the same organ (P < 0.05).

3.1.4 Correlation between ecological stoichiometry and cations in halophytes

In the salt repellent plant *P. communis* (Figure 4), both TC and TP were positively correlated with K^+ content and negatively correlated with Na^+, contrary to the above results, C: P was negatively correlated with K^+ content and positively correlated with Na^+ ($P < 0.05$). In *S. salsa*, TC, C: N, and C: P were negatively correlated with the contents of Ca^{2+}, Na^+, and Mg^{2+}, and TN and N: P were significantly positively correlated with the contents of the above ions, in addition, C: N and C: P were positively correlated with K^+ content, TP was negatively correlated with K^+ content, and positively correlated with Mg^{2+}. The *A. sinensis* TN and TP were significantly positively correlated with the K^+ and Na^+ content, and the TC was negatively correlated with the Ca^{2+} and Mg^{2+} content.

3.2 Ecological stoichiometry and salinity characteristics of different halophyte soils

3.2.1 Distribution characteristics of TC, TN, and TP content in halophyte soil at different soil depths

The TC and TN contents of the three halophytes in the 0-20 cm soil layer were significantly higher than those of the respective 20-40 cm and 40-60 cm soil layers ($P < 0.05$), and the TP contents of the soils were not significantly different ($P > 0.05$) under different soil layers of the same halophytes (Figure 5).

Comparing different halophytes in the same soil layer, it was found that only the contents of TC and TN showed differences in the 0-20 cm soil layer ($P < 0.05$). TC: *A. sinensis* > *P. communis* = *S. salsa*, TN: *P. communis* = *A. sinensis* > *S. salsa*, while the TC and TN contents of three different halophytes were not significantly different in 20-40 cm and 40-60 cm soil layers and TP in three soil layers. ($P > 0.05$).

3.2.2 Ecological stoichiometric ratio characteristics of halophyte soil at different soil depths

The C: N of *P. communis* and *A. sinensis* 0-20 cm soil layer was significantly higher than that of their respective 40-60 cm soil layers (Figure 5), and the C: N of S. salsa 0-20 cm soil layer was significantly higher than that of the 20-40 cm and 40-60 cm soil layers ($P < 0.05$); the C: P and N: P contents of the three halophytes 0-20 cm soil layer were significantly higher than that of their respective 20-40 cm and 40-60 cm soils ($P < 0.05$).

Comparing different halophytes in the same soil layer, it was found that the soil ecological stoichiometric ratios of the three halophytes only varied significantly before the 0-20 cm soil layer, the variability of C: N values was shown by: *S. salsa* > *A. sinensis* > *P. communis*; the C: P content of the *A. sinensis* soil was significantly

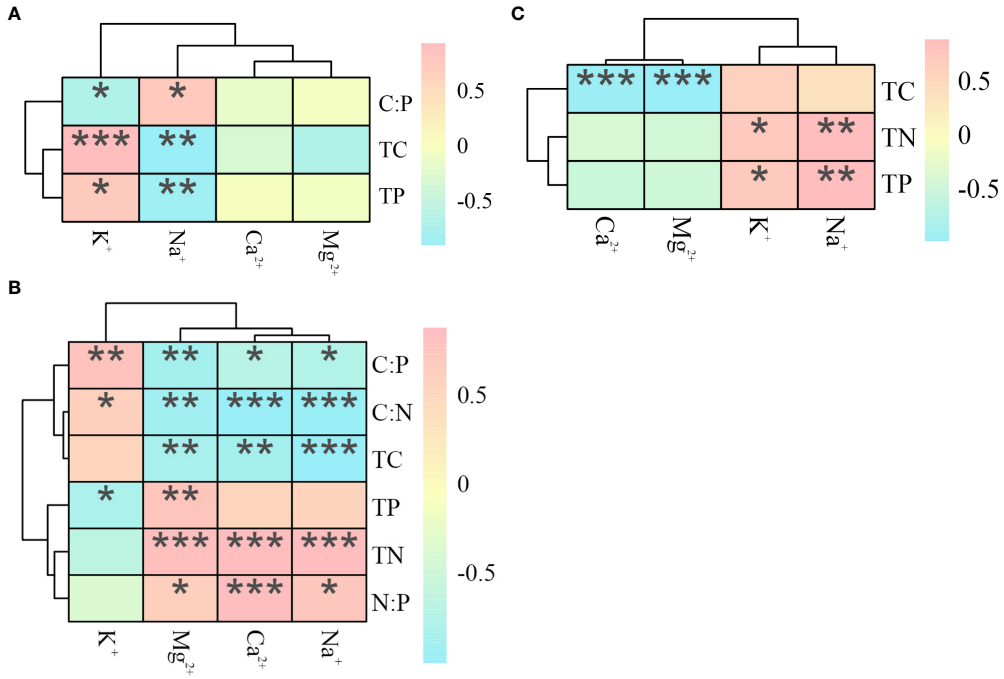

FIGURE 4
Heat map of the correlation between ecological stoichiometry and cations in *P. communis* **(A)**, *S. salsa* **(B)** and *A. sinensis* **(C)**. *, ** and *** represent significant differences at 0.05, 0.01 and 0.001 levels respectively.

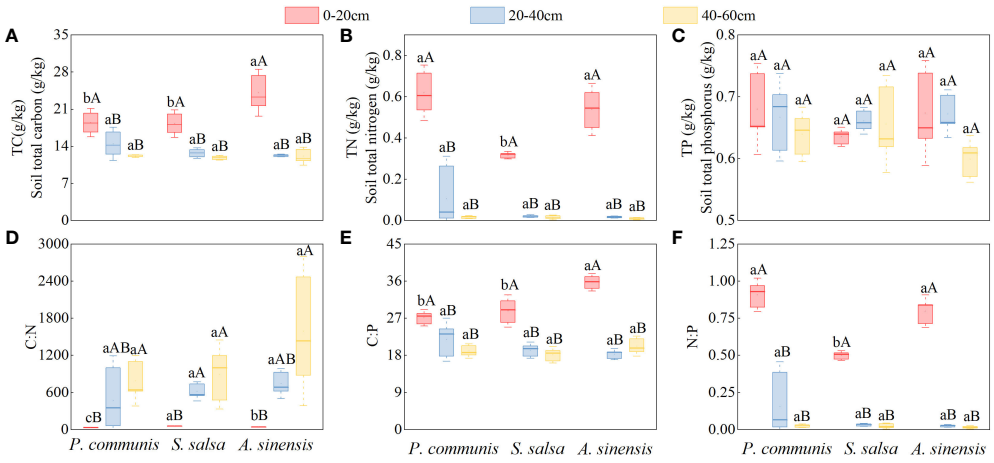

FIGURE 5
Halophytes characteristics of TC **(A)**, TN **(B)** and TP **(C)** contents and C:N **(D)**, C:P **(E)** and N:P **(F)** stoichiometric ratios in soils of different soil layers. Capital letters indicate the difference among different soil layers in the same halophyte, lowercase letters indicate the difference among different halophytes in the same soil layer ($P < 0.05$).

higher than that of *P. communis* and *S. salsa* ($P < 0.05$), and the N: P content of *P. communis* and *A. sinensis* soil was significantly higher than that of *S. salsa* ($P < 0.05$). The C: N, C: P, and N: P contents of the three halophyte soils were not significantly different in the 20-40 cm and 40-60 cm soil layers ($P > 0.05$).

3.2.3 Distribution characteristics of salt content in halophyte soil at different soil depths

As shown in Figure 6, the K^+, Ca^{2+}, and Na^+ contents of *P. communis* and *S. salsa* 0-20 cm soil layers were significantly higher ($P<0.05$) than 20-40 cm and 40-60 cm soil layers, and the Mg^{2+} contents were significantly higher than 40-60 cm soil layers for the same halophyte in different soil layers, while only the K^+ contents of *A. sinensis* 0-20 cm soil layers were significantly higher than the 40-60 cm soil layer.

Comparing the cation contents of different halophytes in the same soil layer (Figures 6), it was found that the K^+, Ca^{2+}, and Mg^{2+} contents of *P. communis* soil were significantly higher than those of *S. salsa* and *A. sinensis* in the 0-20 cm soil layer, and the Na^+ content was only significantly higher than that of *A. sinensis*. The Ca^{2+} and Mg^{2+} contents in the 40-60 cm soil layer were significantly higher in *P. communis* and *A. sinensis* than in *S. salsa* ($P < 0.05$).

As shown in Figure 7, the Cl^-, SO_4^{2-}, and NO_3^- contents in the 0-20 cm soil layers of *P. communis* and *S. salsa* were significantly higher than those of their respective 20-40 cm and 40-60 cm soil layers ($P < 0.05$), and the Cl^- content of the 0-20 cm soil layer of *A. sinensis* was significantly higher than that of other soil layers ($P < 0.05$). When comparing the soil anion contents of different halophytes in the same soil layer, we discovered that the Cl^- and NO_3^- contents of *P. communis* 0-20 cm soil layer were significantly higher than that of *A. sinensis*, and the Cl^- content was significantly higher than that of *S. salsa*. The Cl^- content of *P. communis* in the 20-40 cm soil layer was significantly lower than that of *A. sinensis*; in the 40-60 cm soil layer, the NO_3^- content of *P. communis* and *S. salsa* soil was significantly higher than that of *A. sinensis* ($P < 0.05$), while SO_4^{2-} did not differ significantly among the three halophytes in the same soil layer.

3.2.4 Correlation between soil ecological stoichiometric characteristics and soil salinity factors

The TC, TN, C: P, and N: P values of *P. communis* soil were positively correlated with the contents of K^+, Na^+, Mg^{2+}, SO_4^{2-}, and NO_3^- in the soil, while the C: N was negatively correlated with the above ions, where C: P also showed positive correlations with Ca^{2+}, Cl^-, and soil salinity (Figures 8).

S. salsa soil TC, TN, and C: P values were positively correlated with K^+, Ca^{2+}, Na^+, Cl^-, SO_4^{2-} and salt content, negatively correlated with pH; N: P was positively correlated with K^+, Ca^{2+}, Cl^-, and SO_4^{2-} ions content and negatively correlated with pH; C: N was negatively correlated with K^+ and SO_4^{2-} contents, while TP was positively correlated with pH.

In *A. sinensis* soil, the values of TC, TN, and N: P were positively correlated with SO_4^{2-} content, where TC was also positively correlated with Na^+ content; C: P was positively correlated with K^+ content; TP was positively correlated with Cl^- content, and C: N was negatively correlated with SO_4^{2-} content.

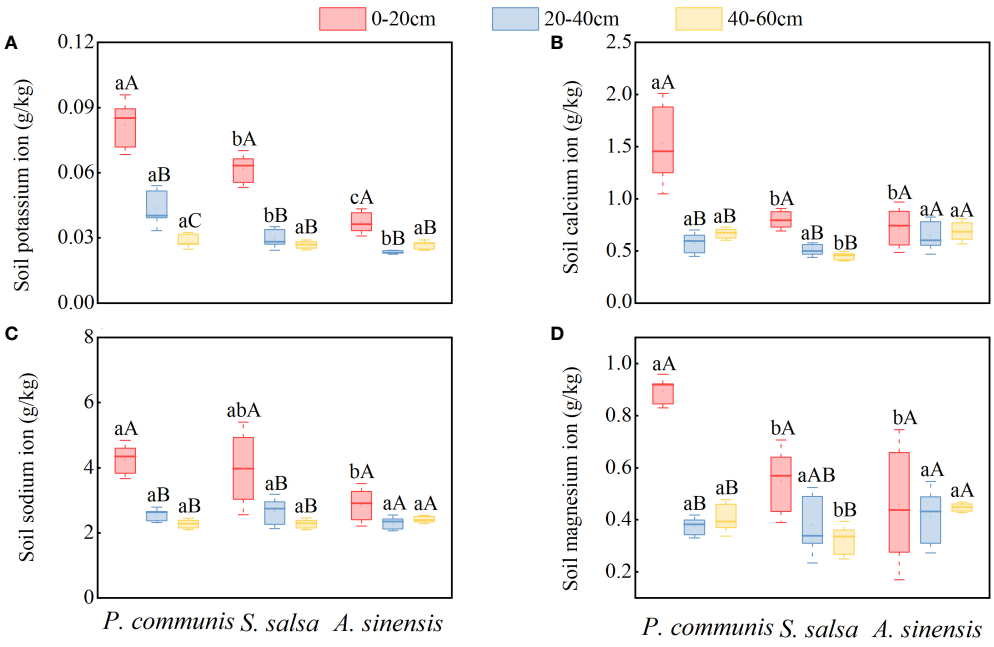

FIGURE 6
K+ **(A)**, Ca2+ **(B)**, Na+ **(C)**, Mg2+ **(D)** cation content in soils of halophyte. Capital letters indicate the difference between different organs in the same halophyte, and lowercase letters donate the difference of different halophytes of the same organ ($P < 0.05$).

3.3 Correlation between plant ecological stoichiometry and soil factors

3.3.1 Correlation between plant ecological stoichiometry and soil ecological stoichiometry

P. communis plant TC was negatively correlated with soil TC, TN, C: P, N: P, and positively correlated with C: N value (Table 1); plant TP was negatively correlated with soil TC.

Plants TC and C: N values in *S. salsa* were positively correlated with soil TC, TN, C: P, N: P, and negatively correlated with soil C: N; plant TN, N: P were negatively correlated with soil TC, TN, C: P, N: P, and plant TN was also positively correlated with soil C: N; plant TP was negatively correlated with soil TC; plant C: P was negatively correlated with soil TC, and negatively correlated with C: N.

The plant TC content of *A. sinensis* was negatively correlated with soil C: P; plant TN and TP were negatively correlated with soil TC, TN, and N:P, and positively correlated with soil C: N. Among them, plant TP was negatively correlated with soil TP; plant C: P was positively correlated with soil TP; plant N: P was negatively correlated with soil TN and N:P, and positively correlated with soil C: N.

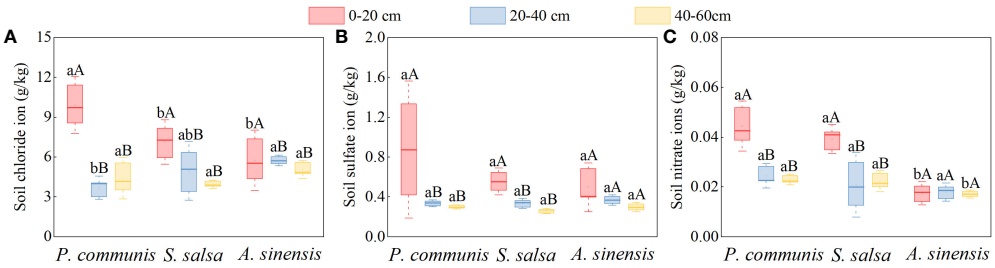

FIGURE 7
Cl- **(A)**, SO42- **(B)**, NO3- **(C)** anion content in soils of halophyte. Capital letters indicate the difference between different organs in the same halophyte, and lowercase letters donate the difference of different halophytes of the same organ ($P < 0.05$).

10.3389/fpls.2022.990246

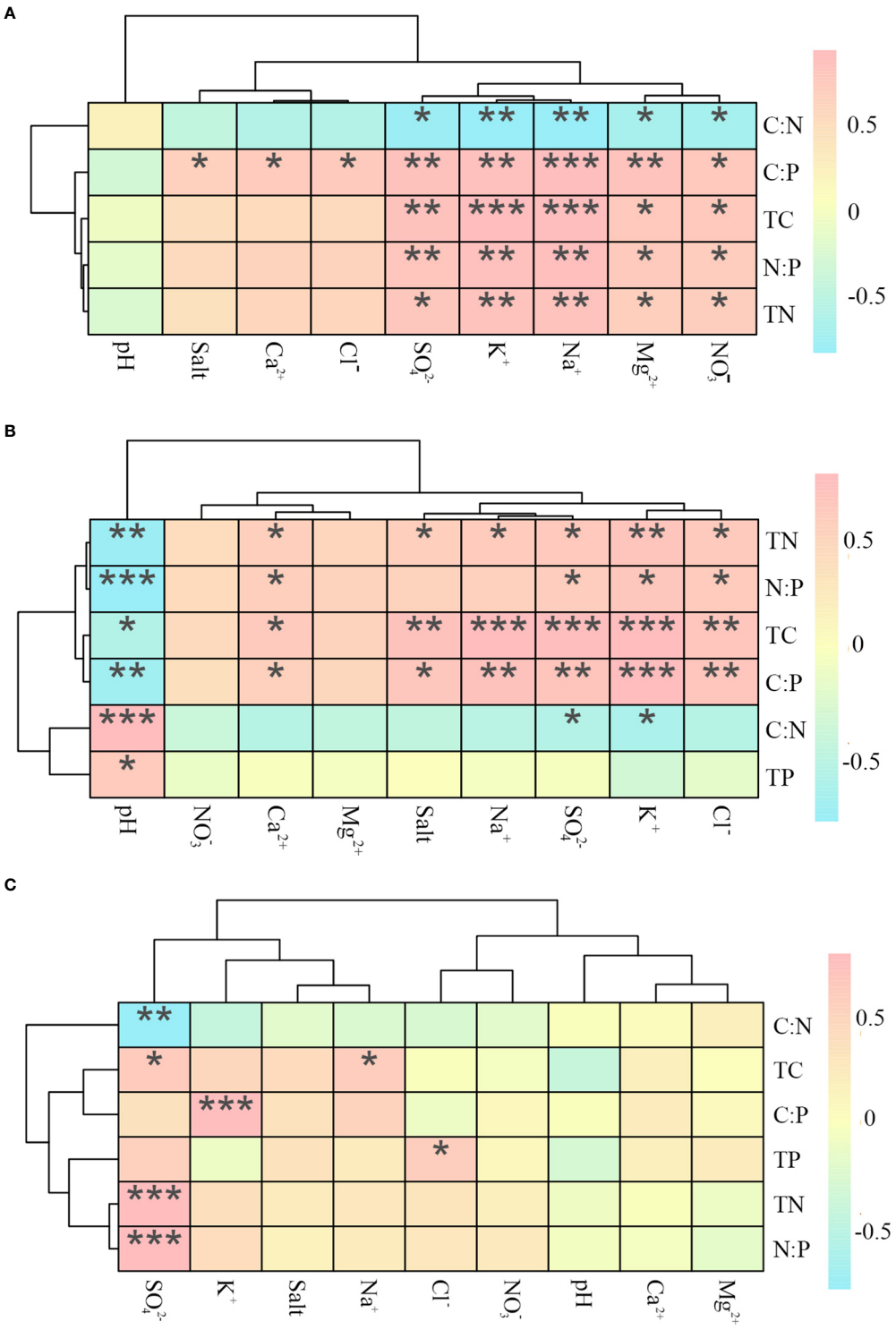

FIGURE 8
Heat map of correlations between ecological stoichiometry and ions in *P. communis* **(A)**, *S. salsa* **(B)** and *A. sinensis* **(C)**. *, ** and *** represent significant differences at 0.05, 0.01 and 0.001 levels respectively.

TABLE 1 Correlation between plant and soil ecological stoichiometry of three different halophytes.

Plant types		Soil TC	Soil TN	Soil TP	Soil C: N	Soil C: P	Soil N: P
P. communis	Plant TC	-0.92***	-0.85**	-0.48	0.85**	-0.83**	-0.83**
	Plant TN	-0.4	-0.23	-0.25	0.23	-0.17	-0.22
	Plant TP	-0.7*	-0.5	-0.62	0.50	-0.37	-0.48
	Plant C: N	0.4	0.23	0.25	-0.23	0.17	0.22
	Plant C: P	0.62	0.42	0.62	-0.42	0.28	0.40
	Plant N: P	-0.02	0.05	0.20	-0.05	-0.07	0.03
S. salsa	Plant TC	0.77*	0.83**	-0.07	-0.72*	0.75*	0.78*
	Plant TN	-0.92***	-0.87**	0.22	0.77*	-0.88**	-0.82**
	Plant TP	-0.7*	-0.52	-0.1	0.57	-0.62	-0.47
	Plant C: N	0.87**	0.92***	-0.25	-0.83**	0.87**	0.88**
	Plant C: P	0.7*	0.63	0	-0.7*	0.65	0.62
	Plant N: P	-0.73*	-0.75*	0.22	0.62	-0.7*	-0.7*
A.sinensis	Plant TC	-0.55	-0.37	0.18	0.4	-0.82**	-0.38
	Plant TN	-0.68*	-0.92***	-0.52	0.92***	-0.42	-0.88**
	Plant TP	-0.77*	-0.88**	-0.73*	0.78*	-0.43	-0.8**
	Plant C: N	0.28	0.62	0.52	-0.63	-0.18	0.57
	Plant C: P	0.23	0.48	0.92***	-0.32	-0.37	0.35
	Plant N: P	-0.38	-0.72*	-0.43	0.73*	-0.02	-0.7*

*, ** and *** showed significance at 0.05, 0.01 and 0.001 levels respectively.

3.3.2 Correlation between plant ecological stoichiometry and soil salinity factor

Compared to the correlations between the three halophytes' ecological stoichiometry and soil salt ion content (Table 2), it was found that the *P. communis* plants' TC content was negatively correlated with K^+, Na^+, SO_4^{2-}, and NO_3^-. *S. salsa* plant TC was positively correlated with soil K^+, Ca^{2+}, SO_4^{2-} and salinity; plant TN and TP were negatively correlated with the content of Ca^{2+}, Na^+, SO_4^{2-} and salinity. In addition, plant TN was positively correlated with soil pH and negatively correlated

TABLE 2 Correlation between organ ecological stoichiometry and soil salt ions in three halophytes.

Plant types		pH	salinity	K^+	Ca^{2+}	Na^+	Mg^{2+}	Cl^-	SO_4^{2-}	NO_3^-
P. communis	Plant TC	0.29	-0.52	-0.93***	-0.52	-0.87**	-0.62	-0.62	-0.95***	-0.88**
	Plant TN	0.08	-0.25	-0.47	0.3	-0.38	0.1	0.17	-0.43	-0.35
	Plant TP	0.03	-0.12	-0.65	0.02	-0.5	-0.08	-0.02	-0.5	-0.4
	Plant C: N	-0.08	0.25	0.47	-0.3	0.38	-0.1	-0.17	0.43	0.35
	Plant C: P	-0.08	0.15	0.58	-0.22	0.4	-0.08	-0.15	0.43	0.35
	Plant N: P	0.19	-0.53	-0.25	0.12	-0.25	-0.03	-0.03	-0.33	-0.32
S. salsa	Plant TC	-0.65	0.73*	0.77*	0.7*	0.67	0.53	0.67	0.82**	0.35
	Plant TN	0.75*	-0.78*	-0.93***	-0.78*	-0.78*	-0.6	-0.68	-0.9***	-0.58
	Plant TP	0.4	-0.78*	-0.6	-0.72*	-0.73*	-0.6	-0.68	-0.82**	-0.18
	Plant C: N	-0.78*	0.77*	0.88**	0.8**	0.75*	0.63	0.7*	0.88**	0.57
	Plant C: P	-0.53	0.8**	0.63	0.78*	0.73*	0.67	0.73*	0.85**	0.27
	Plant N: P	0.63	-0.5	-0.78*	-0.62	-0.53	-0.42	-0.37	-0.67	-0.72*
A.sinensis	Plant TC	-0.37	-0.45	-0.88**	-0.23	-0.65	-0.12	0.37	-0.25	0.22
	Plant TN	0.02	-0.27	-0.38	0.13	-0.33	0.23	-0.08	-0.8**	0.05
	Plant TP	0.08	-0.6	-0.47	-0.27	-0.63	-0.18	-0.3	-0.78*	0.08
	Plant C: N	-0.23	-0.07	-0.27	-0.43	-0.13	-0.45	0.08	0.53	-0.12
	Plant C: P	-0.32	0.33	-0.3	0.15	0.17	0.2	0.53	0.47	-0.05
	Plant N: P	0.18	0.13	0	0.45	0.1	0.57	0.02	-0.7*	-0.1

*, ** and *** showed significance at 0.05, 0.01 and 0.001 levels respectively.

with soil K^+ content; C: N and C: P were positively correlated with soil Ca^{2+}, Na^+, Cl^-, SO_4^{2-} and salinity, among them, C: N was also positively correlated with soil K^+ content, and negatively correlated with soil pH; N: P was negatively correlated with soil K^+, and NO_3^- content. In *A. sinensis*, the plant TC was negatively correlated with soil K^+; the plant TN and TP contents were negatively correlated with SO_4^{2-}.

3.4 Homeostasis characteristics of different types of halophytes

The analysis of the ecological stoichiometry homeostasis of different organs in different halophytes according to the four type intervals delineated by Persson et al. (2010) showed (Figure 9) that the C elements of *P. communis* and *A. sinensis* roots, stems, and leaves were stable, but the C elements of three nutrient organs in *S. salsa* were weakly sensitive; the N and P elements of *P. communis* roots were weakly sensitive, stems were sensitive and leaves were weakly stable, and the N and P elements of *S. salsa* roots, stems and leaves were sensitive, the N elements of *A. sinensis* roots were stable and P elements were weakly stable, the N and P elements of stems were weakly stable and leaves were weakly sensitive. Collectively, the homeostasis of C, N and P elements in three halophytes was: C > N > P.

C: N, C: P, and N: P of *P. communis* roots, stems, and leaves were sensitive; C: N and C: P of *S. salsa* roots and stems were sensitive, leaves were weakly sensitive, and N:P of three organs were sensitive; C: N of *A. sinensis* stems and leaves were sensitive, roots were weakly stable, and C: P of three organs were sensitive, N: P of roots and stems were weakly sensitive, and leaves were sensitive.

The fuzzy mathematics subordinate method was used to comprehensively evaluate the C, N, and P nutrient contents and the C: N, C: P, and N: P ecological stoichiometric indices of three halophytes (Table 3), and obtained three overall means of subordinate functions for halophytes. It was found that the total average values of *A. sinensis*, *P. communis*, and *S. salsa* were 0.75, 0.46, and 0.22, indicating that the salt secreting plant *A. sinensis* had the strongest homeostasis and the salt accumulating plant *S. salsa* had the weakest homeostasis.

4 Discussion

4.1 Salt tolerance characteristics of different halophytes

Relevant studies have found that halophytes adapt to long-term saline-alkali stress mainly by accumulating inorganic ions in the plant, and the salt ion content in the plant gradually increases during transport from the roots to the tip, forming a "salt island" effect (Yong et al., 2016). In our study, the distribution pattern of the total cation content of the salt repellent plant *P. communis* and the salt accumulating plant *S. salsa* was consistent with this, i.e., root < stem < leaf. However, the distribution of salt ion content in *A. sinensis* and their soils showed different patterns, presumably related to the unique salt tolerance strategy of salt secreting: salt glands or salt vesicles are generally present in salt secreting, which can absorb salt ions from the soil through the roots and excrete excess soluble salt ions through salt glands or salt vesicles (Fu et al., 2013), resulting in a high salt ion content in the roots and a low salt ion content in the soil.

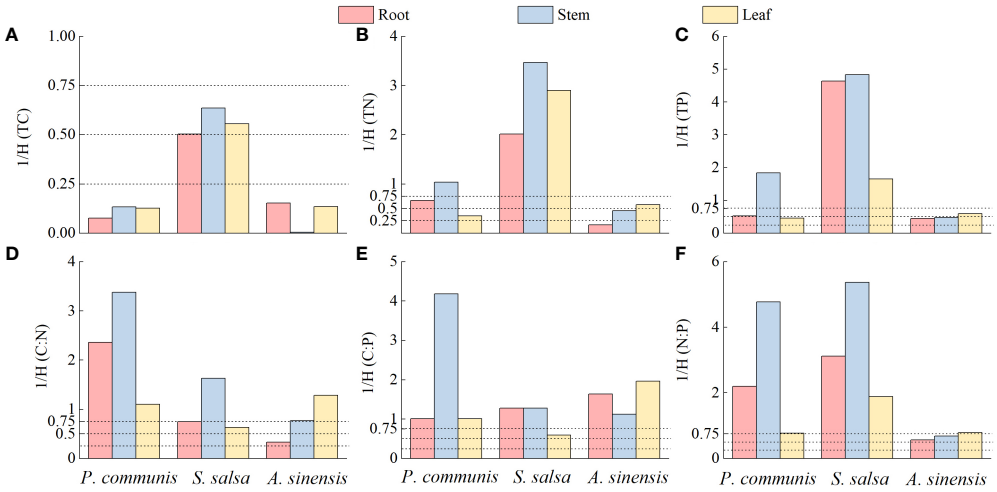

FIGURE 9
Ecological stoichiometric homeostasis indices of TC **(A)**, TN **(B)**, TP **(C)**, C:N **(D)**, C:P **(E)** and N:P **(F)** in three halophytes.

TABLE 3 Fuzzy mathematics subordinate value and homeostasis evaluation of three halophytes.

Halophyte	TC	TN	TP	C: N	C: P	N: P	Average	Rank
P. communis	0.68	0.51	0.68	0.05	0.47	0.37	0.46	2
S. salsa	0	0	0	0.56	0.76	0	0.22	3
A. sinensis	0.77	0.85	0.89	0.67	0.33	0.99	0.75	1

Na^+ is an important inorganic osmoregulatory substance, Parida and Das (2005) have pointed out that one of the mechanisms of salt tolerance in plants is to control the uptake of Na^+ by roots and reduce its translocation to the leaves. The results of this study showed that the salt repellent plant *P. communis* root will limit Na^+ transport to the ground, reduce its translocation to stems and leaves, translocate plant Na^+ to the soil, and balance the osmotic pressure in the plant by absorbing more K^+, fundamentally reducing the toxicity of salt ions to ensure *P. communis* growth in salt-stressed environments, which is consistent with the results of Peng et al. (2017). In addition, the cations in the *S. salsa* accumulated in the leaves of the plants and showed stronger uptake of Na^+ and Mg^{2+} than the other two halophytes. This is because *S. salsa* is a typical salt accumulating plant that can absorb salt from the soil to accumulate in its fleshy stems and leaves (Jia et al., 2021). The accumulation of Na^+ in *S. salsa* leaves is the main reason for leaf succulence, which in turn increases the number of cells in the plant, allowing more Na^+ to enter the vesicles, thereby reducing the osmotic stress caused by Na^+ to the plant, which is conducive to the survival of *S. salsa* in saline soil (Wang et al., 2001).

In the present study, the anion and cation contents of the soils of the salt repellent plant *P. communis* and the salt accumulating plant *S. salsa* were similar in vertical structure, i.e., the salt was concentrated in the top soil layer, in agreement with the view proposed by Su et al. (2022), which is because soil salts mainly originate from groundwater, and under the absorption and transpiration of plants, the salinity in the lower soil migrates to the upper layer, the salinity of the soil surface was higher (Ali et al., 2022). However, there are relatively few ionic species that differ in the vertical structure of the salt secreting plant *A. sinensis* soil, mainly K^+ and Cl^-, which differs from that of Zhang et al. (2016) for the salt secreting plant *T. chinensis*, and the reason for this phenomenon may be related to the depth of the root system of a halophyte, which needs to be further investigated.

4.2 Ecological stoichiometric characteristics of three halophyte organs

The C, N, and P contents in plant organs are one of the important indicators of the nutritional status of plants, which can reflect the adaptive defense responses to the external environment and the growth status of plants (Shi et al., 2021). In our study, we found that the three nutrient elements differed significantly among halophytes and in different organs of the same halophyte, and the results were consistent with the first hypothesis to some extent, which is keep up with the findings of Wen et al. (2021) on different vegetation types in semi-arid regions, Yang et al. (2019) on typical vegetation in temperate deserts, and Zeng et al. (2016) on different vegetation communities in the Loess Plateau. The main reason for this phenomenon is that the different N and P requirements of halophytes affect their photosynthetic and C allocation abilities, resulting in different nutrient contents and ratios among different halophytes (Zechmeister et al., 2015). However, the nutrient changes among roots, stems, and leaves of different types of halophytes showed consistency again during plant growth. For example, three different types of halophytes showed higher N and P contents in their leaves, which is consistent with most studies (Zhang et al., 2021a; Zhang et al., 2021b). On the one hand, this is because the sampling time is summer when the transpiration of leaves is vigorous, and the N and P absorbed by roots are transported upward to the leaves with water, resulting in the enrichment of N and P in the leaves. On the other hand, it is because the plants are in the growth period when the leaves are photosynthetically active and require large amounts of N and P elements to synthesize chlorophyll, proteins, and nucleic acids (Liu et al., 2015). In addition, the higher degree of root and stem fibrillation in all three halophytes resulted in significantly higher C: N values than their respective leaves, which is consistent with the findings of Shi et al. (2021).

Zeng et al. (2015) found that plant leaf C: N and C: P values were proportional to the nutrient use efficiency of plant N and P elements and inversely proportional to plant growth rate, it is clear that the growth rate of *S. salsa* among the three halophytes was relatively faster during this period. In addition, the N and P content of leaves were able to determine the plant nutrient limitation in that environment (Zhang et al., 2019), plant growth was limited by N elements when N: P < 14, by N and P elements when 14 < N: P < 16, and by P elements when N: P > 16. Therefore, the growth of *P. communis* and *S. salsa* is mainly limited by P, *A. sinensis* is limited by both N and P, which is consistent to some extent with the finding of Han et al. (Han et al., 2011) that P is the growth-limiting nutrient element for terrestrial plants in China, and the reason why salt plants are limited by P is mainly related to the availability of soil P. Because

the Yellow River delta region is subject to seawater erosion, the soil is heavily dominated by the calcium adsorbed form of P, which is more stable and difficult to be absorbed and used by plants (Bian et al., 2022).

4.3 Ecological stoichiometric characteristics of three halophytes in different soil layers

The nutrients required by plants to maintain their growth and development are mainly derived from the soil, therefore the soil texture condition has a great influence on plant growth and development. According to Dise et al. (1998), soil texture, nutrient supply capacity, and the decomposition and transformation of nutrient elements by soil microorganisms can be expressed by the stoichiometric characteristics of soil C, N, and P. In our study, the C and N contents of the surface soils of the three different types of halophytes differed from those of other soil layers, but there was no significant variation in P content, which is consistent with the results of Li et al. (2021). The higher C and N content of the soil surface layer is on the one hand due to the return of vegetation residues to the surface soil, high microbial activity, and rapid decomposition rate of dead fallen matter, therefore higher soil nutrient content; on the other hand, it is caused by the C and N reabsorption and transport of the lower soil by the plant roots (Wang and Zheng, 2018). Because the study area is virtually unaffected by anthropogenic tillage activities and because soil P content is mainly associated with the return of soil parent material and plant and animal residues, which are formed over a long period and are difficult to migrate in the soil, P content does not vary significantly in the soil profile (Bian et al., 2022).

Soil C: N values are inversely proportional to soil nutrient cycling rates, and higher C: N values are not conducive to soil organic matter mineralization decomposition and soil organic carbon accumulation (Haney et al., 2004). The present results indicate that the decomposition rate of organic matter is inversely proportional to soil depth, which is consistent with the results of Wang et al. (2021). In addition, soil C: P values were inversely related to soil P effectiveness. Compare to the analysis of soil C: P values in the three halophytes, it is clear that the surface soil P effectiveness of the three halophytes is lower, and the P effectiveness of *P. communis* and *S. salsa* surface soil was higher than that of *A. sinensis*. Plants grow more easily in lower N: P soils (Chen et al., 2009), indicating that deeper soils are more suitable for plant growth, which is because deeper soils are less affected by anthropogenic activities and climatic conditions. Also comparing the N: P values of the surface soil of the three halophytes shows that the *S. salsa* surface soil is more favorable for plant growth than the *P. communis* and *A. sinensis* surface soil. This suggests that the *S. salsa* plant community has certain advantages in improving the surface layer.

4.4 Interrelationship between ecological stoichiometric characteristics and salt ion content

Changes in nutrient elements within the organs of halophytes inevitably affect the transport processes of salt ions (Gupta et al., 2020), and studies have shown that the nutrient element content of halophyte soils can affect the N and P nutrient status within the halophytes, and to a certain extent, it affects the accumulation of total salt in halophytes (Wei et al., 2021). In our study, the interrelationship between ecological stoichiometric characteristics and salt ion content of the three halophytes did not show a consistent pattern, in line with the second hypothesis in the previous paper. The nutrient elements as well as stoichiometric ratios of salt repellent plant *P. communis* soil were mainly correlated with the plant TC content, based on the results of the study, it is clear that under suitable soil nutrient conditions, *P. communis* have enhanced photosynthesis and faster physiological metabolic processes, which promote more Na^+ excretion from plant organs and K^+ absorption from outside to balance osmotic pressure, while the faster metabolic rate of *P. communis* in turn reduces the content of various salt ions in the soil, creating soil conditions more suitable for *P. communis* growth and development.

Due to the different physiological strategies of salt tolerance developed in the process of adaptation to soil salinization in *S. salsa* and *P. communis*, the correlation between TC content and soil indicators in both showed opposite patterns. By analyzing the TN content of *S. salsa* with the salt ion content in the plants and the salt content in the soil, we found that N and salt ions in halophytes have a mutually reinforcing effect, which is consistent with the results of Yong et al. (2016) on the stoichiometry and salt ions of nutrient organs in four halophytes. In addition, it was found that the higher N content in *S. salsa* plants in soils with lower C and N nutrient content could more effectively promote the uptake of salt ions in the soil by halophytes, which is due to the higher NO_3^- storage capacity of *S. salsa* under low N conditions, it can better maintain N metabolism and photosynthetic performance in the plants (Liu et al., 2017), the results provide some theoretical basis for saline soil improvement.

Unlike *P. communis* and *S. salsa*, soil nutrients and stoichiometric ratios of the salt secreting plant, *A. sinensis*, had significant effects on TP content within *A. sinensis*, while no significant correlation existed between soil factors and plant TP content for both the salt repellent plant, *P. communis*, and the salt accumulating plant, *S. salsa*. The phenomenon suggests that *A. sinensis* improves the ability of this halophyte to adapt to external environmental conditions by accumulating more P elements in nutrient-depleted soils compared to *P. communis* and *S. salsa*.

4.5 Evaluation of plant homeostasis

Plants need to maintain relatively stable nutrient ratios (stoichiometric homeostasis) in their bodies for maintaining optimal plant growth levels (Spohn, 2016), and the level of plant stoichiometric homeostasis is influenced by factors such as uptake, transport, distribution, utilization, and release processes of chemical elements in halophyte (Sistla et al., 2015). In our study, the different organs' stoichiometric homeostasis of the three halophytes did not show a consistent pattern, which is consistent with the third hypothesis, but overall, the homeostasis of C, N, and P elements in halophytes was: C > N > P, which was consistent with the results of previous related studies that the homeostasis of massive elements in plants is higher than trace elements and trace elements are higher than non-essential elements (Han et al., 2011). It was found that plants with higher homeostasis were more conservative in nutrient use and could maintain slow growth in poor environments, while plants with lower homeostasis were more adaptable to external soil changes (Persson et al., 2010). A comprehensive evaluation of plant homeostasis through the fuzzy mathematics subordinate method of halophytes showed that *A. sinensis* had the most homeostasis and *S. salsa* had the least homeostasis, which indicated that *A. sinensis* was more adapted to grow in stable environments and *S. salsa* was more advantageous in variable environments compared to the three halophytes. It is speculated that in the future, as the environmental conditions of saline soils gradually improve, *S. salsa* can become the dominant species for saline soil improvement in the region, therefore, it is recommended to plant *S. Salsa* in areas where saline improvement is being carried out and *A. sinensis* in saline areas with more stable soil conditions. Overall, this study provides some theoretical basis for further discussion of ecological adaptation processes, nutrient allocation and utilization strategies, and plant stoichiometry homeostasis characteristics of halophytes in saline areas of the Yellow River Delta.

5 Conclusion

In this area, the salt ion content in the salt repelling plant *P. communis* and the salt accumulating plant *S. salsa* gradually increases during transport from the roots to the tip, forming a salt island effect, and the leaves of *S. salsa* show an extremely strong absorption capacity for Na^+. The N and P elements were enriched in the leaves of the three halophytes, and the C: N and C: P values of *P. communis* and *A. sinensis* leaves were significantly greater than those of *S. salsa*, indicating that the growth rate of *S. salsa* was relatively faster in this period. Based on the N: P values of the halophytes, it is clear that the growth of *P. communis* and *S. salsa* in this area is mainly limited by P, and that *A. sinensis* is limited by both N and P. The contents of C, N, C: P, and N: P in the surface soil (0-20 cm) of the three halophytes were significantly higher than those in the 20-40 cm and 40-60 cm soil layers, indicating that the deeper soils are more suitable for plant growth. The C:P was lower on the surface soil of *P. communis* and *S. salsa*, and N:P was lower in the surface soil of *S. salsa* than in *P. communis* and *A. sinensis*, indicating that the P effectiveness of the surface soil in *P. communis* and *S. salsa* was high, and the surface soil of *S. salsa* was more favorable for plant growth than in the surface soil of *P. communis* and *A. sinensis*. In contrast to *P. communis* and *S. salsa*, *A. sinensis* can improve the ability of halophytes to adapt to external environmental conditions by accumulating more P elements in nutrient-depleted soils. Compared to the three halophytes, *A. sinensis* is more adapted to a stable environment, while *S. salsa* is more advantageous in a variable environment.

Data availability statement

The original contributions presented in the study are included in the article/supplementary material. Further inquiries can be directed to the corresponding author.

Author contributions

YZ and TL analyzed the data and wrote the manuscript. JL performed the experiment, TL and JS designed the experiment. PZ participated in the sample plot survey. All authors contributed to the article and approved the submitted version.

Funding

The funding was supported by the National Natural Science Foundation of China (41871089, 41971119, and 42171059), the "Collection, Conservation, and Accurate Identification of Forest Tree Germplasm Resources" of Shandong Provincial Agricultural Elite Varieties Project (2019LZGC01805), the Natural Science Foundation of Shandong Province (ZR2019MD024, ZR2020QD004), and the Science and Technology Support Plan for Youth Innovation of Colleges and Universities (2019KJD010).

Conflict of interest

The authors declare that the research was conducted in the absence of any commercial or financial relationships that could be construed as a potential conflict of interest.

Publisher's note

References

Agren, G. (2004). The c: N: P stoichiometry of autotrophs: Theory and observation. *Ecol. Lett.* 7, 185–191. 00567. x. doi: 10.1111/j.1461-0248.2004.00567.x

Ali, S. D., Jalil, K., Elham, G. A., and Majid, H. (2022). Evaluating moisture distribution and salinity dynamics in sugarcane subsurface drip irrigation. *Water Sci. Eng.* 5 (17), 1–19. doi: 10.1007/s41101-022-00139-y

Bai, Y., Wu, J., Clark, C. M., Pan, Q., Zhang, L., Chen, S., et al. (2012). Grazing alters ecosystem functioning and c: N: P stoichiometry of grasslands along a regional precipitation gradient. *J. Appl. Ecol.* 49, 1204–1215. 02205. X. doi: 10.1111/j.1365-2664.2012.02205.x

Bao, S. D. (2000). *Soil agricultural chemistry analysis* (Beijing: Chinese agricultural press).

Bian, F. H., Wu, Q. T., Wu, M. D., Guan, B., Yu, J. B., and Han, G. X. (2022). C: N: P stoichiometry in plants and soils of *Phragmites australis* wetland under different water-salt habitats. *J. Appl. Ecol.* 33 (02), 385–396. doi: 10.13287/j.1001-9332.202202.040

Chen, K. H., Yin, H. X., Liu, J. Y., Wang, W., Gong, B. Q., Mei, H. M., et al. (2009). The dynamics of soil total nitrogen content of different vegetation types on alpine kobersia meadow. *Energy Environ. Sci.* 18 (06), 2321–2325. doi: 10.16258/j.cnki.1674-5906.2009.06.065

Dise, N. B., Matzner, E., and Forsius, M. (1998). Evaluation of organic horizon c: N ratio as an indicator of nitrate leaching in conifer forests across Europe. *Environ. pollut.* 102, 453–456. doi: 10.1016/B978-0-08-043201-4.50066-6

Elser, J. J., Fagan, W. F., Denno, R. F., Dobberfuhl, D. R., Folarin, A., Huberty, A., et al. (2000). Nutritional constraints in terrestrial and freshwater food webs. *Nature* 408, 578–580. doi: 10.1038/35046058

Fu, C., Sun, Y. G., and Fu, G. R. (2013). Advances of salt tolerance mechanism in hylophyate plants. *Biol. Bull.* 29 (1), 1–7. 026. doi: 10.13560/j.cnki.biotech.bull.1985.2013.01.026

Gupta, S., Schillaci, M., Walker, R., Smith, P. M. C., Watt, M., and Roessner, U. (2020). Alleviation of salinity stress in plants by endophytic plant-fungal symbiosis: Current knowledge, perspectives and future directions. *Plant Soil* 461, 219–244. doi: 10.1007/s11104-020-04618-w

Haney, R. L., Franzluebbers, A. J., Porter, E. B., Hons, F. M., and Zuberer, D. A. (2004). Soil carbon and nitrogen mineralization. *Soil Sci. Soc Am. J.* 68 (2), 489–492. doi: 10.2136/sssaj2004.4890

Han, W. X., Fang, J. Y., Reich, P. B., Woodward, F. I., and Wang, Z. H. (2011). Biogeography and variability of eleven mineral elements in plant leaves across gradients of climate, soil and plant functional type in China. *Ecol. Lett.* 14 (8), 788–796. 01641. x. doi: 10.1111/j.1461-0248.2011.01641.x

Hood, J. M., and Sterner, R. (2010). Diet mixing: Do animals in-tegrate growth or resources across temporal heterogeneity? *Am. Nat.* 176 (5), 651–663. doi: 10.1111/fwb.13956

Hu, Y. F., Shu, X. Y., He, J., Zhang, Y. L., Xiao, H. H., Tang, X. Y., et al. (2018). Storage of c, n and p affected by afforestation with *Salix cupularis* in an alpine semi-arid desert ecosystem. *Land. Degrad. Dev.* 29, 188–198. doi: 10.1002/ldr.2862

Jia, L., Liu, L. Y., Wang, P. S., Li, Z. M., Zhang, J. L., Tian, X. M., et al. (2021). Salt-tolerance and soil improvement mechanism of *Suaeda salsa*: Research progress. *Chin. Ag. Sci. Bull.* 37 (3), 73–80. doi: 10.11924/j.issn.1000-6850.casb20191200947

Jordi, S., Albert, R. U., and Josep, P. (2012). The elemental stoichiometry of aquatic and terrestrial ecosystems and its relationships with organismic lifestyle and ecosystem structure and function: a review and perspectives. *Biogeochemistry* 111 (1-3), 1–39. doi: 10.1007/s10533-011-9640-9

Koerselman, W., and Meuleman, A. F. M. (1996). The vegetation n: P ratio: a new tool to detect the nature of nutrient limitation. *J. Appl. Ecol.* 33 (6), 1441–1450. doi: 10.2307/2404783

Koojiman, S. A. L. M. (1995). The stoichiometry of animal energetics. *J. Theor. Biol.* 177 (2), 139–149.

Lareen, A., Burton, F., and Schafer, P. (2016). Plant root-microbe communication in shaping root microbiomes. *Plant Mol. Biol.* 90 (6), 575–587. doi: 10.1007/s11103-015-0417-8

Lau, J. A., and Lennon, J. T. (2012). Rapid responses of soil microorganisms improve plant fitness in novel environments. *PNAS* 109 (35), 14058–14062. doi: 10.1073/pnas.1202319109

Li, T., Sun, J. K., and Fu, Z. Y. (2021). Halophytes differ in their adaptation to soil environment in the yellow river delta: Effects of water source, soil depth, and nutrient stoichiometry. *Front. Plant Sci.* 12, 675921. doi: 10.3389/fpls.2021.675921

Liu, R. R., Shi, W. W., Zhang, X. D., and Song, J. (2017). Effects of nitrogen starvation on suaeda salsa from different habitats. *Acta Ecologica Sin.* 37 (06), 1881–1887. doi: 10.5846/stxb201511052251

Liu, W. D., Su, J. R., Li, S. F., Lang, X. D., Zhang, Z. J., and Huang, X. B. (2015). Leaf carbon, nitrogen and phosphorus stoichiometry at different growth stages in dominant tree species of a monsoon broad-leaved evergreen forest in pu'er, yunnan province, China. *Chin. J. Plant Ecol.* 39 (1), 52–62. doi: 10.17521/cjpe.2015.0006

Liu, R., Zhao, H., Zhao, X., and Drake, S. (2011). Facilitative effects of shrubs in shifting sand on soil macro-faunal community in horqin sand land of inner Mongolia, northern China. *Eur. J. Soil Biol.* 47, 316–321. doi: 10.1016/j.ejsobi.2011.07.006

Parida, A. K., and Das, A. B. (2005). Salt tolerance and salinity effects on plants: a review. *Ecotoxicol. Environ. Saf.* 60 (3), 324–349. doi: 10.1016/j.ecoenv.2004.06.010

Peng, Z., He, S. P., Gong, W. F., Pan, Y. E., Jia, Y. H., Lu, Y. L., et al. (2017). Transcriptome analysis of transcription factors in upland cotton seedlings under NaCl stress. *Acta Agronomica Sin.* 43 (3), 354–370. doi: 10.3724/SP.J.1006.2017.00354

Persson, J., Fink, P., and Goto, A. (2010). To be or not to be what you eat: Regulation of stoichiometric homeostasis among autotrophs and heterotrophs. *Oikos* 119, 741–751. 18545. x. doi: 10.1111/j.1600-0706.2009.18545.x

Schade, J. D., Kyle, M., Hobbie, S. E., Fagan, W. F., and Elser, J. J. (2003). Stoichiometric tracking of soil nutrients by a desert insect herbivore. *Ecol. Lett.* 6, 96–101. 00409. x. doi: 10.1046/j.1461-0248.2003.00409.x

Schreeg, L. A., Santiago, L. S., Wright, S. J., and Turner, B. L. (2014). Stem, root, and older leaf n: P ratios are more responsive indicators of soil nutrient availability than new foliage. *Ecology* 95, 2062–2068. doi: 10.1890/13-1671.1

Shi, L. J., Li, Q. K., Fu, X. L., Kou, L., Dai, X. Q., and Wang, H. M. (2021). Foliar, root and rhizospheric soil c: N: P stoichiometries of overstory and understory species in subtropical plantations. *Catena* 198, 105020. doi: 10.1016/j.catena.2020.105020

Sistla, S. A., Appling, A. P., Lewandowska, A. M., Taylor, B. N., and Wolf, A. A. (2015). Stoichiometric flexibility in response to fertilization along gradients of environmental and organismal nutrient richness. *Oikos* 124 (7), 949–959. doi: 10.1111/oik.02385

Spohn, M. (2016). Element cycling as driven by stoichiometric homeostasis of soil microorganisms. *Basic. Appl. Ecol.* 17, 471–478. doi: 10.1016/j.baae.2016.05.003

Sterner, R. W., and Elser, J. J. (2002). Ecological stoichiometry: The biology of elements from molecules to the biosphere. *J. Plankton Res.* 25 (9), 1183. doi: 10.1038/35046058

Sun, J. K., Zhang, W. H., Zhang, J. M., Liu, B. Y., and Liu, X. C. (2006). Response to droughty stresses and drought-resistances evaluation of four species during seed germination. *Acta Botanica Boreali-Occidentalia Sin.* 9, 1811–1818. doi: 1000-4025.2006.09-1811-08

Su, F. M., Wu, J. H., Wang, D., Zhao, H. H., Wang, Y. H., and He, X. D. (2022). Moisture movement, soil salt migration, and nitrogen transformation under different irrigation conditions: Field experimental research. *Chemosphere* 300, 134569. doi: 10.1016/j.chemosphere.2022.134569

Tilman, D. (2004). Niche trade-offs, neutrality, and community structure: a stochastic theory of resource competition, invasion, and community assembly. *PNAS* 101, 10854–10861. doi: 10.1073/pnas.0403458101

Wang, Z. C., He, G. X., Hou, Z. H., Luo, Z., Chen, S. X., Jia, Z., et al. (2021). Soil c: N: P stoichiometry of typical coniferous (*Cunninghamia lanceolata*) and/or evergreen broadleaved (*Phoebe bournei*) plantations in south China. *For. Ecol. Manage.* 486, 118974. doi: 10.1016/j.foreco.2021.118974

Wang, B., Luttge, U., and Ratajczak, R. (2001). Effects of salt treatment and osmotic stress on V-ATPase and V-PPase in leaves of the halophyte. *Suaeda salsa*. *J. Exp. Bot.* 52 (365), 2355–2365. doi: 10.1093/jexbot/52.365.2355

Wang, K. B., Shao, R. X., and Shangguan, Z. P. (2010). Changes in species richness and community productivity during succession on the loess plateau of China. *Pol. J. Ecol.* 58 (3), 549–558. doi: 10.1016/j.polar.2009.11.001

Wang, Z. F., and Zheng, F. L. (2018). C, n, and p stoichiometric characteristics of *Pinus tabulaeformis* plantation in the ziwuling region of the loess plateau. *Acta Ecologica Sin.* 38 (19), 6870–6880. doi: 10.5846/stxb201705090856

Wei, Y. J., Dang, X. H., Wang, J., Zhang, K. H., Gao, Y., and Li, S. Z. (2021). Characterization of the soil ecological stoichiometry of *Nitraria tangutorun* nebkhas during different succession stages. *J. Soil. Water. Conserv.* 35 (2), 377–384. doi: 10.13870/j.cnki.stbcxb.2021.02.050

Wen, C., Yang, Z. J., Yang, L., Li, Z. S., Wei, W., and Zhang, Q. D. (2021). Ecological stoichiometry characteristics of plants and soil under different vegetation types in the semi-arid loess small watershed. *Acta Ecologica Sin.* 41 (5), 1824–1834. doi: 10.5846/stxb202004301056

Xu, Z., Mi, W., Mi, N., Fan, X. G., Zhou, Y., and Tian, Y. (2021). Comprehensive evaluation of soil quality in a desert steppe influenced by industrial activities in northern China. *Sci. Rep.* 11, 17493. doi: 10.1038/s41598-021-96948-7

Yang, Y., Liu, B. R., and An, S. S. (2018). Ecological stoichiometry in leaves, roots, litters and soil among different plant communities in a desertified region of northern China. *Catena* 166, 328–338. doi: 10.1016/j.catena.2018.04.018

Yang, H. T., Wang, Z. R., Li, X. J., and Gao, Y. H. (2019). Vegetation restoration drives the dynamics and distribution of nitrogen and phosphorous pools in a temperate desert soil-plant system. *J. Environ. Manage.* 245 (1), 200–209. doi: 10.1016/j.jenvman.2019.04.08

Yong, Y. H., Zhang, X., Wang, S. M., and Wu, L. (2016). Salt accumulation in vegetative organs and ecological stoichiometry characteristics in typical halophytes in xinjiang, China. *Chin. J. Plant Ecol.* 40 (12), 1267–1275. doi: 10.1016/j.catena.2018.04.018

Zechmeister, S., Keiblinger, K. M., Mooshammer, M., Richter, A., Sardans, J., and Wanek, W. (2015). The application of ecological stoichiometry to plant-microbial-soil organic matter transformations. *Ecol. Monogr.* 85, 133–155. doi: 10.1890/14-0777.1

Zeng, Q. C., Li, X., Dong, Y. H., An, S. S., and Darboux, F. (2016). Soil and plant components ecological stoichiometry in four steppe communities in the loess plateau of China. *Catena* 147, 481–488. doi: 10.1016/j.catena.2016.07.047

Zeng, Z. X., Wang, K. L., Liu, X. L., Zeng, F. P., Song, T. Q., Peng, W. X., et al. (2015). Stoichiometric characteristics of plants, litter and soils in karst plant communities of Northwest guangxi. *Chin. J. Plant Ecol.* 39 (7), 682–693. doi: 10.17521/cjpe.2015.0065

Zhang, L. H., Chen, P. H., Li, J., Chen, X. B., and Feng, Y. (2016). Distribution of soil salt ions around *Tamarix chinensis* individuals in the yellow river delta. *Acta Ecologica Sin.* 36 (18), 5741–5749. doi: 10.5846/stxb201504230839

Zhang, Y. L., Dong, C., Yang, Y. H., and Liu, H. J. (2021b). Ecological stoichiometric characteristics and influencing factors of carbon, nitrogen, and phosphorus in the leaves of *Sophora alopecuroides* l. in the yili river valley, xinjiang. *PeerJ* 9 (1), e11701. doi: 10.7717/peerj.11701

Zhang, W., Liu, W. C., Xu, M. P., Deng, J., Han, X. H., Yang, G. H., et al. (2019). Response of forest growth to c: N: P stoichiometry in plants and soils during *Robinia pseudoacacia* afforestation on the loess plateau, China. *Geoderma* 337 (1), 280–289. doi: 10.1016/j.geoderma.2018.09.042

Zhang, J., Xie, H. J., Biswas, S. A. Y., Qi, X. X., and Cao, J. J. (2021a). Response of different organs' stoichiometry of phragmites australis to soil salinity in arid marshes, China. *Glob. Ecol. Conserv.* 31, e01843. doi: 10.1016/j.gecco.2021.e01843

Zhao, Y. H., Li, T., Shao, P. S., Sun, J. K., Xu, W. J., and Zhang, Z. H. (2022). Variation in bacterial community structure in rhizosphere and bulk soils of different halophytes in the yellow river delta. *Front. Ecol. Evol.* 9, 816918. doi: 10.3389/fevo.2021.816918

frontiers | Frontiers in Plant Science

TYPE Original Research
PUBLISHED 19 October 2022
DOI 10.3389/fpls.2022.1013812

OPEN ACCESS

EDITED BY
Bing Song,
Ludong University, China

REVIEWED BY
Chunhui Zhang,
Qinghai University, China
Yanfu Bai,
Sichuan Agricultural University, China

*CORRESPONDENCE
Huidan He
hehuidan321@163.com
Fawei Zhang
mywing963@126.com

SPECIALTY SECTION
This article was submitted to Functional Plant Ecology, a section of the journal Frontiers in Plant Science

RECEIVED 07 August 2022
ACCEPTED 04 October 2022
PUBLISHED 19 October 2022

CITATION
Zhu J, Li H, He H, Zhang F, Yang Y and Li Y (2022) Interannual characteristics and driving mechanism of CO_2 fluxes during the growing season in an alpine wetland ecosystem at the southern foot of the Qilian Mountains. *Front. Plant Sci.* 13:1013812. doi: 10.3389/fpls.2022.1013812

Interannual characteristics and driving mechanism of CO_2 fluxes during the growing season in an alpine wetland ecosystem at the southern foot of the Qilian Mountains

Jingbin Zhu[1,2], Hongqin Li[3], Huidan He[1,2*], Fawei Zhang[2*], Yongsheng Yang[2] and Yingnian Li[2]

[1]College of Tourism, Resources and Environment, Zaozhuang University, Zaozhuang, China, [2]Key Laboratory of Adaptation and Evolution of Plateau Biota, Northwest Institute of Plateau Biology, Chinese Academy of Sciences, Xining, China, [3]College of Life Sciences, Luoyang Normal University, Luoyang, China

The carbon process of the alpine ecosystem is complex and sensitive in the face of continuous global warming. However, the long-term dynamics of carbon budget and its driving mechanism of alpine ecosystem remain unclear. Using the eddy covariance (EC) technique—a fast and direct method of measuring carbon dioxide (CO_2) fluxes, we analyzed the dynamics of CO_2 fluxes and their driving mechanism in an alpine wetland in the northeastern Qinghai–Tibet Plateau (QTP) during the growing season (May–September) from 2004–2016. The results show that the monthly gross primary productivity (GPP) and ecosystem respiration (Re) showed a unimodal pattern, and the monthly net ecosystem CO_2 exchange (NEE) showed a V-shaped trend. With the alpine wetland ecosystem being a carbon sink during the growing season, that is, a reservoir that absorbs more atmospheric carbon than it releases, the annual NEE, GPP, and Re reached −67.5 ± 10.2, 473.4 ± 19.1, and 405.9 ± 8.9 gCm^{-2}, respectively. At the monthly scale, the classification and regression tree (CART) analysis revealed air temperature (Ta) to be the main determinant of variations in the monthly NEE and GPP. Soil temperature (Ts) largely determined the changes in the monthly Re. The linear regression analysis confirmed that thermal conditions (Ta, Ts) were crucial determinants of the dynamics of monthly CO_2 fluxes during the growing season. At the interannual scale, the variations of CO_2 fluxes were affected mainly by precipitation and thermal conditions. The annual GPP and Re were positively correlated with Ta and Ts, and were negatively correlated with precipitation. However, hydrothermal conditions (Ta, Ts, and precipitation) had no significant effect on annual NEE. Our results indicated that climate warming would be beneficial to the

improvement of GPP and Re in the alpine wetland, while the increase of precipitation can weaken this effect.

KEYWORDS

Alpine wetland, CO_2 fluxes, growing season, driving mechanism, Qinghai–Tibetan plateau

Introduction

Global climate change is predicted to have a substantial influence on the stability of the grassland ecosystem, an ecosystem whose vegetation is dominated by grasses (Piao et al., 2012; Chai et al., 2019; Chen et al., 2021a). The carbon process of the alpine grassland ecosystem is extremely sensitive to and complex in the face of continuous global warming (Shen et al., 2015; Wang et al., 2017). Because the soil of the alpine ecosystem contains a substantial amount of thatch, or undecomposed organic matter, it is particularly vulnerable to changes in the global climate (Shen et al., 2022). Although high-altitude grassland ecosystems have attracted more attention recently, studies on carbon processes based on long-term data have still been lacking (Li et al., 2021).

The unique environmental conditions in the alpine grassland, namely, its high altitude, low temperature, and strong radiation, aid in the carbon fixation of vegetation, whereby vegetation converts inorganic carbon into organic compounds (Shen et al., 2022). However, the differences between biotic and abiotic factors still significantly impacted carbon source/sink dynamics, which will increase the uncertainty of predicting the carbon balance dynamics of the alpine grassland under the background of climate change in the future (Chai et al., 2017). Studies have shown that increases in the temperature and CO_2 concentration improve the photosynthetic production capacity of vegetation, referring to the rate at which vegetation can fix carbon during photosynthesis, in alpine grassland ecosystems (Shen et al., 2015; Kang et al., 2022). However, temperature increases also stimulate the decomposition of soil organic matter and enzymatic activities of microorganisms, thus promoting the release of soil carbon (Li et al., 2019). Furthermore, the temperature increase leads to an increase in soil water evaporation, which worsens drought stress on vegetation and can thus lead to a decrease in the amount of CO_2 fixed by vegetation through photosynthesis (Baldocchi et al., 2021). The balance between these opposing biological and metabolic processes determines the feedback effect of the alpine ecosystem on the climate environment; thus, the influence of climate change on the source/sink dynamics of alpine ecosystems in the QTP is still unclear (Chen et al., 2021a).

Studies have shown that CO_2 fluxes in alpine ecosystems are mainly controlled by the dynamics of carbon balance in the growing season (Chai et al., 2017; Chai et al., 2019). In the context of global climate change, the rise of temperature is expected to promote snow melt and vegetation greening earlier, thus prolonging the length of the growing season (Groendahl et al., 2007; Street et al., 2007; Shen et al., 2022). Wetland ecosystems are fragile and play an important role in the carbon cycle of global terrestrial ecosystems (Temmink et al., 2022; Zhang et al., 2022). The wetland in QTP occupies 33% of China's wetland area (Zheng et al., 2013; Kang et al., 2022). Furthermore, permafrost thawing and glacier retreat may create larger or new wetlands on the QTP (Kang et al., 2014; Shen et al., 2022). Climatic and environmental factors at different time scales may have different impacts on the carbon cycle (Saito et al., 2009; Zhu et al., 2015; Zhu et al., 2020). However, previous studies on the carbon cycle of alpine ecosystems have been conducted over short periods; hence, how the carbon balance in the alpine wetland ecosystem responds over the long term to climate change remains unclear (Li et al., 2021). Hence, in this work, we analyze continuous data of 13 years, measured by the eddy covariance (EC) technique in an alpine wetland of the northeastern QTP. This study aimed to measure the interannual variation of CO_2 fluxes in alpine wetland ecosystems and clarify the driving mechanisms of major environmental factors so as to provide a theoretical basis for predicting the carbon budget of alpine wetland ecosystems amidst climate change in the future.

Materials and methods

Study area

The study site was located at the southern foot of the Qilian Mountains (37°35′N, 101°20′E, 3250 m a.s.l.). The region mainly has a plateau continental monsoon climate. Previous monitoring data found the annual average temperature to be −1.1°C, and the average minimum (−18.3°C) and maximum (12.6°C)

temperature were recorded in January and July, respectively. The mean annual precipitation was approximately 490 mm, and precipitation in the growing period accounted for over 80% of the total annual precipitation. The study area soil is a silty clay loam of Mat-Cryic Cambisols, which is rich in organic matter. *Carex pamirensis* is the alpine wetland's constructive species. Many mounds are scattered across the study site, owing to the seasonal freeze–thaw process (Song et al., 2015; Wang et al., 2017).

Flux and abiotic measurements

The EC sensor array comprised a three-dimensional (3D) ultrasound anemometer (CSAT3, Campbell, Scientific Inc., Logan, UT, USA) and an open-path infrared CO_2/H_2O analyzer (Li7500, Li-cor Inc., Lincoln, Nebraska, USA). The raw data is recorded by the data collector at a frequency of 10 Hz. A data logger (CR5000, Campbell Scientific Inc.) was used to calculate and log the mean, variance, and covariance values of the raw data every 30 min. The growing season is from May to September (Zhang et al., 2008).

Data processing

We applied the flux data processing method from ChinaFLUX (Yu et al., 2008; Fu et al., 2009). We obtained the daily GPP by subtracting the net ecosystem CO_2 exchange (NEE) from the ecosystem respiration (Re) (Equation (1)); daily Re was the sum of nocturnal respiration (Re_n) and daytime respiration (Re_d), which was extrapolated from the exponential regressions of Re_n with nighttime soil temperature to the daytime periods (Yu et al., 2008).

$$GPP = Re - NEE = (Re_d + Re_n) - NEE \quad (1)$$

Statistical analysis

The classification and regression tree (CART) is used to determine which environmental factors—such as air temperature (Ta), soil temperature in 5cm depth (Ts), photosynthetic photon flux density (PPFD), precipitation (PPT), air relative humidity (RH), and vapor pressure deficit (VPD)—function in a major controlling manner in variations in CO_2 fluxes. We used SYSTAT 13.0 (Systat Software Inc, USA) for the CART and linear regression analyses.

Results

Variation characteristics of climatic factors

The average monthly Ta, Ts, VPD, and PPT showed a unimodal trend, but the peak did not occur in consistent months (Figure 1). The peak values of monthly Ta, PPT, and VPD occurred in July, but the maximum value of monthly Ts occurred in August (Figure 1). Only at the beginning of the growing season (May, June), monthly Ts was higher than Ta (Figure 1A). The mean values of annual Ta, Ts, and PPT in the growing season were 7.5 ± 1.0, 9.5 ± 1.2°C, and 418.2 ± 34.0 mm, respectively. Monthly PPFD and RH showed the opposite trend: Monthly PPFD gradually decreased, and monthly RH gradually increased in the growing season (Figures 1B, C).

Variation characteristics of CO_2 fluxes

The average monthly GPP and Re showed a unimodal trend (Figure 2). The peak of the monthly GPP (164.2 ± 15.1gCm^{-2}month^{-1}) occurred in July, but the maximum of the monthly Re (107.0 ± 16.9 gCm^{-2}month^{-1}) occurred in August.

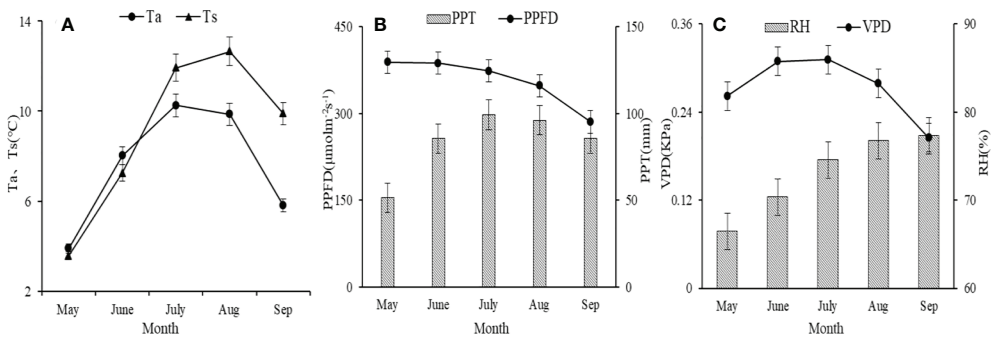

FIGURE 1
The average value of monthly air temperature (Ta) (± its standard deviation) and soil temperature (Ts) **(A)**; photosynthetic photon flux density (PPFD) and precipitation (PPT) **(B)**; vapor pressure deficit (VPD) and air relative humidity (RH) **(C)**.

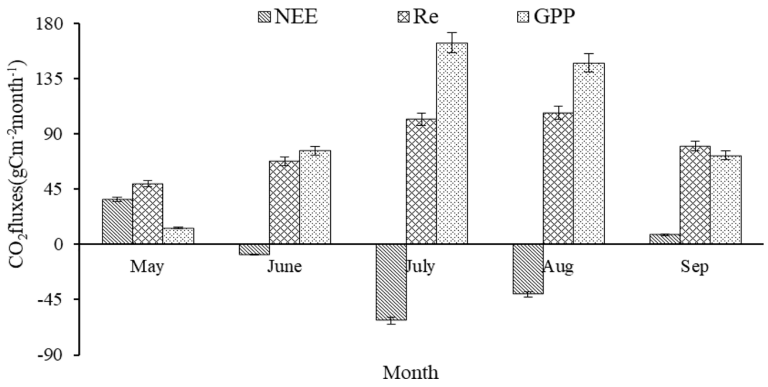

FIGURE 2
The average value of monthly CO_2 fluxes ($gCm^{-2}month^{-1}$) of alpine wetland in the growing season for the period 2004-2016.

The monthly NEE showed a V-shaped trend, and the minimum of the monthly NEE (-62.2 ± 9.5$gCm^{-2}month^{-1}$) appeared in July. Only in May of the growing season, when the NEE was positive, did the alpine wetland act as a carbon source (Figure 2). In addition, the monthly NEE was negatively correlated with both monthly GPP and monthly Re (P<0.001) (Figures 3A, B), while the monthly GPP was positively correlated with monthly Re (P<0.001) (Figure 3C). Compared with monthly Re (R^2 = 0.40), the monthly GPP (R^2 = 0.87) has a stronger control effect on the monthly NEE during the growing season (Figures 3A, B).

The mean values of annual GPP and Re in the growing season of alpine wetland from 2004 to 2016 were 473.4 ± 19.1 gCm^{-2} and 405.9 ± 8.9 gCm^{-2}, respectively (Figure 4). The mean annual NEE of the alpine wetland in the growing season was −67.5 ± 10.2 gCm^{-2} (Figure 4), which represented a carbon sink, with the maximum and minimum values of −22.6 gCm^{-2} (2011) and −105.4 gCm^{-2} (2007), respectively. Linear regression analysis showed that annual GPP was positively correlated with Re (P<0.001), and annual NEE was positively correlated with Re (P=0.003), but NEE was not significantly correlated with GPP (P=0.158). Therefore, annual Re might be more important than GPP for the dominant role of NEE at the interannual scale.

Effects of climatic factors on CO_2 fluxes at the monthly scale

The CART analysis results reveal that Ta and Ts were the main controlling factors of the monthly GPP and Re, respectively (Figures 5A, B). Ta could explain 92.8% of the

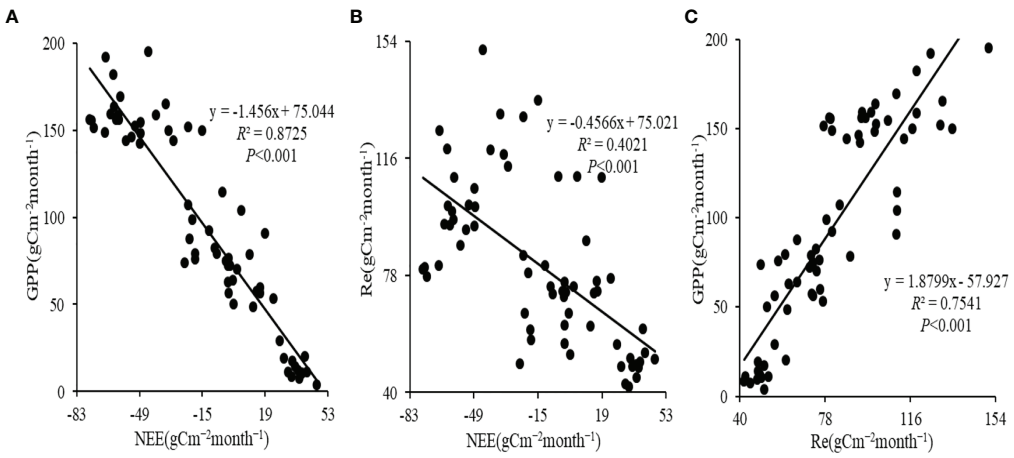

FIGURE 3
Linear regressions between monthly GPP and NEE **(A)**, linear regressions between monthly Re and NEE **(B)**, and linear regressions between monthly GPP and Re **(C)** of alpine wetland in the growing season for the period 2004-2016.

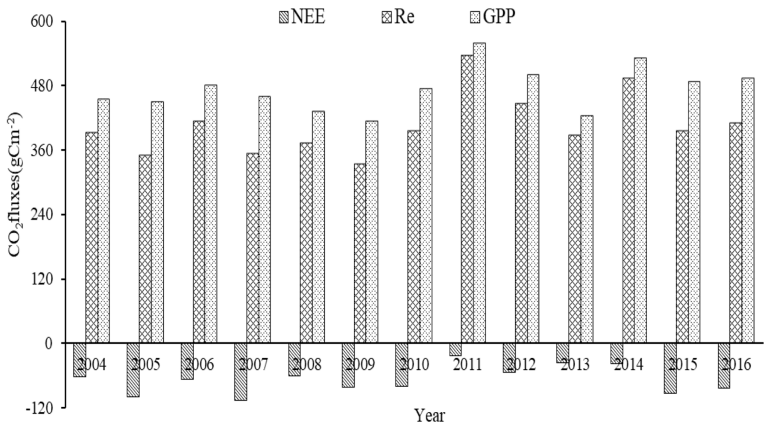

FIGURE 4
The annual CO_2 fluxes of alpine wetland in the growing season for the period 2004-2016.

variation in the monthly GPP (Figure 5A), and Ts could explain 88.1% of the variation in the monthly Re (Figure 5B). The results of CART reveal that Ta was the dominant factor of monthly NEE, and Ta could explain 90.1% of the variation in the monthly NEE (Figure 5C). Linear regression analysis also showed that thermal conditions (Ta, Ts) were the main controlling factors of monthly CO_2 fluxes (Table 1). In sum, Ta had a major impact on the change in the monthly GPP and NEE, and Ts was the main

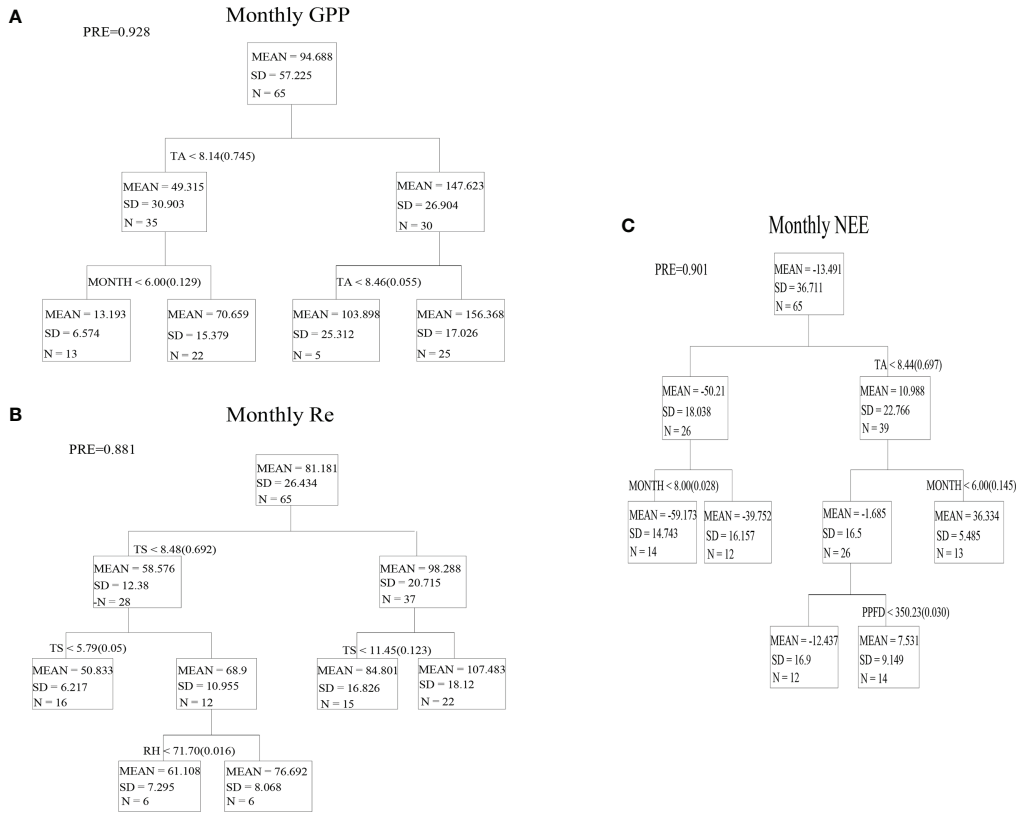

FIGURE 5
Regression trees for monthly GPP **(A)**, Re **(B)** and NEE **(C)** from environmental variables of alpine wetland in the growing season (May-September).

TABLE 1 Linear regressions between monthly CO_2 fluxes and environmental variables of alpine wetland in the growing season (May-September).

Month	GPP Linear Equation	R^2	*P*	Re Linear Equation	R^2	*P*	NEE Linear Equation	R^2	*P*
Ta(x_1)	$y = 19.86x_1$-54.55	0.80	0.000	$y = 7.27x_1 + 26.53$	0.50	0.000	$y = -12.60x_1$+81.16	0.78	0.000
RH(x_2)	$y = 7.14x_2$-427.1	0.37	0.000	$y = 3.34x_2 - 163.12$	0.38	0.000	$y = -3.81x_2$+264.54	0.26	0.000
PPFD(x_3)	$y = -0.15x_3$+149.06	0.02	0.313	$y = -0.17x_3 + 142.93$	0.10	0.011	$y = -0.02x_3$-6.27	0.00	0.835
Ts(x_4)	$y = 12.69x_4$-19.76	0.70	0.000	$y = 5.93x_4 + 27.69$	0.72	0.000	$y = -6.77x_4$+47.53	0.48	0.000
PPT(x_5)	$y = 1.25x_5$-9.72	0.35	0.000	$y = 0.48x_5$+41.25	0.24	0.000	$y = -0.77x_5$+51.03	0.32	0.000
VPD(x_6)	$y = 403.57x_6$-15.77	0.12	0.005	$y = 89.52x_6$+56.68	0.03	0.189	$y = -313.84x_6$+72.40	0.17	0.001

controlling factor of Re. This also reveals that GPP rather than Re was the predominant determinant of the change in NEE at the monthly scale.

Effects of climatic factors on CO_2 fluxes at the interannual scale

At the interannual scale, linear regression analysis showed that VPD, RH, and PPFD had no significant correlation with annual CO_2 fluxes during the growing season ($P>0.05$). The annual GPP and Re were positively correlated with Ta and Ts ($P<0.01$) (Figures 6A, B). However, Ta and Ts had no significant correlation with the annual NEE ($P>0.05$) (Figures 6A, B). The PPT was negatively correlated with the annual GPP and Re ($P<0.05$), but had no significant correlation with the annual NEE ($P>0.05$) (Figure 6C).

Discussion

Driving mechanisms of CO_2 fluxes at the monthly scale

CART and linear regression analysis showed that Ta in the growing season of alpine wetland was the most important controlling factor for the monthly GPP, which might be attributed to the relatively high aboveground biomass of alpine grassland vegetation. Thus, the growing season thermal conditions strongly impacted the photosynthesis of vegetation (Ueyama et al., 2013; Shen et al., 2015). Moreover, the thermal condition is the primary limiting factor to breaking the dormancy of vegetation and is crucial to the phenological development and sustainable metabolic growth of vegetation (Ueyama et al., 2013; Kang et al., 2022). Further, the growth and metabolism of vegetation in the alpine wetland ecosystem have full phenotypic plasticity to thermal conditions (Zhao et al., 2006; Li et al., 2021). In addition, soil microbial and enzyme activities in alpine grassland are extremely sensitive to temperature, and thermal conditions can indirectly affect the nutrient supply of soil for vegetation growth and metabolism by affecting microbial activities and enzyme activities (Li et al., 2021; Shen et al., 2022). The study of alpine meadows, alpine shrubs and alpine wetlands near the study site showed that the daily GPP during the growing season was mainly controlled by Ta and PPFD. However, when PPFD is relatively high and exceeds a certain threshold, GPP is almost unaffected by the increase of PPFD (Zhao et al., 2005). Under the same PPFD condition, the GPP of the three vegetation types from high to low were alpine meadows, alpine shrubs, and alpine wetlands (Zhao et al., 2006; Li et al., 2016). However, studies have shown that climate and environmental factors may have different effects on the photosynthetic production capacity of vegetation at different time scales (Zhu et al., 2020). Because PPFD reaches its peak in June and then begins to decline, there is no significant correlation between monthly PPFD and monthly GPP (R^2 = 0.02, P=0.313) during the growing season.

CART showed that the variation of monthly Re in alpine wetland was mainly controlled by Ts. Many studies have shown that soil temperature in alpine grassland ecosystems significantly affects CO_2 release and nitrogen mineralization, and soil microbial biomass in alpine ecosystems is limited by low temperature (Song et al., 2015; Cao et al., 2019). The high soil temperature can stimulate microbial activities and enzyme activities and promotes soil respiration (Gao et al., 2011). Therefore, soil temperature becomes the primary controlling factor of CO_2 emission from the alpine grassland ecosystem (Kang et al., 2022). However, some research has found that the increase in temperature improves autotrophic respiration, the loss of fixed carbon by plants, and inhibits heterotrophic respiration, the loss of fixed carbon by non-plant species, resulting in the poor response of Re to warming (De et al., 2008; Duan et al., 2019). CART and the linear regression analysis showed that Ts had a stronger controlling effect on the monthly Re in the alpine wetland than Ta, suggesting that soil respiration in the alpine wetland, compared to vegetation respiration, may be more sensitive to thermal conditions (Figure 5 and Table 1).

Only in May of the growing season did the alpine wetland acts as a carbon source (Figure 2). Because the temperature is low and the precipitation is less in the early growing season of

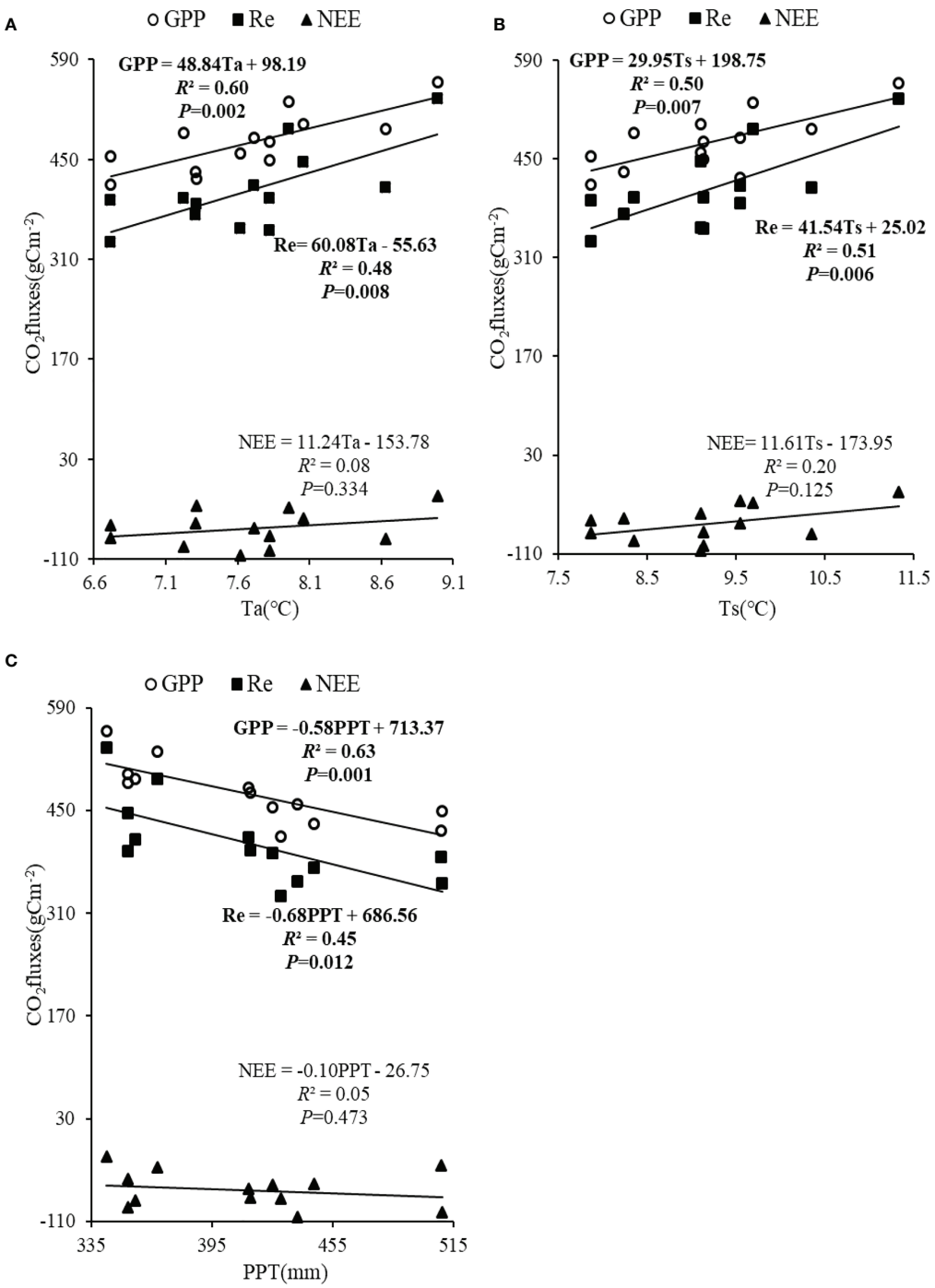

FIGURE 6
Linear regressions between seasonal CO_2 fluxes and Ta **(A)**, linear regressions between seasonal CO_2 fluxes and Ts **(B)**, and linear regressions between seasonal CO_2 fluxes and PPT **(C)**.

the alpine wetland, the vegetation just germinates and grows, and the growth metabolism of vegetation is weak (Zhao et al., 2010). Compared with ecosystem respiration, the photosynthetic production capacity of vegetation is low, so the alpine wetland is a carbon source in May. Linear regression analysis showed that monthly NEE was significantly negatively correlated with the monthly GPP and monthly Re during the growing season of alpine wetland from 2004 to 2016 (P<0.001) (Figures 3A, B), and

compared with the monthly Re (R^2 = 0.40), the monthly GPP (R^2 = 0.87) had a stronger controlling effect on the monthly NEE. CART and linear regression analysis showed that the thermal conditions (Ta and Ts) of the alpine wetland were the dominant factors for the change in the monthly NEE at the monthly scale, and Ta had a stronger controlling effect on the monthly NEE. This is similar to the results of previous studies (Ueyama et al., 2013; Li et al., 2016; Chen et al., 2021a), suggesting that the carbon sequestration of alpine wetlands in the growing season is more dependent on the photosynthetic production capacity of vegetation at the monthly scale.

Driving mechanisms of CO_2 fluxes at the interannual scale

The mean annual NEE of the alpine wetland in the growing season was −67.5 ± 10.2 gCm^{-2} (Figure 4), which represented a carbon sink. Owing to the special climate of the QTP and the favorable water and thermal conditions in the growing season, the grassland plants have high primary production capacity (Kato et al., 2006; Luo et al., 2015). Moreover, owing to the relatively low temperature, especially the low temperature at night, vegetation respiration and soil respiration consume relatively less organic matter (Groendahl et al., 2007; Chai et al., 2017). Linear regression analysis showed that annual Re was more responsible than the GPP for the dominant role of NEE at the interannual scale, which indicates that the dominant factors of NEE are not consistent in different time scales. This may because there is a large amount of thatch in the soil of the alpine wetland, and the process of the microbial decomposition is sensitive to Ts, resulting in a stronger controlling effect of Re on NEE. This result indicates that soil respiration in the alpine wetland is crucial to carbon balance (Zhang et al., 2008; Zhao et al., 2010; Li et al., 2021).

Linear regression analysis showed that the annual GPP and Re were positively correlated with Ta and Ts (P<0.01) (Figure 6A, B). Temperature promoted photosynthetic productivity and autotrophic respiration of vegetation (Ueyama et al., 2013; Chen et al., 2021a). However, soil temperature promoted the decomposition of a large amount of organic matter in the soil and enhanced soil respiration (Zhao et al., 2010). In addition, the decomposition of soil organic matter provides nutrients for vegetation growth, which further strengthens the process of vegetation growth and metabolism (Zhang et al., 2008). The PPT was negatively correlated with the annual GPP, Re (P<0.05) (Figure 6C). The PPT could affect the depth of surface water in the alpine wetland, and the increase of PPT deepens the water depth to a certain extent (Wang et al., 2017). The surface water level of the wetland limits the movement of atmospheric oxygen into soil; thus, the microorganism activity is inhibited, the decomposition rate of soil organic matter is reduced, and soil respiration is reduced (Hirota et al., 2006). Furthermore, the photosynthesis of alpine wetland vegetation is reduced, owing to the reduction of nutrients in the soil (Chimner and Cooper 2003). Furthermore, the saturated zone of soil could also affect the soil heat transfer, thus impacting the change in soil temperature (Zhang et al., 2008; Zhang et al., 2022). Because soil temperature affects the decomposition rate of soil organic matter, water depth may indirectly affect GPP and Re by regulating soil temperatures (Zhao et al., 2010; Song et al., 2015; Chen et al., 2021b). However, owing to the similar responses of GPP and Re to hydrothermal conditions in the alpine wetland, there was no significant correlation between the NEE and hydrothermal conditions, indicating that it is necessary to be more cautious when evaluating the carbon source and sink capacity of alpine wetland. More in-depth studies are needed to verify this result (Niu et al., 2013; Peng et al., 2014; Li et al., 2021).

Conclusions

Based on CO_2 fluxes measured with the EC technique, the alpine wetland ecosystem was found to be a carbon sink during the growing season in the northeastern QTP. At the monthly scale, Ta and Ts played a crucial role in the dynamics of monthly CO_2 fluxes. At the interannual scale, hydrothermal (Ta, Ts and PPT) conditions had significant effects on the GPP and Re, but had no significant effects on the NEE. Our results indicate that climate warming is beneficial to the improvement of GPP and Re during the growing season in the alpine wetland, while the increase of PPT may weaken this effect.

Data availability statement

The raw data supporting the conclusions of this article will be made available by the authors, without undue reservation.

Author contributions

JZ performed the research, analyzed data, and wrote the paper. HL, YY, and YL analyzed data and wrote the paper. HH and FZ conceived of the study. All authors have revised, discussed, and approved the final manuscript.

Funding

This study was supported by Natural Science Foundation of Shandong Province (ZR2021QC222), the National Natural Science Foundation in China (32001185, 41877547), the Chinese Academy of Sciences-People's Government of Qinghai Province Joint Grant on Sanjiangyuan National Park Research (YHZX-2020-07), the National Key R&D Program (2017YFA0604802), and the Qingtan Talent Scholar project in Zaozhuang University.

Acknowledgments

The authors are grateful to Jinlong Wa for the help in obtaining field data.

Conflict of interest

The authors declare that the research was conducted in the absence of any commercial or financial relationships that could be construed as a potential conflict of interest.

Publisher's note

References

Baldocchi, D., Ma, S. Y., and Verfaillie, J. (2021). On the inter-and intra-annual variability of ecosystem evapotranspiration and water use efficiency of an oak savanna and annual grassland subjected to booms and busts in rainfall. *Glob. Change. Biol.* 27, 359–375. doi: 10.1111/gcb.15414

Cao, S. K., Cao, G. C., Chen, K. L., Han, G. Z., Liu, Y., Yang, Y. F., et al. (2019). Characteristics of CO_2, water vapor, and energy exchanges at a headwater wetland ecosystem of the qinghai lake. *Can. J. Soil. Sci.* 99, 227–243. doi: 10.1139/cjss-2018-0104

Chai, X., Shi, P. L., Song, M. H., Zong, N., He, Y. T., Zhao, G. S., et al. (2019). Carbon flux phenology and net ecosystem productivity simulated by a bioclimatic index in an alpine steppe-meadow on the Tibetan plateau. *Ecol. Model.* 394, 66–75. doi: 10.1016/j.ecolmodel. 2018.12.024

Chai, X., Shi, P. L., Zong, N., Niu, B., He, Y. T., and Zhang, X. Z. (2017). Biophysical regulation of carbon flux in different rainfall regime in a northern Tibetan alpine meadow. *J. Resour. Ecol.* 8, 30–41. doi: 10.5814/j.issn.1674-764x.2017.01.005

Chen, H. Y., Xu, X., Fang, C. M., Li, B., and Nie, M. (2021b). Differences in the temperature dependence of wetland CO_2 and CH_4 emissions vary with water table depth. *Nat. Clim. Change.* 11, 766–771. doi: 10.1038/s41558-021-01108-4

Chen, N., Zhang, Y. J., Zhu, J. T., Cong, N., Zhao, G., Zu, J. X., et al. (2021a). Multiple-scale negative impacts of warming on ecosystem carbon use efficiency across the Tibetan plateau grasslands. *Glob. Ecol. Biogeogr.* 30, 398–413. doi: 10.1111/geb.13224

Chimner, R. A., and Cooper, D. J. (2003). Influence of water table levels on CO_2 emissions in a colorado subalpine fen: an *in situ* microcosm study. *Soil. Biol. Biochem.* 35, 345–351. doi: 10.1016/S0038-0717(02)00284-5

De, G. B., Cornelissen, J. H. C., and Bardgett, R. D. (2008). Plant functional traits and soil carbon sequestration in contrasting biomes. *Ecol. Lett.* 11, 516–531. doi: 10.1111/j.1461-0248.2008.01164.x

Duan, M., Li, A. D., Wu, Y. H., Zhao, Z. P., Peng, C. H., Deluca, T. H., et al. (2019). Differences of soil CO_2 flux in two contrasting subalpine ecosystems on the eastern edge of the qinghai-Tibetan plateau: a four-year study. *Atmos. Environ.* 198, 166–174. doi: 10.1016/ j.atmosenv. 2018.10.067

Fu, Y. L., Zheng, Z. M., Yu, G. R., Hu, Z. M., Sun, X. M., Shi, P. L., et al. (2009). Environmental influences on carbon dioxide fluxes over three grassland ecosystems in China. *Biogeosci. Discuss.* 6, 2879–2893. doi: 10.5194/bg-6-2879-2009

Gao, J. Q., Ouyang, H., Lei, G. C., Xu, X. L., and Zhang, M. X. (2011). Effects of temperature, soil moisture, soil type and their interactions on soil carbon mineralization in zoigê alpine wetland, qinghai-Tibet plateau. *Chinese. Geogr. Sci.* 21, 27–35. doi: 10.1007/s11769-011-0439-3

Groendahl, L., Friborg, T., and Soegaard, H. (2007). Temperature and snow-melt controls on interannual variability in carbon exchange in the high Arctic. *Theor. Appl. Climatol.* 88, 111–125. doi: 10.1007/s00704-005-0228-y

Hirota, M., Tang, Y., and Hu, Q. (2006). Carbon dioxide dynamics and controls in a deep-water wetland on the qinghai-Tibetan plateau. *Ecosystems* 9, 673–688. doi: 10.1007/s10021-006-0029-x

Kang, E. Z., Li, Y., Zhang, X. D., Yan, Z. Q., Zhang, W. T., Zhang, K. R., et al. (2022). Extreme drought decreases soil heterotrophic respiration but not methane flux by modifying the abundance of soil microbial functional groups in alpine peatland. *Catena* 212, 106043. doi: 10.1016/j.catena.2022.106043

Kang, X. M., Wang, Y. F., Chen, H., Tian, J. Q., Cui, X. Y., and Rui, Y. C. (2014). Modeling carbon fluxes using multitemporal MODIS imagery and CO_2 eddy flux tower data in zoige alpine wetland, south-west China. *Wetlands* 34, 603–618. doi: 10.1007/s13157-014-0529-y

Kato, T., Tang, Y. H., Gu, S., Hirota, M., Du, M. Y., Li, Y. N., et al. (2006). Temperature and biomass influences on inter-annual changes in CO_2 exchange in an alpine meadow on the qinghai-Tibetan plateau. *Glob. Change Biol.* 12, 1285–1298. doi: 10.1111/j.1365-2486.2006.01153.x

Li, H. Q., Zhang, F. W., Li, Y. N., Wang, J. B., Zhang, L. M., Zhao, L., et al. (2016). Seasonal and inter-annual variations in CO_2 fluxes over 10 years in an alpine shrubland on the qinghai-Tibetan plateau, China. *Agric. For. Meteorol.* 228, 95–103. doi: 10.1016/j.agrformet.2016.06.020

Li, H. Q., Zhang, F. W., Zhu, J. B., Guo, X. W., Li, Y. K., Lin, L., et al. (2021). Precipitation rather than evapotranspiration determines the warm-season water supply in an alpine shrub and an alpine meadow. *Agric. For. Meteorol.* 300, 108318. doi: 10.1016/j.agrformet.2021.108318

Li, H. Q., Zhu, J. B., Zhang, F. W., He, H. D., Yang, Y. S., Li, Y. N., et al. (2019). Growth stagedependant variability in water vapor and CO_2 exchanges over a humid alpine shrubland on the northeastern qinghai-Tibetan plateau. *Agric. For. Meteorol.* 268, 55–62. doi: 10.1016/j.agrformet.2019.01.013

Luo, C. Y., Zhu, X. X., Wang, S. P., Cui, S. J., Zhang, Z. H., Bao, X. Y., et al. (2015). Ecosystem carbon exchange under different land use on the qinghai-Tibetan plateau. *Photosynthetica* 4, 527–536. doi: 10.1007/s11099-015-0142-1

Niu, S. L., Sherry, R. A., Zhou, X. H., and Luo, Y. Q. (2013). Ecosystem carbon fluxes in response to warming and clipping in a tallgrass prairie. *Ecosystems* 16, 948–961. doi: 10.1007/ s10021 -013 -9661-4

Peng, F., You, Q. G., Xu, M. H., Guo, J., Wang, T., and Xue, X. (2014). Effects of warming and clipping on ecosystem carbon fluxes across two hydrologically contrasting years in an alpine meadow of the qinghai-Tibet plateau. *PloS One* 9, e109319. doi: 10.1371/journal.pone.0109319

Piao, S. L., Tan, K., Nan, H. J., Ciais, P., Fang, J. Y., Wang, T., et al. (2012). Impacts of climate and CO_2 changes on the vegetation growth and carbon balance of qinghai–Tibetan grasslands over the past five decades. *Global Planet Change* 98, 73–80. doi: 10.1016/ j.gloplacha. 2012.08.009

Saito, M., Kato, T., and Tang, Y. (2009). Temperature controls ecosystem CO_2 exchange of an alpine meadow on the northeastern Tibetan plateau. *Global. Change. Biol.* 15, 221–228. doi: 10.1111/j.1365-2486.2008.01713.x

Shen, X. J., Liu, Y. W., Zhang, J. Q., Wang, Y. J., Ma, R., Liu, B. H., et al. (2022). Asymmetric impacts of diurnal warming on vegetation carbon sequestration of marshes in the qinghai Tibet plateau. *Global. Biogeochem. Cy* 36(7), e2022GB007396. doi: 10.1029/2022GB007396

Shen, M. G., Piao, S. L., Jeong, S. J., and Yao, T. D. (2015). Evaporative cooling over the Tibetan plateau induced by vegetation growth. *P Natl. Acad. Sci.* 112, 9299–9304. doi: 10.1073/pnas.1504418112

Song, W. M., Wang, H., Wang, G. S., Chen, L. T., Jin, Z. N., Zhuang, Q. L., et al. (2015). Methane emissions from an alpine wetland on the Tibetan plateau: neglected but vital contribution of the nongrowing season. *J. Geophy. Res. Biogeosci.* 120, 1475–1490. doi: 10.1002/2015JG003043

Street, L. E., Shaver, G. R., Williams, M., and Wijk, M. T. (2007). What is the relationship between changes in canopy leaf area and changes in photosynthetic CO_2 flux in arctic ecosystems? *J. Ecol.* 95, 139–150. doi: 10.1111/j.1365-2745.2006.01187.x

Temmink, R. J., Lamers, L. P., Angelini, C., Bouma, T. J., Fritz, C., Koppel, J., et al. (2022). Recovering wetland biogeomorphic feedbacks to restore the world's biotic carbon hotspots. *Science* 376, eabn1479. doi: 10.1126/science.abn1479

Ueyama, M., Iwata, H., Harazono, Y., Euskirchen, E. S., and Oechel, W. C. (2013). Growing season and spatial variations of carbon fluxes of Arctic and boreal ecosystems in Alaska (USA). *Ecol. Appl.* 23, 1798–1816. doi: 10.1890/11-0875.1

Wang, H., Yu, L. F., Zhang, Z. H., Liu, W., Chen, L. T., Cao, G. M., et al. (2017). Molecular mechanisms of water table lowering and nitrogen deposition in affecting greenhouse gas emissions from a Tibetan alpine wetland. *Global Change bio.* 23, 815–829. doi: 10.1111/gcb.13467

Yu, G. R., Zhang, L. M., Sun, X. M., Fu, Y. L., Wen, X. F., Wang, Q. F., et al. (2008). Environmental controls over carbon exchange of three forest ecosystems in eastern China. *Glob. Change Biol.* 14, 2555–2571. doi: 10.1111/j.1365-2486.2008.01663.x

Zhang, F. W., Liu, A. H., Li, Y. N., Liang, Z., and Wang, Q. X. (2008). CO_2 flux in alpine wetland ecosystem on the qinghai-Tibetan plateau. *Acta Ecologica. Sinica.* 28, 453–462. doi: 10.1016/S1872-2032(08)60024-4

Zhang, Y. M., Naafs, B. D., Huang, X. Y., Song, Q. W., Xue, J. T., Wang, R. C., et al. (2022). Variations in wetland hydrology drive rapid changes in the microbial community, carbon metabolic activity, and greenhouse gas fluxes. *Geochim. Cosmochim. Ac.* 317, 269–285. doi: 10.1016/j.gca.2021.11.014

Zhao, L., Li, Y., Xu, S. X., Zhou, H. K., Gu, S., Yu, G. R., et al. (2006). Diurnal, seasonal and annual variation in net ecosystem CO_2 exchange of an alpine shrubland on qinghai-Tibetan plateau. *Glob. Change. Biol.* 12, 1940–1953. doi: 10.1111/j.1365-2486.2006.01197.x

Zhao, L., Li, J., Xu, S. X., Zhou, H. K., Li, Y. N., Gu, S., et al. (2010). Seasonal variations in carbon dioxide exchange in an alpine wetland meadow on the qinghai–Tibetan plateau. *Biogeosciences* 7, 1207–1221. doi: 10.5194/bg-7-1207-2010

Zhao, L., Li, Y. N., Zhao, X. Q., Xu, S. X., Tang, Y. H., Yu, G. R., et al. (2005). Comparative study of the net exchange of CO_2 in 3 types of vegetation ecosystems on the qinghai-Tibetan plateau. *Chin. Sci. Bull.* 50, 1767–1774. doi: 10.1360/04wd0316

Zheng, Y., Niu, Z., Gong, P., Dai, Y., and Shangguan, W. (2013). Preliminary estimation of the organic carbon pool in china's wetlands. *Chin. Sci. Bull.* 58, 662–670. doi: 10.1007/s11434-012-5529-9

Zhu, Z. K., Ma, Y. M., Li, M. S., Hu, Z. Y., Xu, C., Zhang, L., et al. (2015). Carbon dioxide exchange between an alpine steppe ecosystem and the atmosphere on the nam Co area of the Tibetan plateau. *Agr. For. Meteorol.* 203, 169–179. doi: 10.1016/j.agrformet. 2014.12.013

Zhu, J. B., Zhang, F. W., Li, H. Q., He, H. D., Li, Y. N., Yang, Y. S., et al. (2020). Seasonal and interannual variations of CO_2 fluxes over 10 years in an alpine wetland on the qinghai-Tibetan plateau. *J. Geophy. Res. Biogeosci.* 125, e2020JG006011. doi: 10.1029/2020JG006011

frontiers | Frontiers in Plant Science

TYPE Original Research
PUBLISHED 04 January 2023
DOI 10.3389/fpls.2022.990597

OPEN ACCESS

EDITED BY
Rongxiao Che,
Yunnan University, China

REVIEWED BY
Gaosen Zhang,
Northwest Institute of Eco-Environment and Resources (CAS), China
Victoria Cerecetto,
Julius Kühn-Institut, Germany
Gero Benckiser,
University of Giessen, Germany

*CORRESPONDENCE
Hongtao Jia
jht@xjau.edu.cn

†These authors have contributed equally to this work

SPECIALTY SECTION
This article was submitted to Functional Plant Ecology, a section of the journal Frontiers in Plant Science

RECEIVED 10 July 2022
ACCEPTED 25 November 2022
PUBLISHED 04 January 2023

CITATION
Abulaizi M, Chen M, Yang Z, Hu Y, Zhu X and Jia H (2023) Response of soil bacterial community to alpine wetland degradation in arid Central Asia.
Front. Plant Sci. 13:990597.
doi: 10.3389/fpls.2022.990597

Response of soil bacterial community to alpine wetland degradation in arid Central Asia

Maidinuer Abulaizi[1†], Mo Chen[2†], Zailei Yang[1†], Yang Hu[1], Xinping Zhu[1,3] and Hongtao Jia[1,3*]

[1]College of Resources and Environment, Xinjiang Agricultural University, Urumqi, China, [2]College of Grassland Science, Xinjiang Agricultural University, Urumqi, China, [3]Xinjiang Key Laboratory of Soil and Plant Ecological Processes, Urumqi, China

A large number of studies have reported the importance of bacterial communities in ecosystems and their responses to soil degradation, but the response mechanism in arid alpine wetlands is still unclear. Here, the non-degraded (ND), slightly degraded (SD), and heavily degraded (HD) regions of Bayinbuluk alpine wetland were used to analyzed the diversity, structure and function of bacterial communities in three degraded wetlands using 16S rRNA. The results showed that with the increase of degradation degree, the content of soil moisture (SM) and available nitrogen (AN) decreased significantly, plant species richness and total vegetation coverage decreased significantly, Cyperaceae (Cy) coverage decreased significantly, and Gramineae (Gr) coverage increased significantly. Degradation did not significantly affect the diversity of the bacterial community, but changed the relative abundance of the community structure. Degradation significantly increased the relative abundance of Actinobacteria (ND: 3.95%; SD: 7.27%; HD: 23.97%) and Gemmatimonadetes (ND: 0.39%; SD: 2.17%; HD: 10.78%), while significantly reducing the relative abundance of Chloroflexi (ND: 13.92%; SD: 8.68%; HD: 3.55%) and Nitrospirae (ND: 6.18%; SD: 0.45%; HD: 2.32%). Degradation significantly reduced some of the potential functions in the bacterial community associated with the carbon (C), nitrogen (N) and sulfur (S) cycles, such as hydrocarbon degradation (ND: 25.00%; SD: 1.74%; HD: 6.59%), such as aerobic ammonia oxidation (ND: 5.96%; SD: 22.82%; HD: 4.55%), and dark sulfide oxidation (ND: 32.68%; SD: 0.37%; HD: 0.28%). Distance-based redundancy analysis (db-RDA) results showed that the bacteria community was significantly related to the TC (total carbon) and Gr ($P < 0.05$). The results of linear discriminant analysis effect size (LEfSe) analysis indicate significant enrichments of Alphaproteobacteria and *Sphingomonas* in the HD area. The vegetation communities and soil nutrients changed significantly with increasing soil degradation levels, and *Sphingomonas* could be used as potential biomarker of degraded alpine wetlands.

KEYWORDS

degraded wetland, degradation biomarker, bacterial diversity, community structure, bacterial function

Introduction

Although the land surface area of wetland stations is less than one-tenth (Mitsch and Gosselink, 2007), their C storage per unit area accounts more than any other ecosystem (Yarwood, 2018). Wetlands are vital to the preservation of biodiversity and ecological functioning in natural resources (Xia et al., 2015; Wu et al., 2021a). Compared with other ecosystems, alpine wetland ecosystems have relatively singular species, fragile system stability, an extremely sensitive response to human disturbance, and are highly prone to irreversible regional degradation (Chen et al., 2021). Wetland degradation refers to the process of structural changes and functional imbalances of wetland ecosystems under the interference of nature, anthropogenic processes or both (Coban et al., 2022). The degradation of alpine wetlands is mainly caused by climate change, while overgrazing will aggravate the degradation process (Fawzy et al., 2020). Despite the significance of wetlands within the land ecosystem is widely recognized, human factors (e.g., population growth, excessive reclamation, grazing) (Bai et al., 2013) have caused the wetland degradation situation to become increasingly severe and have therefore become an important issue worldwide (Wei and Wu, 2021).

Soil is a complex biological system that serves as a habitat for biogeochemical circulation and enables plant production (Philippot et al., 2013). Soil bacteria is an important driver of the nutrient cycle and energy flow in the ecosystem, and is sensitive to environmental change (Wardle et al., 2004; Peralta et al., 2013; Wagg et al., 2014), thus playing a crucial role in the wetland soil ecosystems (Wu et al., 2021a). Different microbes play different roles in ecosystem environments, such as participating within the C, N, and P cycles, the degradation of cellulose (Xiong et al., 2015), and the production of antibiotics (Chen et al., 2020). The results of many related studies have shown that significant changes in plant biomass, community composition, soil physicochemical properties are the objective manifestations of wetland degradation (Wu et al., 2014; Wang et al., 2015; Chu et al., 2016), as well as important factors that lead to microbial community changes. Soil pH has been shown to be a key factor driving bacterial community diversity and community structure (Wang et al., 2020). Wu et al. (2021a) found that wetland degradation increased the relative abundance of Chloroflexi and Gematimonadetes and significantly reduced the relative abundance of Proteobacteria; However, there were no significant differences in alpha diversity in bacterial communities in different degrees of degraded wetland. In addition, some studies have shown that with the aggravation of degradation, the sulfate respiration process in wetland bacterial community gradually weakens (Liu et al., 2022). The changes in diversity and composition of soil microbial communities reflect the response strategy of microorganisms to adapt to change (Marschner et al., 2003; Segata et al., 2011). The influence mechanism of degradation on alpine grassland was studied from the perspective of plant-soil-microorganism (Zhou et al., 2019). Whether the soil microbial community diversity and composition changes can be used as an indicator of the health or recovery of degraded grassland (Wu et al., 2021b). Li et al. (2022) reported that the degradation of the alpine wetland inhibited the growth of nitrogen-fixing bacteria, leading to the decline of their nitrogen-fixing function. However, there are few reports on the co-change of soil microbial community characteristics and soil environmental factors in different degraded areas of arid alpine wetland under the background of global change. At the same time, this study is the first demonstration of soil bacterial community in different degraded area of Bayinbuluke alpine wetland.

Bayinbuluke alpine wetland is a typical wetland in arid areas of Central Asia, and the only national swan nature reserve in China, which has great ecological strategic value in protecting water resources and biodiversity in this area (Liu et al., 2019; Hu et al., 2022). In the past 20 years, the increasing human disturbance has degraded the Bayinbuluke alpine wetland to varying degrees, which has a profound impact on the plant community and soil nutrient cycle in this area (Zhao et al., 2021). High-cover grassland area decreasing the most, and the number of landscape type patches to low-cover grassland decreased, the landscape fragmentation index of dry land and high-cover grassland was reduced (Shi et al., 2015). Swampy soil with high coverage evolved into sandy land that lead to the loss of soil C (Zhu et al., 2019). Therefore, it is of great significance to study the response mechanism of soil microbial community to the degradation of alpine wetlands in arid areas of Central Asia, for better understanding the wetland ecosystem process under the condition of global environmental change, and providing reference datum for the restoration with sustainable use of degraded alpine wetlands. For this we used high-throughput sequencing technology to analyze the different soil bacterial community characteristics in areas within the Bayinbuluk alpine wetland that have been subjected to different degrees of degradation. The aims of the research are to 1) explore the changing characteristics of the plant community and soil physicochemical properties in wetlands with different degrees of degradation, as well as their relationship to the change of soil bacterial community composition; and 2) elucidate discrepancies in bacterial community structure, and identify microbes that could be employed as alpine wetland degradation biomarkers; 3) to reveal the effects of degradation on the diversity, structure and function of soil bacterial community in alpine wetland.

Materials and methods

Study area information

This research was conducted in the Bayinbuluk National Nature Reserve (E 82°59′-83°31′, N 42°45′-43°00′) in Xinjiang,

China, in August 2019. The Bayinbuluk alpine wetland covers an area of over 770 km^2, with an altitude of 2300-3042 m. The annual average temperature and precipitation in the area are approximately -4.6 °C, 273 mm, respectively. The water source is snow, ice meltwater, and underground diving overflow, and the underground water level is 0.5-1.0 m deep. The Bayinbuluk alpine wetland has been degraded in different degrees in recent years due to the influence of natural and human disturbance factors, such as climate warming and grazing. The study area was divided into three degraded areas with different degrees: ND, SD and HD, according to aboveground plant biomass, total vegetation coverage, and vegetation coverage of Cyperaceae and Gramineae (Zhou et al., 2019). Figure 1 and Table 1 summarizes the overall situation of wetland degradation in the area.

Plant measurement and soil sampling

Three large quadrats (50 × 50 m, distance >100 m) were set in the ND, SD, and HD areas, and then randomly selected three small quadrats (1 × 1 m, distance >10 m) in each large quadrat. The characteristics of plant communities in each quadrat were investigated, including plant coverage, species, and height. Aboveground plants were removed after measuring the plant community. A five-point method (The center point of the square and four points on the diagonal that are the same distance from the center point, distance > 0.5m) was used to collect surface fresh bulk soil (0-10 cm) samples using sterile soil sampler. The composite soil samples obtained from each quadrat were mixed evenly, sieved with a 2 mm mesh size (roots and stones were removed) and divided into four parts on average. Three parts (one for use, two for preparation) were used for measuring the soil physicochemical properties (Air-dried soil samples under natural conditions), and the remaining part was used for high-throughput sequencing (stored at -80°C).

Vegetation characteristics

The aboveground plant biomass is the aboveground plants after drying treatment (30 minutes at 105°C and 48 hours at 65° C). Some samples were ground into fine powder using a freezing ball mill (PM100, Retsch, Germany) sieved with 60 mesh size and total carbon (TC) content was determined by using an element analyzer (Vario El III, Elemental, Germany).

Soil physicochemical properties

A pH meter (FE28-Standard, Switzerland) was used to measure the soil pH (soil-to-water ratio of 1:5). An element analyzer (Vario El III, Elemental, Germany) was used to determine the TC and nitrogen (TN) concentrations in the soil (Chen et al., 2021), and the soil available nitrogen (AN) was measured using the alkaline hydrolysis diffusion method

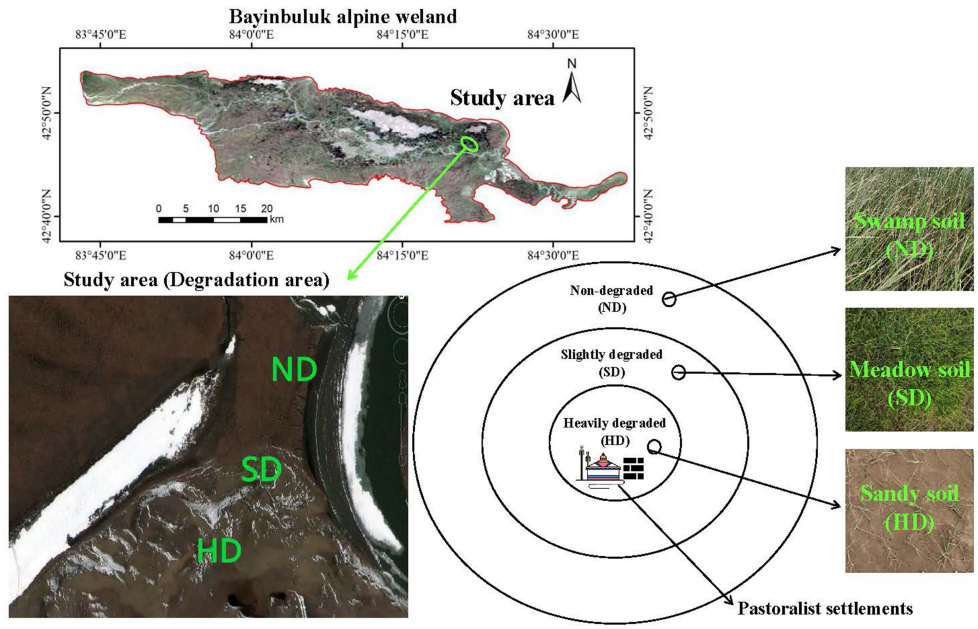

FIGURE 1
General overview of the non-degraded (ND), slightly degraded (SD), and heavily degraded (HD) alpine wetlands.

TABLE 1 General information of the non-degraded (ND), slightly degraded (SD) and heavily degraded (HD) alpine wetland areas.

	ND	SD	HD
Plant coverage	85.00%	70.00%	15.00%
Plant height	48.60 cm	8.20 cm	5.50 cm
Aboveground biomass	107.33 ± 23.92 g/m^2	55.73 ± 3.23 g/m^2	10.20 ± 0.83 g/m^2
Soil type	Swamp	swamp meadow	sandy
Grazing intensity	0.65 head/hm^2	2.09 head/hm^2	4.15 head/hm^2
Dominant plant groups	*Carex tristachya; Potentilla serices*	*Festuca ovina*	*Leymus*

(Lu, 2000). A spectrophotometer (UV-1780, Japan) was used to assess total (TP) and available phosphorus (AP) with $NaHCO_3$ Extraction-Mo-Sb colorimetry (Lu, 2000). Flame photometry (M420, Sherwood, British) was used to estimate total potassium (TK) and available potassium (AK) with NaOH melting method-flame photometer method (Hu et al., 2022). The gravimetric method was used to determine the soil moisture (SM). Bulk density (BD) was determined by the cutting-ring method, which was calculated with the following formula: dry soil weight (g)/soil volume (cm^3) = BD (g cm^{-3}) (Zhou et al., 2019).

DNA extraction and sequencing

The bacterial community was evaluated by high-throughput sequencing of 16S rRNA gene. Soil total community DNA was extracted with the Power Soil DNA Isolation Kit (MO BIO, USA). The DNA quality and quantity was determined using NanoDrop™ One (Thermo Fisher, USA). Using the primer pair 338F(5'-ACTCCTAGGGAGCA-3')/806R (5'-GGACTCHVGGGTWTTAT-3') (Christian et al., 2013). The sequencing and bioinformatics services of all of the samples were completed on the Illumina Hiseq 2500 platform of BMK Cloud (www.biocloud.net, Biomarker Technologies Co. Ltd., Beijing, China) (Chen et al., 2021). SRA (Sequence Read Archive) records will be accessible with the following link after the indicated release date: https://www.ncbi.nlm.nih.gov/sra/PRJNA813909.

Processing of sequencing data

Flash software (version 1.2.11) and Trimmomatic (version 0.33) software were used to obtain high-quality reads. UCHIME (version 8.1) software was used to remove chimera sequence and obtain the final valid data. USEARCH (version 10.0) software was used to cluster the reads (at a similarity level of 97%) to obtain the operational taxonomic units (OTUs). OTUs with polar abundance (abundance less than 0.005%) were removed, and the OTUs were taxonomically annotated based on the 16S bacteria taxonomy database (Silva, release 132).

Data analyses

R (version 4.0.2) was used to perform the univariate and multivariate analyses. Analysis of the variance (ANOVA) and the *post-hoc* test least significant difference test (LSD) were used to test significant differences among different areas using the agricolae package (version 0.11.3) (Mendiburu et al., 2016). Car software package (version 0.1-0) and dplyr software package (version 1.0.10) are used normality and homogeneity of variance were checked. The ggalluvial package (version 0.11.3) was used to draw the stack histogram of the bacterial relative abundances (Aime, 2021). The microeco package (version 0.7.1) (Liu et al., 2021) was used to perform the linear discriminant analysis effect size (LEfSe, from phylum to genus level) in different degradation areas. The bacterial community alpha-diversity indices (with rarefied data) and rarefaction curves were determined using Mothur (version 1.30). Functional prediction of soil bacterial communities under different degradation area was done using the FAPROTAX database (Hu et al., 2022).

We have done the PCoA, the ANOSIM and the RDA with rarefied data. The vegan software package (version 2.5.6) was used to construct a PCoA (principal co-ordinate analysis) based on the Bray-Curtis distance to measure the β-diversity of the bacterial community, and the ANOSIM (analysis of similarities) analysis was used to further test whether there were significant differences in different degrees of degradation. The ggvegan software package (version 0.1-0) was used to construct a db-RDA to analyze the relationship between bacterial community structure and environmental factors. Linket software package (version 0.0.2.9) was used to analyze the Pearson correlation and spearman correlation (Huang, 2021).

Results

Characteristics of alpine wetlands plant communities under different degradation degrees

In this study, the plant characteristics of different degraded areas in alpine wetlands were different (Table 2). In the ND area, species richness was significantly higher than SD and HD areas.

TABLE 2 Plant communities features of the non-degraded (ND), slightly degraded (SD) and heavily degraded (HD) alpine wetland areas.

	ND	SD	HD
Plant species richness	12.00 ± 1.53^{a}	8.00 ± 1.15^{b}	1.00 ± 0.00^{c}
Plant coverage (%)	85.33 ± 0.88^{a}	70.67 ± 0.67^{b}	15.00 ± 0.57^{c}
Gramineae (%)	4.66 ± 0.33^{c}	9.33 ± 0.88^{b}	15.00 ± 0.57^{a}
Cyperaceae (%)	80.67 ± 1.67^{a}	54.67 ± 2.40^{b}	0.00 ± 0.00^{c}
Forb (%)	3.59 ± 0.20^{b}	7.21 ± 0.15^{a}	0.00 ± 0.00^{c}
Plant total carbon (g kg^{-1})	424.37 ± 1.11^{ab}	427.11 ± 10.37^{a}	410.17 ± 9.10^{b}

mean ± standard error (n = 3). The same lowercase letter indicates no significant difference, but the difference is significant at the 0.05 level.

Cyperaceae coverage significantly decreased with increasing degradation level, whereas Gramineae coverage increased. *Leymus* was the only gramineous plant found in the HD area (Table 1). The coverage of Cyperaceae plants in the ND area was the highest, reaching 80.67 ± 1.67%, which was significantly higher than that in SD (54.67 ± 2.40%) and HD (0.00%) areas. The TC content of plants decreased with the aggravation of degradation.

Differences in soil physicochemical properties of alpine wetlands under different degradation levels

There were significant differences in soil physicochemical properties within the different degraded areas of alpine wetlands (Figure 2). The pH in the HD area was significantly higher than that in ND and HD areas, reaching 8.37 ± 0.13. TC, TN and TP in ND area was not different to SD area, but was significantly higher than in HD area. There were no significant differences in TK between the SD and HD areas, but between ND and SD/HD there were. The SM and AN significantly decreased with increasing degradation degree, while the BD was significantly increased with degradation level. AP content was significant different between ND and SD/HD; there was less AP in ND. The AK was significantly higher in SD than in ND/HD.

Diversity of soil bacterial community in degraded wetlands

The library coverage of all of the sequencing samples was higher than 0.99, which was sufficient to detect most bacteria (Table 3). Rarefaction curves reached a plateau trend for all samples and showed that sequencing depth was sufficient to cover the microbial diversity in all samples (Figure S1). After the chimeras were removed, the number of OTUs was 968-1346; after removing unclassified OTUs at domain level, chloroplast and mitochondria, the final number of OTUs was 963-1341. There were no differences in ACE, Chao1, and Simpson indexes among the degraded alpine wetlands. The Shannon index was the lowest in the ND area, and significant different to SD/HD (Table 3). Based on the result of PCoA (Figure 3A), the bacterial communities showed differences among the different degradation areas, and the ANOSIM showed that degradation had a significant effect (R=1, P=0.005) on the bacterial community beta-diversity (Figure 3B). Suggesting that there were obvious differences in bacterial communities under the condition of wetland degradation.

Differences of wetlands soil bacterial community composition under different degradation

At phylum level, the Proteobacteria (ND: 40.62%; SD: 50.61%; HD: 38.03%) was the dominant phylum among all samples (Figure 4A). The second most dominant phylum of the bacterial communities was Actinobacteria (ND: 3.95%; SD: 7.27%; HD: 23.97%). The other dominated phyla were Acidobacteria (ND: 9.20%; SD: 14.80%; HD: 9.55%), Bacteroidetes (ND: 15.17%; SD: 16.37%; HD: 8.87%), Chloroflexi (ND: 13.92%; SD: 8.68%; HD: 3.55%). The relative abundance of Gemmatimonadetes in the HD area was significantly higher than that in ND and SD areas ($P < 0.05$). There were no significant differences in relative abundance of Nitrospirae between the SD and HD areas, but between ND and SD/HD there were ($P < 0.05$).

At class level, Gammaproteobacteria (ND: 22.85%; SD: 22.53%; HD: 10.29%) and Alphaproteobacteria (ND: 2.83%; SD: 12.38%; HD: 25.36%) were the most abundant in the soil of the different degraded wetlands, followed by Deltaproteobacteria, Bacteroidetes, Actinobacteria, Gemmatimonadetes, Anaerolineae, and others (Figure 4B). The abundances of Alphaproteobacteria, Actinobacteria, and Gemmatimonadetes significantly increased with degradation degree. Figure 4C shows the relative abundance of the top 50 bacteria genera in the nine wetland samples and that there were significant differences among soil bacterial genera in the different degraded areas, there are specific communities for HD, ND and SD. There are 20 specific communities with higher relative abundance in HD area, including Sphingomonas, Gemmatimonas and Gemmatirosa etc. Similarly, there are 15 in the ND area (uncultured_bacterium_f_anaerolineae, uncultured_bacterium_o_SJA-15 etc.), and 15 in SD area (uncultured_bacterium_o_Rokubacteria, uncultured_bacterium_c_Subgroup_17 etc.).

10.3389/fpls.2022.990597

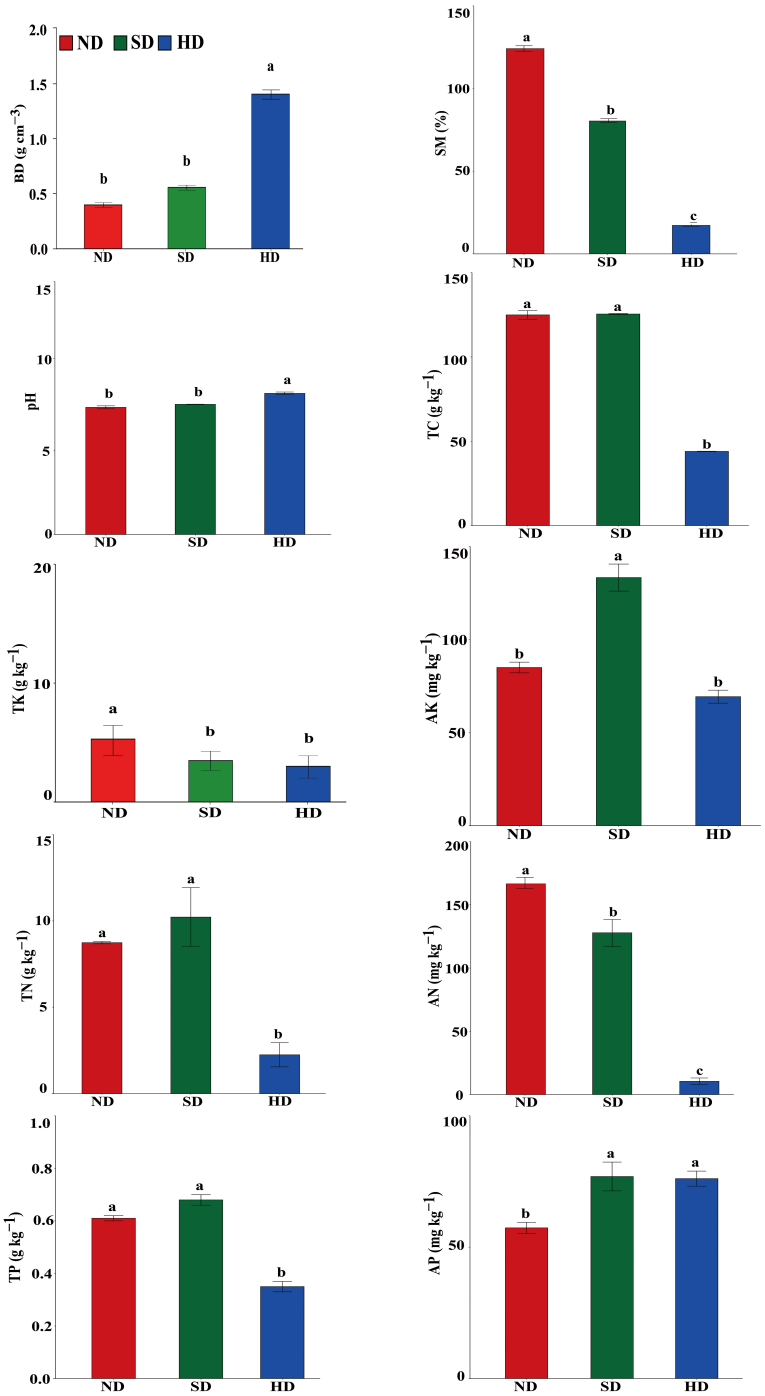

FIGURE 2
Soil physicochemical properties of the non-degraded (ND), slightly degraded (SD) and heavily degraded (HD) alpine wetland areas. Note: mean ± standard error (n = 3). Values within the same line followed by the same letter do not differ at $P < 0.05$. BD, bulk density; SM, soil moisture content; TC, total carbon; TN, total nitrogen; TP, total phosphorus; TK, total potassium; AN, available nitrogen; AP, available phosphorus; AK, available potassium.

10.3389/fpls.2022.990597

TABLE 3 Diversity of the soil bacterial communities of the non-degraded (ND), slightly degraded (SD) and heavily degraded (HD) alpine wetland areas.

	ND	SD	HD
OTUs	1051.33 ± 41.96[b]	1253.33 ± 14.75[a]	1238.33 ± 58.05[a]
Library coverage (%)	99 ± 0.00 [a]	99 ± 0.00 [a]	100 ± 0.00 [a]
ACE index	1332.68 ± 49.58[a]	1487.40 ± 15.91[a]	1436.87 ± 65.09[a]
Chao1 index	1372.74 ± 57.67[a]	1510.97 ± 15.79[a]	1489.6 ± 62.64[a]
Simpson index	0.01 ± 0.0009[a]	0.01 ± 0.0014[a]	0.01 ± 0.0004[a]
Shannon index	5.42 ± 0.07[b]	5.67 ± 0.05[a]	5.65 ± 0.09[a]

mean ± standard error (n = 3). The same lowercase letter indicates no significant difference, but the difference is significant at the 0.05 level.

LEfSe analysis showed that when the LDA threshold was 4.0, there were 72 bacterial taxa (from phylum to genus level) with statistically significant differences among different degradation degrees (Figure 5). In the ND area, 33 biomarkers were found, whereas the SD and HD areas had 13 and 26 biomarkers, respectively. Anaerolineae and Bacteroidales were the ND biomarkers with highest relative abundance. uncultured deltaproteobacteria (NB1-j) was the SD biomarker with highest relative abundance. Alphaproteobacteria was the HD biomarker with highest relative abundance, followed by Sphingomonadales, *Sphingomonadaceae*, *Sphingomonas* and Gemmatimonadetes.

Relationship between the changes in bacterial community and environmental factors

A Pearson correlation analysis was made between environmental factors and the bacterial community alpha diversity indices under different degrees of degraded wetlands. TK and AK were negatively significantly correlated to ACE, Chao1 and Shonnon index, and above-ground biomass was negatively significantly correlated to shannon diversity index (Figure 6).

The results of db-RDA showed that the samples in each group were close, and the groups were distant Figure 7A. Bacterial community structure was significantly correlated with TC and Gr, among which TC had the most significant ($P < 0.01$) influence on bacterial community structure (Table 4). A spearman correlation analysis was made between environmental factors and the bacterial community composition (at phylum level) under different degrees of degraded wetlands, and showed a significant correlation among the dominant phyla (Figure 7B). The results showed a significant correlation between the dominant phyla. The relationships between Gemmatimonadetes and Actinobacteria, Gemmatimonadetes and Chloroflexi, Actinobacteria and Chloroflexi, and Rokubacteria and Acidobacteria were the most significant ones. Relative abundance of Proteobacteria and Chloroflexi were significantly positively correlated with plant coverage, SM, TC and TN; and Acidobacteria was significantly negatively correlated with AK.

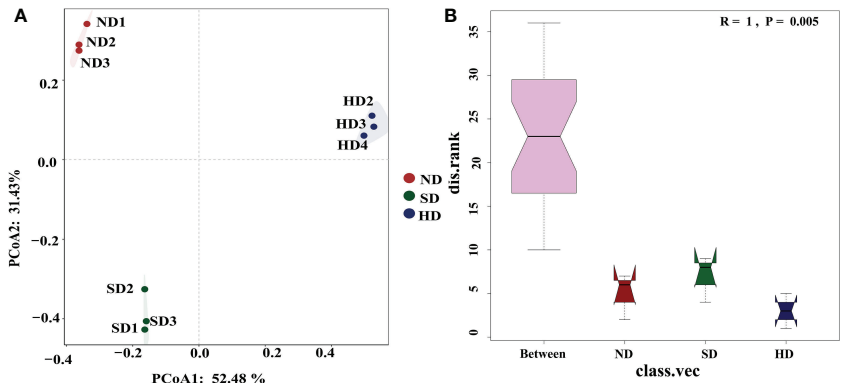

FIGURE 3
(A) Principal coordinate analysis (PCoA) plot of the first two principal components based on soil Bacterial community compositions based on Bray-Curtis distance matrix at each area; **(B)** Bacterial community β-diversity differences; Note: R-value is between (-1,1), R-value > 0, indicating that the difference between groups is significant. R-value = 0, indicating that the difference within the group is greater than the difference between groups. The reliability of statistical analysis is expressed by P-value, and $P < 0.05$ indicates that the statistics are significant.

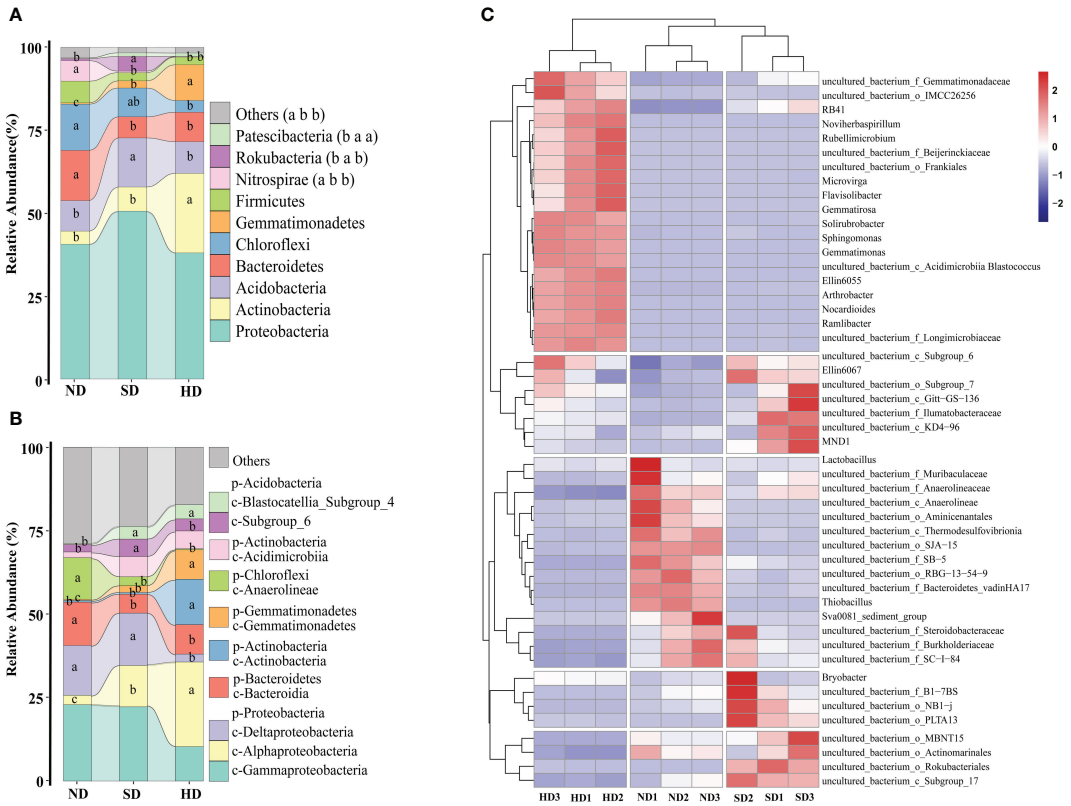

FIGURE 4
Bacterial community composition of the non-degraded (ND), slightly degraded (SD), and heavily degraded (HD) alpine wetland areas. Mean ± standard error (n = 3). **(A)** Bacterial phyla (p), **(B)** classes (c), **(C)** classified genera (top 50). In the stacked diagram, the same lowercase letters indicate no significant difference.

Soil bacterial community functions under different degraded wetlands

A total of 54 function were observed by the FAPROTAX functional annotation (Figure 8). Through the analysis of variance, it was found that 32 of the 54 functional pathways had significant differences in different degrees of degradation. The chemoheterotrophy process is the main bacterial metabolic process in Bayinbuluk alpine wetland, followed by aerobic chemoheterotrophy, fermentation, nitrification, aerobic ammonia oxidation. The above five processes exist in all degraded areas (ND, SD, HD), indicating that soil bacterial in the different degraded area of Bayinbuluk alpine wetland actively participate in the biogeochemical cycle of elements such as C, N, H and S. As can be seen from Figure 8, with the intensification of degradation, the bacterial-dominated fermentation process and most of the sulfur-related functional processes weaken, but its relative abundance is not significantly different. In HD area, chemoheterotrophy, aerobic chemoheterotrophy, ureolysis and chitinolysis are significantly enhanced ($P < 0.05$). SD area showed the highest nitrification and aerobia ammonia oxidation. From the correlation analysis between environmental factors and bacterial community function, 39 functional pathways were significantly affected by environmental factors (Figure 8). SM was significantly negatively correlated with majority functional pathways, followed by soil TC.

Discussion

Response of environmental factors to alpine wetlands

Plant community structure can directly reflect the degree of degradation (Hirsch et al., 2016). In our study, the Cyperaceae proportion and the total vegetation coverage decreased significantly with the intensifying degradation. This result is consistent with the research results of alpine grassland degradation in Qinghai-Tibet Plateau. With the aggravation of grassland degradation, the total vegetation coverage and Cyperaceae coverage decreased from 94.00% and 41.33% to 24.60% and 0.00% respectively (Zhou et al., 2019). The reason

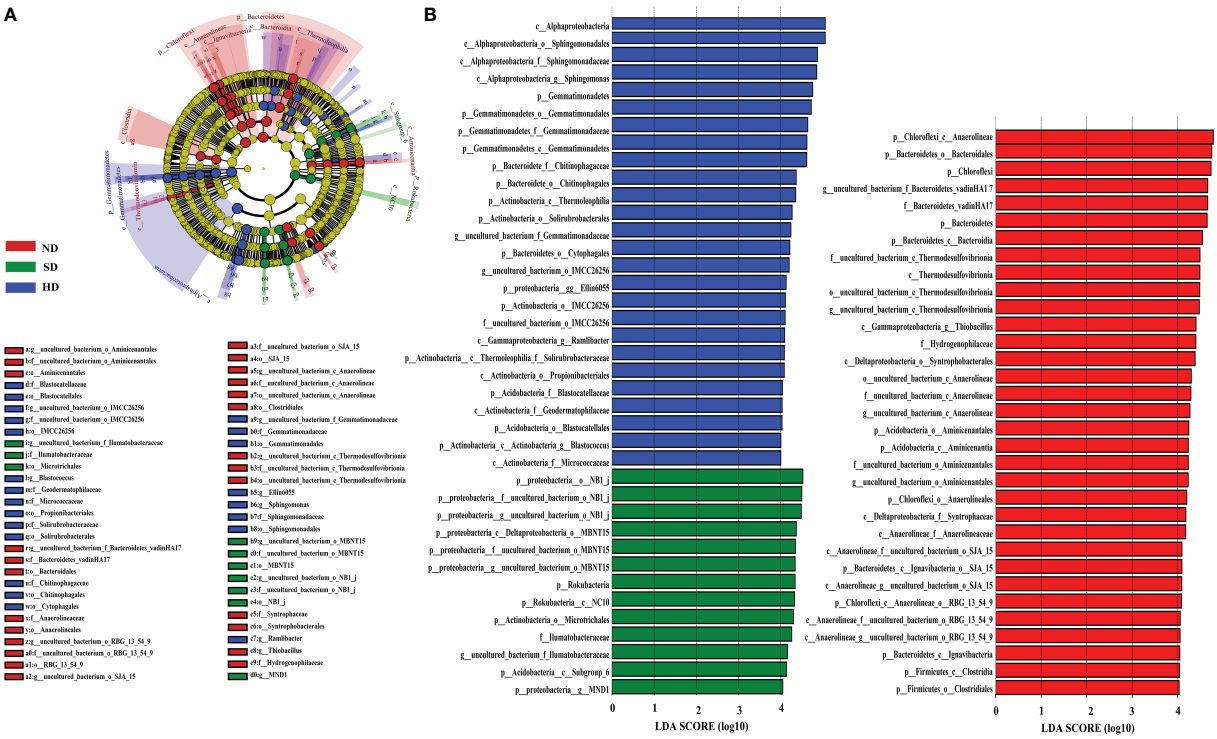

FIGURE 5
LEfSe analysis of the Bacterial abundance in the non-degraded (ND), slightly degraded (SD), and heavily degraded (HD) alpine wetland areas. **(A)** Phylogenetic tree with the ND, SD and HD bacterial biomarkers obtained with LEfSe analysis. **(B)** Histogram of the LDA scores computed for the differentially abundant bacteriaamong the degraded alpine wetlands identified with a threshold value of 4.0. Note: The LEfSe analysis was performed at the phylum to genus levels.

may be that Cyperaceae plants have developed roots and can fully absorb water and nutrients to adapt to wetland environment. However, due to the aggravation of wetland degradation, the soil moisture and nutrient content decrease, which is not favorable for Cyperaceae growth, and is gradually replaced by other grasses (Wang et al., 2018). At the same time, overgrazing (cattle, sheep, horses, etc.) is an important reason to change the physical and chemical properties of wetland plant communities and soil. Specifically, the trampling and nibbling behaviors of animals could explain the changes in the plant community and in the physicochemical properties of wetlands. Chu et al. (2016) reported that increasing soil bulk density will limit the movement of nutrients and water in the soil, and directly affect the absorption of nutrients by plants. In addition, research shows that the succession pattern of alpine meadow plant community changes with the aggravation of degradation degree, and the dominance of the plants of Spartinae and Cyperaceae will decrease, as observed in the studied area (Liu et al., 2018). Similarly, in our study, it was found that the dominance of Cyperaceae plants decreased in SD area, but did not exist in HD area. However, the rhizomatous grass (Leymus chinensis), which is more drought-tolerant, has a greater advantage in the competition (Li et al., 2017) and becomes the dominant species in HD area. At the same time, the difference of plant community structure changes the input of litter, thus affecting the nutrient cycle, changing the soil fertility and further affecting the bacterial community structure (Pereira et al., 2021). Therefore, there are direct and indirect relationships between the characteristics of plant communities and the structure of soil bacterial communities.

The soil physicochemical properties are the key factors that affect the soil bacterial community structure (Gu et al., 2018). Grazing affects the surface soil, gas emissions, and water conduction, increases the surface exposure, and enhances surface transpiration, which leads to reduced soil water content and eventually aggravates soil degradation (Cheng et al., 2016). A reduction of SM is the most direct response to alpine wetland degradation (Lin et al., 2019). Grazing affects the nutrients cycling in the ecosystem and changes the soil chemical structure by increasing the stomping, feeding, and excrement of livestock (Xiong et al., 2015). Previous studies have reported that nitrogen is the main factor that determines the primary

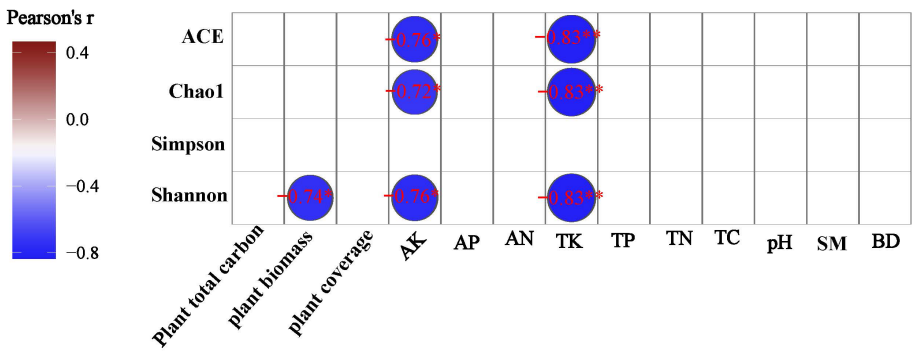

FIGURE 6
Pearson correlation analysis between alpha-diversity indices and environmental factors.

productivity of plants. In our study, with the increase of grazing intensity, TN and AN content in HD area were significantly lower than those in SD and ND areas (Figure 2). This may be because grazing increases the ratio of soil C to N, which leads to nitrogen mineralization (Wang et al., 2014). At the same time, our research found that SM, TC and other soil physical and chemical factors changed significantly with the increase of degradation degree. These results are similar to the research results of Zoige Wetland (Gu et al., 2018). The contents of TC and AN decreased significantly with the increase of degradation degree, while the content of available potassium increased first and then decreased (Gu et al., 2018). Most of the K ingested from animals and plants returns to the soil in the form of AK through excrement, which makes the AK content in SD area higher than that in ND area (Su et al., 2015). In addition, this study found that with the aggravation of degradation, the content of AP increased, while the content of TP decreased, mainly because animals excreted P back to the soil (Wang et al., 2022), which led to the increase of AP. Furthermore, the SM content will decrease after alpine wetland degradation, which affects the SOC (Lin et al., 2019) and ultimately the global C cycle process (Xu et al., 2016). Soil nutrients, including N, may directly or indirectly affect the diversity and structure of soil bacterial communities by affecting plant communities (Gu et al., 2018).

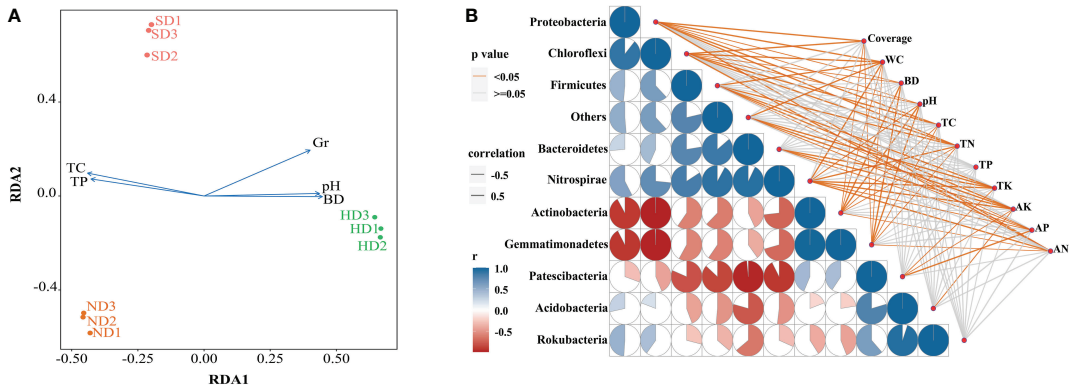

FIGURE 7
Correlation analysis between the bacterial community structure and environmental factors in the non-degraded (ND), slightly degraded (SD), and heavily degraded (HD) alpine wetland areas. **(A)** Distance-based redundancy analysis (db-RDA) of the soil bacterial community with environmental factors. **(B)** Spearman correlation analysis between the dominant bacteria phyla and environmental factors. Pairwise comparisons of the environmental factors are shown with a color gradient denoting the Spearman correlation coefficient. Taxonomic bacteria (based on the phylum level) community composition is related to each environmental factor by partial (geographic distance-corrected) Mantel tests. The edge width corresponds to the Mantel's r statistic for the corresponding distance correlations. The edge color denotes the statistical significance based on 9,999 permutations. Note: n = 3. Coverage: total plan coverage; SM: soil moisture content; BD: bulk density; TC: total carbon; TN: total nitrogen; TP: total phosphorus; TK: total potassium; AK: available potassium; AP: available phosphorus; AN: available nitrogen.

TABLE 4 Effects of environmental factors on bacterial community structure in non-degraded (ND), slightly degraded (SD) and heavily degraded (HD) alpine wetland areas.

Indices	Df	Variance	F	Pr(>F)	Significance
TC	1	0.2660	11.8336	0.003	**
TP	1	0.0257	1.1413	0.372	
pH	1	0.0611	2.7205	0.063	
BD	1	0.0294	1.3099	0.341	
Gr	1	0.0810	3.6019	0.042	*

*: P<0.05; **: P<0.01. TC, total carbon; TP, total phosphorus; BD, bulk density; Gr, Gramineae.

Response of bacterial community to alpine wetlands degradation

In our research, degradation has significant effects on both Shannon index and β-diversity ($P < 0.05$). It was similar to those of Zhou et al. (2019) on degraded alpine grassland, who showed no significant variations in the Chao1 and Shannon indexes among the degraded alpine steppes. Previous studies have found that the change of water conditions caused by wetland degradation has an important impact on soil bacterial community diversity (Mentzer et al., 2006). Wu et al., 2021a found that compared with meadow soil and sandy soil with low water content, the Shannon index of swamp soil with high water content is obviously lower. Too high or too low soil water content is not conducive to the survival and reproduction of bacterial communities (Moche et al., 2015). Therefore, the low shannon index in ND area in this study may be due to the high-water content. SD area is a transitional zone of alpine wetland degradation and a special habitat with frequent changes of groundwater level. The results of PCoA analysis and ANOSIM analysis (Figures 6A, B) showed that there were significant differences in the structure of soil bacterial communities in different degradation areas (R=1, P=0.005). It should be pointed out that although degradation has no significant effect on community richness, it does not mean that there is no significant difference in soil bacterial community structure in different degraded areas.

The bacterial community composition changed significantly with increasing alpine wetland deterioration. Proteobacteria was the dominant phylum in the degraded Bayinbuluk alpine wetland. Proteobacteria widely exist in alpine ecosystems, participate in biogeochemical processes, and have strong survival and adaptability. Although, Proteobacteria was the most abundant phylum in all the different studied areas, there were no significant differences among them. The other dominant phyla were Actinobacteria, Acidobacteria, Bacteroidetes, Chloroflexi, and others. Actinobacteria have strong metabolic and repair functions at low temperatures (Johnson et al., 2007). Studies have shown that Actinobacteria predominate in the dry and cold regions of the arid McMurdo Valley in Antarctica at high altitudes (Goordial et al., 2016). Goordials's results confirm that Actinobacteria can adapt to low temperatures, dry environments, and low nutrient content. Actinobacteria are widely found in sandy degraded soils in the Tibet plateau (Gu et al., 2018), which is consistent with the results obtained here, and its highest relative abundance in the HD area (Figure 4).

The differences in bacterial composition between alpine wetlands and alpine grasslands may be caused by water differences and they have different vegetation (Zhou et al., 2019; Wu et al., 2021a). Zhou et al. (2019) reported that Actinobacteria was the most abundant in degraded grassland. However, Wu et al. (2021a) indicated Proteobacteria was the dominant phylum in degraded alpine wetland. Wetland degradation affects soil moisture content, and the decrease of soil moisture further affects the average relative abundance of Actinobacteria. The results showed that bacterial community abundance responded to water changes in different ways under drought and non-drought conditions. With the decrease of soil water content, the abundance of Actinobacteria will increase. The reason for this is that Actinobacteria have a thick layer of peptidoglycans and the ability to produce endospores helps them become dominant in long-term dry environments (Nicholson et al., 2000; Fabia and Blair, 2009; Fierer et al., 2012; Hernández et al., 2019; Coban et al., 2022). In our research, these two phyla were significantly lower in HD areas in comparison to ND and SD area (Figure 4A). Acidobacteria is terrestrial diderm bacteria (Maestre et al., 2015) and its abundance decreased during drying (Coban et al., 2022). The bacterial communities in alpine regions around the world are similar but there are significant differences in soil bacterial communities with different degradation degrees in different regions. Although soil types and climates are different in different areas, bacterial communities have similar responses to soil moisture changes (Romain et al., 2013). In Qinghai-Tibetan plateau the relative abundance of Bacteroidetes decreased with the decrease of soil moisture (Zhou et al., 2019). Wu et al. (2021a) found the relative abundance of Bacteroidetes were significantly lower in swamp meadow in comparison to meadow wetland. Our research showed, in HD the relative abundance of Bacteroidetes were significantly lower than SD and HD. The relative abundance of Bacteroidetes in this study reached 15.17%-8.87% (Figure 4A), which is higher than that reported in Zhou et al. (2019) (3.724%-2.274%).

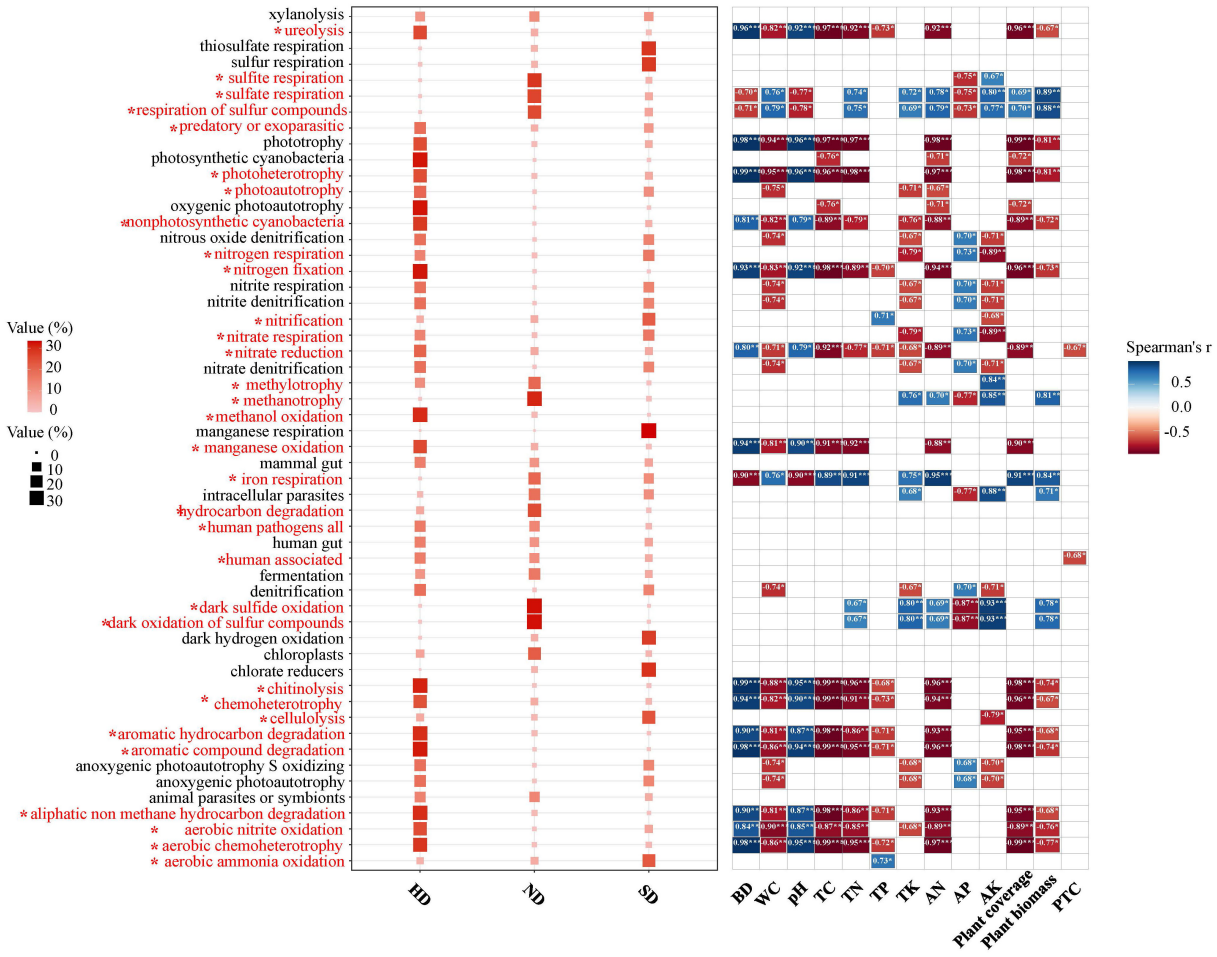

FIGURE 8
Bacterial community functions of the non-degraded (ND), slightly degraded (SD), and heavily degraded (HD) alpine wetland areas. Functional Prediction of Bacterial Communities; Spearman correlation analysis between community function and environmental factors; *: $P<0.05$; **: $P<0.01$; ***$P<0.001$.

C mineralization are strongly affected Bacteroidetes (Fierer et al., 2007), thus the TC and SM were positively correlated with relative abundance of Bacteroidetes (Figure 7B).

LEfSe analysis was used to identify biomarkers of wetlands with different degradation degrees and indicate the difference in soil bacterial community composition (Figure 5). 72 bacterial markers showed significant differences when the LDA threshold was 4.0, as shown in Figure 5. Alphaproteobacteria was the most abundant biomarker in HD, followed by Sphingomonadales (class: Alphaproteobacteria), Sphingomonadaceae (class: Alphaproteobacteria) and *Sphingomonas* (class: Alphaproteobacteria). Their content increased significantly with increasing degradation. Thus, we used *Sphingomonas* as a biomarker in HD. *Sphingomonas* can survive in extreme environments, because *Sphingomonas* has a special metabolic regulation mechanism to adapt to the changeable environment (especially the nutrient-deficient environment), and can efficiently adjust its own growth to resist many adverse environmental changes (Eguchi et al., 1996; Chen et al., 2004; Hu et al., 2007; Roggo et al., 2013). In addition, we used uncultured deltaproteobacteria (SD) and uncultured bacterium anaerolineae (ND) as biomarkers. In summary, our results indicated that the different degraded areas have their own bacterial communities.

Relationship between environmental factors and bacterial communities

The main goal of our research is to understand the relationship between environmental factors and soil bacteria. The response mechanism of soil bacterial communities in fragile ecosystems to degradation has always been the focus of global research. The results of db-RDA showed that environmental

factors, especially TC and Gr, had significant correlation with the changes of bacterial communities. In addition, there are differences in the characteristics of vegetation communities in different degraded regions of alpine wetlands. The degradation leads to the difference of SM in different degraded regions, and the different water-holding capacities of vegetation communities will also lead to the change of bacterial community structure, especially the influence on aerobic and anaerobic bacterial communities will be amplified. Maestre et al. (2015) showed that aridity indirectly affected bacterial community diversity and abundance by strongly affecting pH, SOC and total plant coverage. TN and TK may indirectly affect soil bacterial community composition by affecting plant growth (Wang et al., 2020). In our study, BD increased significantly with the aggravation of degradation (Figure 2), thus directly affecting the survival of soil bacteria by affecting the soil porosity.

Han et al. (2018) found that vegetation coverage may be an important factor affecting the diversity and structure of soil bacterial communities. The Cyperaceae coverage and plant species richness in the HD area were significantly lower than ND and SD areas. In our study, the Proteobacteria, Chloroflexi, Firmicutes, and Nitrospirae are positively correlated with plant coverage. The correlation analysis shows that the vegetation coverage, TC, TN, TP is significantly positively related to Proteobacteria and Chloroflexi, (Figure 7B). This indicates that their suitable for living in an environment with sufficient nutrients (Zhou et al., 2019). Proteobacteria can live in a wide range of environments and a good environment is more conducive to Proteobacteria accumulation (Xia et al., 2019; Yang et al., 2020), which is verified by the reduced abundance of Proteobacteria in the HD area compared with the ND and SD areas (Figure 4). In addition, there are differences in the viability of bacterial groups at the genus level. Similar to Actinobacteria, Gemmatimonadetes can release spores to resist extreme environment (Genderjahn et al., 2018).

In the studied alpine wetlands, Actinobacteria and Gemmatimonadetes are positively correlated with Bacteroidetes, Nitrospirae and Firmicutes, and negatively correlated with Chloroflexi. The result of correlation analysis showed that the Actinobacteria and Gemmatimonadetes were negatively correlated with soil water content, while the Bacteroidetes, Nitrospirae and Firmicutes were positively correlated. This suggests that when the soil water content decreases, the relative abundance of the former will increase, while the average relative abundance of the latter will decrease. This is because Bacteroidetes and Chloroflexi like anaerobic environments (Klatt et al., 2013), so their abundance will decrease when the water content decreases, which is closely related to their own metabolic function. In addition, Acidobacteria is only significantly correlated with AK. Therefore, Acidobacteria can survive better in areas with higher AK content (Fierer et al., 2007).

Through FAPROTAX function prediction, it was found that there are many bacterial taxa that are involved in different elements biogeochemical cycles, such as C, N and S, in the different degraded areas of the Bayinbuluk alpine wetland. Through the analysis of variance, it was found that with the intensification of wetland degradation, the sulfate respiration process of the bacterial community was significantly weakened. Sulfate respiration was positively correlated to the contents of SM, TN, TK AN, above-ground biomass, vegetation coverage, and AK (Figure 8). This means that environmental factors play a key role in the process of sulfate respiration (Ren et al., 2018). In addition, the function of bacterial community is closely related to aboveground plants, because aboveground plants provide different survival materials for bacterial community through litter input and root exudates, which further causes the change of bacterial community function (Tolli and King, 2005). In our research, wetland degradation reduces aerobic heterotrophic and chemical heterotrophic functions. This may be because degradation significantly reduced the aboveground biomass and C input and inhibited the assimilation of carbohydrates by soil bacterial communities (Liang et al., 2019). It shows that bacterial function will be affected by changes in environmental factors mediated by degradation. In this study, there are four key nitrogen metabolism processes: nitrogen fixation, aerobic ammonia oxidation, nitrate denitrification, and denitrification. This can indicate that soil bacterial in different degraded areas of the Bayinbuluk alpine wetland can carry out nitrogen cycling. In HD area, the relative abundance of nitrogen fixation is significantly higher than that of SD and ND, while the relative abundance of aerobic ammonia oxidation is lower than that of SD and ND, which means that the aerobic ammonia oxidation process is affected by HD, resulting in the decrease of TN and AN.

In summary, the results of this study show that there are differences in vegetation community characteristics, soil physicochemical properties, and bacterial community characteristics in different degraded regions of alpine wetlands, and there is a close causal relationship between them. Therefore, the unique bacterial communities in each degraded area can be considered as potential markers of degradation.

Conclusions

This research investigated the vegetation characteristics, soil physicochemical properties, and bacterial community distribution patterns of degraded alpine wetlands in Bayinbuluk. The results showed that the characteristics of the alpine wetland plant community significantly changed with degradation. The coverage of Cyperaceous decreased with increasing degradation of alpine wetland, whereas that of Gramineae gradually increased. The soil TC, SM, and AN significantly decreased with increasing degradation, whereas the pH, AP and BD significantly increased. There were significant differences in the bacterial community structure and composition

in the different degraded areas, but no significant differences were observed in community alpha diversity. LEfSe analysis suggests *Sphingomonas* as HD biomarker. The soil bacterial community was significantly related to the TC and Gr. Degradation significantly affected the functions related to C, N and S cycle in soil bacterial community.

In conclusion, degradation alters the vegetation and soil physicochemical properties characteristics of wetlands. This affects the bacterial community structure and composition. Different methods combined with a multi-omics study can be applied in the future to promote research on alpine wetland interconnection and provide further reference data for the sustainability and restoration of wetland ecosystems.

Data availability statement

The data presented in the study are deposited in the https://www.ncbi.nlm.nih.gov/, accession number PRJNA813909.

Author contributions

MA, MC, and ZY designed the study and wrote the manuscript. YH and XZ are responsible for field survey and experimental determination. MA and HJ are responsible for analysed the data. All authors have read and agreed to the published version of the manuscript.

Funding

This study was supported by the National Natural Science Foundation of China (No.31560171) and Xinjiang Uygur Autonomous Region Graduate Innovation Project of China (XJ2021G167).

Acknowledgments

Thanks to Guangling Yu, Xuyang Wang, Mengfei Cong, Tao Tang, Yunpeng Hu, Mengyao Zhang, Keyi Li for their assistance. We also thank Qin Ren, the head of grassland station in Hejing County, Bayingolin Mongolian Autonomous Prefecture, for his support. We appreciate the linguistic assistance provided by TopEdit (www.topeditsci.com) during the preparation of this manuscript.

Conflict of interest

The authors declare that the research was conducted in the absence of any commercial or financial relationships that could be construed as a potential conflict of interest.

Publisher's note

All claims expressed in this article are solely those of the authors and do not necessarily represent those of their affiliated organizations, or those of the publisher, the editors and the reviewers. Any product that may be evaluated in this article, or claim that may be made by its manufacturer, is not guaranteed or endorsed by the publisher.

Supplementary material

The Supplementary Material for this article can be found online at: https://www.frontiersin.org/articles/10.3389/fpls.2022.990597/full#supplementary-material

SUPPLEMENTARY FIGURE 1
Observed OTUs of non-degraded (ND), slightly degraded (SD), heavily degraded (HD) alpine wetland.

References

Aime, M. C. (2021). Table S1 & figs S1-S2. *Fungal Systematics Evolution.* 7 (1), 21–47. doi: 10.3114/fuse.2021.07.02_supp1

Bai, J., Lu, Q., Wang, J., Zhao, Q., Hua, O., and Li, A. (2013). Landscape pattern evolution processes of alpine wetlands and their driving factors in the zoige plateau of China. *J. Mt Sci.* 10, 54–67. doi: 10.1007/s11629-013-2572-1

Chen, Z., Diana, C., Francisco, A., Guardiola, F. A., and Esteban, M.Á. (2020). Dietary administration of the probiotic shewanella putrefaciens to experimentally wounded gilthead seabream (Sparus aurata l.) facilitates the skin wound healing. *Sci. Rep.* 10, 11029. doi: 10.1038/s41598-020-68024-z

Cheng, J., Jing, G., Wei, L., and Jing, Z. (2016). Long-term grazing exclusion effects on vegetation characteristics, soil properties and bacterial communities in the semi-arid grasslands of China. *Ecol. Eng.* 97, 170–180. doi: 10.1016/j.ecoleng.2016.09.003

Chen, M., Wu, S., Lin, G., Lu, C., Lin, Y., Lin, Y., et al. (2004). Rubrobacter taiwanensis sp. nov, a novel thermophilic, radiation-resistant species isolated from hot springs. *Int. J. Syst. Evol. Microbiol.* 54, 1849–1855. doi: 10.1099/ijs.0.63109-0

Chen, M., Zhu, X., Zhao, C., Yu, P., Abulaizi, M., and Jia, H. (2021). Rapid microbial community evolutn in initial carex litter destructure stages in bayinbuluk alpine wetland during the freeze–thaw period. *Ecol. Indic.* 121, 107180. doi: 10.1016/j.ecolind.2020.107180

Christian, Q., Elmar, P., Pelin, Y., Jan, G., Timmy, S., Pablo, Y., et al. (2013). The SILV a ribosomal RNA gene database project: improved data processing and web-based tools. *Nucleic Acids Res.* 41, D590–D596. doi: 10.1093/nar/gks1219

Chu, H., Sun, H., Binu, M., Jonathan, M., Huang, R., Zhang, Y., et al. (2016). Bacterial community dissimilarity between the surface and subsurface soils equals

horizontal differences over several kilometers in the western Tibetan plateau. *Environ. Microbiol.* 18 (5), 1523–1533. doi: 10.1111/1462-2920.13236

Coban, O., Deyn, G., and Ploeg, M. (2022). Soil microbiota as game-changes in restoration of degraded lands. *Science* 375, 990. doi: 10.1126/science

Eguchi, M., Nishikawa, T., Macdonald, K., Cavicchioli, R., Gottschal, J., Cavicchioli, R, et al. (1996). Responses to stress and nutrient availability by the marine ultramicrobacterium sphingomonas sp. strain RB2256. *Appl. Environ. Microbiol.* 62 (4), 1287–1294. doi: 10.1128/aem.62.4.1287-1294.1996

Fabia, U., and Blair, H. A. (2009). Major clade of prokaryotes with ancient adaptations to life on land. *Mol. Biol. Evol.* 26 (2), 335–343. doi: 10.1093/molbev/msn247

Fawzy, S., Osman, A., Doran, J., and Rooney, D. (2020). Strategies for mitigation of climate change: a review. *Environ. Chem. Lett.* 18, 2069–2094. doi: 10.1007/s10311-020-01059-w

Fierer, N., Bradford, M., and Jackson, R. (2007). Toward an ecological classification of soil bacteria. *Ecology* 88, 1354–1364. doi: 10.1890/05-1839

Fierer, N., Leff, J., Adams, B., Nielsen, U., Bates, S., and Lauber, C. (2012). Cross-biome metagenomic analyses of soil microbial communities and their functional attributes. *Proc. Natl. Acad. Sci. U.S.A.* 109, 21390–21395. doi: 10.1073/pnas.1215210110

Genderjahn, S., Alawi, M., Mangelsdorf, K., Horn, F., and Wagner, D. (2018). Desiccation- and saline-tolerant bacteria and archaea in Kalahari pan sediments. *Front. Microbiol.* 9. doi: 10.3389/fmicb.2018.02082

Goordial, J., Davila, A., Greer, C., Cannam, R., DiRuggiero, J., McKay, C., et al. (2016). Comparative activity and functional ecology of permafrost soils and lithic niches in a hyper-arid polar desert. *Environ. Microbiol.* 19 (2). doi: 10.1111/1462-2920.13353

Gu, Y., Yan, B., Xiang, Q., Yu, X., Zhao, K., Zhang, X., et al. (2018). Degradation shaped bacterial and archaeal communities with predictable taxa and their association patterns in zoige wetland at Tibet plateau. *Sci. Rep.* 8, 3884. doi: 10.1038/s41598-018-21874-0

Han, D., Wang, N., Sun, X., Hu, Y., and Feng, F. (2018). Biogeographical distribution of bacterial communities in changbai mountain, northeast China. *Microbiologyopen* 7 (2), e00529. doi: 10.1002/mbo3.529

Hernández, M., Klose, M., Claus, P., Bastviken, D., Marotta, H., Figureiredo, V., et al. (2019). Structure, function and resilience to desiccation of methanogenic microbial communities in temporarily inundated soils of the Amazon rainforest (Cunia reserve, rondonia). *Environ. Microbiol.* 21 (5), 1702–1717. doi: 10.1111/1462-2920.14535

Hirsch, P., Jhurreea, D., Williams., K., and Murray, J. (2016). Soil resilience and recovery: rapid community responses to management changes. *Plant Soil.* 412, 283–297. doi: 10.1007/s11104-016-3068-x

Huang, H. (2021). *linkET*: *Everything is linkable. R package version 0.0.2.9*. Available at: https://rdrr.io/github/Hy4m/linkET/f/README.md.

Hu, Y., Chen, M., Yang, Z., Cong, M., Zhu, X., and Jia, H. (2022). Soil microbial community response to nitrogen application on a swamp meadow in the arid region of central Asia. *Front. Microbiol.* 12. doi: 10.3389/fmicb.2021.797306

Hu, J., He, X., Li, D., and Liu, Q. (2007). Progress in research of sphingomonas. *Chin. J. Appl. Environ. Biol.* 13 (3), 431–437. doi: 10.3321/j.issn:1006-687X.2007.03.030

Johnson, S., Hebsgaard, M., Christensen, T., Mikhail, M., and Rasmus, N. (2007). Ancient bacteria show evidence of DNA repair. *Proc. Natl. Acad. Sci. U.S.A.* 104, 14401–14405. doi: 10.1073/pnas.0706787104

Klatt, C., Liu, Z., Ludwig, M., Kühl, M., Bryant, A., and Ward, M. (2013). Temporal meta transcriptomic patterning in phototrophic choroflexi inhabiting a microbial mat in geothermal spring. *ISME J.* 7 (9), 1775–1789. doi: 10.1038/ismej.2013.52

Liang, S., Deng, J., Jiang, Y., Wu, S., and Zhu, W. (2019). Functional distribution of bacterial community under different land use patterns based on FAPROTAX function prediction. *Pol. J. Environ. Stud.* 29 (2), 1245–1261. doi: 10.15244/pjoes/108510

Li, X., Chen, X., Xu, Y., and Cao, Y. (2017). Temporo-spatial expressions and prediction of cellulose synthase gene functions with growth of phyllostachys edulis. *J. Zhejiang A&F University*. 34 (4), 565–573. doi: 10.11833/j.issn.2095-0756

Li, C., Li, X., Yang, Y., Shi, Y., and Li, H. (2022). Degradation reduces the diversity of nitrogen-fixing bacteria in the alpine wetland on the Qinghai-Tibet Plateau. *Front. Plant Sci.* 13, 939762. doi: 10.3389/fpls.2022.939762

Lin, C., Li, X., Li, H., Sun, H., and Han, H. (2019). Distribution and storage of soil organic carbon and nitrogen in alpine wetland under different degradation succession. *Acta Agrestia Sinica*. 27, 805–816. doi: 10.11733/j.issn.1007-0435.2019.04.003

Liu, C., Cui, Y., Li, X., and Yao, M. (2021). Microeco: An r package for data mining in microbial community ecology. *FEMS Microbiol. Ecol.* 97 (2), fiaa255. doi: 10.1093/femsec/fiaa255

Liu, Y., Fang, B., Gao, L., Li, L., Wang, S., et al. (2022). Community structure and ecological functions of soil microorganisms in the degraded area of barkol lake. *Acta Microbiol. Sin.* 62 (6), 2053–2073. doi: 10.13343/j.cnki.wsxb.20220269

Liu, H., Wei, W., Yang, Y., and Zhang, Y. (2018). Redundancy analysis on relationships between grassland vegetation and soil factors on degraded alpine meadow. *Acta Agric. Boreali-occidentalis Sinica.* 27 (4), 480–490. doi: 10.7606/j.issn.1004-1389.2018.04.004

Liu, Y., Zhu, X., Li, D., Yan, C., Sun, T., Jia, H., et al. (2019). Soil aggregate and intra-aggregate carbon fractions associated with vegetation succession in an alpine wetland of Northwest China. *Catena.* 181, 104107. doi: 10.1016/j.catena.2019.104107

Lu, R. (2000). *Methods for soil agrochemistry analysis* (Beijing: China Agricultural Science and Technology Press).

Maestre, F., Manuel, D., Jecffries, T., Eldridge, D., Ochoa, A., Gozalo, B., et al. (2015). Increasing aridity reduces soil microbial diversity and abundance in global drylands. *Proc. Natl. Acad. Sci.* 112, 15684–15689. doi: 10.1073/pnas.1516684112

Marschner, P., Kandeler, E., and Marschner, B. (2003). Structure and function of the soil microbial community in a long-term fertilizer experiment. *Soil Biol. Biochem.* 35, 453–461. doi: 10.1016/S0038-0717(02)00297-3

Mendiburu, F. (2016). Statistical procedures for agricultural research: Package "agricolae". *CRAN Repository*, 1–157. Available at: http://tarwi.lamolina.edu.pe/~fmendiburu.

Mentzer, J., Goodman, R., and Balser, T. (2006). Microbial response over time to hydroloyic and fertilization treatments in a simulated wet praire. *Plant soil.* 284 (1/2), 85–100. doi: 10.1007/s11104-006-0032-1

Mitsch, W., and Gosselink, J. (2007). *Wetlands. 4th ed* (New York: Wiley). doi: 10.1007/s10980-012-9758-8

Moche, M., Gutknecht, J., Schulz, E., Langer, U., and Rinklebe, J. (2015). Monthly dynamics of microbial community structure and their controlling factors in three floodplain soils. *Soil Biol. Biochem.* 90, 169–178. doi: 10.1016/j.soilbio.2015.07.006

Nicholson, W., Nobuo, M., Gerda, H., Henry, J., and Peter, S. (2000). Resistance of bacillus endospores to extreme terrestrial and extraterrestrial environments. microbiol. *Mol. Biol.* 64, 548–572. doi: 10.1128/MMBR.64.3.548572.2000

Peralta, R., Ahn, C., and Gillevet, P. (2013). Characterization of soil bacterial community structure and physicochemical properties in created and natural wetlands. *Sci. Total Environ.* 443, 725–732. doi: 10.1016/j.scitotenv.2012.11.052

Pereira, A., Lima, L., Bezerra, W., Pereira, L., Mendes, W., Oliveira, B., et al. (2021). Grazing exclusion regulates bacterial community in highly degraded semiarid soils from Brazilian caatinga biome. *Land Degrad. Dev.* 32, 2210–2225. doi: 10.1002/ldr.3893

Philippot, L., Spor, A., Henault, C., Bru, D., and Bizouard, F. (2013). Loss in microbial diversity affects nitrogen cycling in soil. *ISME J.* 7 (8), 1–11. doi: 10.1038/ismej.2013.34

Ren, M., Zhang, Z., Wang, X., Zhou, Z., Chen, D., Zeng, H., et al. (2018). Diversity and contributions to nitrogen cycling and carbon fixation of soil salinity shaped microbial communities in tarim basin. *Front. Microbiol.* 9. doi: 10.3389/fmicb.2018.00431

Roggo, C., Coronado, E., Moreno, S., Harshman, K., Webber, J., and Roelof, J. (2013). Genome-wide transposon insertion scanning of environmental survival functions in the polycyclic aromatic hydrocarbon degrading bacterium Sphingomonas wittichii RW1. *Environ. Microbiol.* 15 (10), 2681–2695. doi: 10.1111/1462-2920.12125

Romain, L., Catherine, A., and Marry, L. (2013). Responses of soil bacterial and fungal communities to extreme desiccation and rewetting. *ISME J.* 7, 2229–2241. doi: 10.1038/ismej.2013.104

Segata, N., Izard, J., Waldron, L., Gevers, D., Miropolsky, L., Garrett, W., et al. (2011). Metagenomic biomarker discovery and explanation. *Genome Biol.* 12, R60. doi: 10.1186/gb-2011-12-6-r60

Shi, H., Yang, Z., Han, F., Shi, T., and Li, D. (2015). Assessing landscape ecological risk for a world natural heritage site: A case study of bayanbulak in China. *Polish J. Envi. Stu.* 24 (1), 269–283. doi: 10.15244/pjoes/28685

Su, Z., Sun, Y., Fu, J., Chu, X., Xu, Y., Hu, T., et al. (2015). Effects of grazing intensity on soil nutrient of kobresia pygmaea meadow in Tibet plateau. *Prata Sci.* 32 (3), 322–328. doi: 10.11829j.issn.1001-0629.2014-0286

Tolli, J., and King, G. (2005). Diversity and structure of bacterial chemolithotrophic communities in pine forest and agroecosystem soils. *Appl. Environ. Microbiol.* 71 (12), 8411–8418. doi: 10.1128/AEM.71.12.8411-8418.2005

Wagg, C., Bender, S., and Widmer, F. (2014). Soil biodiversity and soil community structure determine ecosystem multifunctionality. *Proc. Natl. Acad. Sci. U.S.A.* 111, 5266–5270. doi: 10.1073/pnas.1320054111

Wang, Y., Tian, L., Ai, Y., Cheng, S., and Mipam, T. (2022). Effects of short-term yak grazing intensity on soil bacterial communities in an alpine meadow of the Northwest sichuan plateau. *Acta Ecol. Sin.* 42 (4), 1549–1559. doi: 10.5846/stxb202011273042

Wang, C., Wang, G., Wang, Y., Rashad, R., Ma, L., Hu, L., et al. (2015). Fire alters vegetation and soil microbial community in alpine meadow. *Land Degrad. Dev.* 27, 1379–1390. doi: 10.1002/ldr.2367

Wang, D., Wu, G., Zhu, Y., and Shi, Z. (2014). Grazing exclusion effects on above- and below-ground C and N pools of typical grassland on the Loess Plateau (China). 123, 113–120. doi: 10.1016/j.catena.2014.07.018

Wang, X., Zhang, Z., Yu, Z., Shen, G., Cheng, H., and Tao, S. (2020). Structure and diversity of soil microbial communities in the alpine wetland and alpine forest ecosystems on the Tibetan plateau. *Sci. Total Environ.* 747, 141358. doi: 10.1016/j.scitotenv.2020.141358

Wang, J., Zhao, C., Zhao, L., Wang, X., and Li, Q. (2018). Response of root morphology and biomass of phragmites australis to soil salinity in in▪ land salt marsh. *Acta Ecol. Sin.* 38 (13), 4843–4851. doi: 10.5846/stxb201707141283

Wardle, D., Bardgett, R., and Klironomos, J. (2004). Ecological linkages between aboveground and belowground biota. *Science* 304, 1629–1633. doi: 10.1126/science.1094875

Wei, X., and Wu, P. (2021). Responses of soil insect communities to alpine wetland degradation on the eastern qinghai-Tibetan plateau, China. *Eur. J. Soil Biolo.* 103, 103276. doi: 10.1016/j.ejsobi.2020.103276

Wu, G., Ren, G., Dong, Q., Shi, J., Wang, Y., and Shi, Y. (2014). Above-and belowground response along degradation gradient in an alpine grassland of the qinghai-Tibetan plateau. *Clean-Soil Air Water.* 42 (3), 319–323. doi: 10.1002/clen.201200084

Wu, Y., Xu, N., Wang, H., Li, J., Zhong, H., Dong, H., et al. (2021a). Variations in the diversity of the soil microbial community and structure under various categories of degraded wetland in sanjiang plain, northeastern China. *Land Degrad. Dev.* 32, 2143–2156. doi: 10.1002/ldr.3872

Wu, X., Yang, J., Ruan, H., Wang, S., Yang, Y., Naeem, I., et al. (2021b). The diversity and co-occurrence network of soil bacterial and fungal communities and their implications for a new indicator of grassland degradation. *Ecol. Indic.* 129, 107989. doi: 10.1016/j.ecolind.2021.107989

Xia, Y., He, X., Feng, Z., Zhang, Q., and Yang, H. (2019). A comprehensive analysis of the microbial diversity in natural and engineered ecosystems based on high-throughput sequencing of 16S rRNA gene. *Int. Biodeter Biodegr.* 140, 160–168. doi: 10.1016/j.ibiod.2019.03.018

Xiong, W., Zhao, Q., Zhao, J., Xun, W., and Li, R. (2015). Dierent continuous cropping spans signifcantly affect microbial community membership and structure in a vanilla-grown soil as revealed by deep pyrosequencing. *Microb. Ecol.* 70, 209–218. doi: 10.1007/s00248-014-0516-0

Xu, F., Cai, T., and Yang, X. (2016). Effect of cultivation and natural restoration on soil bacterial community diversity in marshland in the San jiang plain. *Acta Ecol. Sinica.* 36, 7412–7421. doi: 10.5846/stxb201601040015

Yang, Z., Hollebone, B., Shah, K., Yang, C., and Brown, C. (2020). Biodegradation potential assessment by using autochthonous microorganisms from the sediments from lac mégantic (Quebec, Canada) contaminated with light residual oil. *Chemosphere* 239, 124796. doi: 10.1016/j.chemosphere.2019.124796

Yarwood, S. (2018). The role of wetland microorganisms in plant-litter destructure and soil organic matter formation: a critical review. *FEMS Microbiol. Ecol.* 94 (11). doi: 10.1093/femsec/fiy175

Zhao, Y., Luo, L., Wang, H., Wu, Q., and Liu, C. (2021). Remote sensing monitoring and analysis of landscape pattern in Bayanbulak Heritage Site for nearly 30 years. *J Remote Sen* 25 (12), 2488–2506. doi: 10.11834/jrs.20211193

Zhou, H., Zhang, D., Jiang, Z., Sun, P., Xiao, H., Wu, Y., et al. (2019). Changes in the soil microbial communities of alpine steppe at qinghai-Tibetan plateau under different degradation levels. *Sci. Total Environ.* 651, 2281–2291. doi: 10.1016/j.scitotenv.2018.09.336

Zhu, X., Yu, P., Li, L., Su, J., and Jia, H. (2019). Effect of the water regime on the soil carbon fractions at swan lake alpine wetland in Tianshan mountain, China. *Fresenius Environmental Bulletin* 28 (6), 4529–4536.

Frontiers in
Plant Science

Cultivates the science of plant biology and its applications

The most cited plant science journal, which advances our understanding of plant biology for sustainable food security, functional ecosystems and human health.

Discover the latest Research Topics

See more →

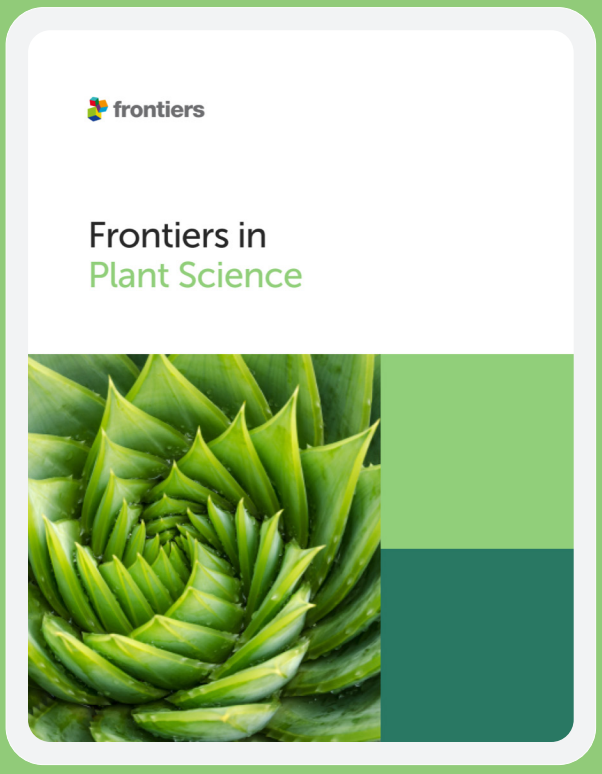

Frontiers

Avenue du Tribunal-Fédéral 34
1005 Lausanne, Switzerland
frontiersin.org

Contact us

+41 (0)21 510 17 00
frontiersin.org/about/contact